Atropisomeric Fragments in Drug Discovery and Probe Compound Development



Benjamin Danet

St Hilda's College

A dissertation presented in partial fulfilment of requirements for the award of the degree

Doctor of Philosophy

of the

University of Oxford

Dedication

I would like to dedicate this thesis to my parents and brothers – Yaël, Vincent, Nathan and Simon Danet.

Declaration

This dissertation describes work carried out in the Chemistry Research Laboratory at the University of Oxford between February 2018 and April 2022. The dissertation is a product of my own work and includes no results obtained through collaboration, unless explicitly stated otherwise in the text.



Benjamin Danet

Acknowledgements

I would like to begin with thanking my supervisors, Paul Brennan and Martin Smith for giving me the opportunity to undertake this project within their research groups. Thank you for your guidance and support all throughout this endeavour. I am also very grateful to my industrial sponsor, Neville McLean (AstraZeneca), for the continued interest he showed in my project and our regular, very helpful meetings.

Having spent most of my time in the Smith Group, I would like to express my gratitude to all the members of the group who crossed my path during these 4 long years. I am extremely grateful to Antti, who helped me find my way in the lab. Thank you Minh for motivating me to train to become a Zumba instructor and Alison for attending my very first classes. Thank you Kat and Liam for getting me on your Nintendo Switch Online family plan, and Yao for the numerous hours spent sat at a screen helping me sort out my dodgy NMRs. I would like to thank Zac and Mihai, my cohort mates, who always showed interest in my projects and kept track of the related literature, sometimes better than I could have done it myself. Thank you to Elliot and Zhuqing, who kept F5 lively during the grim times of Covid shift work, and Ali for being such a great Part II in spite of these dire working conditions. I would like to express my dearest gratitude to Owen, Pearse, Maddie, Jess and Ana, who have been not only great labmates but also good friends to me, I hope we get to keep in touch even after I leave Oxford. I will not forget Mengxue, Xiangqian, Jiyuan, Morgan, Tudor, Nick, Ricky, Ben J., Harriet, Ben W., Yasmine, Ella, Naa, Jay, Dan, Daniella, Michael, Hasanain and Pascal, with whom I remember sharing great moments, in and out of the lab.

I am also grateful to the members of the Brennan Group, despite me not spending much time with them, especially after Covid hit. They always made me feel welcome and a part of their team. Thank you in particular to Katherine, Carmen, Rob, Stéphane and Tryfon, for showing renewed interest in my project and helping me out with insightful suggestions.

My life in Oxford was made easier thanks to the amazing friends I made along the way. I cannot be grateful enough to my friend Nada, who was always there for me when I needed her, in and out of the lab. I don’t remember sharing as many laughs with anyone else in the world. I would like to thank Neja for her constant support and striking generosity. Thank you to my dear friends Sofia and Xinlan, who helped me get through very hard times during the pandemic. I am grateful to

Lucia, who helped me navigate the first years of my life in Oxford by showing me endless support and companionship. Though I was not a Lady Margaret Hall student, I ended up spending a lot of time there and made many friends who have all brightened my days: Vânia, Michael, Claire, Sarah, Kris, Vishnupriya. I won't forget the many other friends who've crossed my path during my time in this town: Sven, Giorgio, Julien, Daniel, Hana, Vid, Llorens, Jaime, Tanya, Niamh, Ndi, and Hamza. Sven, we finally made that burger!

Many of these friends also greatly supported me in my extracurricular endeavours, which allowed me to meet wonderful people. Thank you to Owen, Ana, Sandrine, Eliyah, Damian, Loïc, Adam, Xinlan, and many more for not missing a single of my Zumba classes at the Oxford University Club. Thank you to Sarah at BuzzGym and Eli at FeelFit Gym for calling on me whenever you needed an extra instructor. I would like to thank everyone in the 2019, 2020 and 2021 Oxford Pride committees, especially Dale and Debbie, and the 2021 and 2022 Witney Pride committee, especially Beth, for allowing me to express my artistry for the greater good. Thank you to Fleur Ostojak from the BBC Radio Oxford for the many lovely interviews, and the whole Lockdown Legends cast, especially my mentors, Rose Garden, Tia Kofi and Sum Ting Wong – you all made me feel like a true star in the most trying times.

Special shoutout to my bestie from Basel, Lucas "Jean-Michael" Loredana Donovan Turner Dirson, who never failed to try and bring a smile on my face even in the most difficult times, and my friends back home of Le Noyau (Cindy, Chloé, Christine, Melissa, Morgane and Romane) and les Kurvi (Cloé, Diana, Eléonore, Emeline, Marie-Adeline, Mélanie, Nour, Ondine, Perrine, and Regina) who I could always turn to for a laugh or comforting word.

I would like to extend my thanks to my family, especially my parents and brothers (and their lovely girlfriends), who have always showed unwavering support to my every single endeavour. I am grateful for the love I receive from my grandparents, aunties, and cousins, even being miles away from all of them. You all have given me a reason to keep pushing to be the greatest version of myself and I will always feel nothing but love for all of you.

Finally, I would like to thank anyone who's helped me with this final endeavour. Thank you Owen for collecting the crystallography data for me, thank you Lucia and Alistair for helping me out with collecting experimental data for the first part of this project, and thank you Nada, Maddie, Pearse, Elliot and Morgan for proofreading this thesis.

List of Abbreviations

$\Delta G^{\ddagger}_{T\,(K)}$	Rotational barrier at a given temperature T (in Kelvins)
[Ox]	Oxidant
$[Cp^*RhCl_2]_2$	Pentamethylcyclopentadienylrhodium(III) chloride dimer
4-DMAP	4-Dimethylaminopyridine
Ac	Acetate
ADMET	Absorption, Distribution and Metabolism
ADP	Adenosine Diphosphate
AK	Adenosine kinase
ATP	Adenosine Triphosphate
BIDIME	(*S*)-3-(tert-butyl)-4-(2,6-dimethoxyphenyl)-2,3-dihydrobenzo[*d*][1,3]oxaphosphole
BINAP	2,2'-bis(diphenylphosphino)-1,1'-binaphthyl
BINOL	1,1'-Bi-2-naphthol
Bn	Benzyl
Boc	*tert*-butyloxycarbonyl
B_2pin_2	Bis(pinacolato)diboron
brsm	Based on recovered starting material
BTK	Bruton's Tyrosine Kinase
Bu	Butyl
CASCADE	Chemical shift calculation with deep learning
Cat.	Catalyst
Cbz	Benzyloxycarbonyl
CDI	1,1'-carbonydiimidazole
CDK	Cyclin-dependant kinase
clog*P*	Calculated log*P*
CuAAC	Copper-catalysed alkyne-azide cycloaddition
Cy	Cyclohexyl
Cyoct	Cyclooctyl
s/m/d/h	second(s)/minute(s)/day(s)/hour(s)

Da	Dalton
DCE	1,2-dichloroethane
DDQ	2,3-Dichloro-5,6-dicyano-1,4-benzoquinone
DIPEA	*N,N*-Diisopropyl ethylamine
DMB	Dimethoxybenzyl
DME	1,2-dimethoxyethane
DMF	*N,N*-Dimethylformamide
DMSO	Dimethyl Sulfoxide
e.e./e.r.	Enantiomeric excess/Enantiomeric ratio
ent.	Enantiomer
ERK	Extracellular-signal-regulated kinase
ESI	Electrospray ionisation
eq.	Equivalent(s)
Et	Ethyl
FBDD	Fragment-Based Drug Discovery
FDA	Food and Drug Administration (US)
FTIR	Fourrier-Transform Infrared Spectroscopy
fur	Furyl
GAP	GTPase-activating protein
GEF	Guanine nucleotide Exchange Factor
GDP	Guanosine Diphosphate
GTP	Guanosine Triphosphate
HPLC	High Performance Liquid Chromatography
HRas	Harvey Rat Sarcoma Viral Oncogene Homologue
HRMS	High Resolution Mass Spectrometry
HTS	High Throughput Screening
IPA	2-propanol/isopropyl alcohol/isopropanol
*i*Pent	Isopentyl
*i*Pr	Isopropyl
IUPAC	International Union of Pure and Applied Chemistry
kcal	Kilocalorie
KHMDS	Potassium bis(trimethylsilyl)amide

KRas	Kirsten Rat Sarcoma Viral Oncogene Homologue
Lit.	Literature
logP	Partition coefficient
logD	Distribution coefficient
M	Molar
m-CPBA	*meta*-chloroperbenzoic acid
Me	Methyl
MEK/MAPK	Mitogen Activated Protein Kinase
MIDA	Methyliminodiacetic Acid
mTOR	Mammalian Target of Rapamycin
MW	Molecular Weight/Molecular Mass
N	Normal
NHC	*N*-heterocyclic carbene
NMR	Nuclear Magnetic Resonance
nOe	Nuclear Overhauser Effect
NRas	Neuroblastoma Rat Sarcoma Viral Oncogene Homologue
NSCLC	Non-small-cell lung cancer
PEPPSI	Pyridine-enhanced Precatalyst Preparation Stabilisation and Initiation
Pd/C	Palladium, 10% activated on carbon
$Pddba_2$	Bis(dibenzylidenacetone)palladium(0)
Pd_2dba_3	Tris(dibenzylideneacetone)dipalladium(0)
$Pd(dppf)Cl_2$	(1,1'-bis(diphenylphosphino)ferrocene)dichloropalladium
$Pd(OAc)_2$	Palladium(II) acetate
$Pd(PPh_3)_4$	Tetrakis(triphenylphosphine)palladium(0)
$Pd(PPh_3)_2Cl_2$	Bis(triphenylphosphine)palladium(II) dichloride
PDEδ	Phosphodiesterase, delta subunit
PI3K	Phosphoinositide 3-Kinase
Pin	Pinacolate
PIP2	Phosphatidylinositol bisphosphate
PIP3	phosphatidylinositol (3,4,5)-trisphosphate
Piv	Pivaloyl
Ph	Phenyl

$POCl_3$	Phosphorus(V) oxychloride
PTC	Phase Transfer Catalysis
QSAR	Quantitative Structure Activity Relationship
r.t.	Room temperature
rac.	Racemic mixture/racemate
Raf	Rapidly accelerated fibrosarcoma
Ras	Rat sarcoma virus
R^L	Large substituent
R^S	Small substituent
S-IIP	Switch II pocket (KRas)
S6K	S6 Kinase
SAR	Structure-Activity Relationship
SBDD	Structure-Based Drug Design
SFC	Supercritical Fluid Chromatography
SHP2	(SH2)-containing protein tyrosine phosphatase 2
SM	Starting material
S_NAr	Nucleophilic aromatic substitution
SOS	Son of Sevenless
SPhos	Dicylcohexylphosphino-2,6'-dimethoxy-1,1'-biphenyl
SPR	Surface Plasmon Resonance
$t_{1/2}^{rac}$	Half-life of racemization
TBAF	Tetra-*n*-butylammonium fluoride
t-Bu/*t*Bu	*tert*-butyl
THF	Tetrahydrofuran
TIMSO	Sulfur dioxide 1-methylpyrrolidine adduct
TFA	Trifluoroacetic acid
TLC	Thin-layer chromatography
TMS	Trimethylsilyl
Tol	Toluyl
Ts	Tosyl
TSA	Thermal Shift Assay
w/w	Percent by weight

XantPhos	4,5-Bis(diphenylphosphino)-9,9-dimethylxanthene
XPhos	2-Dicyclohexylphosphino-2’,4’,6’-triisopropylbiphenyl

Abstract

This thesis describes work on the use of atropisomeric biaryl compounds in fragment-based drug discovery (FBDD) and probe compound development. Part I describes the investigation of derivatisation methodologies and fragment growth methodologies to generate axially chiral biarylpyrimidines with high rotational barriers, for potential incorporation in FBDD screening libraries. We explored 6 derivatisation methodologies, yielding 23 examples. When carried out on enantioenriched substrates, conservation of the enantiomeric ratio was observed and the compounds displayed high enantiomeric stability in most cases ($\Delta G_T^{\ddagger}$ > 30 kcal/mol) (**Figure 0.1**).

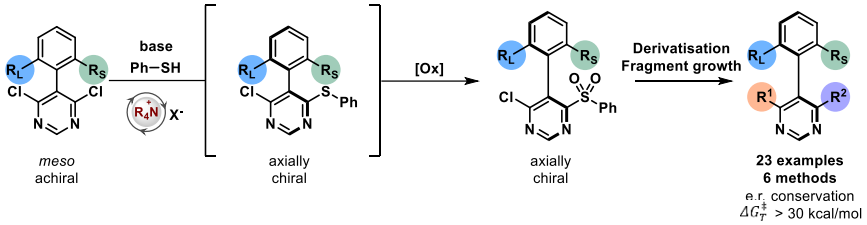


Figure 0.1: *The synthesis of highly stable atropisomeric biarylpyrimidines for the development of FBDD screening libraries.*

Part II describes the exploitation of axially chiral biarylpyrimidine fragments to synthesise molecular probes for KRas G12C covalent inhibition, following the discovery of sotorasib (AMG-510). Probe **120** was synthesised, assessed in biological studies, and optimised to lead to probe **150**, active against KRas G12C in the low micromolar range as a racemate (**Figure 0.2**).

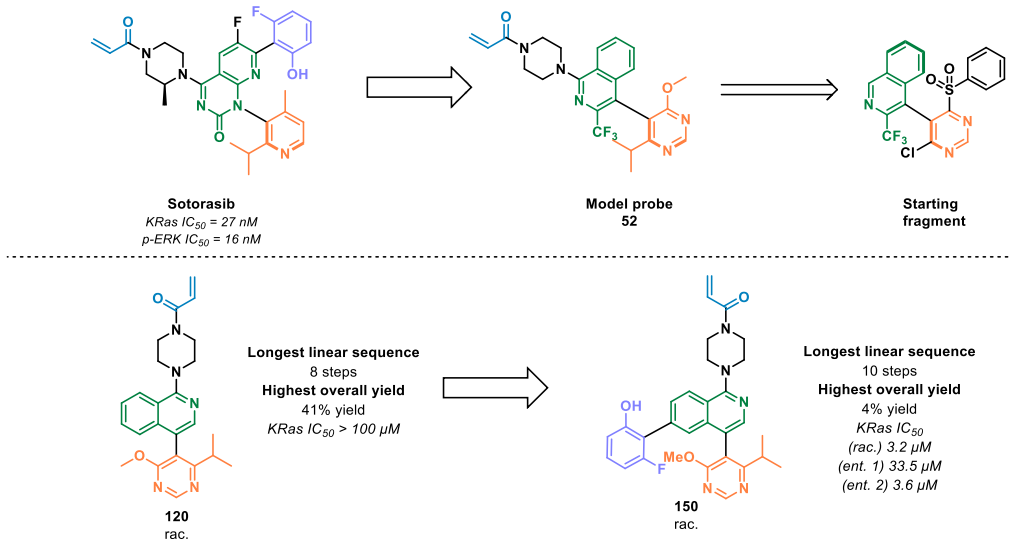


Figure 0.2: *The synthesis of KRas G12C probes containing an axially chiral biarylpyrimidine scaffold.*

Table of Contents

I. Atropisomers in Fragment-Based Drug Discovery 2

I.1 Introduction 2

I.1.1 Fragment-Based Drug Discovery 2

I.1.2 Complexity and three-dimensionality in FBDD 6

I.1.3 Atropisomerism as a source of three-dimensionality 8

I.1.4 The challenges of atropisomerism in drug discovery 10

I.1.4.1 Atropisomerism: a “lurking menace”? 10

I.1.4.2 The different classes of atropisomers 11

I.1.4.3 Giving atropisomers another chance in medicinal chemistry 12

I.1.4.4 Recent successes in the development of single enantiomer axially chiral drugs 14

I.2 Generating atropisomeric fragments for FBDD libraries 16

I.2.1 Project rationale 16

I.2.1.1 The enantioselective synthesis of biaryl pyrimidines 16

I.2.1.2 Biarylpyrimidines in medicinal chemistry 18

I.2.2 Project aims 21

I.3 Results and discussion 22

I.3.1 Precursor synthesis and thermodynamic properties 22

I.3.1.1 Synthesis of the sulfonyl precursor 22

I.3.1.2 Assessing the rotational barrier of the sulfonyl precursor 24

I.3.2 Derivatisation at the chloro site 26

I.3.2.1 Sonogashira cross-coupling 26

I.3.2.2 Other potential derivatisations 34

I.3.3 Derivatisation at the sulfonyl site 39

I.3.3.1 Nucleophilic aromatic substation (SNAr) 40
I.3.3.2 The serendipitous discovery of a solvolysis effect 43
I.3.3.3 One-pot hydrolysis and electrophilic trapping sequence 47
I.3.4 Fragment growth: copper-catalysed azide–alkyne cycloadditions 51
I.3.4.1 Preliminary observations 51
I.3.4.2 Developing the tandem CuAAC/methanolysis sequence 53
I.4 Conclusions & Follow-up Work 55
I.4.1 Conclusions 55
I.4.2 Follow-up work 57
II. The synthesis of atropisomeric biarylpyrimidines for the inhibition of KRAS G12C 62
II.1 Introduction 62
II.1.1 The Ras GTPase family 62
II.1.1.1 Ras oncogenes 62
II.1.1.2 Ras GTPases 63
II.1.2 KRas mutations in human tumours 66
II.1.3 KRas: an undruggable target? 68
II.1.3.1 Direct inhibition of KRas mutants 68
II.1.3.2 Indirect inhibition of KRas mutants 69
II.1.4 KRas G12C: an “Achilles’ heel” in KRas mutant tumours 75
II.1.4.1 The discovery of KRas G12C covalent inhibitors and the switch II pocket (S-IIP) 75
II.1.4.2 The preclinical years 77
II.1.4.3 The development of sotorasib (AMG-510) 79
II.1.4.4 The development of agradasib (MRTX849) 83
II.1.4.5 Other notable KRas G12C inhibitors in the pipeline 86
II.2 The synthesis of an atropisomeric KRas G12C covalent inhibitor 87
II.2.1 Project rationale 87

II.2.2 Project aims 90
II.3 Results and discussion 94
II.3.1 The synthesis of a linchpin precursor 94
II.3.2 Towards the racemic synthesis of probe 52 97
II.3.2.1 Preliminary study 97
II.3.2.2 Synthesis of the pyrimidinyl coupling partners 100
II.3.2.3 The cross-coupling issue: hitting a wall 102
II.3.2.4 Revising the strategy 109
II.3.2.5 Synthesis of a less hindered probe 117
II.3.2.6 Preliminary biochemical and physiochemical analysis 120
II.3.3 Towards the enantioselective synthesis of probe 52 121
II.3.3.1 Issues with the malonate route 121
II.3.3.2 Direct coupling of a dichloropyrimidine on a less hindered isoquinoline? 126
II.3.4 The racemic synthesis of an optimised probe 132
II.3.4.1 Designing an optimised probe 132
II.3.4.2 The synthesis of a new linchpin intermediate 135
II.3.4.3 Anisole demethylation and completing the synthesis of 150 140
II.3.4.4 Refining the route 146
II.3.4.5 Thermodynamics and preliminary biochemical and physiochemical studies 149
II.4 Conclusion and future work 154
II.4.1 Conclusion 154
II.4.2 Future Work 156
III. Experimental Part 162
III.1 Materials and Methods 162
III.1.1 Naming and numbering 162
III.1.2 General conditions 162

III.1.3 Solvents and reagents 162
III.1.4 Thin-layer chromatography 163
III.1.5 Flash column chromatography 163
III.1.6 High-performance liquid chromatography 164
III.1.7 Nuclear Magnetic Resonance (NMR) spectroscopy 164
III.1.7.1 ^{1}H NMR spectroscopy 164
III.1.7.2 ^{13}C NMR spectroscopy 164
III.1.7.3 ^{19}F NMR spectroscopy 165
III.1.7.4 ^{31}P NMR spectroscopy 165
III.1.8 High resolution mass spectrometry 165
III.1.9 Fourier-transform infrared spectroscopy 166
III.1.10 Melting points 166
III.1.11 Specific optical rotations 166
III.1.12 X-Ray crystallography 166
III.1.13 Protein docking 167
III.1.14 Biochemical and physiochemical assays 167
III.2 Experimental procedures and data 168
III.2.1 Part I: Atropisomers in Fragment-Based Drug Discovery 168
III.2.1.1 General procedures 168
III.2.1.2 Experimental data 173
III.2.2 Part II: The synthesis of atropisomeric biarylpyrimidines for the inhibition of KRAS G12C 240
III.2.2.1 General procedures 240
III.2.2.2 Experimental data 244
III.2.2.3 By-products data 350
III.3 Rotational barriers 360

III.4 X-Ray Crystallography 374

IV. Bibliography 378

V. Appendix 408

Appendix A – Origin of rate of racemisation equation 408

Appendix B – Failed attempts at SNAr on the sulfonyl group 411

Appendix C – MPLS PGR Student Log – Impact of the Coronavirus (COVID-19) Public Health Emergency 412

Part I

Atropisomers in Fragment-Based Drug Discovery

I. Atropisomers in Fragment-Based Drug Discovery

I.1 Introduction

I.1.1 Fragment-Based Drug Discovery

A key step in the development of small-molecule drugs is the identification of a lead chemical compound. A chemical lead should display high potency in biological assays, as well as physical and biological properties that will provide it with an optimal absorption, distribution and metabolism profile (ADMET).[1] Methods to identify chemical leads have been evolving alongside the rapid development of new chemical technologies, which have allowed chemists to move from designing chemical leads by deriving them from natural products, to using high throughput screening (HTS) as a tool to rapidly screen millions of drug-like molecules against specific targets of interest (**Figure 1.1**).[1,2]

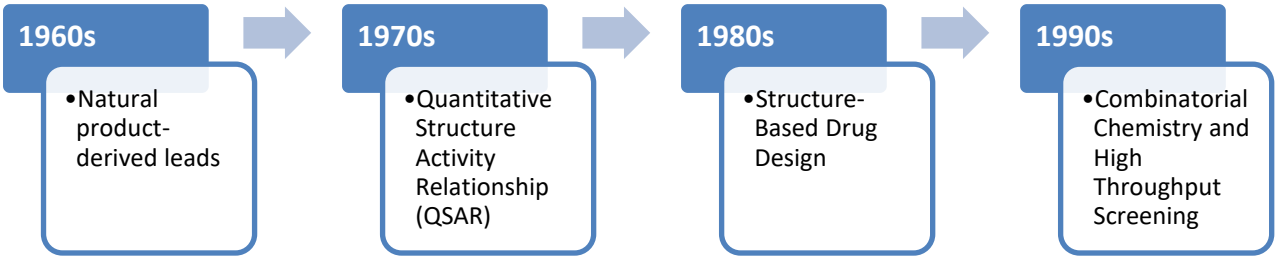


Figure 1.1: *Chemical lead identification methods have evolved alongside the rapid development of new chemical technologies.*[1]

A lead compound not displaying an appealing ADMET profile is one of the main causes of attrition in the drug discovery process. A basic set of rules, known as "Lipinski's rule of five", was established to guide medicinal chemists in their quest for lead compounds.[1,3] A small molecule should display a better oral absorption profile if its molecular weight (MW) is less than 500 Da, its

calculated log*P* (or clog*P*, an indicator of lipophilicity, where *P* is the partition coefficient between octanol and water) is less than 5 (or measured log*P* < 4.15), it possesses no more than 5 hydrogen bond donors (the total number of N-H and O-H bonds) and no more than 10 hydrogen bond acceptors (the total number of N and O atoms).[3] Indeed, multiple clinical studies have established a link between high-MW/high lipophilicity and disappointing ADMET profiles or increased likelihood of toxic events.[4–9] These rules, albeit not universal (many natural product or natural-product-like oral drugs, such as the immunosuppressant cyclosporine,[1] do not comply with the rule of 5), have helped chemists identify a plethora of drug-like molecules.

HTS has established itself as the dominant paradigm in chemical lead identification and world-leading pharmaceutical companies are now equipped with multimillion drug-like compound libraries that they can swiftly screen upon discovery of new biological targets.[10] However, the total of drug-like molecules (*i.e.* with a molecular weight < 500 Da and up to 30 non-hydrogen – or "heavy" – atoms) is estimated to be on the order of 10^{63} (the number of stars in the universe is estimated to be between 10^{22} and 10^{24}).[11] The proportion of the chemical space explored by a library with tens-of-millions compounds (10^7) is therefore extremely small, rendering finding hit compounds with HTS a tedious endeavour for some biological targets (especially targets with a shallow pocket, often deemed undruggable).[12] Moreover, the aforementioned issues caused by high molecular mass and lipophilicity are likely to arise after hit-to-lead optimisation campaigns, a process which usually starts with the derivatisation of a molecule with a molecular mass already close to 500 Da.[1,2,10]

These observations have led the scientists of the 2000s to diversify their approach to lead compound identification, by exploiting much smaller libraries of smaller molecules for their preliminary hit identification campaigns. This new approach was named "Fragment-based Drug

Discovery" (FBDD). A fragment is usually defined as a weakly-binding molecule of less than 20 heavy atoms (the general consensus being around 17 heavy atoms).[1,2,10] In 2012, Reymond *et al.* calculated that the number of organic molecules containing up to 17 key heavy atoms (carbon, nitrogen, oxygen, sulfur, chlorine, bromine, iodine and fluorine) reaches around 166 billion (1.66×10^9).[13] Albeit still being a considerable number of compounds, it makes up a chemical space that can be explored by multimillion fragment libraries in a more exhaustive way than the one explored by HTS campaigns. Indeed, Novartis reported in 2005 that the preliminary hit rates for NMR-based fragment screens was around 10 to 1,000 times higher than for regular HTS campaigns.[14] With analogy to successful chemical leads being likely of fulfilling Lipinski's "rule of five", fragments are more likely to yield good results in a screening campaign if they comply with the "rule of three". This means that their MW should not exceed 300 Da, their clog*P* should be lower than 3, and they should contain fewer than 3 hydrogen bond donors, hydrogen bond acceptors and rotatable bonds. [15,16]

Despite being initially weakly binding, fragments have been estimated to contribute to over half of the favourable binding energy of the final drug they are incorporated into.[1] However, this low affinity is at the root of one the main challenges of FBDD, which is the need for specialized biophysical methods to detect fragment binding. This challenge has been tackled by advances in X-Ray crystallography, NMR spectroscopy, Surface Plasmon Resonance (SPR) and, more recently, microscale thermophoresis, thermal shift assays (TSAs) and weak affinity chromatography.[1,10] Once screened, preliminarily successful fragments are confirmed as "hits" and then developed into potential leads, either by being "grown", "hopped" or "linked" together.[10,12] Fragment growth is the most commonly used strategy to develop lead compounds *via* FBDD and entails adding chemical groups to an existing fragment. Fragment hopping (or fragment "merging") is applied to different fragments which display overlapped binding sites and refers to combining/merging their

chemical features together. Finally, fragment linking is considered as the most powerful way to develop potent leads from fragments and consists of liking two or more weakly binding fragments together.[12] Analysis suggests that following this process generates smaller, less lipophilic leads than those emerging from HTS.[17] The whole process of FBDD and how it falls within the greater process of Drug Discovery is illustrated in **Figure 1.2**.[12]

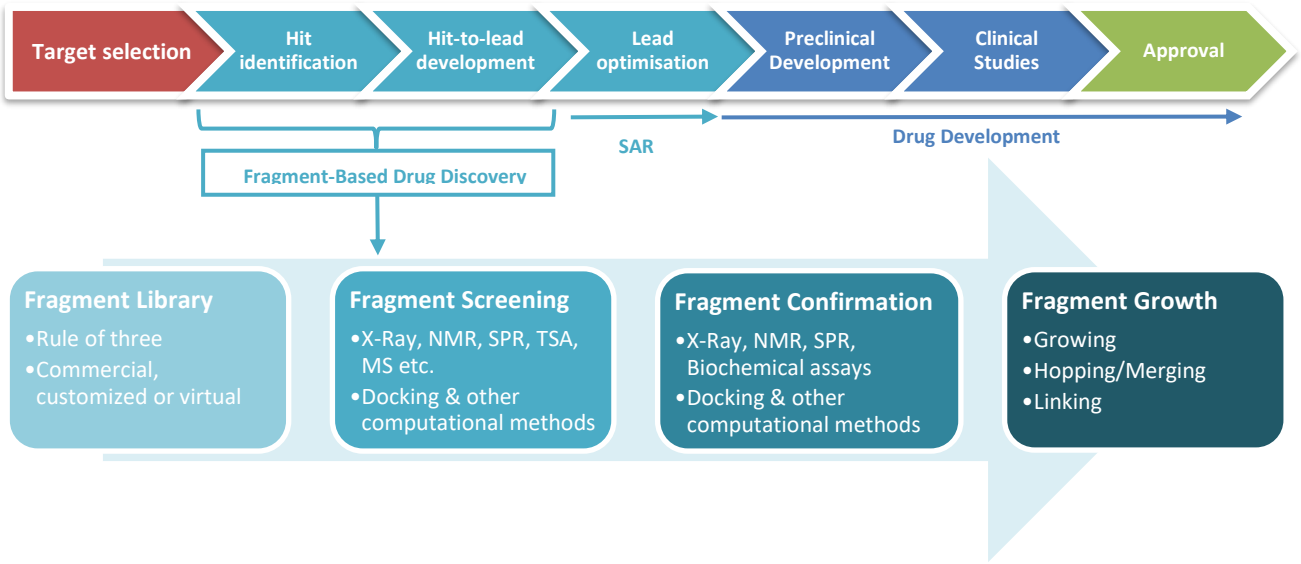


Figure 1.2: *A flow chart of FBDD and its place within the Drug Discovery process. Inspired by Li, 2020.*[12]

FBDD has only recently started to bear fruit, with the approval of the very first *BRAF*-mutant cancer drug, Zelboraf® (Vemurafenib), for late-stage metastatic melanoma in 2011 (**Figure 1.3A**).[18] Since then, dozens of drug candidates discovered *via* FBDD have entered the clinic.[10] Only a few of them have been approved so far, with one of the most notable examples being the selective Bcl-2 (despite Bcl-2 and Bcl-X_L having very similar sequences) inhibitor Venclyxto®/Venclexta® (venetoclax), approved in 2016 for the treatment of chronic lymphocytic leukemia for patients with a chromosomal 17p deletion (**Figure 1.3B**), after having been stuck in development for decades.[19–21] In 2019, Turalio® (pexidartinib) was approved for patients with symptomatic tenosynovial giant cell tumours (**Figure 1.3A**),[12,22] and Balversa® (erdafitinib) was

approved as the first targeted therapy for metastatic bladder cancer (**Figure 1.3C**).[12,23] In May 2021, Lumakras®/Lumykras® (sotorasib or AMG-510), was approved as the first targeted therapy for patients with lung cancer caused by the previously considered resistant KRAS G12C mutation (**Figure 1.3D**).[24–26] Sotorasib (AMG-510) was studied in further detail in the second part of this project.

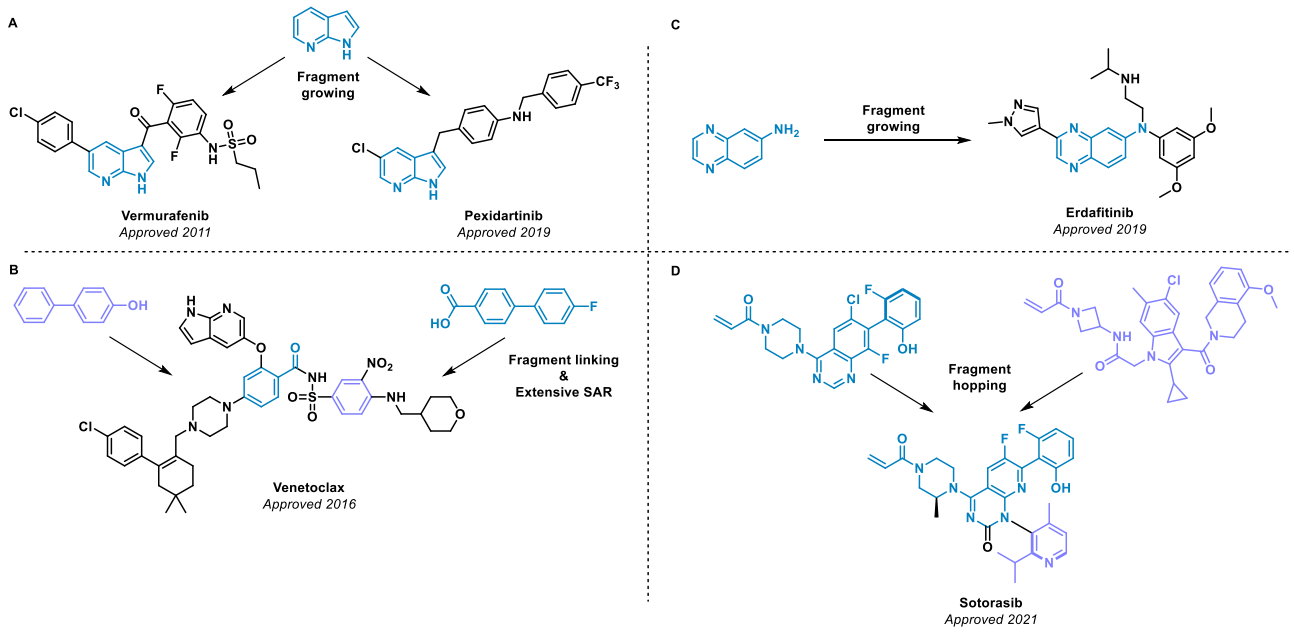


Figure 1.3: *Approved drugs that resulted from FBDD and their initial hit fragments.* ***(A)*** *Vermurafenib (2011) and Pexidartinib (2019).* ***(B)*** *Venetoclax (2016).* ***(C)*** *Erdafitinib (2019).* ***(D)*** *Sotorasib (2021).*

I.1.2 Complexity and three-dimensionality in FBDD

The early days of FBDD led to many discussions on the topic of what makes an efficient fragment library. From these discussions arose the heavy atom count limitations as well as the "rule of three" mentioned earlier.[1,15] Additionally, Hann *et al.* suggested that compound libraries built for FBDD should contain compounds of reduced complexity to allow for better molecular recognition between a ligand and its receptor.[27] However, a few years down the line, medicinal chemists observed an imbalance regarding FBDD success rates across all target classes, and analytical

studies led by pharmaceutical companies such as GSK and Pfizer suggested that stepping away from the all-aromatic/all-achiral formula in drug design and increasing the proportion of sp^3 centres in hit/lead candidates might result in improvements in profile and project progression.[28,29] Furthermore, Jorgensen *et al.*, AstraZeneca and Astex, sparked similar discussions when they evidenced that the ring dearomatisation and addition of a methyl group on their fragments/compounds resulted in a significant increase in their potency (and ligand efficiency), by allowing conformational changes for better access to receptor pockets.[30,31] Indeed, the complexity model suggested by Hann *et al*. deals with matching the number of pharmacophoric points on the ligand and the receptor, rather than matching their 3D arrangements. Therefore, the use of 3D structures that comprise of equal numbers of pharmacophoric points to their 2D counterparts should not necessarily have a negative impact on molecular recognition between a ligand and its receptor.[32] The 3D Fragment Consortium (founded by 9 UK leading not-for-profit drug discovery research institutions*) suggested that the overall "flatness" of most FBDD libraries might explain why they are less successful in identifying hits for targets that might require ligands bearing alternative substitution vectors for optimal molecular recognition, and decided to start building a shared library of 500 to 3000 compounds. This database would include compounds found in many existing libraries but would also incorporate a complementary set of fragments with greater three-dimensionality, with hopes of making FBDD more universally suitable for hit identification.[32]

---

* *The 3D Fragment Consortium was founded in 2013 under the leadership of the Drug Discovery Unit (University of Dundee) and counts as it members University College London, the Medical Research Council Technology, the Beatson Institute for Cancer Research UK, the Paterson Institute for Cancer Research, the Institute of Cancer Research, Cancer Research Technology, the University of Cambridge, and the Structural Genomics Consortium (University of Oxford).*

I.1.3 Atropisomerism as a source of three-dimensionality

Atropisomerism (or "axial chirality") is a dynamic type of chirality that arises from restricted rotation about a bond due to a hindered substitution pattern. George Hallatt Christie and James Kenner discovered this phenomenon at the University of Sheffield in 1923 while studying the molecular conformations of the *ortho*-tetrasubstituted biaryl system of 6,6'-dinitro-[1,1'-biphenyl]-2,2'-dicarboxylic acid **1** (**Figure 1.4**).[33]

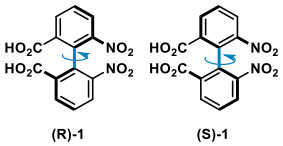


Figure 1.4: *The two enantiomers of 6,6'dinitro-[1,1'-biphenyl]-2,2'-dicarboxylic acid **1** were isolated in 1923.[33]*

In addition to hindered biaryl systems, atropisomerism has been observed in hindered amides, puckered medium-sized (7/8-membered) rings formed under conformational restrictions and macrocyclic compounds containing large moieties unable to swing through the plane of the macrocyclic ring (**Figure 1.5**).[34–37]

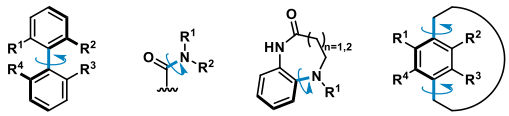


Figure 1.5: *Axial chirality can be found in (from left to right): biaryl compounds, hindered amides, puckered medium-size rings and macrocyclic compounds.*

Axial chirality is widely observed in natural products, such as gossypol, viriditoxin or longithorone B (**Figure 1.6**).[36,38–40]

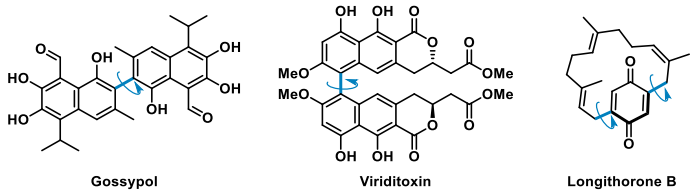


Figure 1.6: *Examples of axially chiral natural products.*

Perhaps the widest application of atropisomers, however, is their use in asymmetric synthesis as chiral ligands or auxiliaries for enantioselective reactions.[41,42] BINAP has cemented itself as a go-to ligand for the enantioselective reduction of π bonds using ruthenium,[43,44] and the chiral phosphoric acid TRIP has been widely used as a catalyst for asymmetric transfer hydrogenations,[45] Diels Alder reactions,[46] Pictet-Spengler reactions[47] and more (**Figure 1.7**).[48]

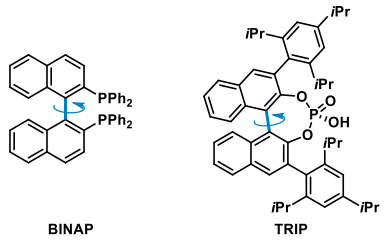


Figure 1.7: *BINAP, an axially chiral ligand, and TRIP an axially chiral catalyst.*

The inclusion of polyaryl fragments in FBDD libraries has proven successful, with hits from such fragments leading to the design of venetoclax and sotorasib (**Section I.1.1**, **Figure 1.3**).[19,20,25,32] Due to steric hindrance about the chiral axis, biaryl atropisomers cannot exist as flat systems, and are therefore an undeniable source of three-dimensionality. Therefore, interest in exploiting atropisomerism for the construction of 3D compound libraries for FBDD has been growing.[32]

I.1.4 The challenges of atropisomerism in drug discovery

I.1.4.1 Atropisomerism: a "lurking menace"?

In essence, atropisomers are conformers that interconvert slowly enough that they can be isolated as two different stereoisomers. Unlike classical point chiral compounds, which require bond breaking and making to enantiomerise, atropisomers interconvert *via* a dynamic process that only involves single bond rotation. The interconversion rate of two atropisomers is quantified by their half-life of racemisation ($t_{1/2}^{rac}$). $t_{1/2}^{rac}$ is calculated while determining the rotational barrier ($\Delta G_T^{\ddagger}$) at a given temperature. $\Delta G_T^{\ddagger}$ represents the amount of energy required to interconvert one mole of atropisomer into the opposite enantiomer. It is generally assumed not to be temperature dependant and is usually just written as $\Delta G^{\ddagger}$ (however, the extrapolation of $t_{1/2}^{rac}$, and thus $\Delta G_T^{\ddagger}$, at temperatures different from that of the measurement is not recommended. This is due to the temperature-related changes in entropy).[49] Oki arbitrarily decided that, for a compound to be considered atropisomeric, its half-life of racemisation at r.t. should be above 1000 s.[50]

Atropisomers may generate geometrical isomers, diastereoisomers or enantiomers which also have a potential to readily interconvert at biological temperatures (typically around 37 °C). The effect of chirality on the biological activity, pharmacokinetics and toxicity of pharmaceutical compounds is well documented and illustrated by the infamous examples thalidomide and perhexiline.[51–54] The US Food and Drug Administration (FDA) recommends that chiral drugs be developed as a single enantiomer in cases where this leads to improved safety.[55] Nonetheless, drugs like Ibuprofen, or even the axially chiral Iomperol, showcase acceptable toxicological profiles when used as a mixture and are approved to be sold as racemates.[56,57] However, guidance was established with solely classical, point chiral molecules in mind. In the case of axially chiral pharmaceuticals, the ability to develop the compound as a single enantiomer or a racemate is

heavily influenced by its rotational barrier, and exerting control over this thermodynamic value is not trivial. This practical challenge and the lack of regulatory guidance has led medicinal chemists to eschew atropisomerism, deemed a "lurking menace", and many projects were abandoned upon the discovery that the identified chemical leads existed as isolable atropisomers.[55,57,58]

I.1.4.2 The different classes of atropisomers

When LaPlante discovered a very potent axially chiral HIV-integrase inhibitor during his time at Boehringer Ingelheim (Canada), he initiated a collaboration with the FDA to issue guidance for medicinal chemists who encounter atropisomeric compounds during their lead identification campaigns (**Figure 1.8**).[39,57] LaPlante *et al.* had previously proposed to differentiate axially chiral compounds into three different classes, depending on the size their rotational barrier.[59] Class 1 atropisomerism describes molecules with rapid axial rotation ($\Delta G_T^{\ddagger} <$ 20 kcal/mol; nanoseconds $< t_{1/2}^{rac} <$ minutes) and which cannot usually be isolated as different enantiomers. Class 2 atropisomerism describes molecules with moderate to slow interconversion rates (20 kcal/mol $< \Delta G_T^{\ddagger} <$ 30 kcal/mol; hours $< t_{1/2}^{rac} <$ days) and which can be isolated as separate enantiomers, but for which racemisation is observable on human timescales. Class 3 atropisomerism describes molecules with slow interconversion rates ($\Delta G_T^{\ddagger} >$ 30 kcal/mol; $t_{1/2}^{rac} \sim$ years) and which are rotationally stable (kinetically inert), meaning that they will show little to no racemisation on human timescales.[39,59]

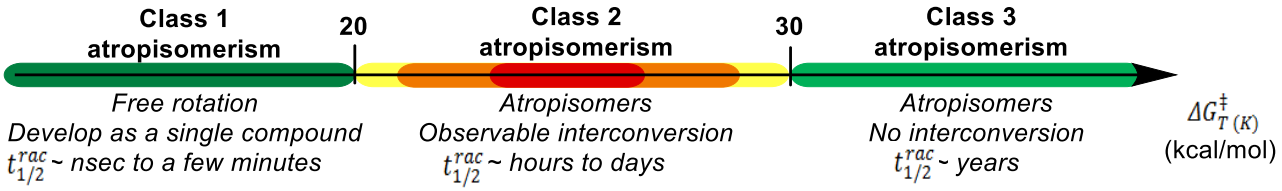


Figure 1.8: *The three different classes of atropisomerism, as described by LaPlante et al.*[58]

I.1.4.3 Giving atropisomers another chance in medicinal chemistry

Class 1 atropisomers, due to their relatively fast rotation rates, do not display any axial chirality and can therefore be considered as a single entity that will not lead to stereoisomers. Class 3 compounds, on the other hand, display such slow interconversion rates that they can easily be isolated *via* chiral separation methods, without loss of their stereochemical integrity, and can therefore be developed in a similar fashion to conventional stereoisomers that result from point chiral centres. Class 2 atropisomers pose more of a conundrum when it comes to their development as drugs, as their moderate interconversion rates compromises their stereochemical integrity over time. Problems of stability could cause the mis-interpretation of biochemical assays, and instability during production and storage. A compound developed as a single eutomer (most active enantiomer), but with a half-life of racemisation at biological temperatures that is much faster than its half-life of *in vivo* elimination, will cause inevitable patient exposure to its other enantiomer (and thus, to a different toxicology profile).[39] Four strategies are recommended to mitigate the effects of intermediate atropisomeric stability in a lead candidate and are described below.[37,39,55]

I.1.4.3a Raise $\Delta G_T^{\ddagger}$ by increasing bond rigidity

Several examples of structure redesign upon recognition of a class 2 chiral axis during early lead development were reported. Raising $\Delta G_T^{\ddagger}$ by increasing steric hindrance to produce stable separable atropisomers of negligible interconversion was used in the development of locked NK_1 antagonist **3** by the rigidification of lead compound **2** ($t_{1/2}^{rac} \sim$ days), a class 2 atropisomer, *via* linking of the amide and the naphthyl moieties into a methylated eight-membered ring (**Figure 1.9**).[60,61]

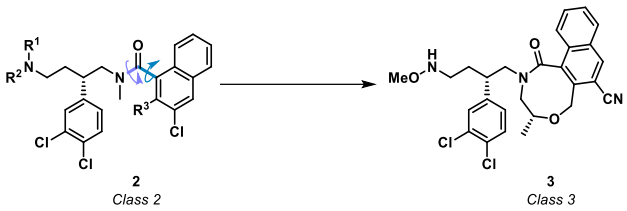


Figure 1.9: *The development of a locked NK_1 antagonist by rigidification of the rotatable bonds.*[59,60] *Quickly rotating bonds are shown in lavender, bonds with a slower rotation rate are shown in blue.*

I.1.4.3b Lower $\Delta G_T^{\ddagger}$ to equilibration

The approach of steric hindrance reduction was fruitful in the case of the human-gonado-tropin-releasing hormone receptor antagonist **5**, where the removal of a methyl group in the uracil region of compound **4** rendered it non-atropisomeric (**Figure 1.10**).[62]

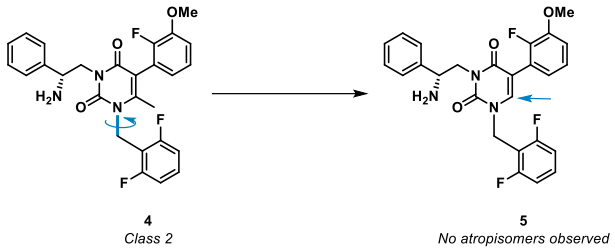


Figure 1.10: *Reducing steric hindrance allows for the development of a potent non-chiral human-gonado-tropin-releasing hormone receptor antagonist.*[61]

I.1.4.3c Symmetrise the molecule to remove the chiral axis

In the case of SCH 351125 (**7**), a CCR5 antagonist that inhibits HIV entry into host cells, four diastereoisomers arose in precursor **6** due to a hindered rotation around the N–CO and Ar–CO axes in the amide region of the inhibitor, and the two pairs of enantiomers displayed half-lives of interconversion of around 5 hours at 37 °C. Symmetrising the Ar–CO bond resulted in elimination of the chiral Ar–CO axis, leaving only a chiral N–CO axis that interconverted extremely rapidly, transforming the compound in a class 1 atropisomer (**Figure 1.11**).[63]

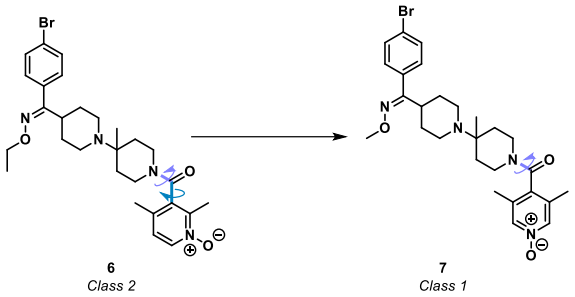


Figure 1.11: *Symmetrising as a tool to develop a class 1 axially chiral compound for the treatment of HIV.*[62] *Quickly rotating bonds are shown in lavender, bonds with a slower rotation rate are shown in blue.*

I.1.4.3d Shift the equilibrium to a single desired atropisomer by introducing another stereochemical element

Bristol-Myers Squibb (BMS) reported the discovery of the atropisomerically stable Bcl-2 inhibitor **9**. The atropisomeric axes of the lead BMS compound, **8**, were not stereochemically stable, but the addition of a point chiral centre generated a Bcl-2 active atropisomer (**9**) that was more stable than its other diastereoisomers, leading to an equilibration at room temperature to a mixture that primarily contained the active atropisomer (**Figure 1.12**).[64,65]

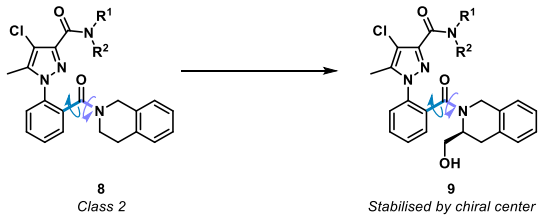


Figure 1.12: *The introduction of a point chiral centre drives the equilibrium to the more active, stable atropisomer of a Bcl-2 inhibitor.*[63,64] *Quickly rotating bonds are shown in lavender, bonds with a slower rotation rate are shown in blue.*

I.1.4.4 Recent successes in the development of single enantiomer axially chiral drugs

LaPlante and co-workers' guidance allowed for a better understanding of axial chirality and provided medicinal chemists with new means of tackling issues related to atropisomerism in drug

discovery. They opened the gates to the development of single enantiomer, axially chiral compounds. Atropisomerism has proven useful in the field of kinase inhibition, where the development of selective probes is of crucial interest but extremely difficult. In 2018, it was estimated by Gustafson *et al.* that up to 80% of FDA-approved kinase inhibitors contained an atropisomeric axis (mostly class 1).[58,66] His team had also evidenced a few years prior that increased kinase selectivity can be achieved by using only one atropisomer instead of the racemic mixture, and that the complementary enantiomer usually displayed higher off-target activity.[67] Stéphane Perreault and co-workers at Gilead computationally engineered and subsequently synthesized the selective, highly stable ($\Delta G^{\ddagger}_{393}$= 35.0 kcal/mol at 120°C) Phosphoinositide 3-Kinase (PI3K) β inhibitor **10,** for the treatment of cancer (**Figure 1.13**).[68] An atropisomeric Bruton's Tyrosine Kinase (BTK) inhibitor developed by Bristol-Myers Squibb completed phase II clinical trials for the treatment of rheumatoid arthritis in 2019 (**11**, **Figure 1.13**).[69,70] In other therapy areas, axially chiral Sotorasib was approved in May 2021 as the first inhibitor for the previously deemed undruggable lung cancer caused by the G12C mutation of KRas (**Figure 1.13**).[24,25]

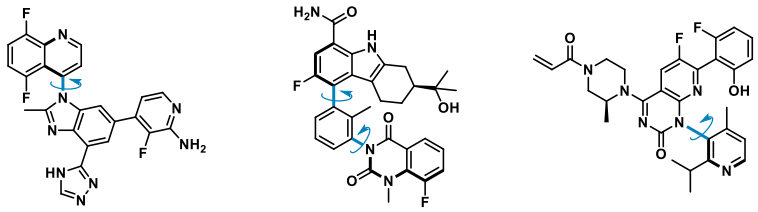


Figure 1.13: *Examples of single-enantiomer high-barrier drugs in the clinic or already approved.*

I.2 Generating atropisomeric fragments for FBDD libraries

I.2.1 Project rationale

I.2.1.1 The enantioselective synthesis of biaryl pyrimidines

The enantioselective synthesis of atropisomeric compounds using phase-transfer catalysis has been an area of interest in the Smith group over the last decade.[71–74] Racemic atropisomeric mixtures were used to enantioselectively generate a single enantiomer of a desired compound in a biphasic mixture by performing kinetic resolutions employing a chiral cinchona alkaloid derived catalyst (**$R_4N^+X^-$**, **Figure 1.14**). A kinetic resolution is a method allowing the differentiation of a pair of enantiomers in a racemic starting material by exploiting the different reactivities of the two enantiomers. The theoretical maximum yield of a kinetic resolution is of 50% as only one of the two enantiomers is consumed.[75] In a dynamic kinetic resolution, the non-reactive enantiomer of the racemic starting material epimerises quickly to its reactive counterpart which increases the theoretical yield to 100%.[76]

For example, Jolliffe and Armstrong were able to exploit the tight ion pair formed by the deprotonated racemic 2-tetralone analogues and the chiral phase-transfer catalyst to achieve the enantioselective dynamic kinetic resolution of the former *via* *O*-alkylation (**Figure 1.14A**).[72] Cation-directed *O*-alkylation was also used by Fugard in the enantioselective dynamic kinetic resolution of naphthol anilides (**Figure 1.14B**),[73] and by Balan, Jones and Jolliffe for the enantioselective kinetic resolution of C_2- and non C_2-symmetric BINOLs (**Figure 1.14C**).[74]

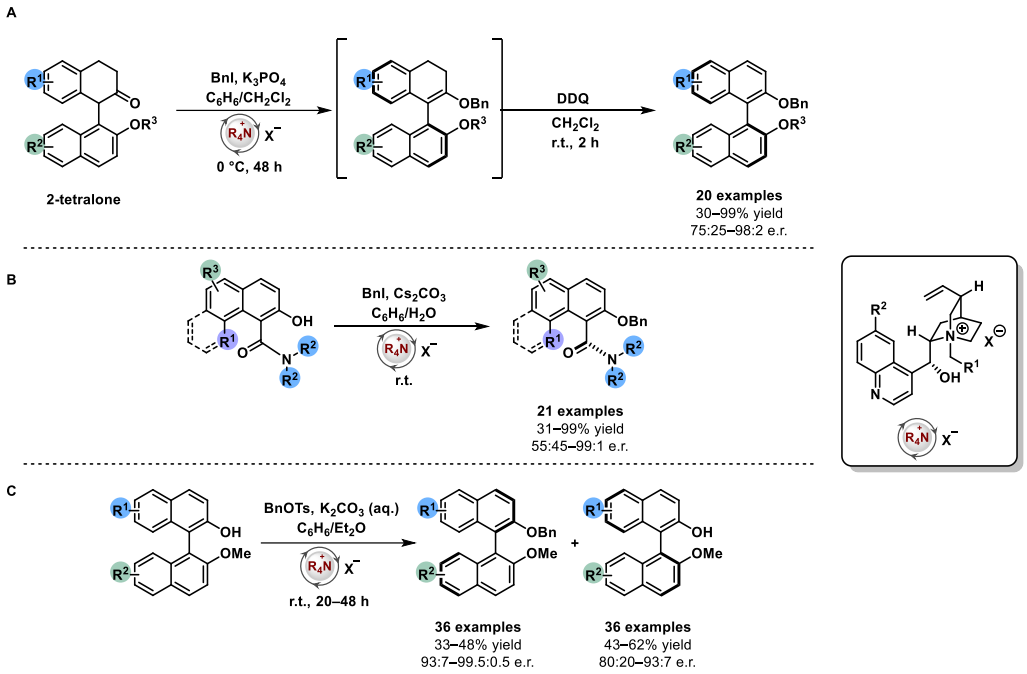


Figure 1.14: ***(A)*** *Jolliffe and Armstrong's enantioselective dynamic kinetic resolution of 2-tetralone derivatives.*[71] ***(B)*** *Fugard's enantioselective dynamic kinetic resolution of naphthol anilides.*[72] ***(C)*** *Balan, Jones and Jolliffe's kinetic resolution of BINOLs.*[73]

Most notably, Armstrong reported the desymmetrisation of pro-atropisomeric biaryl dichloropyrimidines using a cation-directed nucleophilic aromatic substitution (SNAr) reaction. Armstrong utilised the idea that, under asymmetric phase-transfer conditions, the tight ion pair formed between a deprotonated thiophenol and a chiral cation allows for a stereo-controlled attack on the electron-poor and sterically encumbered dichloropyrimidine. Twelve different pyrimidines were reacted in tetrachloromethane in the presence of aqueous potassium carbonate and thiophenol to yield the desymmetrised SNAr products in moderate to high yields and with enantiomeric ratios (e.r.) ranging from 85:15 to 97:3 (**Figure 1.15A**). Armstrong also explored the derivatisation of enantioenriched naphthylpyrimidine **12** (97:3 e.r.) *via* oxidation, SNAr, and Suzuki cross-coupling (**Figure 1.15B**).[71] All of these attempts showed that it was possible to achieve derivatisation of the enantioenriched atropisomer without loss of stereochemical integrity. The absolute configuration of compound **12** was determined by X-Ray crystallography and it was

postulated by analogy that all the other products obtained with the same chiral catalyst were of the same absolute configuration. The rotational barrier of the least hindered compound (R_L = OBn, R_S = H, **Figure 1.15A**) was determined to be 28.0 kcal/mol at room temperature ($\Delta G^{\ddagger}_{298}$ = 28.0 kcal/mol), which indicates that the more hindered substrates in this family of compounds the may potentially be class 3 atropisomers. This result also implied that the moderate enantioselectivity observed in the desymmetrisation step resulted from low enantioinduction from the catalyst, rather than thermal racemisation of the product.[49]

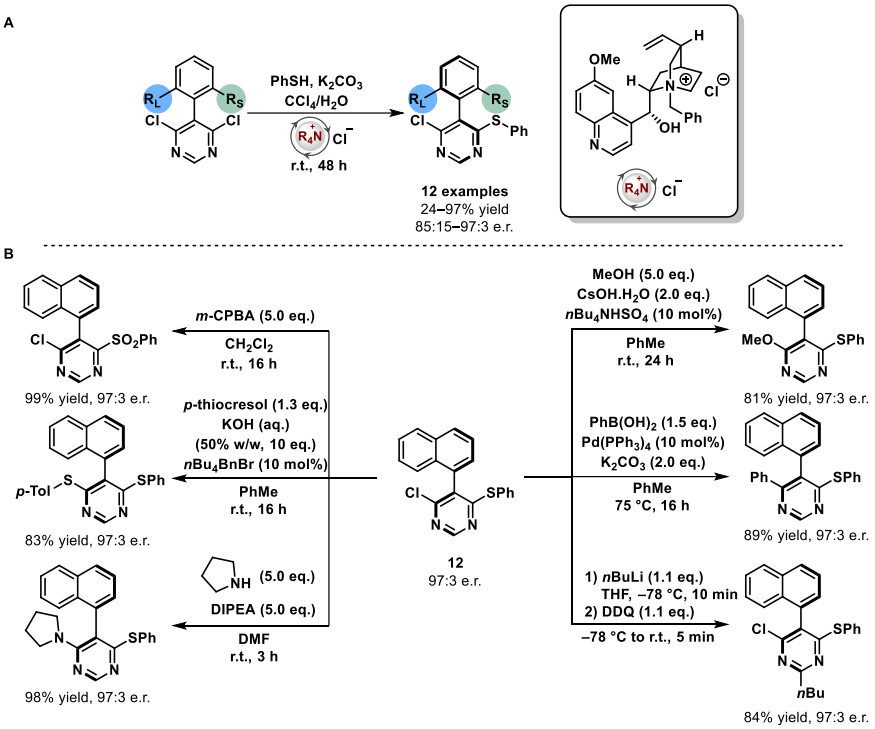


Figure 1.15: ***(A)*** *Armstrong's enantioselective desymmetrisation of dichloropyrimidines via a cation-directed SNAr.*[70,76] ***(B)*** *Armstrong's derivatisation of enantioenriched substituted biaryl pyrimidines.*[70]

I.2.1.2 Biarylpyrimidines in medicinal chemistry

Of all molecular classes involved in drug discovery, heteroaromatics are probably the most crucial. Despite the numerous examples of approved small-molecule drugs that contain one or several heterocyclic moieties, a sizeable portion of the chemical space they make up remains

unexplored.[77,78] Although examples of biarylpyrimidines in drug discovery are few, they demonstrate the potential for using this class of molecules to inhibit difficult targets, such as kinases or "undruggable" KRas.[79–82]

Zheng, Matulenko and co-workers at Abbott Laboratories showed the potential of pyridopyrimidines as oral adenosine kinase (AK) inhibitors, for the treatment of pain (*via* neuroprotective, antinociceptive and anti-inflammatory properties).[79] This discovery resulted in the chemical lead ABT-702, which was further optimised into biarylpyrimidine **13** (**Figure 1.16**) in a effort to reduce toxicological and CNS side effects.

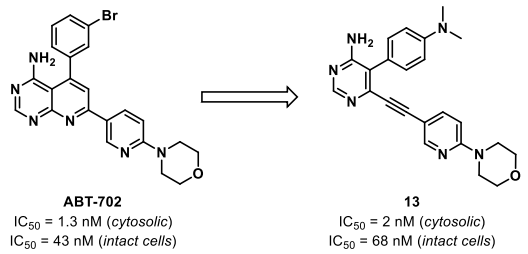


Figure 1.16 *Abbott Laboratories' work on adenosine kinase inhibitors allowed the identification of biarylpyrimidines as potential drug candidates.*[79,80]

Compound **13** turned out to be a comparable *in vitro* AK inhibitor to ABT-702, and performed well in the formalin animal assay of inflammatory pain, but did not show any activity in the Chung animal model of pain.[80] This study, however, highlighted biarylpyrimidines as a potent alternative to nucleoside-based compounds in the treatment of nucleoside kinases such as AK, especially since these compounds adopt a different binding mode that channels an increased number of stabilising interactions as compared with the binding mode of adenosine (**Figure 1.17**).[80]

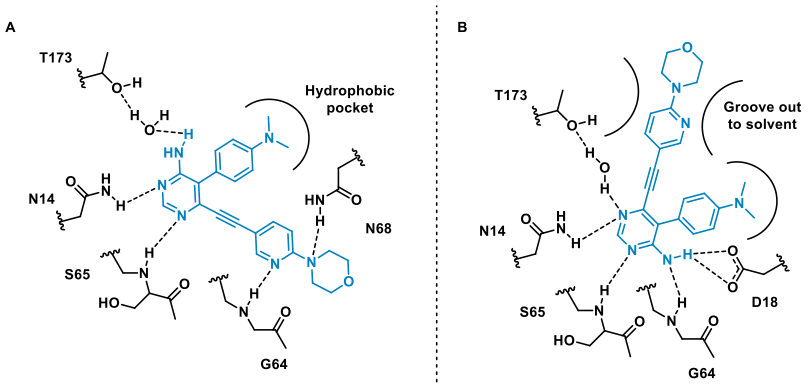


Figure 1.17: ***(A)*** *Predicted binding mode of* ***13*** *in AK based on the interactions of adenosine.* ***(B)*** *Observed binding mode (X-Ray crystallography) of* ***13*** *in AK.*[80]

The discovery process of sotorasib also highlighted biarylpyrimidines as strong contenders for the development of covalent inhibitors of the "undruggable" KRas G12C.[25,81,82] Amgen reported numerous examples of active, symmetrical (non-atropisomeric) biarylpyrimidines with encouraging activity profiles in both KRas inhibition biochemical assays and the *p*-ERK1/ 2 cellular immunoassay. Examples of compounds with comparable potency to sotorasib are highlighted in **Figure 1.18** (**14a–c**).[25,81,82] One atropisomeric example, **14d**, was also reported as one of their final optimisation attempts. Despite having lower cellular potency than its pyridine counterparts, **14d**, exhibited the best aqueous solubility (lowest logD).[25]

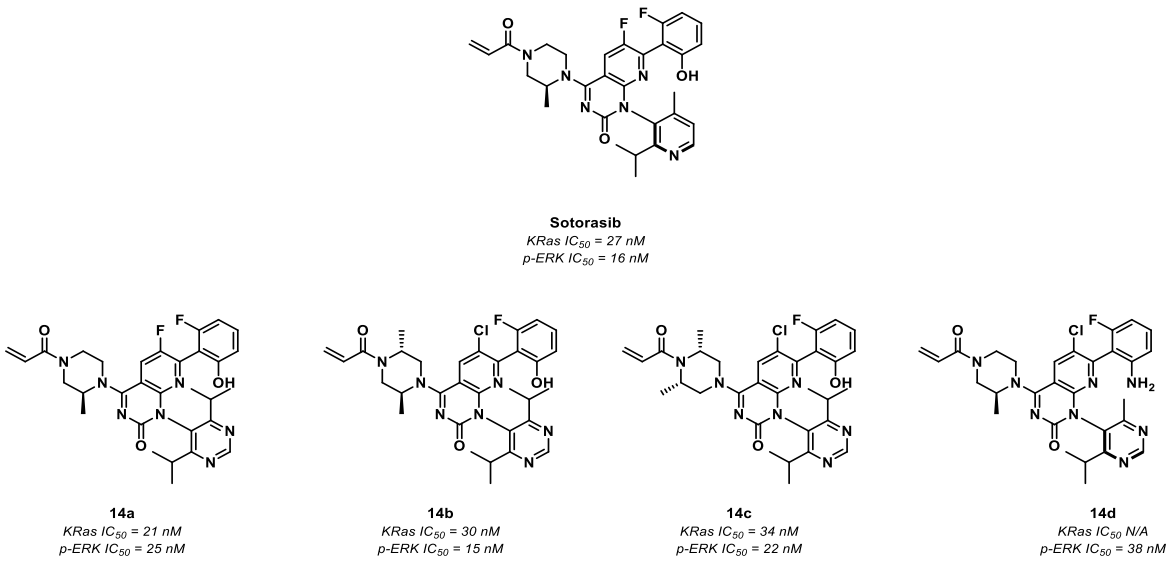


Figure 1.18: *Examples of biarylpyrimidine KRas G12C covalent inhibitors and their potencies against KRas G12C (biochemical potency) and in the p-ERK1/ 2 immunoassay (cellular potency), compared with sotorasib.*[25,82]

I.2.2 Project aims

Albeit scarce, the examples of biarylpyrimidines in drug discovery show the relevance of this class of compounds in the lead identification process and makes them a useful asset to FBDD libraries. We therefore decided to exploit Armstrong's enantioselective desymmetrisation of pro-atropisomeric biarylpyrimidines to generate a high-barrier axially chiral precursor **iii** (**Figure 1.19**). That precursor could then, in turn, be derivatised at the remaining chloro site or at the newly-generated sulfonyl site *via* orthogonal methods to generate an array of compounds that could be added to 3D libraries designed for fragment-based sceening. Derivatisation methods could include SNAr-type reactions or cross-coupling reactions, as Armstrong demonstrated such methodologies are likely to preserve the stereochemical integrity of the atropisomeric precursors.[71]

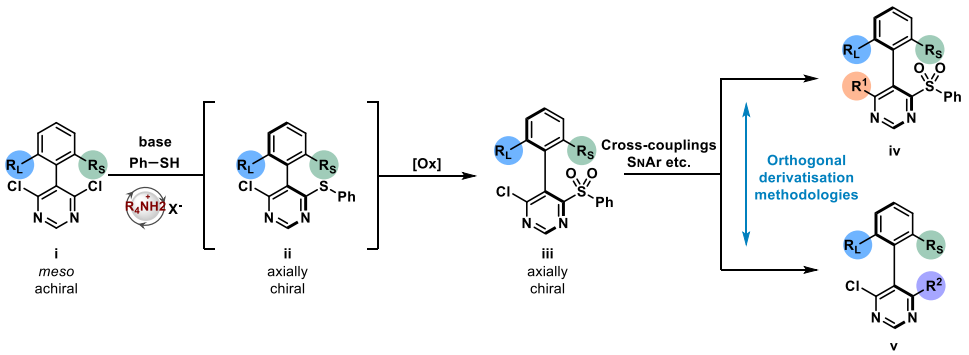


Figure 1.19: *Generating atropisomeric fragments for FBDD libraries.*

I.3 Results and discussion

I.3.1 Precursor synthesis and thermodynamic properties

I.3.1.1 Synthesis of the sulfonyl precursor

For this study, we decided to focus on the synthesis of *ortho*-trifluorophenyl pyrimidines. The trifluoromethyl group is widely employed in medicinal chemistry for its unique chemical and physiological properties, especially its ability to protect a position from metabolic degradation, thus increasing a compound's metabolic stability.[83] Examples of drugs where the insertion of an aryl-trifluoromethyl group was a key development step include the selective serotonin reuptake inhibitor, fluoxetine (Prozac®),[84] and the cyclooxygenase 2 inhibitor celecoxib (Celebrex®) (**Figure 1.20**).[85] Moreover, an *ortho*-trifluoromethyl group generates enough steric bulk to restrict rotation about a bond formed with a di-*ortho*-substituted pyrimidine and will therefore allow for the synthesis of atropisomeric compounds.[83]

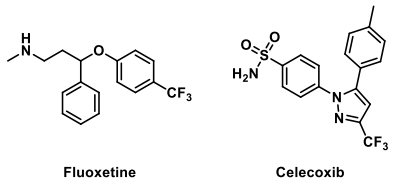


Figure 1.20: *Fluoxetine and celecoxib.*

We completed the synthesis of sulfonyl precursor **20** by adapting Armstrong's procedure for the enantioselective synthesis of atropisomeric biarylpyrimidines.[71,80] Commercially available diethyl malonate **16a** was α-arylated *via* heating to 50 °C in 1,4-dioxane in the presence of trifluoromethyliodobenzene **15**, caesium carbonate and catalytic amounts of copper iodide and 2-picolinic acid, to yield malonate **17** in moderate to high yields (**Figure 1.21**).[71,86] Formamidine hydrochloride was then condensed onto malonate **17** by heating to 80 °C in a 3:2 methanol/tetrahydrofuran mixture in the presence of *in situ*-generated sodium methoxide. The resulting crude was precipitated in concentrated hydrochloric acid and subsequently heated to 90 °C in phosphorus (V) oxychloride to yield pro-atropoisomeric dichloropyrimidine **18** in moderate yields (**Figure 1.21**).[71,80]

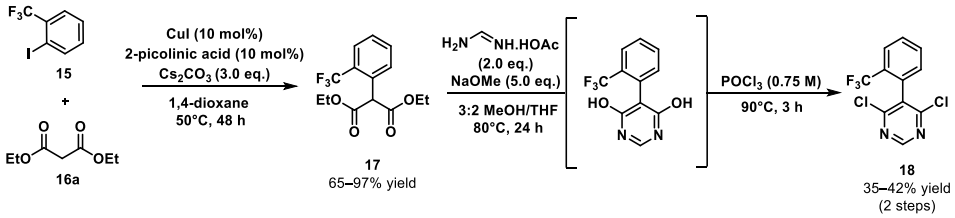


Figure 1.21: *Synthesis of the pro-atropisomeric dichloropyrimidine **18***

The desymmetrisation product **19** was synthesised both as a racemic mixture and an enantioenriched mixture. Both mixtures were synthesised *via* a phase-transfer catalysed (PTC) SNAr. Racemic **19** was obtained in moderate to high yields by vigorously stirring dichloropyrimidine **18** in toluene at room temperature in the presence of thiophenol, catalytic amounts of tributylammonium bromide and aqueous potassium hydroxide (50% w/w)

(**Figure 1.22A**).[71] Enantioenriched **19** was obtained in high yields and moderate e.e. (81:19–89:11 e.r.) by vigorously stirring dichloropyrimidine **18** in tetrachloromethane at room temperature in the presence of thiophenol, catalytic amounts of *N*-benzylquininium bromide and aqueous potassium carbonate (50% w/w) (**Figure 1.22B**).[71] The absolute configuration of the major enantiomer was determined by Armstrong.[49,71] The oxidation of sulfide **19** was performed on both the racemic and enantioenriched mixtures by stirring them at room temperature in dichloromethane with an excess of *meta*-chloroperbenzoic acid to yield sulfone **20** in quantitative yields and with no erosion of the enantioenriched substrate (**Figure 1.22**).[71] We decided to work with sulfone **20** rather than sulfide **19** as the arylsulfonyl moiety would be easier to displace once it had served its desymmetrisation purpose.

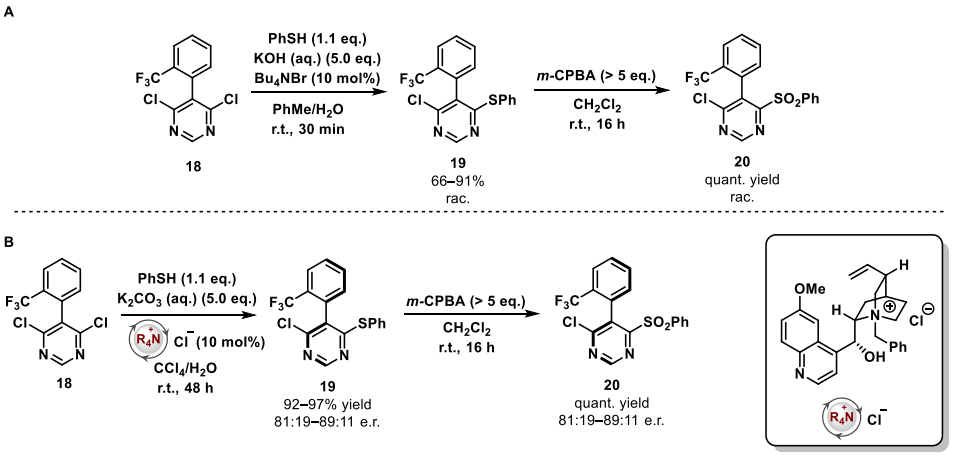


Figure 1.22: ***(A)*** *Synthesis of the racemic precursor* ***20****.* ***(B)*** *Synthesis of the enantioenriched precursor* ***20****.*

I.3.1.2 Assessing the rotational barrier of the sulfonyl precursor

To determine whether the compounds resulting from a derivatisation of **20** (**Figure 1.22**) would make for suitable high-barrier atropisomeric fragments, its rotational barrier was assessed. Rotation student Lucia Staroňova dissolved a small quantity of an 88:12 e.r. sample in *meta*-xylene. Heating the sample to 80 °C and removing aliquots at regular intervals over the

course of several days lead to measurable racemisation. As a result, the mixture was heated to 130 °C and, by withdrawing and analysing aliquots by chiral HPLC over the course of 27 hours, a reduction of the e.r. to 86:14 was observed (**Figure 1.23**).[87]

Plotting $ln\frac{1}{ee} = f(t)$ for such data should result in a straight line with a gradient of $2k_{ent} = k_{rac}$ (where k_{rac} is the rate constant of racemisation and k_{ent} is the rate constant of enantiomerisation)†.[49] Staroňova's data was plotted in this manner and allowed us to determine that k_{rac} = 5.32 × 10^{-7} s^{-1}, corresponding to a half-life of racemisation $t_{1/2}^{rac}$ of 15 days at this temperature. Using the Eyring equation, we calculated that the rotational barrier of sulfonylpyrimidine **20** at this given temperature ($\Delta G_{403}^{\ddagger}$), is approximatively 36.0 kcal/mol (**Figure 1.23**). Compound **20**, thanks to the bulk generated by the sulfonyl and trifluoromethyl groups around its chiral axis, is therefore an extremely stable class 3 atropisomer.

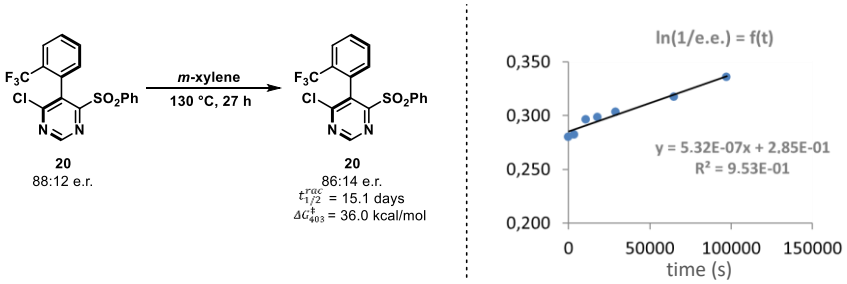


Figure 1.23: *Experiment to determine the rate of racemisation of compound **20**. Data collected by Lucia Staroňova.*[86]

† It can be shown that $ln\frac{1}{ee} = 2k_{ent}t + constant$. For a derivation of this equation, please refer to **Appendix A**.

I.3.2 Derivatisation at the chloro site

I.3.2.1 Sonogashira cross-coupling

I.3.2.1a Preliminary results

Taking inspiration from Matulenko and co-workers' AK inhibitors (**Section I.2.1.2**, **Figure 1.16**), we decided to explore the possibility of derivatising the chloro site of pyrimidine **20** using a Sonogashira cross-coupling. The Sonogashira reaction, named after Kenkichi Sonogashira, is a useful tool in the creation of carbon–carbon bonds between aryl (or vinyl) halides and terminal alkynes, involving a palladium catalyst and a copper co-catalyst.[88] As the acetylene group is a gateway a multitude of chemical transformations (cycloadditions, electrophilic and nucleophilic substitutions, etc.), it is a useful group to equip our fragments with for potential fragment growth (see **Section I.3.4**).

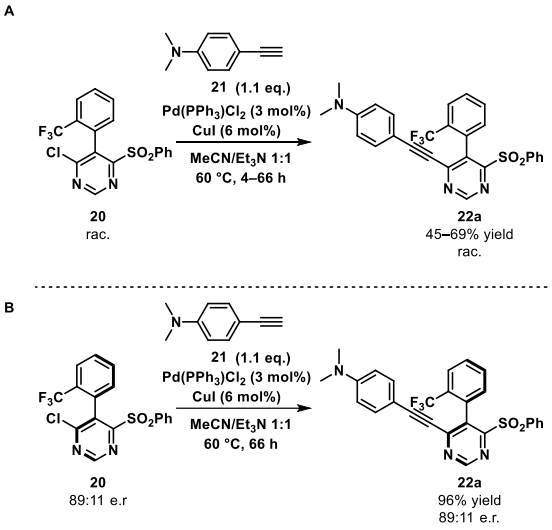


Figure 1.24: *Application of Matulenko's Sonogashira conditions to substrate **20**.*[80] ***(A)*** *On a racemic mixture.* ***(B)*** *On an enantioenriched mixture (89:11 e.r.).*

As a preliminary investigation, we decided to couple racemic pyrimidine **20** with 4-ethynyl-*N,N*-dimethylaniline **21**, one of the alkynes that gave the best results on coupling with Matulenko and

co-wokers' substrate (**Figure 1.24**).[80] Chloropyrimidine **20** and terminal alkyne **21** were coupled at 60 °C in a 1:1 acetonitrile/triethylamine mixture in the presence of bis(triphenylphosphine)palladium(II) dichloride and copper iodide. An initial reaction time of 4 hours yielded 45% of the desired cross-coupling product **22a**.[80] Considering that the oxidative addition on a carbon–chloride bond is usually slow due to the greater strength of such a bond,[89] we extended the reaction time to 66 hours, which allowed the yield to be increased to 69% (**Figure 1.24A**). The reaction was also performed on an enantioenriched sample of chloropyrimidine **20** (89:11 e.r.) and yielded compound **22a** in excellent yield (96%) and with no loss of stereochemical integrity (**Figure 1.24B**).

Rotation student Lucia Staroňova also studied the racemisation of compound **22a** by heating it in *meta*-xylene at 130 °C for 5 hours, withdrawing aliquots at regular intervals. An erosion of the e.r. was identified (from 86:14 to 83:17) and plotting $ln\frac{1}{ee} = f(t)$ allowed to determine that k_{rac} = 5.25 × 10^{-6} s^{-1}, corresponding to a half-life of racemisation at 130 °C ($t_{1/2}^{rac}$) of 1.5 days. This means that the barrier to rotation of compound **22a** at 130 °C ($\Delta G_{403}^{\ddagger}$) is 34.1 kcal/mol, which corresponds to class 3 atropisomerism (**Figure 1.25**).[87]

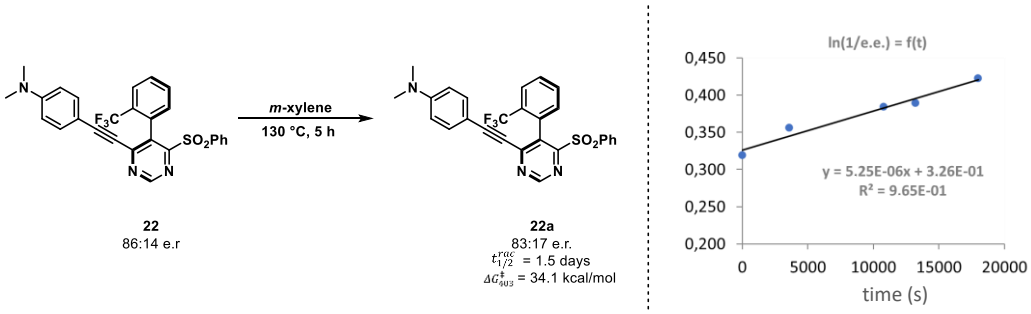


Figure 1.25: *Experiment to determine the rate of racemisation of compound **22a**. Data collected by Lucia Staroňova.*[86]

We grew crystals of **22a** by slow evaporation of an isopropanol solution and fellow DPhil student Owen Smith analysed them by single-crystal X-Ray diffraction to obtain a crystal structure, thus elucidating the absolute configuration of 22**a** and confirming Roly Armstrong's observation of the enantioselectivity of the dichloropyrimidine desymmetrisation (**Figure 1.26**).[49]

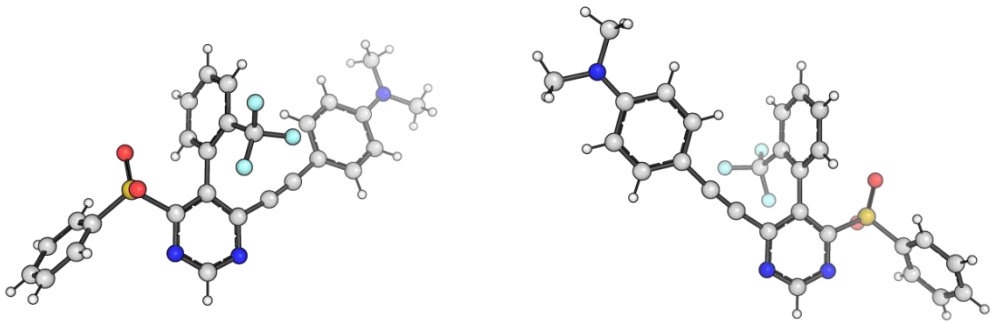


Figure 1.26: *Crystal structure of compound **22a**. The absolute configuration is the same as that reported by Armstrong.[76] Data collected by Owen Smith*

I.3.2.1b Scope-ability issues

Considering the encouraging preliminary results we obtained using the methodology developed by Matulenko *et al.* for the Sonogashira coupling of a biaryl halopyrimidine, we decided to try to apply these conditions to substrate **20** using other terminal alkynes. Another example found in the Abbott Laboratories' reports is trimethylsilylacetylene,[80] which we reacted with **20** for 24 hours under the same conditions as previously reported. Disappointingly, we were only able to obtain compound **22b** in 7% yield (**Figure 1.27A**). Electron-rich arylalkynes such as 4-ethynyl-anisole (**Figure 1.27B**) and electron-poor arylalkynes, such as 1-ethynyl-3-fluorobenzylacetylene and 1-ethynyl-4-nitrobenzylacetylene (**Figure 1.27C**) did not react at all.

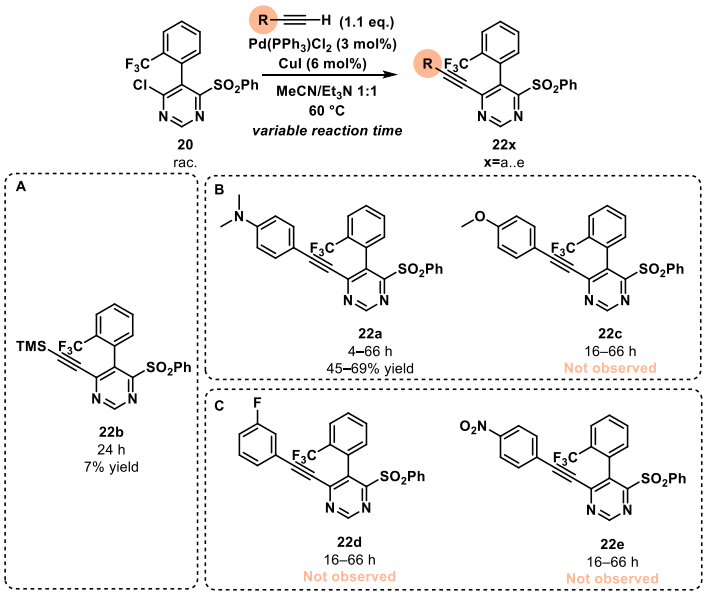


Figure 1.27: *Attempts at scoping Matulenko and co-workers' Sonogashira reaction on substrate **20**.[80] **(A)** On aliphatic substrates. **(B)** On electron-rich arylacetylenes. **(C)** On electron-poor arylacetylenes.*

I.3.2.1c Fixing the reaction

Despite the heartening results obtained with 4-ethynyl-*N,N*-dimethylaniline **21** (**Section I.3.2.1a**, **Figure 1.24**), no other terminal alkyne gave encouraging results with the conditions reported by Abbott Laboratories, making these conditions unsuitable for a scope study of the Sonogashira reaction. Katherine England (Brennan group) reported in her PhD thesis that using tetrakis(triphenylphosphine)palladium(0) ($Pd(PPh_3)_4$), in combination with the addition of catalytic amounts of triphenylphosphine helped her to dramatically increase the yield of a Sonogashira cross-coupling reaction between a chloropyrimidine and trimethylsilylacetylene.[90] Looking at the mechanism of our reaction if it were carried out using $Pd(PPh_3)_4$ as a palladium source, we can see that the oxidative addition step of the mechanism generates triphenylphosphine, while the reductive elimination step uses this free triphenylphosphine for the recycling of the palladium catalyst (**Figure 1.28**).[89] Therefore, we can assume that introducing triphenylphosphine into the reaction mixture would increase the rate of the reductive elimination step, at the expense of the

rate of the oxidative addition step. As mentioned in **Section 1.3.2.1a**, carbon–chloride oxidative additions tend to be slower due to the greater bond strength.[89] Nonetheless, as we did not recover any starting material from both our successful and unsuccessful Sonogashira coupling attempts, we postulated that the issue with the reaction conditions might reside in the transmetallation or reductive elimination steps, rather than in the oxidative addition of the catalyst on **20**, and opted for applying England's optimised conditions to our substrates.

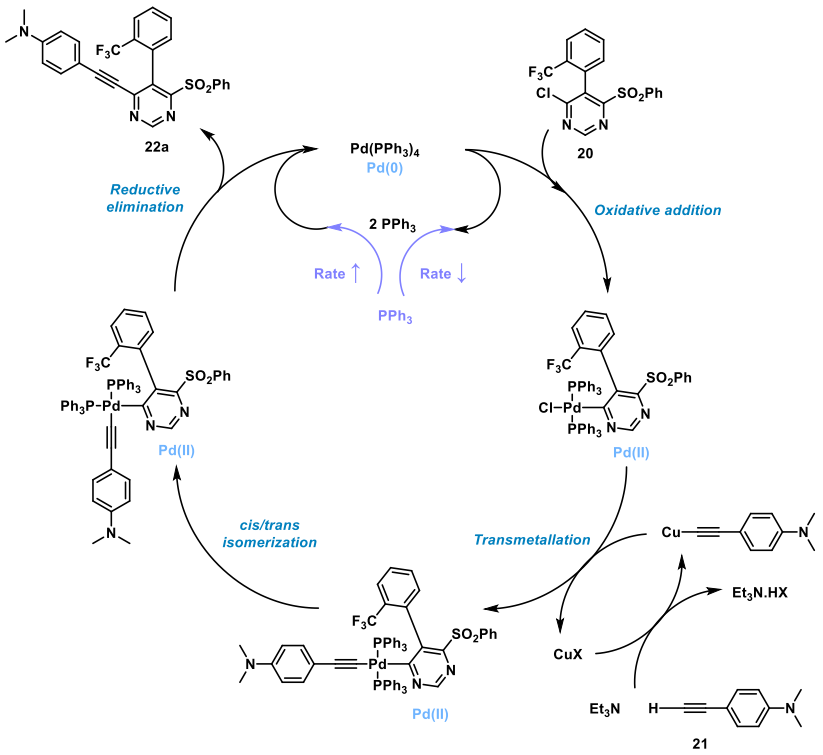


Figure 1.28: *Mechanism of the Sonogashira cross-coupling and the influence of adding triphenylphosphine on the rates of the oxidative addition and the reductive elimination steps.*

We dissolved racemic **20** and 4-ethynyl-*N,N*-dimethylaniline **21** in a 1:2 mixture of *N,N*-dimethylformamide and triethylamine and heated the resulting solution to 50 °C in presence of tetrakis(triphenylphosphine)palladium(0), copper iodide and an additional 20 mol% of triphenylphosphine (**Figure 1.29**).[90] Contrary to our previous set of conditions, where we would not observe full consumption of the starting material before a minimum of 2.5 days, these

conditions allowed for full completion of the reaction overnight, yielding product **22a** almost quantitatively (99% yield). This result comforted us in the idea that the reductive elimination step was one of the limiting steps of this cross-coupling, and that the extra triphenylphosphine helped accelerate it without too much of a negative impact on the oxidative addition step.

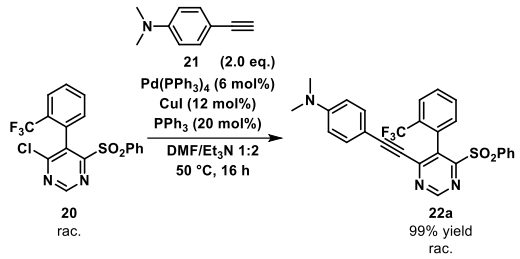


Figure 1.29: *Applying England's conditions for the Sonogashira reaction, using our initial acetylene **21**.*[89]

We also decided to apply these conditions to the coupling of trimethylsilylacetylene with racemic compound **20**, for which the previous set of conditions were very low-yielding (7% yield). These conditions allowed for an extremely quick reaction (3 hours), affording product **22b** with a high yield of 83% (**Figure 1.30A**). The coupling of trimethylsilylacetylene with an enantioenriched sample of compound **20** (81:19 e.r.) also led to a quick reaction (3 hours), with an almost quantitative yield (98%) and no erosion of the enantiomeric ratio (**Figure 1.30B**).

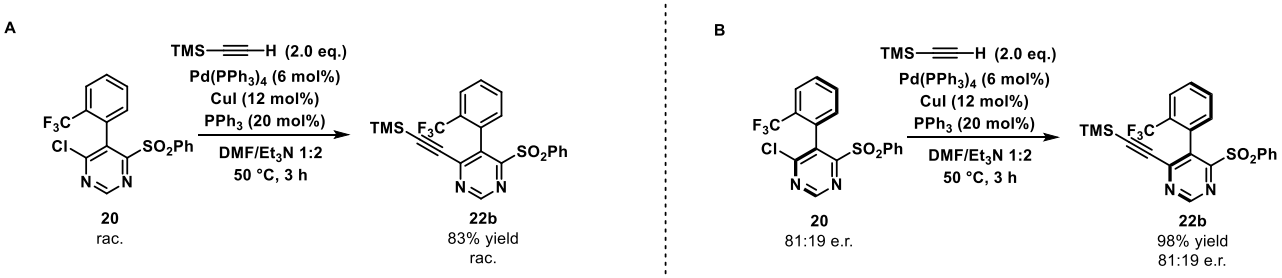


Figure 1.30: *Applying England's conditions for the Sonogashira reaction, using our initial acetylene **21**.*[89]*: **(A)** Using trimethylsilylacetylene on a racemic **20**. **(B)** Using trimethylsilylacetylene on an enantioenriched **20***

The trimethylsilylacetyl moiety being a rather small group, we decided to evaluate the rotational barrier of compound **22b**. An enantioenriched sample of **22b** (81:19 e.r.) was dissolved in *meta*-xylene and heated to 80 °C, with regular aliquot sampling. After 4 days, the e.r. had dropped to 78:22, allowing us to plot $ln\frac{1}{ee} = f(t)$ to determine that k_{rac} = 3.57 × 10 $^{-7}$ s^{-1}, corresponding to a half-life of racemisation at 80 °C ($t_{1/2}^{rac}$) of 22.4 days and $\Delta G_{353}^{\ddagger}$ = 31.9 kcal/mol (**Figure 1.31**). Despite the small size of the trimethylsilylacetylenyl group, the steric hindrance generated by the trifluoromethyl and phenylsulfonyl groups allow **22b** to be a class 3 atropisomer.

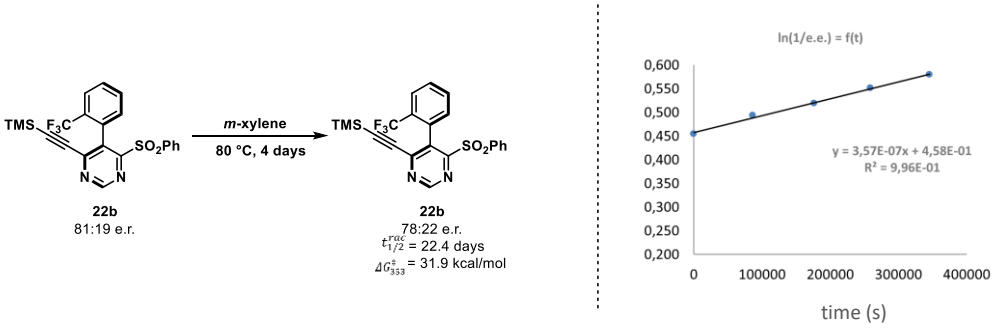


Figure 1.31: *Experiment to determine the rate of racemisation of compound **22b**.*

I.3.2.1d Reaction scope

We decided to evaluate the functional group tolerance of the newly-optimised Sonogashira reaction conditions for substrate **20**. Chloropyrimidine **20** was coupled to eight terminal alkynes, split into three categories: aliphatic acetylenes (2), electron-rich arylacetylenes (3), and electron-poor arylacetylenes (3). Chloropyrimidine **20** and the corresponding alkyne were heated to 50 °C in a 1:2 mixture of *N,N*-dimethylformamide and triethylamine, in the presence of $Pd(PPh_3)_4$, copper iodide and an additional 20 mol% of triphenylphosphine (**Figure 1.32**).[90] Trimethylsilylacetylene gave compound **22b** with a short reaction time and high yield (83%) and cyclopropylacetylene gave compound **22f** in moderate yield (71%) (**Figure 1.32A**). Electron-rich arylalkynes reacted readily with **20** under these conditions, with 4-ethynyl-*N,N*-dimethylaniline

yielding compound **22a** in 99% yield. Methyl and methoxy groups were also tolerated, with 1-ethynyl-4-methylbenzene yielding compound **22g** in 93% yield and 1-ethynyl-anisole yielding compound **22c** in 84% yield (when the previous set of conditions had led to no product formation at all) (**Figure 1.32B**). Electron-poor arylalkynes showed less compatibility with these reaction conditions. The tolerance of the fluorine group was confirmed by using 1-ethynyl-3-fluorobenzylacetylene, yielding compound **22d** in 63% yield (when the previous set of conditions had led to no product formation at all) and the methyl ester was also tolerated in methyl-4-ethynylbenzoate, yielding compound **22h** in 46% yield. These more moderate yields testified for the reduced reactivity of electron-poor arylalkynes, and 1-ethynyl-4-nitrobenzylacetylene was therefore not reactive under these conditions (**Figure 1.32C**). Indeed, we can postulate that, during the reaction process, electron-withdrawing groups on the arylacetylene stabilise the electron-rich Pd(II) metal centre, thus rendering the whole metal complex more resistant to reductive elimination.[91]

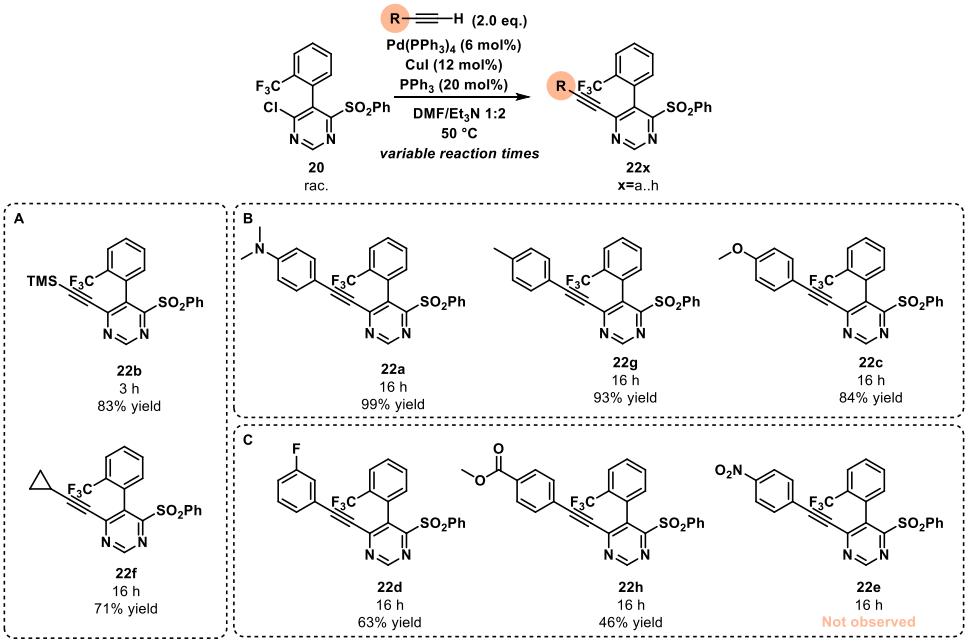


Figure 1.32: *Attempts at scoping England's Sonogashira reaction on substrate **20**.*[89] ***(A)*** *On aliphatic substrates.* ***(B)*** *On electron-rich arylacetylenes.* ***(C)*** *On electron-poor arylacetylenes.*

The optimised Sonogashira reaction allowed for the generation of a respectable range of atropisomeric fragments with acceptable functional group tolerance. When applied to enantioenriched samples, the conditions did not lead to any loss of stereochemical integrity. Fragments with even a small acetylene moiety such as trimethylsylilacetylene still displayed a high rotational barrier.

I.3.2.2 Other potential derivatisations

Although we did not explore other transformations at the chloro site in as much depth as the Sonogashira reaction, we still report our preliminary investigations in this section.

I.3.2.2a Suzuki-Miyaura cross-coupling

Taking inspiration from Armstrong's successful Suzuki-Miyaura coupling of phenylboronic acid with substrate **12** (**Section I.2.1.1**, **Figure 1.15**), we decided to explore the derivatisation of compound **20** using these conditions.[71] First published in 1979 by Suzuki and Miyaura,[92] the eponymous reaction is the most commonly used carbon–carbon bond forming reaction in the pharmaceutical industry and shares a Nobel prize with the Negishi coupling.[93,94] Due to its ability to generate a wide range of $C(sp^2)$–$C(sp^2)$ bonds, it has established itself as the go-to reaction to synthesise multiaryl motifs with a high level of functional group tolerance and is therefore of great relevance in the context of generating atropisomeric fragments for fragment-based screening.

We started by assessing whether our sulfonyl precursor **20** would react as readily as Armstrong's sulfide **12** with phenylboronic acid. Chloropyrimidine **20** was heated to 75 °C in toluene in the presence of phenylboronic acid, potassium carbonate, and catalytic amounts of tetrakis(triphenylphosphine)palladium(0) (**Figure 1.33**).[71] The reaction yielded phenylpyrimidine **23a** in high yield (88%) and we therefore proceeded to assess this set of conditions on other substrates.

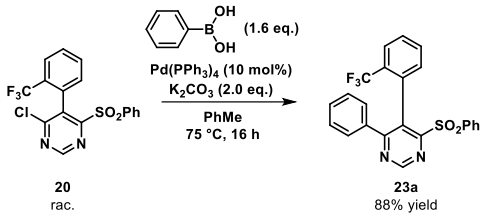


Figure 1.33: *Preliminary attempt at a Suzuki-Miyaura coupling on **20**.*[70]

Upon being subjected to the same set of conditions, allylboronic acid and chloropyrimidine **20** reacted to yield compound **23b** in 16% yield (**Figure 1.27**). Compound **23b**, despite having been obtained with a mediocre yield, makes for an interesting fragment, as it is of small size (the "rule of three" for FBDD advising the use of molecules no bigger than 300 Da for fragment-based screening[15]) and, allows for potential fragment growth after hit-identification by introducing a terminal alkene handle onto the molecule. However pyridin-4-ylboronic acid and (1-methyl-1*H*-pyrazol-4-yl)boronic acid did not show any reactivity with **20** under these conditions and only a trace amount of compound **23e** was detected upon reaction with (1*H*-pyrazol-4-yl)boronic acid (**Figure 1.34**).

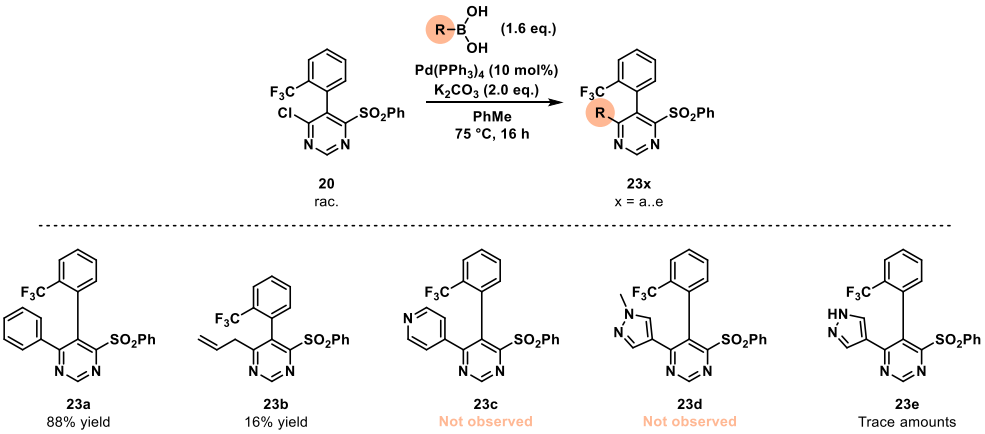


Figure 1.34: *Attempts at expanding the scope of the Suzuki-Miyaura derivatisation of **20***

Heterocyclic boronic acids such as the three we experimented with earlier (**Figure 1.34**) are known to easily undergo proto-deborylation under Suzuki-Miyaura coupling conditions. If such

degradation occurred at a faster rate than the oxidative addition of the palladium catalyst onto the aryl halide, then there would be no boronic acid left for transmetallation onto the palladium–aryl complex and no product would be observed. To prevent this from happening, David M. Knapp *et al.* developed a method for the slow-release of a boronic acid into a Suzuki-Miyaura reaction medium, by exploiting the slow hydrolysis of MIDA boronates by aqueous tripotassium phosphate in 1,4-dioxane.[95] We had at our disposal (1H-pyrazol-4-yl)-MIDA boronate and (thiazol-5-yl)-MIDA boronate and decided to try to apply Knapp and co-workers' strategy to the coupling of these boronates and our precursor **20**. Chloropyrimidine **20** and the MIDA boronates were heated to 60 °C in 1,4-dioxane in the presence of aqueous tripotassium phosphate, and catalytic amounts of palladium(II) acetate and dicylcohexylphosphino-2,6'-dimethoxy-1,1'-biphenyl (SPhos) (**Figure 1.35**). Although we did not observe any reactivity between **20** and (thiazol-5-yl)-MIDA boronate, (1H-pyrazol-4-yl)-MIDA boronate did react with our substrate, but it did not yield the expected compound (**23e**). Instead, we isolated the product of both the Suzuki-Miyaura coupling of the boronate at the chloro position and the hydrolysis of the phenylsulfonyl moiety **23f**. Spectroscopic data evidenced the preferred tautomeric state of this product as the pyrimidone form instead of the hydroxypyrimidine. The solvolysis of the sulfone in aqueous basic media is described in further detail in **Sections I.3.3** and **I.3.4**.

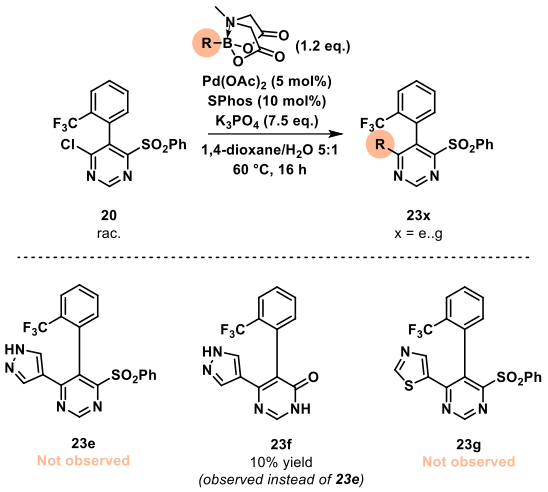


Figure 1.35: *Attempts at improving the derivatisation of **20** by Suzuki-Miyaura coupling, replacing unstable boronic acids by their MIDA boronate counterpart.*[92]

Considering it drastically improved the Sonogashira reaction (see **Section I.3.2.1**), adding extra triphenylphosphine (33 mol%) to Armstrong's conditions was explored.[71,90] Chloropyrimidine **20** was heated to 75 °C in toluene in the presence of the boronic acid of choice, potassium carbonate, and catalytic amounts of tetrakis(triphenylphosphine)palladium(0) and triphenylphosphine. However, this resulted in the deterioration of the yield in compound **23a** when carried out with phenylboronic acid, which dropped to 33% (with quantitative recovery of remaining starting material). These conditions and resulted in full recovery of starting material with both allylboronic acid and (1*H*-pyrazol-4-yl)boronic acid) (**Figure 1.36**). This hinted that the effect of the extra triphenyl phosphine on slowing down the oxidative addition step prevailed over the effect of speeding up the reductive elimination step.

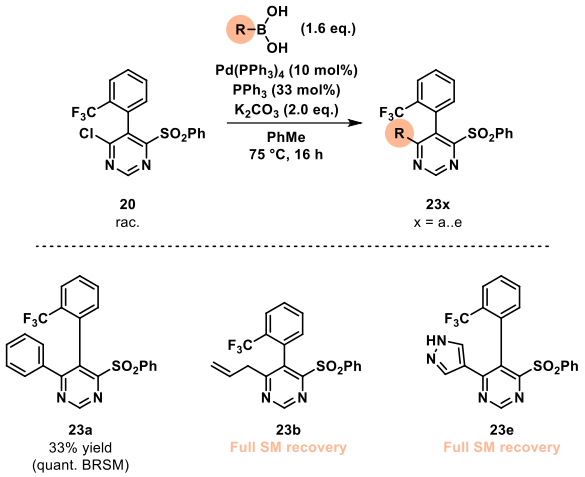


Figure 1.36: *Attempts at improving the derivatisation of **20** by Suzuki-Miyaura with PPh_3.*[70,89]

Despite proving successful in the coupling of phenyl boronic acid with **20** and leading to the obtainment of useful fragments with the likes of allylpyrimidine **23b**, the Suzuki-Miyaura reaction was not developed any further as it appeared considerably more sensitive and substrate-specific than the Sonogashira reaction.

I.3.2.2b Nucleophilic aromatic substitution (SNAr)

Armstrong's successful derivatisation of compound **12** by SNAr using pyrrolidine (**Section I.2.1.1**, **Figure 1.15**) inspired us to try the same strategy with our sulfide substrate **19**.[71] A racemic mixture of chloropyrimidine **19** was stirred in *N,N*-dimethylformamide in the presence of *N,N*-diisopropylethylamine at room temperature to yield the desired SNAr product **24** in good yield (89%) (**Figure 1.37A**). Sulfide **24** could not be converted into sulfone **25** using excess *meta*-chloroperbenzoic acid, and this transformation necessitated milder conditions. Therefore, a racemic mixture of sulfide **24** was stirred in trifluoroacetic acid at room temperature in the presence of aqueous dihydrogen peroxide (30 wt.%) to yield sulfone **25** in moderate yield (68%) (**Figure 1.37A**). This sequence was also applied to an enantioenriched sample of compound **19** (85:15 e.r.) and yielded an enantioenriched sample of sulfone **25**, without any loss of stereochemical integrity (**Figure 1.37B**).

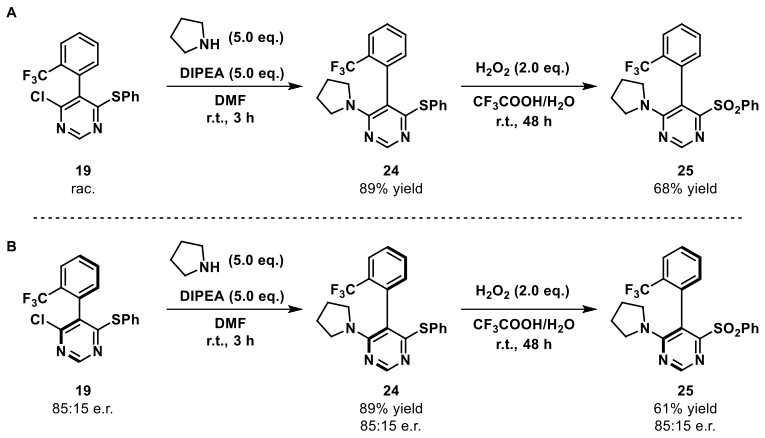


Figure 1.37: *Assessing the potential of sulfide **19** to be derivatised by SNAr.*[70] ***(A)*** *On a racemic sample.* ***(B)*** *On an enantioenriched sample.*

The rate of racemisation of compound **25** was studied by stirring an enantioenriched sample (85:15 e.r.) in *meta*-xylene at 120 °C for 24 hours. By sampling aliquots at regular intervals, we observed a decrease of the e.r. to 79:21 e.r., allowing us to plot $ln\frac{1}{ee} = f(t)$ and determine that k_{rac} = 2.00 × 10 $^{-6}$ s^{-1}, corresponding to a half-life of racemisation at 120 °C ($t_{1/2}^{rac}$) of 4.0 days and $\Delta G_{393}^{\ddagger}$ = 34.0 kcal/mol (**Figure 1.38**).

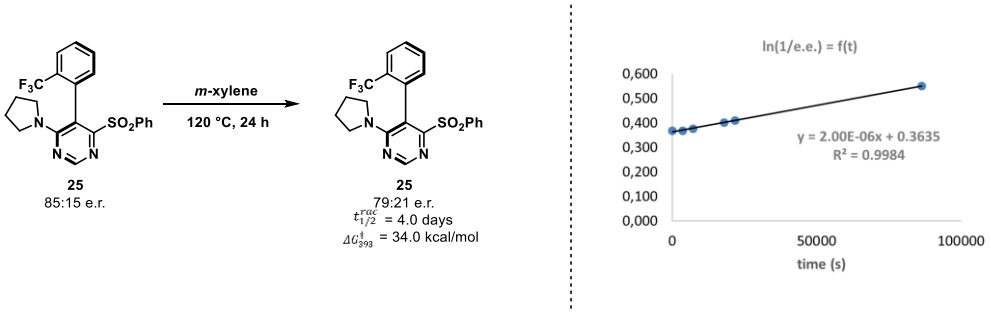


Figure 1.38: *Experiment to determine the rate of racemisation of compound **25**.*

I.3.3 Derivatisation at the sulfonyl site

Though it contributes greatly to the steric hindrance about the chiral axis in our compounds, the high molecular weight (141 Da) of the phenylsulfonyl group renders most of our atropisomeric fragments non-compliant with the "rule of three".[15] Additionally, several reports have shown the

usefulness of an amino substituent *ortho* to one of the nitrogen atoms of the pyrimidine ring in the development of kinase inhibitors (adenosine, Src and Brk kinases, amongst others).[80,96] We decided to explore the possibility to substitute the arylsulfonyl group on our compounds by smaller moieties, making our compounds more amenable to use as fragments and, potentially more drug-like.

I.3.3.1 Nucleophilic aromatic substation (SNAr)

Several examples in the literature describe the phenylsulfonyl and *para*-toluene sulfonyl groups as good leaving groups for aromatic nucleophilic substitution.[96–100] However, due to the softness of the C–S electrophilic site, substituting an arylsulfonyl group with a simple nitrogen or oxygen nucleophile usually requires harsh conditions. Most of the reported methodologies call for temperatures exceeding 120 °C for several hours in strong basic media,[97–100] which would lead to an erosion of the enantiomeric excess of the generated products if they were to be carried out on our substrates. Cardenas *et al.* adapted the conditions of Armstrong's cation-directed desymmetrisation of biarylpyrimidines to the kinetic resolution of 3-substituted pyrrolopyrimidines, for an enantioselective synthesis of known Scr/Brk kinase inhibitors (**Figure 1.32A**).[96] They were able to oxidise the resulting atropisomeric sulfides **26a–d** using *meta*-chloroperbenzoic acid and, by stirring the resulting sulfones in neat 2,4-dimethoxybenzylamine at room temperature for 72 to 96 hours, obtained the desired protected amines.[96] Subsequent treatment with trifluoroacetic acid in dichloromethane for a few hours at room temperature yielded the desired kinase inhibitors **27a-d** with no loss of stereochemical integrity over the whole sequence (**Figure 1.39**).

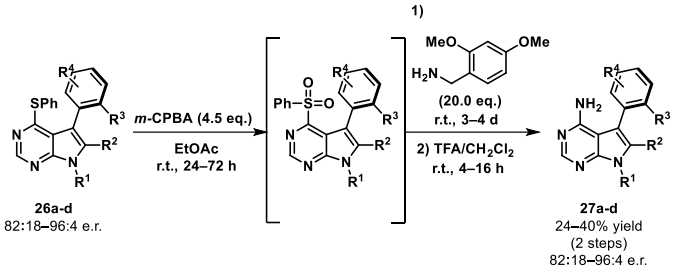


Figure 1.39: ***(A)*** *Cardenas and co-workers' conditions for the derivatisation of sulfonyl pyrrolopyrimidines vial SNAr.*[93]

We attempted to apply Cardenas and co-workers' conditions to both sulfone **22a** and sulfone **25**. The racemic sulfones were stirred in neat 2,4-dimethoxybenzylamine at room temperature for 3.5 to 4 days (**Figure 1.40**).[96] We observed no reaction for sulfone **25**, for which a similar reaction with diethylamine was also attempted but did not lead to any reactivity at all. In the case of sulfone **22a**, we did observe the formation of a new product, which was subsequently treated with trifluoroacetic acid in dichloromethane for 4 hours to yield compound **29**. **29** was identified as the deprotection product resulting from the addition of 2,4-dimethoxybenzylamine onto the alkyne site of compound **22a**, indicating that the desired SNAr at the sulfonyl site had not taken place. Harsher methodologies consisting of heating sulfone **25** to high temperatures (above 100 °C) with either neat or diluted diethylamine or morpholine, in the presence or absence of a base, were also attempted, but did not lead to any reactivity (see **Appendix B**).

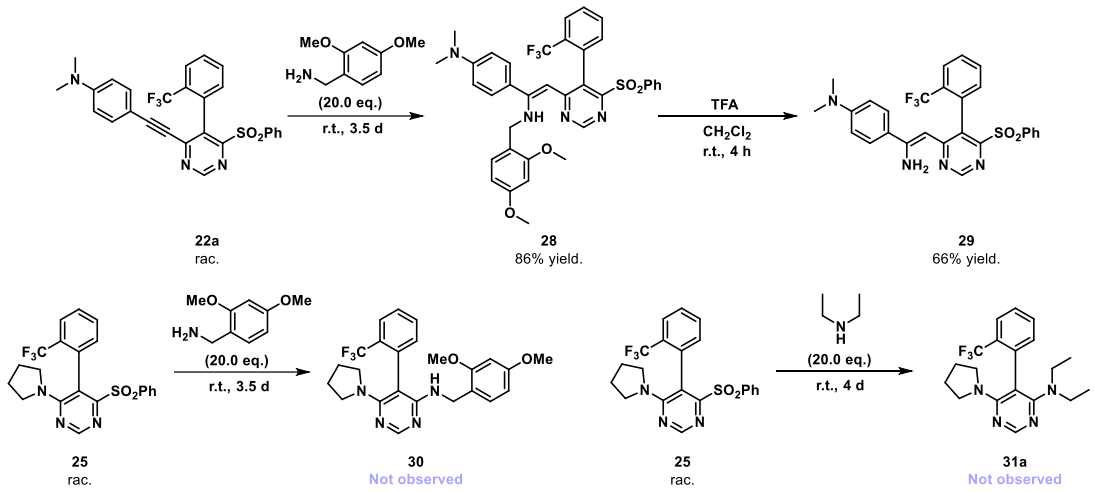


Figure 1.40: *Attempts to apply Cardenas and co-workers' conditions to substrates **22a** and **25**.*[93]

An alternative to the use of high temperatures in the SNAr of amines onto sulfonyl electrophiles is to deprotonate the amine. Lithium amides have proven successful in the displacement of phenylsulfonyl groups on aromatic compounds, sometimes even favouring the attack on a sulfonyl electrophilic centre over a halide electrophilic centre, due to the softness of the C–S bond.[97] Matulenko and co-workers also reported the use of lithium amide ($LiNH_2$) to synthesise their amino-pyrimidine AK inhibitor **13**.[80] We used *n*-butyllithium to deprotonate morpholine, *N*-ethylpiperazine and methylimidazole at –78 °C in anhydrous tetrahydrofuran. We also dissolved some lithium amide salt in anhydrous tetrahydrofuran. These solutions were added to a solution of sulfone **25** in anhydrous tetrahydrofuran and refluxed overnight (**Figure 1.41**). The reactions with lithium morpholinide and lithium *N*-ethylpiperazinide were successful and respectively afforded compounds **32b** and **32c** in moderate to good yield. The reaction with lithium amide did not yield any of the desired product **32d**. The reaction with the deprotonated methylimidazole did not yield any of the desired product **32e**, but we were expecting such a result as we would imagine a carbon–lithium substrate would more readily act as a base than a nucleophile.

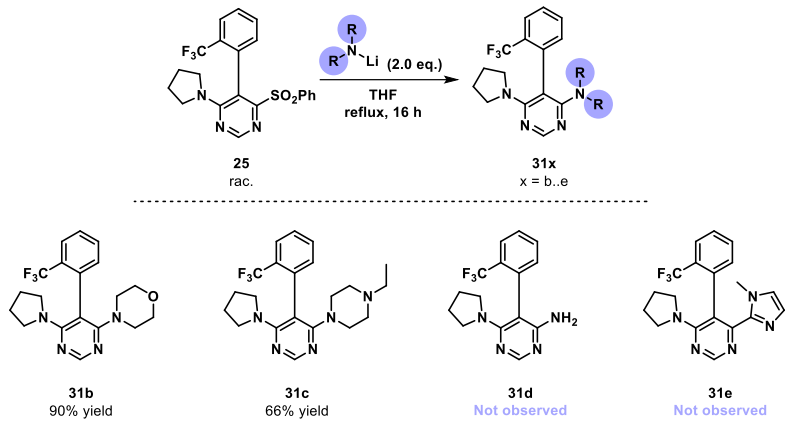


Figure 1.41: *Attempts at derivatising the sulfonyl moiety of compound **25** via SNAr using lithium adducts*

Lucia Staroňova also attempted these conditions on Sonogashira product **22a**, using both lithium morpholinide and lithium amide, but did not observe any formation of the desired products (**Figure 1.42**).[87]

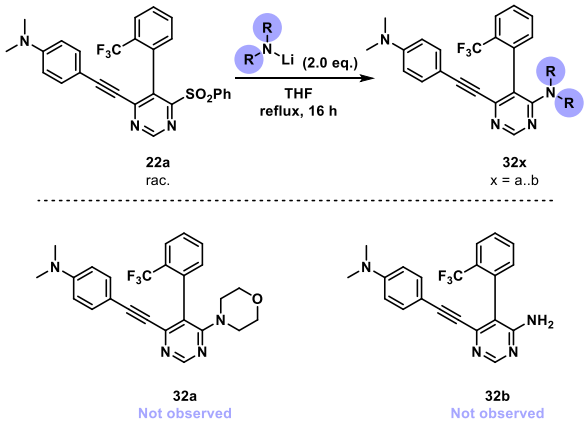


Figure 1.42: *Attempts at derivatising the sulfonyl moiety of compound **22a** via SNAr using lithium amides.*
Data collected by Lucia Staroňova.[86]

I.3.3.2 The serendipitous discovery of a solvolysis effect

With the potential of the acetylene group to serve as a handle for fragment growth we decided to investigate the deprotection of trimethylsilylalkyne **22b**. Classic deprotection conditions for silyl alkynes include the use of fluoride anions, in the form of tetra-*n*-butylammonium fluoride (TBAF),

at low temperatures.[101] We decided to dissolve **22b** in tetrahydrofuran and stir it at –5 °C in the presence of TBAF (**Figure 1.43**). In such conditions, we obtained fluoroalkene **33** as a single isomer (assigned by nOe NMR spectroscopy). Buffering the TBAF solution with acetic acid in tetrahydrofuran allowed for milder reaction conditions,[102] leading to slower conversion, but the deprotected alkyne was also attacked, yielding acetylalkene **34** as a single isomer (confirmed by nOe NMR spectroscopy) (**Figure 1.43**).

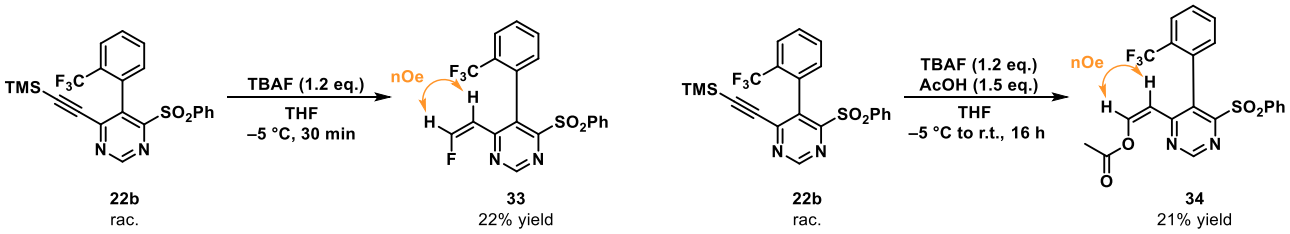


Figure 1.43: *Deprotection attempts on the trimethylsilyl alkyne **22b** using TBAF.*[98,99]

Matulenko *et al.* reported the deprotection of their TMS-alkyne substrate by using aqueous potassium carbonate in methanol.[80] Sulfone **22b** was therefore dissolved in methanol and stirred at room temperature in the presence of aqueous potassium carbonate (1 M), and we quickly observed the formation of compound **35**, which showed the removal of the trimethylsilyl group but also the replacement of the phenylsulfonyl group by a methoxy group (**Figure 1.44**). Such observation came as a surprise, as the phenylsulfonyl group had proven so difficult to remove under classic SNAr conditions. The reported yield was low (36%), but a portion of the starting material was recovered, leading us to believe that extending the reaction time could potentially increase the yield of the transformation.

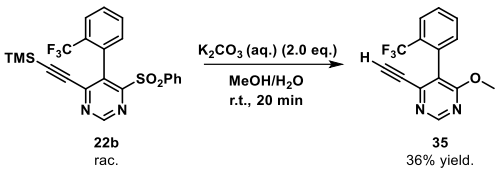


Figure 1.44: *Deprotection attempts on the trimethylsilyl alkyne **22b** using potassium carbonate in methanol.*[80]

We decided to investigate this serendipitously-discovered transformation further, particularly on substrates which did not display a trimethylsilylacetylene group, such as compounds **23a** and **22a** (**Figure 1.45A** and **Figure 1.45B**). We stirred sulfones **23a** and **22a** in methanol in the presence of aqueous potassium carbonate (1M) at room temperature overnight.[80] In both instances, the corresponding methanolysis products, respectively **36** and **37a**, were obtained, with respective yields of 56% and 93%. We also evaluated the reaction conditions on an enantioenriched sample of **22a** (85:15 e.r.) and were pleased to obtain methanolysis product **37a** without any erosion of the enantiomeric ratio (**Figure 1.45C**).

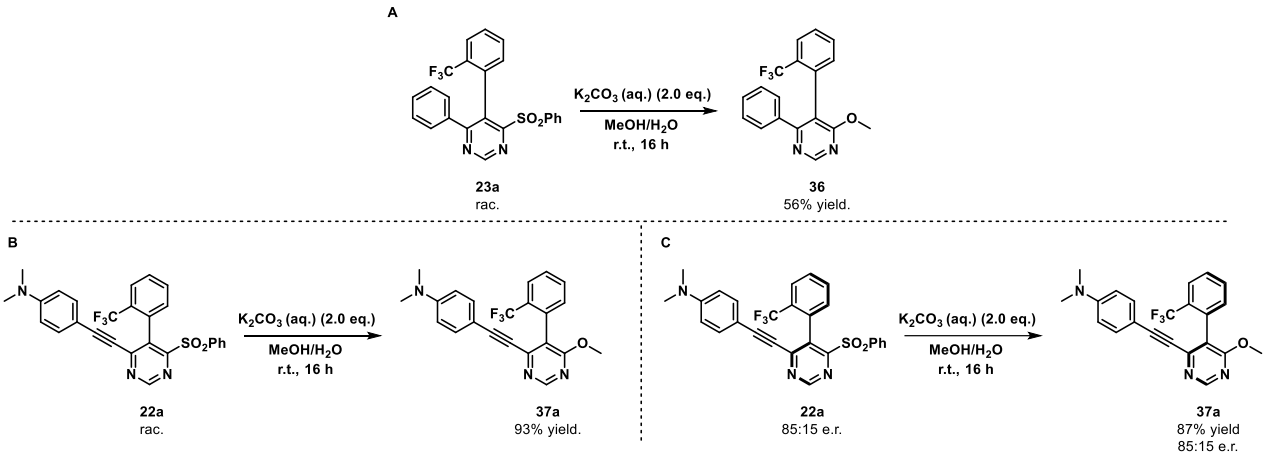


Figure 1.45: *Assessing the solvolysis conditions on non TMS-protected compounds. **(A)** On racemic **23a**. **(B)** On racemic **22a**. **(C)** On enantioenriched **22a**.*

Recalling compound **23f** (**Section I.3.2.2a**, **Figure 1.35**), which resulted from the hydrolysis of the phenylsulfonyl group initially present on compound **20** whilst trying to perform a Suzuki-Miyaura coupling, we decided to examine if more alcohol solvents could generate such effect. Sulfone **22a**

was dissolved or suspended in an array of different alcohols (and water) and stirred overnight at room temperature in the presence of aqueous potassium carbonate (1M) (or 1M NaOH in the case of the reaction in water) (**Figure 1.46**). We only observed successful formation of product when using water (**37b**) and methanol (**37a**) as solvents. The hydrolysis of sulfone **22a** generated compound **37b** in quantitative yield, and spectroscopic analysis allowed us to determine that the preferred tautomeric state of the compound is the pyrimidone instead of the hydroxypyrimidine. The methanolysis of compound **22a** generated compound **37a** in excellent yield (93%), but the ethanolysis, isopropanolysis and *tert*-butanolysis of sulfone **22a** did not occur. We therefore assumed that steric hindrance was a crucial element in the solvolysis of the sulfone, and only water and methanol were small enough for the transformation to happen.

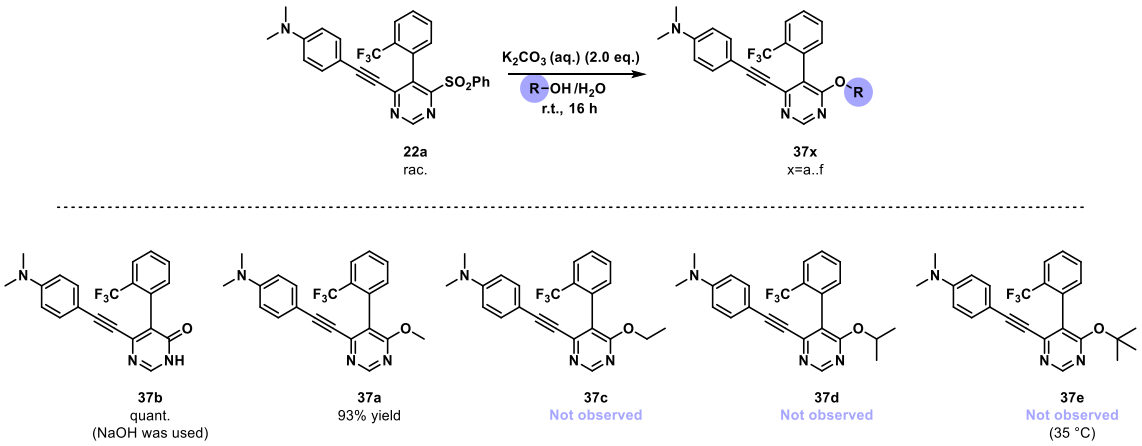


Figure 1.46: *Assessing the scope of the solvolysis effect.*

The rate of racemisation of methanolysis product **37a** was evaluated by dissolving an enantioenriched sample (85:15 e.r.) in *meta*-xylene and heating it to 80 °C for 8 hours. Regular aliquoting allowed us to observe erosion of the enantiomeric ratio to 59:41 (**Figure 1.47**). Plotting $ln\frac{1}{ee} = f(t)$ allowed us to determine that k_{rac} = 4.83 × 10 $^{-5}$ s^{-1}, corresponding to a half-life of racemisation at 80 °C ($t_{1/2}^{rac}$) of 4.0 hours and $\Delta G_{353}^{\ddagger}$ = 28.4 kcal/mol. The removal of the sulfone did indeed result in a dramatic drop of the configurational stability of our atropisomeric fragments.

However, to truly assess whether the fragments would not be viable at all for drug discovery, we would have to evaluate their half-life of racemisation and barrier to rotation at 37 °C, as the entropic factor might allow for increased stability at lower temperatures.

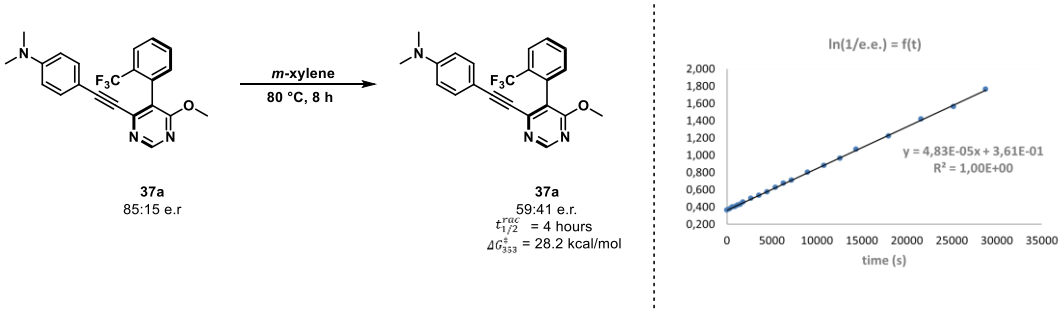


Figure 1.47: *Experiment to determine the rate of racemisation of compound **37a***

I.3.3.3 One-pot hydrolysis and electrophilic trapping sequence

We decided to probe whether we could use the newly-discovered solvolysis effect as an efficient way to derivatise the phenylsulfonyl site of our probes. We postulated that the hydrolysis of the sulfone in the presence of sodium hydroxide was orthogonal to derivatisations at the chloro-site of the pyrimidine ring, and that we could devise a strategy that would derivatise the sulfonyl moiety of biaryl pyrimidines **iii** without affecting the carbon–chlorine bond (**Figure 1.48**). Despite having established that the preferred tautomeric state of the hydrolysed compounds was the pyrimidone, we suggested they should exist as pyrimidinolates **vi** in basic media and could potentially trap an electrophile (R–X) at the newly-generated nucleophilic *O* site to yield *O*-substituted products **vii** in a one-pot hydrolysis-alkylation sequence (**Figure 1.48**).

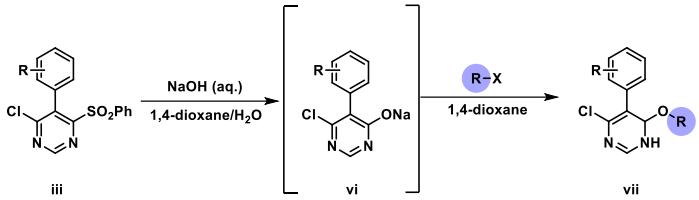


Figure 1.48: *Conceptualising a one-pot hydrolysis and electrophilic trapping sequence of phenylsulfonyl pyrimidines **iii**.*

We decided to apply these conditions to racemic sulfone **20** by stirring it at room temperature in 1,4-dioxane in the presence of aqueous sodium hydroxide (50% w/w) (**Figure 1.49**). We confirmed the hydrolysis of the phenylsulfone took place without affecting the chloro-site of the pyrimidine ring by isolating pyrimidone **39** after an acidic work-up.

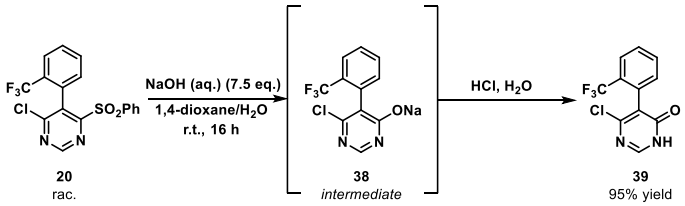


Figure 1.49: *Isolating pyrimidone **39**.*

Alternatively, we spiked the racemic **38** reaction mixture with benzylbromide and heated it to 50 °C for an hour (**Figure 50A**). We managed to isolate compound **40a** in decent yield (76%). However, spectroscopic analysis (infrared & ^{13}C), along with DFT calculations,[103] allowed us to determine that **40a** was the *N*-alkylation product, and the expected *O*-alkylation product was not observed at all. Despite not observing the expected product, we still decided to attempt the reaction on an enantioenriched sample of **20**, as *N*-alkylated pyrimidines could still display a high rotational barrier and present themselves as interesting drug-like atropisomeric fragments. We applied the aforementioned conditions to an enantioenriched sample of **20** (88:12 e.r.) and were able to obtain an enantioenriched sample of **40a**, with no loss of stereochemical integrity in the process (**Figure 1.50B**).

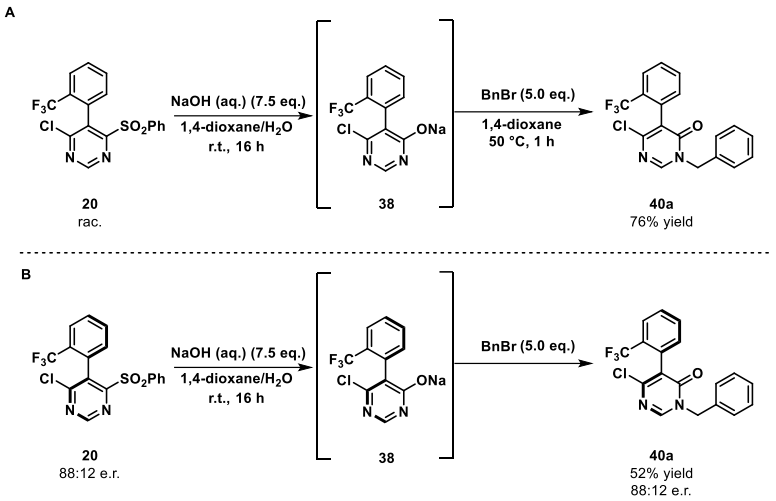


Figure 1.50: *First attempt at the one-pot hydrolysis and electrophilic trapping using **20** and benzyl bromide. **(A)** On a racemic substrate. **(B)** On an enantioenriched substrate.*

The rate of racemisation of the enantioenriched *N*-benzyl pyrimidone **40a** was measured by dissolving an enantioenriched sample in *meta*-xylene and heating it to 80 °C for 24 hours. Withdrawing aliquots at regular intervals allowed us to observe a decrease in enantiomeric ratio, from 88:12 to 75:25 (**Figure 1.51**). We plotted $ln\frac{1}{ee} = f(t)$, which allowed us to calculate k_{rac} = 4.88 × 10 $^{-6}$ s^{-1}, corresponding to $t_{1/2}^{rac}$ = 1.6 days at 80 °C and a rotational barrier ($\Delta G_{353}^{\ddagger}$) of 29.8 kcal/mol. Although at the border between class 2 and class 3 atropisomerism at such a temperature, we can assume these fragments would be configurationally stable at biological temperatures (37 °C).

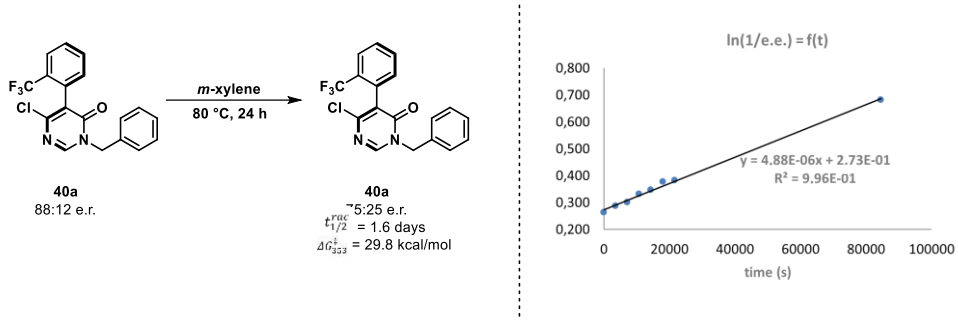


Figure 1.51: *Experiment to determine the rate of racemisation of compound **40a**.*

We then proceeded with the evaluation of the potential scope of this transformation. Sulfone **20** was stirred at room temperature in 1,4-dioxane in the presence of aqueous sodium hydroxide (50% w/w) and then immediately spiked with a bromide electrophile and heated to 50 °C for an hour. If no formation of product was observed, the heating was increased to 80 °C and the reaction mixtures were stirred for an extra 22 hours (**Figure 1.52**). We observed good reactivity with benzyl bromides, both electron rich and electron poor. For instance, benzyl bromide, 4-*tert*-butylbenzyl bromide and 3,5-di-*tert*-butylbenzyl bromide, 4-fluorobenzylbromide, 4-nitrobenzyl bromide and 2-(bromomethyl)naphthalene yielded compounds **40a–f** in moderate to good yields (64–91%) (**Figure 1.52A**). Allylbromide and propargylbromide yielded *N*-alkylated pyrimidines **40g** and **40h** respectively in moderate yields (52% and 48%, respectively), generating two fragments with high growth potential, thanks to the useful synthetic handles that the terminal alkene and alkyne make up (**Figure 1.52B**). Smaller alkyl electrophiles such as isopropyl bromide and bromonitromethane, and electrophilic aromatic rings such as bromobenzene, 1-bromo-4-nitrobenzene, 2-bromopyridine and 2-bromo-5-nitropyridine did not lead to any reactivity, even with higher temperatures and longer reaction times (**Figure 1.52C** and **Figure 1.52D**).

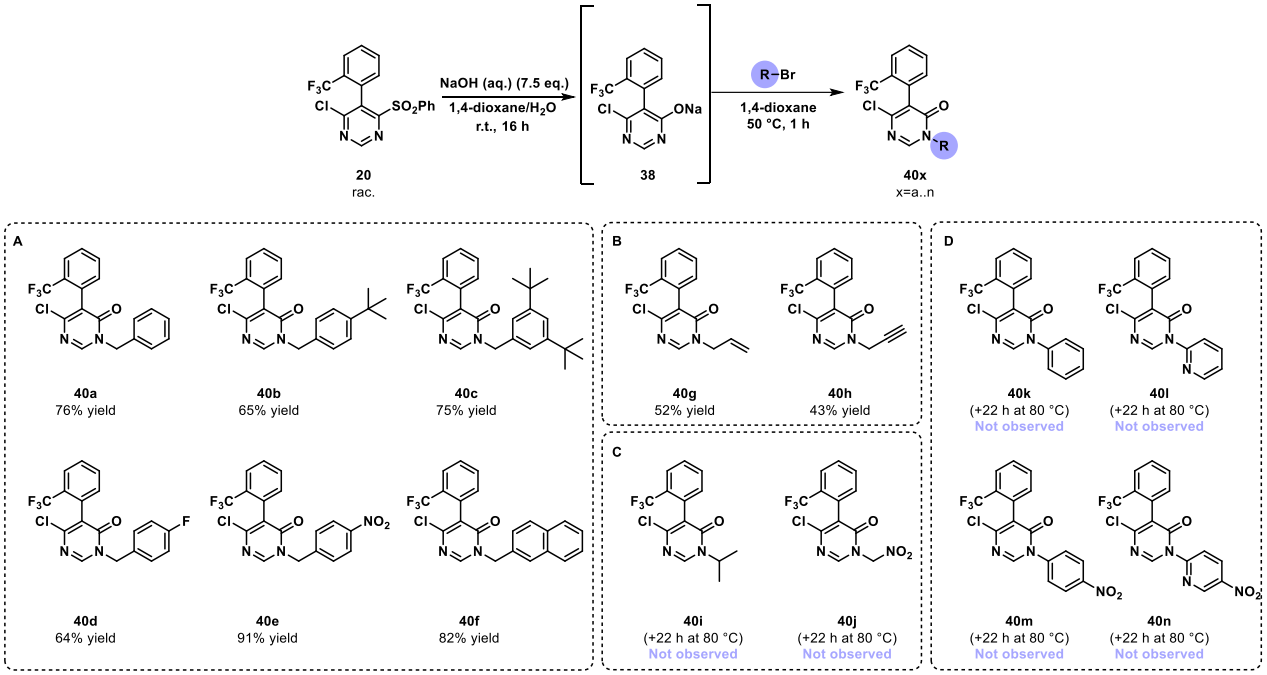


Figure 1.52: *Evaluation of the scope of the one-pot hydrolysis and electrophilic trapping of sulfone* ***20****.* ***(A)*** *On electron rich and electron poor benzylbromides.* ***(B)*** *On unsaturated aliphatic handles.* ***(C)*** *On small alkyl bromides.* ***(D)*** *On aromatic electrophiles prone to SNAr.*

I.3.4 Fragment growth: copper-catalysed azide–alkyne cycloadditions

I.3.4.1 Preliminary observations

As detailed in **Section I.1**, once a fragment has been identified as a hit during fragment-based screening, it will be developed as a chemical lead candidate. One way of doing this is by "growing" said fragment. Fragment growth is the most commonly used way of developing chemical leads and consists of adding more functional groups to the hit fragment using various chemical transformations.[12] We reported in **Section I.3.2.1** the successful derivatisation of chloropyrimidine **20** *via* Sonogashira cross-coupling reactions, and, in particular, the synthesis of trimethylsilylalkyne **22b** (**Figure 1.30**). Compound **22b** presented itself as an ideal substrate for a copper-catalysed azide–alkyne cycloaddition (CuAAC), or "Click" reaction. Developed by Sharpless *et al.* in the early 2000s, the Click reaction is a facile, single-step reaction that does not generate any problematic by-products and displays high yields thanks to a strong thermodynamic driving

force.[104] The Click reaction generates 1,2,3-triazoles, a class of molecule which have found a sizeable number of applications in drug discovery, from their use as linkers[105] or as pharmacophores of their own, such as in antibiotics tazobactam and cefatrizine (**Figure 1.53**).[90,106]

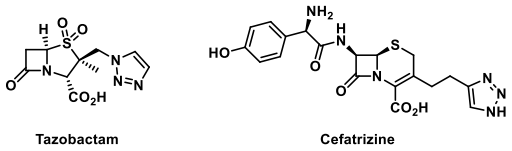


Figure 1.53: *Examples of antibiotics with an 1,2,3-triazole moiety.*

We heated a racemic mixture of TMS-alkyne **22b** and benzylazide to 33 °C in a 1:1 mixture of water and *tert*-butyl alcohol in the presence of tetra-*n*-butylammonium fluoride (TBAF), sodium *L*-ascorbate, an excess of pyridine, and a catalytic amount of copper sulfate pentahydrate (**Figure 1.54A**).[90] The resulting 1,2,3-triazole **41** was obtained in moderate yield (65%). Changing the deprotection system to aqueous potassium carbonate in methanol, *ceteris paribus,* afforded the product of the one-pot CuACC at the alkyne site and methanolysis at the phenylsulfonyl site, **42a**, albeit in a rather low yield (23%) (**Figure 1.54A**).[107] When applying the CuAAC conditions using the TBAF/*t*-BuOH deprotection system to an enantioenriched (81:19 e.r.) sample of **22b**, we obtained an enantioenriched sample of **41** without observing any erosion of the enantiomeric excess.

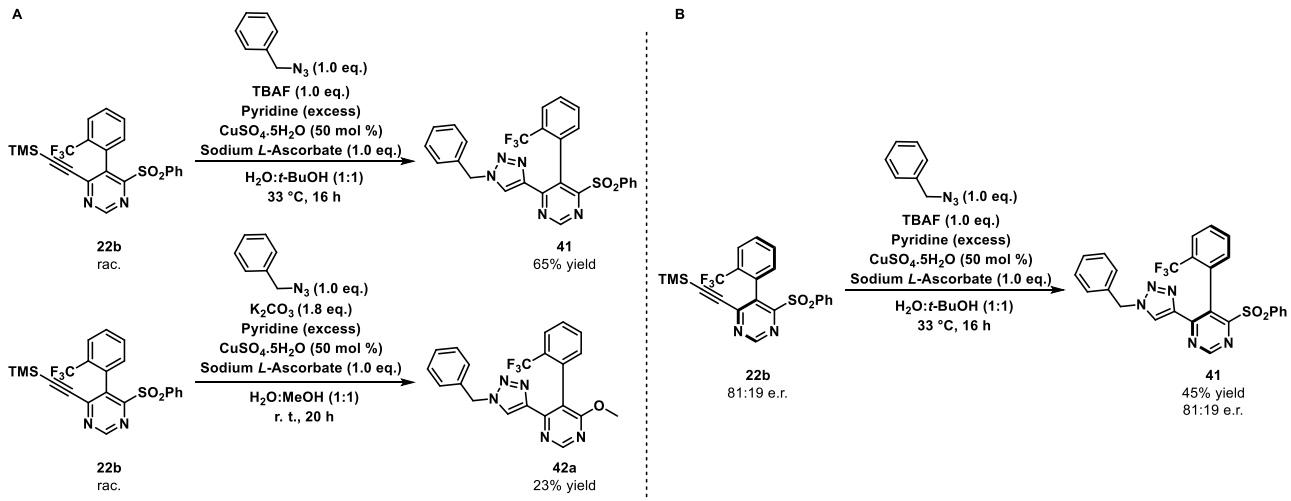


Figure 1.54: *Tandem deprotection/CuAAC of TMS-alkyne **22b**. **(A)** On a racemic substrate, assessing two different deprotections systems. **(B)** On an enantioenriched substrate.*

I.3.4.2 Developing the tandem CuAAC/methanolysis sequence

Under our supervision, part II student Alistair Ross investigated the tandem CuAAC/methanolysis sequence in further detail.[108] Firstly, the rate of racemisation of 1,2,3-triazole **42a** was determined. Ross isolated an enantioenriched sample of **42a** by purifying a racemate mixture *via* chiral semi-preparative HPLC. The resulting 96:4 e.r. sample was heated to 120 °C in *meta*-xylene and, over the course of 5 hours, aliquots were withdrawn at regular intervals (**Figure 1.55**). By plotting $ln\frac{1}{ee} = f(t)$, we were able to determine that k_{rac} = 6.37 × 10 $^{-5}$ s^{-1}, corresponding to a half-life of racemisation at 120 °C ($t_{1/2}^{rac}$) of 3.0 hours, and a subsequent rotational barrier $\Delta G_{393}^{\ddagger}$ = 31.3 kcal/mol. Despite having substituted the phenylsulfonyl group with a methoxy group in compound **42a**, which had resulted in a dramatic drop of enantiomeric stability in the case of **37a** (**Section I.3.3.2**, **Figure 1.47**), the bulk of the 1,2,3-triazole moiety allowed compound **42a** to maintain a high rotational barrier. This result prompted us to further examine the tandem CuAAC/methanolysis of compound **22b**.

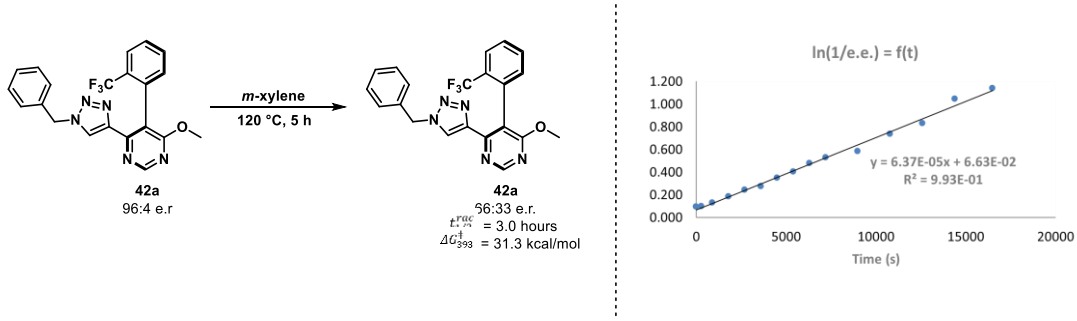


Figure 1.55: *Experiment to determine the rate of racemisation of compound **42a**. Data collected by Alistair Ross*[108]

Ross also briefly investigated a potential azide scope for the one-pot CuAAC/methanolysis sequence (**Figure 1.56**).[108] By stirring racemic TMS-alkyne **22b** and different benzylazide derivatives together at room temperature in a 1:1 mixture of water and methanol in the presence of aqueous potassium carbonate (1M), sodium *L*-ascorbate, an excess of pyridine, and a catalytic amount of copper sulfate pentahydrate, Ross generated 1,2,3-triazoles **42a–c** in moderate yields (29–43%).

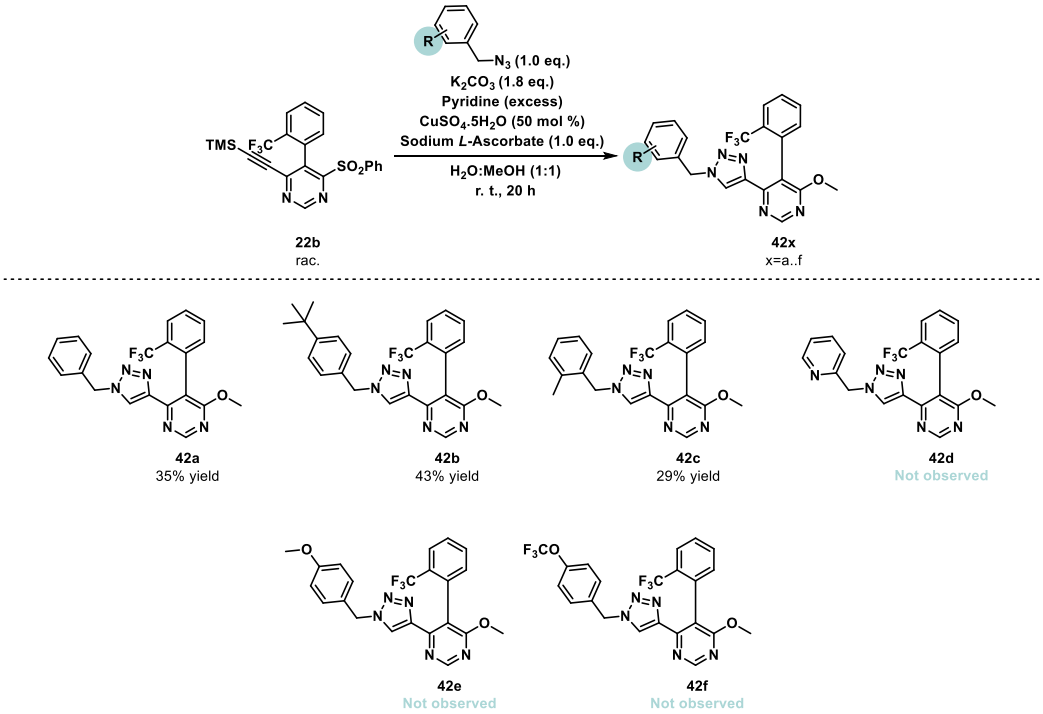


Figure 1.56: *Preliminary study to determine the scope-ability of the one-pot CuAAC/methanolysis sequence on **22b**. Data collected by Alistair Ross*[108]

Ross also showed that, other than *via* methanolysis, the sulfonyl group could be displaced by refluxing **41** overnight in tetrahydrofuran in the presence of lithium morpholide to yield morpholine-substituted product **43** in low yield (20%) (**Figure 1.57**).[108]

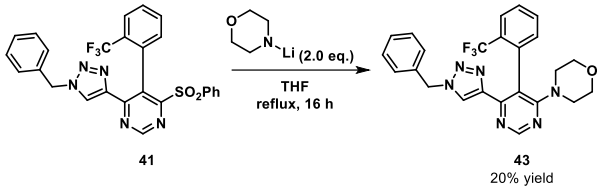


Figure 1.57: *SNAr of lithium morpholide onto **41**.*
Data collected by Alistair Ross[108]

I.4 Conclusions & Follow-up Work

I.4.1 Conclusions

We synthesised highly stable atropisomeric biarylpyrimidine scaffolds **19** and **20** both as racemic and enantioenriched mixtures. These scaffolds were readily transformed *via* orthogonal methodologies that selectively affected either the carbon–chlorine or the carbon–sulfur bond of the pyrimidine ring. Transformations selective of the chloro site included cross-coupling chemistry (Sonogashira and Suzuki-Miyaura) and SNAr. The sulfur site, in the form of a phenylsulfonyl group, was selectively hydrolysed or methanolysed in basic media. The subsequent pyrimidone was *N*-alkylated by trapping with a range of bromo electrophiles. The phenylsulfonyl group was also removed successfully in different instances by lithium amides (**Figure 1.58**).

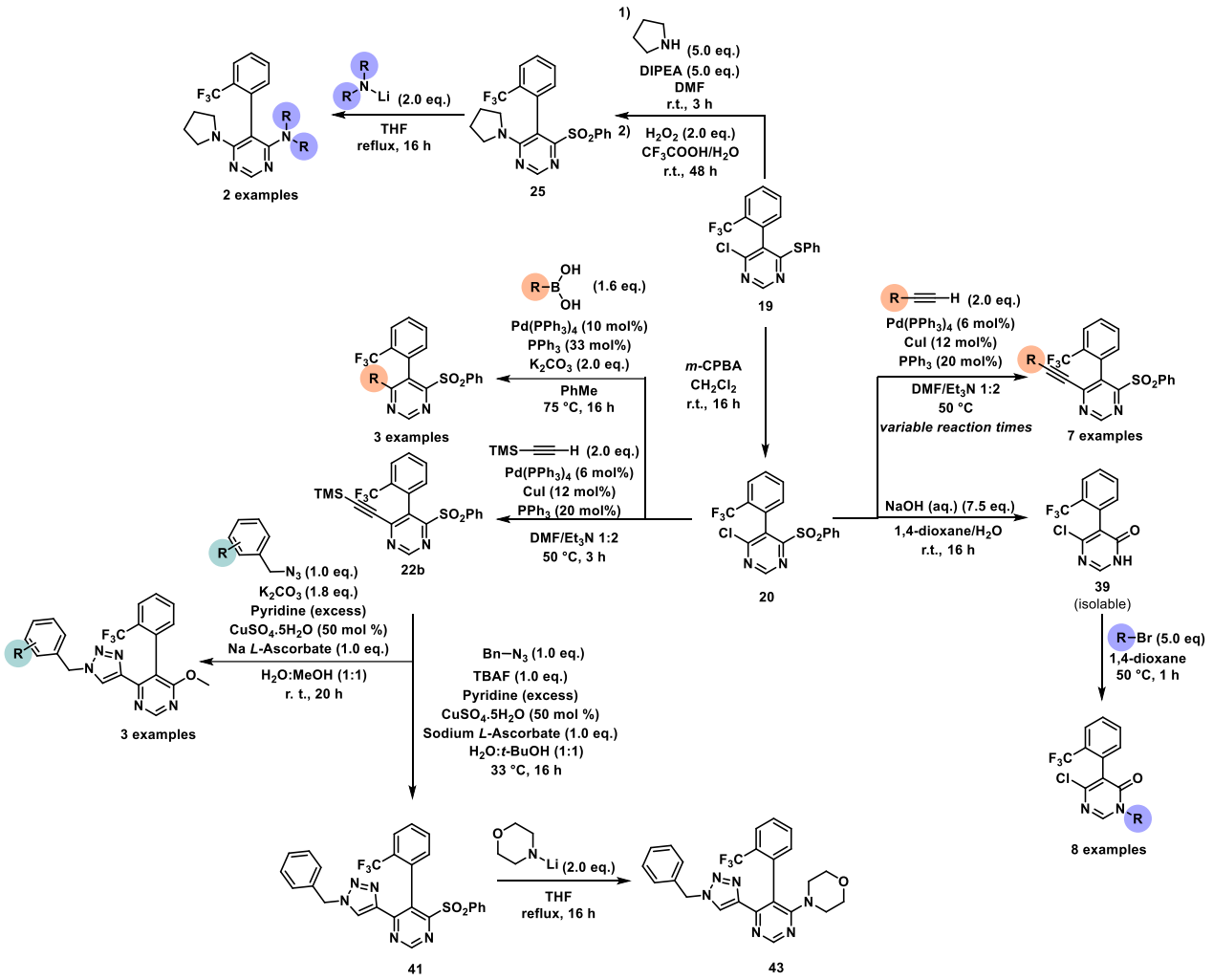


Figure 1.58: *Summary of the different transformations described in Part I.*

When performed on enantioenriched samples, none of these transformations led to loss of stereochemical integrity. The rotational barriers of various enantioenriched compounds remained relatively high at elevated temperatures ($28.2 \leq \Delta G_T^{\ddagger} \leq 35.0$ kcal/mol), and fragment growth in the vicinity the chiral axis (*e.g.* with a CuAAC reaction) allowed for the increase of previously reduced enantiomeric stabilities.

With these various transformations, we were able to generate several classes of stable atropisomeric compounds for potential incorporation in 3D libraries for fragment-based screening. These fragments could prove useful in the screening of targets such as kinases or Ras proteins, which have been shown to be readily inhibited by compounds with a chiral axis.[25,37,57,96] However,

the majority of these fragments, besides sulfone hydrolysis product **39**, are heavier than 300 Da and hence do not adhere to the "rule of three", recommended for compounds used in fragment-based screening.[15]

I.4.2 Follow-up work

The Suzuki-Miyaura and SNAr transformations (both at the chloro and sulfur site) of compounds **19** and **20** (**Figure 1.58**) were studied only succinctly and warrant further investigating. If successfully optimised, these transformations would allow for the insertion of smaller substituents at both of the synthetic handles of the pyrimidine ring, thus generating compounds that would be more readily amenable to FBDD.

When trying to develop a one-pot hydrolysis and electrophilic trapping of compound **20** (**Section I.3.3.1c**), we encountered a regioselectivity issue. Although we expected the alkylation to happen at the newly-generated nucleophilic *O*- centre, the hydrolysed intermediate was selectively *N*-alkylated. *O*- *versus* *N*-selectivity in the nucleophilic substitution of heterocyclic lactams has been studied extensively. Tosylate electrophiles have been shown to react faster with *O*-nucleophiles than with softer *N*- or *S*- nucleophiles.[109] Mitsunobu conditions have allowed scientists to drive the nucleophilic additions of 2-pyridones and isoquinolines onto alcohols at either the *N*- or the *O*- site depending on which additives were used.[110,111] Alternatively, silver salts, such as silver carbonate and silver nitrate, have helped chemists to selectively *O*-alkylate 2-pyridones and pyrimidine-diones.[112,113] In a preliminary study, we were able to observe the competition between *O*-alkylation and *N*-alkylation when sulfone **20** was heated to 50 °C in *N,N*-dimethylformamide in the presence of silver carbonate and benzyl bromide.[112,113] The *N*-alkylation product **22a** was still observed as the major product, but the *O*-alkylation product **22o**

was found in a mixture with the recovered starting material **20**, opening the doors to a potential *O*-selective method, complementary to the *N*-selective method we developed (**Figure 1.59**).

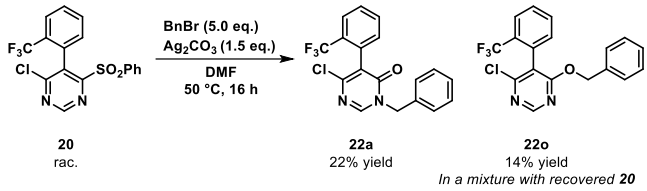


Figure 1.59: *Silver salts open the door to a potentially O-selective alkylation of sulfone **20**.*

Taking inspiration from sotorasib (AMG-510), we decided to focus the second half of this project on the synthesis of a potential covalent inhibitor for KRAS G12C, by growing a biarylpyrimidine fragment analogous to the ones synthesised in **Part I** (**Figure 1.60**).

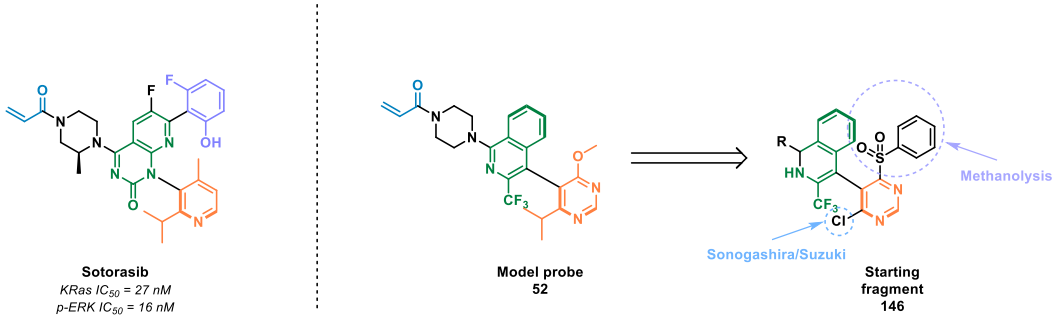


Figure 1.60: *Design of model probe **52**, inspired by sotorasib which could be derived from a starting fragment synthesised using the chemistry developed in **Part I**.*

Part II

The synthesis atropisomeric biarylpyrimidines for the inhibition of KRAS G12C

II. The synthesis of atropisomeric biarylpyrimidines for the inhibition of KRAS G12C

II.1 Introduction

II.1.1 The Ras GTPase family

II.1.1.1 Ras oncogenes

In the past decades, the extensive study of human cancers has allowed researchers to identify numerous oncogenes (mutated genes that contribute to the development of a cancer by inducing uncontrolled cell growth, proliferation and/or survival). Discovered in the 1960s by Harvey and Kirsten,[114,115] Ras oncogenes (from "rat sarcoma virus") were the first mutated genes to have been identified in human cancer.[116] In humans, the three Ras genes encode for four different, but highly homologous proteins: HRas (H for "Harvey"), NRas (N for "Neuroblastoma"), and two types of KRas proteins (K for "Kirsten"): KRas4A and KRas4B, where KRas4B is the dominant form in human cells and is simply referred to as KRas in this text.[117] Ras is considered as the most mutated gene family in human cancers, with Ras mutations being identified in 25–30% of human tumours.[118–120] Scientists have identified three main sites of mutation in Ras oncogenes: at the codons coding for glycine 12 (G12), glutamine 61 (Q61), and glycine 13 (G13). Mutations at G12 are the most prevalent mutations in KRas (65%) and HRas (35%), whereas mutations at Q61 are the most observed mutations in NRas (62%), but are also highly prevalent in HRas (34%).[121]

II.1.1.2 Ras GTPases

The Ras proteins encoded by the Ras oncogenes are a family of membrane-bound GTPase transductor proteins expressed in all animals and humans.[122] Ras proteins function as "molecular switches", where their binding status to guanosine diphosphate (GDP) or guanosine triphosphate (GTP) determines whether they are inactive ("switch off") or active ("switch on"), respectively.[120] In the active state, Ras becomes the origin of numerous signalling pathways from the cell membrane to the nucleus, ultimately activating transcription factors that regulate cell growth and differentiation.[120] Ras proteins have three major domains: the G-domain, the C-terminal domain and the C-terminal CAAX box (C: cysteine, A: aliphatic amino acid and X: amino acid dictating prenylation mode for membrane anchoring).[123] The G-domain, containing the switch I and switch II loops, is a highly-conserved domain responsible for the GDP–GTP exchange.[124] The C-terminal domain, including the CAAX box, is highly variable between the Ras family members and is essential for post-translational modifications allowing membrane association.[124,125]

The main signalling pathways involving Ras activation, described in the following paragraphs, are illustrated in **Figure 2.1** below.[119,120] Signalling typically begins when an upstream receptor, such as a tyrosine kinase receptor (typically the epidermal growth factor receptor, EGFR) is activated. Typically monomeric, tyrosine kinase receptors dimerise upon binding to their assigned ligand and proceed with auto-phosphorylation mechanisms.[126] Once phosphorylated, the receptor binds to signal transducing adaptor proteins (STAPs) (such as growth-factor receptor-bound protein 2, Grb2), which in turn recruit guanine nucleotide exchange factors (GEFs) to the plasma membrane (most frequently son of sevenless, SOS) (**Figure 2.1**).[127] GEFs are capable of displacing GDP from Ras proteins, allowing Ras–GTP interactions that induce conformational changes in the switch I

and II loops, hence activating Ras. Henceforth, the downstream signalling pathway cascade will take place until the bound GTP molecule is hydrolysed to a GDP.

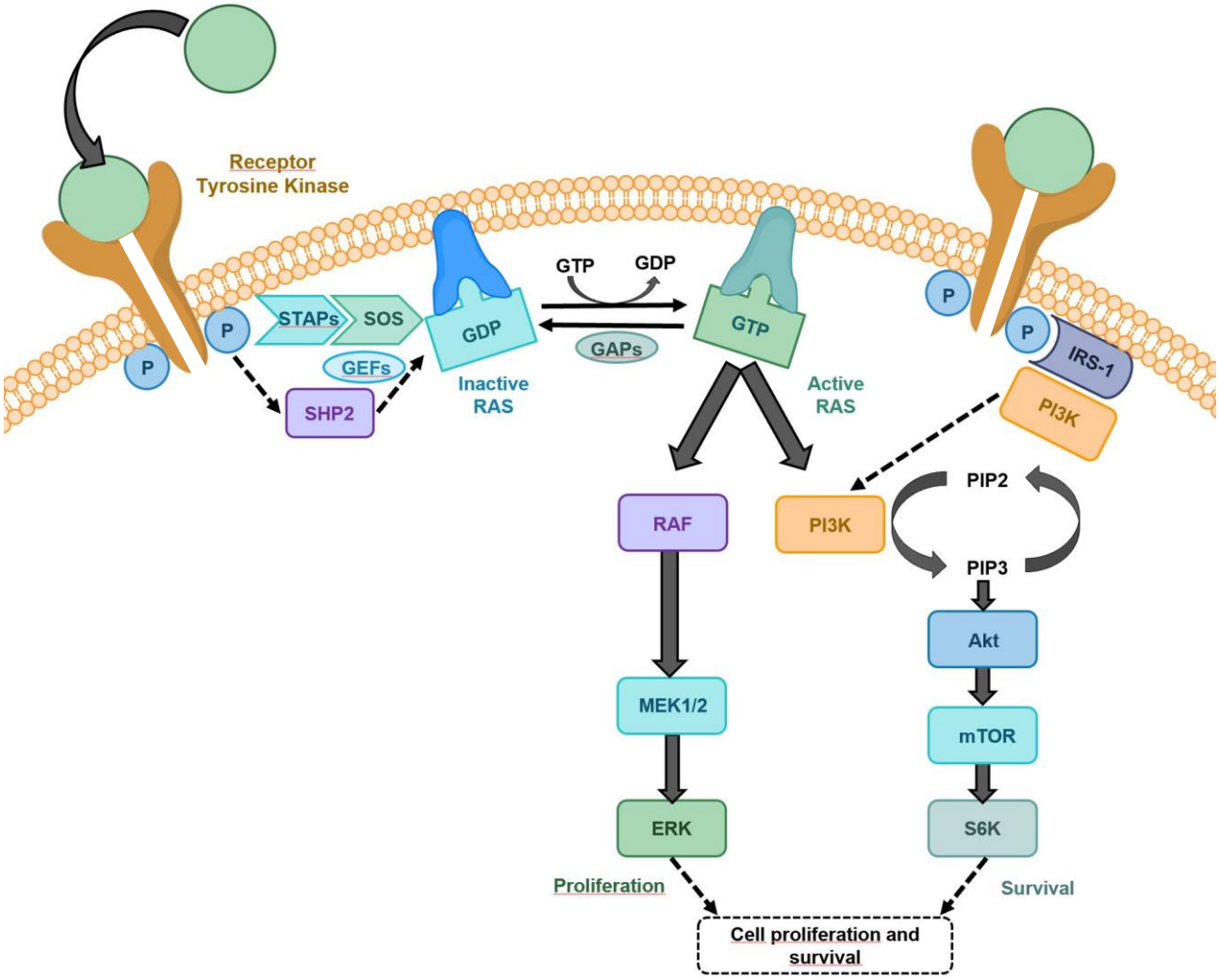


Figure 2.1: *Simplified scheme of RAS GTPase activation and signalling pathways. Inspired by Adjei et al.*[120]

Ras proteins have inherently low GTPase activity and need to be stimulated by GTPase Activating Proteins (GAPs), such as p120-GAP and NF1-GAP (**Figure 2.1**).[128] GAPs are coded by a class of genes called tumour suppressor genes, due to their ability to help switch off Ras and avoid prolonged cell growth and proliferation activity.[120] The aforementioned G12, G13 and Q61 mutations in Ras genes are considered as "gain-of-function" mutations, which prevent Ras from successfully completing its GTPase activity and therefore leaves it permanently switched on.

Oncogenic mutations of Q61 interfere with the water molecule required for the hydrolysis of the phosphate group, thus preventing the hydrolysis of Ras-bound GTP.[129] Oncogenic mutations at G12 and G13 prevent Van der Waals interactions between Ras and GAPs through steric encumbrance, which drastically attenuates the GTPase activity of Ras.[130]

An activated (*i.e.* GTP-bound) Ras protein can trigger numerous effector modules which are involved in several signalling pathways, all of which not being understood at equal levels. Amongst them, Raf (for "rapidly accelerated fibrosarcoma") kinase and phosphoinositide 3-kinase (PI3K) have been the most studied (**Figure 2.1**).[124,131] Raf is a serine/threonine kinase that is recruited to the cell membrane following the activation of Ras. Upon recruitment, Raf is dimerised and phosphorylated, allowing it to phosphorylate MEK (Mitogen activated protein kinase), which in turn phosphorylates ERK (extracellular-signal-regulated kinase), which enters the nucleus and promotes cell proliferation.[119,120] The most relevant activation mechanism for PI3K in the context of this work is its direct activation of by GTP-bound RAS. The activated PI3K then migrates further into the cell membrane to induce the phosphorylation of phosphatidylinositol bisphosphate (PIP2) to phosphatidylinositol (3,4,5)-trisphosphate (PIP3).[132] This results in the activation of an Akt protein kinase, which in turn activates mTOR (Mammalian Target of Rapamycin).[132,133] The activation of mTOR ultimately results in the activation of the translation factor S6 kinase (S6K), which, amongst other things, binds to the larger ribosomal subunit and induces mRNA translation into proteins that in turn signal for cell growth and survival.[133]

II.1.2 KRas mutations in human tumours

Ras is considered as the most mutated oncogene in human cancers, and amongst all three members of the Ras family, KRas is the most mutated isoform. KRas mutations constitute 86% of all Ras mutations.[119] KRas mutations are estimated to be at the origin of 90% of pancreatic cancers, 44% of colorectal cancers, 35% of small bowel cancers, 26% of biliary tract cancers, 17% of endometrium cancer and 30% of lung cancers (mostly non-small-cell lung cancers (NSLCs)) (**Table 2.1**).[119,121,134] For all the aforementioned pathologies, KRas mutations are almost the exclusive Ras mutation observed. KRas mutations are also observed in cervical, bladder, breast and liver cancer, as well as myeloid leukaemia, but at lesser proportions.

Primary tissue	KRas (%)	HRas (%)	NRas (%)	Total (%)
Pancreas	90	0	<1	90
Colon	44	1	6	50
Small intestine	35	0	<1	35
Biliary tract	26	0	2	28
Endometrium	17	<1	5	22
Lung	30	<1	1	31
Skin (melanoma)	1	1	18	20
Cervix	8	9	2	19
Urinary tract	5	10	1	16

Table 2.1 : *Frequency of Ras isoform mutations in human cancers.*[119,121,134]

As with the other two isoforms of the Ras family, the most prevalent mutations in KRas are observed at glycine 12 and 13 (G12 & G13) and glutamine 61 (Q61). Mutations at G12 make up 83% of KRas mutations *vs.* 14% for G13 and 2% for Q61.[121] Mutations also occur at codons 63, 117, 119 and 146 but only make up for *circa* 1% of all KRas mutations (**Figure 2.2**).[121,135]

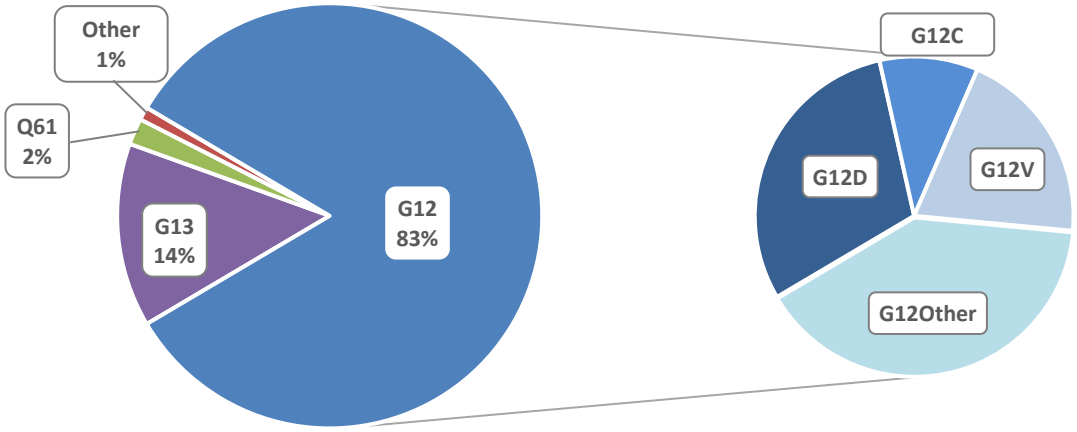


Figure 2.2: *Distribution of mutations in KRas.*[121] *The proportions of the subtypes of G12 mutations were established from rough estimates.*[139-142]

The most common mutations at codon 12 in KRas are (in order): G12D ("glycine-to-aspartic acid", where a guanine is replaced by an adenine at position 35 of the coding DNA sequence), G12V ("glycine-to-valine", where a guanine is replaced by a thymine at position 35 for the coding DNA sequence), and G12C ("glycine-to-cysteine", where a guanine is replaced by a thymine at position 34 for the coding DNA sequence).[136] Each mutation is associated with a different prognosis, for example, the G12V mutant has been associated with a worse prognosis than the G12D mutant in colorectal and lung cancers.[137,138] KRas G12D is most widely spread in pancreatic (36%, *circa* 70,000 patients in the US and Europe) and colorectal cancer (12%, *circa* 80,000 patients in the US and Europe), whereas KRas G12V is widely spread in pancreatic cancer (26%, *circa* 50,000 patients in the US and Europe). KRas G12C is not observed as frequently as its two counterparts, however, it is worth noting is makes up 14% of all NSCLC adenocarcinomas, affecting 44,000 patients in the US and Europe (**Table 2.2**).[139–142]

Primary tissue	G12D (patients*)	G12V (patients*)	G12C (patients*)	Total KRas (patients)
Pancreas	36% (70,000)	26% (50,000)	2% (4,000)	90% (175,000)
Colon	12% (80,000)	9% (60,000)	3–4% (20,000)	44% (293,000)
Lung	4% (13,000)	5% (16,000)	14% (44,000)	30% (98,000)
Endometrium	6% (15,000)	6% (15,000)	<1% (< 2,500)	17% (42,000)

Table 2.2: *Frequency of the most common G12 mutations in some human cancers.*[139–142] **Patients estimates in the US and Europe, truncated to the nearest thousands.*

II.1.3 KRas: an undruggable target?

II.1.3.1 Direct inhibition of KRas mutants

Three factors justify KRas as a valid therapeutic target. Firstly, as mentioned in **Section II.1.1.1**, Ras mutations are estimated to make up 25–30% of human cancers, and KRas mutations make up 86% of all Ras mutations.[118–120] Secondly, the link between mutant KRas and direct tumorigenesis has been established by preclinical transfection and/or activation of mutants in mouse models.[143,144] Thirdly, KRas mutant cancer cells are KRas-dependent, and the preclinical abrogation of mutant KRas in mice with both primary and metastatic pancreatic cancer inhibited tumour growth and proliferation.[145] These factors make a compelling argument for targeting KRas in cancer therapy.

Considering KRas is equipped with a binding site meant to host GTP for hydrolysis, it should be possible to design small-molecule inhibitors that directly bind to it. This strategy has been successful in the development of ATP-competitive inhibitors for protein kinases. However, kinase–ATP affinities range from low micromolar to millimolar, whereas KRas–GTP affinities are around 10 picomolar (three orders of magnitude higher on average),[119,146] and GTP abundance in the cytoplasm is high (*circa* 0.5 mmol/L). Added together, these factors have made all efforts targeting

the GTP-binding pocket in KRas vain. These experiences, added to the absence of well-defined hydrophobic pockets on the relatively smooth surface of Ras proteins, rendering allosteric binding implausible, have led scientists to consider KRas "untargetable" and "undruggable".[118–121]

II.1.3.2 Indirect inhibition of KRas mutants

To tackle the "untargetability" issues mentioned in section **II.1.3.1**, several strategies have been explored to develop small molecules as therapeutic tools for KRas-dependent cancers. They involve targeting KRas membrane association, pan-Ras inhibition (both upstream and downstream signalling), or inducing synthetic lethality. Each of these strategies will be discussed more in depth below.

II.1.3.2a Targeting KRas membrane association

Targeting KRas membrane association consists of stopping the post-translational modifications that associate mutant KRas to the cell membrane. Prenylation is a post-translational rate-limiting step that consists of the addition of a farnesyl or a geranylgeranyl moiety to KRas that help its membrane localisation.[125] Farnesyltransferase inhibitors such as tipifarnib (Zanestra®) and lonafarnib (Zokinvy®) (**Figure 2.3**) were developed with hopes to prevent Ras membrane localisation, thus inhibiting Ras-mediated cell proliferation.[147] Several phase II and phase III clinical studies were conducted, both for tipifarnib[148–151] and lonafarnib,[152–154] sometimes in combination with other anti-cancer agents. These studies failed to demonstrate any benefit in KRas-dependent cancers, likely because KRas can be alternatively prenylated by geranylgeranyltransferases.

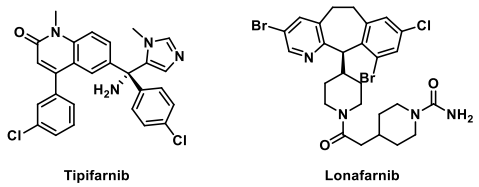


Figure 2.3: *Examples of farnesyltransferase inhibitors.*

The development of geranylgeranyltransferase inhibitors has proven difficult, with only GGTI-2418 (**Figure 2.4**) showing good *in vitro* activity. However, after a phase I clinical study, no objective response was observed and the compound was abandoned for lack of efficacy.[155]

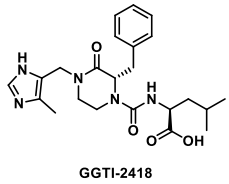


Figure 2.4: *GITI-2418, a geranylgeranyltransferase inhibitor.*

Since inhibiting prenylation itself failed, medicinal chemists attempted to stop membrane localisation of prenylated-KRas *via* inhibiting prenyl-binding protein PDE*δ* (phosphodiesterase, delta subunit). PDE*δ* binds and solubilises prenylated-Ras proteins, thereby enhancing their diffusion in the cell cytoplasm. In 2016, Bastiaens *et al.* at the Max Planck Institute evidenced deltazinone 1 (**Figure 2.5**) as a potent inhibitor of PDE*δ*.[156] However, *in vivo* anticancer activity was not assessed due to stability issues and more chemical optimisation work is to be done to fully evaluate this new approach.

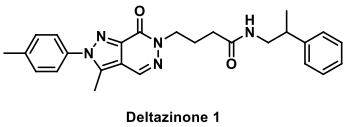


Figure 2.5: *Delazinone 1, a potent PDEδ inhibitor.*

II.1.3.2b Inhibiting downstream Ras signalling

Downstream signalling inhibition of KRas has probably yielded the most drug candidates out of all the attempted strategies to tackle KRas-dependent tumours, mostly because of all the diverse effectors in the KRas cascade (**Section II.1.1.2**, **Figure 2.1**). The first kinase to be phosphorylated after Ras activation is Raf. Numerous Raf kinase inhibitors have been approved for various tumour types, such as sorafenib (Nexavar®),[157–159] dabrafenib (Tafinlar®/Rafinlar®),[160,161] vemurafenib (Zelboraf®),[18,162] and encorafenib (Braftovi®) (**Figure 2.6**).[163,164] Sorafenib is a multikinase inhibitor that is not particularly specific or potent,[165] and has shown no clinical activity in cancers with high KRas mutation prevalence such as pancreatic cancer.[166,167] Dabrafenib, vemurafenib and sorafenib are selective inhibitors of a Raf subtype, B-Raf. Counter-intuitively, in KRas mutant cells, B-Raf inhibition activates upstream proteins that eventually lead to the activation of ERK through an alternative pathway,[168] thus rendering these treatments not suitable for KRas mutant tumours.

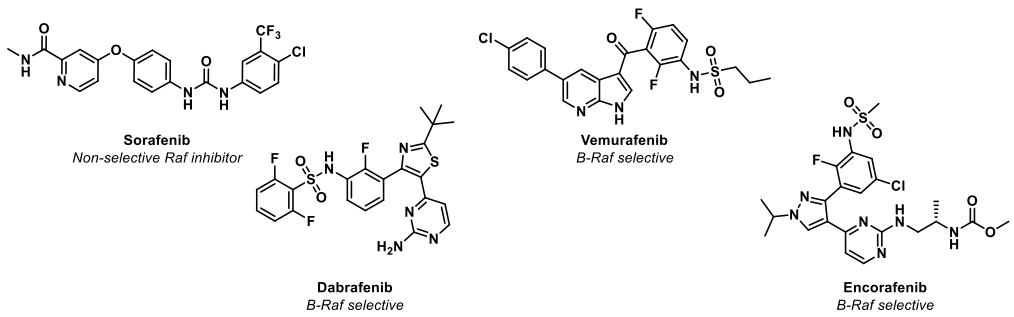


Figure 2.6*: Examples of Raf inhibitors.*

The next effector to be considered in the cascade is MEK. MEK inhibitors are mostly used in conjunction with B-Raf inhibitors as such combination leads to better results in B-Raf mutant cancers.[161,163,164,169] Three MEK inhibitors are approved for this purpose: trametinib (Mekinist®/Meqsel®),[161,169] cobimetinib (Cotellic®),[170] and binimetinib (Mektovi®) (**Figure 2.7**).[163,164] Another notable MEK inhibitor is selumetinib (Koselugo®), approved for the treatment

of neurofibromas in children (**Figure 2.7**).[171] MEK inhibitors alone have shown disappointing results in various tumour types,[172,173] and did not show any efficacy in the treatment of KRas mutant tumours.[174–176] Moreover, inhibiting MEK induces PI3K activation, thus triggering the alternative Ras signalling pathway.[177]

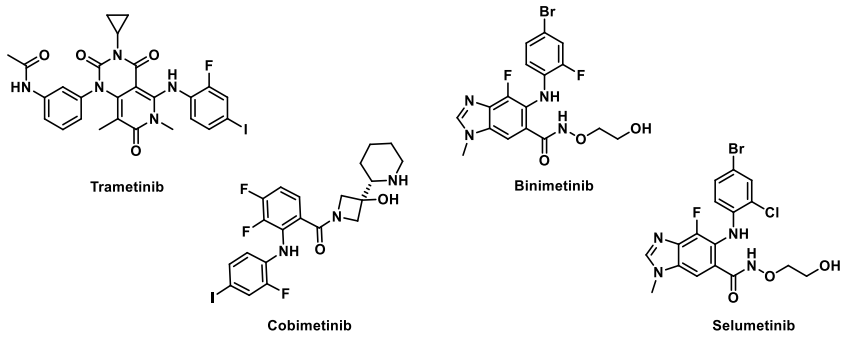


Figure 2.7*: Examples of MEK inhibitors.*

The final downstream kinase of the Raf/MEK pathway is ERK. Preclinical data supported the hypothesis that ERK inhibitors could be effective in KRas mutant tumours and temuterkib is currently being investigated in phase II clinical trials for this purpose (**Figure 2.8**).[178] Other ERK inhibitors: ulixertinib, MK-8353 and KO-947, are currently in early phase of clinical studies (**Figure 2.8**).[120]

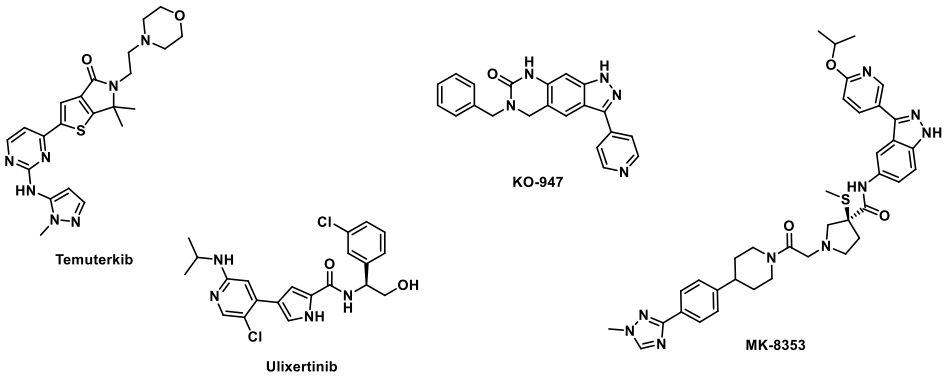
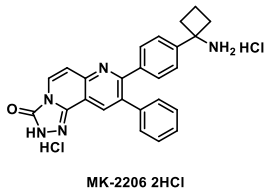


Figure 2.8*: Examples of ERK inhibitors.*

The alternative PI3K pathway is also being explored. KRas mutations have been shown to mediate resistance to PI3K inhibition,[179] and MEK inhibition has been shown to further activate PI3K/Akt signalling.[177] It was preclinically suggested that the simultaneous inhibition of PI3K and MEK may be synergistic and could help counter these effects.[180] A phase I trial treated patients with KRas mutated tumours a combinatorial treatment comprising Akt inhibitor MK-2206 (**Figure 2.9**) and MEK inhibitor selumetinib (**Figure 2.7**). The combination exhibited heartening results with 23% of patients from the NSCLC cohort showing an objective response.[181] However, phase II trials showed the combination increased the risk of adverse events in patients.[182]

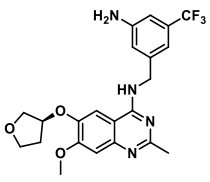


MK-2206 2HCl

Figure 2.9*: MK-2206, a PI3K/Akt inhibitor.*

II.1.3.2c Inhibiting upstream Ras signalling

Inhibiting upstream Ras signalling consists of targeting pre-activation Ras regulators, most notably, guanine nucleotide exchange factors (GEFs), such as son of sevenless (SOS). BI-3406 (**Figure 2.10**) from Boehringer-Ingelheim was identified as a selective inhibitor of SOS, that showed activity in G12 and G13 KRas mutant cancers by reducing GTP–KRas levels. BI 1701963, a BI-3406 analogue (structure undisclosed), is currently being investigated in phase II clinical trials.[183]



BI-3406

Figure 2.10*: BI-3406, a selective SOS inhibitor.*

Another notable target of pan-Ras protein inhibition is (SH2)-containing protein tyrosine phosphatase 2 (SHP2), that relays stimulatory signals from various membrane receptor tyrosine kinases to the MAPK (MEK) kinase signalling pathway. Developing traditional inhibitors for SHP2 has proven difficult, however, SHP099 (**Figure 2.11**) was discovered as the first allosteric inhibitor of SHP2 and showed promising results in patient-derived tumour xenograft models.[184] This discovery sparked an interest in the development of SHP2 allosteric inhibitors, leading to the development of TNO155, RMC-4630, JAB-3068 and JAB-3312 (structures undisclosed), all currently undergoing clinical testing (phase I and/or phase II) (**Figure 2.11**).[185–187]

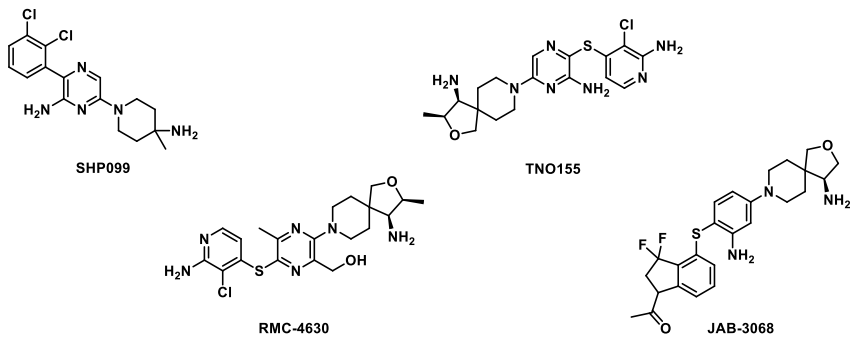


Figure 2.11*: Examples of SHP2 inhibitors.*

II.1.3.2d Inducing synthetic lethality

Synthetic lethality describes a type of genetic interaction where the combination of two genetic events leads to cell death. In case of KRas-driven oncogenesis, the effect of inhibiting cyclin-dependant kinases (CDKs) 4 and 6 to induce synthetic lethality has been investigated. CDK4 and CDK6 are important mediators of the normal cell cycle. In human malignancies, cell-cycle control is frequently dysregulated,[188] and CDKs are essential for KRas-driven oncogenesis. CDK4 inhibition has been shown to induce selective death of KRas mutant cancer cells.[189] Abemaciclib (Verzenio®/Ramiven®) (**Figure 2.12**) is a CDK4/6 inhibitor currently approved for a subtype of breast cancer. Abemaciclib showed a better response rate than tyrosine kinase inhibitor erlotinib

in phase III trial on patients with stage IV, platin-doublet resistant, KRas mutant NSCLC. However, despite the better response rate, the overall survival rate of the patients did not increase.[190]

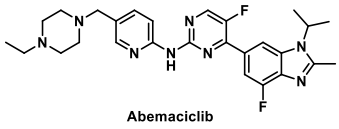


Figure 2.12*: Abemaciclib, a selective CDK4/6 inhibitor that induces synthetic lethality with KRas.*

Amongst all these alternative ways of trying to medicate KRas mutant tumours with small molecules, some of them did show some promising results and are being investigated further. Nevertheless, the high attrition rates due to relatively disappointing results in clinical trials are a testament to how difficult this endeavour is. This has led scientists to turn to alternative medication pathways, such as immunotherapy,[191,192] recombinant protein vaccines and,[193] the identification of mRNA vaccines.[194] Additionally, a random T7 phage display technology has allowed to identify a short artificial peptide, KRpep-2d, as a highly potent and selective KRas G12D inhibitor, that inspired the development of *in vivo*-active KS-58, likely to enter clinical trials for KRas G12D-driven tumours soon.[195–198] Spring *et al.* also reported the use of 5–6 mer peptides in targeting a novel KRas binding site, subsequently blocking nucleotide exchange.[199]

II.1.4 KRas G12C: an "Achilles' heel" in KRas mutant tumours

II.1.4.1 The discovery of KRas G12C covalent inhibitors and the switch II pocket (S-IIP)

By exploiting the nucleophilic nature of the mutant cysteine in KRas G12C, Ostrem, Shokat and co-workers made a breakthrough discovery in 2013. They were able to synthesise compounds that covalently and irreversibly bind to the abnormal amino acid. Initially screening compounds aimed at linking to the mutant cysteine by disulfide tethering, they found hit **44** that was later optimised

into the more potent compound **45**, which used an acrylamide warhead instead of the disulfide electrophile (**Figure 2.13**). Acrylamide warheads covalently bond with cysteine 12 *via* Michael addition, and are stabilised by an extra carbonyl interaction with the NH_3^+ group on lysine 16.[200]

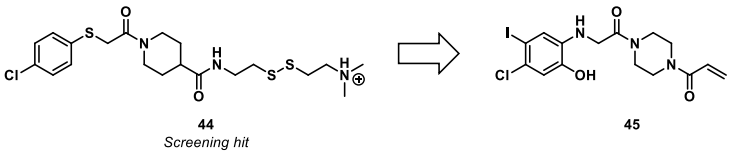


Figure 2.13: *The discovery of KRas covalent inhibitor by Ostrem, Shokat and colleagues.*[200]

Hit **45** was identified to bind with low affinity to an allosteric shallow pocket, located beneath the switch II loop, in close enough vicinity of mutant cysteine 12 to trigger a covalent tethering reaction. This new pocket, initially not observed in apo-crystal structures, but apparently induced and/or stabilised by Shokat and co-workers' compounds, was named the switch II pocket (S-IIP).[200] This new inhibition strategy was all the more interesting considering it targeted a mutant amino acid, thus solely targeting the mutant forms of the protein and leaving the wild-type untouched. This should, theoretically, reduce the toxicities and side effects associated with the resulting therapeutic agents.

Further analysis demonstrated that compound **45** preferentially bound to the GTP-bound (thus inactive) state of KRas G12C.[200] Targeting the inactive state of KRas might seem counter-intuitive, considering the active form is involved in tumour proliferation. However, recent evidence showed the GTPase activity of KRas mutants at codon 12 (KRas G12) is not drastically reduced compared to their wild-type counterparts and that GAP-stimulated GTP hydrolysis and GEF-stimulated nucleotide exchange rates in mutant KRas might play a crucial part in tumour development.[201–203] Moreover, it was shown that compound **45** decreased KRas affinity for GTP, impaired SOS-

catalysed nucleotide exchange from GDP to GTP and blocked the KRas–Raf effector interaction in mutant cells.[200] Thus, irreversibly binding to the inactive state of the KRAs G12C mutant ultimately resulted in the decrease of GTP-bound KRAs mutants in the cell.

II.1.4.2 The preclinical years

Despite its promising initial results, compound **45** presented sub-optimal pharmacologic properties and subsequent studies showed it was incapable of engaging with KRas G12C cancer cells, even at high doses and long incubations times.[201,203] The compound was licensed to Wellspring Biosciences, a subsidiary of Araxes Pharma (both co-founded by Shokat in 2012). Further optimisation of **45** led to the discovery of ARS-853 (**Figure 2.14**).

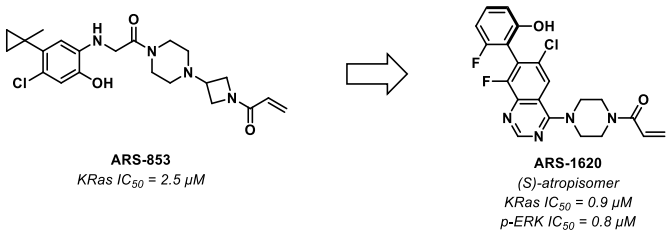


Figure 2.14: *The development of ARS-2620.*
KRas IC_{50} indicates biochemical assay potency, p-ERK IC_{50} indicates cellular potency.

ARS-853 presented itself as the first selective KRas G12C inhibitor, with a potency within the range of a potential drug candidate. ARS-853 was found to bind to KRas G12C 600 times quicker than compound **45** in biochemical assays, and demonstrated low micromolar potency in cellular assays.[201,203] The newly-discovered inhibitor was also shown to inhibit KRas-G12C-mutant cell growth. Studied in greater depth, ARS-853 was shown to inhibit GEF–KRas interaction, thus blocking GDP to GTP nucleotide exchange. The blockade of the Ras/MEK/ERK and PI3K/Akt signalling pathways was also observed, most likely due to the failure of loading GTP onto the drugged KRas.[201,203] These effects were not observed on non-KRas-G12C-mutants, even at concentrations ten-fold higher than on KRas-G12C-mutant cells, confirming the selectivity of the

compound for the specific mutation. Off-target activity was assessed by testing the compound against 2,740 surface-exposed cysteine residues from 1,584 protein profiles. Only two off-targets were identified: FAM213A and Reticulon-4.[201,203] ARS-853 was thus identified as a selective, covalent inhibitor of low micromolar potency in KRas G12C-driven tumour cells.

Although it displayed many selling points, ARS-853 lacked *in vivo* potency in mouse tumour models, partially because of its poor bioavailability and low metabolic plasma stability. However, efficient tweaking of its structure the development ARS-1620 (**Figure 2.14**), a covalent KRAs G12C inhibitor that was potent, selective, orally available and well tolerated in mice. ARS-1620 exhibited both *in vitro* and *in vivo* efficacy, with a therapeutic window within the range of a drug candidate. Most notably, its improved pharmacological properties allowed it to be highly potent in both human cancer cell lines and patient-derived mouse xenografts.[204] The binding mode of ARS-1620 is similar to that described for ARS-853 (see **Section II.1.4.1**) and is illustrated in **Figure 2.15**.[205] ARS-1620 established itself as the first small molecule providing *in vivo* evidence that targeting S-IIP is a viable strategy for the development of a treatment for patients with KRas G12C-driven cancers. In the context of this work, it is also worth noting that ARS-1620 is atropisomeric and that only the (*S*) atropisomer showed activity in the biological assays. The (*S*) atropisomer showed no sign of interconversion after 3 weeks at 37 °C and was therefore considered stable at biological temperatures.[204]

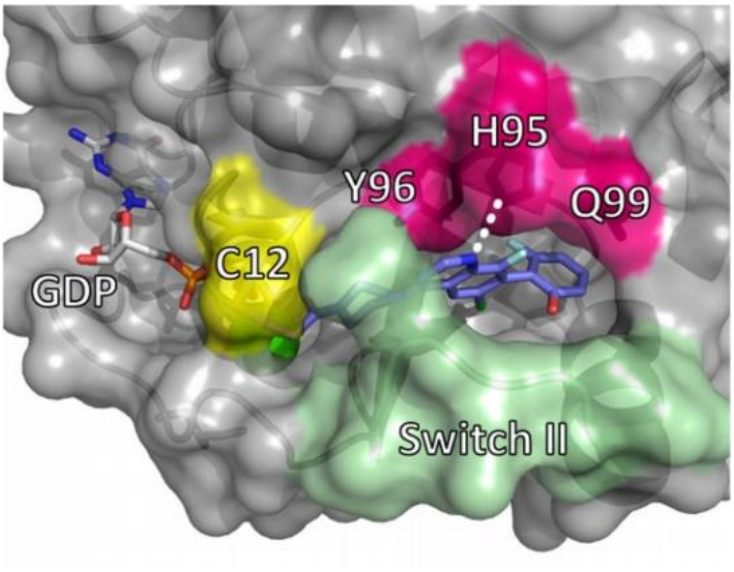


Figure 2.15: *X-ray cocrystal structure of ARS-1620 (blue, PDB code: 5V9U) and GDP in complex with KRas G12C.*
Extracted from Nature ***2019****, 575, 217-223.*[205]

II.1.4.3 The development of sotorasib (AMG-510)

Prior to the discovery of covalent inhibitor **45** by Shokat *et al.*, Amgen had partnered with Carmot Therapeutics in an effort to discover KRas G12C covalent inhibitors. Carmot Therapeutics had developed the Chemotype Evolution platform, a custom library synthesis and screening platform, allowing for the rapid generation and testing of compounds based around a given fragment. Utilising this platform in combination with structure-based drug design (SBDD), the scientists at Amgen were able to identify initial hit **46** (**Figure 2.16**).

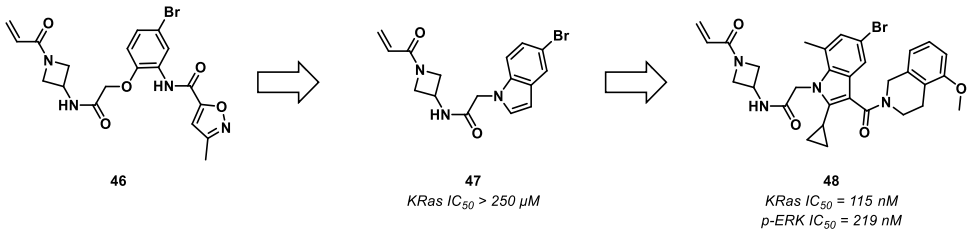


Figure 2.16: *The development of lead compound* ***48*** *by Amgen and Carmot.*[26]

This hit compound inspired the design of precursor **47**, of a smaller size, and containing fewer rotatable bonds, thus making it the perfect fragment candidate for another iteration of Carmot's Chemotype Evolution. Subsequent SAR studies culminated into lead compound **48** (**Figure 2.16**).[26] Compound **48** was revealed to interact with the S-IIP, similarly to **45** and the ARS compounds. However, it did so by exploiting a cryptic pocket on the surface of KRas that had been recently identified by Gentile *et al.* in 2017.[206] The inclusion of the tetrahydoisoquinoline ring in **48** promoted the rotation of the H95 (histidine 95) side chain, which allowed the access to said pocket, bordered by the H95, Y96, and Q99 side chains (**Figure 2.17**). Engagement with this pocket led to a non-negligeable increase of cellular potency compared to ARS-1620.

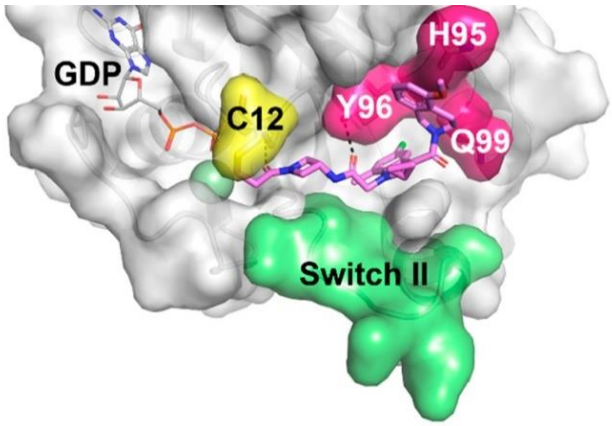


Figure 2.17: *X-ray cocrystal structure of advanced lead **48** (pink, PDB code: 6P8Z) and GDP in complex with KRas G12C.*
*Extracted from ACS Med. Chem. Lett. **2019**, 10, 1302−1308.*[26]

However, lead compound **48** could not be clinically developed due to low oral bioavailability and rapid clearance in *in vivo* mice and rats models.[26] Lanman *et al.* took a closer look at both ARS-1620 and lead compound **48**, and, by superimposing them, established it would be possible to create a hybrid compound that further explored the S-IIP whilst also binding within the histidine 95 groove. Thus, by adding substituents to the benzylpyrimidine ring on ARS-1620 and optimising

the thermodynamic properties of the resulting axially chiral molecule, as well as its pharmacokinetic profile, AMG-510 (later named sotorasib) was discovered (**Figure 2.18**).[25]

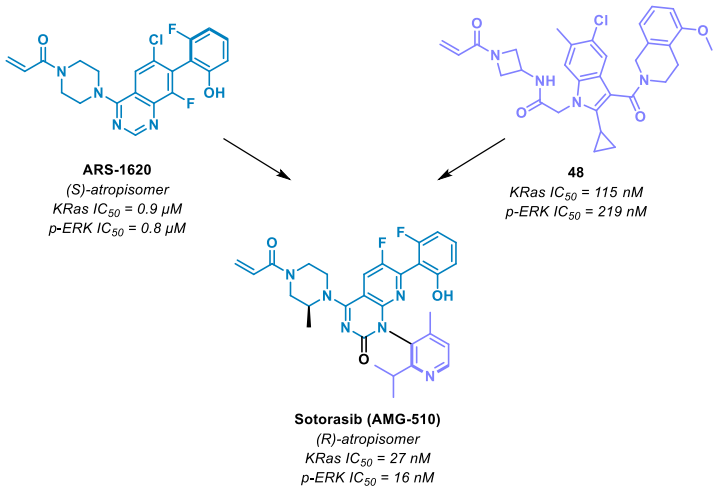


Figure 2.18: *The hybridisation of ARS-1620 and **48** to produce AMG-510.*[25]

AMG-510 was found to follow the binding mode of previous quinazoline lead ARS-1620, but with its pyridinyl ring accessing and properly filling the H95 cryptic pocket, establishing close contacts with H95, Y96 and Q99 thanks to its isopropyl substituent, even inducing a side chain rotation of the H95 residue. In total, sotorasib occupying the histidine 95 groove engaged 25 Van der Waals weak interactions, which extended from the backbone of helix 2 (H95-Y96) to the backbone of the flexible switch II loop. The (*S*)-methylpiperazine ring adopted a twist boat conformation, giving the methyl group close interactions with both C12 and Y96 (**Figure 2.19**). These newly-generated interactions provided sotorasib with an exceptional potency.[25]

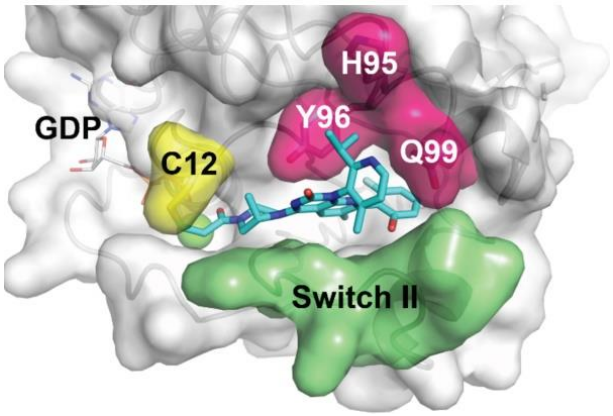


Figure 2.19: *X-ray cocrystal structure of AMG-510 (cyan, PDB code: 6OIM) and GDP in complex with KRas G12C.*
Extracted from J. Med. Chem. ***2020****, 63, 52−65.*[25]

Canon *et al.* published an extensive preclinical study investigating the combinations of sotorasib and various inhibitors of the MAPK/MEK and PI3K/Akt signalling pathways. Multiple combinations resulted in synergistic activity. The combination of sotorasib and the MEK inhibitor trametinib, for example, resulted in increased antitumor activity in both cell culture models and mouse tumour models, as compared with using either agent alone. Combining sotorasib with carboplatin, a standard-of-care chemotherapeutic agent in lung cancers, resulted in peak anti-tumour activity. Moreover, the authors evidenced the role of sotorasib in driving anti-tumour immunity. Indeed, the use of sotorasib on patient-derived colorectal cancer mouse xenografts led to tumour regression with long-term cure in mouse models equipped with T cells, and tumour regression without long-term cure in mouse models deprived of T cells (immunocompromised). Further experiments allowed Canon *et al.* to prove that sotorasib increased T cell priming, antigen recognition of tumours cells harbouring a KRas G12C mutation, and led to the potential establishment of long-term tumour-specific T cell adaptive immune responses.[205]

In August 2018, sotorasib became the first KRas G12C covalent inhibitor to enter human clinical trials and demonstrate clinical safety and efficacy. A Phase I study, completed in June 2020,

established that sotorasib had a relatively tolerable safety profile, with low-grade toxic effects and no dose-limiting toxic effects.[207] Additionally, sotorasib showed promising anti-cancer activity in patients with heavily pre-treated KRas G12C mutant solid tumours, particularly NSCLC. A year later, in June 2021, Skoulidis *et al.* reported the results of the multicentre, single-group, open-label phase II trial, which confirmed the safety observations made in the phase I study and established the durable clinical benefits of sotorasib.[208] In May 2021, sotorasib (under the brand name Lumakras®) was approved as the first treatment for adult patients with NSCLC harbouring the KRas G12C mutation, who had received at least one prior systemic therapy, thus becoming the first commercialised drug to directly inhibit a Ras protein.[24]

II.1.4.4 The development of agradasib (MRTX849)

In collaboration with Array BioPharma, Mirati Therapeutics conducted a covalent fragment screen of the Array BioPharma library and identified a series of tetrahydropyridopyrimidines as irreversible KRas G12C covalent inhibitors.[209] Subsequent fragment growth led to lead compound **49**, which demonstrated encouraging cellular activity, with low micromolar *p*-ERK inhibition (**Figure 2.20**).[209,210] Despite originating from an independent fragment screening, **49** turned out to have a very similar structure to ARS-1620 and AMG-510, and therefore triggered the regular interactions with C12 and K16 *via* its acrylamide warhead and H95 and Y96 *via* the pyrimidine ring. Further SBDD led to compound **50**, introducing a C2 tail that triggered a salt bridge with glutamic acid 62 (E62). The introduction of the cyanomethyl substituent on the piperazine ring allowed newly-generated compound **51** to develop H-bonding with glycine 10 (G10) and increased cellular potency enough to allow for removal of the hydroxyl group on the naphthyl ring, for a better ADMET profile (avoiding sulfonation and glucuronidation). Substitution of the naphthyl moiety with a methyl group allowed the resulting MRTX1257 to fill a hydrophobic pocket. Although

extremely potent, with sub-nanomolar cellular activity, MRTX1257 displayed poor bioavailability and distribution volume. Further SAR and covalent warhead optimisation led to the less potent but of better ADMET profile drug candidate, MRTX849, later named agradasib (**Figure 2.20**).[210,211]

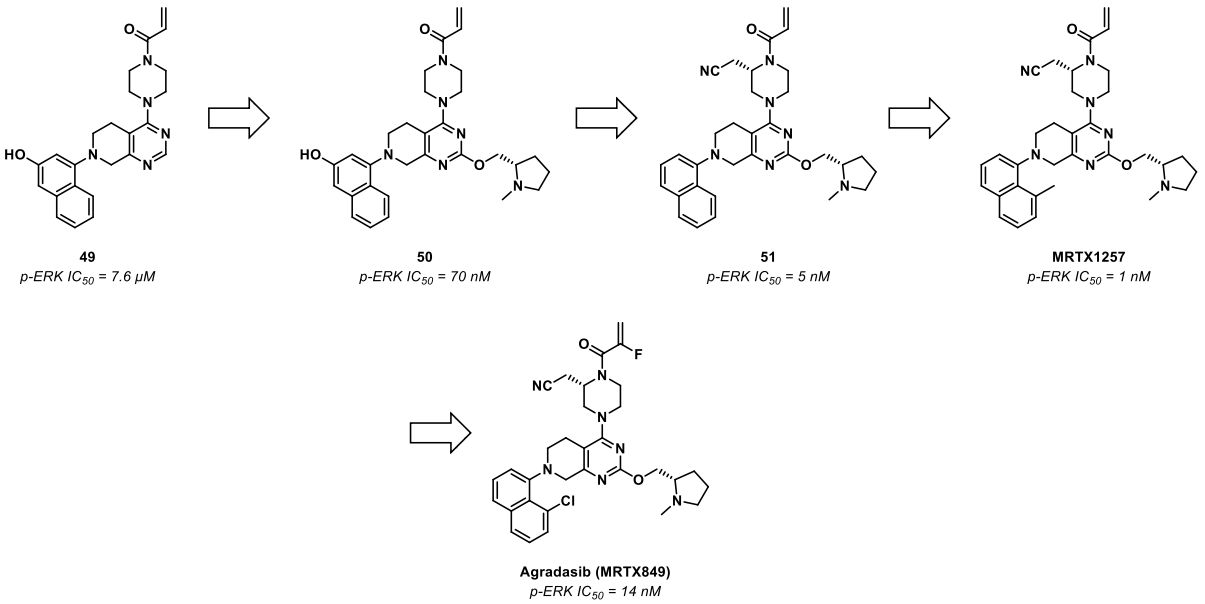


Figure 2.20: *The development of agradasib (MRTX849) from compound **49**.[210,211]*

Hallin *et al.* provided detailed preclinical study of agradasib, elucidating its activity, response and resistance mechanisms, and identified effective combinations.[212] Namely, in a panel of human KRas-G12C-mutant-cell-line-derived xenografts and patient-derived xenograft models (lung, colon and pancreatic cancers), they observed broad tumour regression (exceeding 30% regression from baseline in 17 of 26 KRas G12C-derived xenografts).[210,211] Most other preclinical results were coherent with previous ARS-1620 results, with a therapeutic response observed in the regulators of the Ras pathway. Combination with CDK4/6, mTOR and SHP2 inhibitors resulted in an augmented response that led to substantial tumour regression in multiple tumour models, including those that had previously been resistant to agradasib monotherapy.[210,212]

Agradasib entered phase I/II clinical testing in January 2019, 5 months later than sotorasib. The study was carried out on patients with advanced or metastatic solid tumours harbouring a KRas

G12C mutation, who had been previously treated with unsuccessful chemotherapy. The NSCLC cohort of the study evidenced a positive response for 45% of patients, with 96% of patients showing disease control.[213] 17% of patients with colorectal cancer showed an objective response (*i.e.* a measurable response), with 94% of patients showing disease control.[214] Toxicity was limited to majorly grade 1/2 adverse events for both cohorts. A small number of patients with endometrial and pancreatic cancer also showed a partial response.[214] Agradasib completed phase II clinical trials for monotherapy in NSCLC, colorectal and pancreatic cancers harbouring the KRAs G12C mutation in the fourth quarter of 2021 and the results are set to be reviewed by the FDA for approval in last quarter 2022.[215,216] This has led Mirati Therapeutics to fall behind in the stock exchange market compared to its competitor Amgen.[217] Agradasib is also currently undergoing phase III clinical testing in combination with chemotherapy agent docetaxel (Taxotere®) for the broad treatment of NSCLC, as well as phase II/III trials in combination with various immunotherapies.[216,218]

Despite falling behind in the race for the development of KRas G12C inhibitors, Mirati Therapeutics revealed earlier in 2022 their breakthrough in the development of KRas G12D non-covalent inhibitors. KRas G12D is the most observed mutant in KRas-derived tumours (see **Section II.1.1.2**). By reproducing and optimising the multiple Van der Waals weak interactions developed in the KRas G12C S-IIP by agradasib and its analogues, as well as exploiting the fact that the free nitrogen on the bicyclic piperazine would be protonated at biological pH, thus interacting *via* hydrogen bonding with the deprotonated mutant aspartic acid in KRas G12D, Marx *et al.* were able to develop MRTX1133 (**Figure 2.21**).[219] MRTX1133 was identified as a potent, selective non-covalent KRas G12D inhibitor with nanomolar cellular activity and is currently undergoing investigational new drug application (IND-enabling) for approval for first-in-human studies.[216]

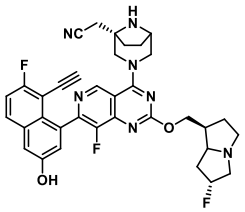


Figure 2.21: The first small-molecule *KRas G12D inhibitor MRTX1133*

II.1.4.5 Other notable KRas G12C inhibitors in the pipeline

Following in Amgen's and Mirati's footsteps, many pharmaceutical and biopharmaceutical companies have been developing their own KRas G12C inhibitors. Eli Lilly and Company, who were initially considered to directly compete with Amgen and Mirati in the run for obtaining the first approved KRas G12C covalent inhibitor, experienced a major setback when the phase I clinical trial for their highly selective and potent compound LY499446 was abruptly terminated due to unexpected toxicity issues.[220] However, the company started recruiting for a phase I trial of their backup compound LY3537982 in July 2021.[221] Genentech, Novartis, Inventis Biotech and Boehringer-Ingelheim also reported they were recruiting patients for the phase I testing of their respective compounds: GDC-6036, JDQ443, D-1553 and BI 1823911 (structures undisclosed).[218,222–225]

The identification of KRas G12C mutants as an "Achilles' heel" in previously deemed undruggable KRas, thanks to the ability to target the mutant cysteine with covalent warheads, allowed for the development of small molecule cancer therapies for tumours harbouring such mutation. These advances have rekindled an interest in targeting Ras oncoproteins, a research field marred with decades of failures. Moreover, in identifying and exploring the S-IIP binding site in KRas G12C, scientists have developed compounds that maximise weak interactions with it, thus opening the

door to finding therapies for other KRas mutants, such as KRas G12D, which is estimated to be behind twice as many tumours as its G12C counterpart.[139,141,216,226]

II.2 The synthesis of an atropisomeric KRas G12C covalent inhibitor

II.2.1 Project rationale

In the context of exploring the relevance of atropisomeric biarylpyrimidines in drug discovery, we reported in **Part I** the enantioselective synthesis of atropisomeric fragments of high rotational barrier. In June 2019, Amgen revealed the promising results of their phase I clinical trials for sotorasib, unveiling its chemical structure and that of various analogues in a subsequent patent.[82,227] Sotorasib (AMG-510), was revealed to be an extremely stable atropisomeric compound, containing a hindered isopropylpyridine ring and a rotational barrier measured at 25 °C of $\Delta G_T^{\ddagger}$ > 31.0 kcal/mol ($t_{1/2}^{rac}$ > 180 years).[25] Lanman and co-workers, who pulished most of the chemistry work related to sotorasib, revealed experimenting with non-atropisomeric biarylpyrimidines before settling for the asymmetric pyridines, which showcased higher cellular potencies. Nonetheless, some of the pyrimidine compounds expressed satisfactory potencies in both biochemical and cellular assays, the most notable examples being reported in **Figure 2.22** below.[81,82]

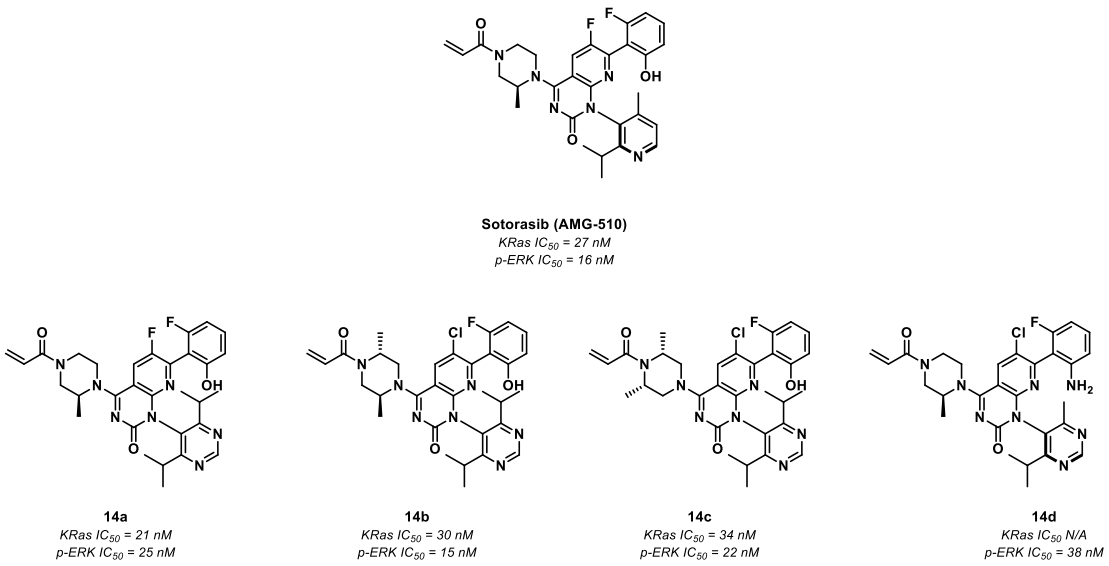


Figure 2.22: *Examples of biarylpyrimidine KRas G12C covalent inhibitors and their potencies against KRas G12C (biochemical potency) and in the p-ERK1/ 2 immunoassay (cellular potency), compared with sotorasib.*[25,81,82]

As mentioned in **Section II.1.1.4**, several structural properties of sotorasib are essential for its potency. The pyridopyrimidinone ring, inspired by the benzopyrimidine ring on ARS-1620, allows for close interactions with the S-IIP, the piperazine adopts a twist-boat conformation to guide the acrylamide towards not only C12 for covalent binding, but also K16 for carbonyl interaction (hydrogen bond).[25,205] The atropisomeric hindered pyridine ring fills the H95 cryptic groove by inducing a rotation of the side chain in that area and allows for multiple stabilising Van der Waals interactions, including π-π stacking between the pyridopyrimidone moiety and Y96. Keeping these interactions in mind, we decided to design a compound that exhibited structural similarities with both the biarylpyrimidine atropisomers we generated in **Part I**, and sotorasib (**Figure 2.23**). We designed model probe **52** which would be built around an isoquinoline ring, that should still display π-π interactions with Y96. Atropisomerism would be caused by the steric encumbrance generated by the trifluoromethyl substituent on the isoquinoline ring and the isopropyl and methoxy group on the pyrimidine ring, all in the *ortho* position relative to the chiral axis. The pyrimidine would therefore be locked in a conformation mimicking that of the pyridine ring on

sotorasib. Such a hindered pyrimidine should induce the same effects in the H95 cryptic pocket that were observed in the case of sotorasib. Finally, we would keep a piperazine ring as a linker between the isoquinoline ring and the covalent warhead, which would remain an acrylamide group. A methoxy group was chosen instead of a methyl group on the pyrimidine ring for synthetic reasons, resulting from the observations we made on the methanolysis of sulfonyl pyrimidines in **Section I.3.3**. Probe **52** could be generated enantioselectively from starting fragment **146**, replacing the usual trifluoromethylphenyl ring we used in **Part I** by a trifluoromethyl isoquinolinone, and utilising our orthogonal cross-coupling (see **Section I.3.2**) and methanolysis (see **Section I.3.3**) derivatisation reactions as a starting point for fragment growth (**Figure 2.23**).

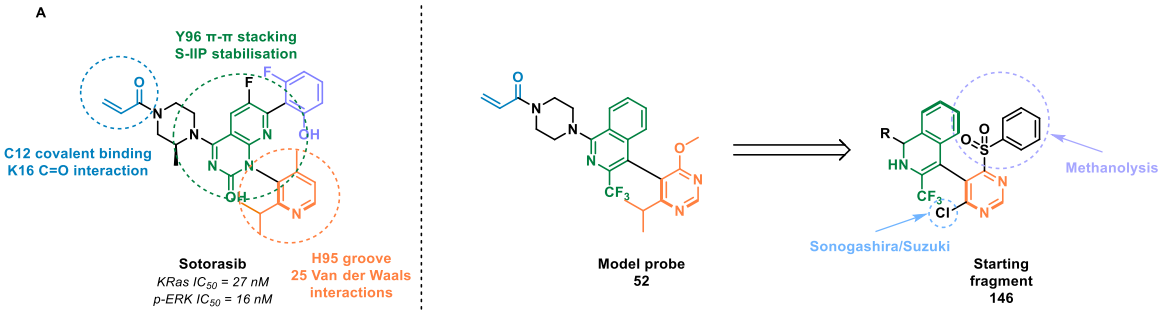


Figure 2.23: *Design of model probe **52**, inspired by sotorasib and that could be synthesised from starting fragment **146** (or analogue) using the chemistry developed in **Part I**.*

To further support these assumptions, we decided to dock our target probe **52** against sotorasib (AMG-510) in its X-Ray cocrystal with GDP and KRas G12C (PDB code: 6OIM), using Schrödinger's CovDock tool. The docking model's accuracy was assessed by docking sotorasib against itself in the X-Ray crystal (**Figure 2.24A**).[25] The superimposition of the parts of the molecule involved in the key interactions with KRas G12C was satisfactory enough for us to apply the docking to model probe **52** (**Figure 2.24B**). Probe **52** showed satisfactory superimposition with sotorasib and conserved the key interactions, including the filling of the cryptic H95 groove by the isopropyl group on the pyrimidine moeity, the π-π stacking of the isoquinoline ring with Y96 and hydrogen

bond between K16 and the carbonyl of the acrylamide warhead. This docking structure allowed us to predict that the active enantiomer would be the (*S*) atropisomer. This docking study served as a proof of concept and allowed us to move onto devising synthesis plans for probe **52**.

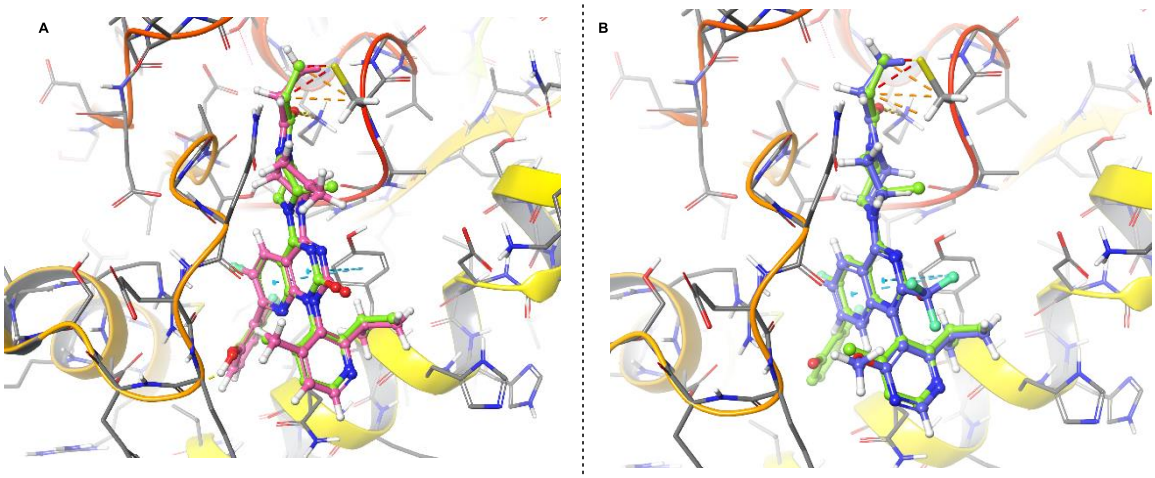


Figure 2.24: ***(A)*** *Docked structure of AMG-510 (magenta), compared with AMG-510 in its cocrystal with KRas (green, PBD code: 6OIM).*[25] ***(B)*** *Docked structure of model probe* ***52*** *(blue), compared with AMG-510 in its cocrystal with KRas (green, PDB code: 6OIM).*[25]

II.2.2 Project aims

With this project, we were aiming to synthesise probe **52** and assess its biological and physiochemical properties. Depending on the results of the biochemical assays, we also considered to optimise **52** *via* SAR studies. Model probe **52** would be synthesised both in racemic and enantioselective fashion. The enantioselective synthesis of **52** would be attempted using the methodologies described in **Part I**, namely by attempting to generate fragment **146** (**Section II.2.1**, **Figure 2.23**) in an enantioselective fashion and subsequently growing it.

Before setting out on developing retrosynthetic routes for both the racemic and enantioselective synthesis of probe **52**, we took a look at the forward synthesis of compound **14d**, which was reported by Lanman *et al.* as part of one of the final contenders for a chemical lead with AMG-510 and exhibits an atropisomeric biaryl pyrimidine (**Figure 2.25A**).[25] Starting with

2,4,6-trichloronicotinic acid **57**, Lanman and co-workers formed 2,4,6-trichloronicotinic amide **58** by pre-treating with coupling agent 1,1'-carbonyldiimidazole (CDI) at 90 °C in 2-methyltetrahydrofuran, followed by the addition of ammonium hydroxide an stirring at room temperature (yield unreported). Amide **58** was dissolved in 1,2-dichloroethane (DCE) and treated with oxalyl chloride at 80 °C, to subsequently by reacted with 4-Isopropyl-6-methylpyrimidin-5-amine **56** in acetonitrile at room temperature to yield urea **59** in high yield (82%). The subsequent treatment of **59** with potassium bis(trimethylsilyl)amide (KHMDS) in tetrahydrofuran at room temperature yielded the intramolecular cyclisation product, pyridopyrimidine-dione **60** (yield unreported, but was of 92% for an analogue). Chlorination with phosphorus(V) oxychloride in acetonitrile at 80 °C, in the presence of *N,N*-diisopropylethylamine (DIPEA), followed by the addition of (S)-4-N-Boc-2-methyl piperazine *via* SNAr at room temperature in the presence of DIPEA afforded substituted pyridopyrimidone **61** (yield unreported, but was of 97% over 2 steps for an analogue). The Suzuki-Miyaura coupling of chloropyridopyrimidone **61** with 2-fluoro-6-hydroxyphenylboronic acid **62** at 80 °C in 1,4-dioxane, in the presence of (1,1'-bis(diphenylphosphino)ferrocene)dichloropalladium and potassium acetate, yielded product **63** (yield unreported, but was of 96% for an analogue). The treatment of Boc-piperazine **63** with trifluoroacetic acid (TFA) at room temperature in dichloromethane, followed by the *N*-acylation of the resulting free amine with acryloyl chloride in dichloromethane at 0 °C, yielded racemic compound **14d**. The active (*R*)-atropisomer was isolated by chiral supercritical fluid chromatography (SFC).

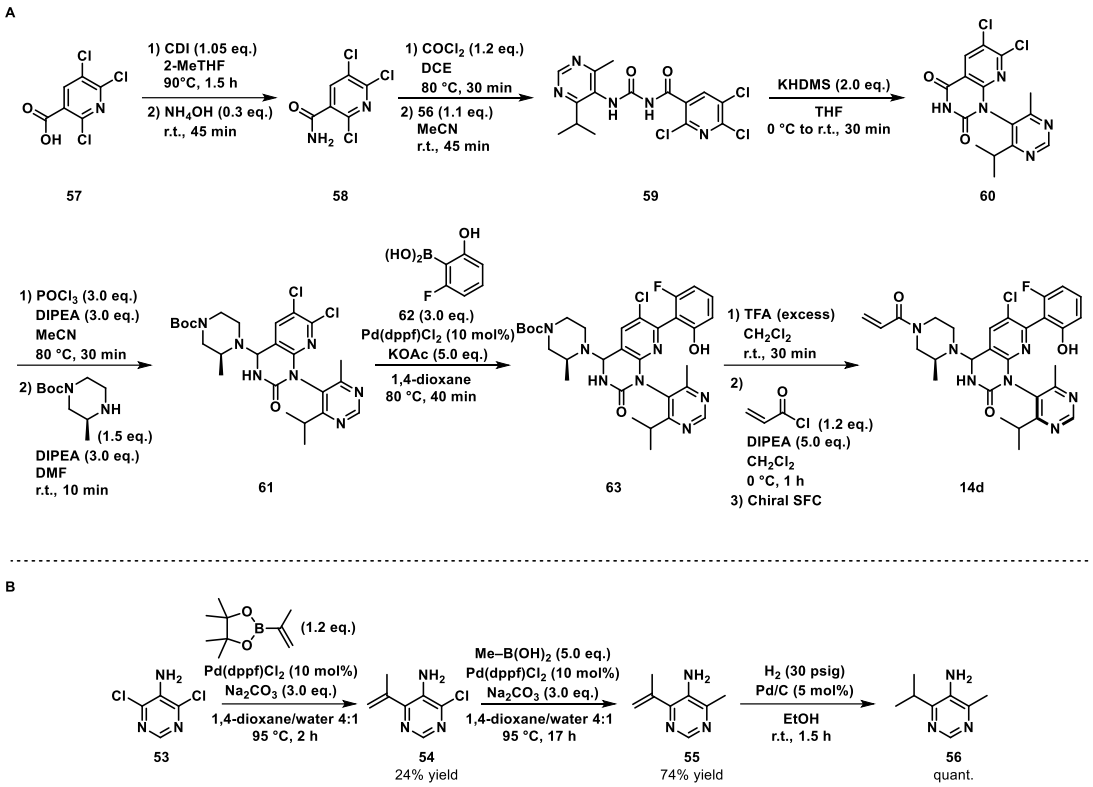


Figure 2.25: ***(A)*** *The synthesis of sotorasib analogue* ***14b*** *(yields unreported).*[25] ***(B)*** *The synthesis of aminopyrimidine* ***56****.*[25]

The synthesis of 4-Isopropyl-6-methylpyrimidin-5-amine **56** was also reported by Lanman *et al.* and, as it was also of interest to us, is detailed in **Figure 2.25B**.[25] 4,6-dichloro-5-aminopyrimidine **53** was dissolved in a 4:1 1,4-dioxane/water mixture and heated to 95 °C in the presence of , 2-isopropenylboronic acid, pinacol ester, sodium carbonate and Pd(dppf)Cl_2. The Suzuki-Miyaura coupling yielded chloropyrimidine **54** in low yield (24%), which was in turn subjected to the same conditions, but with methylboronic acid as a coupling partner. Aminopyrimidine **55** was obtained in higher yield (74%) and its alkyne moiety was hydrogenated in ethanol, in the presence of palladium (10% activated on carbon, Pd/C), to afford 4-Isopropyl-6-methylpyrimidin-5-amine **56** in quantitative yield.

The main difference between our probe **52** and sotorasib is the chiral axis being a C–C bond instead of a C–N bond, as we chose to use an isoquinoline ring as a base for our compound instead

of a pyridopyrimidone. Although the creation of C–C aryl–aryl bonds can be considered difficult, numerous cross-coupling methodologies have emerged to help chemists in this endeavour.[88,92,94,228,229] The retrosynthetic approach of the racemate synthesis of probe **52** exploited the idea that such methodologies allowed for the design a convergent route, by sequentially anchoring the piperazine ring *via* SNAr, followed by the addition of a fully substituted pyrimidine ring *via* cross-coupling chemistry (ideally a Suzuki-Miyaura reaction) onto "linchpin" type intermediate **71** (**Figure 2.26**). By possessing an iodine or bromine atom *meta* to the isoquinoline nitrogen, and a chlorine atom *ortho* to this same nitrogen, intermediate **71** could theoretically be derivatised by orthogonal transformations. The chloro site would be more susceptible to nucleophilic attacks, whereas the iodo/bromo site would be more susceptible to oxidative additions onto a metal centre. This intermediate would be obtained after halogenating the product of the condensation-elimination sequence between homophthalic acid **64** and trifluoroacetic anhydride **65**.

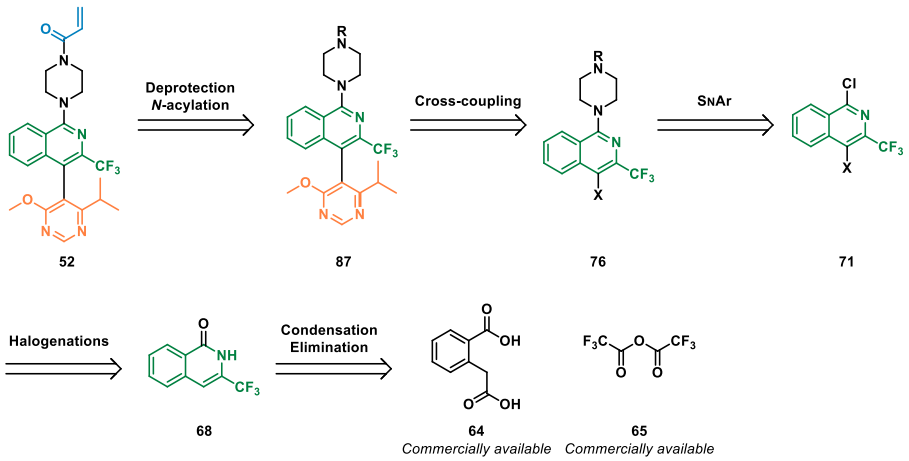


Figure 2.26: *Retrosynthetic approach of racemic **52**.*

The enantioselective retrosynthetic approach of probe **52** was devised around the same concept (**Figure 2.27**). However, instead of introducing a fully substituted pyrimidine ring onto intermediate **76**, we would generate dichloropyrimidine **146** *via* malonate **123**, following the

synthetic route developed by Armstrong.[71] The dichloropyrimidine would then in turn be desymmetrised using thiophenol and undergo subsequent derivatisations, following the methodologies developed in **Section I.3.2** and **Section I.3.3**. The isopropyl group on the pyrimidine could be introduced following Lanman and co-workers' Suzuki-Miyaura/hydrogenation sequence (**Figure 2.25B**),[25] or, if it proves a better option, Sonogashira cross-coupling using trimethylsilylacetylene,[80,90] followed by a carboalumination/hydrogenation sequence.[230] The methoxy group would be introduced by methanolysis of the sulfone (see **Section I.3.3**).

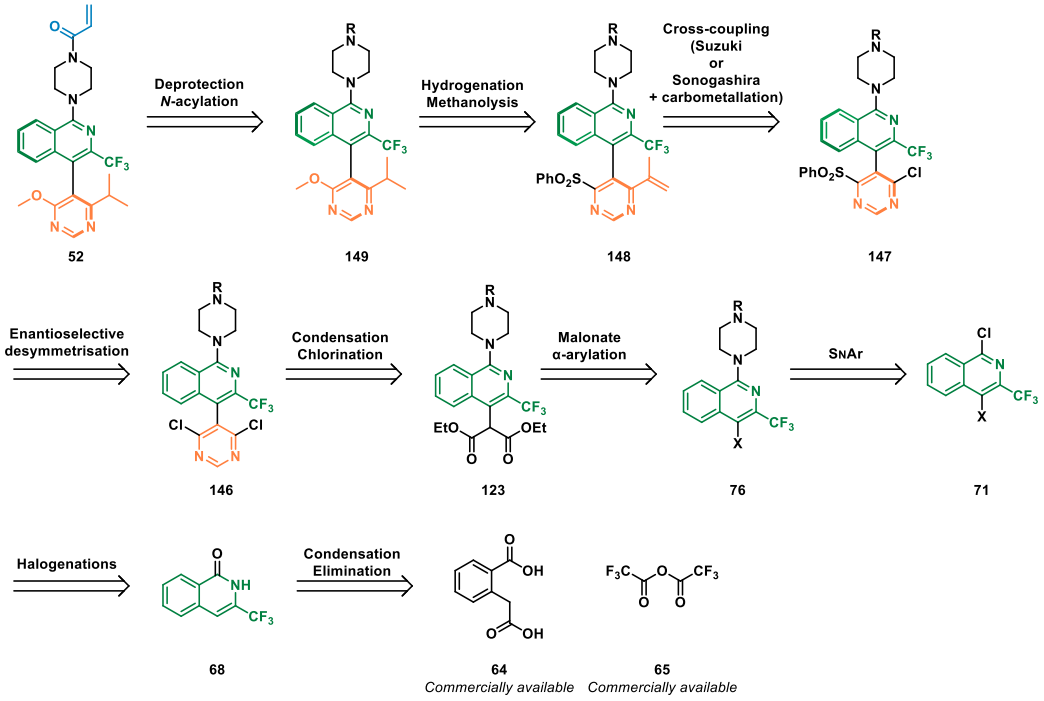


Figure 2.27: *Retrosynthetic approach of enantioenriched **52**.*

II.3 Results and discussion

II.3.1 The synthesis of a linchpin precursor

The synthesis of 3-trifluoromethyl-1-isoquinolinone **68** was reported in the context of α4-integrin inhibition for the treatment of immune or inflammatory disorders by Langham and co-workers

(**Figure 2.28A**).[231] Langham and colleagues condensed trifluoroacetic anhydride **65** and homophthalic acid **64** by stirring the latter in an excess of the former at 110 °C for a day, and then 140 °C for an extra day. The resulting crude mixture of isochromenes was suspended in aqueous ammonium hydroxide and stirred at 100 °C for 5 days, to yield **68** in 70% yield (**Figure 2.28A**).[231]

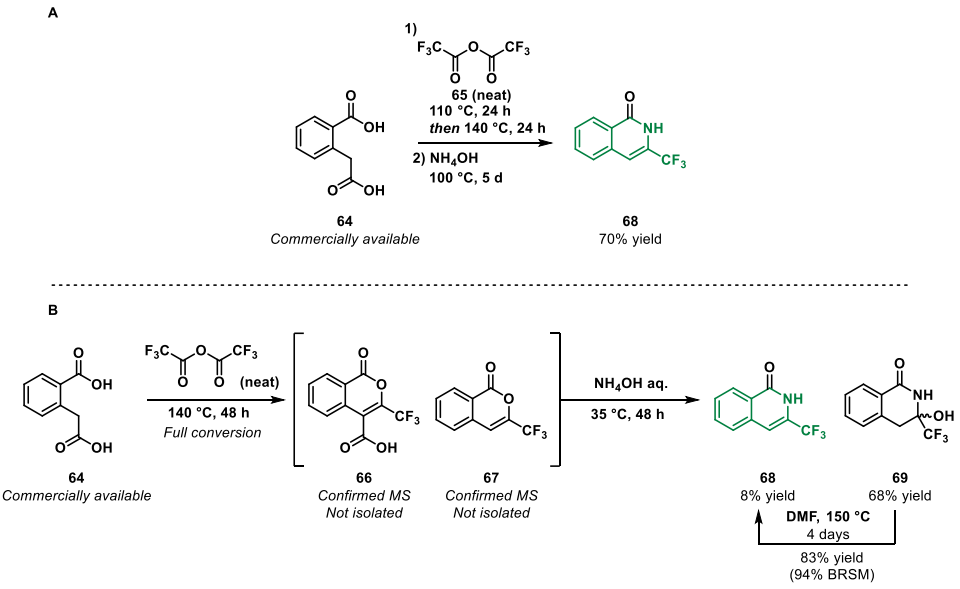


Figure 2.28: *Synthesis of isoquinolinone **68**: **(A)** As reported by Langham et al.[231] **(B)** As attempted by us.*

We were able to repeat the first step of this transformation by stirring **64** in an excess of **65** at 140 °C for 2 days. The boiling point of trifluoroacetic anhydride (**65**) being 40 °C, the reaction had to be conducted with minimal amounts in a sealed pressure tube (**Figure 2.28B**). The transformation of the resulting isochromenes **66** and **67** into **68** required dilute reaction conditions in ammonium hydroxide, the boiling point of which being 35 °C. Thus, it necessitated the use of pressure-resistant equipment with a sizeable amount of headspace that we did not possess. We decided to attempt the reaction at reflux conditions, and heated **67** to 35 °C in aqueous ammonium hydroxide for two days. These conditions only yielded isoquinolinone **68** in 8% yield. However, we identified the major product of the reaction as the corresponding hemi-aminal **69**, which we decided to heat up to 150 °C in *N,N*-dimethylformamide for several days to provoke its

dehydration into the desired isquinolinone **68**. Such a transformation, though incomplete after 4 days, allowed us to increase the total isolated yield in compound **68** to 64% (as 83% of the hemiaminal **69** were converted into desired product **68**).

With isoquinolinone **68** in hand, the subsequent transformations to reach linchpin precursor **71** were found in the literature. The halogenation of 3-subsituted isoquinolinones at position 4 by *N*-bromosuccinimide has been reported by Usifoh,[232] and the chlorination of the remaining carbonyl bond by phosphorus(V) oxychloride is well documented.[233,234] We repeated the synthesis of isquinolinone **68** by prolonging the dehydration step, allowing us to bring the total yield to a slightly higher value than the one reported by Langham and co-workers (83% *vs.* 70% (lit.)) (**Figure 2.29**).[231] Isoquinolinone **68** was subsequently dissolved in *N,N*-dimethylformamide and heated to 80 °C in the presence of *N*-iodosuccinimide. Alternatively, **68** was kept at room temperature in the presence of *N*-bromosuccinimide to afford the corresponding 4-haloisoquinolinones **70a** and **70b** in high yields (77–94% and 71–84% respectively).[232] The resulting isoquinolinones **70a–b** were taken up in phosphorus(V) oxychloride and heated to 90 °C for two days, to yield the desired linchpin intermediates: iodoisquinoline **71a** (93% to quantitative yield) and bromoisoquinoline **71b** (quantitative yield).[234]

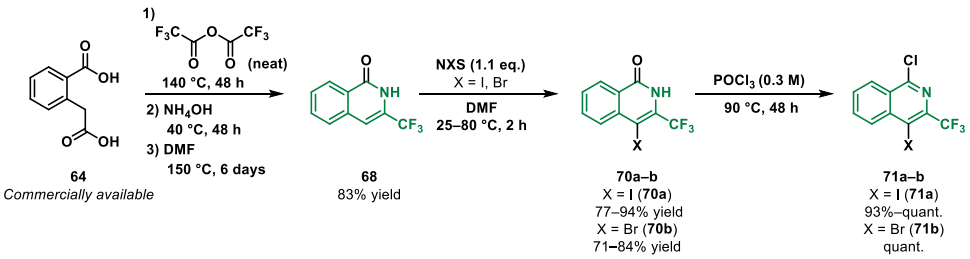


Figure 2.29: *The synthesis of linchpin precurors **71a–b**.*

II.3.2 Towards the racemic synthesis of probe 52

II.3.2.1 Preliminary study

The retrosynthetic approach of racemic model probe **52** (**Section II.2.2**, **Figure 2.26**) being less linear than its enantioselective counterpart, we decided to investigate it first. With linchpin precursors **71a–b** at our disposal, the key transformation of this sequence would be the cross-coupling of the pyrimidine and the isoquinoline. This step, though conceptually simple, generates a tetra-*ortho*-substituted biaryl scaffold, and was thus expected to be synthetically challenging. Indeed, sterically-demanding cross-couplings, most notably Suzuki-Miyaura couplings, are notoriously difficult.[235–238] Moreover, heterocyclic coupling partners, especially heterocyclic boronic acids, are prone to proto-deborylation.[95,239,240]

We thus decided to probe the aptitude of an unsubstituted pyrimidinylboronic acid to couple with intermediate **71a** as a model substrate, before increasing steric hindrance (**Figure 2.30**). Intermediate **71a** was stirred at 100 °C in a 2:1 mixture of 1,2-dimethoxyethane and water, in the presence of 5-pyrimidinylboronic acid **72**, sodium carbonate and catalytic amounts of Pd(dppf)Cl_2 (in complex with dichloromethane) to yield the Suzuki-Miyaura cross-coupling product **73** in moderate yield (67%).[241] The subsequent treatment of chloroisoquinoline **73** with piperazine in *N,N*-dimethylformamide at 80 °C in the presence of potassium carbonate yielded SNAr product **74**,[242] which was in turn *N*-acylated by acryloyl chloride at room temperature in dichloromethane in the presence of triethylamine, to yield compound **75** in moderate yield (51%, 2 steps).[243] This 3-step sequence, with a 29% overall yield, served as a proof of concept for a convergent synthesis of racemic probe **52**.

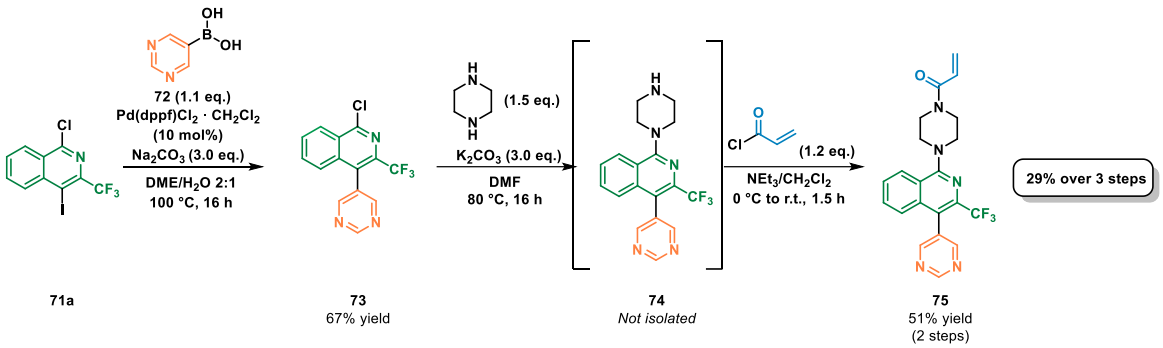


Figure 2.30: *Synthesis of unsubstituted biarylpyrimidine **75**.*

In an effort to increase the overall yield of the sequence, we decided to examine whether changing the order of the steps (*i.e.* switching the SNAr and the Suzuki-Miyaura reactions) could be beneficial (**Figure 2.31**). Considering nitrogen bases are known for poisoning palladium catalysts,[244,245] we decided to introduce the piperazine as a protected entity to ensure the catalyst in the following Suzuki-Miyaura coupling would not be deactivated by the presence of a free nitrogen on our substrate. In the context of this sequence, we established a *tert*-butyloxycarbonyl (Boc) protecting group would be the easiest to work with. We therefore heated intermediate **71a** and 1-Boc-piperazine to 80 °C in *N,N*-dimethylformamide, in the presence of potassium carbonate, to yield compound **76a** in moderate to high yields (56–96%).[242] Moderate yields were obtained when pouring the crude mixture onto ice cold water upon reaction completion and filtering the resulting sticky precipitate, whereas higher yields were obtained after an aqueous workup followed by purification by column chromatography. The resulting iodoisoquinoline (**76a**) was stirred at 100 °C in a 2:1 mixture of 1,2-dimethoxyethane and water, in the presence of 5-pyrimidinylboronic acid **72**, sodium carbonate and catalytic amounts of Pd(dppf)Cl_2 (in complex with dichloromethane), to yield the Suzuki-Miyaura cross-coupling product **77** in high yield (85%).[241] The subsequent removal of the Boc protecting group by stirring **77** in a hydrogen chloride solution in methanol (1.5 M) at room temperature, followed by *N*-acylation at room temperature in dichloromethane in the presence of acryloyl chloride and

triethylamine, afforded compound **75** in high yield (93% over two steps).[243] Despite introducing an extra deprotection step, this sequence had overall yields comprised between 51 and 76%, and thus considerably higher than in the sequence described previously (**Figure 2.30**). We therefore decided that, moving forward, we would derivatise intermediates **71a–b** at the chloro site *via* SNAr before attempting derivatisation at the iodo/bromo site.

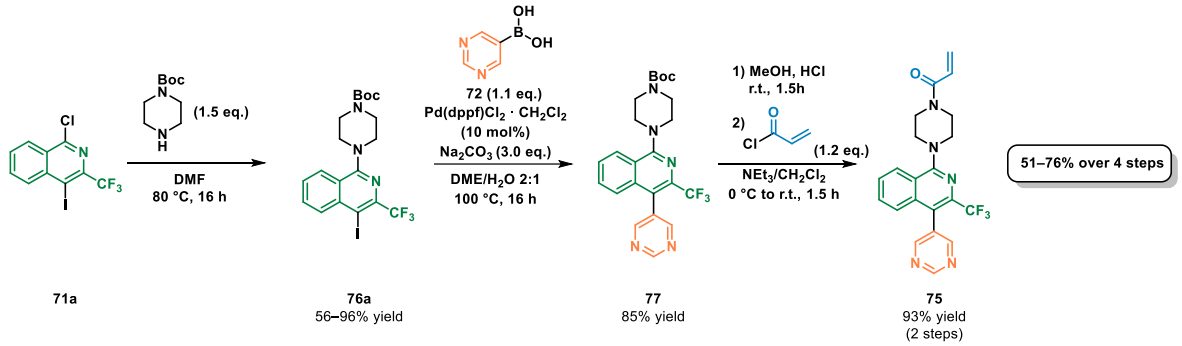
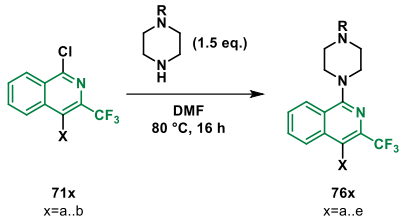


Figure 2.31: *Alternative synthesis of unsubstituted biarylpyrimidine **75**.*

In the aforementioned sequences, the Boc group seemed like a natural choice, as no reaction except the deprotection step required the use of acidic conditions. However, in the case of our planned asymmetric synthesis, a protecting group resisting harsher conditions would be required. Therefore, we explored the SNAr derivatisation of intermediate **71a** with various protected piperazines, using the same conditions as described earlier (**Table 2.3**).[242] Boc-protected **76a** was obtained in moderate yield when isolated by precipitation and subsequent filtration (56%), but a higher yield was obtained when isolating it by column chromatography (96%). Benzyloxycarbonylpiperazine (1-Cbz-piperazine) yielded product **76b** in almost quantitative yield (99%) when isolated by precipitation and, therefore, isolating it by column chromatography was not attempted. Finally, tosylpiperazine (1-Ts-piperazine) afforded product **76c** in similar yields, whether it was isolated by precipitation or column chromatography (79% and 77% respectively). Bromoisoquinoline **71b** was also subjected to the same reaction conditions in the presence

of -Boc-piperazine and 1-Ts-piperazine. The respective bromo products **76d** and **76e** were isolated in high yields, using the highest yielding purification method observed for their iodo counterparts.



71x
x=a..b

76x
x=a..e

Product	R	X	Precipitation	Column chromatography
76a	Boc	I	56% yield	96% yield
76b	Cbz	I	99% yield	N/A
76c	Ts	I	79% yield	77% yield
76d	Boc	Br	N/A	88% yield
76e	Ts	Br	69% yield	N/A

Table 2.3: *Influence of the protecting group and the isolation method on the SNAr of a protected piperazine on compounds **71a–b**.*

II.3.2.2 Synthesis of the pyrimidinyl coupling partners

The Suzuki-Miyaura coupling of an unsubstituted pyrimidine with our isoquinoline intermediates **71a** and **76a** proving successful, we decided to synthesise a pyrimidine coupling partner exhibiting the desired *ortho*-isopropyl and *ortho*-methoxy groups. In June 2020, Brenneman *et al.* at KSQ Therapeutics reported the synthesis of pyrazolopyrimidines as ubiquitin-specific protease 1 inhibitors.[246] The synthesis of their compounds involved the cross coupling of a chloro-pyrazolopyrimidine with di-*ortho*-substituted pyrimidinylboronic acids.[246] We thus decided to replicate the synthesis of their boronic acids for the synthesis of *ortho*-isopropyl *ortho*-methoxy pyrimidinyl coupling partner (**Figure 2.32**).

We obtained hydroxypyrimidine **79** in moderate yields (43–70%) by stirring the commercially available ethyl isobutyrylacetate **78** in anhydrous methanol at room temperature, in the presence of *in situ*-generated sodium methoxide and formamidine acetate (**Figure 2.32**). Hydroxypyrimidine

79 was brominated in ethanol at room temperature in the presence of bromine to yield hydroxypyrimidine **80** in moderate to high yields (55–83%), which was in turn chlorinated by heating to 100 °C in 1,2-dicholoethane in the presence of an excess of phosphorus(V) oxychloride, to afford chloropyrimidine **81** in high yields (84–86%). Finally, the SNAr reaction involving chloropyrimidine **81** and solid sodium methoxide in methanol at room temperature yielded bromopyrimidine precursor **82** in high yields (80–93%).[246]

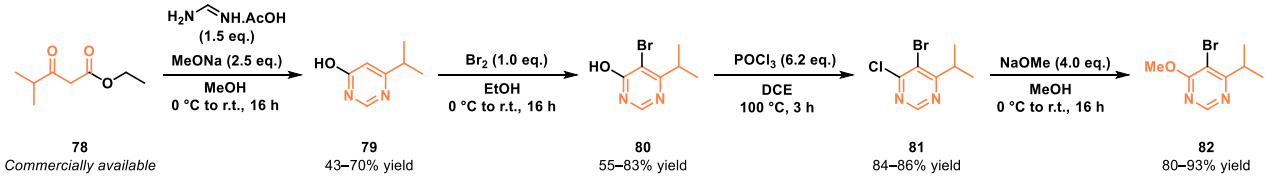


Figure 2.32: *Synthesis of bromopyrimidine precursor **82**.[246]*

We then proceeded to transform boromopyrimidine **82** in various organometallic species for use in different cross-coupling reactions (**Figure 2.33**). The first step of all these derivatisations consisted in performing a lithium-bromine exchange on **82** using *n*-butyllithium at –78 °C. Boronic acid **83** was synthesised by trapping the newly-generated organolithium with triisopropyl borate in a 5:1 toluene/tetrahydrofuran mixture at room temperature, and subsequently hydrolysing it by spiking the solution with 2 N hydrochloric acid at room temperature.[246] Boronic acid **83** was obtained in moderate yields (29–39%), but was found to readily undergo proto-deborylation at room temperature. Such unstable boronic acids are recommended to be used as their MIDA-complexed (MIDA = methyliminodiacetic acid) counterparts.[95] MIDA-boronate **84** was easily obtained in high yield (70%, 89% brsm) by complexing boronic acid **83** with MIDA in *N,N*-dimethylformamide at 90 °C under non-inert atmosphere.[247] The Suzuki-Miyaura cross-coupling reaction being notoriously difficult for heavily hindered systems,[235–238] we also decided to synthesise lithium sulfinate **85** and tributyltinpyrimidine **86.** Both compounds were

obtained by trapping the nucleophile generated by the lithium-halogen exchange in anhydrous tetrahydrofuran at room temperature. Lithium sulfinate **85** was obtained in moderate yields (27–49%) by using sulfur dioxide 1-methylpyrrolidine adduct (TIMSO) as a trapping agent,[239,240] and tributyltinpyrimidine **86** was obtained in quantitative yields using tributyltin chloride as a trapping agent.[248]

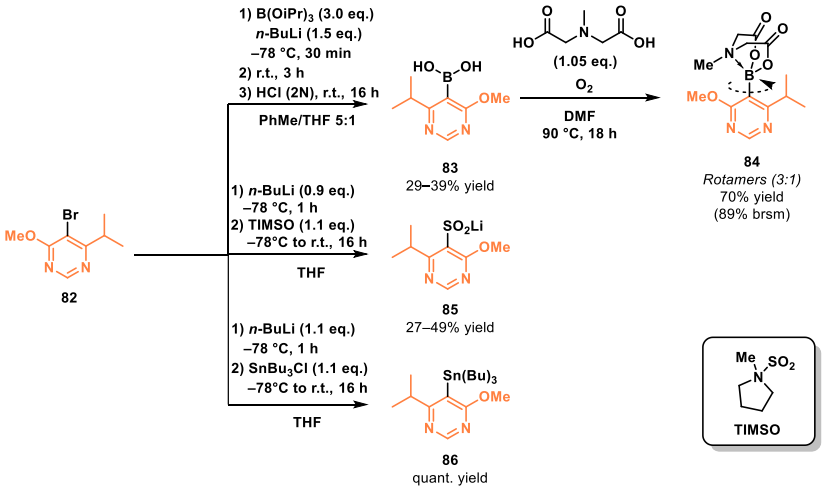


Figure 2.33: *Synthesis of pyrimidinyl organometallic cross-coupling-partners.*

II.3.2.3 The cross-coupling issue: hitting a wall

With pyridiminyl coupling partners **83–86** in hand, we decided to attempt using them in cross-coupling reactions. The conditions used in **Section II.3.2.1** for the coupling of **71a** and **76a** with 5-pyrimidinyl boronic acid **72** being successful, we decided to probe them for the coupling of isoquinoline **76a** with boronic acid **83** (**Figure 2.34**). Iodoisoquinoline **76a** and boronic acid **83** were suspended in a 2:1 mixture of 1,2-dimethoxyethane and water, and heated to 100 °C in the presence of sodium carbonate, and catalytic amounts of palladium, until complete consumption of **76a** was observed. However, after analysis, only deiodination product **88** was collected. Such an observation suggested that the oxidative addition of the palladium catalyst onto iodoisoquinoline **76a** did happen, but that the following transmetallation/reductive elimination steps would not

occur. The steric hindrance generated by the *ortho*-methyl and *ortho*-isopropyl groups on the pyrimidinylboronic acid, as well as the ortho-trifluoromethyl group and the general bulk of the isoquinoline ring could be a potential reason for this outcome.

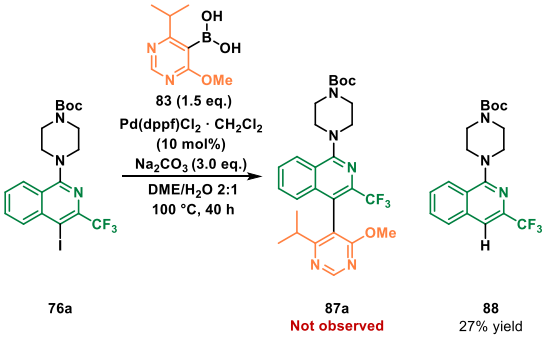


Figure 2.34: *First attempt generating compound **87** via Suzuki-Miyaura coupling.*

As mentioned in **Section II.3.2.2**, we did expect such a result, partly due to this steric hindrance issue, but also due to the general instability of pyrimidinylboronic acid **83**. Therefore, we investigated whether we would be able to overcome these two main issues in our system. Our first idea was to look into Suzuki-Miyaura cross-coupling conditions for the synthesis of tetra-*ortho*-substituted biaryl systems. In 2011, Dorta *et al.* found that the synthesis of tetra-*ortho*-substituted biaryls was facilitated by using *N*-heterocyclic carbene (NHC) palladium complexes such as Pd-PEPPSI-*i*Pent, which allowed to couple di-*ortho*-substituted aryl (and heteroaryl) halides with di-*ortho*-substituted boronic acids, sometimes up to the point of not needing to heat up their reaction mixtures (**Figure 2.35**).[249]

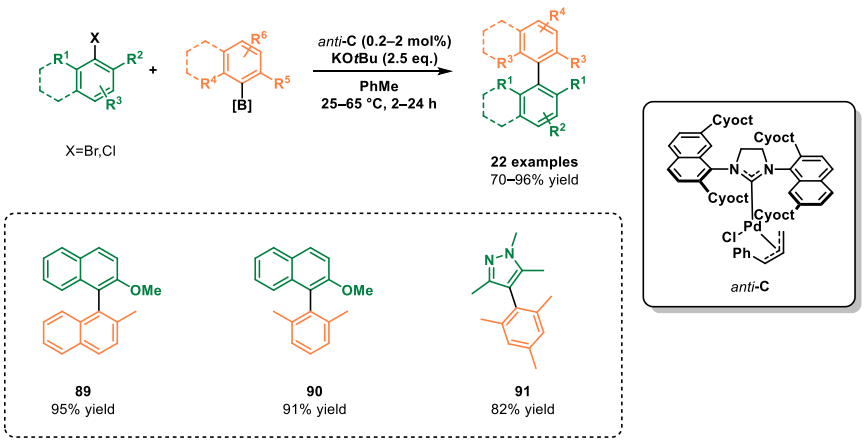


Figure 2.35: *Dorta and colleagues' Suzuki-Miyaura cross-coupling conditions using (NHC)-palladium complexes and notable examples.*[249]

In 2020, Tang and co-workers reported the asymmetric synthesis of numerous tetra-*ortho*-substituted biaryl systems, including heterocyclic biaryl systems, using a Suzuki-Miyaura cross-coupling reaction catalysed by a classic palladium source and P-chiral monophosphorous ligands (**Figure 2.36**).[238] The use of di and trialkybiarylphosphine ligands such as SPhos, Xphos and the ones used by Tang and co-workers has been associated with higher success-rates for Suzuki couplings, especially the ones involving heterocyclic species and sterically-demanding systems.[250] Such ligands can also be paired with MIDA boronates (instead of regular boronic acids/esters) to facilitate the Suzuki-Miyaura coupling of unstable nucleophilic species, such as pyridinylboronic or isoxazoloboronic acids, with aryl halides.[95] Knapp, Burke *et al.* showed MIDA-boronates can slowly release their boronic acid counterpart into the reaction medium *via* a mild hydrolysis enabled by aqueous tripotassium phosphate, thus avoiding the degradation of boronic acids or esters that would be awaiting catalyst turnover to react.

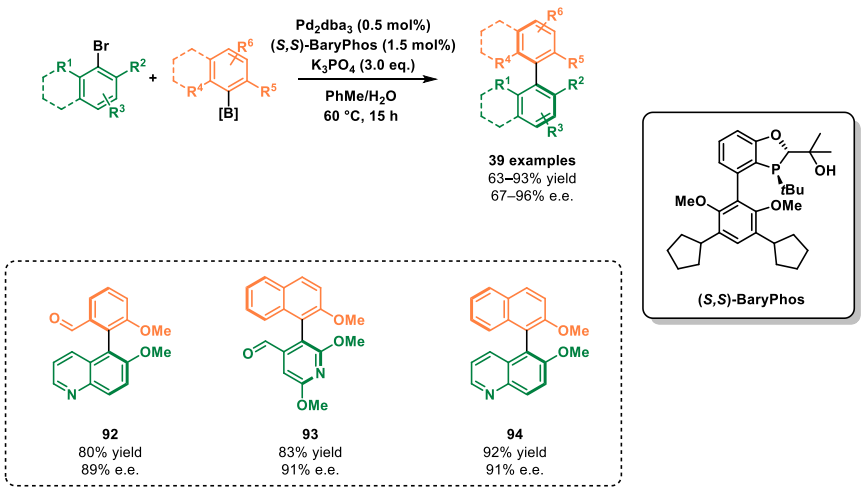


Figure 2.36: *Tang and co-workers' Suzuki-Miyaura cross-coupling conditions using trialkylbiarylphosphines as ligands and notable examples.*[238]

We also decided to explore alternative cross-coupling reactions to the Suzuki-Miyaura coupling. In 2017, Tim Markovic *et al.* of the Willis group reported in two different articles the use of lithium/sodium heteroaryl sulfinates as nucleophilic substitutes for boronic acids in a Suzuki-Miyaura-like cross-coupling reaction (**Figure 2.37A & 2.37B**).[239,240] The harshness of the conditions depended on the ligand used: P(*t*-Bu)Me_2·HBF_4 required milder temperatures, whereas or PCy_3 required higher temperatures, but nonetheless allowed for a wide substrate scope. Such coupling partners would allow us to get around the instability issue pyrimidinylboronic acids raise, and the increased temperatures would potentially help overcome the activation energy arising from the steric hindrance in our system. Aside from Markovic and co-worker's conditions, the use of a tributyltinpyrimidine in a palladium-catalysed Stille cross-coupling was seen as an alternative. Developed in 1986 by John K. Stille, the Stille reaction is considered one of the most reliable cross-coupling reactions, and is usually privileged for more demanding systems, despite the many drawbacks of organotin species (toxicity, difficulty to isolate from products etc.).[228,248,251]

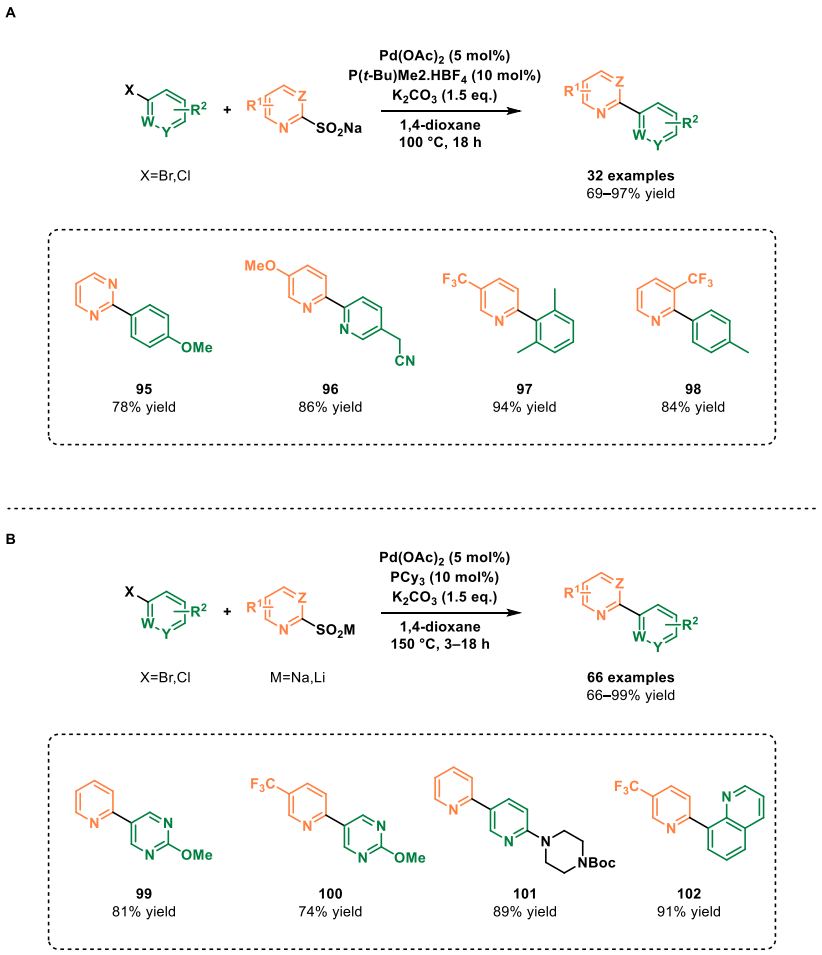
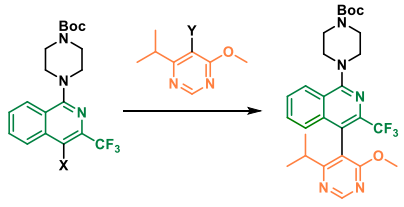


Figure 2.37: *Markovic and colleagues' (Willis group) conditions for the synthesis of heterobiaryl system and notable examples:* ***(A)*** *Using P(t-Bu)Me$_2$·HBF$_4$ as a ligand.*[239] ***(B)*** *Using PCy$_3$ as a ligand.*[240]

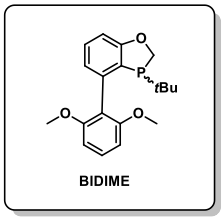
These sets of conditions in hands, we attempted to apply them to our system. These experiments are summed up in **Table 2.4**. Dorta and co-workers' conditions were applied to iodioisoquinoline **76a** using catalytic amounts of (NHC)Pd(allyl)Cl **103**, the NHC-based catalyst that gave Dorta *et al.* a first hit in the development of their reaction (**Table 2.4, entry 2**).[249] The two species, as well as boronic acid **83**, were suspended in toluene in the presence of potassium *tert*-butoxide, and heated to both 65 °C and reflux. In both instances, only deiodination of **76a** was observed. We then proceeded with trying Tang and colleagues' conditions on our system, using (*S*)-BIDIME, the dialkylbiarylmonophosphorous ligand that gave a first hit in the development of

their reaction.[238] Compound **76a** and boronic acid **83** were suspended in a 9:1 mixture of toluene and water iandaqueous tripotassium phosphate and, catalytic amounts of tris(dibenzylideneacetone)dipalladium(0) (Pd_2dba_3) and (*S*)-BIDIME were added. The resulting mixture was stirred at either 60 °C or reflux, but only de-halogenation of **76a** was observed in both instances (**Table 2.4, entry 3**). The failure of these conditions, usually efficient for sterically-demanding systems, drove us to attempt coupling methods where the pyrimidinyl coupling partner is more stable.

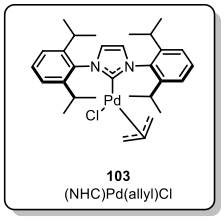


76a–b **87a**

Entry	Coupling	X	Y	Catalytic system	Additive(s)	Solvent	Temperature(s)	Observation
1	Suzuki	I	$B(OH)_2$	$Pd(dppf)Cl_2.CH_2Cl_2$	Na_2CO_3	DME/H_2O 2:1	100 °C	Dehalogenation
2	Suzuki	I	$B(OH)_2$	(NHC)Pd(allyl)Cl	KO*t*-Bu	PhMe	65 °C/ Reflux	Dehalogenation
3	Suzuki	I	$B(OH)_2$	Pd_2dba_3 (*S*)-BIDIME	K_3PO_4	PhMe/H_2O 9:1	60 °C/ Reflux	Dehalogenation
4	Suzuki	I	B(MIDA)	$Pd(OAc)_2$ SPhos	K_3PO_4	1,4-dioxane/H_2O 5:1	60/ 80 °C	Dehalogenation
5	Suzuki	I	B(MIDA)	Pd_2dba_3 (*S*)-BIDIME	K_3PO_4	PhMe/H_2O 9:1	60 °C/ Reflux	Dehalogenation
6	"Willis"	Br	SO_2Li	$PdOAc_2$ $P(t\text{-}Bu)_2Me.HBF_4$	K_2CO_3	1,4-dioxane	110 °C/ 130 °C	Dehalogenation
7	"Willis"	Br	SO_2Li	$Pd(OAc)_2$ PCy_3	K_2CO_3	1,4-dioxane	150 °C	Dehalogenation
8	Stille	I	$SnBu_3$	$Pd(PPh_3)_4$ CuI	CsF	DMF	65/ 80/ 100/ 120 °C	Dehalogenation



BIDIME



103
(NHC)Pd(allyl)Cl

Table 2.4: *Summary of the various sets of conditions attempted for the cross-coupling of **76a–b** with pyrimidinyl coupling partners **83**, **84**, **85** and **86**.*

We decided to apply Knapp, Burke and colleagues' strategy for the slow release of our pyrimidinylboronic acid **83** by using its MIDA-boronate counterpart **84**. By dissolving iodoisoquinoline **76a** and MIDA-boronate **84** in a 5:1 mixture of 1,4-dioxane and water, and stirring it in the presence of aqueous tripotassium phosphate, and catalytic amounts of palladium

acetate and SPhos, heated to either 60 or 80 °C, we observed no formation of the desired product (**Table 2.4, entry 4**). Similarly to all previous attempts, only deiodination of **76a** was observed. Considering Tang and colleagues' conditions also used aqueous potassium phosphate, we decided to merge them with Knapp and co-workers' conditions, by taking **76a** and **84** in a 9:1 mixture of toluene and water, adding aqueous tripotassium phosphate and, catalytic amounts of tris(dibenzylideneacetone)dipalladium(0) (Pd_2dba_3) and (*S*)-BIDIME. Stirring this mixture at either 60 °C or reflux did not lead to anything but dehalogenation of iodoisoquinoline **76a** (**Table 2.4, entry 5**). Since boron-derived pyrimidinyl coupling partners did not appear fit for purpose, we investigated the use of lithium sulfinate **85**, following the Willis group's coupling conditions. We first attempted the set of conditions that used P(*t*-Bu)Me_2·HBF_4 as a ligand, which consisted in taking bromoisoquinoline **76b** and lithium sulfinate **85** in 1,4-dioxane with potassium carbonate and, catalytic amounts of palladium(II) acetate and said ligand.[239] We heated the mixture to both the recommended 110 °C and the tolerated 130 °C, but neither temperatures yielded the desired product and only debromination of **76b** was observed (**Table 2.2, entry 6**). Using the same set of conditions, but replacing the ligand by tricyclohexylphosphine and heating up to 150 °C, led to the same observations (**Table 2.4, entry 7**).[240] In an last attempt, we turned to the more reliable Stille cross-coupling of iodoisoquinoline **76a** and tributyltinpyrimidine **86**. The two coupling partners were dissolved in *N,N*-dimethylformamide and stirred at 65, 80, 100 or 120 °C, in the presence of caesium fluoride, and catalytic amounts of $Pd(PPh_3)_4$ and copper iodide (**Table 2.2, entry 8**).[251] Unfortunately, the desired product **87a** was observed in none of these attempts and only the de-halogenation of iodoisoquinoline **76a** was observed.

II.3.2.4 Revising the strategy

II.3.2.4a Switching the cross-coupling electrophile and nucleophile?

Considering our unsuccessful attempts at using various classes of pyrimidinyl coupling partners for their cross-coupling with **76a–b** (**Section II.3.2.3**, **Table 2.4**), we briefly investigated if using an isoquinoline nucleophile and a 5-halopyrimidine would give better results. The cross coupling of aromatic boronic acids with 5-halopyrimidines has been reported by Merck for the synthesis of BTK inhibitor evobrutinib and its analogues (**Figure 2.38**).[252]

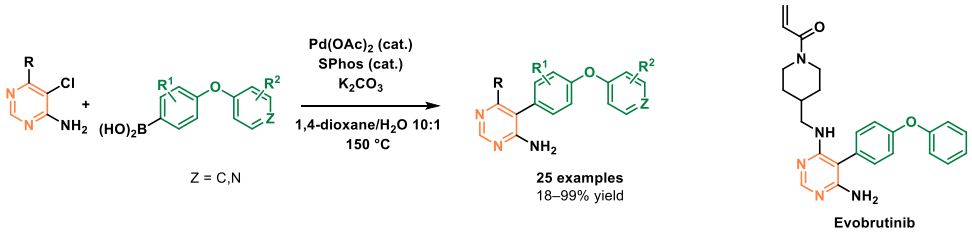
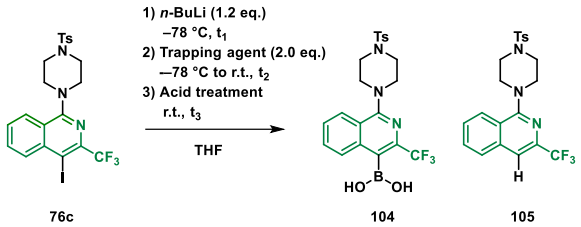


Figure 2.38: *The Suzuki-Miyaura coupling of 5-chloropyrimidines with aromatic boronic acids for the synthesis of BTK inhibitor Evobrutinib.*[252]

Our first efforts consisted in attempting to synthesise boronic acid **104** or boronic acid pinacol ester **107a** from isquinoline **76c** (**Table 2.5** and **Figure 2.39**). The lithium-halogen exchange and subsequent trapping method used in **Section II.3.2.1** for the synthesis of pyrimidinylboronic acid **83** has been reported for bicyclic fused pyridine compounds.[253] However, these techniques did not yield any of the desired boronic acid **104** in high enough purity when applied to **76c** (**Table 2.5**).



t_1	Trapping agent	t_2	Acid	t_3	104	105
5 min	$B(OiPr)_3$	30 min	10% H_2SO_4	5 min	Not observed	Detected
1 h	$B(OiPr)_3$	3 h	HCl (2N)	10 min	Complex mixture	Detected
1 h	$B(OiPr)_3$	3 h	HCl (2N)	16 h	Complex mixture	Detected
1 h	$B(OMe)_3$	3 h	HCl (1N)	5 min	Complex mixture	Detected

Table 2.5: *Attempts at generating boronic acid **104** by lithium-halogen exchange and subsequent boronate trapping.*

We therefore decided to attempt making boronic acid pinacol ester **107a** from isoquinoline **76c** using Miyaura's borylation reaction.[254,255] Iodosoquinoline **76c** was heated to 100 °C in 1,4-dioxane with bis(pinacolato)diboron (B_2pin_2), potassium acetate, and catalytic amounts of Pd(dppf)Cl_2 (dichloromethane adduct) (**Figure 2.39**). Although carrying out this experiment overnight gave 18% of desired product **106a** and only 4% of dehalogenation/proto-deborylation product **105** (with recovery of starting material), increasing the reaction time only resulted in the sole isolation of dehalogenation/proto-deborylation product **105**.

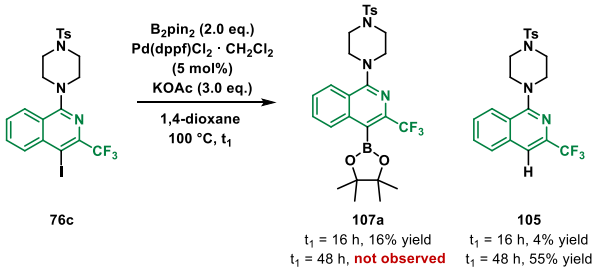


Figure 2.39: *The synthesis of boronic acid pinacol ester **107a** using Miyaura's borylation.[255]*

Interestingly, subjecting intermediate **71a** to these conditions allowed for longer reaction times with increased yields in product **106** (55–61%) (**Figure 2.40**). Optimal reaction times for substrate

71a were comprised between 3 and 5 days, with extending the reaction time to 10 days only marginally increasing the yield.

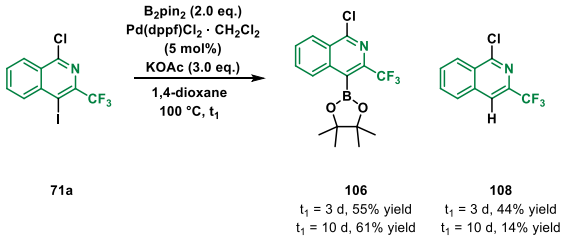
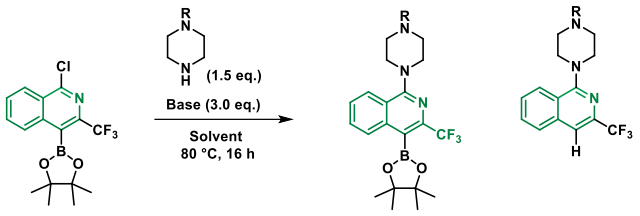


Figure 2.40: *The synthesis of boronic acid pinacol ester **106** using Miyaura's borylation.*[255]

Once obtained, chloroisoquinoline **106** could react with protected piperazines *via* SNAr to afford products **107a**–**b**.[242] However, in this case, the use of our usual potassium carbonate/*N,N*-dimethylformamide system did not yield any of the desired product **107a**, but only the deborylation product **105** (**Table 2.6, entry 1**). We therefore decided to stir isoquinoline **106** at 80 °C in dimethylsufloxide with *N,N*-diisopropylethyl amine and a protected piperazine.[256] In the case of 1-Ts-piperazine, product **107a** was isolated by either precipitation or column chromatography purification, the latter giving a much better yield than the former (71% *vs* 46%) (**Table 2.6, entries 2 & 3**). No deborylation of the SNAr product was observed in this case. The reaction of 1-Boc-piperazine with **106** to give product **107b** proved more difficult, with only 56% yield of product obtained, and higher proportions of proto-deborylation of the product were observed (21%) (**Table 2.6, entry 4**).



Entry	Product	R	Base	Solvent	Purification method	Yield	De-borylated by-product
1	**107a**	Ts	K_2CO_3	DMF	Precipitation	Not observed	50%
2	**107a**	Ts	DIPEA	DMSO	Precipitation	46%	Not observed
3	**107a**	Ts	DIPEA	DMSO	Column Chromatography	71%	Not observed
4	**107b**	Boc	DIPEA	DMSO	Column Chromatography	56%	21%

Table 2.6: *Using SNAr to add protected piperazines onto isoquinoline **106**.*

Recently reported Suzuki-Miyaura reactions involving bicyclic fused pyridinylboronic acid pinacol esters or pyrimidine electrophiles involve the use of microwave synthesis, including the synthesis of Bruton's Tyrosine Kinase inhibitor, evobrutinib (**Figure 2.38**).[252,257,258] Microwave reactions have been associated with milder conditions, reaction rate acceleration, increased yields, and reduced amounts of by-product formation.[259–262] We decided to apply microwave conditions to the Suzuki-Miyaura coupling of isquinolinyl boronic ester **107a** with halopyrimidine **82** (**Figure 2.41**). In a first attempt, **107a** and **82** were stirred at 120 °C for 1 hour in a 3:1 mixture of 1,4-dioxane and water, in the presence of sodium carbonate and catalytic amounts of $Pd(PPh_3)_4$.[257] In a second attempt, **107a** and **82** were stirred at 150 °C for 90 minutes in a 10:1 mixture of 1,4-dioxane and water with caesium carbonate, and catalytic amounts of palladium(II) acetate and SPhos.[258] Unfortunately, nothing but proto-deborylation product **105** was observed in both instances. We assumed that the failure of microwave conditions on our system indicated that succeeding in this strategy would be difficult and proceeded with investigating other options to troubleshoot the cross-coupling of our isoquinoline and pyrimidine precursors.

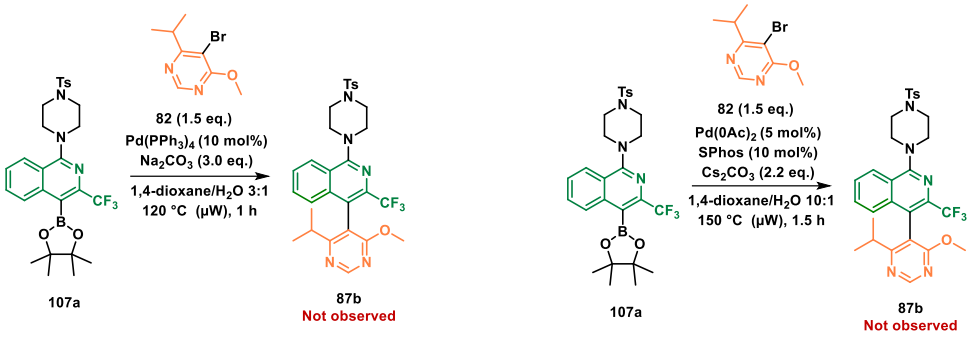


Figure 2.41: *Suzuki-Miyaura cross-coupling attempts using **107a** and **82** as coupling partners.*

II.3.2.4b Reducing the steric hindrance

The Suzuki-Miyaura coupling of the isoquinoline and pyrimidine moieties of target probe **52** so far proving difficult, we decided to explore whether reducing the steric hindrance of the system would increase our chances at successfully joining those two moieties. As mentioned in **Section II.3.2.3**, the generation of tetra-*ortho*-substituted biaryl systems using the Suzuki-Miyaura reaction remains a laborious endeavour. We decided to investigate if the coupling methodologies explored in **Section II.3.2.3** would allow to generate a tri-*ortho*-substituted system instead, either by removing the *ortho*-methoxy substituent on the pyrimidine coupling partner, or by removing the *ortho*-trifluoromethyl group on the isoquinoline coupling partner.

The synthesis of the *ortho*-isopropyl pyrimidinyl coupling partners was similar to that of our di-*ortho*-substituted pyrimidinyl coupling partners described in **Section II.3.2.2**, starting from 5-bromopyrimidine **108** (**Figure 2.42**). The silver-catalysed decarboxylative alkylation of **108** was performed following Qu and colleagues' procedure.[263] Pyrimidine **108** was stirred with isobutyric acid in a 1:1 mixture of dichloromethane and water at room temperature, in the presence of potassium persulfate and catalytic amounts of silver nitrate to yield isopropylpyrimidine **109**. The resulting bromopyrimidine was then subjected to lithium-halogen exchange using *n*-butyllithium at –78 °C in dry tetrahydrofuran (in conjunction with toluene in the case of the boronic acid

synthesis, 5:1 toluene/tetrahydrofuran). Trapping the resulting organolithium with triisopropyl borate and subsequently hydrolysising the *in situ* intermediate with aqueous hydrogen chloride yielded highly unstable boronic acid **110** in a complex mixture (presence confirmed by HRMS ESI$^+$),[246] which was immediately treated with MIDA in *N,N*-dimethylformamide at 90 °C but did not yield any of the desired MIDA boronate **111**.[95] Trapping with TIMSO and tributyltin chloride yielded lithium sulfinate **112** and organotin **113** respectively, with moderate yields (49% and 41% respectively).[239,240,248]

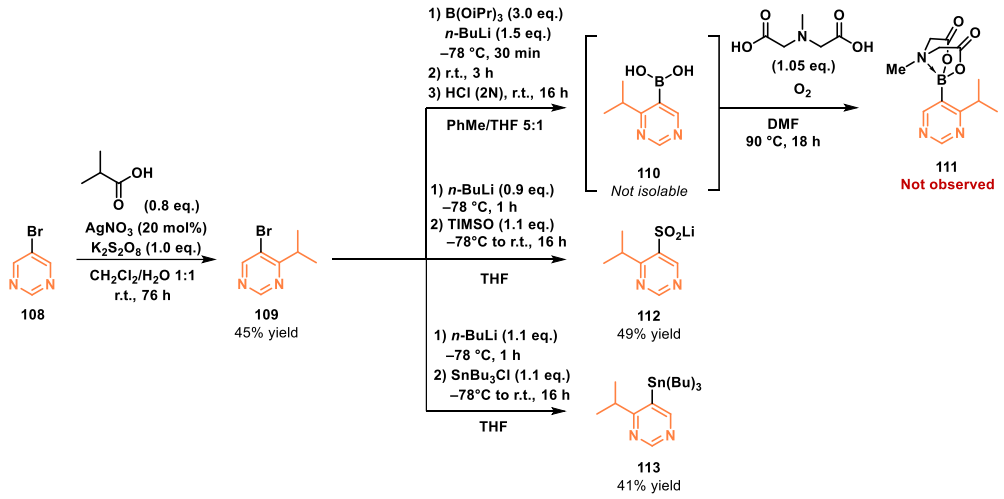


Figure 2.42: *Synthesis of mono-ortho-substituted pyrimidine coupling partners from 5-bromopyrimidine **108**.*

The mono-*ortho*-substituted isoquinoline partners **117a–e** were synthesised from isocarbostyril **114** (1-isoquinolinol), following an identical synthetic route to isoquinolines **76a–e** (**Figure 2.43**). Isocarbostyril **114** was first halogenated using either *N*-iodosuccinimide at 80 °C or *N*-bromosuccinimide at room temperature in *N,N*-dimethylformamide.[232] Resulting haloisoquinolines **115a–b** were chlorinated using neat phosphorus(V) oxychloride at 90 °C to yield chloroisoquinolines **116a–b** in high yields.[234]

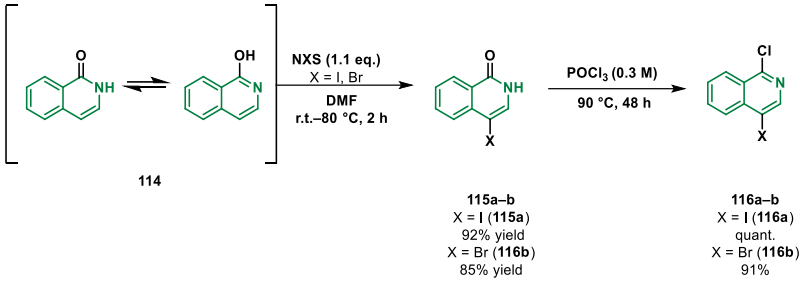
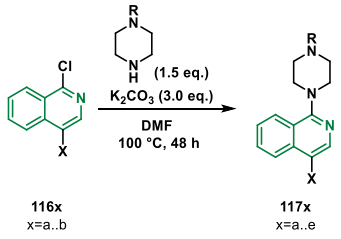


Figure 2.43: *Synthesis of mono-ortho-substituted isoquinolines **116a–b** from isocarbostyril **114**.*

Piperazines protected with either a Boc, Cbz or Ts group were then added onto chloroisoquinolines **116a–b** *via* SNAr. These substrates required higher temperatures and longer reaction times than their trifluoromethylated counterparts, with needing to be stirred for two days at 100 °C in *N,N*-dimethylformamide in the presence of potassium carbonate to observe similar yields. This observation can be explained by the absence of the electron withdrawing trifluoromethyl group, the presence of which rendered the isoquinoline ring electron-deficient and thus stabilised negative charges during the SNAr reaction. The results of these reactions were compiled in **Table 2.7**.

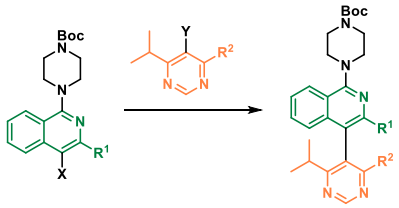


Product	X	R	Yield(s)
117a	I	Boc	71%
117b	I	Cbz	69–77%
117c	I	Ts	86%
117d	Br	Boc	51%
117e	Br	Ts	quant.

Table 2.7: *Addition of protected piperazines onto **116a–b** by SNAr reaction.*

Once obtained, the precursors were used in the same cross-coupling reactions described in **Section II.3.2.3** (**Table 2.8**). As the synthesis of *ortho*-isopropylboronic acid **110** and its MIDA derivative **111** failed, they could not be used in a Suzuki-Miyaura cross-coupling. The use of

Markovic's and co-workers' conditions on lithium sulfinate **112**,[239,240] and Stille conditions for organotin **113** did not yield to anything but dehalogenation of isoquinolines **76a–b** (**Table 2.8, entries 1–3**).[251] However, the absence of the trifluoromethyl group on isoquinolines **117a** and **117d** led to more promising results. Stirring isoquinoline **117a** with di-*ortho*-substituted pyrimidinylboronic acid **83** at 100 °C in a 2:1 mixture of 1,2-dimethoxyethane and water, in the presence of sodium carbonate, and catalytic amounts of Pd(dppf)Cl_2 (dichloromethane adduct), did not lead to anything but dehalogenation of the starting isoquinoline (**Table 2.8, entry 4**).[241] However, when isoquinoline **117d** was stirred with lithium sulfinate **85** at 150 °C in 1,4-dioxane in the presence of potassium carbonate, and a catalytic amount of palladium(II) acetate and tricyclohexylphosphine, we observed the formation of trace amounts of the desired coupling product **119** (**Table 2.8, entry 5**).[240] Eventually, by stirring organostannane **86** with iodoisoquinoline **117a** at 80 °C in *N,N*-dimethylformamide in the presence of caesium fluoride, and catalytic amounts of Pd(PPh_3)$_4$ and copper iodide, we observed the formation of the desired Stille coupling product **119** in moderate yield (66%) (**Table 2.8, entry 6**).[251] These last two experiments highlighted the trifluoromethyl group as the main hurdle to the coupling of our isoquinoline and pyrimidine moieties, most likely due to the steric encumbrance it generated. We decided to work without it for the remainder of the synthesis, with potential plans of reintroducing it at a later stage of the synthesis via C–H functionalisation, if need be.



Entry	Coupling	X	Y	R^1	R^2	Catalytic system	Additive(s)	Solvent	Temperature(s)	Expected product	Observation
1	"Willis"	Br	SO_2Li	CF_3	H	$PdOAc_2$ $P(t\text{-}Bu)_2Me.HBF_4$	K_2CO_3	1,4-dioxane	110/ 130 °C	118	Dehalogenation
2	"Willis"	Br	SO_2Li	CF_3	H	$Pd(OAc)_2$ PCy_3	K_2CO_3	1,4-dioxane	150 °C	118	Dehalogenation
3	Stille	I	$SnBu_3$	CF_3	H	$Pd(PPh_3)_4$ CuI	CsF	DMF	80/ 100/ 120 °C	118	Dehalogenation
4	Suzuki	I	$B(OH)_2$	H	OMe	$Pd(dppf)Cl_2.CH_2Cl_2$	Na_2CO_3	DME/H_2O 2:1	100 °C	119	Dehalogenation
5	"Willis"	Br	SO_2Li	H	OMe	$Pd(OAc)_2$ PCy_3	K_2CO_3	1,4-dioxane	150 °C	119	Trace amounts
6	Stille	I	$SnBu_3$	H	OMe	$Pd(PPh_3)_4$ CuI	CsF	DMF	80 °C	119	66% yield

Table 2.8: *Summary of the various sets of cross-coupling conditions attempted for the generation of tri-ortho-substituted biaryl systems.*

II.3.2.5 Synthesis of a less hindered probe

II.3.2.5a Mastering the Stille coupling

With Stille coupling product **119** in hand (see **Section II.3.2.4b**, **Table 2.8**), we optimised the work-up and purification methods to ensure Sn(IV) residues were efficiently removed without major erosion of the yield. Indeed, by stirring isoquinoline **117a** and organostannane **86** at 80 °C in *N,N*-dimethylformamide with caesium fluoride, and catalytic amounts of $Pd(PPh_3)_4$ and copper iodide, washing the resulting crude mixture with generous amounts of aqueous potassium fluoride (1 M solution) and purifying it *via* two consecutive flash column chromatography purifications, we were able to isolate product **119** in 98% yield (**Figure 2.44**).[251]

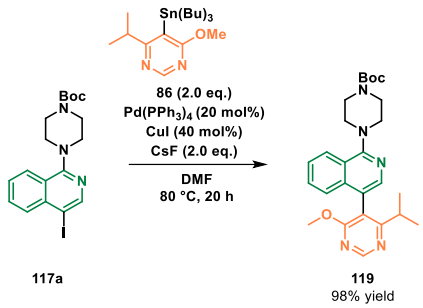


Figure 2.44: *Stille coupling of **117a** and **86**.*

By eluting **119** on a chiral HPLC column, we identified it as a racemic mixture of two atropisomers. We thus decided to evaluate the half-life of racemisation of **119** by separating its two enantiomers by chiral semi-preparative HPLC. One of the resulting enantioenriched samples was dissolved in *meta*-xylene and heated to 80 °C for 6 hours. Withdrawing aliquots at regular intervals allowed us to observe a decrease in enantiomeric ratio, from 100:0 to 74:26 (**Figure 2.45**). Plotting $ln\frac{1}{ee} = f(t)$ allowed us to calculate k_{rac} = 3.97 × 10 $^{-5}$ s^{-1}, corresponding to $t_{1/2}^{rac}$ = 4.9 hours at 80 °C and a rotational barrier ($\Delta G_{353}^{\ddagger}$) of 28.4 kcal/mol. This half-life of racemisation, though probably much longer at biological temperatures (around 37 °C), might warrant further derivatisation work to increase the steric bulk around the chiral axis on compound **119** and ensure it would not racemise when used as a therapeutic agent.

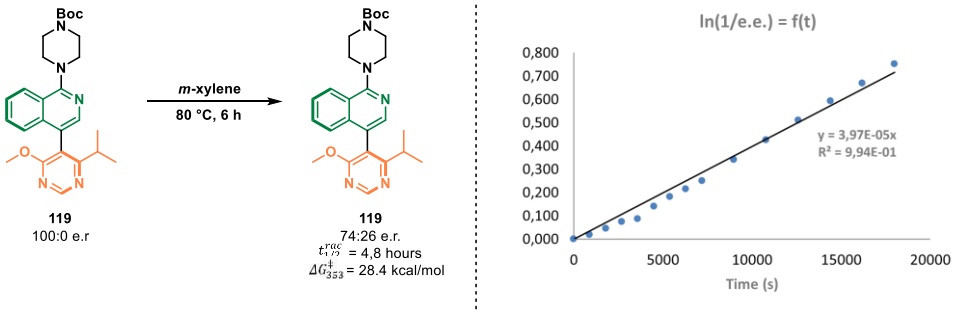


Figure 2.45: *Experiment to determine the half-life of racimesation of compound **119**.*

II.3.2.5b Completing the synthesis

The isoquinoline and pyrimidine moieties finally coupled, we proceeded with deprotecting piperazine **119** and installing the acrylamide warhead to generate probe **120** (**Figure 2.46**). The Boc deprotection of piperazine **119** was achieved by stirring in a hydrogen chloride solution in methanol (1.5 M) at room temperature. The resulting crude mixture was transferred into dichloromethane and stirred with acryloyl chloride in the presence of triethylamine at room temperature, to yield alternative probe **120** in moderate to high yields (61–89% over two steps).[243]

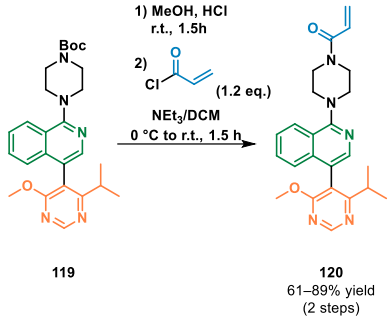


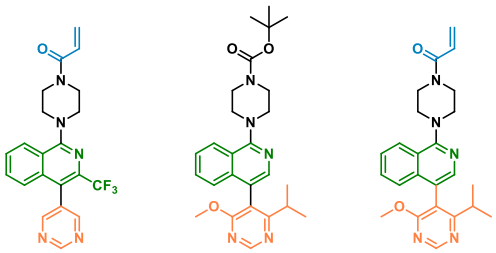
Figure 2.46: *Finalising the synthesis of alternative probe **120**.*

Alternative probe **120** was therefore obtained by a convergent synthetic route, with a longest linear sequence of 8 steps (ethyl isobutyrylacetate **78** to probe **120**), and overall yields ranging from 6 to 41%.

II.3.2.6 Preliminary biochemical and physiochemical analysis

With the help of Neville McLean, compound **120** was submitted to AstraZeneca, along with "control" compounds **75** and **119** for preliminary biochemical and physiochemical analysis. Mean solubility, plasma protein binding, logD, clearance and KRas G12C i*n vitro* IC_{50} were determined using Kettle and co-workers' methods.[264] The results from these preliminary studies were compiled in **Table 2.9**.

Compound **120** was more soluble in DMSO than both unsubstituted pyrimidine **75** and its non-covalent counterpart **119** (252 µM *vs* 4 and 62 µM respectively), however, this solubility was three orders of magnitude lower than that of sotorasib, which is around 178 mM in DMSO (90–100 mg/mL).[265,266] Compound **120** showed similar plasma protein binding and lipophilicity to sotorasib, with both molecules being reported to be 89% protein-bound and of logD/logP comprised between 3 and 4 (3.30 and 4.11 respectively).[265,266] However, the clearance (human liver microsomes) of all of our compounds was much higher than that of sotorasib,[265] and no tangible activity in KRas G12C biochemical assays was detected.



75 **119** **120**

Compound	Mean solubility DMSO (mM)	Mean protein binding (% free)	Mean IC_{50} (µM)	Median CL_{int} (µL/min/mg)	Mean LogD
75	0.004	-	> 100	> 300	3.10
119 (rac)	0.062	0.20	> 100	87.1	5.10
120 (rac)	0.252	11	> 100	126	3.30
Sotorasib (literature)	178	11	0.027	17	4.11*

Table 2.9: *Preliminary biochemical and physiochemical analysis results.*
**logP in this case.*

These disappointing results confirmed further optimisation and SAR work would be required to generate active atropisomeric biarylpyrimidine-based KRAS G12C covalent inhibitors.

II.3.3 Towards the enantioselective synthesis of probe 52

In parallel with our studies aiming at synthesising **52** as a racemic mixture, we also investigated potential routes to generate enantioenriched samples of **52** (see **Section II.2.2**). For reading clarity, **Figure 2.27**, depicting the enantioselective retrosynthetic approach to probe **52**, is repeated below.

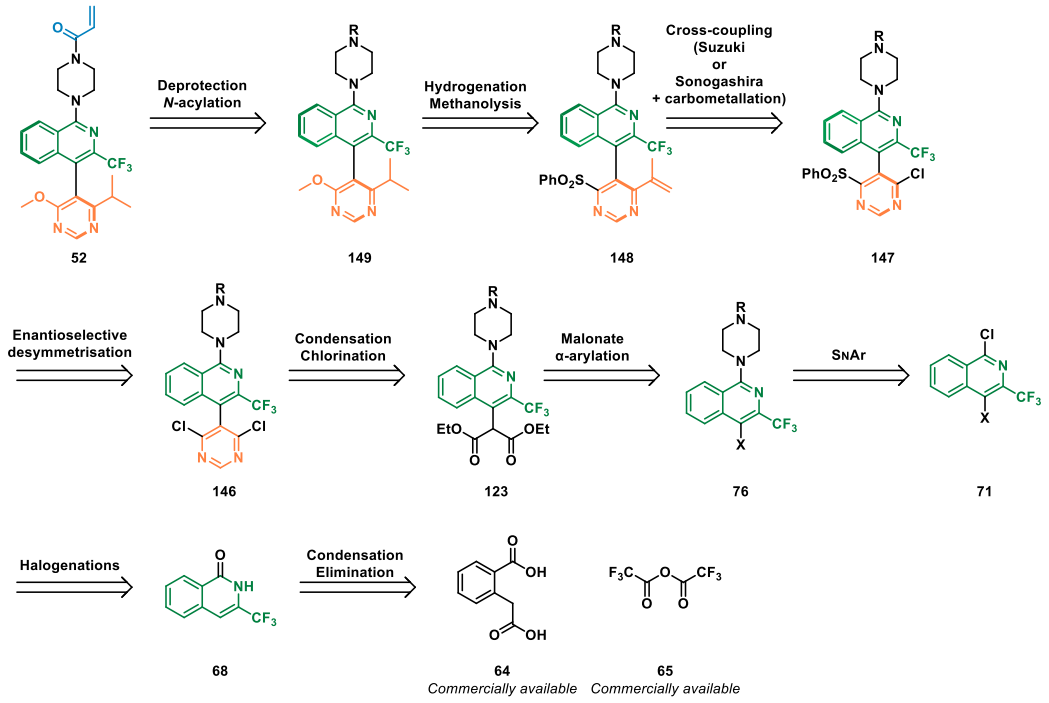


Figure 2.27: *Retrosynthetic approach of enantioenriched **52**.*

II.3.3.1 Issues with the malonate route

Linchpin intermediates **71a–b** in hand, the main difference with our racemic retrosynthetic approach and our enantioselective retrosynthetic approach resided on the moiety that would be coupled onto it. If the pyrimidine ring could already be equipped with the desired substituents prior to the coupling in our racemic synthesis, it would have to be pro-atropisomeric in the case of

the enantioselective synthesis. This would be achieved by generating dichloropyrimidine intermediate **146** (**Section II.3.3**, **Figure 2.27**), ready for desymmetrisation using Armstrong's method.[71]

As exhibited in **Part I**, our privileged method for the synthesis of biaryl dichloropyrimidine derivatives involved the preliminary α-arylation of a malonate. We thus decided to investigate this transformation in the context of our synthesis. Similarly to our preliminary study in **Section II.3.2.1**, we explored whether to derivatise intermediate **71a** at the chloro or at the iodo site first. Derivatisation at the iodo site *via* α-arylation of dialkylmalonates **16a–b** using compound **71a** was carried out by following a general procedure involving stirring in 1,4-dioxane at 50 °C in the presence of caesium carbonate, and catalytic amounts of copper iodide and 2-picolinic acid (**Figure 2.47**).[86] Compound **121a**, resulting from reacting malonate **16a**, was obtained in moderate to high yields (61–84%). Compound **121b**, resulting from reacting malonate **16b**, was obtained in quantitative yield. However, the subsequent treatment of diethylmalonate **121a** with 1-tosylpiperazine hydrochloride and 4-dimethylaminopyridine (4-DMAP) in dimethylsulfoxide at 100 °C yielded amide **122a** instead of the expected SNAr product (56% yield) (**Figure 2.43**).[256] This observation allowed us to retrospectively realise that compounds **121a–b** were in fact the products of the subsitution of intermediate **71a** at the chloro site, instead of the iodo site (which was confirmed by the presence of characteristic C–I signals on ^{13}C NMR on compounds **121a–b** and **122a–b**). This came as a surprise to us as transition-metal-catalysed reactions had privileged the iodo site to the chloro site in previous instances (see **Section II.3.2.1**). Nonetheless, the SNAr of the nucleophilic deprotonated malonates **16a–b** onto the C–Cl bond might have prevailed over the oxidative addition of the copper(I) enolate complexes onto the C–I bond, which is normally observed in such a reaction.[86] This was probably due to the steric encumbrance caused by the trifluoromethyl group around the C–I bond (as observed in **Sections II.3.2.4** and **II.3.2.5**). In the

case of diisopropyl malonate **121b**, no formation of the amide was obtained, highlighting the higher stability of this substrate to nucleophilic attack.

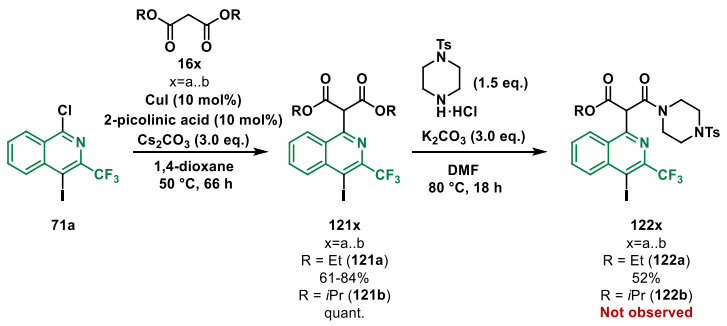


Figure 2.47: *Attempts to synthesise malonate intermediates from intermediate **71a** by derivatising the iodo site first.*

Performing the SNAr reaction of 1-Ts-piperazine hydrochloride with **71a** first, and the subsequent attempt at α-arylation of diethylmalonate did not give any formation of the desired arylation product **123** (**Figure 2.48**). In this instance, the chloro site having been already derivatised, we assumed the accessibility of the iodo site would be slightly higher. However, the transformation still not taking place, we were comforted in the idea that the trifluoromethyl group might play a part in the reaction not proceeding.

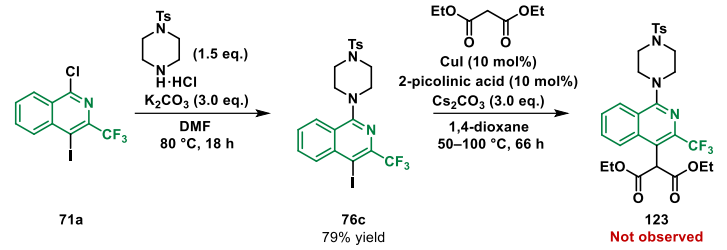


Figure 2.48: *Attempts to synthesise malonate intermediates from intermediate **71a** by derivatising the chloro site first.*

Having learned from our previous experience with cross-couplings in our system (see **Section II.3.2.4**), we decided to examine whether the trifluoromethyl group had been a hindrance to the α-arylation of dialkylmalonates with **71a**. We carried out the reaction using non 3-substituted

iodoisoquinoline **116a** and diethylmalonate **16a**, stirred at 50 °C in 1,4-dioxane with caesium carbonate and catalytic amounts of copper iodide and 2-picolinic acid (**Figure 2.49**).[86] These conditions yielded diethylmalonate **124** in almost quantitative yield (99%), confirming our hypothesis that the bulk of the trifluoromethyl group was obstructing the iodo site in our previous attempts. However, subsequent treatment with 1-Ts-piperazine hydrochloride and potassium carbonate in *N,N*-dimetylformamide at 80 °C yielded amide **125** instead of the expected SNAr product (20% yield).

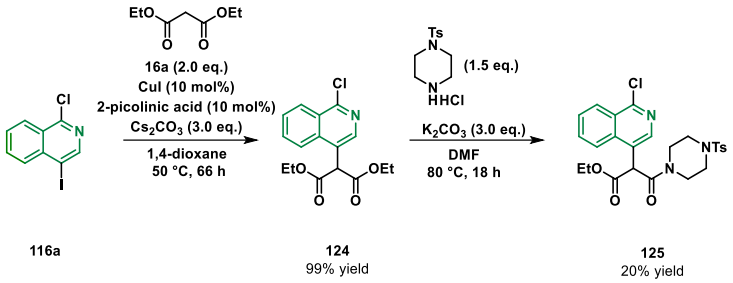


Figure 2.49: *Attempts to synthesise malonate intermediates from intermediate **116a** by derivatising the iodo site first.*

We therefore decided to carry out the malonate arylation on compounds **117a–c**, generated in **Section II.3.2.4b** (**Figure 2.50**). Boc-protected piperazine **126a** and Cbz-protected **126b** were obtained in moderate yields (56% and 51% respectively), but with high recovery of starting material (92% and 84% brsm yield respectively). The formation of Ts-protected piperazine **126c** was not observed.

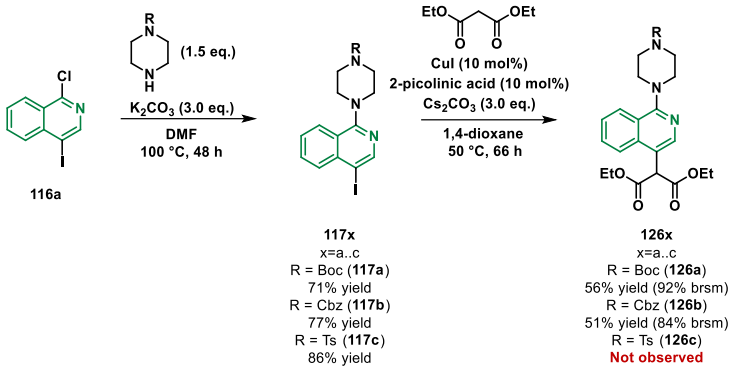


Figure 2.50: *Attempts to synthesise malonate intermediates from intermediate **116a** by derivatising the chloro site first.*

Considering the synthesis of a pyrimidine ring from malonates would involve acidic treatment, we decided to use Cbz-protected piperazine **126c** for the remainder of the synthesis (**Figure 2.51**). Compound **126c** was stirred at 80 °C in a 3:2 mixture of methanol and tetrahydrofuran, in the presence of *in situ* generated sodium methoxide and formamidine hydrochloride. The resulting crude mixture was precipitated in concentrated hydrochloric acid and the filtrate was also isolated and worked up. The resulting solids were treated with phosphorus(V) oxychloride at 90 °C. After isolation of the various species generated by these transformation, none of them were identified as the desired dichloropyrimidine **127b**. The transformation was attempted several times but the desired product was never observed. Several factors could be at the origin of such a failure, for example, the drastic changes in pH prior to chlorination could be protonating the isoquinoline ring and/or deprotonating the hydroxy groups in suggested intermediate **127c**, thus generating zwitterionic species (**Figure 2.51**).[49] This would render the precipitation step or even the isolation of the product from the recovered filtrate difficult.

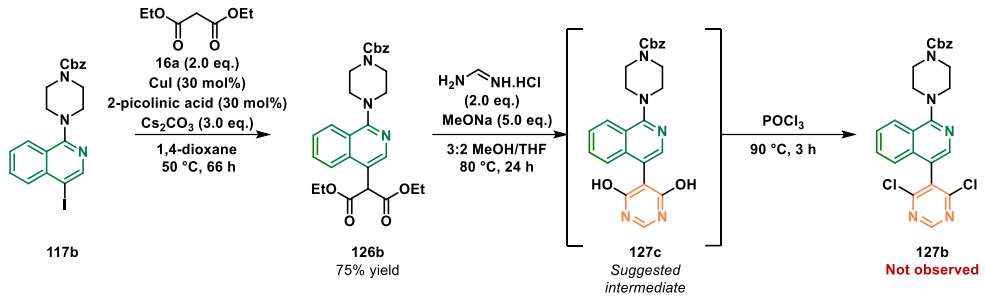


Figure 2.51: *Attempting to synthesise dichloropyrimidine **127** from malonate **126b**.*

II.3.3.2 Direct coupling of a dichloropyrimidine on a less hindered isoquinoline?

II.3.3.2a Pyrimidine nucleophiles and isoquinoline electrophiles

Considering attempting to generate a pyrimidine ring from a di-alkyl(isoquinolinyl)malonate such as compound **126b** (**Figure 2.51**) proved difficult, we hoped to exploit our previous successes at cross-coupling chemistry (see **Sections II.3.2.1** and **II.3.2.4b**) to directly couple a dichloro (or dihydroxo) pyrimidine onto our isoquinoline derivatives. Our first investigations consisted in trying to couple a nucleophilic pyrimidine to a haloisoquinoline, such as isoquinolines **117a–c** (**Section II.3.2.4b**, **Table 2.7**). We therefore attempted to apply the conditions we used in **Section II.3.2.2** to synthesise the desired pyrimidinyl nucleophilic coupling partners (**Figure 2.52**).[240,246,248,254] Unfortunately, neither 5-bromo-4,6-dichloropyrimidine **128a** or 5-bromo-4,6-dihydroxopyrimidine **129b** were readily turned into their boronic ester, boronic acid, lithium sulfinate or tributylstannane counterparts.

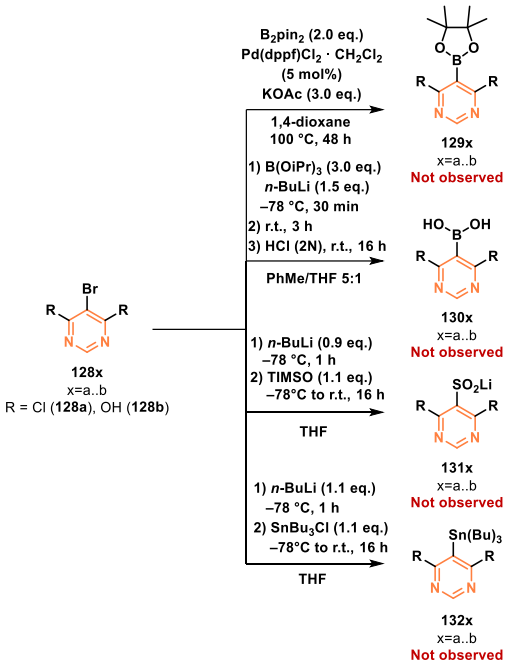


Figure 2.52: *Attempts at applying previously successful methodologies to synthesise pyrimidinyl coupling partners to compounds **128a–b**.*

Knochel *et al.* reported in 2013 the use of acidic aryls such as 4,6-dichloropyrimidine **133** for the development of organozinc species, using their base "TMPZnOPiv·LiCl" **137** (**Figure 2.53**).[267] The resulting organometallics were then used in several Negishi cross-coupling reactions with various aryl and vinyl electrophiles to yield the corresponding coupling products in moderate to high yields, with the examples involving pyrimidinylzinc pivalate **134** being especially successful (**Figure 2.53**). Organozincs hold a special place amongst organometallics as they are reputed to be compatible with multiple functional groups.[268] We therefore decided to try and use compound **134** for the synthesis of dichlorpyrimidine **127a** (see **Figure 2.55** below).

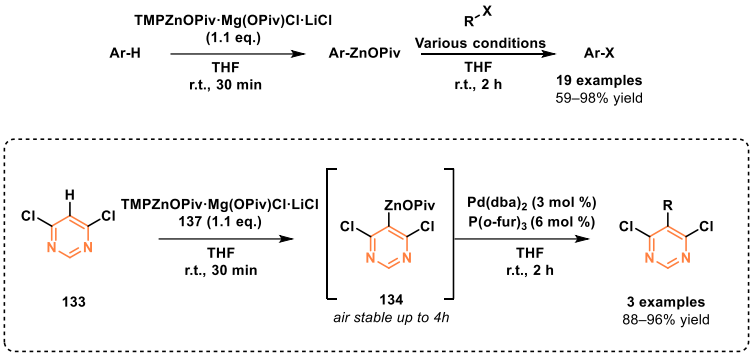


Figure 2.53: *Knochel and co-workers' use of TMPZnOPiv·LiCl **137** to generate organozincs for Negishi couplings.*[267]

The first step of this synthesis involved making Knochel and co-workers' base **137** (**Figure 2.54**). Following a literature procedure,[269] we took Turbo Grignard at room temperature in tetrahydrofuran and slowly added 2,2,6,6-tetramethylpiperidine **135**. The reaction mixture was stirred until the gas evolution stopped and the concentration of the resulting solution of **136** in tetrahydrofuran was determined to be 1.0 M upon titration. Subsequent treatment with zinc pivalate in tetrahydrofuran at room temperature yielded TMPZnOPiv·LiCl **137** as a 0.63 M solution in tetrahydrofuran.[267]

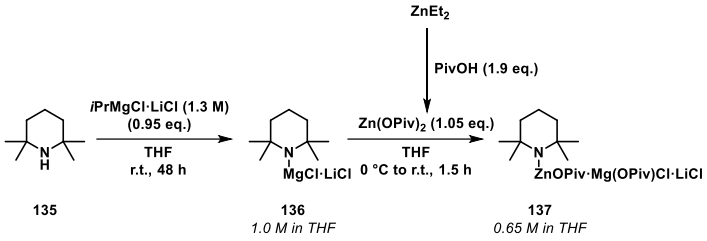


Figure 2.54: *The synthesis of TMPZnOPiv·LiCl **137**.*[267,269]

Adding base **137** to a solution of 4,6-dichloropyrimidine **133** in tetrahydrofuran at room temperature yielded organozinc **134** (**Figure 2.55**).[267] To test the reactivity of **134**, we dissolved it in tetrahydrofuran and stirred it at room temperature with literature substrate 4-iodothioanisole **138**, and catalytic amounts of bis(dibenzylidenacetone)palladium(0) (Pddba$_2$), and tris(2-furyl)phosphine (P(*o*-fur)$_3$). Negishi cross-coupling product **139** was obtained in 15% yield

(*vs.* 91% in the literature).[267] This result, however disappointing, testified for the reactivity of our intermediate **134**. We thus took **134** and isoquinoline **117a** in tetrahydrofuran and stirred it at room temperature in the presence of catalytic amounts of bis(dibenzylidenacetone)palladium(0) ($Pddba_2$) and tris(2-furyl)phosphine (P(*o*-fur)$_3$) (**Figure 2.55**). However, no reaction was observed and this strategy was abandoned.

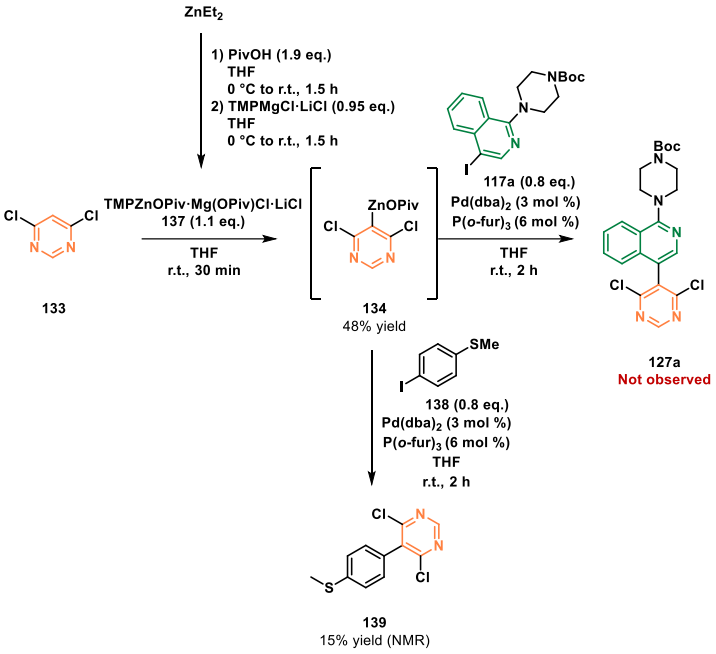


Figure 2.55: *Attempting to synthesise dichloropyrimidine **127a** using Knochel and colleagues' methodology.*[267]

II.3.3.2b Isoquinoline nucleophiles and pyridimidine electrophiles

Since pyrimidine-derived nucleophilic coupling partners proved very difficult to synthesise, we briefly investigated whether using isoquinoline nucleophiles in our cross-couplings would be easier to generate pro-atropoisomeric dichloropyrimidines **127a–c** (see **Figure 2.57**).

Considering our previous success at making isoquinolinylboronic esters (see **Section II.3.2.4a**), we decided to investigate this option first (**Figure 2.56**). Bromoisoquinoline **116b** and B_2pin_2 were stirred in 1,4-dioxane at 100 °C with catalytic amounts of $Pd(dppf)Cl_2$ (dichloromethane adduct) and potassium acetate to yield boronic acid pinacol ester **140**, which was immediately dissolved in

dimethylsulfoxide in the presence of *N,N*-diisopropylethylamine and 1-Boc-piperazine without further purification. The resulting mixture was heated at 80 °C to yield boronic ester **141** in low yield (13% over two steps). Xu *et al.* reported their ability to drive the cross-coupling of boronic acids onto the bromo site of pyrimidine **142a** by using specific solvent systems, we therefore decided to apply their conditions to our system.[270] Upon reaction with bromopyrimidine **142a** at 120 °C in a 4:1:1 mixture of toluene, ethanol and water, in the presence of potassium carbonate, and catalytic amounts of $Pd(PPh_3)_4$, compound **141** yielded compound **143**.[270] Compound **143** resulted from of the cross-coupling of **141** with **142a** at one of the two chloro positions and the subsequent SNAr reaction of ethanol with the remaining C–Cl bond. The desired dichloropyrimidine **127a** was not observed. Removing ethanol from the mixture led to no reaction at all. This result showed, however, that isoquinoline-derived boronic esters such as **141** are potential coupling partners to halopyrimidines. Nonetheless, considering the low-yields obtained in the synthesis of **141**, we decided not to explore this strategy further.

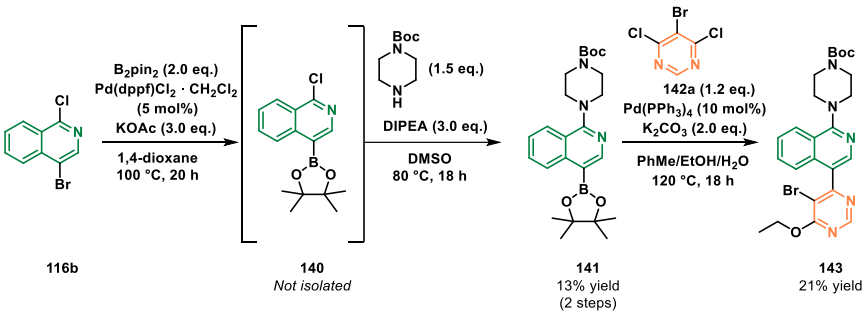


Figure 2.56: *Isoquinolinyl boronic esters in Suzuki-Miyaura reactions for the synthesis of a pro-atropisomeric biarylpyrimidine.*

The Stille reaction having established itself as a reliable cross-coupling method in our system, we decided to probe whether isoquinoline-derived tributylstannane **144** and bromopyrimidines **142a–b** would be amenable to it (**Figure 2.57**). Bromoisoquinoline **117e** was lithiated *via* lithium-halogen exchange using *n*-butyllithium in anhydrous tetrahydrofuran at –78 °C and the *in*

situ generated organolithium was trapped using tributyltin chloride at room temperature.[248] Tibutyltinstannane **144** was obtained in rather low yield (17%). When dissolved in *N,N*-dimethylformamide with bromopyrimidines **142a–b** in the presence of caesium fluoride and, catalytic amounts of $Pd(PPh_3)_4$ and copper iodide, compound **144** did not yield any of the desired products.[251]

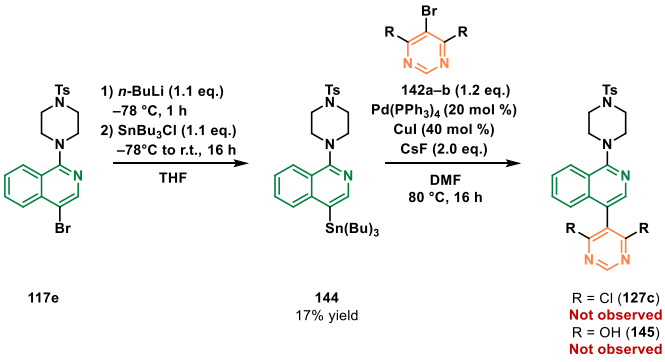


Figure 2.57: *Isoquinolinyl stannanes in Stille reactions for the synthesis of a pro-atropisomeric biarylpyrimidine.*

Considering the apparent difficulty of the synthesis of dichloropyrimidines **127a–c**, we decided to focus on the synthesis and optimisation of probes **52** and **120** *via* racemic routes for the remainder of this project.

II.3.4 The racemic synthesis of an optimised probe

II.3.4.1 Designing an optimised probe

In light of the disappointing results in the preliminary biochemical and physiochemical tests carried out by the researchers at AstraZeneca on probe **120** (see **Section II.3.2.6**), we decided to investigate whether we could rework its design to potentially increase its potency.

Using our KRas G12C covalent docking model (see **Section II.2.1**), we decided to compare docked probe **120** to sotorasib (AMG-510), taken in its X-Ray cocrystal with GDP and KRas G12C (PDB code: 6OIM) (**Figure 2.58B**).[205] Compared to initial probe **52** (**Figure 2.58A**), the absence of a trifluoromethyl group to restrict the rotation of the pyrimidine ring on probe **120** allows it to sit out of place. This might lead to different interactions with the H95 cryptic pocket in *in vitro* models, and explain why **120** did not show a satisfying potency on KRas G12C in biochemical assays. As evidenced in **Section II.1.4.3**, the numerous Van der Waals interactions developed in the H95 pocket are crucial to the high potency of sotorasib.[25]

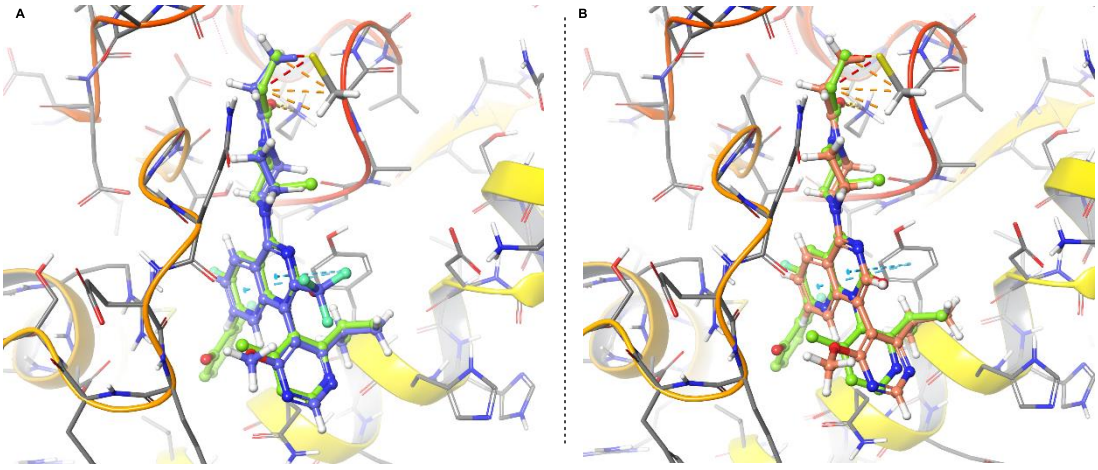


Figure 2.58: ***(A)*** *Docked structure of model probe* ***52*** *(blue), compared with AMG-510 in its cocrystal with KRas (green, PBD code: 6OIM).*[25] ***(B)*** *Docked structure of less hindered probe* ***120*** *(orange), compared with AMG-510 in its cocrystal with KRas (green, PDB code: 6OIM).*[25]

If reintroducing a 3-trifluoromethyl group in the probe might help with this issue, the steric encumbrance around the chiral axis makes this position difficulty accessible. Additionally, the trifluoromethyl group considerably reduced reactivity at the iodo/bromo sites on intermediates **71a–b** and **76a–c** (see **Section II.3.2.3** and **Section II.3.3.1**). We therefore decided to investigate whether we could increase favourable interactions in the S-IIP area of KRas G12C, before studying trifluoromethylation reactions. A common feature of ARS-1620 and sotorasib are the phenol ring, that establishes a hydrogen bond with glutamic acid 63 (E63) in the S-IIP.[205] Even though phenol groups are susceptible to oxidation and glucuronidation,[271] the developments of agradasib and sotorasib showed a replacement of such moieties by typical bioisosteres such as benzopyrazoles led to a reduction in activity and cellular permeability.[25,211] In the case of ARS-1620 and sotorasib, the phenol group was considered as the most optimal group to maximise interactions in the S-IIP of KRas G12C. We therefore decided to design probe **150** (**Figure 2.59**), which would majorly be inspired by probe **120**, but would showcase this additional fluorophenol group.

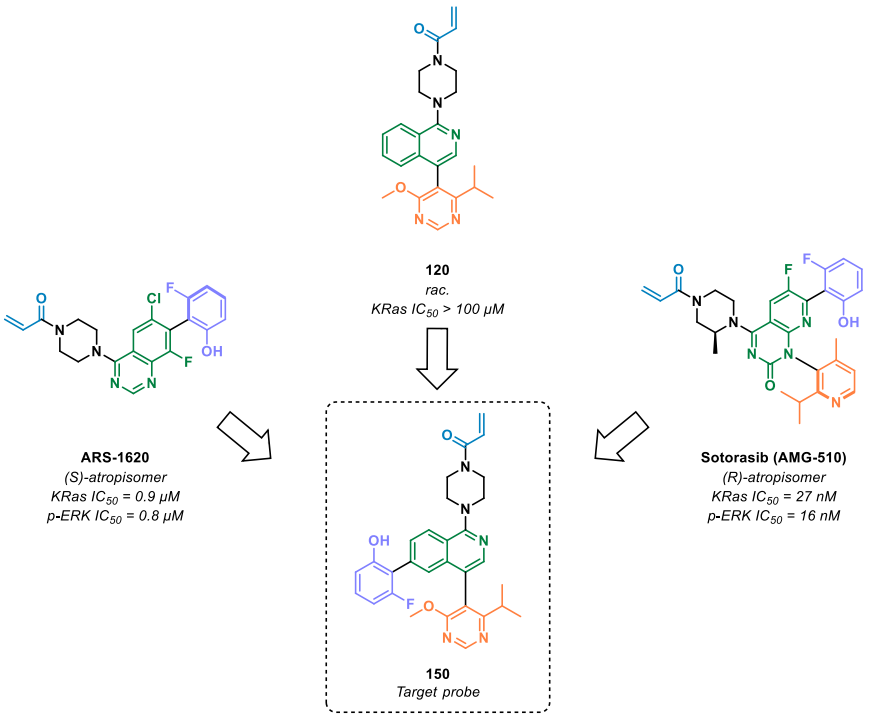


Figure 2.59: *Designing target probe **150** taking inspiration from ARS-1620 and sotorasib.*

Docking our newly-designed probe against sotorasib in its X-Ray cocrystal with GDP and KRas, we still observed the effect of the absence of a trifluoromethyl group (though at a slightly lesser extent) (**Figure 2.60**). However, **150** should indeed develop new interactions with the S-IIP thanks to the newly-introduced fluorophenol group which would hence grant probe **150** a higher affinity for KRAs G12C than probe **120**. Similarly to probe **52**, the most active enantiomer for probe **150** is expected to the (*S*) atropisomer.

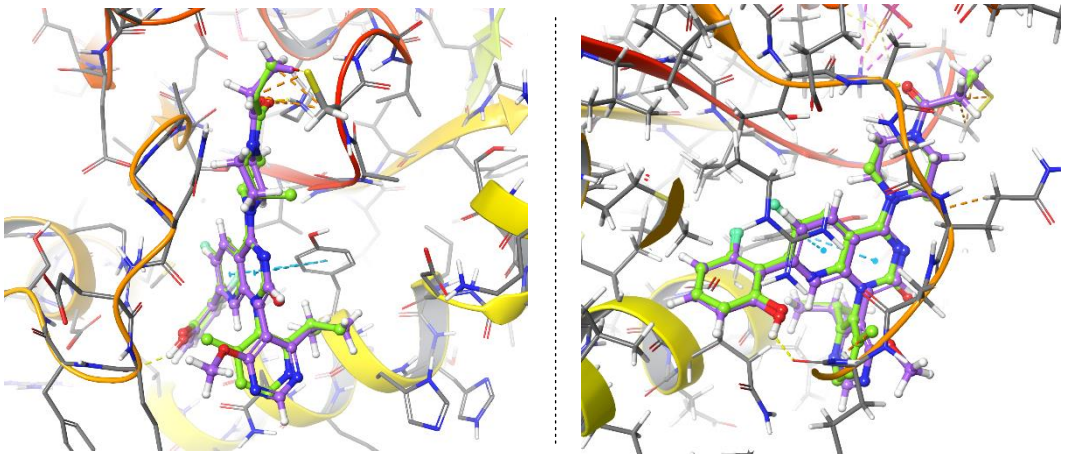


Figure 2.60: *Docked structure of optimised probe **150** (purple), compared with AMG-510 in its cocrystal with KRas (green, PBD code: 6OIM) at two different angles.*[25]

The retrosynthetic approach to probe **150** was similar to that of probe **120** (**Figure 2.61**), and consisted of a convergent route using key linchpin intermediate **164**, onto which a protected piperazine and di-*ortho*-substituted pyrimidine **86** would be sequentially anchored by SNAr and Stille coupling, respectively. The main new key steps would include the introduction of the protected phenolic coupling partner on intermediates **155a–b**, and the deprotection of said phenol in the later stages of the forward synthesis. The synthesis of intermediates **156a–b** is reported in the literature using commercially available acyl chlorides **154a–b**.[272]

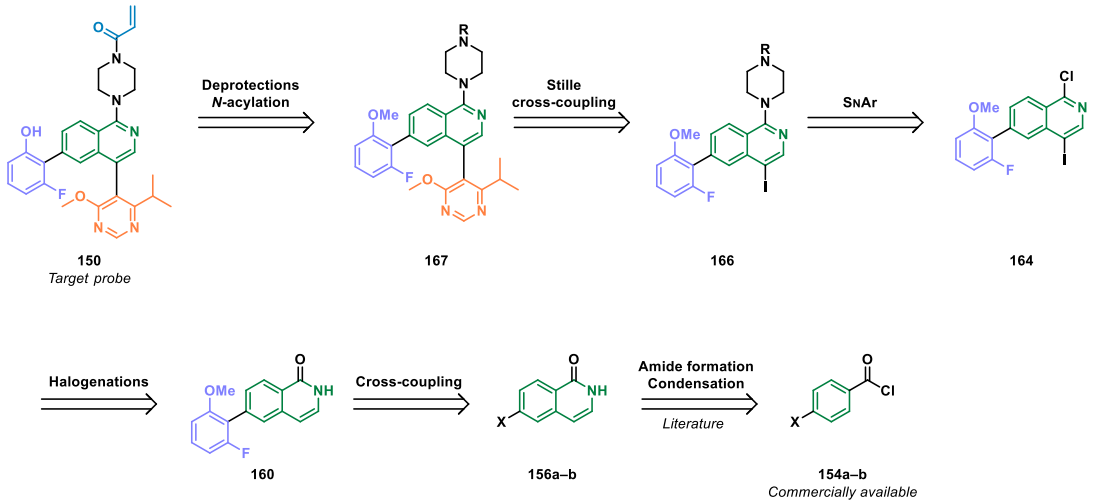


Figure 2.61: *Retrosynthetic approach of racemic probe **150**.*

II.3.4.2 The synthesis of a new linchpin intermediate

II.3.4.2a Synthesis of 6-haloisoquinolinones 156a–b

In 2011, the Fagnou[273] and Glorius[274] groups reported the synthesis of isoquinolin-2-one and dihydroisoquinolin-2-one derivatives *via* rhodium(III)-catalysed C–H activation/annulation sequences utilising an oxidising directing group (**Figure 2.62A** & **Figure 2.62B**). In 2014, Webb and Marsden at the University of Leeds, in collaboration with Raw at AstraZeneca, took inspiration from these transformations to use vinyl esters as acetylene equivalents in a rhodium(III)-catalysed directed C–H activation/annulation sequence to synthesise multiple *N*-heterocycles, including 16 isoquinolinones (**Figure 2.62C**).[272]

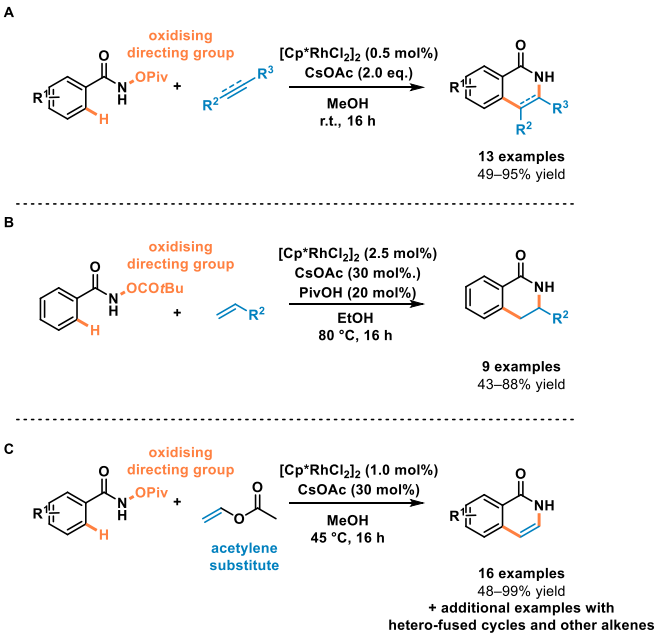


Figure 2.62: *Literature reports of rhodium(III)-catalysed C–H activation/annulation sequences using an oxidising activating group:* ***(A)*** *As reported by Fagnou et al.*[273] ***(B)*** *As reported by Glorius et al.*[274] ***(C)*** *As reported by Raw et al.*[272]

We decided to replicate Webb and co-workers' synthesis of 6-haloisoquinolinones **156a–b**, so that we could use them in cross cross-coupling reactions to generate compound **160** (**Section II.3.4.1**, **Figure 2.61**). The first step of this synthesis involved synthesising *O*-(pivaloyl)hydroxylammonium chloride **153** from *tert*-butylhydroxycarbamate **151** (**Figure 2.63**).[273,275] Hydroxycarbamate **151** was refluxed in chloroform at room temperature in the presence of pivalic anhydride and the resulting *tert*-butyl (pivaloyloxy)carbamate **152** was stirred at room temperature for several days in a 2 M hydrogen chloride in anhydrous diethyl ether solution to afford *O*-(pivaloyl)hydroxylammonium chloride **153** in yields ranging from 7 to 45% (22% average).

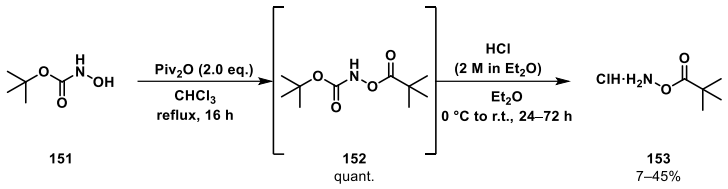


Figure 2.63: *The Synthesis of O-(pivaloyl)hydroxylammonium **153**.*[272,274,275]

Commercially available acyl chlorides **154a** and **154b** were then each suspended with **153** and triethylamine in tetrahydrofuran and stirred at 0 °C to yield *N*-(pivaloyl)benzamides **155a** and **155b** respectively, in moderate yields (58–69% for **155a** and 57% for **155b**) (**Figure 2.64**).[272] Compounds **155a** and **155b** were each suspended in methanol with vinyl acetate and stirred at 45 °C in the presence of catalytic amounts of pentamethylcyclopentadienylrhodium(III) chloride dimer ($[Cp^*RhCl_2]_2$) and caesium acetate to yield 6-haloisoquinolines **156a** and **156b** respectively, in moderate yields (52–66% for **156a** (lit. yield 83%) and 67% for **156b** (lit. yield 70%)).

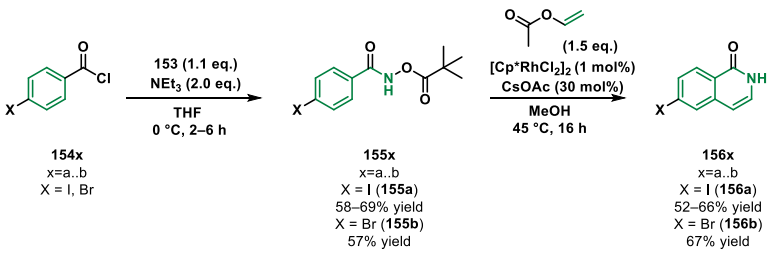


Figure 2.64: *The synthesis of 6-haloisoquinolinones **156a–b**.*[272]

II.3.4.2b Adding the phenol ring

The Suzuki-Miyaura cross-coupling has been reported as the method of choice to tether the phenol ring onto prospective KRas G12C inhibitors. When introduced at later stages of the synthesis, the phenolic acids can be used, as illustrated in **Section II.2.2** with the synthesis of sotorasib analogues by Lanman *et al.* (**Figure 2.65A**).[25,82] However, it is recommended to use the anisole-derived boronic acids when the group is introduced at earlier stages of the synthesis, an

anisole moiety being less reactive than its phenolic counterpart, as illustrated by Liu *et al.* (**Figure 2.65B**).[276]

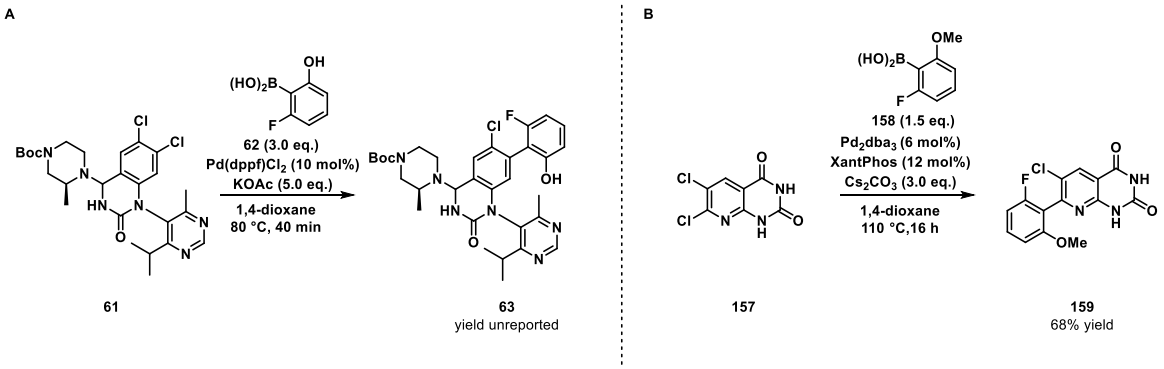


Figure 2.65: *Suzuki-Miyaura cross-coupling conditions to introduce the phenol/anisole moiety:* ***(A)*** *As described my Lanman et al.*[25] ***(B)*** *As described by Liu et al.*[276]

We decided to apply the conditions described by both Lanman *et al.* and Liu *et al.* to our system, using 6-haloisoquinolinones **156a–b** and (2-fluoro-6-methoxyphenyl)boronic acid **158** (**Figure 2.66A**). When **156a–b** and **158** were stirred in 1,4-dioxane at 80 °C with potassium acetate and catalytic amounts of Pd(dppf)Cl_2, the desired cross-coupling product **160** was not observed.[25] Similarly, compound **160** was not observed either when **156a–b** and **158** were stirred in 1,4-dioxane at 110 °C with caesium carbonate, and catalytic amounts of Pd_2dba_3 and 4,5-Bis(diphenylphosphino)-9,9-dimethylxanthene (XantPhos) (**Figure 2.66B**).[276]

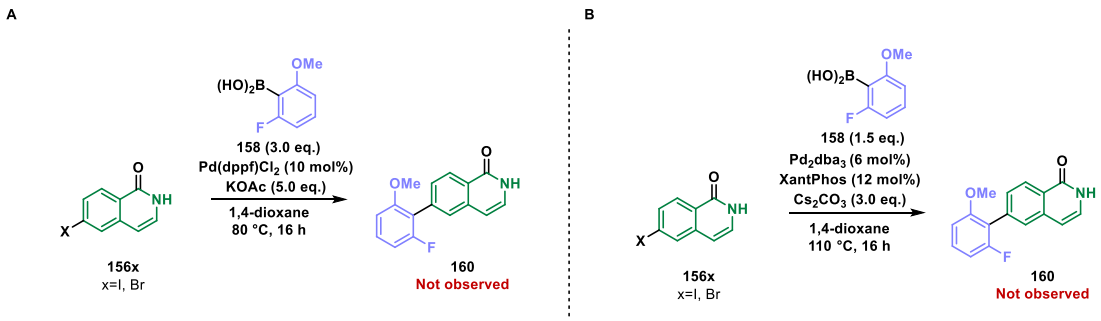


Figure 2.66: *Suzuki-Miyaura cross-coupling attempts to introduce the phenol/anisole moiety on compounds* ***156a–b****:* ***(A)*** *Using Lanman and co-workers' methodology.*[25] ***(B)*** *Using Liu and colleagues' methodology.*[276]

Given our previous experience with the application of cross-coupling chemistry to our substrates (**Sections II.3.2.3** and **II.3.2.4**), we decided to turn to the Stille reaction for this transformation (**Figure 2.67**). Tributyltinstannane **162** was obtained in 91% yield by performing a lithium-boron exchange reaction on 2-bromo-3-fluoroanisole **161** using *n*-butyllithium in anhydrous tetrahydrofuran, followed by electrophilic trapping using tributyltin chloride.[248] The newly-generated organometallic was suspended in *N,N*-dimethylformamide with 6-iodoisoquinolinone **156a** and caesium fluoride, and heated to 80 °C in the presence of catalytic amounts of $Pd(PPh_3)_4$ and copper iodide, to yield compound **160** in moderate yields (59–66%).[251] This reaction demonstrated poor scalability potential but was considered satisfactory enough to be used as our go-to method for the coupling of haloisoquinolinones **156a–b** and anisole-derived nucleophilic coupling partners.

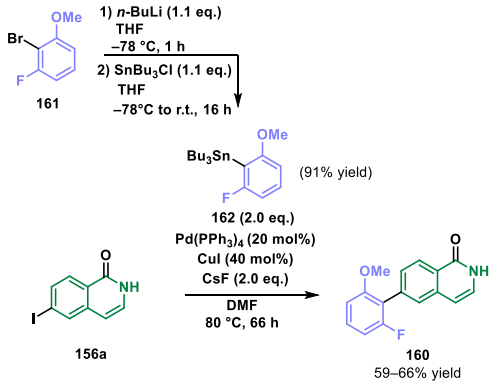


Figure 2.67: *Applying the Stille coupling reaction to isoquinolinone **156a** and organostannane **162**.*

II.3.4.2c Completing the synthesis of linchpin intermediate 164

Once obtained, methoxybenzylisoquinolinone **160** was easily turned into linchpin intermediate **164** by sequential halogenation reactions (**Figure 2.68**). Isoquinolinone **160** was stirred with *N*-iodosuccinimide in *N,N*-dimethylformamide at 80 °C to yield iodoisoquinolinone **163** in high yields (81–91%),[232] which was in turn chlorinated using neat phosphorus(V) oxychloride at 90 °C, to yield chloroisoquinoline **164** in high yields (86–93%).[234] It is worth noting that both compound

163 and compound **164** were obtained as solids that would readily sublime when heated to 40 °C under reduced pressure (rotary evaporation). Chloroisoquinoline **164** would also slowly de-iodinate when heated in acidic medium.

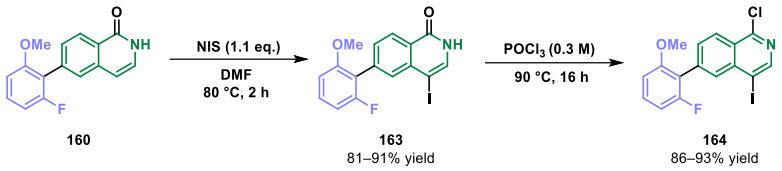


Figure 2.68: *Completing the synthesis of linchpin intermediate **164**.*

II.3.4.3 Anisole demethylation and completing the synthesis of 150

II.3.4.3a Demethylation strategy

Apart from the cross-coupling of protected phenol **162** onto haloisoquinoline **156a** (**Section II.3.4.2b**, **Figure 2.67**), another key step of this synthetic strategy was the demethylation of said phenol. When introduced as an anisole moiety in patented KRas G12C inhibitors, the phenol group was obtained by demethylation using boron tribromide at low temperatures as the final step of the synthesis, following the *N*-acylation of the deprotected piperazine.[82,276] However in our case, considering a demethylation reaction anytime past the final Stille cross-coupling, poses a regioselectivity problem, as two methoxy groups are present in Stille coupling product **ii** (**Figure 2.69**, **route I**). The demethylation of aryl methylethers usually involves harsh conditions, such as the Zeisel-Prey ether cleavage using molten pyridine hydrochloride at temperatures ranging from 180 to 220 °C, or refluxing in hydrogen bromide (or hydrogen iodide) in acetic acid, or using boron tribromide at various temperatures.[277–280] Such conditions might be detrimental to the protecting group used on the piperazine, especially the ones we have been using so far (namely Boc and Cbz).[281–283] Thus, considering a demethylation reaction anytime past the SNAr of a protected piperazine onto our substrate might pose chemoselectivity issues (**Figure 2.69**, **route II**). Finally, if

demethylating prior to any of the aforementioned transformations might appear as the most optimal option in terms of regioselectivity and chemoselectivity, a free phenol **v** might negatively impact the following transformations due to its reactivity, or the handling issues it induces (stickiness to solvent etc.) (**Figure 2.69**, **route III**).[276]

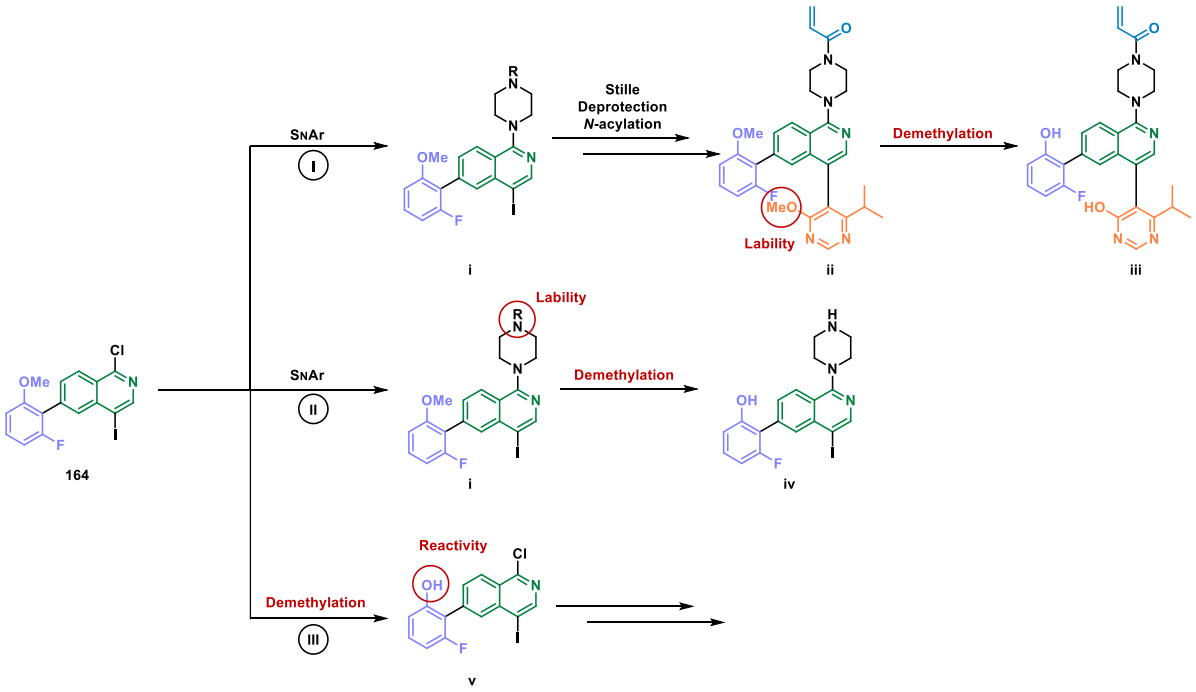


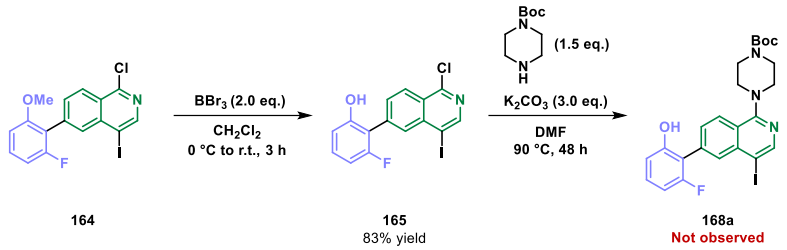
Figure 2.69: *Strategic approaches to determine the optimal placement of the anisole demethylation reaction in the synthesis of probe **150**.*

II.3.4.3b Demethylation attempts

Considering the observation we made on the volatility of compounds **163** and **164** (**Section II.3.4.2c**), we established boron tribromide as our demethylating agent of choice, as it was shown to be active at lower temperatures (between –78 °C and room temperature in most instances).[276,284,285]

Based on the considerations made in the previous paragraph (**Section II.3.4.3a**), we decided to firstly investigate whether the execution of the demethylation in earlier stages of the synthesis would prove viable (**Figure 2.70**). We dissolved methoxybenzylisoquinoline **164** in

dichloromethane at 0 °C in the presence of boron tribromide and allowed the reaction mixture to warm up to room temperature for a few hours.[276] Although the resulting phenol **165** was obtained in high yield (83%), it did not show any reactivity during the SNAr reaction with 1-Boc-piperazine and potassium carbonate in *N,N*-dimethylformamide at 90 °C.[242]



164 **165** 83% yield **168a** Not observed

Figure 2.70: *Attempting to demethylate the anisole moiety at an early stage of the synthesis.*

This previous strategic approach proving unsuccessful, we decided to explore the demethylation of the anisole once the piperazine moiety had been introduced in the molecule (**Figure 2.71**). In a preliminary study, we decided to use Boc-protected piperazine **166a**, even if the acidic medium of such a transformation would most likely result in the deprotection of the piperazine ring. Chloroisoquinoline **164** was stirred with 1-Boc-piperazine at 90 °C in *N,N*-dimethylformamide with potassium carbonate to yield compound **166a** in moderate yields (64–79%).[242] We took compound **166a** in dichloromethane at 0 °C in the presence of boron tribromide and allowed the reaction to warm up to room temperature for a few hours and stir until full disappearance of the starting material.[276] Monitoring was carried out by NMR spectroscopy, with the total disappearance of signal corresponding to the methoxy group as an indicator of reaction completion. Both NMR spectroscopy and positive electrospray ionisation (ESI^+) mass spectrometry indicated the exclusive presence of compound **167**, showing deprotection of both the phenol and piperazine moieties. To avoid the poisoning of the palladium catalyst in the subsequent Stille cross-coupling reaction,[244,245] we decided to reintroduce the Boc protecting group by stirring intermediate **167** in tetrahydrofuran at 40 °C in the presence of di-*tert*-butyl dicarbonate.[286]

Product **168a** was identified by ESI^+ mass spectrometry and NMR spectroscopy, but we were unable to determine an accurate isolated yield for it, as it would exist in complex mixtures with solvents, even after purification and desiccation.

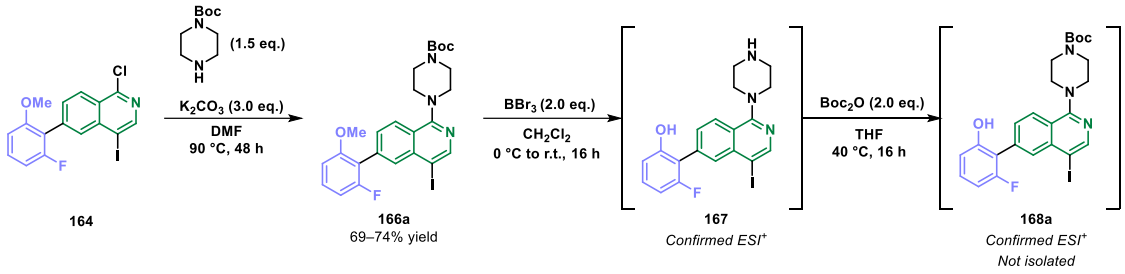


Figure 2.71: *Demethylation and subsequent re-protection of compound **166a**.*

II.3.4.3c Completing the synthesis of 150

We took the crude mixture of product **168a** and decided to subject it to our Stille cross-coupling conditions with pyrimidine **86** (**Figure 2.72**). After prolonged drying and subsequent degassing of compound **168a** in *N,N*-dimethylformamide to eliminate as much as the solvent impurities, stannylpyrimidine **86** was added to the solution, which was heated to 80 °C and stirred in the presence of caesium fluoride, and catalytic amounts of $Pd(PPh_3)_4$ and copper iodide.[251] These conditions allowed us to elucidate that the reprotection of intermediate **167a** with Boc anhydride described earlier (**Figure 2.71**) had not reached completion. Indeed, cross-coupling product **169a** was obtained in a mixture with an unknown compound (81% NMR and HPLC purity), which, after semi-prep HPLC purification was identified as deprotected piperazine **170** *via* NMR spectroscopy (21% yield in **169a**, 5% yield in **170**).

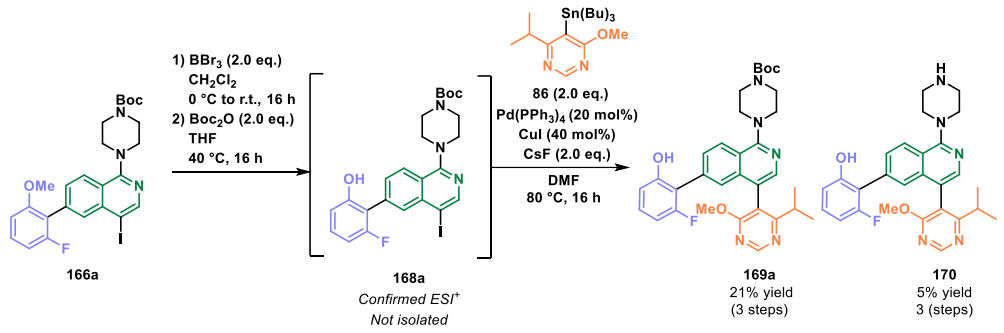


Figure 2.72: *Application of the Stille coupling to **168a**.*

We therefore decided to revise our Boc-protection conditions (**Figure 2.72**). After the concerted demethylation-deprotection of compound **166a** by boron tribromide in dichloromethane, we took intermediate **167** with di-*tert*-butyl dicarbonate and triethylamine in *N,N*-dimethylformamide and stirred at room temperature to yield **168a** as an isolable oil (44% yield).[287] Subjecting this mixture to the conditions described above allowed us to obtain **169a** in 92% purity (59% yield). The remaining 8% were identified as deprotected piperazine **170** (7% yield). The yield in **169a** over 3 steps using this reprotection method was of 26%, which was only slightly higher than that obtained previously (21% over 3 steps).

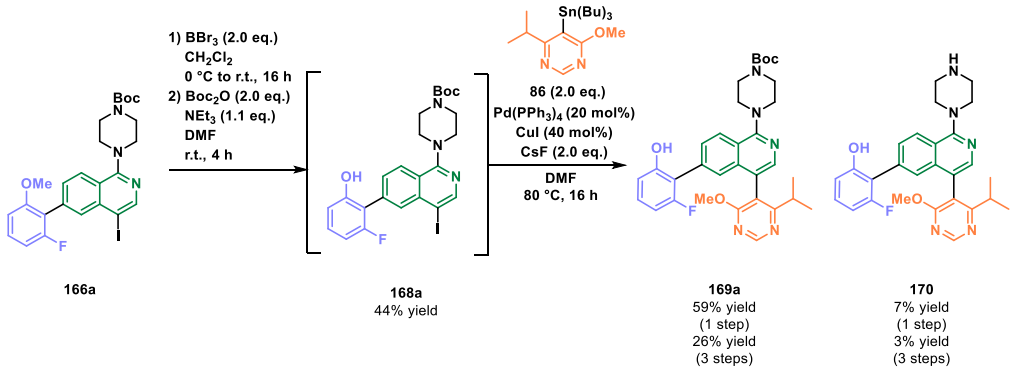


Figure 2.73: *Application of the Stille coupling to **168a**, obtained using optimised Boc-reprotection conditions.*

We decided to use the mixtures of **169a** and **170** in the final deprotection-*N*-acylation sequence to generate our target compound **150**. In a first instance, we deprotected the remaining **169a** by stirring it in a hydrogen chloride solution in methanol (1.5 M) at room temperature (**Figure 2.74**).[243] The resulting deprotected compound **170** could then be suspsended in dichloromethane and triethylamine with acryloyl chloride and stirred at room temperature. However, these conditions only afforded *O*-acylation product **171** (27% yield) and double acylation product **172** (25% yield).

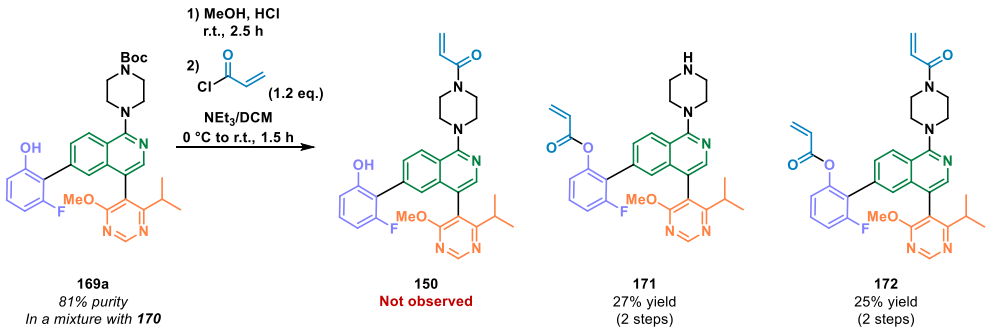


Figure 2.74: *Final deprotection-N-acylation sequence for the synthesis of **150**, using triethylamine.*

When omitting triethylamine (**Figure 2.74**), we exclusively obtained the desired *N*-acylation product **150** in moderate yield (67%), and only trace amounts of the double acylation product were observed by mass spectrometry (ESI^+, low resolution). We were unable to explain this effect and further experimentation would be required to confirm its repeatability.

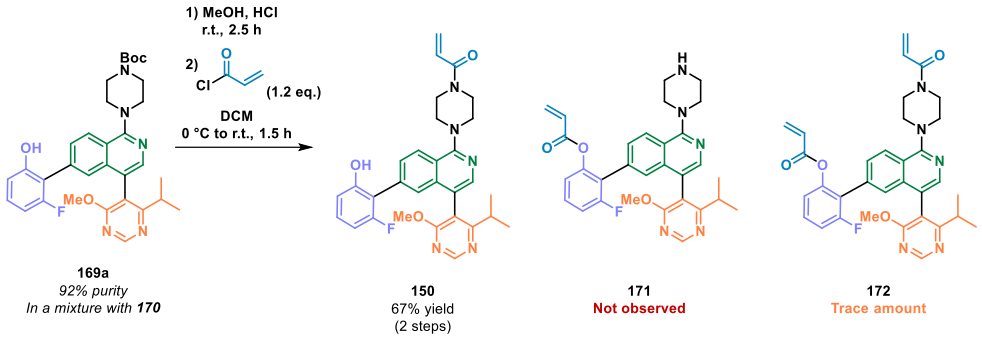


Figure 2.75: *Final deprotection-N-acylation sequence for the synthesis of **150**, without triethylamine.*

II.3.4.4 Refining the route

II.3.4.4a Finding an alternative protecting group

Despite its appealing versatility and easiness to introduce and remove, the Boc protecting group proved inefficient in our synthesis due to its lability to the acidic conditions of the boron-tribromide-mediated demethylation step (see **Section II.3.4.3b**). Though not widespread, the trifluoroacetyl protecting group has been reported as an orthogonal protecting group to Boc and Cbz, as it is easily deprotected in mild basic conditions but resistant to acidic conditions (as long as temperatures remain below 100 °C).[283,288] Replacing the Boc group with a trifluoroacetyl group should therefore allow us to optimise our route without drastically altering it, as simple basic aqueous conditions should allow to deprotect it prior to *N*-acylation.

We dissolved chloroisoquinoline **164** in *N,N*-dimethylformamide at 90 °C in the presence of *N,N*-diisopropylethyl amine and 1-triluoroacteylpiperazine (**Figure 2.76**).[242] Desired SNAr product **166b** was obtained in a rather low yield (24%) with an extra 24% of by-product **173**, resulting from the thermal decomposition of *N,N*-dimethylformamide and addition of the resulting dimethylamine onto **164**.

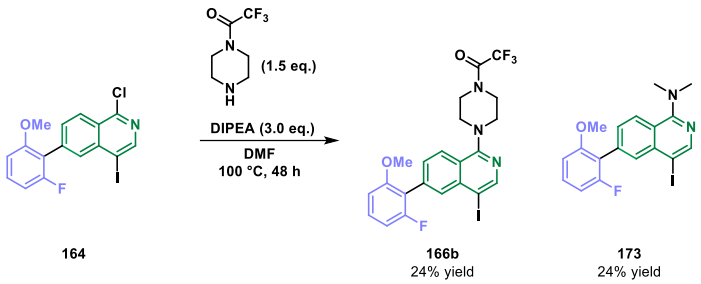


Figure 2.76: *The SNAr of trifluoroacetylpiperazine on **164**, using N,N-dimethylformamide as a solvent.*

To prevent this secondary transformation from taking place, we repeated the reaction in dimethylsulfoxide, *ceteris paribus* (**Figure 2.77**).[256] This allowed us to obtain trifluoroacetyl protected **166b** in moderate yield (54%).

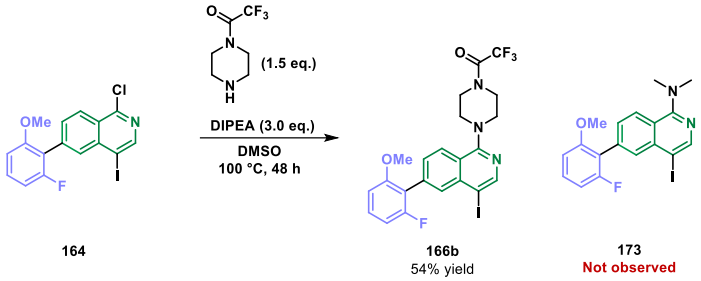


Figure 2.77: *The SNAr of trifluoroacetylpiperazine on **164**, using dimethylsulfoxide as a solvent.*

II.3.4.4b Completing the synthesis

With trifluoroacetylpiperazine **166b** in our hands, we decided to investigate its performance as a substrate in the remainder of the synthesis (**Figure 2.78**). We proceeded with the demethylation of the anisole moiety of **166b** using boron tribromide in dichloromethane at room temperature.[276] The demethylation reaction proved much faster than with Boc-piperazine **166a** and yielded intermediate **168b**. Intermediate **168b** was also much easier to handle than its Boc-protected counterpart **168a**, and was obatined as a solid, but was not purified. Crude phenol **168b** was coupled with tributylstannylpyrimidine **86** at 80 °C in *N,N*-dimethylformamide in the presence of cesium fluoride, and catalytic amounts of $Pd(PPh_3)_4$ and copper iodide to yield

biarylpyrimidine **169b** in moderate yield (33%). The subsequent removal of the trifluoroacetyl protecting group was achieved by stirring **169b** with potassium carbonate in a 4:1 mixture of methanol and water at 50 °C overnight.[289] The resulting crude mixture was immediately suspended in dichloromethane in the presence of acryloyl chloride and stirred at room temperature to yield our target probe **150** in high yield (86% yield over 2 steps).

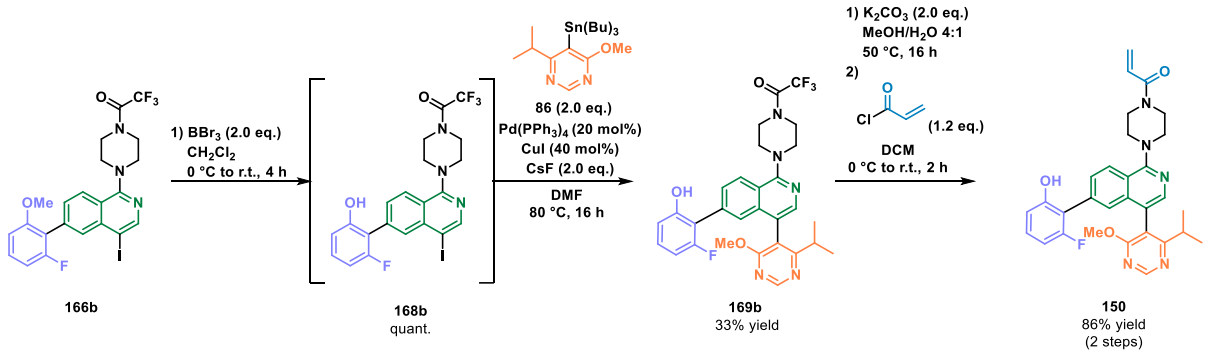


Figure 2.78: *Completing the synthesis of probe **150** using a trifluoroacetyl protecting group.*

Using the Boc-protecting group, the 6-step sequence allowing to transform linchpin intermediate **164** into probe **150** had a maximum yield of 13% (**Figure 2.79**). The use of a trifluoroacetyl group allowed to reduce the total number of steps to 5, with an overall yield of 15%. Even though the overall yield increase was not as important as expected, the trifluoroacetyl-protected compounds were easier to handle than their Boc-protected counterparts.

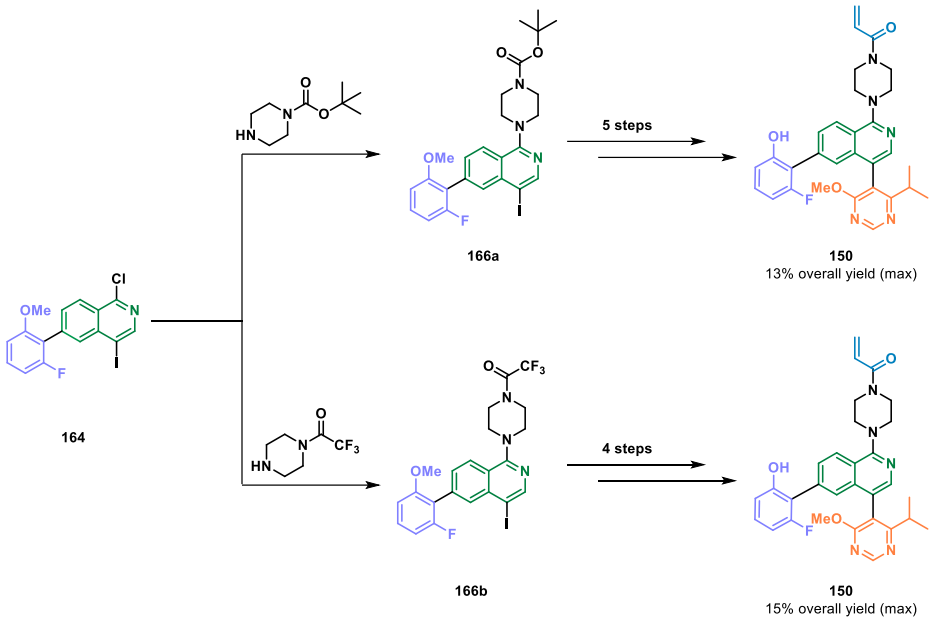


Figure 2.79: *Summary of the synthesis of probe **150** from linchpin intermediate **164**.*

II.3.4.5 Thermodynamics and preliminary biochemical and physiochemical studies

II.3.4.5a Atropisomerism and enantiomeric stability

When ran through various analytic chiral HPLC columns, Stille coupling precursors **168a–b** did not show any separation, confirming the hypothesis that the phenol–isoquinoline bond was not a source of axial chirality. However, compounds **169a–b** and probe **150** were identified as a racemic mixture of two enantiomers *via* chiral analytical HPLC. As expected, only the pyrimidine–isoquinoline bond was identified to be atropisomeric in these compounds, as is the case with sotorasib (**Figure 2.80**).[25]

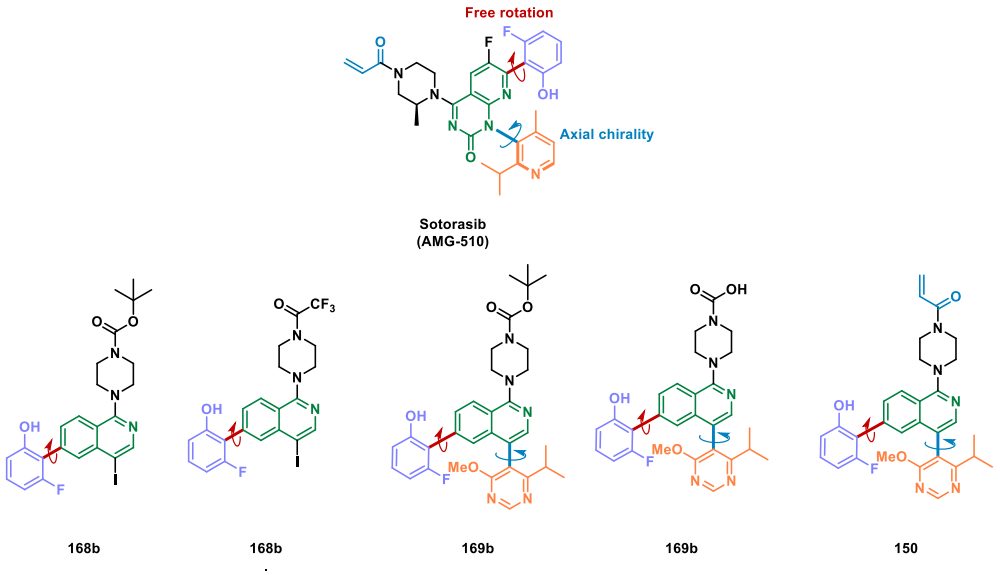


Figure 2.80: *Axial chirality was only observed at the pyrimidine–isoquinoline bond in compounds **169a–b** and **150**. Red curly arrows represent free bond rotation, and blue curly arrows represent hindered bond rotation (axial chirality).*

A chiral semi-preparative HPLC purification allowed to isolate the two atropisomers of probe **150**. A single enantiomer sample of **150** was dissolved in *meta*-xylene and allowed to stir at 80 °C for 6 hours. Regular aliquot sampling allowed us to observe a decrease of the enantiomeric ratio, from 100:0 to 74:26 (**Figure 2.81**). Plotting $ln\frac{1}{ee} = f(t)$ allowed us to calculate k_{rac} = 3.97 × 10^{-5} s^{-1}, corresponding to $t_{1/2}^{rac}$ = 4.9 hours at 80 °C and a rotational barrier ($\Delta G_{353}^{\ddagger}$) of 28.4 kcal/mol. This rotational barrier was identical to that of compound **119**, and is not high enough to consider **150** as a class 3 atropisomer. However, the same study would have to be carried out at 37 °C to completely rule compound **150** out of being suitable for pharmaceutical use.

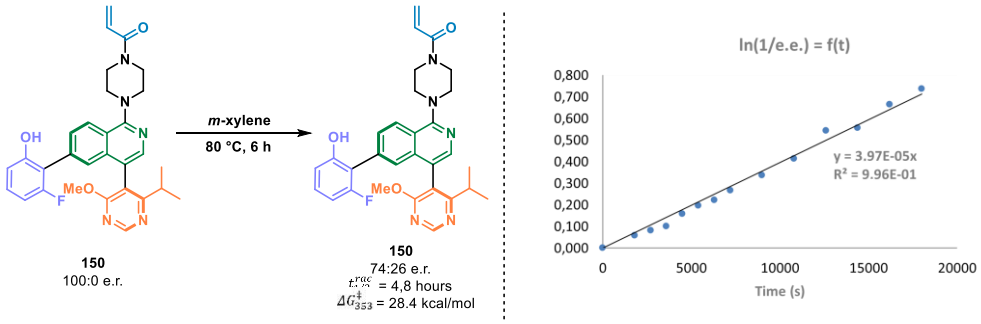
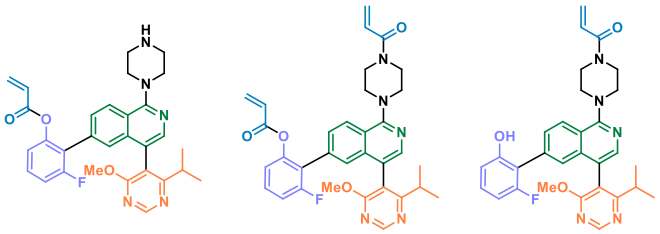


Figure 2.81: *Experiment to determine the half-life of racemisation of compound **150**.*

II.3.4.5b Preliminary biochemical and physiochemical studies

With the help of Neville McLean, compounds **171**, **172** and probe **150** were submitted to AstraZeneca for preliminary biochemical and physiochemical analysis. Probe **150** was submitted both as a racemic and as two separate enantiomers. Mean DMSO solubility, plasma protein binding, logD, clearance and KRas G12C i*n vitro* IC_{50} were determined using Kettle and co-workers' methods.[264] The results from these preliminary studies were compiled in **Table 2.10** (**ent. 1** refers to the **150** enantiomer that eluted the fastest on HPLC, and **ent. 2** was therefore the slowest eluting **150** enantiomer on HPLC).

Compounds **171** and **172** were submitted principally as "negative controls" and thus, only their *in vitro* activity against KRas G12C was assessed. After *in vitro* biochemical activity assessment, there was not enough racemic **150** left for the measurement of its mean solubility, protein binding, clearance and logD, therefore, only the separate enantiomers underwent physiochemical assessment.



171 172 150

Compound	Mean solubility DMSO (mM)	Mean protein binding (% free)	Mean IC_{50} (μM)	Median CL_{int} (μL/min/mg)	Mean LogD
171 (rac)	N/A	N/A	> 100	N/A	N/A
172 (rac)	N/A	N/A	> 100	N/A	N/A
150 (rac)	N/A	N/A	3.2	N/A	N/A
150 (ent. 1)	0.073	0.49	33.5	126	>3.7 (4.4 calculated)
150 (ent. 2)	0.083	0.37	3.6	169	>3.7 (4.4 calculated)
Sotorasib (literature)	178	11	0.027	17	4.11*

Table 2.10: *Preliminary biochemical and physiochemical analysis results. *logP in this case.*

Unsurprisingly, compounds **171** and **172** did not lead to any *in vitro* activity on KRas G12C (IC_{50} > 100 μM) (**Table 2.10**). However, we were pleased to observe low micromolar range activity of racemic **150** on KRas G12C (IC_{50} = 3.2 μM, repeated twice). The separate **150** enantiomers, **ent. 1** and **ent. 2**, were both less active than racemate **150**, showcasing respective IC_{50}s of 33.5 μM (repeated once), and 3.6 μM (repeated twice). It is commonly accepted that biologically active chiral compounds developed as single enantiomers will show different activities than their racemic counterpart.[290] One enantiomer should be more active than the racemate (eutomer), and the other less active than the racemate (dystomer), thus, having both **ent. 1** and **ent. 2** display inferior activities to racemic **150** was unexpected. However, this result is most likely due to the error of the assay, considered to be two-fold: the activities obtained for **ent. 2** and racemic **150** being very close, it can be assumed that an increased amount of readings would indicate that **ent. 2** is more active than the racemate (the researchers at AstraZeneca usually repeat the biochemical assay 6 times). These activities, though much lower than that of sotorasib (IC_{50} = 0.027 μM), showed that

the optimisation of **120** (see **Figure 2.82** below) into **150** successfully yielded a functioning KRas G12C inhibitor.

Although *in vitro* biochemical assays yielded heartening results, preliminary physiochemical studies suggested **150** would need further optimisation (**Table 2.10**). Indeed, both enantiomers were way less soluble than sotorasib in DMSO (0.073 mM for **ent. 1** and 0.083 mM for **ent. 2** *vs*. 178 mM for sotorasib).[265,266] Sotorasib was reported to be 89% bound to plasma protein, leaving 11% free for pharmacologic effect,[266]L but in the case of **150**, only 0.49% of **ent. 1** and 0.37% of **ent. 2** were found to be free for pharmacologic effect. Moreover, clearance by human liver microsomes was one order of magnitude higher for both enantiomers of **150** than that of sotorasib (126 µL/min/mg for **ent. 1** and 169 µL/min/mg for **ent. 2** *vs.* 17 µL/min/mg for sotorasib).[266] Both enantiomers of **150** were determined to have logD > 3.7 (calculated logD = 4.4), which indicated **150** and sotorasib (logP = 4.11) are of similar lipophilicity.

III. Conclusion and future work

III.1.1 Conclusion

We started this project aiming at synthesising a KRas G12C inhibitor displaying an axially chiral biaryl pyrimidine moiety, probe **52**. Due to steric hindrance issues, we were only able to synthesise probe **120**, and optimised it into probe **150** (**Figure 2.82**).

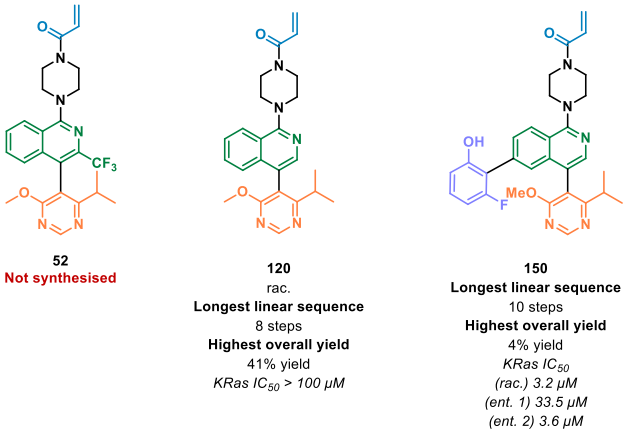


Figure 2.82: *Summary of the synthesis of probe **150**.*

We synthesised probe **120** using a convergent synthetic route, with a longest linear sequence of 8 steps and overall maximum yield of 41% (**Figure 2.83**). The synthetic strategy was centred around a "linchpin" intermediate (**116a**) which could be derivatised orthogonally at two different sites depending on the methodology used. The chloro site, *ortho* to the nitrogen atom in the isoquinoline ring was more reactive in nucleophilic aromatic substitution reactions whereas the iodo site, *meta* to the nitrogen in the isoquinoline ring was more reactive in cross-coupling transformations such as the Stille reaction. Preliminary *in vitro* biochemical assays were disappointing in terms of activity (IC_{50} > 100 μM) and solubility. However, **120** showed comparable lipophilicity, and mean plasma protein binding to sotorasib.

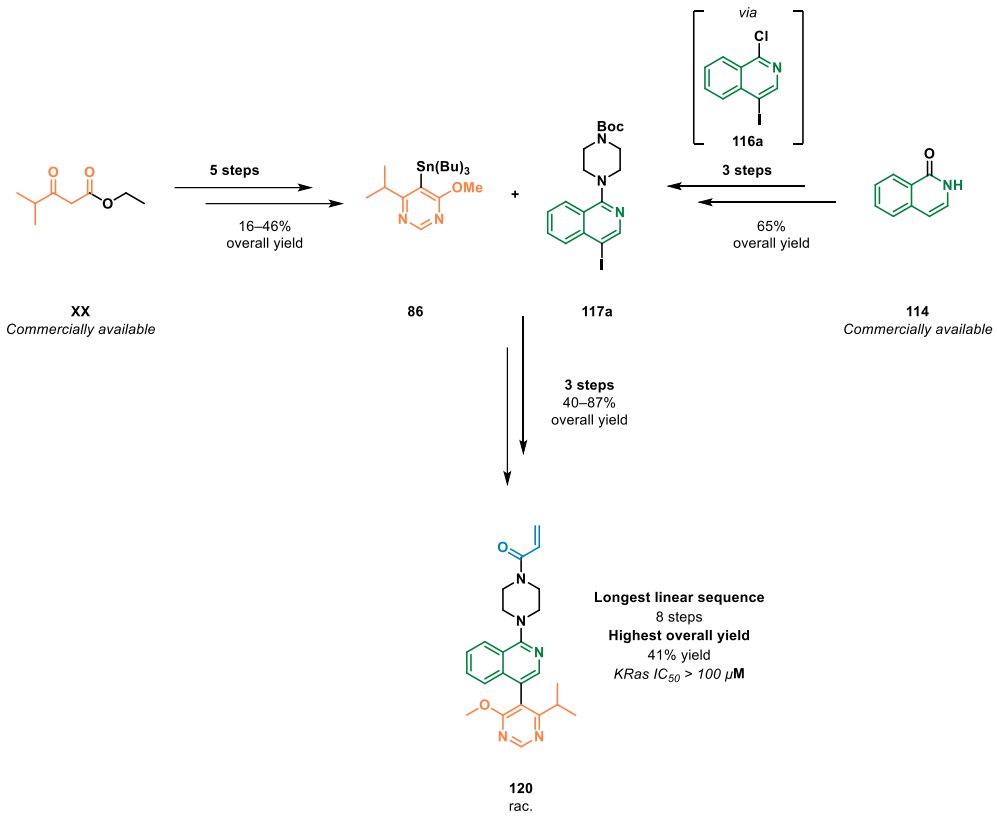


Figure 2.83: *Summary of the synthesis of probe **120**.*

In an effort to increase KRas G12C activity, we synthesised an optimised probe (**150**) using a convergent synthetic route that differed only slightly from that used to synthesise probe **120**. The longest linear sequence of this synthesis was of 10 steps and the maximum overall yield was of 4% (**Figure 2.84**). Nitrogen protecting group optimisation played an important role in this synthesis and we assume optimising the way the trifluoroacetyl protecting group is introduced in the molecule might help increase the overall yield. Racemic **150** was active *in vitro* against KRas G12C in low micromolar range (IC_{50} = 3.2 µM). After separation by preparative chiral HPLC, both the atropisomer with the shortest retention time (**ent. 1**), and that with the longest retention time (**ent**. **2**) were found to be less active than the racemate (IC_{50} = 33.5 µM and 3.6 µM respectively). Both **150** enantiomers showed comparable lipophilicity to sotorasib, but disappointing clearance, mean plasma protein binding and DMSO solubility.

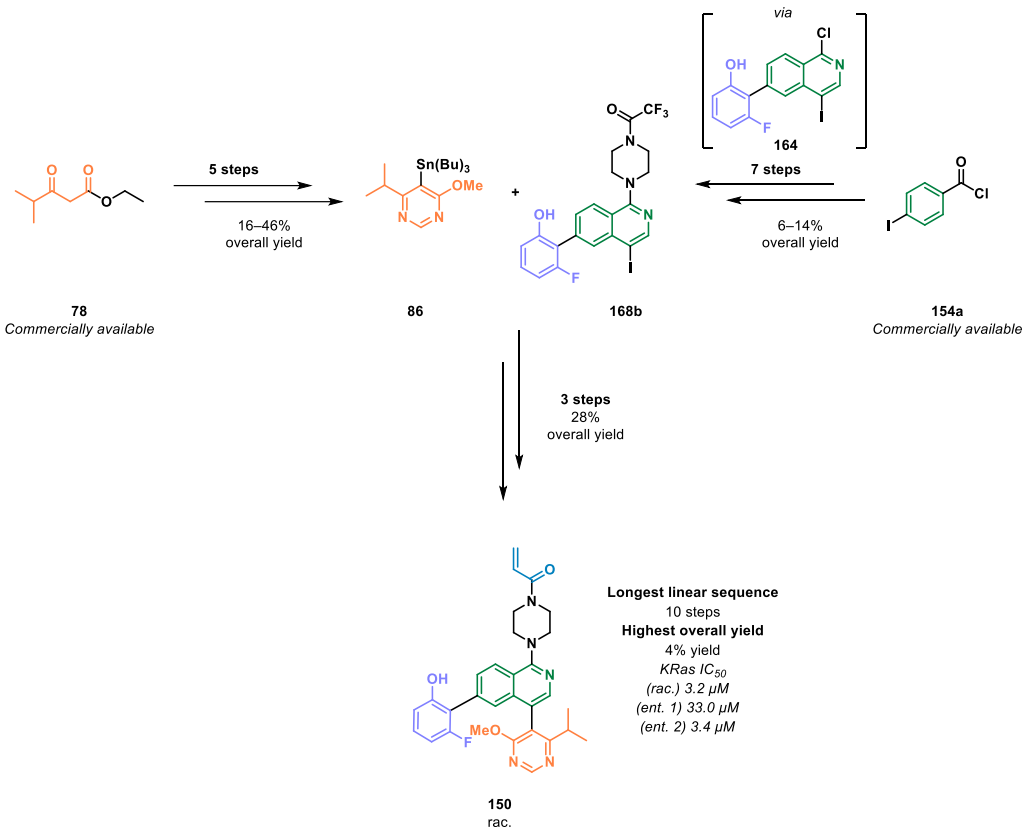


Figure 2.84: *Summary of the synthesis of probe **150**.*

Both probes **120** and **150** were identified to be atropisomeric due to hindered rotation around their isoquinoline–pyrimidine axes. Their identical barriers to rotation (28.4 kcal/mol) make them high-class 2 atropisomers. Such enantiomeric stability might be considered too low for pharmaceutical use. However, weekslong studies of the barrier at 37 °C would be needed to rule them out completely based on this criteria.

III.1.2 Future Work

In order to maximise its potency on KRas G12C, its stereochemical integrity, and its physiochemical properties, compound **150** will require optimisation. The convergent synthetic approach allows for easy SAR studies by introducing variability on the various fragments that are linked together in the course of the synthesis (**Figure 2.85**). The isoquinoline ring could be

synthesised as a more complex moiety, introducing groups prior to any other transformation, or in more late-stage functionalisation transformations. The piperazine ring could be substituted with small chiral functional groups that have proven useful in the optimisation processes of sotorasib and agradasib.[25,210] The phenol ring could be further substituted prior to coupling or altogether replaced by a naphthol or indazole (bioisostere) group. Failures to increase bulk on the isoquinoline moiety for a maximisation of stereochemical integrity could be compensated by increasing the bulk of the pyrimidine moiety.[246] Additionally, further substitution of the pyrimidine moiety with functional groups such as a free amine could increase weak interactions with the H95 cryptic pocket. Finally, the development of agradasib elucidated that substituted acrylamides could stabilise the covalent inhibitors they were incorporated in and might be worth trying in SAR studies around compound **150**.[211]

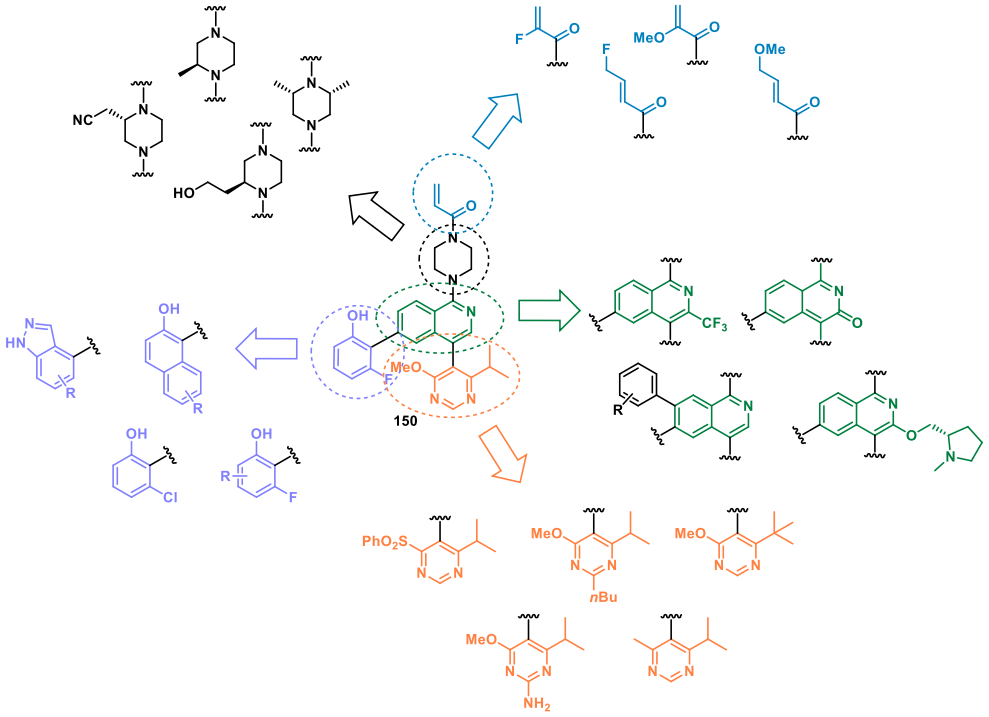


Figure 2.85: *Potential directions for SAR studies around probe **150**.*

On the topic of late stage functionalisation of the isoquinoline ring with hopes of increasing stereochemical integrity (*i.e.* increasing steric bulk around the chiral axis), we initiated attempts to re-introduce the trifluoromethyl group onto probe **120** (and thus make probe **52**) by exploiting a recent methodology developed my McNally and colleagues.[291] Indeed, in 2021, the McNally group, in collaboration with the Paton group, reported the use of phosphorus-mediated sp^2–sp^3 couplings for the selective fluoroalkylation of *N*-heterocycles (**Figure 2.86**).

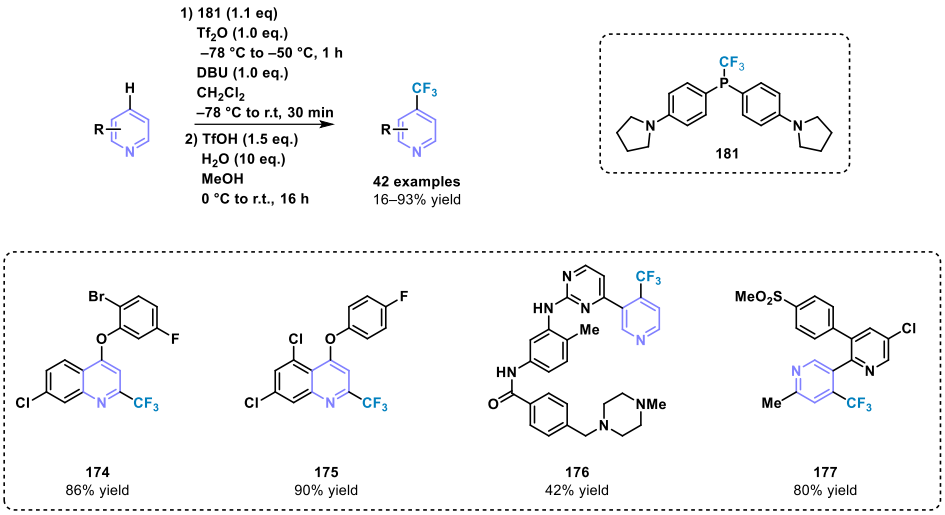


Figure 2.86: *McNally and co-workers' phosphorus mediated sp^2–sp^3 couplings for the selective fluoroalkylation of N-heterocycles.*[291]

We decided to synthesise McNally and co-workers' phosphorus-based trifluoromethylation from 4-bromoaniline (**Figure 2.87A**) and briefly investigated the application of their reaction conditions to our precursors **117a** and **119** (**Figure 2.87B**). Our efforts have so far been in vain, but the idea of exploiting C–H functionalisation for the late-stage reintroduction of steric bulk around the chiral axis of our compounds should be further explored. Indeed, our docking studies suggested the removal of the trifluoromethyl group on probe **52** might have been at the origin of the low potency observed for probe **120** (see **Section II.3.4.1**, **Figure 2.58**).

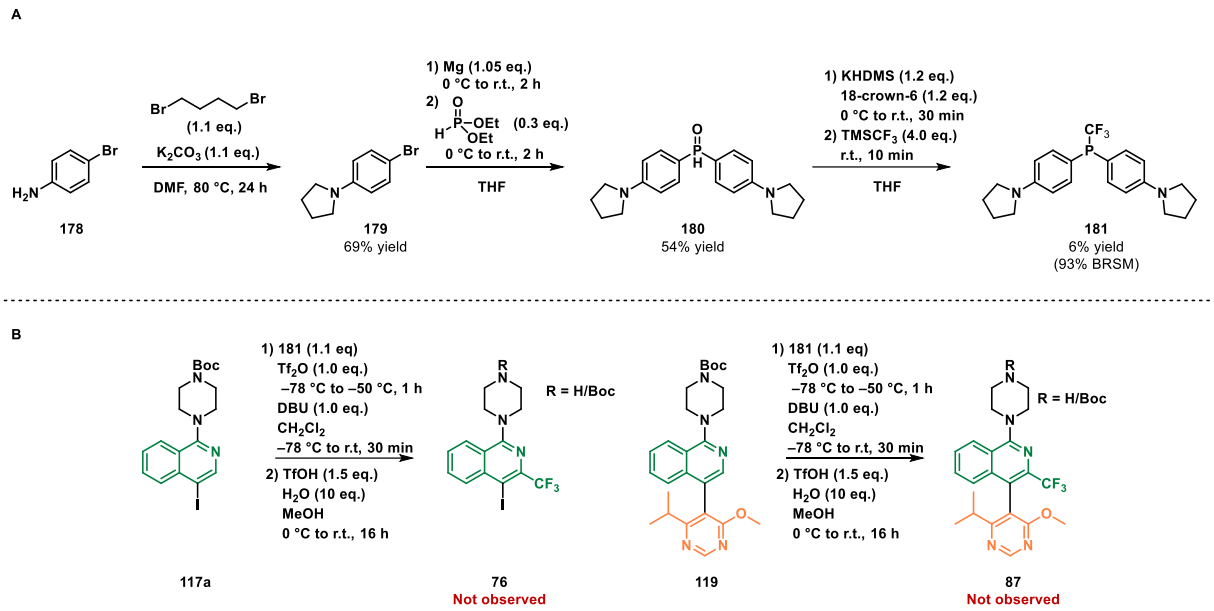


Figure 2.87: ***(A)*** *The synthesis of McNally and co-workers' trifluoromethylating agent* ***181****.*[291] ***(B)*** *Attempts to reintroduce a trifluoromethyl group on precursors* ***117a*** *and* ***119*** *using McNally and colleagues' method.*[291]

Part III

Experimental Part

IV. Experimental Part

IV.1 Materials and Methods

IV.1.1 Naming and numbering

Chemical compounds have been named according to IUPAC convention or commonly used names when appropriate. The numbering of compounds does not correspond to IUPAC recommendations, it has been arbitrarily chosen to aid assignment of ^{1}H and ^{13}C NMR spectra.

IV.1.2 General conditions

Reactions were carried out under ambient conditions unless specified in the procedures. Glassware for reactions carried under inert atmosphere (N_2 or Ar) was flamed-dried under vacuum prior to use. Room temperature (r.t.) refers to temperatures comprised within a 20–25 °C range. Temperatures of 0 °C were obtained using an ice/water bath. Temperatures between –10 and 0 °C were achieved using an salt/ice/water bath with different salt/ice weight ratios. Temperatures of –78 °C were obtained using a dry ice/acetone bath. Temperatures between –78 and –10 °C were achieved using a cryostat. Reactions were heated using oil baths, sand baths or DrySyn® heating blocks when appropriate, and a contact thermometer probe.

IV.1.3 Solvents and reagents

Anhydrous 1,4-dioxane, diethyl ether, tetrahydrofuran, *N,N*-dimethylformamide, dichloromethane, acetonitrile, pyridine and triethylamine were purified using an MBraun SPS5 purification system. Anhydrous methanol was obtained by drying over activated molecular sieves for 3 days. The molecular sieves were activated by heating at 230 °C for 16–20 h. All other solvents

and chemicals were reagent grade, purchased from usual chemical suppliers, and were used without further purification. Petrol 40–60 °C refers to the fractions of petroleum ether which boil in the range 40–60 °C. Where mixtures of solvents are described, the stated ratios are volume:volume (v/v). Copper iodide was purified according to Kauffman and co-worker's methodology.[292] All other solvents and reagents were used as supplied without further purification, unless stated in the procedure. Brine refers to a saturated aqueous solution of sodium chloride in water.

IV.1.4 Thin-layer chromatography

Analytical thin layer chromatography was carried out using pre-coated, aluminium-backed plates (60 F_{254} 0.25 mm, *Merck Kieselgel*). Revelation was achieved using ultraviolet irradiation (254 nm) or staining with solutions of basic potassium permanganate, vanillin or ferric chloride as appropriate. The basic potassium permanganate solution was prepared by dissolving potassium permanganate (2.5 g), potassium carbonate (13 g) and sodium hydroxide (0.63 g) in water (250 mL). The vanillin solution was prepared by dissolving food-grade vanillin (12 g) in absolute ethanol (190 mL) and conc. sulfuric acid (3 mL). The ferric chloride solution was prepared by dissolving iron(III) chloride (4 g) in 0.5 N aqueous hydrochloric acid (200 mL).

IV.1.5 Flash column chromatography

Column chromatography was carried out manually using *Merck Geduran®* Silica gel (40-63 μm particle size). Appropriate amounts of Silica gel were calculated based upon thin-layer chromatography separation and expected product mass. Pressurisation (0.2–0.4 bar) was achieved using in-house N_2 supply. The solvent systems used are stated in the procedures.

IV.1.6 High-performance liquid chromatography

Analytical and semi-preparative HPLC was carried out using a *Dionex Ultimate 3000* HPLC system, comprising *a Dionex LPG 3400A* pump*, WPS-3000SL* autosampler*,* a *TCC-3000SD* column compartment and a *Daicel Chiralpak* column (0.46 cm × 25 cm), equipped with an appropriate guard column 124 (0.4 cm × 1 cm). The columns and solvent systems used for each separation are stated in the procedures.

IV.1.7 Nuclear Magnetic Resonance (NMR) spectroscopy

IV.1.7.1 ^{1}H NMR spectroscopy

^{1}H NMR spectroscopy was carried out using either a *Brücker AV700* (700 MHz), *NEO600 (600 MHz), AV500* (500 MHz), *AV400* (400 MHz), or *DPX200* (200 MHz) spectrometer using the non-deuterated residual solvent signal as the internal reference. Chemical shifts are quoted in ppm, based on appearance rather than interpretation. ^{1}H NMR spectra were reported as follows: **^{1}H NMR (spectrometer frequency, solvent)** δ_H = *chemical shift/ppm (multiplicity of peak, coupling constant, integration, assignment)*. The assignment refers to the numbering scheme shown in the diagrams prefacing each experimental procedure. The multiplicity of the signals was given as follows: *s* (singlet), *d* (doublet), *t* (triplet), *q* (quartet), *m* (multiplet) and *br* (broad signal).

IV.1.7.2 ^{13}C NMR spectroscopy

^{13}C NMR spectroscopy was carried out using either a *Brücker AV700* (176 Mz)*, NEO600 (151 MHz), AV500* (126 MHz) or *AV400* (101 MHz) spectrometer using the non-deuterated residual solvent signal as the internal reference. ^{13}C NMR spectra were reported as follows: **^{13}C NMR (spectrometer frequency, solvent)** δ_C = *chemical shift/ppm (multiplicity, coupling constant, assignment)*. Multiplicities are assigned as *Quat., CH, CH_2* or *CH_3*. Assignments given refer to a

combination of the numbering schemes shown along with other generic labels. A variety of additional spectroscopic techniques including COSY, HSQC, HMBC and nOe were used to assign the one-dimensional spectra. Ambiguous signals could be attributed using the Paton's group CASCADE tool, which also helped with identifying the regioselectivity of some reactions.[103]

IV.1.7.3 ^{19}F NMR spectroscopy

^{19}F NMR spectroscopy was carried out using either a *Brücker, AV500* (470 MHz) or *AV400* (376 MHz) spectrometer, using $CFCl_3$ as an external reference (0 ppm). ^{19}F NMR spectra were reported as follows: **^{19}F NMR (spectrometer frequency, solvent)** δ_F *= chemical shift/ppm (multiplicity, coupling constant, assignment when relevant)*.

IV.1.7.4 ^{31}P NMR spectroscopy

^{31}FPNMR spectroscopy was carried out using *AV400* (162 MHz) spectrometer, using 85% H_3PO_4 in water as an external reference (0 ppm). ^{31}F NMR spectra were reported as follows: **^{31}P NMR (spectrometer frequency, solvent)** δ_P *= chemical shift/ppm (multiplicity, coupling constant, assignment when relevant)*.

IV.1.8 High resolution mass spectrometry

High resolution mass spectra were obtained by Electron Spray Ionisation (ESI) (*LCT Premier Reflectron TOF* and *Brücker MicroTOF*) using tetraoctylammonium bromide or sodium dodecyl sulfate as lock mass. Values are quoted as ratio of mass to charge in Daltons. HRMS was not necessarily collected for literature compounds.

IV.1.9 Fourier-transform infrared spectroscopy

Infrared spectra were recorded using a *Brücker Tensor 27* FTIR spectrometer. Spectra were reported as follows: **FTIR (solvent)** λ/cm^{-1} *= absorption maxima/*cm^{-1}. The additional abbreviation *br = broad* is used where appropriate. FTIR analysis was not necessarily carried out for literature compounds.

IV.1.10 Melting points

Melting points were determined using a *Griffin Education MELTP* melting point apparatus and are uncorrected.

IV.1.11 Specific optical rotations ($[\alpha]_D^{25}$)

Specific optical rotations were recorded on a Schmidt-Haensch Unipol L2000 polarimeter at 25°C, using the sodium D line wavelength of 529 nm. They were calculated using the following formula:

$$[\alpha]_D^{25} = \frac{100 \times \alpha}{l \times c}$$

Where α is the average value of the measured rotation in degrees (out of ten readings), *l* is the length of the cell in decimetres (typically, 1.00 dm) and *c* is the concentration of the sample, in g/100 mL.

IV.1.12 X-Ray crystallography

Single crystal X-ray diffraction was carried out by Owen A. Smith using a (Rigaku) Oxford Diffraction/Agilent Supernovae A diffractometer (Cu-K_α radiation, λ = 1.54180 Å) equipped with a graphite monochromator within the Department of Chemistry, University of Oxford. Samples were mounted in perfluoropoly-ethyl ether oil and cooled to 150 K during the data collection by a N_2

Crysostream open-flow cooling device.[293] The raw frame data was integrated and reduced using CrysalisPro. CRYSTALS[294,295] was used to obtain an *ab initio* solution using SuperFlip[296] embedded within CRYSTALS and for structure refinement. The images of the structure solutions were created using Pymol and represent thermal displacement ellipsoid plots of the best fit model drawn at 50% probability. For enantiopure crystals, the flack x parameter[297,298] was refined and Bayesian analysis of the Bijvoet pairs was use to give the Hooft y parameter.[299] Analysis of the Flack x and Hooft y parameters was used to determine the absolute structure of the crystal.

IV.1.13 Protein docking

Compounds were docked into protein crystal structures using Maestro 12.5 from the Schrödinger suite (2020-3 release). Protein crystal structures were obtained from the Protein Data Bank.[300] Covalent docking was carried out using the CovDock feature in Maestro, following a preliminary Glide docking. Protein, ligand and grid preparation for the Glide docking were carried out following Schrödinger's "A Chemist's Guide to Maestro" tutorial.[301] Distance restraints were used to constrain the binding mode to be consistent with the binding mode of closely related ligands.

IV.1.14 Biochemical and physiochemical assays

The biochemical and physiochemical properties of KRas G12C probe compounds were carried out by scientists at AstraZeneca, Sweden. They followed the protocols developed by Kettle *et al.*[264]

IV.2 Experimental procedures and data

IV.2.1 Part I: Atropisomers in Fragment-Based Drug Discovery

IV.2.1.1 General procedures

General procedure A

*For the Sonogashira reaction of **20** with terminal alkynes using Matulenko and co-workers' conditions.*[80]

Chloropyrimidine **20** (40 mg, 0.10 mmol, 1.0 eq.), bis(triphenylphosphine)palladium(II) dichloride (2 mg, 0.003 mmol, 3 mol%), copper (I) iodide (1 mg, 0.006 mmol, 6 mol%) and, if a solid, the appropriate alkyne (0.11 mmol, 1.1 eq.) were added into a flame-dried Schlenk tube. The vessel was purged with argon three times and the solids were dissolved in argon-sparged anhydrous acetonitrile and triethylamine (0.5 mL, 1:1 v/v, 0.2 M) under argon atmosphere. If a liquid, the appropriate alkyne (0.11 mmol, 1.1 eq.[‡]) was added. The reaction mixture was heated to 60 °C and stirred under argon until full consumption of the starting material was observed (TLC and/or quantitative ^{19}F NMR monitoring) (4–66 h). The resulting mixture was concentrated *in vacuo* and the crude product was purified by column chromatography.

General procedure B

*For the Sonogashira reaction of **20** with terminal alkynes using England's conditions.*[90]

Chloropyrimidine **20** (25 mg, 0.062[*] mmol, 1.0 eq.), copper (I) iodide (1.4 mg, 0.008 mmol, 12 mol%), triphenylphosphine (3.3 mg, 0.013 mmol, 20 mol%), tetrakis(triphenylphosphine)palladium

[‡] Unless stated otherwise

(4.4 mg, 0.004 mmol, 6 mol%), and, if a solid, the appropriate alkyne (0.125 mmol, 2.0 eq.) were added into a previously flame-dried Schlenk tube. The vessel was purged with argon five times and the solids were dissolved in argon-sparged anhydrous *N,N*-dimethylformamide and triethylamine (0.3 mL, 1:2 v/v, 0.2 M). If a liquid, the appropriate alkyne (0.125 mmol, 2.0 eq.) was added and the reaction mixture was heated to 50 °C and stirred for 16 h* under argon atmosphere. The resulting mixture was concentrated *in vacuo* and the crude product was purified by column chromatography.

General procedure C

*For the Suzuki reaction of **20** with boronic acids using Armstrong's conditions.*[71]

A flame-dried Schlenk tube was charged with chloropyrimidine **20** (30 mg, 0.075 mmol, 1.0 eq.), the appropriate boronic acid (0.12 mmol, 1.6 eq.), potassium carbonate (21 mg, 0.15 mmol, 2.0 eq.) and tetrakis(triphenylphosphine)palladium(0) (9 mg, 0.008 mmol, 10 mol%). The vessel was purged with argon three times and argon-sparged anhydrous toluene (0.5 mL) was added. The resulting mixture was stirred at 75 °C overnight under argon atmosphere. The reaction mixture was diluted with dichloromethane (3 mL) and quenched with aqueous saturated ammonium chloride (3 mL). The phases were separated and the aqueous layer was extracted with dichloromethane (2 × 5 mL). The combined organic layers were dried with anhydrous magnesium sulfate, filtered and concentrated *in* vacuo. The resulting crude mixture was purified by column chromatography.

General procedure D

*For the SNAr reaction of lithium amides and sulfonylpyrimidine **25**.*[97]

In a flame-dried round bottom flask, *n*-butyllithium (1.12 mL, 0.28 mmol, 1.0 eq.) was added under nitrogen atmosphere to a stirred solution of the appropriate secondary amine (0.28 mmol, 1.0 eq.) in dry tetrahydrofuran (12 mL) at –78 °C. The resulting reaction mixture was stirred at –78 °C for 1 h and was then allowed to warm to room temperature. A round bottom flask, a stirrer bar and a condenser were dried with a heat gun under vacuum and the flask was loaded with racemic sulfonylpyrimidine **25** (15 mg, 0.035 mmol, 1.0 eq.). The reaction medium was backfilled with argon 3 times and put under argon atmosphere. The previously made lithium amide solution (0.023 M in THF, 3 mL, 0.07 mmol, 2.0 eq.) was added, and the resulting mixture was heated to reflux overnight under argon atmosphere. The reaction mixture was allowed to cool down to room temperature, diluted with dichloromethane (20 mL), and slowly poured onto water (20 mL). The resulting biphasic mixture was diluted with brine (10 mL) and the organic layer was separated. The aqueous layer was extracted with dichloromethane (3 × 10 mL) and the combined organic layers were washed with brine (20 mL), dried over anhydrous magnesium sulfate, filtered and concentrated under reduced pressure. The resulting crude product was purified by column chromatography.

General procedure E

*For the solvolysis of sulfonylpyrimidine **37a**.*

*S*ulfonylpyrimidine **37a** (10 mg, 0.02 mmol, 1.0 eq.) was weighed into a small vial, dissolved in an alcohol solvent (0.2 mL) and 1 M aqueous potassium carbonate (40 µL, 0.04 mmol, 2.0 eq.) was added. The resulting yellow suspension was stirred at room temperature for 18 h. If no progress was observed, the reaction mixture was heated to 75 °C and stirred for an extra 48 h. Water (1 mL)

and dichloromethane (1 mL) were added and the phases were separated. The aqueous layer was extracted with dichloromethane (3 × 2 mL) and the combined organic layers were washed with brine (5 mL), dried over anhydrous magnesium sulfate, filtered and concentrated. The resulting crude mixture was purified by preparative thin-layer chromatography.

General procedure F

*For the one-pot hydrolysis and electrophilic trapping of sulfonylpyrimidine **20**.*

Sulfonylpyrimidine **20** (15 mg, 0.038 mmol, 1.0 eq.) was weighed into a vial and dissolved in 1,4-dioxane (0.2 mL). Aqueous sodium hydroxide (50% w/w, 25 µL, 0.456 mmol, 12.0 eq.) was added and the resulting colorless mixture was stirred at room temperature overnight. Upon completion, the reaction mixture had turned yellow. The reaction mixture was quenched with the appropriate bromide electrophile (5.0 eq.), heated to 50 °C and stirred for 1 h. If no progress was observed after that time, the reaction mixture was heated to 80 °C and stirred for an extra 22 h. The resulting reaction mixture was diluted with dichloromethane (1 mL) and water (1 mL). The aqueous layer was extracted with dichloromethane (3 × 2 mL). The combined organic extracts were washed with brine (5 mL), dried over anhydrous magnesium sulfate, filtered and concentrated *in vacuo*. The resulting crude mixture was purified by column chromatography.

General procedure G

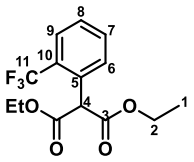
*For the one-pot methanolysis/CuAAC sequence on compound **22b**.*[107,108]

In a small vial, (trimethylsilyl)acetylene-pyrimidine **22b** (30 mg, 0.065 mmol, 1.0 eq.) was dissolved in methanol (0.4 mL) and the corresponding benzyl azide (0.072 mmol, 1.1 eq.) was added. In another small vial, copper(II) sulfate pentahydrade (8 mg, 0.032 mmol, 50 mol%), potassium carbonate (17 mg, 0.12 mmol, 1.8 eq.) and sodium-*L*-ascorbate (13 mg, 0.065 mmol, 1.0 eq.) were dissolved in water (0.4 mL). The resulting orange aqueous solution was added slowly to

the previous methanol solution and pyridine (32 µL) was slowly added to the mixture. The resulting black solution was stirred at room temperature for 20 h. The reaction mixture was diluted with water (3 mL) and extracted with dichloromethane (3 × 3 mL). The combined organic layers were dried over anhydrous magnesium sulfate, filtered and concentrated under reduced pressure. The crude reaction mixture was purified by column chromatography. Only the compounds synthesised by us were characterised in this work, for more information, see Alistair Ross' Part II thesis.[108]

IV.2.1.2 Experimental data

Diethyl 2-(2-(trifluoromethyl)phenyl)malonate, 17:



Following a literature procedure.[71] In a flame-dried Schlenk tube, copper iodide (262 mg, 1.38 mmol, 10 mol%), 2-picolinic acid (169 mg, 1.38 mmol, 10 mol%) and caesium carbonate (13.4 g, 41.3 mmol, 3.0 eq.) were added in sequence. The vessel was purged three times with argon and anhydrous 1,4-dioxane (14 mL) was added, followed by 2-iodobenzotrifluoride **15** (1.93 mL, 13.8 mmol, 1.0 eq.), and freshly distilled diethyl malonate **16** (4.2 mL, 27.5 mmol, 2.0 eq.). The resulting green slurry was heated to 50 °C and stirred for 40 h. The reaction mixture was allowed to cool to room temperature, diluted in ethyl acetate (40 mL) and saturated aqueous ammonium chloride (50 mL) was added. The aqueous layer was washed with ethyl acetate (3 × 25 mL). The combined organic layers were washed with brine (2 × 25 mL), dried over anhydrous magnesium sulfate, filtered and concentrated *in vacuo*. The resulting amber oil was purified by column chromatography (400 g silica, 1:49 ethyl acetate/toluene to 2:8 ethyl acetate/toluene). The desired diethyl malonate **17** was obtained as a colourless oil (3.61 g, 86%).

^{1}H NMR (400 MHz, Chloroform-*d*) *δ_H = 7.67 (t, J = 7.2 Hz, 2H, H_6 and H_9), 7.59 (t, J = 7.6 Hz, 1H, H_7), 7.45 (t, J = 7.5 Hz, 1H, H_8), 5.08 (s, 1H, H_4), 4.23 (m, 4H, H_2), 1.26 (t, J = 7.1, 6H, H_1).*

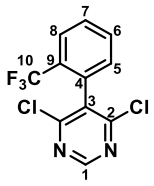
^{13}C NMR (101 MHz, Chloroform-*d*) *δ_C = 167.9 (Quat., C_3), 131.4 (q, J = 1.7 Hz, Quat., C_5), 132.2 (CH, C_6), 131.2 (CH, C_7), 129.1 (d, J = 29.8 Hz, Quat., C_{10}), 128.3 (CH, C_8), 126.0 (q, J = 5.7 Hz, CH, C_9), 124.2 (q, J = 273.9 Hz, Quat., C_{11}), 62.3 (CH_2, C_2), 53.7 (q, J = 3.0 Hz, CH, C_4), 14.1 (CH_3, C_1).*

^{19}F NMR (377 MHz, Chloroform-*d*) *δ_F = -58.9.*

LRMS (ESI$^+$) *calculated for $C_{14}H_{15}O_4F_3Na$ = 327.1, mass found = 327.1.*

The spectral data matches that reported in the literature.[49]

4,6-Dichloro-5-(2-(trifluoromethyl)phenyl)pyrimidine, 18



Following a literature procedure.[71,80]

Pyrimidine formation: To a stirred suspension of sodium methoxide at room temperature, prepared *in situ* by the portionwise addition of metallic sodium (1.67 mg, 72.5 mmol, 5.0 eq.) to anhydrous methanol (35 mL), formamidine hydrochloride (1.67 g, 29.0 mmol, 2.0 eq.) was added in a single portion. The resulting white suspension was stirred at room temperature for 45 minutes and was then diluted in tetrahydrofuran (20 mL). A solution of diethyl malonate **17** (4.4 g, 14.5 mmol, 1.0 eq.) in tetrahydrofuran (20 mL) and methanol (35 mL) was added and the resulting off-white suspension was stirred under nitrogen atmosphere at 80 °C for 23 h. The reaction mixture was then cooled to room temperature and concentrated to dryness under reduced pressure. The residue was suspended in 1 M hydrochloric acid solution (*ca.* 0.5 mL/mmol malonate), acidified with concentrated hydrochloric acid and stored in the fridge for 2 days. The resulting solid was isolated by vacuum filtration and then dried under high vacuum for 2 h to yield the corresponding dihydroxypyrimidine (4.97 g, crude) as a light-brown solid.

Chlorination: A suspension of crude dihydroxypyrimidine (4.7 g, 18.3 mmol, 1.0 eq.) in phosphorus(V) oxychloride (25 mL, 0.75 M) was stirred at 90 °C for 3 h and then cooled to room temperature. The mixture was poured onto ice (60 g ice/mL $POCl_3$) and was stirred until the ice had completely melted. The resulting aqueous solution was neutralized with 35% ammonium hydroxide (*ca*. 50 mL) and extracted with dichloromethane (3 × 100 mL). The combined organic layers were dried over anhydrous magnesium sulfate, filtered and concentrated under reduced

pressure. The resulting crude was purified by column chromatography (200 g silica, 1:19 ethyl acetate/pentane) and dried under high vacuum for 2 hours to yield dichloropyrimidine **18** as a white solid (1.77 g, 42% over 2 steps).

^{1}H NMR (400 MHz, Chloroform-*d*) *δ_H = 8.84 (s, 1H, H_1), 7.84 (d, J = 7.1 Hz, 1H, H_8), 7.72 (t, J = 7.6 Hz, 1H, H_6), 7.65 (t, J = 7.8, 1H, H_7), 7.28 (d, J = 7.3 Hz, 1H, H_5).*

^{13}C NMR (101 MHz, Chloroform-*d*) *δ_C = 161.7 (Quat., C_2), 157.7 (CH, C_1), 132.7 (CH, C_6), 132.0 (Quat., C_3), 131.3 (q, J = 2.1 Hz, Quat., C_4), 130.8 (CH, C_5), 130.1 (CH, C_7), 128.7 (q, J = 30.9 Hz, Quat., C_9), 127.0 (q, J = 4.9 Hz, CH, C_8), 123.5 (q, J = 273.8 Hz, Quat., C_{10}).*

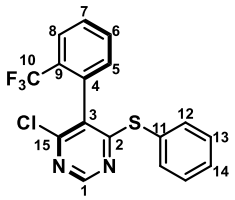
^{19}F NMR (470 MHz, Chloroform-*d*) *δ_F = -61.1.*

HRMS (ESI$^+$) *calculated for $C_{11}H_5Cl_2F_3N_2$ = 292.9855, mass found = 292.9856.*

Melting point *108–110 °C.*

The spectral data matches that reported in the literature.[49]

(*S*)-4-Chloro-6-(phenylthio)-5-(2-(trifluoromethyl)phenyl)pyrimidine, 19



Racemic: As previously reported in the literature.[71] In a 14 mL screw-cap vial, dichloropyrimidine **18** (300 mg, 1.02 mmol, 1.0 eq.) was dissolved in toluene (10.2 mL) and tetrabutylammonium bromide (33 mg, 0.102 mmol, 0.10 eq.), thiophenol (114 µL, 1.12 mmol, 1.1 eq.) and 50% (w/w) aqueous potassium hydroxide (0.38 mL, 5.1 mmol, 5.0 eq.) were added sequentially. The biphasic reaction mixture was rapidly stirred at room temperature for 30 min and then saturated aqueous ammonium chloride (15 mL) and dichloromethane (15 mL) were added. The organic layer was separated and the aqueous layer was extracted with dichloromethane (2 x 20 mL). The combined organic extracts were dried over anhydrous magnesium sulfate, filtered and concentrated under reduced pressure. The crude reaction mixture was purified by column chromatography (100 g Silica, 7.5:92.5 ethyl acetate/pentane). The pure fractions of the desired product were combined, concentrated under reduced pressure and dried under high vacuum to yield sulfide **19** as a white solid (340 mg, 91%).

Asymmetric: As previously reported in the literature.[71] In a 14 mL screw-cap vial, dichloropyrimidine **18** (300 mg, 1.02 mmol, 1.0 eq.) was dissolved in carbon tetrachloride (10.2 mL). *N*-benzylquininium (48 mg, 0.102 mmol, 0.1 eq.), thiophenol (114 µL, 1.12 mmol, 1.1 eq.) and 50% (w/w) aqueous potassium carbonate (0.62 mL, 3.37 mmol, 3.3 eq.) were added sequentially. The atmosphere was purged with nitrogen, and the biphasic reaction mixture was rapidly stirred at room temperature for 140 hours. Upon completion of the reaction, saturated aqueous ammonium chloride (15 mL) and dichloromethane (15 mL) were added. The organic layer was

separated and the aqueous layer was extracted with dichloromethane (2 x 20 mL). The combined organic extracts were dried over anhydrous magnesium sulfate, filtered and concentrated under reduced pressure. The crude reaction mixture was purified by column chromatography (100 g silica, 7.5:92.5 ethyl acetate/pentane). The pure fractions of the desired product were combined, concentrated under reduced pressure and dried under high vacuum to yield sulfide **19** as a white solid (345 mg, 92%, 89:11 e.r.).

^{1}H NMR (400 MHz, Chloroform-*d*) *δ_H = 8.62 (s, 1H, H_1), 7.89 (d, J = 7.8 Hz, 1H, H_8), 7.75 (tdd, J = 7.7, 1.4, 0.7 Hz, 1H, H_6), 7.67 (tt, J = 7.5, 1.1 Hz, 1H, H_7), 7.46 (m, 5H, H_{12-14}), 7.38 (d, J = 7.6 Hz, 1H, H_5).*

^{13}C NMR (101 MHz, Chloroform-*d*) *δ_C = 172.1 (Quat., C_2), 158.7 (Quat., C_{15}), 157.3 (CH, C_1), 135.6 (CH, C_{12}), 132.8 (CH, C_6), 131.7 (CH, C_5), 131.5 (q, J = 2.0 Hz, Quat., C_4), 130.1 (CH, C_{14}), 130.0 (CH, C_7), 129.5 (CH, C_{13}), 129.2 (d*, J = 31.0 Hz, Quat., C_9), 128.4 (Quat., C_{11}), 127.9 (Quat., C_3), 127.4 (q, J = 5.0 Hz, CH, C_8), 123.7 (d*, J = 274.2 Hz, Quat., C_{10}).*

^{19}F NMR (376 MHz, Chloroform-*d*) *δ_F = -61.0.*

LRMS (ESI$^+$) *calculated for $C_{17}H_{11}N_2ClF_3S$ = 367.0278, mass found = 367.0.*

Chiral HPLC *(Chiralpak IC, 2 % IPA, 98 % hexane, 1.0 mL/min, λ = 230 nm, 10 μL injection) τ_R^{minor} = 6.5 min, τ_R^{major} = 7.3 min (89:11 e.r.).*

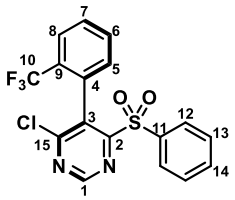
$[\alpha]_D^{25}$ *= -7 (c = 0.1, chloroform) for the 89:11 e.r. mixture.*

* In this section, some ^{13}C signals expected to be quartets (q) were reported as doublets (d) when observed as such on the spectra. This can be due to low concentrations of substrate or signals merging together.

Melting point *121–123 °C (rac. and ent.).*

The spectral data matches that reported in the literature.[49]

(*S*)-4-Chloro-6-(phenylsulfonyl)-5-(2-(trifluoromethyl)phenyl)pyrimidine, 20



Racemic: As previously reported in the literature.[71] In a 14 mL screw-cap vial. To a stirred solution of sulfidylpyrimidine **19** (rac.) (250 mg, 0.68 mmol, 1.0 eq.) in dichloromethane (6.8 mL), *m*-CPBA (>77%, 760 mg, > 5.0 eq.) was added in one portion at room temperature. The reaction mixture was stirred at room temperature for 16 h. Dichloromethane (10 mL) was added and the reaction mixture was quenched with saturated aqueous sodium thiosulfate (10 mL). The organic layer was separated and the aqueous layer was extracted with dichloromethane (3 x 12 mL). The combined organic extracts were washed with saturated aqueous sodium bicarbonate (2 x 25 mL) and brine (25 mL), dried over anhydrous magnesium sulfate, filtered and concentrated under reduced pressure. After drying under high vacuum for several hours, the crude mixture yielded sulfone **20** as a white solid (280 mg, quant.).

Enantioenriched: As previously reported in the literature.[71] In a 7 mL screw-cap vial. To a stirred solution of sulfidylpyrimidine **19** (89:11 e.r.) (150 mg, 0.41 mmol, 1.0 eq.) in dichloromethane (4 mL), *m*-CPBA (>77%, 460 mg, > 5.0 eq.) was added in one portion. The reaction mixture was stirred at room temperature for 16 h. Dichloromethane (10 mL) was added and the reaction mixture was quenched with saturated aqueous sodium thiosulfate (10 mL). The organic layer was separated and the aqueous layer was extracted with dichloromethane (3 x 12 mL). The combined organic extracts were washed with saturated aqueous sodium bicarbonate (2 x 25 mL) and brine (25 mL), dried over anhydrous magnesium sulfate, filtered and concentrated under reduced pressure. After

drying under high vacuum for several hours, the crude mixture yielded the desired sulfone **20** as white sticky oil (175 mg, quant., 89:11 e.r.).

^{1}H NMR (400 MHz, Chloroform-*d*) *δ_H = 8.98 (s, 1H, H_1), 7.90 (dd, J = 8.5, 1.3 Hz, 2H, H_{12}), 7.85 (dd, J = 7.8, 1.6 Hz, 1H, H_8), 7.74 (m, 1H, H_6), 7.69 (m, 2H, H_7 & H_{14}), 7.56 (dd, J = 8.3, 7.4 Hz, 2H, H_{13}), 7.36 (d, J = 7.5 Hz, 1H, H_5).*

^{13}C NMR (126 MHz, Chloroform-*d*) *δ_C = 164.8 (Quat., C_2), 164.5 (Quat., C_{15}), 157.6 (CH, C_1), 137.2 (Quat., C_{11}), 134.8 (CH, C_{14}), 132.1 (CH, C_6), 131.1 (CH, C_5), 130.2 (CH, C_7), 130.2 (Quat., C_3), 130.1 (CH, C_{12}), 129.3 (q, J = 2.3 Hz, Quat., C_4), 129.2 (CH, C_{13}), 128.7 (q, J = 30.7 Hz, Quat., C_9), 127.0 (q, J = 4.6 Hz, CH, C_8), 123.8 (d*, J = 274.1 Hz, Quat., C_{10}).*

^{19}F NMR (377 MHz, Chloroform-*d*) *δ_F = -59.6.*

FTIR (neat) *ν/cm^{-1} = 2981, 2889, 1583, 1543, 1393, 1361, 1316, 1264, 1233, 1167, 1444, 1110, 1079, 1062, 996, 956, 803, 771, 752, 715, 678, 644, 616.*

HRMS (ESI$^+$) *calculated for $C_{17}H_{10}ClF_3N_2O_2S$ = 399.0176, mass found = 399.0175.*

Chiral HPLC *(Chiralpak ADH, 20 % IPA, 80 % hexane, 1.0 mL/min, λ = 250 nm, 10 μL injection) τ_R^{minor} = 23.8 min, τ_R^{major} = 7.4 min (89:11 e.r.).*

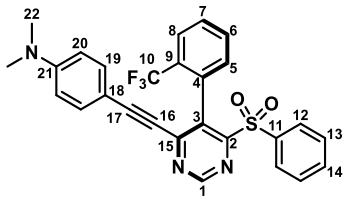
$[\boldsymbol{\alpha}]_{\boldsymbol{D}}^{\mathbf{25}}$ *= -48 (c = 0.1, chloroform) for the 89:11 e.r. mixture.*

Melting point *104–105 °C (rac. and ent.).*

The spectral data matches that reported in the literature.[49]

* In this section, some ^{13}C signals expected to be quartets (q) were reported as doublets (d) when observed as such on the spectra. This can be due to low concentrations of substrate or signals merging together.

(*S*)-*N,N*-Dimethyl-4-((6-(phenylsulfonyl)-5-(2-(trifluoromethyl)phenyl)pyrimidin-4-yl)ethynyl)aniline, 22a



Racemic: *Following general procedure A*, on a two-fold scale, using 4-ethynyl-*N,N*-dimethylaniline **21** (32 mg, 0.22 mmol, 1.1 eq.) and racemic chloropyrimidine **20**. The reaction mixture was stirred at 60 °C under argon atmosphere for 66 h. The crude product was purified by column chromatography (40 g silica, 8:2 ethyl acetate/pentane to 7:3 ethyl acetate/pentane). Alkyne **22a** was obtained as a bright yellow/orange solid (70 mg, 69%).

Following general procedure B, using 4-ethynyl-*N,N*-dimethylaniline **21** (18 mg, 0.125 mmol, 2.0 eq.) and racemic chloropyrimidine **20**. The resulting crude mixture was purified by column chromatography (15 g silica, 2:8 ethyl acetate/pentane). Alkyne **22a** was obtained as a bright yellow/orange solid (32 mg, 99%).

Enantioenriched: *Following general procedure A,* on a 1.75-fold scale (0.17 mmol), using 4-ethynyl-*N,N*-dimethylaniline **21** (28 mg, 0.19 mmol, 1.1 eq.) and enantioenriched chloropyrimidine **20** (89:11 e.r.). The crude product was purified by column chromatography (40 g silica, 8:2 ethyl acetate/pentane). Alkyne **22a** was obtained as a bright yellow/orange solid (86 mg, 96%, 89:11 e.r.).

^{1}H NMR (400 MHz, Chloroform-*d*) *δ_H = 9.09 (s, 1H, H_1), 7.91 (m, 2H, H_{12}), 7.87 (dd, J = 7.3, 2.0 Hz, 1H, H_8), 7.71 (m, 3H, H_{13} & H_6), 7.66 (m, 1H, H_{14}), 7.54 (t, J = 7.9 Hz, 1H, H_7), 7.40 (dd, J = 7.2, 1.8 Hz, 1H, H_5), 6.90 (d, J = 9.0 Hz, 2H, H_{20}), 6.50 (d, J = 9.0 Hz, 2H, H_{19}), 2.98 (s, 6H, H_{22}).*

^{13}C NMR (101 MHz, Chloroform-*d*) *δ_C = 162.4 (Quat., C_2), 157.8 (CH, C_1), 155.1 (Quat., C_{15}), 151.6 (Quat., C_{21}), 137.9 (Quat., C_{11}), 134.4 (CH, C_{14} & C_{19}), 131.7 (CH, C_6), 131.6 (d*, J = 1.9 Hz, Quat., C_4), 131.8 (CH, C_5), 130.9 (Quat., C_3), 129.9 (CH, C_{12}), 129.3 (CH, C_7), 129.3 (q, J = 30.3 Hz, Quat., C_9), 129.0 (CH, C_{13}), 126.7 (q, J = 4.6 Hz, Quat., C_8), 123.9 (d*, J = 274.1 Hz, Quat., C_{10}), 122.6 (Quat., C_{18}), 111.5 (CH, C_{20}), 106.3 (d, J = 3.1 Hz, Quat., C_{17}), 86.2 (Quat., C_{16}), 40.1 (CH_3, C_{22}).*

^{19}F NMR (377 MHz, Chloroform-*d*) *δ_F = -59.0.*

FTIR (neat) *ν/cm^{-1} = 2981, 2888, 2182, 1603, 1540, 1462, 1382, 1252, 1152, 1081, 955, 810, 720, 684.*

HRMS (ESI$^+$) *calculated for $C_{27}H_{20}F_3N_3O_2S$ = 508.1262, mass found = 508.1298.*

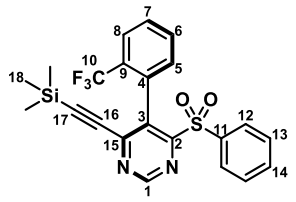
Chiral HPLC *(Chiralpak ADH, 40 % IPA, 60 % hexane, 1.3 mL/min, λ = 250 nm, 10 μL injection) τ_R^{minor} = 13.0 min, τ_R^{major} = 15.7 min (89:11 e.r.).*

$[\boldsymbol{\alpha}]_{\boldsymbol{D}}^{\mathbf{25}}$ *= -27 (c = 0.1, chloroform).*

Melting point *200–202 °C (rac.), 140–143 °C (ent.).*

* In this section, some ^{13}C signals expected to be quartets (q) were reported as doublets (d) when observed as such on the spectra. This can be due to low concentrations of substrate or signals merging together.

(*S*)-4-(Phenylsulfonyl)-5-(2-(trifluoromethyl)phenyl)-6-((trimethylsilyl)ethynyl)pyrimidine, 22b



Racemic: *Following general procedure A*, using trimethylsilylacetylene (75 µL, 0.50 mmol, 5.0 eq.) and racemic chloropyrimidine **20**. The crude product was purified by column chromatography (20 g silica, ethyl acetate/pentane, 8:2 to 1:1). The fractions of pure product were collected to yield a dark, amber solid (11 mg). Further NMR and TLC analyses showed that two products were present in the amber mixture. The mixture was further purified by preparative thin-layer chromatography (98:2 toluene/diethyl ether) to yield the desired alkyne **22b** as brown solid (3.4 mg, 7%).

Following general procedure B, on a ten-fold scale (0.63 mmol), using trimethylsilylacetylene (192 µL, 1.38 mmol, 2.2 eq.) and racemic chloropyrimidine **20**. The reaction mixture was stirred at 50 °C under argon atmosphere for 3 h. The crude product was purified by column chromatography (28 g silica, 15:85 ethyl acetate/pentane). The fractions of product were collected to yield alkyne **22b** as a brown solid (239 mg, 83%).

Enantioenriched: *Following general procedure B,* on a three-fold scale (0.21 mmol), using trimethylsilylacetylene (65 µL, 0.47 mmol, 2.2 eq.) and enantioenriched chloropyrimidine **6** (81:19 e.r.). The reaction mixture was stirred at 50 °C under argon atmosphere for 3 h. The crude product was purified by column chromatography (10 g silica, 15:85 ethyl acetate/pentane). The fractions of product were collected to yield alkyne **22b** as a brown solid (96 mg, 98%, 81:19 e.r.).

^{1}H NMR (400 MHz, Chloroform-*d*) *δ_H = 9.14 (s, 1H, H_1), 7.88 (dd, J = 8.5, 1.2 Hz, 2H, H_{12}), 7.81 (dd, J = 7.7, 1.5 Hz, 1H, H_8), 7.67 (m, 3H,H_6 & H_7 & H_{14}), 7.53 (dd, J = 8.2, 7.3 Hz, 2H, H_{13}), 7.34 (dd, J = 6.9, 0.8 Hz, 1H, H_5),-0.03 (s, 9H, H_{18}).*

^{13}C NMR (101 MHz, Chloroform-*d*) *δ_C = 163.2 (Quat., C_2), 157.8 (CH, C_1), 153.8 (Quat., C_{15}), 137.5 (Quat., C_{11}), 134.6 (CH, C_{14}), 132.5 (Quat., C_3), 131.7 (CH, C_6), 131.3 (CH, C_5), 130.7 (q, J = 2.1 Hz, Quat., C_4), 129.9 (CH, C_{12}), 129.9 (Quat., C_9) 129.7 (CH, C_7), 129.1 (CH, C_{13}), 126.7 (q, J = 4.6 Hz, CH, C_8), 123.9 (q, J = 273.8 Hz, Quat., C_{10}), 109.8 (Quat., C_{16}), 99.4 (Quat., C_{17}), -1.0 (CH_3, C_{18}).*

^{19}F NMR (377 MHz, Chloroform-*d*) *δ_F = -58.9.*

FTIR (neat) *ν/cm^{-1} = 1542, 1506, 1412, 1362, 1314, 1252, 1170, 1151, 1125, 1084, 1067, 997, 909, 846, 811, 758, 722, 687, 657.*

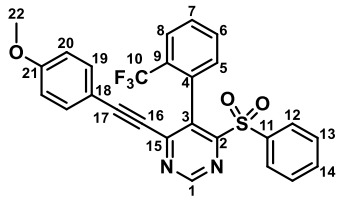
HRMS (ESI$^+$) *calculated for $C_{22}H_{19}F_3N_2O_2SSi$ = 461.0962, mass found = 461.0960.*

Chiral HPLC *(Chiralpak ADH, 5% IPA, 95% hexane, 1.0 mL/min, λ = 250 nm, 10 μL injection) τ_R^{minor} = 9.36 min, τ_R^{major} = 14.10 min (81:19 e.r.).*

$[\boldsymbol{\alpha}]_{\boldsymbol{D}}^{\mathbf{25}}$ *= -39 (c = 0.1, chloroform).*

Melting point *92–95 °C (rac. and ent.).*

4-((4-Methoxyphenyl)ethynyl)-6-(phenylsulfonyl)-5-(2-(trifluoromethyl)phenyl)pyrimidine, 22c



Following general procedure B, using 4-ethynylanisole (16 µL, 0.125 mmol, 2.0 eq.). The resulting crude mixture was purified by column chromatography (15 g silica, ethyl acetate/pentane, 2:8 to 1:1). Alkyne **22c** was obtained as a yellow/orange solid (26 mg, 84%).

^{1}H NMR (400 MHz, Chloroform-*d*) *δ_H = 9.14 (s, 1H, H_1), 7.92 (m, 2H, H_{12}), 7.87 (dd, J = 7.3, 1.9 Hz, 1H, H_8), 7.72 (m, 2H, H_6 & H_7), 7.66 (m, 1H, H_{14}), 7.54 (t, J = 7.8 Hz, 2H, H_{13}), 7.41 (dd, J = 7.3, 1.7 Hz, 1H, H_5), 7.00 (d, J = 8.9 Hz, 2H, H_{19}), 6.77 (d, J = 8.9 Hz, 2H, H_{20}), 3.78 (s, 3H, H_{22}).*

^{13}C NMR (101 MHz, Chloroform-*d*) *δ_C = 162.8 (Quat., C_2), 161.5 (Quat., C_{21}), 157.7 (CH, C_1), 154.6 (Quat., C_{15}), 137.6 (Quat., C_{11}), 134.4 (CH, C_{14}/C_{19}), 134.4 (CH, C_{14}/C_{19}), 131.6 (CH, C_5), 131.6 (CH, C_6), 131.4 (Quat., C_3), 131.1 (d*, J = 2.2 Hz, Quat., C_4), 129.8 (CH, C_{12}), 129.4 (CH, C_7), 129.1 (d, J = 31.0 Hz, Quat., C_9), 128.9 (CH, C_{13}), 126.6 (q, J = 4.5 Hz, CH, C_8), 123.8 (d*, J = 274.2 Hz, Quat., C_{10}), 114.2 (CH, C_{20}), 112.2 (Quat., C_{18}), 102.9 (Quat., C_{17}), 85.4 (Quat., C_{16}), 55.4 (CH_3, C_{22}).*

^{19}F NMR (377 MHz, Chloroform-*d*) *δ_F = -58.9.*

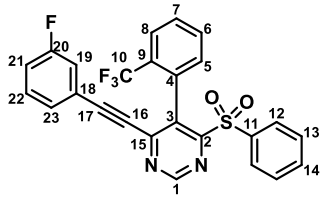
FTIR (Chloroform-*d*) *ν/cm^{-1} = 2200, 1603, 1541, 1512, 1447, 1418, 1377, 1314, 1295, 1255, 1167, 1148, 1124, 1083, 1067, 1033, 996, 910, 834, 810, 770, 724, 686, 643.*

* In this section, some ^{13}C signals expected to be quartets (q) were reported as doublets (d) when observed as such on the spectra. This can be due to low concentrations of substrate or signals merging together.

HRMS (ESI$^+$) *calculated for $C_{26}H_{17}F_3N_2O_3S$ = 495.0961, mass found = 495.0982.*

Melting point *139–142 °C.*

4-((3-Fluorophenyl)ethynyl)-6-(phenylsulfonyl)-5-(2-(trifluoromethyl)phenyl)pyrimidine, 22d



Following general procedure B, using 1-ethynyl-3-fluorobenzene (15 µL, 0.125 mmol, 2.0 eq.). The resulting crude mixture was purified by column chromatography (15 g silica, ethyl acetate/pentane, 2:8 to 1:1). Alkyne **22d** was obtained as a yellow/orange solid (19 mg, 63%).

^{1}H NMR (400 MHz, Chloroform-*d*) *δ_H = 9.19 (s, 1H, H_1), 7.92 (m, 2H, H_{12}), 7.89 (dd, J = 7.3, 1.9 Hz, 1H, H_8), 7.74 (td, J = 7.2, 6.9, 1.7 Hz, 2H, H_6 & H_7), 7.68 (m, 1H, H_{14}), 7.55 (t, J = 7.9 Hz, 2H, H_{13}), 7.43 (dd, J = 7.2, 1.7 Hz, 1H, H_5), 7.23 (m, 1H, H_{22}), 7.07 (tdd, J = 8.5, 2.6, 1.0 Hz, 1H, H_{21}), 6.88 (dt, J = 7.6, 1.0 Hz, 1H, H_{23}), 6.73 (ddd, J = 8.9, 2.6, 1.4 Hz, 1H, H_{19}).*

^{13}C NMR (101 MHz, Chloroform-*d*) *δ_C = 163.5 (Quat., C_2), 162.2 (d, J = 239.2 Hz, Quat, C_{20}), 157.9 (CH, C_1), 154.1 (Quat., C_{15}), 137.5 (Quat., C_{11}), 134.6 (CH, C_{14}), 132.1 (Quat., C_3), 131.8 (CH, C_6), 131.6 (CH, C_5), 130.8 (q, J = 2.1 Hz, Quat., C_4), 130.4 (d, J = 8.4 Hz, CH, C_{22}), 130.0 (CH, C_{12}), 129.8 (CH, C_7), 129.2 (d, J = 30.1 Hz, Quat., C_9), 129.1 (CH, C_{13}), 128.4 (d, J = 3.2 Hz, CH, C_{23}), 126.8 (q, J = 4.4 Hz, CH, C_8), 123.9 (d[*], J = 274.3 Hz, Quat., C_{10}), 122.2 (d, J = 9.5 Hz, Quat., C_{18}), 119.2 (d, J = 23.1 Hz, CH, C_{19}), 118.0 (d, J = 21.3 Hz, C_{21}), 99.7 (d, J = 3.3 Hz, Quat., C_{17}), 86.1 (Quat., C_{16}).*

^{19}F NMR (377 MHz, Chloroform-*d*) *δ_F = -58.9 (Ar–CF_3), -111.8 (td, J = 8.9, 5.8 Hz, Ar–F).*

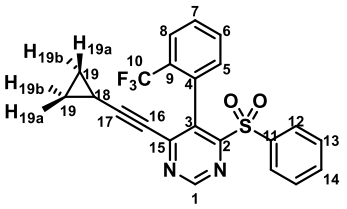
FTIR (Chloroform-*d*) *ν/cm^{-1} = 2981, 2219, 1607, 1581, 1505, 1488, 1414, 1371, 1267, 1240, 1218, 1152, 1126, 1082, 1066, 1035, 963, 874, 789, 756, 726, 710, 680, 645.*

[*] In this section, some ^{13}C signals expected to be quartets (q) were reported as doublets (d) when observed as such on the spectra. This can be due to low concentrations of substrate or signals merging together.

HRMS (ESI$^+$) *calculated for $C_{25}H_{14}F_4N_2O_2S$ = 483.0785, mass found = 483.0784.*

Melting point *106–109 °C.*

4-(Cyclopropylethynyl)-6-(phenylsulfonyl)-5-(2-(trifluoromethyl)phenyl)pyrimidine, 22f



Following general procedure B, using 2-cyclopropylacetylene (12 µL, 0.138 mmol, 2.2 eq.). The resulting crude mixture was purified by column chromatography (15 g silica, 2:8 ethyl acetate/pentane). Alkyne **22f** was obtained as an orange solid (19 mg, 71%).

^{1}H NMR (400 MHz, Chloroform-*d*) *δ_H = 9.07 (s, 1H, H_1), 7.88 (m, 2H, H_{12}), 7.80 (dd, J = 7.9, 1.3 Hz, 1H, H_8), 7.67 (m, 2H, H_6 & H_7), 7.64 (m, 1H, H_{14}), 7.52 (t, J = 7.8 Hz, 2H, H_{13}), 7.31 (d, J = 6.7 Hz, 1H, H_5), 1.20 (tt, J = 8.2, 4.9 Hz, 1H, H_{18}), 0.78 (m, 2H, H_{19a}/ H_{19b}), 0.44 (m, 1H, H_{19a}/ H_{19b}), 0.30 (m, 1H, H_{19a}/ H_{19b}).*

^{13}C NMR (126 MHz, Chloroform-*d*) *δ_C = 162.8 (Quat., C_2), 157.7 (CH, C_1), 154.8 (Quat., C_{15}), 137.7 (CH, C_{11}), 134.4 (CH, C_6/C_7), 131.7 (CH, C_6/C_7), 131.7 (Quat., C_3), 131.4 (CH, C_5), 131.2 (q, J = 2.3 Hz, Quat., C_4), 129.9 (CH, C_{12}), 129.4 (CH, C_{14}), 129.0 (CH, C_{13}), 128.9 (d*, J = 30.5 Hz, Quat., C_9), 126.6 (q, J = 4.5 Hz, CH, C_8), 123.9 (d*, J = 274.0 Hz, Quat., C_{10}), 109.3 (Quat., C_{17}), 73.2 (Quat., C_{16}), 9.9 (CH, C_{19}), 9.7 (CH, C_{19}), 0.3 (CH, C_{18}).*

^{19}F NMR (377 MHz, Chloroform-*d*) *δ_F = -59.0.*

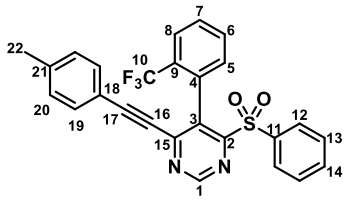
* In this section, some ^{13}C signals expected to be quartets (q) were reported as doublets (d) when observed as such on the spectra. This can be due to low concentrations of substrate or signals merging together.

FTIR (Chloroform-*d*) *ν/cm^{-1} = 2981, 2625, 2222, 1601, 1582, 1543, 1504, 1448, 1424, 1382, 1314, 1268, 1197, 1169, 1152, 1124, 1083, 1067, 1034, 982, 861, 811, 772, 716, 687, 644.*

HRMS (ESI^+) *calculated for $C_{22}H_{15}F_3N_2O_2S$ = 429.0879, mass found = 429.0878.*

Melting point *124–127 °C.*

4-(Phenylsulfonyl)-6-(p-tolylethynyl)-5-(2-(trifluoromethyl)phenyl)pyrimidine, 22g



Following general procedure B, using 4-ethynyltoluene (16 µL, 0.125 mmol, 2.0 eq.). The reaction mixture was stirred at 50 °C under argon atmosphere for 16 h. The crude product was purified by column chromatography (12 g silica, 2:8 ethyl acetate/pentane) to yield alkyne **22g** as an amber oil (28 mg, 93%).

^{1}H NMR (400 MHz, Chloroform-*d*) *δ_H = 9.16 (s, 1H, H_1), 7.92 (dd, J = 8.4, 1.3 Hz, 2H, H_{12}), 7.87 (dd, J = 7.8, 1.5 Hz, 1H, H_8), 7.72 (m, 2H, H_6 & H_7), 7.67 (m, 1H, H_{14}), 7.54 (t, J = 7.8 Hz, 2H, H_{13}), 7.41 (d, J = 7.2 Hz, 1H, H_5), 7.07 (d, J = 7.8 Hz, 2H, H_{19}), 6.96 (d, J = 8.2 Hz, 2H, H_{20}), 2.32 (s, 3H, H_{22}).*

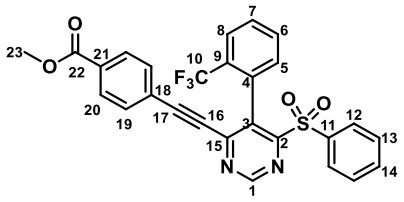
^{13}C NMR (126 MHz, Chloroform-*d*) *δ_C = 163.0 (Quat., C_2), 157.9 (Quat., C_1), 154.7 (Quat., C_{15}), 141.4 (Quat., C_{11}), 137.6 (Quat., C_{21}), 134.5 (CH, H_{14}), 132.6 (CH, C_{20}), 131.8 (CH, C_5), 131.7 (Quat., C_3), 131.6 (CH, C_6), 131.1 (q, J = 2.4 Hz, Quat., C_4), 129.9 (CH, C_{12}), 129.6 (CH, C_7), 129.4 (CH, C_{19}), 129.2 (q, J = 24.1 Hz, Quat., C_9), 129.1 (CH, C_{13}), 126.7 (q, J = 4.6 Hz, Quat., C_8), 123.9 (q, J = 274.2 Hz, Quat., C_{10}), 117.4 (Quat., C_{18}), 102.5 (Quat., C_{17}), 85.5 (Quat., C_{16}), 21.8 (CH_3, C_{22}).*

^{19}F NMR (377 MHz, Chloroform-*d*) *δ_F = -58.9.*

FTIR (Chloroform-*d*) *ν/cm^{-1} = 3066, 2980, 2923, 2235, 2205, 1605, 1583, 1541, 1512, 1502, 1448, 1418, 1376, 1314, 1268, 1228, 1171, 1149, 1125, 1067, 1035, 995, 813, 756, 702, 686.*

HRMS (ESI$^+$) *calculated for $C_{26}H_{17}F_3N_2O_2S$ = 479.1036, mass found = 479.1031.*

Methyl 4-((6-(phenylsulfonyl)-5-(2-(trifluoromethyl)phenyl)pyrimidin-4-yl)ethynyl)benzoate, 22h



Following general procedure B, using methyl 4-ethynylbenzoate (20 mg, 0.125 mmol, 2.0 eq.). The resulting crude mixture was purified by column chromatography (15 g silica, 2:8 ethyl acetate/pentane). Alkyne **22h** was obtained as an amber solid (15 mg, 46%).

^{1}H NMR (400 MHz, Chloroform-*d*) *δ_H = 9.12 (s, 1H, H_1), 7.85 (d, J = 8.6 Hz, 2H, H_{20}), 7.85 (dd, J = 8.4, 1.3 Hz, 2H, H_{12}), 7.81 (dd, J = 7.4, 1.7 Hz, 1H, H_8), 7.66 (m, 2H, H_6 & H_7), 7.60 (m, 1H, H_{14}), 7.48 (t, J = 7.8 Hz, 2H, H_{13}), 7.36 (dd, J = 7.3, 1.8 Hz, 1H, H_5), 7.07 (d, J = 8.6 Hz, 2H, H_{19}), 3.83 (s, 3H, H_{23}).*

^{13}C NMR (101 MHz, Chloroform-*d*) *δ_C = 166.0 (Quat., C_{22}), 163.3 (Quat., C_2), 157.8 (CH, C_1), 153.9 (Quat., C_{15}), 137.3 (Quat., C_{11}), 134.5 (CH, C_{14}), 132.3 (CH, C_{19}), 132.0 (Quat., C_3), 131.7 (CH, C_5), 131.5 (CH, C_6), 130.7 (q, J = 2.3 Hz, Quat., C_4), 129.9 (CH, C_{12}), 129.6 (Quat., C_{21}), 129.5 (CH, C_7), 129.1 (d*, J = 30.8 Hz, Quat., C_9), 129.0 (CH, C_{13} & C_{20}), 126.7 (q, J = 4.7 Hz, CH, C_8), 124.7 (CH, C_{18}), 123.8 (d*, J = 274.1 Hz, Quat., C_{10}), 99.8 (Quat., C_{17}), 87.5 (Quat., C_{16}), 52.4 (CH_3, C_{23}).*

^{19}F NMR (377 MHz, Chloroform-*d*) *δ_F = -58.8.*

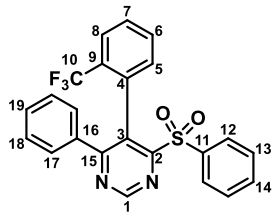
FTIR (Chloroform-*d*) *ν/cm^{-1} = 2981, 2211, 1723, 1606, 1541, 1505, 1437, 1418, 1374, 1314, 1277, 1172, 1150, 1115, 1083, 1067, 1035, 810, 769, 719, 687, 646.*

* In this section, some ^{13}C signals expected to be quartets (q) were reported as doublets (d) when observed as such on the spectra. This can be due to low concentrations of substrate or signals merging together.

HRMS (ESI$^+$) *calculated for $C_{27}H_{17}F_3N_2O_4S$ = 495.0961, mass found = 495.0982.*

Melting point *41–44 °C.*

4-Phenyl-6-(phenylsulfonyl)-5-(2-(trifluoromethyl)phenyl)pyrimidine, 23a



Following general procedure C, using phenylboronic acid (15 mg, 0.12 mmol, 1.6 eq.). The resulting yellow crude mixture was purified by column chromatography (2.5 g silica, 1:9 ethyl acetate/pentane) to yield pyrimidine **23a** as an off-white solid (29 mg, 88%)

^{1}H NMR (500 MHz, Chloroform-*d*) *δ_H = 9.24 (s, 1H, H_1), 7.89 (dd, J = 8.4, 1.3 Hz, 2H, H_{12}), 7.66 (m, 2H, H_6 & H_{14}), 7.63 (d, J = 6.3 Hz, 1H, H_8), 7.59 (m, 2H, H_5 & H_7), 7.54 (dd, J = 8.4, 7.4 Hz, 2H, H_{13}), 7.30 (d, J = 7.4 Hz, 3H, H_{17} & H_{19}), 7.21 (dd, J = 8.4, 7.1 Hz, 2H, H_{18}).*

^{13}C NMR (126 MHz, Chloroform-*d*) *δ_C = 168.2 (Quat., C_2), 164.4 (Quat., C_{15}), 157.5 (Quat., C_1), 137.9 (Quat., C_{11}), 136.8 (Quat., C_{16}), 134.3 (CH, C_{14}), 133.5 (CH, C_5), 131.2 (CH, C_6), 130.4 (q, J = 2.2 Hz, Quat., C_4), 130.1 (CH, C_{19}), 129.9 (CH, C_{17}), 129.8 (CH, C_{12}), 129.7 (CH, C_7), 129.0 (q, J = 30.4 Hz, Quat., C_9), 129.0 (CH, C_{13}), 128.2 (CH, C_{18}), 128.1 (Quat., C_3), 127.1 (q, J = 4.5 Hz, CH, C_8), 123.7 (q, J = 274.4 Hz, Quat., C_{10}).*

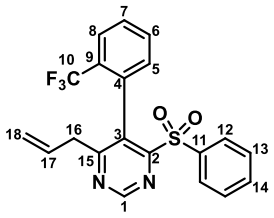
^{19}F NMR (470 MHz, Chloroform-*d*) *δ_F = -58.97.*

FTIR (Chloroform-*d*) *ν/cm^{-1} = 1541, 1511, 1448, 1417, 1363, 1314, 1267, 1152, 1125, 1088, 1067, 1035, 998, 808, 761, 719, 687, 649.*

HRMS (ESI$^+$) *calculated for $C_{23}H_{15}F_3N_2O_2S$ = 441.0840, mass found = 441.0875.*

Melting point *133–135 °C.*

4-Allyl-6-(phenylsulfonyl)-5-(2-(trifluoromethyl)phenyl)pyrimidine, 23b



Following general procedure C, using allylboronic acid pinacol ester (20 mg, 0.12 mmol, 1.6 eq.). The resulting yellow crude mixture was purified by column chromatography (2.5 g silica, 1:9 ethyl acetate/pentane) to yield a light-yellow sticky oil (25 mg). This oil was then further purified by preparative thin-layer chromatography (99:1 toluene/ether) to yield allylpyrimidine **9b** as a light-yellow oil (5 mg, 16%).

^{1}H NMR (500 MHz, Chloroform-*d*) δ_H = 9.04 (s, 1H, H_1), 7.88 (d, *J* = 7.9 Hz, 2H, H_{12}), 7.85 (d, *J* = 7.9 Hz, 1H, H_8), 7.71 (t, *J* = 7.2, Hz, 1H, H_6), 7.66 (m, 2H, H_7 & H_{14}), 7.52 (t, *J* = 7.7 Hz, 2H, H_{13}), 7.34 (d, *J* = 7.8 Hz, 1H, H_5), 7.31 (m, 1H, H_{17}), 5.90 (d, *J* = 15.1 Hz, 1H, H_{18b}), 5.15 (d, *J* = 17.0 Hz, 1H, H_{18a}), 1.82 (dd, *J* = 7.0, 1.7 Hz, 2H, H_{16}).

^{13}C NMR (126 MHz, Chloroform-*d*) *δ_C = 164.2 (Quat., C_2), 163.8 (Quat., C_{15}), 157.3 (CH, C_1), 140.7 (CH, C_{17}), 138.1 (Quat., C_{11}), 134.2 (CH, C_{14}), 132.0 (CH, C_5), 131.9 (CH, C_6), 130.6 (q, J = 2.7 Hz, Quat., C_4), 129.9 (CH, C_{12}), 129.6 (CH, C_7), 129.3 (q, J = 30.3 Hz, Quat., C_9), 129.0 (CH, C_{13}), 126.0 (Quat., C_3), 126.8 (q, J = 4.9 Hz, CH, C_8), 125.8 (CH, C_{18}), 123.8 (d*, J = 274.1 Hz, Quat., C_{10}), 18.9 (CH_2, C_{16}).*

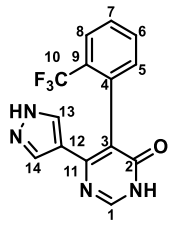
^{19}F NMR (470 MHz, Chloroform-*d*) *δ_F = -59.3.*

* In this section, some ^{13}C signals expected to be quartets (q) were reported as doublets (d) when observed as such on the spectra. This can be due to low concentrations of substrate or signals merging together.

FTIR (Chloroform-*d*) *ν/cm^{-1} = 2917, 2849, 2362, 1564, 1528, 1449, 1399, 1367, 1316, 1265, 1172, 1128, 1036, 793, 764.*

HRMS (ESI^+) *calculated for $C_{20}H_{15}F_3N_2O_2S$ = 405.0840, mass found = 405.0873.*

6-(1*H*-Pyrazol-5-yl)-5-(2-(trifluoromethyl)phenyl)pyrimidin-4-ol, 23f[95]



Chloropyrimidine **20** (15 mg, 0.0375 mmol, 1.0 eq.), 1*H*-pyrazole-4-boronic acid (10 mg, 0.045 mmol, 1.2 eq.), SPhos (1.6 mg, 0.00375 mmol, 0.1 eq.) and palladium (II) acetate (0.4 mg, 0.0019 mmol, 0.05 eq.) were added into a vial. The vial was sealed with a rubber septum, purged with argon three times and dioxane (0.47 mL) was added under argon atmosphere. The resulting mixture was stirred for 10 minutes and an aqueous solution of potassium phosphate (sparged with argon for 30 min) (3 M, 0.094 mL, 0.28 mmol, 7.5 eq.) was added. The reaction mixture was heated to 60 °C and stirred for 16 h. The reaction mixture was cooled to room temperature, diluted with 1 M aqueous sodium hydroxide (1 mL) and extracted with diethyl ether (3 × 1 mL). The combined organics were dried on anhydrous magnesium sulfate, filtered and concentrated *in vacuo*. The crude mixture was purified by preparative TLC (2:8 ethyl acetate/pentane) and compound **23f** was isolated as a white sticky solid (1 mg, 10%).

^{1}H NMR (500 MHz, Chloroform-*d*) *δ_H = 8.86 (s, 1H, H_1), 8.51 (s, 1H, H_{13}), 7.74 (d, J = 7.8 Hz, 1H, H_8), 7.66 (t, J = 7.6 Hz, 1H, H_6), 7.58 (t, J = 7.7 Hz, 1H, H_7), 7.34 (d, J = 7.7 Hz, 1H, H_5), 6.34 (s, 1H, H_{14}).*

^{13}C NMR (126 MHz, Chloroform-*d*) *δ_C* = 163.9 (Quat., C_2), 157.3 (CH, C_1), 155.2 (Quat., C_{11}), 143.7 (CH, C_{14}), 133.3 (q, J = 2.6 Hz, Quat., C_4), 131.9 (CH, C_5), 131.8 (CH, C_6), 130.0 (CH, C_{13}), 128.8 (CH,*

* Not enough material to observe splitting on C_9 and C_{10}.

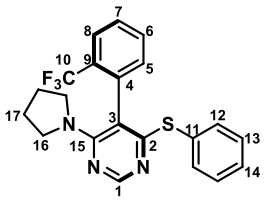
C_7) , 128.5 (Quat., C_9), 126.4 (q, J = 5.0 Hz, CH, C_8), 125.0 (Quat., C_{10}), 120.9 (Quat., C_{12}), 108.5 (Quat., C_3).

^{19}F NMR (470 MHz, Chloroform-*d*) *δ_F = -61.5.*

FTIR (Chloroform-*d*) *ν/cm^{-1} = 2917, 2849, 2362, 1564, 1528, 1449, 1399, 1367, 1316, 1265, 1172, 1128, 1036, 793, 764.*

HRMS (ESI$^+$) *calculated for $C_{14}H_9F_3N_4O$ = 307.0762, mass found = 307.0372.*

***(R)*-4-(Phenylthio)-6-(pyrrolidin-1-yl)-5-(2-(trifluoromethyl)phenyl)pyrimidine, 24**[71]



Racemic: A solution of racemic chloropyrimidine **20** (200 mg, 0.55 mmol, 1.0 eq.), pyrrolidine (228 µL, 2.72 mmol, 5.0 eq.) and *N,N*-diisopropylethylamine (472 µL, 2.72 mmol, 5.0 eq.) in *N,N*-dimethylformamide (4.0 mL) was stirred at room temperature for 15 h under nitrogen atmosphere. Then, saturated aqueous ammonium chloride (4 mL) and ethyl acetate (10 mL) were added. The organic layer was separated, and the aqueous layer was extracted with ethyl acetate (2 × 15 mL). The combined organic extracts were washed with brine (15 mL), dried over anhydrous magnesium sulfate, filtered and concentrated under reduced pressure. Purification of the residue *via* column chromatography (20 g silica, 1:3 ethyl acetate/petroleum ether 40–60) afforded the desired product **24** as a white solid (194 mg, 89%).

Enantioenriched: A solution of enantioenriched chloropyrimidine **20** (85:15 e.r.) (77 mg, 0.21 mmol, 1.0 eq.), pyrrolidine (79 µL, 1.05 mmol, 5.0 eq.) and *N,N*-diisopropylethylamine (182 µL, 1.05 mmol, 5.0 eq.) in *N,N*-dimethylformamide (1.5 mL) was stirred at room temperature for 8 h under nitrogen atmosphere. Then, saturated aqueous ammonium chloride (2 mL) and ethyl acetate (2 mL) were added. The organic layer was separated, and the aqueous layer was extracted with ethyl acetate (2 × 6 mL). The combined organic extracts were washed with brine (10 mL), dried over anhydrous magnesium sulfate, filtered and concentrated under reduced pressure. Purification of the residue *via* column (10 g silica, 1:3 ethyl acetate/petroleum ether 40–60) afforded the desired product **24** as a white solid (75 mg, 89%, 85:15 e.r.).

^{1}H NMR (500 MHz, Chloroform-*d*) *δ_H = 8.33 (s, 1H, H_1), 7.79 (d, J = 6.2 Hz, 1H, H_8), 7.61 (t, J = 7.5 Hz, 1H, H_6), 7.58 (d, J = 7.5 Hz, 1H, H_5), 7.54 (t, J = 6.1 Hz, 1H, H_7), 7.42 (m, 2H, H_{12}), 7.34 (m, 3H, H_{13} & H_{14}), 3.14 (m, 4H, H_{16}), 1.71 (m, 4H, H_{17}).*

^{13}C NMR (126 MHz, Chloroform-*d*) *δ_C = 167.3 (Quat. C_2), 159.1 (Quat., C_{15}), 156.7 (CH, C_1), 135.2 (q, J = 2.0 Hz, Quat., C_4), 135.1 (CH, C_{12}), 134.7 (CH, C_7), 131.4 (CH, C_6), 130.7 (q, J = 29.6 Hz, Quat., C_9), 130.7 (Quat., C_{11}), 129.1 (CH, C_5/C_{14}), 129.1 (CH, C_5/C_{14}), 128.8 (CH, C_{13}), 126.6 (q, J = 5.1 Hz, CH, C_8), 124.0 (q, J = 274.3 Hz, Quat., C_{10}), 111.1 (Quat. C_3), 48.9 (CH_2, C_{16}), 25.4 (CH_2, C_{17}).*

^{19}F NMR (376 MHz, Chloroform-*d*) *δ_F = -61.3.*

FTIR (neat) ν/cm^{-1} *= 2971, 2873, 1544, 1520, 1475, 1455, 1310, 1161, 1126, 1107, 785, 748, 691.*

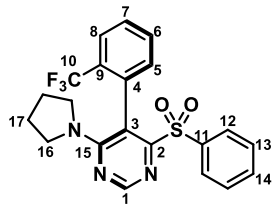
HRMS (ESI$^+$) *calculated for $C_{21}H_{19}F_3N_3S$ = 402.1246, mass found = 402.1255.*

Chiral HPLC *(Chiralpak AD, 20 % IPA, 90 % hexane, 1.0 mL/min, λ = 226 nm, 10 μL injection) τ_R^{major} = 9.88 min, τ_R^{minor} = 19.49 min.*

$[\alpha]_D^{25}$ = *-62 (c = 0.1, $CHCl_3$) for the 85:15 e.r. mixture.*

Melting point *108–113 °C.*

(*R*)-4-(Phenylsulfonyl)-6-(pyrrolidin-1-yl)-5-(2-(trifluoromethyl)phenyl)pyrimidine, 25[71,302]



Racemic: Pyrrolidinyl(sulfidyl)pyrimidine **24** (100 mg, 0.24 mmol, 1.0 eq.) was taken up in trifluoroacetic acid (7 mL). Hydrogen peroxide (30 wt. %, 222 µL, 0.94 mmol, 4.0 eq.) was added at room temperature and the reaction mixture was stirred for 40 h. The reaction mixture was quenched with 1 M sodium hydroxide solution (50 mL) and taken up in diethyl ether (30 mL). The organic layer was separated, and the aqueous layer was extracted with diethyl ether (2 × 30 mL). The combined organic layers were dried over anhydrous magnesium sulfate, filtered and concentrated under reduced pressure. The crude mixture was purified by column chromatography (30 g silica, ethyl acetate/petroleum ether 40–60, 1:1 to 3:1). The pure fractions of the desired sulfone were combined, concentrated under reduced pressure and dried under high vacuum to yield pyrrolidinyl(sulfonyl)pyrimidine **25** as an off-white solid (71 mg, 68%).

Enantioenriched: Hydrogen peroxide (30 wt. %) (29 µL, 0.25 mmol, 2.0 eq.) was added to a stirred solution of chiral phenylthiopyrimidine **24** (85:15 e.r.) (50 mg, 0.12 mmol, 1.0 eq.) in trifluoroacetic acid (2 mL). The reaction mixture was stirred at room temperature for 24 h (a drop of hydrogen peroxide was added after 20 h to push the reaction to completion). The reaction mixture was quenched with 1 M sodium hydroxide solution (10 mL) and taken up in diethyl ether (10 mL). The organic layer was separated, and the aqueous layer was extracted with ether (2 × 15 mL). The combined organic layers were dried over anhydrous $MgSO_4$, filtered and concentrated under reduced pressure. The crude mixture was purified by column chromatography (10 g silica, ethyl acetate/petroleum ether 40–60, 1:1 to 9:1). The pure fractions of the desired sulfone were

combined, concentrated under reduced pressure and dried under high vacuum to yield **25** as an off-white solid (33.1 mg, 61%, 85:15 e.r.).

^{1}H NMR (500 MHz, Chloroform-*d*) *δ_H = 8.46 (s, 1H, H_1), 7.83 (m, 2H, H_{12}), 7.74 (d, J = 6.8 Hz, 1H, H_8), 7.62 (m, 2H, H_6 & H_{14}), 7.59 (m, 2H, H_5 & H_7), 7.48 (t, J = 7.8 Hz, 2H, H_{13}), 3.15 (s, br, 4H, H_{16}), 1.74 (m, br, 4H, H_{17}).*

^{13}C NMR (126 MHz, Chloroform-*d*) *δ_C = 162.3 (Quat., C_2), 159.1 (Quat., C_{15}), 156.8 (CH, C_1), 139.1 (Quat., C_{11}), 134.4 (CH, C_{14}), 133.6 (CH, C_5), 131.7 (d, J = 1.8 Hz, Quat., C_4), 130.8 (CH, C_6), 130.7 (d, J = 29.7 Hz, Quat., C_9), 129.5 (CH, C_{12}), 129.4 (CH, C_7), 128.7 (CH, C_{13}), 126.1 (q, J = 4.9 Hz, CH, C_8), 124.0 (q, J = 274.2 Hz, quat., C_{10}), 112.6 (Quat., C_3), 49.6 (CH_2, C_{16}), 25.3 (CH, C_{17}).*

^{19}F NMR (470 MHz, Chloroform-*d*) *δ_F = -60.1*

HRMS (ESI$^+$) *calculated for $C_{21}H_{18}F_3N_3O_2S$ = 434.1145, mass found = 434.1145.*

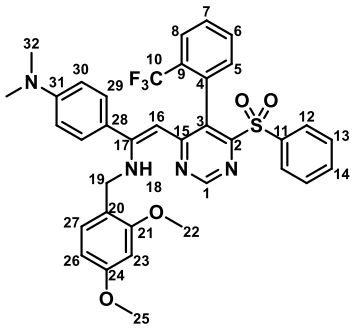
FTIR (neat) *ν/cm^{-1} = 2981, 2804, 1552, 1513, 1479, 1451, 1309, 1167, 1143, 1123, 1109, 801, 774, 733, 721, 682.*

Chiral HPLC *(Chiralpak AD, 30 % IPA, 70 % hexane, 1.0 mL/min, λ = 226 nm, 10 μL injection) τ_R^{major} = 8.38 min, τ_R^{minor} = 21.85 min.*

$[\alpha]_D^{25}$ *= -50 (c = 0.1, $CHCl_3$) for the 85:15 e.r. mixture.*

Melting point *180–183 °C.*

(*Z*)-4-(1-((2,4-Dimethoxybenzyl)amino)-2-(6-(phenylsulfonyl)-5-(2-(trifluoromethyl)phenyl)pyrimidin-4-yl)vinyl)-*N*,*N*-dimethylaniline, 28[96]



In a small vial, sulfonylpyrimidine **22a** (20 mg, 0.04 mmol, 1.0 eq.) was suspended in 2,4-dimethoxybenzylamine (118 µL, 0.8 mmol, 20.0 eq.) and dichloromethane (0.1 mL) was added. The vial was sealed and the resulting dark orange mixture was stirred vigorously at room temperature for 3.5 days. The reaction mixture was quenched with saturated aqueous citric acid (1 mL) and diluted with dichloromethane (1 mL). The reaction mixture was extracted with dichloromethane (3 × 2 mL) and the combined organic extracts were washed with brine (5 mL), dried over anhydrous magnesium sulfate, filtered and concentrated *in vacuo*. The resulting bright yellow crude material was purified *via* column chromatography (2 g silica, ethyl acetate/pentane, 2:8 to 1:0). The bright-yellow fractions were combined to afford enamine **28** as a yellow/orange solid (23 mg, 86%).

^{1}H NMR (400 MHz, Chloroform-*d*) *δ_H = 10.93 (t, J = 6.5 Hz, 1H, H_{18}), 8.66 (s, 1H, H_1), 7.87 (m, 2H, H_{12}), 7.75 (d, J = 7.6 Hz, 1H, H_8), 7.58 (m, 2H, H_6 & H_{14}), 7.49 (m, 3H, H_7 & H_{13}), 7.24 (d, J = 7.9 Hz, 1H, H_5), 7.07 (d, J = 8.9 Hz, 2H, H_{29}), 6.99 (d, J = 8.2 Hz, 1H, H_{23}), 6.60 (d, J = 8.9 Hz, 2H, H_{30}), 6.44 (d, J = 2.3 Hz, 1H, H_{27}), 6.40 (dd, J = 8.2, 2.4 Hz, 1H, H_{26}), 4.38 (s, 1H, H_{16}), 4.35 (d, J = 6.5 Hz, 2H, H_{19}), 3.81 (s, 3H, H_{22}/H_{25}), 3.81 (s, 3H, H_{22}/H_{25}), 2.95 (s, 6H, H_{32}).*

^{13}C NMR (101 MHz, Chloroform-*d*) *δ_C = 165.5 (Quat., C_2), 163.7 (Quat., C_{28}) , 160.6 (Quat. ,C_{21}), 158.7 (Quat., C_{15}), 158.3 (Quat., C_{24}), 156.0 (CH, C_1), 151.1 (Quat., C_{31}), 139.4 (Quat., C_{11}), 133.6 (CH, C_{14}), 132.3 (Quat., C_4), 131.9 (CH, C_6), 131.9 (CH, C_5), 129.4 (CH, C_{12}), 129.3 (CH, C_{29}), 129.1 (Quat., C_9), 128.9 (CH, C_7), 128.7 (CH, C_{13} & C_{23}[*]), 126.8 (q, J = 4.9 Hz, CH, C_8), 124.2 (q, J = 274.0 Hz, Quat., C_{10}), 123.8 (Quat., C_3/C_{17}), 123.8 (Quat., C_3/C_{17}), 120.0 (Quat., C_{20}), 111.4 (CH, C_{30}), 104.0 (CH, C_{26}), 98.6 (CH, C_{27}), 93.1 (CH, C_{16}), 55.5 (CH_3, C_{22}/C_{25}), 55.4 (CH_3, C_{22}/C_{25}), 44.9 (CH_2, C_{19}), 40.3 (CH_3, C_{32}).*

^{19}F NMR (377 MHz, Chloroform-*d*) *δ_F = -59.3.*

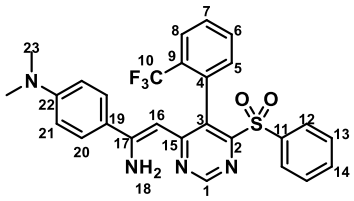
FTIR (Chloroform-*d*) *ν/cm^{-1} = 2918, 1608, 1590, 1544, 1511, 1484, 1447, 1359, 1315, 1287, 1208, 1196, 1159, 1124, 1082, 1065, 1035, 993, 813, 772, 721, 688, 650.*

HRMS (ESI$^+$) *calculated for $C_{36}H_{33}F_3N_4O_4S$ = 675.2239, mass found = 675.2247.*

Melting point *78–80 °C.*

[*] *Broad signal, couples with both H_{13} and H_{23} on HSQC.*

(*Z*)-4-(1-Amino-2-(6-(phenylsulfonyl)-5-(2-(trifluoromethyl)phenyl)pyrimidin-4-yl)vinyl)-*N*,*N*-dimethylaniline, 29[96]



Protected amine **28** (15 mg, 0.022 mmol, 1.0 eq.) was taken up in trifluoroacetic acid (0.19 mL, 2.4 mmol, 0.12 M) and dichloromethane (0.07 mL, 0.3 M) was added. The resulting reaction mixture was stirred at room temperature for 4 hours. The deep red mixture was cooled down to 0 °C and diluted with dichloromethane (1 mL) and the reaction was carefully quenched with a saturated aqueous sodium bicarbonate (2 mL) and allowed to slowly warm up to room temperature. The resulting orange mixture was separated and the aqueous layer was extracted with dichloromethane (2 mL) and the combined organic extracts were washed with brine (5 mL), dried over anhydrous magnesium sulfate, filtered and concentrated *in vacuo*. The crude mixture was purified by preparative TLC and amine **29** was obtained as an orange solid (8 mg, 66%).

^{1}H NMR (400 MHz, Chloroform-*d*) *δ_H = 8.72 (s, 1H, H_1), 7.82 (m, 2H, H_{12}), 7.75 (d, J = 7.4 Hz, 1H, H_8), 7.58 (m, 1H, H_6), 7.52 (m, 2H, H_7 & H_{14}), 7.43 (m, 2H, H_{13}), 7.22 (m, 1H, H_5), 7.12 (d, J = 8.9 Hz, 2H, H_{21}), 6.53 (d, J = 9.0 Hz, 2H, H_{20}), 4.66 (s, 1H, H_{16}), 2.89 (s, 6H, H_{23}).*

^{13}C NMR (126 MHz, Chloroform-*d*) *δ_C = 166.6 (Quat., C_2), 159.4 (Quat., C_{17}), 159.0 (Quat., C_{15}), 156.2 (CH, C_1), 151.9 (CH, C_{22}), 139.2 (Quat., C_{11}), 133.7 (CH, C_{14}), 132.2 (q, J = 2.2 Hz, Quat., C_4), 132.0 (CH, C_6), 131.9 (CH, C_5), 129.5 (CH, C_{12}), 129.3 (d*[*], J = 30.4 Hz, Quat., C_9), 128.9 (CH, C_{13}),*

[*] In this section, some ^{13}C signals expected to be quartets (q) were reported as doublets (d) when observed as such on the spectra. This can be due to low concentrations of substrate or signals merging together.

128.8 (CH, C_7), 127.4 (CH, C_{21}), 126.8 (q, J = 4.8 Hz, CH, C_8), 124.3 (Quat, C_3), 124.1 (d, J = 274.3 Hz, Quat., C_{10}), 112.1 (Quat., C_{19}), 111.9 (CH, C_{20}), 90.3 (CH, C_{16}), 40.3 (CH_3, C_{23}).*

^{19}F NMR (377 MHz, Chloroform-*d*) *δ_F = -59.3.*

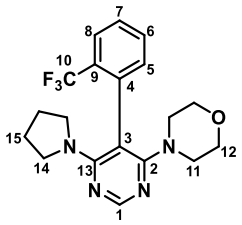
FTIR (Chloroform-*d*) *ν/cm^{-1} = 3423 (br), 2925, 1607, 1542, 1517, 1478, 1445, 1396, 1362, 1315, 1201, 1158, 1124, 1085, 1064, 1035, 992, 947, 909, 811, 774, 727, 687.*

HRMS (ESI$^+$) *calculated for $C_{27}H_{23}F_3N_4O_2S$ = 525.1527, mass found = 525.1561.*

Melting point *169–172 °C.*

* In this section, some ^{13}C signals expected to be quartets (q) were reported as doublets (d) when observed as such on the spectra. This can be due to low concentrations of substrate or signals merging together.

4-(6-(Pyrrolidin-1-yl)-5-(2-(trifluoromethyl)phenyl)pyrimidin-4-yl)morpholine, 31b



Following general procedure D, using morpholine (24.5 µL, 0.28 mmol, 1.0 eq.). The resulting crude product was purified by column chromatography (0.6 g silica, ethyl acetate/petroleum ether 40–60, 1:1 to 8:2). Compound **31b** was obtained as a light-yellow solid (12 mg, 90%).

^{1}H NMR (400 MHz, Chloroform-*d*) *δ_H = 8.39 (s, 1H, H_1), 7.72 (dd, J = 7.8, 1.5 Hz, 1H, H_8), 7.54 (td, J = 7.5, 1.5 Hz, 1H, H_6), 7.48 (m, 1H, H_7), 7.45 (m, 1H, H_5), 3.38 (m, 4H, H_{12}), 3.05 (m, 4H, H_{14}), 2.91 (m, 4H, H_{11}), 1.69 (m, 4H, H_{15}).*

^{13}C NMR (101 MHz, Chloroform-*d*) *δ_C = 165.4 (Quat., C_2), 159.8 (Quat., C_{13}), 156.4 (CH, C_1), 134.7 (CH, C_5), 131.7 (q, J = 2.3 Hz, Quat., C_4), 131.0 (CH, C_6), 130.9 (q, J = 29.7 Hz, Quat., C_9), 128.2 (CH, C_7), 126.9 (d, J = 5.0 Hz, CH, C_8), 124.1 (q, J = 274.3 Hz, Quat., C_{10}), 104.0 (Quat., C_3), 66.7 (CH_2, C_{12}), 49.4 (CH_2, C_{14}), 49.4 (CH_2, C_{11}), 25.5 (CH_2, C_{15}).*

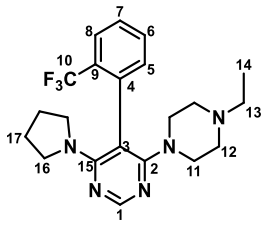
^{19}F NMR (376 MHz, Chloroform-*d*) *δ_F = -60.3.*

FTIR (neat) *ν/cm^{-1} =2981, 2804, 2708, 1553, 1527, 1452, 1422, 1382, 1365, 1310, 1254, 1165, 1102, 1031, 954, 813, 773.*

HRMS (ESI$^+$) *calculated for $C_{19}H_{21}F_3N_4O$ = 379.1740, mass found = 379.1732.*

Melting point *95–100 °C.*

4-(4-Ethylpiperazin-1-yl)-6-(pyrrolidin-1-yl)-5-(2-(trifluoromethyl)phenyl)pyrimidine, 31c



Following general procedure D, using *N*-ethylpiperazine (35.6 µL, 0.28 mmol, 1.0 eq.). The resulting crude product was purified by column chromatography (1.0 g silica, 98:2 dichloromethane/methanol to 96:4 dichloromethane/methanol). Compound **31c** was obtained as an amber solid (9 mg, 66%).

^{1}H NMR (400 MHz, Chloroform-*d*) *δ_H = 8.36 (s, 1H, H_1), 7.70 (d, J = 7.8 Hz, 1H, H_8), 7.52 (m, 1H, H_6), 7.45 (m, 2H, H_7 & H_5), 3.03 (m, 8H, H_{11} & H_{12}), 2.32 (q, J = 7.2 Hz, 2H, H_{13}), 2.19 (m, 4H, H_{16}), 1.67 (td, J = 5.9, 3.0 Hz, 4H, H_{17}), 1.01 (t, J = 7.2 Hz, 3H, H_{14}).*

^{13}C NMR (101 MHz, Chloroform-*d*) *δ_C = 160.2 (Quat., C_2), 159.8 (Quat., C_{15}), 156.1 (CH, C_1), 134.8 (CH, C_5), 134.3 (d, J = 2.0 Hz, Quat., C_4), 130.9 (CH, C_6), 129.4 (q, J = 30.1 Hz, Quat., C_9), 128.0 (CH, C_7), 126.7 (q, J = 5.2 Hz, CH, C_8), 124.0 (q, J = 275.7 Hz, Quat., C_{10}), 103.1 (Quat., C_3), 52.4 (CH_2, C_{16}), 52.3 (CH_2, C_{13}), 49.2 (CH_2, C_{11}/C_{12}), 48.3 (CH_2, C_{11}/C_{12}), 25.4 (CH_2, C_{17}), 11.6 (CH_3, C_{14}).*

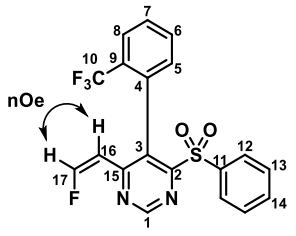
^{19}F NMR (376 MHz, Chloroform-*d*) *δ_F = -60.3.*

FTIR (neat) *ν/cm^{-1} = 2923, 2851, 2360, 1559, 1523, 1481, 1458, 1421, 1370, 1343, 1311, 1256, 1232, 1201, 1163, 1108, 1062, 1022, 991, 962, 803, 781, 770, 665.*

HRMS (ESI$^+$) *calculated for $C_{19}H_{26}F_3N_5$ = 406.2213, mass found = 406.2213.*

Melting point *70–73 °C.*

(*Z*)-4-(2-Fluorovinyl)-6-(phenylsulfonyl)-5-(2-(trifluoromethyl)phenyl)pyrimidine, 33[101]



In a flame-dried and argon backfilled vial was added a solution of TMS-alkyne **22b** (23 mg, 0.05 mmol, 1.0 eq.) in anhydrous tetrahydrofuran (2.0 mL). The bright orange solution was cooled to –5 °C and stirred vigorously. *Tetra-n*-butylammonium fluoride (TBAF) (1.0 M in THF, 60 µL, 0.06 mmol, 1.2 eq.) was added at –5 °C and the resulting dark brown mixture was stirred for 30 min under argon, when TLC monitoring showed complete conversion of the starting material. The resulting dark brown solution was quenched with saturated aqueous ammonium chloride (1.0 mL) and extracted with dichloromethane (3 × 3 mL). The combined organic layers were washed with brine (2 × 3 mL), dried over anhydrous sodium sulfate, filtered and concentrated. The crude mixture was purified by column chromatography (1.2 g silica, 2:8 ethyl acetate/pentane). Fluorovinylpyrimidine **33** was isolated as an amber oil (4.3 mg, 21%).

^{1}H NMR (500 MHz, Chloroform-*d*) *δ_H = 8.88 (d, J = 1.6 Hz, 1H, H_1), 7.90 (dd, J = 7.6, 1.6 Hz, 1H, H_8), 7.85 (m, 2H, H_{12}), 7.72 (m, 2H, H_6 & H_7), 7.71 (d, J = 14.7 Hz, 1H, H_{17}), 7.65 (tt, J = 7.5 Hz, 1.2 Hz, 1H, H_{14}), 7.55 (dd, J = 8.4, 7.2 Hz, 2H, H_{13}), 7.29 (m, 1H, H_5), 7.09 (d, J = 14.6 Hz, 1H, H_{16}).*

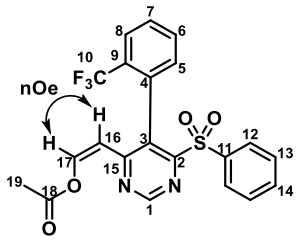
^{13}C NMR (126 MHz, Chloroform-*d*) *δ_C = 167.9 (d, J = 254.8 Hz, Quat., C_{17}), 160.1 (d, J = 4.7 Hz, Quat., C_{15}), 158.3 (Quat., C_2), 158.2 (CH, C_1), 139.2 (Quat., C_{11}), 134.2 (CH, C_{14}), 133.8 (d, J = 5.6 Hz, CH, C_{16}), 132.7 (CH, C_6), 132.1 (q, J = 2.7 Hz, Quat., C_4), 131.8 (CH, C_5), 130.5 (CH, C_7), 129.9 (q, J = 30.6 Hz, Quat., C_9), 129.7 (CH, C_{13}), 128.2 (CH, C_{12}), 127.2 (q, J = 5.0 Hz, Quat., C_8), 123.5 (q, J = 273.8 Hz, Quat., C_{10}), 119.8 (d, J = 27.7 Hz, Quat., C_3).*

^{19}F NMR (377 MHz, Chloroform-*d*) *δ_F = -57.3 (s, -CF_3), -60.4 (d, J = 3.9 Hz, CH=C(H)F).*

FTIR (Chloroform-*d*) *v/cm^{-1} = 3062, 2916, 2361, 1590, 1530, 1436, 1392, 1316, 1177, 1127, 1085, 1069, 1035, 991, 965, 859, 833, 796, 773, 755, 730, 687.*

HRMS (ESI$^+$) *calculated for $C_{19}H_{12}F_4N_2O_2S$ = 409.0589, mass found = 409.0629.*

(*Z*)-2-(6-(Phenylsulfonyl)-5-(2-(trifluoromethyl)phenyl)pyrimidin-4-yl)vinyl acetate, 34[102]



In a flame-dried and argon backfilled vial was added solution of TMS-alkyne **22b** (23 mg, 0.05 mmol, 1.0 eq.) in anhydrous tetrahydrofuran (1.1 mL). The orange solution was cooled to –5 °C and stirred vigorously. Acetic acid (2% v/v in THF, 0.22 mL, 0.075 mmol, 1.5 eq.) and TBAF (1.0 M in THF, 60 µL, 0.06 mmol, 1.2 eq.) were added at –5 °C. The reaction mixture was allowed to slowly warm up to room temperature and stirred for 16 h under argon. The resulting dark solution was quenched with saturated aqueous sodium bicarbonate (0.1 mL), diluted with water (2 mL) and extracted with dichloromethane (3 × 2 mL). The combined organic layers were washed with brine (10 mL), dried over anhydrous sodium sulfate, filtered and concentrated. The crude mixture was purified by column chromatography (1.2 g silica, 2:8 ethyl acetate/pentane). Vinyl acetate **34** was obtained as a red solid (5 mg, 22%).

^{1}H NMR (500 MHz, Chloroform-*d*) *δ_H = 9.02 (s, 1H, H_1), 8.68 (d, J = 12.1 Hz, 1H, H_{17}), 7.89 (dd, J = 8.4, 1.3 Hz, 2H, H_{12}), 7.86 (d, J = 7.7 Hz, 1H, H_8), 7.72 (t, J = 7.2 Hz, 1H, H_6), 7.66 (m, 3H, H_{13} & H_{14}), 7.53 (t, J = 7.9 Hz, 1H, H_7), 7.35 (d, J = 7.5 Hz, 1H, H_5), 5.79 (d, J = 12.0 Hz, 1H, H_{16}), 2.15 (s, 3H, H_{19}).*

^{13}C NMR (126 MHz, Chloroform-*d*) *δ_C = 166.9 (Quat., C_{18}), 163.9 (Quat., C_2), 163.8 (Quat., C_{15}), 157.2 (CH, C_1), 146.3 (CH, C_{17}), 137.9 (Quat., C_{11}), 134.3 (CH, C_{14}), 132.1 (CH, C_6), 131.8 (CH, C_5), 130.3 (q, J = 1.9 Hz, Quat., C_4), 129.9 (CH, C_{12}), 129.7 (CH, C_{13}), 129.2 (q, J = 30.3 Hz, Quat., C_9),*

129.0 (CH, C_7), 126.9 (q, J = 4.8 Hz, C_8), 126.3 (Quat., C_3), 123.8 (q, J = 274.2 Hz, C_{10}), 109.4 (CH, C_{16}), 20.7 (CH_3, C_{19}).

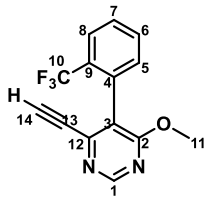
^{19}F NMR (377 MHz, Chloroform-*d*) *δ_F = -59.3.*

FTIR (Chloroform-*d*) *ν/cm^{-1} = 2923, 2852, 1776, 1650, 1545, 1509, 1448, 1422, 1372, 1315, 1173, 1151, 1108, 811, 772, 726, 687.*

HRMS (ESI$^+$) *calculated for $C_{21}H_{15}F_3N_2O_4S$ = 449.0738, mass found = 449.07763.*

Melting point *61–63 °C.*

4-Ethynyl-6-methoxy-5-(2-(trifluoromethyl)phenyl)pyrimidine, 35[80]



In a small vial, TMS-alkynyl(sulfonyl)pyrimidine **22b** (50 mg, 0.11 mmol, 1.0 eq.) was dissolved in methanol (0.8 mL), 1 M aqueous potassium carbonate (0.22 mL, 0.22 mmol, 2.0 eq.) was added and the resulting brown suspension was stirred at room temperature for 20 minutes. Water (5 mL) and dichloromethane (5 mL) were added and the phases were separated. The aqueous layer was extracted with dichloromethane (2 × 5 mL) and the combined organic layers were dried over anhydrous magnesium sulfate, filtered and concentrated. The resulting crude mixture was purified by column chromatography (1.5 g silica, ethyl acetate/pentane, 2:8 to 1:1). The deprotected, methanolysed pyrimidine **35** was isolated as an off-white solid (11 mg, 36%).

^{1}H NMR (500 MHz, Chloroform-*d*) *δ_H = 8.76 (s, 1H, H_1), 7.79 (d, J = 7.9 Hz, 1H, H_8), 7.63 (t, J = 7.4 Hz, 1H, H_6), 7.56 (t, J = 7.7 Hz, 1H, H_7), 7.29 (d, J = 7.5 Hz, 1H, H_5), 3.92 (s, 3H, H_{11}), 3.11 (s, 1H, H_{14}).*

^{13}C NMR (126 MHz, Chloroform-*d*) *δ_C = 167.3 (Quat., C_2), 158.0 (CH, C_1), 148.2 (Quat., C_{12}), 132.0 (CH, C_6), 131.7 (CH, C_5), 131.3 (q, J = 2.2 Hz, Quat., C_4), 129.5 (q, J = 30.5 Hz, Quat., C_9), 129.0 (CH, C_7), 126.6 (q, J = 4.9 Hz, CH, C_8), 123.8 (q, J = 273.8 Hz, Quat., C_{10}), 123.1 (Quat., C_3), 84.4 (CH, C_{14}), 79.6 (Quat., C_{13}), 54.6 (CH, C_{11}).*

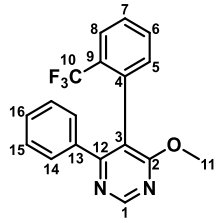
^{19}F NMR (470 MHz, Chloroform-*d*) *δ_F = -60.8.*

FTIR (Chloroform-*d*) *ν/cm^{-1} = 1607, 1562, 1469, 1419, 1384, 1314, 1170, 1127, 1062, 1036, 997, 833, 770.*

HRMS (ESI$^+$) *calculated for $C_{14}H_9F_3N_2O$ = 279.0701, mass found = 279.07388.*

Melting point *104–106 °C.*

4-Methoxy-6-phenyl-5-(2-(trifluoromethyl)phenyl)pyrimidine, 36



Sulfonylpyrimidine **23a** (10 mg, 0.02 mmol, 1.0 eq.) was weighed into a small vial, dissolved in methanol (0.1 mL) and 1 M aqueous potassium carbonate (40 µL, 0.04 mmol, 2.0 eq.) was added. The resulting colourless suspension was stirred at room temperature for 16 h. Water (1 mL) and dichloromethane (1 mL) were added and the phases were separated. The aqueous layer was extracted with dichloromethane (3 × 2 mL) and the combined organic layers were washed with brine (5 mL), dried over anhydrous magnesium sulfate, filtered and concentrated. The resulting crude mixture was purified by preparative TLC (2:8 ethyl acetate/pentane). Methoxypyrimidine **36** product was isolated as a white solid (4 mg, 53%).

^{1}H NMR (500 MHz, Chloroform-*d*) *δ_H = 8.89 (s, 1H, H_1), 7.71 (dd, J = 7.4, 1.9 Hz, 1H, H_8), 7.47 (m, 2H, H_6 & H_7), 7.34 (m, 2H, H_{14}), 7.24 (d, J = 7.3 Hz, 1H, H_5), 7.20 (t, J = 7.3 Hz, 2H, H_{15}), 7.15 (dd, J = 7.3, 1.8 Hz, 1H, H_{16}), 3.94 (s, 3H, H_{11}).*

^{13}C NMR (126 MHz, Chloroform-*d*) *δ_C = 167.9 (Quat., C_2), 163.5 (Quat., C_{12}), 157.6 (CH, C_1), 137.6 (Quat., C_{13}), 132.8 (CH, C_{16}), 132.5 (q, J = 2.1 Hz, Quat., C_4), 131.8 (CH, C_6), 129.8 (q, J = 30.1 Hz, Quat., C_9), 129.5 (CH, C_{14}), 129.1 (CH, C_5), 128.4 (CH, C_7), 128.0 (CH, C_{15}), 127.0 (q, J = 4.8 Hz, CH, C_8), 124.0 (d, J = 274.2 Hz, Quat., C_{10}), 118.1 (Quat., C_3), 54.5 (CH_3, C_{11}).*

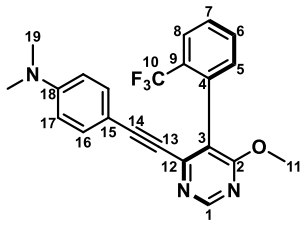
^{19}F NMR (470 MHz, Chloroform-*d*) *δ_F = -60.4.*

FTIR (Chloroform-*d*) *v/cm^{-1} = 2959, 2917, 2362, 1606, 1562, 1544, 1496, 1468, 1422, 1382, 1314, 1169, 1131, 1035, 696.*

HRMS (ESI^{+}) *calculated for $C_{18}H_{13}F_3N_2O$ = 331.1014, mass found = 331.1050.*

Melting point *98–101 °C.*

(*S*)-4-((6-Methoxy-5-(2-(trifluoromethyl)phenyl)pyrimidin-4-yl)ethynyl)-*N*,*N*-dimethylaniline, 37a



Racemic: *Following general procedure E*, using racemic sulfonylpyrimidine **22a** and methanol. Methoxypyrimidine **37a** was isolated as a light yellow solid (7.3 mg, 93%). Starting material **22a** was also recovered (0.7 mg, 7%).

Enantioenriched: *Following general procedure E*, using enantioenriched sulfonylpyrimidine **22a** (85:15 e.r.) and methanol. Methoxypyrimidine **37a** was isolated as a light yellow solid (7 mg, 87%, 85:15 e.r.). Starting material **22a** was also recovered (0.7 mg, 7%).

^{1}H NMR (500 MHz, Chloroform-*d*) *δ_H = 8.74 (s, 1H, H_1), 7.81 (d, J = 7.8 Hz, 1H, H_8), 7.66 (t, J = 7.2 Hz, 1H, H_6), 7.58 (t, J = 7.7 Hz, 1H, H_7), 7.37 (d, J = 7.5 Hz, 1H, H_5), 6.96 (d, J = 8.9 Hz, 2H, H_{16}), 6.51 (d, J = 9.0 Hz, 2H, H_{17}), 3.93 (s, 3H, H_{11}), 2.95 (s, 6H, H_{19}).*

^{13}C NMR (126 MHz, Chloroform-*d*) *δ_C = 167.0 (Quat., C_2), 157.8 (CH, C_1), 151.0 (Quat., C_{12}) , 150.4 (Quat., C_{18}), 133.7 (CH, C_{16}), 132.5 (q, J = 2.1 Hz, Quat., C_4), 132.3 (CH, C_5), 131.8, (CH, C_6) 129.8 (q, J = 30.5 Hz, Quat., C_9), 128.6 (CH, C_7), 126.5 (q, J = 4.9 Hz, CH, C_8), 124.0 (q, J = 274.0 Hz, Quat., C_{10}), 121.2 (Quat., C_3), 111.6 (CH ,C_{17}), 107.7 (Quat., C_{15}), 100.3 (Quat., C_{14}), 85.2 (Quat., C_{13}), 54.4 (CH_2, C_{11}), 40.2 (CH_3, C_{19}).*

^{19}F NMR (377 MHz, Chloroform-*d*) *δ_F = -60.7.*

FTIR (neat) *ν/cm^{-1} = 2918, 2360, 2201, 1607, 1560, 1537, 1466, 1426, 1390, 1367, 1314, 1166, 1127, 1061, 1034, 996, 946, 814, 770.*

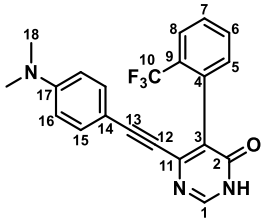
HRMS (ESI$^+$) *calculated for $C_{22}H_{18}F_3N_3O$ = 398.1436, mass found = 398.1482.*

Chiral HPLC *(Chiralpak ADH, 20% IPA, 80% hexane, 1.0 mL/min, λ = 250 nm, 10 μL injection) τ_R^{minor} = 10.66 min, τ_R^{major} = 12.39 min (85:15 e.r.).*

$[\alpha]_D^{25}$ *= 27 (c = 0.1, chloroform).*

Melting point *187–190 °C (rac.), 194–197 °C (ent.).*

6-((4-(Dimethylamino)phenyl)ethynyl)-5-(2-(trifluoromethyl)phenyl)pyrimidin-4(3*H*)-one, 37b



*S*ulfonylpyrimidine **22a** (10 mg, 0.02 mmol, 1.0 eq.) was weighed into a small vial, suspended in 1,4-dioxane(0.2 mL), and sodium hydroxide (50% w/w aqueous solution, 10 µL) was added and the resulting yellow suspension was stirred at room temperature for 18 h. The reaction mixture was neutralized with 1 M hydrogen chloride (a few drops) and water (1 mL) and dichloromethane (1 mL) were added and the phases were separated. The aqueous layer was extracted with dichloromethane (3 × 2 mL) and the combined organic layers were washed with brine (5 mL), dried over anhydrous magnesium sulfate, filtered and concentrated. The crude mixture, a light-yellow solid was identified to be pyrimidone **37b** (7 mg, 93%).

^{1}H NMR (500 MHz, Chloroform-*d*) *δ_H = 13.00 (s, 1H, NH), 8.08 (s, 1H, H_1), 7.84 (d, J = 7.9 Hz, 1H, H_8), 7.68 (t, J = 7.3 Hz, 1H, H_6), 7.60 (t, J = 7.7 Hz, 1H, H_7), 7.42 (d, J = 7.6 Hz, 1H, H_5), 6.93 (d, J = 8.9 Hz, 2H, H_{15}), 6.50 (d, J = 9.0 Hz, 2H, H_{16}), 2.95 (s, 6H, H_{18}).*

^{13}C NMR (126 MHz, Chloroform-*d*) *δ_C = 162.7 (Quat., C_2), 151.2 (Quat., C_{17}), 148.3 (Quat., C_{11}), 148.2 (CH, C_1), 133.8 (CH, C_{15}), 132.4 (q, J = 2.4 Hz, Quat., C_4), 132.3 (CH, C_5), 132.2 (CH, C_6), 130.1 (q, J = 30.4 Hz, Quat., C_9), 128.8 (CH, C_7), 127.5 (Quat., C_3), 126.7 (q, J = 4.8 Hz, CH, C_8), 124.1 (q, J = 274.1 Hz, Quat., C_{10}), 111.6 (CH, C_{16}), 107.4 (Quat., C_{14}), 103.1 (CH, C_{13}), 85.6 (CH, C_{13}), 40.1 (CH_3, C_{18}).*

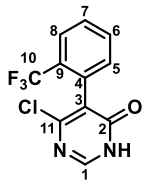
^{19}F NMR (377 MHz, Chloroform-*d*) *δ_F = -60.5.*

FTIR (Chloroform-*d*) *ν/cm^{-1} = 2980, 2918, 2191, 1650, 1591, 1523, 1446, 1409, 1368, 1315, 1265, 1065, 1035, 1017, 817, 769, 732.*

HRMS (ESI^+) *calculated for $C_{21}H_{16}F_3N_3O$ = 384.1318, mass found = 384.1317.*

Melting point *203–206 °C.*

6-Chloro-5-(2-(trifluoromethyl)phenyl)pyrimidin-4(3*H*)-one, 39



Sulfonyl pyrimidine **20** (15 mg, 0.038 mmol, 1.0 eq.) was weighed into a vial and dissolved in 1,4-dioxane (0.2 mL). Aqueous sodium hydroxide (50% w/w) (25 µL, 0.456 mmol, 12.0 eq.) was added and the resulting colourless mixture was stirred at room temperature overnight. Upon completion, the reaction mixture had turned yellow. The reaction mixture was acidified with 1 M hydrogen chloride (a few drops), diluted with dichloromethane (1 mL) and water (1 mL). The aqueous layer was extracted with dichloromethane (3 × 2 mL) and the combined organic extracts were washed with brine (5 mL), dried over anhydrous magnesium sulfate, filtered and concentrated *in vacuo*. The crude mixture, an off-white solid, was identified as pyrimidone **39** (9 mg, 95%).

^{1}H NMR (500 MHz, Chloroform-*d*) *δ_H = 12.99 (s, 1H, NH), 8.02 (s, 1H, H_1), 7.82 (d, J = 7.8 Hz, 1H, H_8), 7.68 (t, J = 7.6 Hz, 1H, H_6), 7.60 (t, J = 7.7 Hz, 1H, H_7), 7.29 (d, J = 7.6 Hz, 1H, H_5).*

^{13}C NMR (126 MHz, Chloroform-*d*) *δ_C = 162.8 (Quat., C_2), 158.5 (Quat., C_{11}), 147.7 (CH, C_1), 132.5 (CH, C_6), 131.3 (CH, C_5), 130.4 (q, J = 2.2 Hz, Quat., C_4), 129.4 (CH, C_7), 129.3 (q, J = 30.8 Hz, Quat., C_9), 126.8 (q, J = 4.9 Hz, CH, C_8), 125.0 (Quat., C_3), 123.7 (q, J = 273.8 Hz, Quat., C_{10}).*

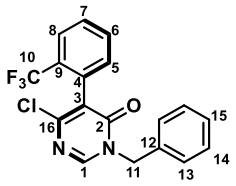
^{19}F NMR (471 MHz, Chloroform-*d*) *δ_F = -61.2.*

FTIR (Chloroform-*d*) *ν/cm^{-1} = 3660, 2981, 2917, 2849, 1661, 1590, 1552, 1462, 1380, 1316, 1252, 1166, 1131, 1067, 1036, 995, 953, 798, 733, 685, 647.*

HRMS (ESI$^+$) *calculated for $C_{11}H_6ClF_3N_2O$ = 275.0194, mass found = 275.0194.*

Melting point *163–165 °C.*

(*R*)-3-Benzyl-6-chloro-5-(2-(trifluoromethyl)phenyl)pyrimidin-4(3*H*)-one, 40a



Racemic: *Following general procedure F,* using racemic chloropyrimidine **20**, the reaction mixture was quenched with benzyl bromide (24 µL, 0.20 mmol, 5.0 eq.), and stirred at 50 °C for 1 h. The crude mixture was purified by column chromatography (7.5 g silica, 2:8 ethyl acetate/pentane) and the desired benzyloxypyrimidine **40a** obtained as a white solid (10.5 mg, 76%).

Enantioenriched: *Following general procedure F,* using enantioenriched chloropyrimidine **20** (88:12 e.r.), the reaction mixture was quenched with benzyl bromide (24 µL, 0.20 mmol, 5.0 eq.), and stirred at 50 °C for 1 h. The crude mixture was purified by column chromatography (7.5 g silica, 2:8 ethyl acetate/pentane) and the desired benzylpyrimidinone **40a** obtained as a white solid (7 mg, 52%, 88:12 e.r.).

^{1}H NMR (400 MHz, Chloroform-*d*) *δ_H = 8.10 (s, 1H, H_1), 7.78 (d, J = 7.9 Hz, 1H, H_8), 7.64 (tdd, J = 7.6, 1.4, 0.7 Hz, 1H, H_6), 7.55 (tt, J = 7.6, 1.1 Hz, 1H, H_7), 7.38 (m, 3H, H_{13} & H_{15}), 7.33 (dd, J = 7.6, 2.0 Hz, 2H, H_{14}), 7.28 (d, J = 7.6 Hz, 1H, H_5), 5.19 (d, J = 14.5 Hz, 1H, H_{11}), 5.08 (d, J = 14.5 Hz, 1H, H_{11}).*

^{13}C NMR (101 MHz, Chloroform-*d*) *δ_C = 159.9 (Quat. ,C_2), 156.0 (Quat., C_{16}), 149.7 (CH, C_1), 134.6 (Quat., C_{12}), 132.5 (CH, C_6), 131.5 (CH, C_5), 131.2 (q, J = 2.1 Hz, Quat., C_4), 129.5 (Quat., C_9), 129.4*

(CH, C_{13}), 129.2 (CH, C_{15}), 129.0 (CH, C_7), 128.4 (CH, C_{14}), 126.8 (q, J = 5.0 Hz, CH, C_8), 124.6 (Quat., C_3), 123.9 (d, J = 274.0 Hz, Quat., C_{10}), 50.5 (CH_2, C_{11}).*

^{19}F NMR (377 MHz, Chloroform-*d*) *δ_F = -61.2.*

FTIR (Chloroform-*d*) *ν/cm^{-1} =2981, 1668, 1587, 1544, 1381, 1315, 1267, 1222, 1171, 1126, 1076, 1044, 1035, 969, 945.*

HRMS (ESI$^+$) *calculated for $C_{18}H_{12}ClF_3N_2O$ = 365.0663, mass found = 365.0663.*

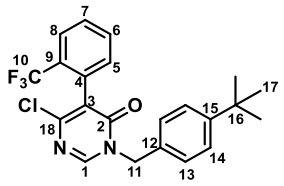
Chiral HPLC *(Chiralpak ADH, 20% IPA, 80% hexane, 1.0 mL/min, λ = 250 nm, 10 μL injection) τ_R^{major} = 9.06 min, τ_R^{minor} = 10.06 min (88:12 e.r.).*

$[\alpha]_D^{25}$ *= – 13 (c = 0.1, chloroform) for the 88:12 e.r. mixture.*

Melting point *94–96 °C (rac.), 73–76 °C (ent.).*

* In this section, some ^{13}C signals expected to be quartets (q) were reported as doublets (d) when observed as such on the spectra. This can be due to low concentrations of substrate or signals merging together.

3-(4-(*tert*-Butyl)benzyl)-6-chloro-5-(2-(trifluoromethyl)phenyl)pyrimidin-4(3*H*)-one, 40b



Following general procedure F, the reaction mixture was quenched with 4-*tert*-butylbenzyl bromide (37 µL, 0.20 mmol, 5.0 eq.). The crude mixture was purified by column chromatography (3 g silica, 2:8 ethyl acetate/pentane) and product **40b** was obtained as a white solid (10 mg, 65%).

^{1}H NMR (500 MHz, Chloroform-*d*) *δ_H = 8.08 (s, 1H, H_1), 7.78 (d, J = 7.9 Hz, 1H, H_8), 7.64 (t, J = 7.5 Hz, 1H, H_6), 7.55 (t, J = 7.7 Hz, 1H, H_7), 7.41 (d, J = 8.3 Hz, 2H, H_{13}), 7.29 (d, J = 8.2 Hz, 1H, H_5), 7.27 (d, J = 8.8 Hz, 2H, H_{14}), 5.14 (d, J = 14.5 Hz, 1H, H_{11}), 5.07 (d, J = 14.5 Hz, 1H, H_{11}), 1.32 (s, 9H, H_{17}).*

^{13}C NMR (126 MHz, Chloroform-*d*) *δ_C = 159.9 (Quat., C_2), 156.0 (Quat., C_{18}), 152.1 (Quat., C_{15}), 149.8 (CH, H_1), 132.5 (CH, C_6), 131.5 (CH, C_5 & Quat., C_{12}), 131.3 (q, J = 2.3 Hz, Quat., C_4), 129.3 (q, J = 30.6 Hz, Quat., C_9), 129.2 (CH, C_7), 128.3 (CH, C_{14}), 126.8 (q, J = 5.0 Hz, CH, C_8), 126.4 (CH, C_{13}), 124.5 (Quat., C_3), 123.9 (q, J = 273.9 Hz, Quat., C_{10}), 50.1 (CH_2, C_{11}), 34.8 (Quat., C_{16}), 31.4 (CH_3, C_{17}).*

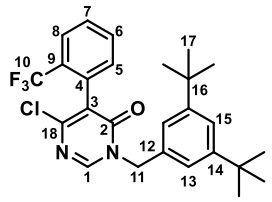
^{19}F NMR (377 MHz, Chloroform-*d*) *δ_F = -61.2.*

FTIR (Chloroform-*d*) *ν/cm^{-1} = 2963, 1669, 1587, 1543, 1403, 1380, 1315, 1267, 1221, 1170, 1128, 1076, 1036, 969, 768, 648, 618.*

HRMS (ESI$^+$) *calculated for $C_{22}H_{20}ClF_3N_2O$ = 421.12890, mass found = 421.1288.*

Melting point *168–170 °C.*

6-Chloro-3-(3,5-di-*tert*-butylbenzyl)-5-(2-(trifluoromethyl)phenyl)pyrimidin-4(3*H*)-one, 40c



Following general procedure F, the reaction mixture was quenched with 3,5-di-*tert*-butylbenzyl bromide (57 mg, 0.20 mmol, 5.0 eq.). The crude mixture was purified by column chromatography (3 g silica, 2:8 ethyl acetate/pentane) and benzylpyrimidinone **40c** was obtained as a white solid (13 mg, 75%).

^{1}H NMR (500 MHz, Chloroform-*d*) *δ_H = 8.07 (s, 1H, H_1), 7.79 (d, J = 7.9 Hz, 1H, H_8), 7.65 (t, J = 7.6 Hz, 1H, H_6), 7.56 (t, J = 7.7 Hz, 1H, H_7), 7.43 (t, J = 1.8 Hz, 1H, H_{15}), 7.29 (d, J = 7.6 Hz, 1H, H_5), 7.16 (d, J = 1.8 Hz, 2H, H_{13}), 5.33 (d, J = 14.5 Hz, 1H, H_{11}), 4.95 (d, J = 14.5 Hz, 1H, H_{11}), 1.32 (s, 18H, H_{17}).*

^{13}C NMR (126 MHz, Chloroform-*d*) *δ_C = 160.0 (Quat., C_2), 155.9 (Quat., C_{18}), 152.2 (Quat., C_{14}), 149.9 (CH, C_1), 133.9 (Quat., C_{12}), 132.5 (CH, C_6), 131.5 (CH, C_5), 131.4 (q, J = 2.2 Hz, Quat., C_4), 129.4 (q, J = 30.5 Hz, Quat., C_9), 129.2 (CH, C_7), 127.8 (d*, J = 277.3 Hz, Quat., C_{10}), 126.8 (q, J = 4.9 Hz, CH, C_8), 124.4 (Quat., C_3), 123.1 (CH, C_{15}), 122.7 (CH, C_{13}), 50.7 (CH_2, C_{11}), 35.0 (Quat., C_{16}), 31.5 (CH_3, C_{17}).*

^{19}F NMR (377 MHz, Chloroform-*d*) *δ_F = -61.1.*

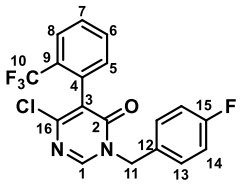
* In this section, some ^{13}C signals expected to be quartets (q) were reported as doublets (d) when observed as such on the spectra. This can be due to low concentrations of substrate or signals merging together.

FTIR (Chloroform-*d*) *ν/cm^{-1} = 2963, 1667, 1588, 1543, 1478, 1403, 1379, 1364, 1315, 1220, 1171, 1130, 1076, 1036, 974, 941, 794, 768, 734, 712.*

HRMS (ESI^+) *calculated for $C_{26}H_{28}ClF_3N_2O$ = 477.1915, mass found = 477.19153.*

Melting point *139–142 °C.*

6-Chloro-3-(4-fluorobenzyl)-5-(2-(trifluoromethyl)phenyl)pyrimidin-4(3*H*)-one, 40d



Following general procedure F, the reaction mixture was quenched with 4-fluorobenzyl bromide (25 µL, 0.20 mmol, 5.0 eq.). The crude mixture was purified by column chromatography (3 g silica, 2:8 ethyl acetate/pentane) and a light-yellow viscous oil was obtained (18 mg, quant.). After triturating the crude mixture in pentane, product **40d** was obtained as a white solid (9 mg, 64%).

^{1}H NMR (500 MHz, Chloroform-*d*) *δ_H = 8.11 (s, 1H, H_1), 7.78 (d, J = 7.9 Hz, 1H, H_8), 7.64 (t, J = 7.5 Hz, 1H, H_6), 7.55 (t, J = 7.7 Hz, 1H, H_7), 7.34 (dd, J = 8.5, 5.3 Hz, 2H, H_{13}), 7.27 (d, J = 8.5 Hz, 1H, H_5), 7.07 (t, J = 8.6 Hz, 2H, H_{14}), 5.16 (d, J = 14.5 Hz, 1H, H_{11}), 5.04 (d, J = 14.5 Hz, 1H, H_{11}).*

^{13}C NMR (126 MHz, Chloroform-*d*) *δ_C= 163.0 (d, J = 248.4 Hz, Quat., C_{15}), 159.8 (Quat., C_2), 156.1 (Quat., C_{16}), 149.5 (CH, C_1), 132.6 (Quat., C_{12}), 132.5 (CH, C_6), 131.5 (CH, C_5), 131.1 (q, J = 2.1 Hz , Quat., C_4), 130.5 (d, J = 8.5 Hz, CH, C_{13}), 129.3 (q, J = 30.5 Hz, Quat., C_9), 129.3 (CH, C_7), 126.9 (q, J = 5.0 Hz, CH, C_8), 124.7 (Quat., C_3), 123.9 (q, J = 273.8 Hz., Quat., C_{10}), 116.4 (d, J = 21.6 Hz, CH, C_{14}), 49.9 (CH_2, C_{11}).*

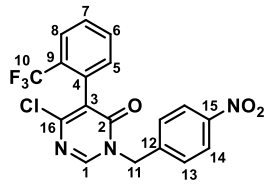
^{19}F NMR (377 MHz, Chloroform-*d*) *δ_F = -61.2 (CF_3), -112.5 (m, CF).*

FTIR (Chloroform-*d*) *ν/cm^{-1} = 2923, 1669, 1587, 1544, 1511, 1404, 1380, 1316, 1267, 1226, 1172, 1127, 1077, 1043, 970, 942, 797.*

HRMS (ESI$^+$) *calculated for $C_{18}H_{11}ClF_4N_2O$ = 383.05689, mass found = 383.0571.*

Melting point *89–92 °C.*

6-Chloro-3-(4-nitrobenzyl)-5-(2-(trifluoromethyl)phenyl)pyrimidin-4(3*H*)-one, 40e



Following general procedure F, the reaction mixture was quenched with 4-nitrobenzyl bromide (43 mg, 0.20 mmol, 5.0 eq.). The crude mixture was purified by column chromatography (7.5 g silica, 2:8 ethyl acetate/pentane to 1:0 ethyl acetate/pentane) and benzylpyrimidinone **40e** was obtained as a yellow oil (14 mg, 91%).

^{1}H NMR (500 MHz, Chloroform-*d*) *δ_H = 8.24 (d, J = 8.8 Hz, 2H, H_{14}), 8.18 (s, 1H, H_1), 7.77 (d, J = 1.3 Hz, 1H, H_8), 7.64 (t, J = 7.5 Hz, 1H, H_6), 7.56 (t, J = 7.8 Hz, 1H, H_7), 7.50 (d, J = 8.7 Hz, 2H, H_{13}), 7.27 (d, J = 8.2 Hz, 1H, H_5), 5.31 (d, J = 15.0 Hz, 1H, H_{11}), 5.13 (d, J = 14.9 Hz, 1H, H_{11}).*

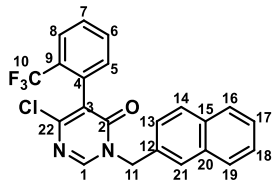
^{13}C NMR (126 MHz, Chloroform-*d*) *δ_C = 159.7 (Quat., C_2), 156.5 (Quat., C_{16}), 149.4 (CH, C_1), 148.2 (Quat., C_{15}), 141.5 (Quat., C_{12}), 132.6 (CH, C_6), 131.4 (CH., C_5), 130.7 (q, J = 2.2 Hz, Quat., C_4), 129.4 (CH, C_7), 129.2 (q, J = 30.5 Hz, Quat., C_9), 129.0 (CH, C_{13}), 126.9 (q, J = 5.0 Hz, CH, C_8), 125.0 (Quat., C_3), 124.5 (CH, C_{14}), 123.9 (d, J = 273.8 Hz, Quat., C_{10}), 50.1 (CH_2, C_{11}).*

^{19}F NMR (377 MHz, Chloroform-*d*) *δ_F = -61.2.*

FTIR (Chloroform-*d*) *ν/cm^{-1} = 2923, 2853, 1670, 1588, 1544, 1521, 1403, 1380, 1346, 1315, 1267, 1222, 1171, 1127, 1078, 1046, 1036, 975, 938, 857, 808, 770, 732.*

HRMS (ESI$^+$) *calculated for $C_{18}H_{11}ClF_3N_3O_3$ = 410.0514, mass found = 410.0515.*

6-Chloro-3-(naphthalen-2-ylmethyl)-5-(2-(trifluoromethyl)phenyl)pyrimidin-4(3*H*)-onene, 40f



Following general procedure F, the reaction mixture was quenched with 2-(bromomethyl)naphtalene (44 mg, 0.20 mmol, 5.0 eq.). The crude mixture was purified by column chromatography (3 g silica, 2:8 ethyl acetate/pentane) and naphtaleneylmethylpyrimidinone **40f** was obtained as a white solid (14 mg, 92%).

^{1}H NMR (500 MHz, Chloroform-*d*) *δ_H = 8.17 (s, 1H, H_1), 7.87 (d, J = 8.4 Hz, 1H, H_{13}), 7.84 (m, 2H, H_{17} & H_{21}), 7.79 (d, J = 7.7 Hz, 2H, H_8 & H_{18}), 7.64 (t, J = 7.4 Hz, 1H, H_6), 7.56 (t, J = 7.8 Hz, 1H, H_7), 7.52 (m, 2H, H_{16} & H_{19}), 7.42 (dd, J = 8.4, 1.9 Hz, 1H, H_{14}), 7.29 (d, J = 7.6 Hz, 1H, H_5), 5.36 (d, J = 14.5 Hz, 1H, H_{11}), 5.24 (d, J = 14.6 Hz, 1H, H_{11}).*

^{13}C NMR (126 MHz, Chloroform-*d*) *δ_C = 159.9 (Quat., C_2), 156.1 (Quat., C_{22}), 149.8 (CH, C_1), 133.4 (Quat., C_{15}/C_{20}), 133.3 (Quat., C_{15}/C_{20}), 132.5 (CH, C_6), 131.9 (Quat., C_{12}), 131.5 (CH, C_5), 131.2 (q, J = 2.3 Hz, Quat., C_4), 129.5 (CH, C_{13}), 129.2 (CH, C_7), 128.9 (d*, J = 32.9 Hz, Quat., C_9), 128.1 (CH, C_{21}), 127.9 (CH, C_{17}), 127.8 (CH, C_{18}), 126.9 (CH, C_{16}/C_{19}), 126.9 (CH, C_{16}/C_{19}), 126.8 (q, J = 5.0 Hz, CH, C_8), 125.5 (CH, C_{14}), 124.6 (Quat., C_3), 123.9 (q, J = 273.8 Hz, Quat., C_{10}), 50.6 (CH_2, C_{11}).*

^{19}F NMR (377 MHz, Chloroform-*d*) *δ_F = -61.1.*

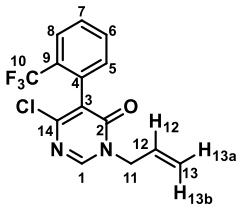
* In this section, some ^{13}C signals expected to be quartets (q) were reported as doublets (d) when observed as such on the spectra. This can be due to low concentrations of substrate or signals merging together.

FTIR (Chloroform-*d*) *ν/cm^{-1} = 2981, 2920, 2851, 1670, 1587, 1543, 1403, 1378, 1315, 1267, 1221, 1127, 1077, 1037, 978, 954, 941, 797, 768.*

HRMS (ESI^+) *calculated for $C_{22}H_{14}ClF_3N_2O$ = 415.0820 , mass found = 415.0818.*

Melting point *45–48 °C.*

3-Allyl-6-chloro-5-(2-(trifluoromethyl)phenyl)pyrimidin-4(3*H*)-one, 40g



Following general procedure F, the reaction mixture was quenched with 3-bromopropene (17 µL, 0.20 mmol, 5.0 eq.). The crude mixture was purified by preparative thin-layer chromatography (1:1 ethyl acetate/pentane) allylpyrimidinone **40g** was obtained as a colourless oil (6 mg, 52%).

^{1}H NMR (500 MHz, Chloroform-*d*) *δ_H = 8.06 (s, 1H, H_1), 7.78 (d, J = 7.9 Hz, 1H, H_8), 7.64 (t, J = 7.4 Hz, 1H, H_6), 7.55 (t, J = 7.7 Hz, 1H, H_7), 7.28 (d, J = 7.6 Hz, 1H, H_5), 5.96 (ddt, J = 16.2, 10.3, 5.9 Hz, 1H, H_{12}), 5.38 (d, J = 10.3 Hz, 1H, H_{13a}), 5.31 (d, J = 17.2 Hz, 1H, H_{13b}), 4.58 (dddt, J = 44.8, 15.6, 6.1, 1.6 Hz, 2H, H_{11}).*

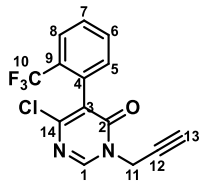
^{13}C NMR (126 MHz, Chloroform-*d*) *δ_C = 159.6 (Quat., C_2), 156.1 (Quat., C_{14}), 149.6 (CH, C_1), 132.5 (CH, C_6), 131.5 (CH, C_5), 131.2 (q, J = 2.3 Hz, Quat., C_4), 130.8 (CH, C_{12}), 129.3 (q, J = 30.5 Hz, Quat., C_9), 129.2 (CH, C_7), 126.8 (q, J = 4.9 Hz, CH, C_8), 124.5 (Quat., C_3), 123.9 (q, J = 273.8 Hz, Quat., C_{10}), 120.4 (CH_2, C_{13}), 49.3 (CH_2, C_{11}).*

^{19}F NMR (377 MHz, Chloroform-*d*) *δ_F = -61.2.*

FTIR (Chloroform-*d*) *ν/cm^{-1} = 2960, 2921, 2851, 1723, 1673, 1587, 1544, 1511, 1462, 1380, 1315, 1269, 1227, 1171, 1128, 1075, 1039, 969, 797, 768.*

HRMS (ESI$^+$) *calculated for $C_{14}H_{10}ClF_3N_2O$ = 315.0507, mass found = 315.0507.*

6-Chloro-3-(prop-2-yn-1-yl)-5-(2-(trifluoromethyl)phenyl)pyrimidin-4(3H)-one, 40h



Following general procedure F, the reaction mixture was quenched with 3-bromopropene (17 µL, 0.20 mmol, 5.0 eq.). The crude mixture was purified by column chromatography (3 g silica, 4:6 ethyl acetate/pentane) and the resulting oil was further purified by thin-layer chromatography (1:1 toluene/diethyl ether) to yield product **40h** as a white sticky solid (5 mg, 43%).

^{1}H NMR (500 MHz, Chloroform-*d*) *δ_H = 8.46 (s, 1H, H_1), 7.79 (d, J = 8.0 Hz, 1H, H_8), 7.65 (t, J = 7.6 Hz, 1H, H_6), 7.56 (t, J = 7.7 Hz, 1H, H_7), 7.28 (d, J = 7.9 Hz, 1H, H_5), 4.76 (qd, J = 18.1, 2.6 Hz, 2H, H_{11}), 2.65 (s, 1H, H_{13}).*

^{13}C NMR (126 MHz, Chloroform-*d*) *δ_C = 159.1 (Quat., C_2), 156.5 (Quat., C_{14}), 148.6 (CH, C_1), 132.5 (CH, C_6), 131.5 (CH, C_5), 130.9 (d, J = 1.9 Hz, Quat., C_4), 129.7 (d*, J = 35.7 Hz, Quat., C_9), 129.3 (CH, C_7), 126.9 (q, J = 4.7 Hz, CH, C_8), 124.0 (Quat., C_3), 123.9 (q, J = 273.8 Hz, Quat., C_{10}) 77.7 (CH, C_{13}), 74.9 (Quat., C_{12}), 36.4 (CH_2, C_{11}).*

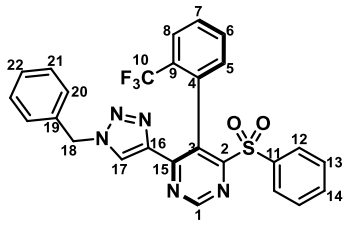
^{19}F NMR (377 MHz, Chloroform-*d*) *δ_F = -61.2.*

FTIR (Chloroform-*d*) *ν/cm^{-1} = 3658, 2981, 2889, 1676, 1589, 1545, 1473, 1462, 1382, 1316, 1252, 1154, 1078, 954.*

HRMS (ESI$^+$) *calculated for $C_{14}H_8ClF_3N_2O$ = 313.0350, mass found = 313.0351.*

* In this section, some ^{13}C signals expected to be quartets (q) were reported as doublets (d) when observed as such on the spectra. This can be due to low concentrations of substrate or signals merging together.

(*S*)-4-(1-Benzyl-1*H*-1,2,3-triazol-4-yl)-6-(phenylsulfonyl)-5-(2-(trifluoromethyl)phenyl)pyrimidine, 41[90,107]



Racemic: In a small vial, racemic (trimethylsilyl)acetylene-pyrimidine **22b** (30 mg, 0.065 mmol, 1.0 eq.) was dissolved in *tert*-butyl alcohol (1.0 mL) at 33 °C and benzyl azide (9.6 µL, 0.072 mmol, 1.1 eq.) was added. In another small vial, copper(II) sulfate pentahydrade (8 mg, 0.032 mmol, 50 mol %), and sodium-*L*-ascorbate (13 mg, 0.065 mmol, 1.0 eq.) were dissolved in water (1.0 mL). The resulting orange aqueous solution was added slowly to the previous organic solution. Pyridine (32 µL) and TBAF (1.0 M in THF, 65 µL, 0.065 M, 1.0 eq.) were slowly added to the mixture in sequence. The resulting brown solution was stirred at 33 °C under nitrogen atmosphere for 16 h. The reaction mixture was quenched with saturated aqueous ammonium chloride (1 mL) and extracted with dichloromethane (3 × 5 mL). The combined organic layers were washed with brine (2 × 10 mL), dried over anhydrous magnesium sulfate, filtered and concentrated under reduced pressure. The crude reaction mixture was purified by column chromatography (3 g silica, 1:1 ethyl acetate/pentane) and 1,2,3-triazolylpyrimidine **41** was isolated as an amber solid (22 mg, 65%).

Enantioenriched: In a small vial, enantioenriched (trimethylsilyl)acetylene-pyrimidine **22b** (81:19 e.r.) (30 mg, 0.065 mmol, 1.0 eq.) was dissolved in *tert*-butyl alcohol (1.0 mL) at 33 °C, and benzyl azide (9.6 µL, 0.072 mmol, 1.1 eq.) was added. In another small vial, copper(II) sulfate pentahydrade (8 mg, 0.032 mmol, 50 mol %), and sodium-*L*-ascorbate (13 mg, 0.065 mmol, 1.0 eq.) were dissolved in water (1.0 mL). The resulting orange aqueous solution was added slowly to the previous organic solution. Pyridine (32 µL) and TBAF (1.0 M in THF, 65 µL, 0.065 M, 1.0 eq.)

were slowly added to the mixture in sequence. The resulting brown solution was stirred at 33 °C under nitrogen atmosphere for 16 h. The reaction mixture was quenched with saturated aqueous ammonium chloride solution (1 mL) and extracted with dichloromethane (3 × 5 mL). The combined organic layers were washed with brine (2 × 10 mL), dried over anhydrous magnesium sulfate, filtered and concentrated under reduced pressure. The crude reaction mixture was purified by column chromatography (5 g silica, 1:1 ethyl acetate/pentane). The desired product **41** was isolated as a brown-red solid (15 mg, 45%, 81:19 e.r.).

^{1}H NMR (400 MHz, Chloroform-*d*) *δ_H = 9.19 (s, 1H, H_1), 7.89 (dd, J = 8.4, 1.3 Hz, 2H, H_{12}), 7.69 (d, J = 7.8 Hz, 1H, H_8), 7.65 (m, 2H, H_6 & H_7), 7.59 (m, 1H, H_{14}), 7.53 (m, 2H, H_{13}), 7.41 (m, 1H, H_5), 7.36 (m, 3H, H_{21} & H_{22}), 7.12 (m, 2H, H_{20}), 6.94 (s, 1H, H_{17}), 5.40 (sextet, J = 17.0 Hz, 2H, H_{18}).*

^{13}C NMR (101 MHz, Chloroform-*d*) *δ_C = 164.6 (Quat., C_2), 158.6 (Quat., C_{15}), 157.8 (CH, C_1), 145.1 (Quat., C_{16}), 137.7 (Quat., C_{11}), 134.4 (CH, C_6), 133.7 (Quat., C_{19}), 132.0 (CH, C_5), 131.9 (CH, C_7), 130.6 (q, J = 1.8 Hz, Quat., C_4), 129.9 (CH, C_{14}), 129.8 (CH, C_{12}), 129.4 (CH, C_{13}), 129.2 (CH, C_{22}), 129.1 (q, J = 34.9 Hz., Quat. C_9), 129.0 (CH, C_{21}), 128.4 (CH, C_{20}), 126.8 (q, J = 4.7 Hz, CH, C_8), 126.4 (Quat., C_3), 126.0 (CH, C_{17}), 123.8 (q, J = 274.5 Hz, Quat., C_{10}), 54.4 (CH_2, C_{18}).*

^{19}F NMR (377 MHz, Chloroform-*d*) *δ_F = -59.5.*

FTIR (Chloroform-*d*) *ν/cm^{-1} = 2981, 2361, 1544, 1448, 1415, 1315, 1267, 1241, 1153, 1123, 1080, 1035, 997, 956, 810, 767, 722, 687.*

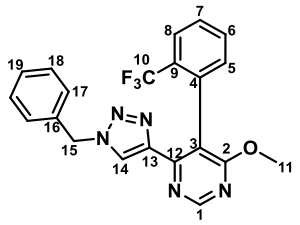
HRMS (ESI$^+$) *calculated for $C_{26}H_{18}F_3N_5O_2S$ = 522.1167, mass found = 522.1207.*

Chiral HPLC *(Chiralpak IC, 40% IPA, 60% hexane, 1.3 mL/min, λ = 250 nm, 10 μL injection) τ_R^{minor} = 28.48 min, τ_R^{major} = 21.92 min (81:19 e.r.).*

$[\boldsymbol{\alpha}]_{\boldsymbol{D}}^{\mathbf{25}}$ *= -14 (c = 0.1, chloroform) for the 81:19 e.r. mixture.*

Melting point *145–147 °C (rac.), 65–68 °C (ent.).*

4-(1-Benzyl-1*H*-1,2,3-triazol-4-yl)-6-methoxy-5-(2-(trifluoromethyl)phenyl)pyrimidine, 42a [107]



Following general procedure G, using benzyl azide (9.6 µL, 0.072 mmol, 1.1 eq.). The crude reaction mixture was purified by column chromatography (2 g silica, 1:1 ethyl acetate/pentane). An amber oil (15 mg) was isolated and further purified by preparative thin-layer chromatography to yield 1,2,3-triazolyl(methoxy)pyrimidine **42a** as a yellow oil (6 mg, 23%).

^{1}H NMR (500 MHz, Chloroform-*d*) *δ_H = 8.84 (s, 1H, H_1), 7.73 (d, J = 7.8 Hz, 1H, H_8), 7.58 (t, J = 8.4 Hz, 1H, H_6), 7.49 (m, 1H, H_7), 7.34 (m, 3H, H_{18} & H_{19}), 7.22 (d, J = 7.3 Hz, 1H, H_5), 7.14 (m, 3H, H_{17} & H_{14}), 5.40 (s, 2H, H_{15}), 3.92 (s, 3H, H_{11}).*

^{13}C NMR (126 MHz, Chloroform-*d*) *δ_C = 167.8 (Quat., C_2), 157.9 (CH, C_1), 154.3 (Quat., C_{12}), 146.0 (Quat., C_{13}), 134.1 (Quat., C_{16}), 132.2 (CH, C_5), 132.2 (CH, C_6), 131.9 (q, J = 2.3 Hz, Quat., C_4), 131.2 (CH, C_{19}), 129.2 (CH, C_{18}), 129.0 (CH, C_7), 128.8 (q, J = 30.8 Hz, C_9), 128.4 (CH, C_{17}), 126.6 (q, J = 4.2 Hz, CH, C_8), 124.9 (CH, C_{14}), 123.8 (q, J = 274.0 Hz, Quat., C_{10}), 116.6 (Quat., C_3), 54.6 (CH_3, C_{11}), 54.3 (CH_2, C_{15}).*

^{19}F NMR (470 MHz, Chloroform-*d*) *δ_F = -61.2.*

FTIR (Chloroform-*d*) *ν/cm^{-1} = 1733, 1607, 1579, 1470, 1422, 1314, 1167, 1110, 1036, 993, 815, 769, 718.*

HRMS (ESI$^+$) *calculated for $C_{21}H_{16}F_3N_5O$ = 412.1340, mass found = 412.1381.*

*For the synthesis and characterisation of 1,2,3-triazolyl(methoxy)pyrimidines **42b–c**, see Alistair Ross' work.*[108]

IV.2.2 Part II: The synthesis of atropisomeric biarylpyrimidines for the inhibition of KRAS G12C

IV.2.2.1 General procedures

General procedure H

*For the iodination of isoquinolinones **68**, **114**, **160** with N-iodosuccinimide.*[232]

N-Iodosuccinimide (1.1 eq.) was added to a solution of a given isoquinolinone (1.0 eq.) in *N,N*-dimethylformamide (0.22 M). The reaction mixture was heated to 80 °C and stirred for 2 h. The reaction mixture was allowed to cool down to room temperature and was then poured onto cold water (0.044 M). The resulting precipitate was filtered, washed abundantly with water and dried under low vacuum for several hours to yield the corresponding 4-iodoisoquinolinone, which was used in the next step without further purification.

General procedure I

*For the bromination of isoquinolinones **68**, **114** with N-bromosuccinimide.*[232]

N-Bromosuccinimide (1.1 eq.) was added to a solution of a given isoquinolinone (1.0 eq.) in *N,N*-dimethylformamide (0.22 M). The reaction mixture was stirred at room temperature for 2 h and was then poured onto ice-cold water (0.044 M). The resulting precipitate was filtered, washed abundantly with water and dried under low vacuum for several hours to yield the corresponding 4-bromoisoquinolinone, which was used in the next step without any further purification.

General procedure J

*For the chlorination of isoquinolinones **70a–b**, **115a–b**, **163** with phosphorus(V) oxychloride.*[234]

A given isoquinolinone (1.0 eq.) was suspended in phosphorus (V) oxychloride (0.3 M). The resulting suspension was heated to 90 °C and stirred until full consumption of the starting material was observed by TLC (16–48 h). The resulting brown solution was allowed to cool down to room temperature and poured onto ice (60 g/mL $POCl_3$). The mixture was stirred until it had warmed up to room temperature and extracted with dichloromethane (× 3). The combined organic layers were washed with brine, dried over anhydrous magnesium sulfate, filtered and concentrated *in vacuo* to yield the corresponding chloroisoquinoline, which was used in the next step without any further purification.

General procedure K

*For the SNAr reaction of chloroisoquinolines **71a–b**, **116a–b**, **164**, **165** with protected piperazines.*[242]

A mixture of a given chloroisoquinoline (1.0 eq.), a given protected piperazine (1.5 eq.) and potassium carbonate (3.0 eq.) in *N,N*-dimethylformamide (0.3 M) was allowed to stir between 80 and 100 °C until full consumption of the starting material had been observed by TLC (16–48 h).

Precipitation "purification": The reaction mixture was allowed to cool down to room temperature and poured onto ice water. The resulting precipitate was filtered off, washed abundantly with water and dried under high-vacuum for several hours to yield the desired piperazinylisoquinoline.

Flash column chromatography purification: The reaction mixture was allowed to cool down to room temperature and poured onto ice water. The resulting slurry was diluted and extracted with ethyl acetate (× 3). The combined organic layers were washed with water (× 3) and brine (× 3),

dried over anhydrous magnesium sulfate, filtered and concentrated *in vacuo*. The resulting crude mixture was purified by column chromatography to yield the desired piperazinylisoquinoline.

General procedure L

*For the SNAr reaction of chloroisoquinolines **106**, **140**, **164** with protected piperazines.*[256]

A mixture of a given chloroisoquinoline (1.0 eq.), a given protected piperazine (1.5 eq.) and *N,N*-diisopropylethylamine (3.0 eq.) in dimethylsulfoxide (0.3 M) was allowed to stir between 80 and 100 °C until full consumption of the starting material was observed by TLC (16–48 h).

Precipitation "purification": The reaction mixture was allowed to cool down to room temperature and poured onto ice water. The resulting precipitate was filtered off, washed abundantly with water and dried under high-vacuum for several hours to yield the desired piperazinylisoquinoline.

Flash column chromatography purification: The reaction mixture was allowed to cool down to room temperature and poured onto ice water. The resulting slurry was diluted and extracted with ethyl acetate (× 3). The combined organic layers were washed with water (× 3) and brine (× 3), dried over anhydrous magnesium sulfate, filtered and concentrated *in vacuo*. The resulting crude mixture was purified by column chromatography to yield the desired piperazinylisoquinoline.

General procedure M

*For the Stille cross-coupling iodoisoquinolines **76a**, **117a**, **156a**, **168a–b** with organostannylpyrimidines **86**, **113** and **162**.*[251]

A flame-dried Schlenk tube was loaded with a given iodoisoquinoline (1.0 eq.), a given pyrimidinylstannane (2.0 eq), cesium fluoride (2.0 eq.), tetrakis(triphenylphosphine) palladium(0) (20 mol%) and copper iodide (40 mol%), the reaction vessel was sealed and purged with argon five times. *N,N*-dimethylformamide (0.1 M) was added and the reaction mixture was heated to 80 °C

and stirred under argon for 20 h[§]. The reaction mixture was allowed to cool down to room temperature and the resulting solution was extracted with ethyl acetate (× 3). The combined organic layers were washed with water (× 3), 1 M aqueous potassium fluoride (× 3, at least 1 min per wash) and brine (× 3), dried over anhydrous magnesium sulfate, filtered and concentrated under reduced pressure. The resulting crude mixture was purified by column chromatography to yield the desired cross-coupling product.

General procedure N

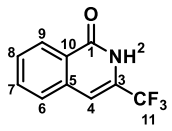
*For the α-arylation of malonates **16a–b**, with haloisoquinolines **71a**, **76c**, **116a**, **117a–c**.*[86]

In a flame-dried Schlenk tube, a given iodoisoquinoline (1.0 eq.), copper iodide (10 mol%), 2-picolinic acid (10 mol%) and caesium carbonate (3.0 eq.) were added in sequence. The vessel was purged three times with argon and anhydrous 1,4-dioxane (0.6 M) was added, followed by a given diethyl malonate (2.0 eq.). The resulting yellow slurry was heated to 50 °C and stirred for 66 h (the temperature was increased to 80–100 °C for **76c** and **117c**, when no reaction had been observed after 66 h at 50 °C). The reaction mixture was allowed to cool down to room temperature and diluted ten-fold in ethyl acetate, and saturated aqueous ammonium chloride was added. The aqueous layer was washed with ethyl acetate (× 3). The combined organic layers were washed with brine, dried over anhydrous magnesium sulfate, filtered and concentrated *in vacuo*. The resulting solid was purified by column chromatography to yield the desired arylated malonate.

[§] *Unless stated otherwise.*

IV.2.2.2 Experimental data

3-(Trifluoromethyl)isoquinolin-1(2*H*)-one, 68[231]



Condensation: Homophthalic acid **64** (98%, 4.1 g, 22.2 mmol, 1.0 eq.) was introduced in a pressure tube and dissolved in trifluoroacetic anhydride **65** (25 mL). The mixture was heated to 140 °C and stirred for 48 h. The black reaction mixture was poured onto water (400 mL) and stirred for 1 h at room temperature. Ethyl acetate (200 mL) was added to the resulting white precipitate and the layers were separated. The aqueous layer was extracted with ethyl acetate (3 × 200 mL). The combined organic layers were dried over anhydrous magnesium sulfate, filtered and concentrated under reduce pressure to yield a light brown solid (5.9 g). MS analysis confirmed the solid to be a mixture of 1-oxo-3-(trifluoromethyl)-1*H*-isochromene-4-carboxylic acid (major) and 3-trifluoromethyl-1*H*-isochrom-1-one (minor).

Lactam formation: The solid was dissolved in concentrated ammonium hydroxide (35%, 250 mL), heated to 35 °C, and stirred for 48 h under nitrogen atmosphere. The reaction mixture was allowed to cool to room temperature, carefully neutralised with concentrated hydrogen chloride (*ca.* 200 mL) and extracted with ethyl acetate (3 × 200 mL). The combined organic layers were dried over anhydrous magnesium sulfate and concentrated under reduced pressure to yield a light brown solid. NMR and MS analysis confirmed the solid to be a 9:1 mixture of 3-hydroxy-3-(trifluoromethyl)-3,4-dihydroisoquinolin-1(2*H*)-one and title compound (3-(trifluoromethyl)isoquinolin-1(2*H*)-one) **68**.

Dehydration: The solid was taken up in *N,N*-dimethylformamide (50 mL) and the resulting solution was refluxed for 6 days. The reaction mixture was allowed to cool down to room temperature and poured onto ice water (200 mL). The resulting beige precipitate was filtrated and washed abundantly with water (2 L). The resulting beige solid was dried *in vacuo* for an hour and identified to be the pure, desired product **68** (3.9 g, 83%).

^{1}H NMR (500 MHz, Dimethyl sufloxide-d_6) *δ_H = 12.27 (s, 1H, H_2), 8.21 (d, J = 8.0 Hz, 1H, H_9), 7.83 (d, J = 7.9 Hz, 1H, H_6), 7.78 (td, J = 7.8, 1.4 Hz, 1H, H_8), 7.63 (t, J = 7.4 Hz, 1H, H_7), 7.19 (s, 1H, H_4).*

^{13}C NMR (126 MHz, Dimethyl sufloxide-d_6) *δ_C = 162.2 (Quat., C_1), 135.7 (Quat., C_5), 133.6 (CH, C_8), 129.6 (CH, C_7), 128.5 (CH, C_6 & Quat., C_{10}), 127.6 (q, J = 21.1 Hz, Quat., C_3), 127.2 (CH, C_9), 120.9 (q, J = 272.3 Hz, Quat., C_{11}), 105.6 (CH, C_4).*

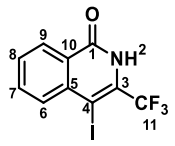
^{19}F NMR (377 MHz, Chloroform-*d*) *δ_F = -67.5.*

FTIR (neat) ν/cm^{-1} *= 2822 (br), 1670, 1606, 1561, 1475, 1387, 1340, 1329, 1310, 1213, 1182, 1129, 1083, 947, 885, 842, 757, 721, 673, 636.*

HRMS (ESI$^+$) *calculated for $C_{10}H_6F_3NO$ = 214.0474, mass found = 214.0475.*

Melting point *185–187 °C.*

4-Iodo-3-(tri fluoromethyl)isoquinolin-1(2*H*)-one, 70a



Following general procedure H, using isoquinolinone **68** (2.0 g, 9.4 mmol). The desired 4-iodoisoquinoline **70a** was obtained as a white solid (2.78 g, 87%).

^{1}H NMR (500 MHz, Chloroform-*d*) *δ_H = 9.59 (s, 1H, H_2), 8.46 (d, J = 7.9 Hz, 1H, H_9), 8.13 (d, J = 8.2 Hz, 1H, H_6), 7.87 (t, J = 7.3 Hz, 1H, H_7), 7.70 (t, J = 7.6 Hz, 1H, H_8).*

^{13}C NMR (126 MHz, Chloroform-*d*) *δ_C = 161.2 (Quat., C_1), 137.4 (Quat., C_5), 134.6 (CH, C_7), 133.2 (CH, C_6), 130.4 (q, J = 33.3 Hz, Quat., C_3), 130.1 (CH, C_8), 128.2 (CH, C_9), 126.8 (Quat., C_{10}), 120.1 (q, J = 275.6 Hz, Quat., C_{11}), 74.9 (Quat., C_4).*

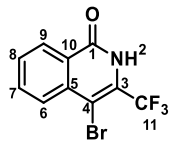
^{19}F NMR (377 MHz, Chloroform-*d*) *δ_F = -63.4.*

FTIR (Chloroform-*d*) ν/cm^{-1} *= 2916, 1687, 1647, 1605, 1465, 1317, 1273, 1238, 1201, 1156, 1138, 764, 725.*

HRMS (ESI$^+$) *calculated for $C_{10}H_5F_3INO$ = 339.9441, mass found = 339.9440.*

Melting point *236–238 °C.*

4-Bromo-3-(trifluoromethyl)isoquinolin-1(2*H*)-one, 70b



Following general procedure I, using isoquinolinone **68** (500 mg, 2.4 mmol). The desired 4-bromoisoquinoline **70b** was obtained as a white solid (577 mg, 84%).

^{1}H NMR (500 MHz, Chloroform-*d*) *δ_H = 9.56 (s, 1H, H_2), 8.48 (dd, J = 8.0, 1.4 Hz, 1H, H_9), 8.15 (d, J = 8.6 Hz, 1H, H_6), 7.88 (ddd, J = 8.4, 7.2, 1.4 Hz, 1H, H_7), 7.71 (ddd, J = 8.2, 7.2, 1.1 Hz, 1H, H_8).*

^{13}C NMR (126 MHz, Chloroform-*d*) *δ_C = 160.8 (Quat., C_1), 135.6 (Quat., C_5), 134.4 (CH, C_7), 130.2 (CH, C_8), 128.3 (Quat., C_{10}), 127.9 (CH, C_9), 127. (CH, C_6), 126.7 (q, J = 34.0 Hz, Quat., C_3), 120.2 (q, J = 274.9 Hz, Quat., C_{11}), 102.1 (q, J = 2.6 Hz, Quat., C_4).*

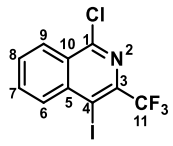
^{19}F NMR (377 MHz, Chloroform-*d*) *δ_F = -63.7.*

FTIR (Chloroform-*d*) ν/cm^{-1} *= 2917, 1685, 1648, 1603, 1559, 1467, 1332, 1320, 1278, 1240, 1161, 1140, 766.*

HRMS (ESI$^+$) *calculated for $C_{10}H_5BrF_3NO$ = 291.9579, mass found = 291.9580.*

Melting point *238–240 °C.*

1-Chloro-4-iodo-3-(trifluoromethyl)isoquinoline, 71a



Following general procedure J, using iodoisoquinolinone **70a** (250 mg, 0.75 mmol). The reaction mixture was stirred at 90 °C for 48 h. Chloroisoquinoline **71a** was obtained as a white solid (246 mg, 93%).

^{1}H NMR (400 MHz, Chloroform-*d*) *δ_H = 8.43 (d, J = 8.4 Hz, 1H, H_9), 8.38 (d, J = 8.3 Hz, 1H, H_6), 7.95 (m, 1H, H_7), 7.88 (m, 1H, H_8).*

^{13}C NMR (126 MHz, Chloroform-*d*) *δ_C = 152.0 (Quat., C_1), 143.1 (q, J = 33.9 Hz, Quat., C_3), 140.1 (Quat., C_5), 133.8 (CH, C_9), 133.8 (CH, C_7), 131.6 (CH, C_8), 128.2 (Quat., C_{10}), 127.3 (CH, C_6) , 121.5 (q, J = 275.5 Hz, Quat., C_{11}), 94.9 (Quat., C_4).*

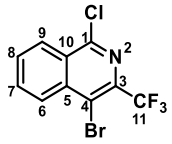
^{19}F NMR (377 MHz, Chloroform-*d*) *δ_F = -63.1.*

FTIR (Chloroform-*d*) ν/cm^{-1} *= 2923, 2853, 1551, 1485, 1447, 1392, 1358, 1298, 1259, 1236, 1174, 1133, 1123, 981, 864, 768, 754, 688, 622.*

HRMS (ESI$^+$) *calculated for $C_{10}H_4ClF_3IN$ = 357.9102, mass found = 357.9102.*

Melting point *103–105 °C.*

4-Bromo-1-chloro-3-(trifluoromethyl)isoquinoline, 71b



Following general procedure J, using bromoisoquinoline **70b** (500 mg, 1.7 mmol, 1.0 eq). The reaction mixture was at 90 °C for 48 h. Chloroisoquinoline **71b** was obtained as a light-yellow solid (524 mg, 99%).

^{1}H NMR (400 MHz, Chloroform-*d*) *δ_H = 8.47 (d, J = 8.5 Hz, 1H, H_9), 8.41 (d, J = 7.5 Hz, 1H, H_6), 7.97 (ddd, J = 8.5, 7.0, 1.3 Hz, 1H, H_8), 7.89 (ddd, J = 8.2, 7.0, 1.2 Hz, 1H, H_7).*

^{13}C NMR (101 MHz, Chloroform-*d*) *δ_C = 150.5 (Quat., C_1), 139.1 (q, J = 34.8 Hz, Quat., C_3), 137.5 (Quat., C_5), 133.5 (CH, C_8), 131.5 (CH, C_7), 128.8 (Quat. C_{10}), 128.2 (CH, C_9), 127.2 (CH, C_6), 121.5 (q, J = 275.0 Hz, Quat., C_{11}), 118.5 (Quat., C_4).*

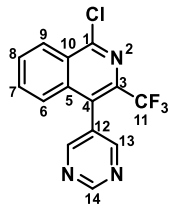
^{19}F NMR (377 MHz, Chloroform-*d*) *δ_F = -63.8.*

FTIR (Neat) ν/cm^{-1} *= 2916, 2849, 1557, 1395, 1302, 1260, 1238, 1196, 1169, 1150, 1127, 985, 865, 768, 754, 720, 624.*

HRSM (ESI$^+$) *calculated for $C_{10}H_4BrClF_3N$ = 311.9218, mass found = 311.9218.*

Melting point *98–100 °C.*

1-Chloro-4-(pyrimidin-5-yl)-3-(trifluoromethyl)isoquinoline, 73[241]



Iodoisoquinoline **71a** (50 mg, 0.14 mmol, 1.0 eq.), pyrimidin-5-yl boronic acid **72** (19 mg, 0.15 mmol, 1.1 eq.), sodium carbonate (44 mg, 0.42 mmol, 3.0 eq.), and 1,1'-bis[(diphenylphosphino)ferrocene]dichloropalladium(II) complex with dichloromethane (11 mg, 0.014 mmol, 0.1 eq.) were added to a Schlenk tube. The vessel was purged with argon three times and 1,2-dimethoxyethane (0.6 mL) and water (0.3 mL) were added under argon atmosphere. The resulting red mixture was heated to 100 °C and stirred for 16 h. The reaction mixture was allowed to cool down to room temperature and water (3 mL) was added. The layers were separated and the aqueous layer was extracted with ethyl acetate (3 × 3 mL). The combined organic layers were dried over anhydrous magnesium sulfate, filtered and concentrated under reduced pressure. The resulting red solid was purified by column chromatography (10 g silica, pentane/ethyl acetate, 9:1 to 1:1) to yield the desired product **73** as a red solid (27 mg, 62%).

^{1}H NMR (500 MHz, Chloroform-*d*) *δ_H = 9.41 (s, 1H, H_{14}), 8.76 (s, 2H, H_{13}), 8.56 (d, J = 8.3 Hz, 1H, H_9), 7.92 (ddd, J = 8.4, 6.9, 1.2 Hz, 1H, H_8), 7.85 (ddd, J = 8.4, 6.9, 1.3 Hz, 1H, H_7), 7.42 (d, J = 8.4 Hz, 1H, H_6).*

^{13}C NMR (126 MHz, Chloroform-*d*) *δ_C = 159.2 (CH, C_{14}), 157.2 (CH, C_{13}), 153.0 (Quat., C_1), 139.0 (q, J = 33.3 Hz, Quat., C_3), 137.8 (Quat., C_5), 133.2 (CH, C_7), 131.1 (CH, C_8), 128.3 (Quat., C_{12}), 127.8 (Quat., C_{10}), 127.3 (CH, C_9), 126.2 (CH, C_6), 126.0 (Quat., C_4), 121.7 (q, J = 275.5 Hz, Quat., C_{11}).*

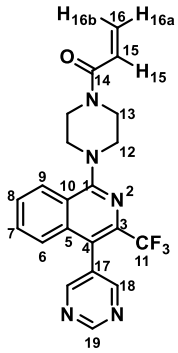
^{19}F NMR (377 MHz, Chloroform-*d*) *δ_F = -59.7.*

FTIR (Chloroform-*d*) *ν/cm^{-1} = 2918, 1548, 1501, 1451, 1420, 1400, 1351, 1325, 1278, 1235, 1185, 1170, 1129, 1098, 1049, 986, 915, 871, 771, 730, 689, 637.*

HRMS (ESI^+) *calculated for $C_{14}H_7ClF_3N_3$ = 310.0353, mass found = 310.0353.*

Melting point *151–153 °C.*

1-(4-(4-(Pyrimidin-5-yl)-3-(trifluoromethyl)isoquinolin-1-yl)piperazin-1-yl)prop-2-en-1-one, 75[242,243]



Starting from compound 74: A mixture of chloroisoquinoline **73** (25 mg, 0.08 mmol, 1.0 eq.), piperazine (10 mg, 0.12 mmol, 1.5 eq.) and potassium carbonate (33 mg, 0.24 mmol, 3.0 eq.) in *N,N*-dimethylformamide (0.5 mL) was allowed to stir at 80 °C for 16 h. The reaction mixture was allowed to cool down to room temperature and poured onto ice water. The resulting red precipitate was filtered, washed abundantly with water, dried under low vacuum and used without any further purification (17 mg). The crude amine (15 mg, 0.04 mmol, 1.0 eq.) was dissolved in triethylamine (62 µL, 0.44 mmol, 11.1 eq.) and dichloromethane (3.3 mL). The resulting solution was cooled to 0 °C and a solution of acryloyl chloride in dichloromethane (0.011 M, 4.7 mL) was added carefully to the mixture. The ice bath was removed and the mixture was stirred at room temperature for 2 h. The reaction was quenched with saturated sodium bicarbonate (5 mL) and extracted with dichloromethane (3 × 5 mL). The combined organic layers were washed with saturated sodium bicarbonate (2 × 8 mL) and brine (8 mL), dried over anhydrous magnesium sulfate, filtered and concentrated *in vacuo*. The resulting yellow crude solid was purified by column chromatography (10 g silica, 97:3 dichloromethane/methanol) to yield the desired product **75** as a light-red solid (15 mg, 51% over two steps).

Starting from compound 77: A solution of isoquinoline **77** (15 mg, 0.03 mmol, 1.0 eq.) in hydrogen chloride (1.25 M in methanol, 1.5 mL) was stirred in a vial at room temperature for 1.5 h. The resulting mixture was concentrated *in vacuo* and the crude yellow solid obtained was taken to the next step without any purification. The crude deprotected amine was dissolved in triethylamine (52 µL, 0.37 mmol, 11.1 eq.) and dichloromethane (2.25 mL). The resulting solution was cooled to 0 °C and a solution of acryloyl chloride in dichloromethane (0.011 M, 3.75 mL) was added carefully to the mixture. The ice bath was removed and the mixture was stirred at room temperature for 1.5 h. The reaction was quenched with saturated sodium bicarbonate (3 mL) and extracted with dichloromethane (3 × 3 mL). The combined organic layers were washed with saturated sodium bicarbonate (5 mL) and brine (5 mL), dried over anhydrous magnesium sulfate, filtered and concentrated *in vacuo*. The resulting yellow crude solid was purified by column chromatography (7g silica, 97: 3 dichloromethane/methanol) to yield the desired product **75** as a light-brown solid (13 mg, 93% over two steps).

^{1}H NMR (500 MHz, Chloroform-*d*) *δ_H = 9.35 (s, 1H, H_{19}), 8.72 (s, 2H, H_{18}), 8.20 (m, 1H, H_9), 7.70 (dddd, J = 15.0, 8.4, 7.0, 1.5 Hz, 2H, H_7 & H_8), 7.32 (dd, J = 8.0, 1.6 Hz, 1H, H_6), 6.65 (dd, J = 16.8, 10.6 Hz, 1H, H_{15}), 6.36 (dd, J = 16.7, 1.9 Hz, 1H, H_{16b}), 5.77 (dd, J = 10.6, 1.9 Hz, 1H,H_{16a}), 3.92 (d, J = 41.7 Hz, 4H, H_{13}), 3.64 (s, 4H, H_{12}).*

^{13}C NMR (126 MHz, Chloroform-*d*) *δ_C = 165.9 (Quat., C_{14}), 160.6 (Quat., C_1), 158.5 (CH, C_{19}), 157.7 (CH, C_{18}), 138.4 (Quat., C_5), 138.2 (q, J = 31.8 Hz, Quat., C_3), 131.5 (CH, C_8), 129.6 (Quat., C_{17}), 128.6 (CH_2, C_{16}), 128.6 (CH, C_7), 127.4 (CH, C_{15}), 126.2 (CH, C_6), 125.7 (CH, C_9), 122.3 (q, J = 275.2 Hz, Quat., C_{11}), 121.6 (Quat., C_{10}), 119.8 (Quat., C_4), 51.9 (CH_2, C_{12}), 50.4 (CH_2, C_{12}), 45.6 (CH_2, C_{13}), 42.0 (CH_2, C_{13}).*

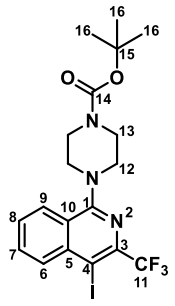
^{19}F NMR (377 MHz, Chloroform-*d*) *δ_F = -60.1.*

FTIR (Chloroform-*d*) ν/cm^{-1} *= 2919, 2851, 1648, 1613, 1575, 1550, 1507, 1460, 1434, 1413, 1391, 1349, 1238, 1176, 1125, 1097, 1049, 1015, 974, 778, 731.*

HRMS (ESI$^+$) *calculated for $C_{21}H_{30}F_3N_5O$ = 414.1536, mass found = 414.1532.*

Melting point *139–142 °C.*

tert-Butyl 4-(4-iodo-3-(trifluoromethyl)isoquinolin-1-yl)piperazine-1-carboxylate, 76a



Following general procedure K, using chloroisoquinoline **71a** (100 mg, 0.28 mmol, 1.0 eq) and 1-Boc-piperazine (78 mg, 0.42 mmol, 1.5 eq.). The reaction mixture was stirred at 80 °C for 16 h. When poured onto ice water and filtrated, title compound **76a** was obtained as an off-white solid (75 mg, 56%) (additional compound **76a** was identified dissolved in the aqueous filtrate). When purified by column chromatography (12 g silica, 85:15 pentane/ethyl acetate), the title compound was obtained as a light-yellow solid (136 mg, 96%).

^{1}H NMR (500 MHz, Chloroform-*d*) *δ_H = 8.33 (dd, J = 8.6, 1.2 Hz, 1H, H_9), 8.03 (dd, J = 8.4, 1.3 Hz, 1H, H_6), 7.78 (ddd, J = 8.4, 6.9, 1.3 Hz, 1H, H_7), 7.68 (ddd, J = 8.2, 6.9, 1.2 Hz, 1H, H_8), 3.68 (m, 4H, H_{12}), 3.47 (m, 4H, H_{13}), 1.50 (s, 9H, H_{16}).*

^{13}C NMR (126 MHz, Chloroform-*d*) *δ_C = 160.1 (Quat., C_1), 155.0 (Quat., C_{14}), 142.2 (q, J = 32.9 Hz, Quat., C_3), 140.1 (Quat., C_5), 133.7 (CH, C_9), 132.0 (CH, C_7), 129.0 (CH, C_8), 125.8 (CH, C_6), 122.7 (Quat., C_{10}), 122.2 (q, J = 275.3 Hz, Quat., C_{11}), 86.3 (CH, C_4), 80.2 (Quat., C_{15}), 51.6 (CH_2, C_{12}), 50.6 (CH_2, C_{12}), 44.0 (CH_2, C_{13}), 43.2 (CH_2, C_{13}), 28.6 (CH_3, C_{16}).*

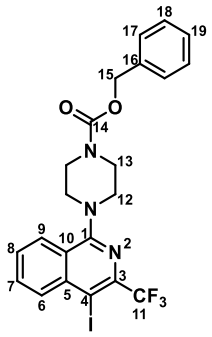
^{19}F NMR (377 MHz, Chloroform-*d*) *δ_F = -63.4.*

FTIR (Chloroform-*d*) ν/cm^{-1} *= 2977, 2924, 1694, 1563, 1498, 1457, 1412, 1339, 1247, 1166, 1129, 1017, 949, 868, 766, 732, 681.*

HRMS (ESI$^+$) *calculated for $C_{19}H_{21}F_3IN_3O_2$ = 508.0703, mass found = 508.0702.*

Melting point *161–163 °C.*

Benzyl 4-(4-iodo-3-(trifluoromethyl)isoquinolin-1-yl)piperazine-1-carboxylate, 76b



Following general procedure K, using chloroisoquinoline **71a** (100 mg, 0.28 mmol, 1.0 eq) and 1-Cbz-piperazine (79 µL, 0.42 mmol, 1.5 eq.). The reaction mixture was stirred at 80 °C for 16 h. When poured onto ice water and filtrated, title compound **76b** was obtained as an off-white solid (151 mg, 99%).

^{1}H NMR (500 MHz, Chloroform-*d*) *δ_H = 8.34 (d, J = 8.4 Hz, 1H, H_9), 8.02 (d, J = 8.4 Hz, 1H, H_6), 7.78 (ddd, J = 8.4, 6.9, 1.3 Hz, 1H, H_7), 7.69 (ddd, J = 8.2, 6.9, 1.2 Hz, 1H, H_8), 7.38 (m, 4H, H_{17} & H_{18}), 7.34 (m, 1H, H_{19}), 5.19 (s, 2H, H_{15}), 3.76 (m, 4H, H_{12}), 3.50 (m, 4H, H_{13}).*

^{13}C NMR (126 MHz, Chloroform-*d*) *δ_C = 160.0 (Quat., C_1), 155.5 (Quat., C_{14}), 142.2 (q, J = 32.7 Hz, Quat., C_3), 140.1 (Quat., C_5), 136.7 (Quat., C_{16}), 133.7 (CH, C_9), 132.1 (CH, C_7) 129.1 (CH, C_8), 128.7 (CH, C_{19}), 128.3 (CH, C_{17}/C_{18}), 128.1 (CH, C_{17}/C_{18}), 125.7 (CH, C_6), 122.7 (Quat., C_{10}), 122.1 (q, J = 275.3 Hz), 86.5 (Quat., C_4), 67.5 (CH_2, C_{15}), 51.0 (d, J = 103.6 Hz, CH_2, C_{13}), 43.8 (CH_2, C_{12}).*

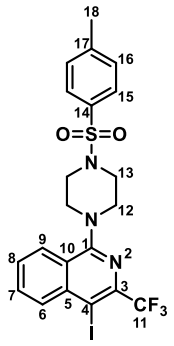
^{19}F NMR (377 MHz, Chloroform-*d*) *δ_F = -63.4.*

FTIR (Chloroform-*d*) ν/cm^{-1} *= 1699, 1563, 1498, 1414, 1242, 1185, 1128, 1014, 765*.

HRMS (ESI$^+$) *calculated for $C_{22}H_{19}F_3IN_3O_2$ = 542.0547, mass found = 542.0547.*

Melting point *> 280 °C.*

4-Iodo-1-(4-tosylpiperazin-1-yl)-3-(trifluoromethyl)isoquinoline, 76c



Following general procedure K, using chloroisoquinoline **71a** (100 mg, 0.28 mmol, 1.0 eq) and 1-tosylpiperazine hydrochloride (116 mg, 0.42 mmol, 1.5 eq.). The reaction mixture was stirred at 80 °C for 16 h. When poured onto ice water and filtrated, title compound **76c** was obtained as an off-white solid (124 mg, 79%). When purified by column chromatography (12 g silica, 85:15 pentane/ethyl acetate), the title compound was obtained as an off-white solid (121 mg, 77%).

^{1}H NMR (500 MHz, Chloroform-*d*) *δ_H = 8.31 (d, J = 8.5 Hz, 1H, H_9), 7.88 (d, J = 8.1 Hz, 1H, H_6), 7.75 (t, J = 7.9 Hz, 1H, H_7), 7.70 (d, J = 7.8 Hz, 2H, H_{15}), 7.63 (t, J = 7.5 Hz, 1H, H_8), 7.37 (d, J = 7.7 Hz, 2H, H_{16}), 3.60 (t, J = 4.7 Hz, 4H, H_{12}), 3.25 (t, J = 4.7 Hz, 4H, H_{13}), 2.46 (s, 3H, H_{18}).*

^{13}C NMR (126 MHz, Chloroform-*d*) *δ_C = 159.5 (Quat., C_1), 144.1 (Quat., C_{17}), 142.1 (q, J = 32.8 Hz, Quat., C_3), 140.1 (Quat., C_{14}), 133.7 (CH, C_9), 132.7 (Quat., C_5), 132.1 (CH, C_7), 130.0 (CH, C_{16}), 129.1 (CH, C_8), 128.0 (CH, C_{15}), 125.5 (CH, C_6), 122.5 (Quat., C_{10}), 122.0 (q, J = 275.1 Hz, Quat., C_{11}), 86.7 (CH, C_4), 50.5 (CH_2, C_{12}), 45.8 (CH_2, C_{13}), 21.7 (CH_3, C_{18}).*

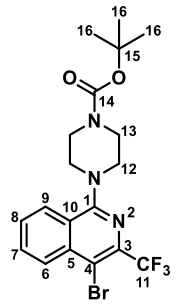
^{19}F NMR (377 MHz, Chloroform-*d*) *δ_F = -63.5.*

FTIR (Chloroform-*d*) ν/cm^{-1} *= 1456, 1342, 1326, 1312, 1284, 1269, 1163, 1127, 1100, 1060, 1021, 931, 800, 768, 729, 652.*

HRMS (ESI$^+$) *calculated for $C_{21}H_{19}F_3IN_3O_2S$ = 562.0268, mass found = 562.0267.*

Melting point *258–261 °C.*

***tert*-Butyl 4-(4-bromo-3-(trifluoromethyl)isoquinolin-1-yl)piperazine-1-carboxylate, 76d**



Following general procedure K, using chloroisoquinoline **71b** (100 mg, 0.32 mmol, 1.0 eq) and 1-Boc-piperazine (78 mg, 0.42 mmol, 1.5 eq.). The reaction mixture was stirred at 80 °C for 16 h. When purified by column chromatography (12 g silica, 85:15 pentane/ethyl acetate), title compound **76d** was obtained as a light-yellow solid (131 mg, 88%).

^{1}H NMR (400 MHz, Chloroform-*d*) *δ_H = 8.4 (d, J = 8.3 Hz, 1H, H_9), 8.1 (d, J = 7.7 Hz, 1H, H_6), 7.8 (ddd, J = 8.4, 7.0, 1.3 Hz, 1H, H_7), 7.7 (ddd, J = 8.3, 7.0, 1.2 Hz, 1H, H_8), 3.7 (m, 4H, H_{12}), 3.5 (m, 4H, H_{13}), 1.5 (s, 9H, H_{16}).*

^{13}C NMR (101 MHz, Chloroform-*d*) *δ_C = 159.2 (Quat. C_1), 155.0 (Quat., C_{14}), 138.1 (q, J = 33.0 Hz, Quat., C_3), 137.7 (Quat., C_5), 131.7 (CH, C_7), 128.9 (CH, C_8), 128.2 (CH, C_9), 125.7 (CH, C_6), 123.2 (Quat., C_{10}), 122.1 (q, J = 275.0 Hz, Quat., C_{11}), 111.3 (Quat., C_4), 80.2 (Quat., C_{15}), 51.2 (CH_2, C_{13}), 44.0 (CH_2, C_{12}), 28.6 (CH_3, C_{16}).*

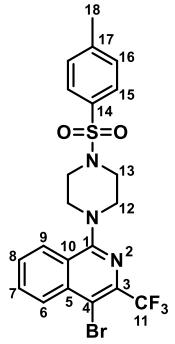
^{19}F NMR (377 MHz, Chloroform-*d*) *δ_F = 64.0.*

FTIR (Chloroform-*d*) ν/cm^{-1} *= 2980, 1693, 1556, 1500, 1410, 1366, 1246, 1165, 1129, 1017, 960, 873, 768, 733, 682.*

HRMS (ESI$^+$) *calculated for $C_{19}H_{21}BrF_3N_3O_2$ = 482.0661, mass found = 482.0659.*

Melting point *160–162 °C.*

4-Bromo-1-(4-tosylpiperazin-1-yl)-3-(trifluoromethyl)isoquinoline, 76e



Following general procedure K, using chloroisoquinoline **71b** (100 mg, 0.32 mmol, 1.0 eq) and 1-tosylpiperazine hydrochloride (116 mg, 0.42 mmol, 1.5 eq.). The reaction mixture was stirred at 80 °C for 16 h. When poured onto ice water and filtrated, title compound **76e** was obtained as an off-white solid (115 mg, 69%).

^{1}H NMR (500 MHz, Chloroform-*d*) *δ_H = 8.36 (d, J = 7.9 Hz, 1H, H_9), 7.94 (dd, J = 8.3, 1.3 Hz, 1H, H_6), 7.79 (ddd, J = 8.3, 6.9, 1.2 Hz, 1H, H_7), 7.70 (d, J = 8.3 Hz, 2H, H_{15}), 7.64 (ddd, J = 8.3, 6.9, 1.2 Hz, 1H, H_8), 7.37 (d, J = 8.0 Hz, 2H, H_{16}), 3.58 (m, 4H, H_{12}), 3.26 (t, J = 4.9 Hz, 4H, H_{13}), 2.46 (s, 3H, H_{18}).*

^{13}C NMR (126 MHz, Chloroform-*d*) *δ_C = 158.6 (Quat., C_1), 144.1 (Quat., C_{17}), 138.0 (q, J = 33.2 Hz, Quat., C_3), 137.7 (Quat., C_5), 132.8 (Quat.,C_{14}), 131.8 (CH, C_7), 130.0 (CH, C_{16}), 129.0 (CH, C_8), 128.3 (CH, C_{15}), 128.0 (CH, C_9), 125.5 (CH, C_6), 123.0 (Quat., C_{10}), 122.0 (q, J = 274.8 Hz, Quat., C_{11}), 111.7 (Quat., C_4), 50.5 (CH_2, C_{12}), 45.8 (CH_2, C_{13}), 31.1 (CH_3, C_{18}).*

^{19}F NMR (377 MHz, Chloroform-*d*) *δ_F = 64.1.*

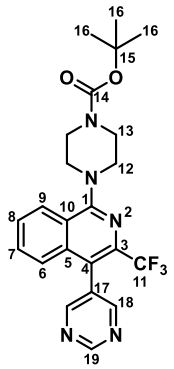
FTIR (Chloroform-*d*) ν/cm^{-1} *= 2923, 2854, 1598, 1557, 1499, 1415, 1327, 1311, 1273, 1238, 1187, 1132, 1103, 1019, 933, 868, 816, 728, 682.*

HRMS (ESI$^+$) *calculated for $C_{21}H_{19}BrF_3N_3O_2S$ = 516.0386, mass found = 516.0383.*

Melting point *238–240 °C.*

<u>*tert*-Butyl-4-(4-(pyrimidin-5-yl)-3-(trifluoromethyl)isoquinolin-1-yl)piperazine-1-carboxylate,</u>

<u>77</u>[241]



Iodoisoquinoline **76a** (25 mg, 0.05 mmol, 1.0 eq.), pyrimidin-5-yl boronic acid **72** (7 mg, 0.06 mmol, 1.1 eq.), sodium carbonate (16 mg, 0.15 mmol, 3.0 eq.), and 1,1'-bis[(diphenylphosphino)ferrocene]dichloropalladium(II) complex with dichloromethane (4 mg, 0.005 mmol, 0.1 eq.) were added to a Schlenk tube. The vessel was purged with argon three times and 1,2-dimethoxyethane (0.2 mL) and water (0.1 mL) were added under argon. The resulting red mixture was heated to 100 °C and stirred for 16 h. The reaction mixture was allowed to cool down to room temperature and water (1 mL) was added. The layers were separated and the aqueous layer was extracted with ethyl acetate (3 × 1 mL). The combined organic layers were dried over anhydrous magnesium sulfate, filtered and concentrated under reduced pressure. The resulting red solid was purified by column chromatography (1 g silica, 6:4 pentane/ethyl acetate) to yield title compound **77** as a red solid (19 mg, 85%).

^{1}H NMR (500 MHz, Chloroform-*d*) *δ_H = 9.34 (s, 1H, H_{19}), 8.71 (s, 2H, H_{18}), 8.18 (dd, J = 7.4, 2.4 Hz, 1H, H_9), 7.67 (m, 2H, H_7/H_8), 7.30 (dd, J = 7.5, 2.2 Hz, 1H, H_6), 3.72 (m, 4H, H_{12}), 3.57 (m, 4H, H_{13}), 1.50 (s, 9H, H_{16}).*

^{13}C NMR (126 MHz, Chloroform-*d*) *δ_C = 160.9 (Quat., C_1), 158.5 (CH, C_{19}), 157.7 (CH., C_{18}), 155.0 (Quat., C_{14}), 138.4 (Quat., C_5), 138.2 (q, J = 31.9 Hz, Quat., C_3), 131.3 (CH, C_7), 129.7 (Quat., C_{17}), 128.4 (CH, C_8), 126.1 (CH, C_6), 125.8 (CH, C_9), 122.4 (q, J = 275.3 Hz, Quat., C_{11}), 121.6 (Quat., C_{10}), 119.4 (Quat., C_4), 80.2 (Quat., C_{15}), 51.1 (d, J = 131.0 Hz, CH_2, C_{13}), 43.7 (d, J = 103.9 Hz, CH_2, C_{12}), 28.6 (CH_3, C_{16}).*

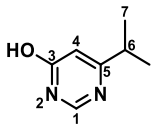
^{19}F NMR (377 MHz, Chloroform-*d*) *δ_F = -60.1.*

FTIR (Chloroform-*d*) ν/cm^{-1} *= 2977, 2924, 1694, 1563, 1498, 1412, 1366, 1339, 1247, 1166, 1129, 1017, 868, 76, 733, 681.*

HRMS (ESI$^+$) *calculated for $C_{23}H_{24}F_3N_5O_2$ = 460.1955, mass found = 460.1951.*

Melting point *143–145 °C.*

6-Isopropylpyrimidin-4-ol, 79



Following a literature procedure.[246] Anhydrous methanol (40 mL) was added to an oven-dried round bottom flask and stirred at room temperature. Sodium metal (1.5 g, 65 mmol, 2.5 eq.) was added portionwise and stirred until fully dissolved (*ca.* an hour). The solution was cooled to 0 °C, formamidine acetate (4.1 g, 39.0 mmol, 1.5 eq.) was added, and the reaction mixture was stirred 0 °C for 15 minutes. Ethyl isobutyrylacetate **78** (4.2 mL, 26.0 mmol, 1.0 eq.) was added at 0 °C. The reaction mixture was allowed to slowly warm up to room temperature (melting ice bath), and stirred for 16 h. The reaction was quenched with water (20 mL), and the pH was adjusted to 4 using glacial acetic acid (*ca.* 100 mL). The mixture was concentrated under reduced pressure, and the resulting crude mixture was taken up in water (40 mL) and extracted with 10% methanol in dichloromethane (3 × 50 mL). The combined organic layers were dried over anhydrous magnesium sulfate, filtered, and concentrated *in vacuo*. The resulting orange crude mixture was purified by column chromatography (185 g silica, 5:95 methanol/dichloromethane) to yield the desired pyrimidine **79** as a light yellow solid (1.96 g, 54%).

^{1}H NMR (400 MHz, Chloroform-*d*) *δ_H = 8.14 (d, J = 1.0 Hz, 1H, H_1), 6.31 (s, 1H, H_4), 2.79 (hept, J = 6.9 Hz, 1H, H_6), 1.23 (d, J = 6.9 Hz, 6H, H_7).*

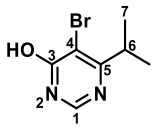
^{13}C NMR (101 MHz, Chloroform-*d*) *δ_C = 175.5 (Quat., C_5), 165.1 (Quat., C_3), 148.1 (CH, C_1), 110.7 (CH, C_4), 35.8 (CH, C_6), 21.1 (CH_3, C_7).*

FTIR (neat) ν/cm^{-1} = *2958 (br), 1644, 1593, 1541, 1469, 1416, 1177, 1123, 1072, 977, 861*.

HRMS (ESI$^+$) *calculated for $C_7H_{10}N_2O$ = 139.0866, mass found = 139.0865.*

Melting point *108–111 °C.*

5-Bromo-6-isopropylpyrimidin-4-ol, 80



Following a literature procedure.[246] Bromine (0.73 mL, 14.3 mmol, 1.0 eq.) was slowly added to a stirred solution of pyrimidine **79** (1.98 g, 14.3 mmol, 1.0 eq.) in ethanol (40 mL) at 0 °C. The orange reaction mixture was allowed to slowly warm up to room temperature (melting ice bath) and stirred for 16 h. The reaction mixture was concentrated under reduced pressure and the resulting solid was quenched with aqueous saturated sodium sulfite (50 mL). The resulting off-white precipitate was filtered, washed abundantly with aqueous saturated sodium sulfite and dried under vacuum to yield the desired bromopyrimidine **80** as an off-white solid (2.19 g, 70%) which was used in the next step without further purification.

^{1}H NMR (400 MHz, Chloroform-*d*) *δ_H = 13.35 (s, 1H, OH), 8.17 (s, 1H, H_1), 3.49 (hept, J = 6.8 Hz, 1H, H_6), 1.22 (d, J = 6.8 Hz, 6H, H_7).*

^{13}C NMR (101 MHz, Chloroform-*d*) *δ_C = 172.5 (Quat., C_5), 161.3 (Quat., C_3), 146.4 (CH, C_1), 111.5 (Quat., C_4), 34.6 (CH, C_6), 20.2 (CH_3, C_7).*

FTIR (neat) ν/cm^{-1} *= 2966, 1649, 1606, 1465, 1405, 1373, 1211, 1062, 1006, 978, 931, 877, 795, 782.*

HRMS (ESI$^+$) *calculated for $C_7H_9BrN_2O$ = 217.9878, mass found = 238.9793.*

Melting point *160–163 °C.*

5-Bromo-4-chloro-6-isopropylpyrimidine, 81



Following a literature procedure.[246] Phosphorus(V) oxychloride (5 mL) was added to a stirred solution of bromopyrimidine **81** (2.2 g, 10.0 mmol, 1.0 eq.) in 1,2-dichloroethane (30 mL) and the reaction mixture was heated to 100 °C and stirred for 3 h. The reaction mixture was allowed to cool down to room temperature and concentrated under reduced pressure. The resulting solid was taken up in water (20 mL), and the pH was adjusted to 8 using saturated aqueous sodium bicarbonate (*ca.* 12 mL). The aqueous solution was extracted with ethyl acetate (3 × 30 mL) and the combined organic layers were dried over anhydrous magnesium sulfate, filtered and concentrated *in vacuo* to yield the desired chloropyrimidine **81** as an amber liquid (1.99 g, 84%), which was used in the next step without further purification.

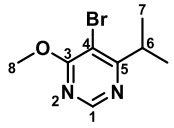
^{1}H NMR (400 MHz, Chloroform-*d*) *δ_H = 8.79 (s, 1H, H_1), 3.58 (hept, J = 6.8 Hz, 1H, H_6), 1.28 (d, J = 6.8 Hz, 6H, H_7).*

^{13}C NMR (101 MHz, Chloroform-*d*) *δ_C = 176.0 (Quat., C_5), 160.9 (Quat., C_3), 156.1 (CH, C_1), 120.3 (Quat., C_4), 35.3 (CH, C_6), 20.8 (CH_3, C_7).*

FTIR (neat) ν/cm^{-1} *= 2970, 1537, 1503, 1416, 1353, 1271, 1196, 1025, 906, 808, 780.*

HRMS (ESI$^+$) *calculated for $C_7H_8BrClN_2$ = 235.9539, mass not found. The rest of the data matches literature data.*[246]

5-Bromo-4-isopropyl-6-methoxypyrimidine, 82



Following a literature procedure.[246] Sodium methoxide (1.83 g, 33.8 mmol, 4.0 eq) was added to a stirred solution of chloropyrimidine **81** (1.99 g, 8.5 mmol, 1.0 eq.) in methanol (50 mL) at 0 °C. The reaction mixture was allowed to slowly warm up to room temperature (melting ice bath) and stirred for 18 h. The reaction mixture was concentrated under reduced pressure. The resulting solid was taken up in water (20 mL) extracted with ethyl acetate (3 × 30 mL). The combined organic layers were washed with brine (50 mL), dried over anhydrous magnesium sulfate, filtered and concentrated *in vacuo* to yield the desired methoxypyrimidine **82** as an amber liquid (1.82 g, 93%), which was used in the next step without further purification.

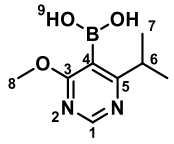
^{1}H NMR (400 MHz, Chloroform-*d*) *δ_H = 8.58 (s, 1H, H_1), 4.03 (s, 3H, H_8), 3.52 (hept, J = 6.8 Hz, 1H, H_6), 1.23 (d, J = 6.8 Hz, 6H, H_7).*

^{13}C NMR (101 MHz, Chloroform-*d*) *δ_C = 173.3 (Quat., C_5), 165.7 (Quat., C_3), 155.8 (CH, C_1), 105.9 (Quat., C_4), 55.1 (CH_3, C_8), 33.6 (CH, C_6), 20.8 (CH_3, C_7).*

FTIR (neat) ν/cm^{-1} *= 2967, 1566, 1521, 1465, 1376, 1323, 1276, 1046, 1016, 859, 791, 656.*

HRMS (ESI$^+$) *calculated for $C_8H_{11}BrN_2O$ = 231.0128, mass found = 231.0127.*

(4-Isopropyl-6-methoxypyrimidin-5-yl)boronic acid, 83



Following a literature procedure.[246] Triisopropyl borate (4.5 mL, 19.5 mmol, 3.0 eq) was added to a stirred solution of bromopyrimidine **82** (1.5 g, 6.5 mmol, 1.0 eq.) in 5:1 toluene/tetrahydrofuran (48 mL) under argon atmosphere and the reaction mixture was cooled to –78 °C. *n*-Butyllithium (2.5 M in hexanes, 3.9 mL, 9.7 mmol, 1.5 eq.) was added dropwise over 45 min and the resulting reaction mixture was stirred for an additional 30 min at –78 °C. The reaction mixture was allowed to warm up to room temperature and stirred for an additional 2.5 hours. The reaction was then quenched with 2 N aqueous hydrochloric acid (20 mL) and was stirred at room temperature for 16 h. The pH of the reaction mixture was adjusted to 8 using solid potassium carbonate and the resulting biphasic mixture was extracted with ethyl acetate (3 × 80 mL). The combined organic layers were washed with brine (2 × 80 mL), dried over anhydrous magnesium sulfate, filtered and concentrated *in vacuo*. The crude amber oil was triturated in 2:3 diethyl ether/*n*-pentane (15 mL), the resulting solid was filtered and dried under vacuum to yield boronic acid **83** as an off-white solid (490 mg, 39%).

^{1}H NMR (600 MHz, Dimethylsulfoxide-d_6) *δ_H = 8.66 (s, 1H, H_1), 8.36 (s, 2H, H_9), 3.86 (s, 3H, H_8), 2.86 (p, J = 6.8 Hz, 1H, H_6), 1.18 (d, J = 6.8 Hz, 6H, H_7).*

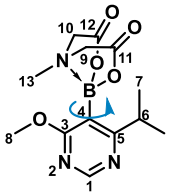
^{13}C NMR (151 MHz, Dimethylsulfoxide-d_6) *δ_H = 175.6 (Quat., C_5), 170.5 (Quat., C_3), 157.2 (CH, C_1), 104.0 (Quat., C_4), 53.2 (CH_3, C_8), 35.6 (CH, C_6), 21.7 (CH_3, C_7).*

FTIR (neat) ν/cm^{-1} *= 3222 (br), 2959, 1568, 1552, 1462, 1372, 1256, 1050, 821, 696.*

HRMS (ESI$^+$) *calculated for $C_8H_{13}BN_2O_3$ = 197.1092, mass found = 197.1095.*

Melting point *95–80 °C.*

8-(4-Isopropyl-6-methoxypyrimidin-5-yl)-4-methyldihydro-4l4,8l4-[1,3,2]oxazaborolo[2,3-b][1,3,2]oxazaborole-2,6(3*H*,5*H*)-dione, 84[247]



A mixture of boronic acid **83** (250 mg, 1.27 mmol, 1.0 eq.) and *N*-methyliminodiacetid acid (197 mg, 1.34 mmol, 1.05 eq.) in *N,N*-dimethylformamide (15 mL) was heated to 90 °C and stirred for 20 h under air. The reaction was cooled to room temperature and toluene (45 mL) was added. The resulting solution was concentrated *in vacuo* and the resulting orange slurry was taken up in ethyl acetate (40 mL) and stored in the fridge for 30 minutes. The resulting precipitate was filtered off and the filtrate was concentrated *in vacuo* to yield a light-yellow solid that was adsorbed onto Celite *in vacuo* from an acetone suspension. The resulting solid was purified by column chromatography (12 g silica, diethyl/ether acetone, 1:0 to 1:1) to yield the desired MIDA-boronate **84** as an off-white solid (274 mg, 70%).

^{1}H NMR (400 MHz, Acetonitrile-d_3) *δ_H = 8.65 (s, 1H, H_1), 4.09 (d, J = 17.2 Hz, 2H, H_9/H_{10} major rotamer), 3.99 (d, J = 17.2 Hz, 2H, H_9/H_{10} major rotamer), 3.92 (d, J = 16.9 Hz, (2H)/3, H_9/H_{10} minor rotamer), 3.87 (s, 3H, H_8), 3.76 (d, J = 16.9 Hz, (2H)/3, H_9/H_{10} minor rotamer), 3.64 (hept, J = 6.7 Hz, 1H, H_6), 2.84 (s, (3H)/3, H_{13} minor rotamer), 2.70 (s, 3H, H_{13} major rotamer), 1.20 (d, J = 6.7 Hz, 6H, H_7).*

^{13}C NMR (101 MHz Acetonitrile-d_3) *δ_C = 181.8 (Quat., C_5), 173.4 (Quat. C_3), 169.5 (Quat., C_{11} & C_{12}), 169.2 (Quat., C_4), 158.7 (CH, C_1), 65.0 (CH_2, C_9/C_{10} major rotamer), 62.7 (CH_2, C_9/C_{10} minor*

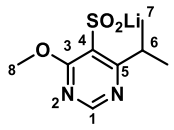
rotamer), 54.1 (CH_3, C_8), 48.8 (CH_3, C_{13} minor rotamer), 46.5 (CH_3, C_{13} major rotamer), 33.6 (CH, C_6), 22.8 (CH_3, C_7).

FTIR (neat) ν/cm^{-1} = *2957, 1782, 1737, 1564, 1532, 1454, 1412, 1367, 1339, 1284, 1251, 1147, 1093, 1036, 982, 889, 870, 780, 653.*

HRMS (ESI$^+$) *calculated for $C_{13}H_8BN_3O_5$ = 308.1412, mass found = 308.1410.*

Melting point *186–190 °C.*

Lithium 4-isopropyl-6-methoxypyrimidine-5-sulfinate, 85[239,240]



A flame-dried round-bottom flask was loaded with bromopyrimidine **82** (250 mg, 1.1 mmol, 1.0 eq.) and anhydrous tetrahydrofuran (5.5 mL). The resulting solution was cooled to –78 °C and *n*-butyllithium (1.6 M in hexanes, 610 µL, 1.0 mmol, 0.9 eq.) was slowly added under inert atmosphere. The resulting dark-orange solution was allowed to stir at –78 °C for 1 h. *N*-methylpyrrolidine SO_2 adduct *TIMSO* (139 µL, 1.1 mmol, 1.0 eq.) was added dropwise and the resulting light-yellow mixture was allowed to warm up to room temperature and stirred overnight. The resulting precipitate was filtered, washed with acetone (2 × 20 mL) and diethyl ether (2 × 20 mL) and dried under vacuum to be collected as a fine white powder, identified as lithium pyrimidinylsulfinate **85** (135 mg, 56%).

^{1}H NMR (500 MHz, Deuterium oxide) *δ_H = 8.57 (s, 1H, H_1), 4.03 (s, 3H, H_8), 3.87 (hept, J = 6.9 Hz, 1H, H_6), 1.25 (d, J = 6.9 Hz, 6H, H_7).*

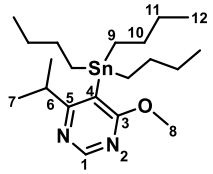
^{13}C NMR (126 MHz, Deuterium oxide) *δ_C = 172.6 (Quat., C_5), 165.9 (Quat., C_3), 157.5 (CH, C_1), 129.2 (Quat., C_4), 54.2 (CH_3, C_8), 29.9 (CH, C_6), 20.7 (CH_3, C_7).*

FTIR (neat) ν/cm^{-1} *= 2980, 1562, 1531, 1468, 1426, 1375, 1320, 1084, 1049, 1030, 984, 943, 896, 810.*

HRMS (ESI$^+$) *calculated for $C_8H_{11}LiN_2O_3SNa$ = 245.0543, mass found = 245.0544 $[M+Na]^+$.*

Melting point *> 300 °C.*

4-Isopropyl-6-methoxy-5-(tributylstannyl)pyrimidine, 86[248]



A flame-dried round-bottom flask was loaded with bromopyrimidine **82** (500 mg, 1.1 mmol, 1.0 eq.) and anhydrous tetrahydrofuran (20 mL) under argon atmosphere. The resulting solution was cooled to –78 °C and *n*-butyllithium (2.5 M in hexanes, 0.96 mL, 2.4 mmol, 1.1 eq.) was slowly added under argon. The resulting dark-orange solution was allowed to stir at –78 °C for 1 h. Tributyltin chloride (0.64 mL, 2.4 mmol, 1.1 eq.) was added dropwise and the resulting mixture was stirred at –78 °C for an hour and allowed to warm up to room temperature and stirred for an extra 16 h. The reaction mixture was quenched with saturated aqueous ammonium chloride (20 mL) and extracted with dichloromethane (2 × 30 mL). The combined organic layers were washed with 1 M aqueous potassium fluoride (3 × 30 mL, at least 1 min per wash), brine (50 mL), dried over anhydrous magnesium sulfate and concentrated *in vacuo.* The resulting crude mixture was dried under high vacuum to yield the desired tributylstannylpyrimidine **86** as an amber oil (1.09 g, quant.), which was used in the subsequent Stille coupling reactions without further purification.

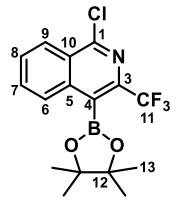
^{1}H NMR (400 MHz, Chloroform-*d*) *δ_H = 8.70 (s, 1H, H_1), 3.90 (s, 3H, H_8), 2.77 (p, J = 6.7 Hz, 1H, H_6), 1.48 (m, 6H, H_{11}), 1.31 (m, 6H, H_{10}), 1.23 (d, J = 6.9 Hz, 6H, H_7), 1.07 (m, 6H, H_9), 0.89 (m, 9H, H_{12}).*

^{13}C NMR (101 MHz, Chloroform-*d*) *δ_C = 181.9 (Quat., C_5), 174.2 (Quat., C_3), 158.4 (CH, C_1), 117.0 (Quat., C_4), 53.6 (CH_3, C_8), 37.8 (CH, C_6), 29.2 (CH_2, C_{11}), 27.4 (CH_2, C_{10}), 22.5 (CH_3, C_7), 13.8 (CH_3, C_{12}), 11.7 (CH_2, C_9).*

FTIR (Chloroform-*d*) ν/cm^{-1} *= 2956, 2923, 1558, 1522, 1454, 1411, 1362, 1288, 1052, 855, 807, 670.*

HRMS (ESI$^+$) *calculated for $C_{20}H_{38}N_2OSn$ = 443.2081, mass found = 443.2077.*

1-Chloro-4-(4,4,5,5-tetramethyl-1,3,2-dioxaborolan-2-yl)-3-(trifluoromethyl)isoquinoline, 106[254]



Iodoisoquinoline **71a** (100 mg, 0.28 mmol, 1.0 eq.), bis(pinacolato)diboron (138 mg, 0.56 mmol, 2.0 eq.), potassium acetate (82 mg, 0.84 mmol, 3.0 eq.) and [1,1'-bis(diphenylphosphino)ferrocene]dichloropalladium(II), complex with dichloromethane (11.4 mg, 0.014 mmol, 5 mol%) were weighed into a flame-dried two-necked round bottom flask, equipped with a condenser. The reaction vessel was purged with argon three times, and argon-sparged anhydrous 1,4-dioxane (2.5 mL) was added. The resulting slurry was heated to 100 °C and stirred for 10 days. The black reaction mixture was filtered over Celite® and the solid was washed with ethyl acetate (25 mL). The resulting organic solution was washed with water (3 × 25 mL) and brine (25 mL), dried over anhydrous magnesium sulfate and concentrated *in vacuo*. The resulting brown solid was purified by column chromatography (15 g silica, ethyl acetate/pentane, 5:95 to 2:8) to yield boronic ester **106** as a white solid (61 mg, 61%).

^{1}H NMR (500 MHz, Chloroform-*d*) *δ_H = 8.44 (d, J = 8.0 Hz, 1H, H_9), 8.06 (d, J = 7.5 Hz, 1H, H_6), 7.85 (ddd, J = 8.3, 7.0, 1.6 Hz, 1H, H_8), 7.81 (ddd, J = 8.3, 7.0, 1.4 Hz, 1H, H_7), 1.49 (s, 12H, H_{13}).*

^{13}C NMR (126 MHz, Chloroform-*d*) *δ_C = 153.4 (Quat., C_1), 143.1 (q, J = 34.3 Hz, Quat., C_3), 140.1 (Quat., C_5), 132.3 (CH, C_8), 130.4 (CH, C_7), 128.3 (CH, C_6), 127.1 (CH, C_9), 127.0 (Quat., C_{10}), 122.1 (q, J = 274.1 Hz, Quat., C_{11}), 85.7 (Quat., C_{12}), 25.3 (CH_3, C_{13}).*

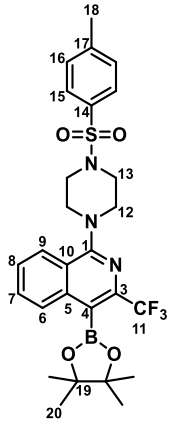
^{19}F NMR (377 MHz, Chloroform-*d*) *δ_F = -63.7.*

FTIR (Chloroform-*d*) ν/cm^{-1} = *2990, 1502, 1379, 1351, 1333, 1292, 1241, 1134, 1121, 1013, 848, 759*.

HRSM (ESI$^+$) *calculated for $C_{16}H_{16}BClF_3NO_2$ = 358.0988, mass found = 358.0989.*

Melting point *153–156 °C.*

4-(4,4,5,5-Tetramethyl-1,3,2-dioxaborolan-2-yl)-1-(4-tosylpiperazin-1-yl)-3-(trifluoromethyl) isoquinoline, 107a



Using 76c as starting material:[254] Iodoisoquinoline **76c** (100 mg, 0.18 mmol, 1.0 eq.), bis(pinacolato)diboron (69 mg, 0.27 mmol, 1.5 eq.), potassium acetate (52 mg, 0.53 mmol, 3.0 eq.) and [1,1'-bis(diphenylphosphino)ferrocene]dichloropalladium(II) complex with dichloromethane (7.3 mg, 0.009 mmol, 5 mol%) were weighed into a flame-dried two-necked round bottom flask, equipped with a condenser. The reaction vessel was purged with argon three times, and argon-sparged anhydrous 1,4-dioxane (1.5 mL) was added. The resulting orange slurry was heated to 100 °C and stirred for 16 h. The black reaction mixture was filtered over Celite® and the solid was washed with ethyl acetate (25 mL). The resulting organic solution was washed with water (2 × 20 mL) and brine (20 mL), dried over anhydrous magnesium sulfate and concentrated *in vacuo*. The resulting oil was triturated in hexane and the solid was filtered away. Quantitative NMR analysis of the precipitate showed the presence of two species (1:2). Preparative TLC of the mixture gave two species, identified as boronic ester **107a** (16 mg, 16%) and dehalogenation/proto-deborylation product **105** (3 mg, 4%) (see **Section III.2.2.3**).

Using 106 as starting material: *Following general procedure L*, using chloroisoquinoline **106** (50 mg, 0.14 mmol, 1.0 eq.) and 1-tosylpiperazine hydrochloride (58 mg, 0.21 mmol, 1.5 eq.). The

reaction mixture was stirred at 80 °C for 16 h. When isolated by precipitation, piperazinylisoquinoline **107a** was isolated as an orange solid (18 mg, 46%). When purified by column chromatography (15 g Silica, 8:2 pentane/ethyl acetate), piperazinylisoquinoline **107a** was isolated as yellow solid (56 mg, 71%).

^{1}H NMR (400 MHz, Chloroform-*d*) *δ_H = 7.94 (m, 2H, H_9 & H_6), 7.68 (d, J = 8.3 Hz, 1H, H_{15}), 7.65 (m, 1H, H_7), 7.54 (m, 1H, H_8), 7.35 (d, J = 7.9 Hz, 1H, H_{16}), 3.62 (t, J = 4.9 Hz, 4H, H_{12}), 3.22 (t, J = 4.9 Hz, 4H, H_{13}), 2.45 (s, 3H, H_{18}), 1.46 (s, 12H, H_{20}).*

^{13}C NMR (126 MHz, Chloroform-*d*) *δ_C = 160.7 (Quat., C_1), 144.0 (Quat., C_{14}), 142.6 (q, J = 32.9 Hz, Quat., C_3), 140.8 (Quat., C_5), 132.6 (Quat., C_{17}), 130.7 (CH, C_7), 129.9 (CH, C_{16}), 128.5 (CH, C_9), 128.4 (CH, C_{15}), 128.0 (CH, C_8), 127.9 (Quat., C_4), 125.5 (CH, C_6) 122.6 (q, J = 274.1 Hz, Quat., C_{11}), 120.8 (Quat., C_{10}), 85.1 (Quat., C_{19}), 50.3 (CH_2, C_{12}), 45.7 (CH_2, C_{13}), 25.2 (CH_3, C_{20}), 21.7 (CH_3, C_{18}).*

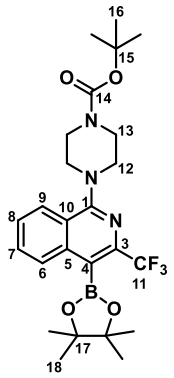
^{19}F NMR (377 MHz, Chloroform-*d*) *δ_F = -64.3.*

FTIR (Chloroform-*d*) ν/cm^{-1} *= 2918, 1505, 1393, 1354, 1326, 1260, 1240, 1165, 1132, 1101, 1020, 943, 911, 850, 816, 729, 650.*

HRMS (ESI$^+$) *calculated for $C_{27}H_{31}BF_3N_3O_4S$ = 562.2157, mass found = 562.2157.*

Melting point *49–52 °C.*

***tert*-Butyl-4-(4-(4,4,5,5-tetramethyl-1,3,2-dioxaborolan-2-yl)-3-(trifluoromethyl)isoquinolin-1-yl)piperazine-1-carboxylate, 107b**



Following general procedure L, using **106** (50 mg, 0.14 mmol, 1.0 eq.) and 1-Boc-piperazine (39 mg, 0.21 mmol, 1.5 eq.). The reaction mixture was stirred at 80 °C for 16 h. The crude mixture was purified by column chromatography (15 g Silica, 9:1 pentane/ethyl acetate) to yield piperazinylisoquinoline **107b** as a white solid (40 mg, 56%). The proto-deborylation product **88** was also isolated (11 mg, 21%) (see **Section III.2.2.3**).

^{1}H NMR (500 MHz, Chloroform-*d*) *δ_H = 8.08 (dd, J = 8.5, 1.3 Hz, 1H, H_6), 7.98 (d, J = 8.2 Hz, 1H, H_9), 7.68 (ddd, J = 8.2, 6.9, 1.3 Hz, 1H, H_8), 7.60 (ddd, J = 8.3, 6.8, 1.2 Hz, 1H, H_7), 3.66 (m, 4H, H_{12}), 3.46 (m, 4H, H_{13}), 1.49 (s, 9H, H_{16}), 1.47 (s, 12H, H_{18}).*

^{13}C NMR (126 MHz, Chloroform-*d*) *δ_C = 161.4 (Quat., C_1), 154.8 (Quat., C_{14}), 142.7 (q, J = 32.7 Hz, Quat., C_3), 140.6 (Quat., C_5), 130.5 (CH, C_8), 128.3 (CH, C_9), 127.6 (CH, C_7), 125.6 (CH, C_6), 125.3 (Quat., C_4), 122.6 (q, J = 273.9 Hz, Quat., C_{11}), 121.0 (Quat., C_{10}), 84.9 (Quat., C_{17}), 79.9 (Quat., C_{15}), 50.9 (d, J = 96.9 Hz, CH_2, C_{13}), 43.5 (d, J = 107.7 Hz, CH_2, C_{13}), 28.5 (CH_3, C_{16}), 25.1 (CH_3, C_{18}).*

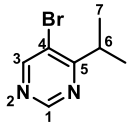
^{19}F NMR (377 MHz, Chloroform-*d*) *δ_F = -64.2.*

FTIR (Chloroform-*d*) ν/cm^{-1} *= 2979, 1697, 1582, 1505, 1392, 1366, 1324, 1247, 1165, 1130, 1021, 851, 731.*

HRMS (ESI$^+$) *calculated for $C_{25}H_{33}BF_3N_3O_4$ = 508.2591, mass found = 508.2591.*

Melting point *128–131 °C.*

5-Bromo-4-isopropylpyrimidine, 109



Following a literature procedure.[263] 5-pyrimidine **108** (1.0 g, 6.3 mmol, 1.3 eq.), isobutyric acid (0.47 mL, 5.0 mmol, 1.0 eq.), silver nitrate (0.21 g, 1.3 mmol, 20 mol %), and potassium persulfate (1.7 g, 6.3 mmol, 1.3 eq.) were loaded in a round bottom flask equipped with a stirrer bar. Dichloromethane (35 mL) and water (35 mL) were added and the resulting mixture was stirred vigorously at room temperature under atmospheric pressure for 76 h, when TLC monitoring indicated complete consumption of the starting material. The solvent was evaporated under reduced pressure and the resulting suspension was extracted with ethyl acetate (100 mL). The organic layer was washed with water (100 mL) and brine (100 mL), dried over anhydrous magnesium sulfate, filtered, and concentrated *in vacuo*. The resulting orange oil was purified by column chromatography (90 g silica, ethyl acetate/pentane 5:95) to yield the desired isopropylpyrimidine **109** as a light-yellow oil (565 mg, 45%).

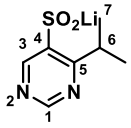
^{1}H NMR (400 MHz, Chloroform-*d*) *δ_H = 9.01 (s, 1H, H_3), 8.69 (s, 1H, H_1), 3.46 (hept, J = 6.8 Hz, 1H, H_6), 1.27 (d, J = 6.8 Hz, 6H, H_7).*

^{13}C NMR (101 MHz, Chloroform-*d*) *δ_C = 173.1 (Quat., C_5), 158.5 (CH, C_1), 157.0 (CH, C_3), 120.9 (Quat., C_4), 33.9 (CH_2, C_6), 20.7 (CH_3, C_7).*

FTIR (Chloroform-*d*) ν/cm^{-1} = *2969, 1559, 1518, 1469, 1436, 1390, 1271, 1159, 1066, 1018, 780, 688.*

HRSM (ESI$^+$) *calculated for $C_7H_9BrN_2$ = 201.0023, mass found = 201.0022.*

Lithium 4-isopropylpyrimidine-5-sulfinate, 112[239,240]



A flame-dried round-bottom flask was loaded with bromopyrimidine **109** (220 mg, 1.1 mmol, 1.0 eq.) and anhydrous tetrahydrofuran (5.5 mL). The resulting solution was cooled to –78 °C and *n*-butyllithium (2.5 M in hexanes, 400 µL, 1.0 mmol, 0.9 eq.) was slowly added under inert atmosphere. The resulting dark-orange solution was allowed to stir at –78 °C for 1 h. *N*-methylpyrrolidine SO_2 adduct *TIMSO* (145 µL, 1.1 mmol, 1.0 eq.) was added dropwise and the resulting light-yellow mixture was allowed to warm up to room temperature and stirred for an additional 16 h. The solvent was evaporated and the resulting amber oil was taken up in 2:3 acetone/diethyl ether and stored in the fridge for 30 min. The resulting light-yellow precipitate was filtered, dried under vacuum and identified as lithium pyrimidinylsulfinate **112** (103 mg, 49%)

^{1}H NMR (500 MHz, Deuterium oxide) *δ_H = 9.05 (s, 1H, H_3), 8.92 (s, 1H, H_1), 3.72 (hept, J = 6.8 Hz, 1H, H_6), 1.30 (d, J = 6.8 Hz, 6H, H_7).*

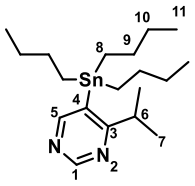
^{13}C NMR (126 MHz, Deuterium oxide) *δ_C = 173.5 (Quat., C_5), 158.1 (CH, C_1), 151.8 (CH, C_3), 143.9 (Quat., C_4), 30.9 (CH, C_6), 20.6 (CH_3, C_7).*

FTIR (neat) ν/cm^{-1} *= 2965, 1638, 1570, 1466, 1199, 1109, 940, 894, 631.*

HRMS (ESI$^-$) *calculated for $c_7H_9N_2O_2S$ = 185.0390, mass found = 185.0382 $[M\text{-}Li]^-$.*

Melting point *> 300 °C.*

4-Isopropyl-5-(tributylstannyl)pyrimidine, 113[248]



A flame-dried Schlenk tube was loaded with bromopyrimidine **109** (250 mg, 1.2 mmol, 1.0 eq.) and anhydrous tetrahydrofuran (12 mL) under argon atmosphere. The resulting solution was cooled to –78 °C and *n*-butyllithium (1.6 M in hexanes, 0.88 mL, 1.4 mmol, 1.1 eq.) was slowly added under argon. The resulting dark-orange solution was allowed to stir at –78 °C for 1 h. Tributyltin chloride (0.37 mL, 1.4 mmol, 1.1 eq.) was added dropwise and the resulting mixture was stirred at –78 °C for an hour, and allowed to warm up to room temperature and stirred for an extra 16 h. The reaction mixture was quenched with saturated aqueous ammonium chloride (10 mL) and extracted with dichloromethane (2 × 20 mL). The combined organic layers were washed 1 M aqueous potassium fluoride (3 × 20 mL, at least 1 min per wash) and brine (50 mL), dried over anhydrous magnesium sulfate, and concentrated *in vacuo*. The resulting crude mixture was dried under high vacuum to yield stannylpyrimidine **113** as an amber oil that was taken to the next step without further purification (421 mg, 41% yield, 50% NMR purity).

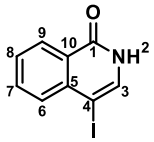
^{1}H NMR (400 MHz, Chloroform-*d*) *δ_H = 9.07 (s, 1H, H_1), 8.53 (s, 1H H_5), 2.74 (pd, J = 7.2, 3.8 Hz, 1H, H_6), 1.63 (m, H_9), 1.32 (m, H_8 & H_{10}), 1.25 (s, H_7), 0.92 (m, H_{11}).*

^{13}C NMR (101 MHz, Chloroform-*d*) *δ_C = 181.0 (Quat., C_3), 163.6 (CH, C_5), 158.7 (CH, C_1), 132.4 (Quat., C_4), 39.2 (CH, H_6), 28.0 (CH_2, C_9), 27.0 (CH_2, C_8/C_{11}), 22.6 (CH_2, C_8/C_{11}), 17.7 (CH_3, C_7), 13.7 (CH_3, C_{10}).*

FTIR (neat) ν/cm^{-1} = *2956, 2922, 2871, 2583, 1627, 1463, 1419, 1377, 1179, 1075, 1020, 876, 672.*

HRMS (ESI$^+$) *calculated for $C_{19}H_{36}N_2Sn$ = 413.1975, mass found = 413.1973.*

4-Iodoisoquinolin-1(2*H*)-one, 115a



Following general procedure H, using isocarbostyril **114** (2.0 g, 13.7 mmol, 1.0 eq.). The desired 4-iodoisoquinolinone **115a** was obtained as a white solid (3.5 g, 82%).

^{1}H NMR (400 MHz, Dimethylsulfoxide-*d_6*) *δ_H = 11.46 (s, 1H, H_2), 8.14 (ddd, J = 7.9, 1.4, 0.6 Hz, 1H, H_9), 7.77 (ddd, J = 8.3, 7.1, 1.4 Hz, 1H, H_7), 7.59 (m, 1H, H_6), 7.56 (s, 1H, H_3), 7.51 (ddd, J = 8.1, 7.1, 1.1 Hz, 1H, H_8).*

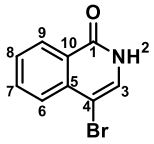
^{13}C NMR (101 MHz, Dimethylsulfoxide-*d_6*) *δ_C = 161.2 (Quat., C_1), 137.5 (Quat., C_5), 135.6 (CH, C_3), 133.6 (CH, C_7), 129.9 (CH, C_6), 127.5 (CH, C_8), 127.3 (CH, C_9), 126.7 (Quat., C_{10}), 70.4 (Quat., C_4).*

FTIR (neat) ν/cm^{-1} *= 2981, 1670, 1615, 1497, 1381, 1260, 867, 789, 682, 632.*

HRMS (ESI$^+$) *calculated for C_9H_6INO = 271.9570, mass found = 271.9565.*

Melting point *248–250 °C.*

4-Bromoisoquinolin-1(2*H*)-one, 115b



Following general procedure I, using isocarbostyril **114** (2.0 g, 13.7 mmol, 1.0 eq.). The desired 4-bromoisoquinolinone **115b** was obtained as an off-white solid (2.6 g, 85%).

^{1}H NMR (400 MHz, Dimethylsulfoxide-*d_6*) *δ_H = 11.58 (s, 1H, H_2), 8.23 (dd, J = 8.0, 1.4 Hz, 1H, H_9), 7.84 (ddd, J = 8.4, 7.1, 1.4 Hz, 1H, H_7), 7.75 (dd, J = 8.2, 1.2 Hz, 1H, H_6), 7.59 (ddd, J = 8.2, 7.1, 1.2 Hz, 1H, H_8), 7.55 (s, 1H, H_3).*

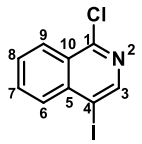
^{13}C NMR (101 MHz, Dimethylsulfoxide-*d_6*) *δ_C = 160.9 (Quat., C_1), 135.7 (Quat., C_5), 133.4 (CH, C_7), 130.2 (CH, C_3), 127.5 (CH, C_8), 127.4 (CH, C_9), 126.5 (Quat., C_{10}), 125.3 (CH, C_6), 97.5 (Quat., C_4).*

FTIR (neat) ν/cm^{-1} *= 3001, 2857, 1658, 1624, 1602, 1550, 1470, 1369, 863, 789, 767, 731, 640.*

HRMS (ESI$^+$) *calculated for C_9H_6BrNO = 223.9706, mass found = 223.9706.*

Melting point *238–240 °C.*

1-Chloro-4-iodoisoquinoline, 116a



Following general procedure J, using 4-iodoisoquinolinone **115a** (1.00 g, 3.7 mmol, 1.0 eq.). The reaction mixture was stirred at 90 °C for 48 h. The desired chloroisoquinoline **116a** was obtained as a light-brown solid (1.07 g, quant.).

^{1}H NMR (400 MHz, Chloroform-*d*) *δ_H = 8.67 (s, 1H, H_3), 8.27 (ddd, J = 8.4, 1.2, 0.6 Hz, 1H, H_9), 8.02 (ddd, J = 8.4, 1.1, 0.6 Hz, 1H, H_6), 7.82 (ddd, J = 8.4, 7.0, 1.3 Hz, 1H, H_7), 7.73 (ddd, J = 8.3, 6.9, 1.2 Hz, 1H, H_8).*

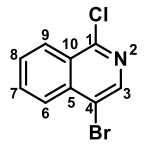
^{13}C NMR (101 MHz, Chloroform-*d*) *δ_C = 152.6 (Quat., C_1), 149.1 (CH, C_3), 138.6 (Quat., C_5), 132.9 (CH, C_7), 131.5 (CH, C_6), 129.8 (CH, C_8), 128.0 (Quat., C_{10}), 127.2 (CH, C_9), 95.8 (Quat., C_4).*

FTIR (Chloroform-*d*) ν/cm^{-1} *= 1556, 1482, 1360, 1254, 1213, 1146, 978, 906, 760, 730, 677, 641.*

HRMS (ESI$^+$) *calculated for C_9H_5ClIN = 289.9228, mass found = 289.9228.*

Melting point *56–58 °C.*

4-Bromo-1-chloroisoquinoline, 116b



Following general procedure J, using 4-bromoisoquinolinone **115b** (1.00 g, 4.5 mmol, 1.0 eq.). The reaction mixture was stirred at 90 °C for 48 h. The desired bromoisoquinoline **116b** was obtained as a light-brown solid (981 mg, 91%).

^{1}H NMR (400 MHz, Chloroform-*d*) *δ_H = 8.46 (s, 1H, H_3), 8.32 (dd, J = 8.4, 0.6 Hz, 1H, H_9), 8.17 (d, J = 8.1 Hz, 1H, H_6), 7.86 (ddd, J = 8.4, 7.0, 1.2 Hz, 1H, H_7), 7.74 (ddd, J = 8.3, 7.0, 1.2 Hz, 1H, H_8).*

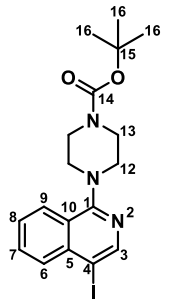
^{13}C NMR (101 MHz, Chloroform-*d*) *δ_C = 151.1 (Quat., C_1), 143.0 (CH, C_3), 136.4 (Quat., C_5), 132.5 (CH, C_7), 129.6 (CH, C_8), 128.0 (Quat., C_{10}), 127.1 (CH, C_9), 126.8 (CH, C_6), 119.2 (Quat., C_4).*

FTIR (Chloroform-*d*) ν/cm^{-1} *= 1615, 1561, 1484, 1329, 1319, 1295, 1271, 1218, 1210, 1150, 981, 758, 678, 640.*

HRMS (ESI$^+$) *calculated for C_9H_5BrClN = 243.9344, mass found = 243.9345.*

Melting point *84–86 °C.*

***tert*-Butyl 4-(4-iodoisoquinolin-1-yl)piperazine-1-carboxylate, 117a**



Following general procedure K, using chloroisoquinoline **116a** (580 mg, 2.0 mmol, 1.0 eq.) and 1-Boc-piperazine (560 mg, 3.0 mmol, 1.5 eq.). The reaction mixture was stirred at 100 °C for 48 h. Purification of the crude mixture by column chromatography (30 g silica, 85:15 pentane/ethyl acetate) yielded the desired piperazinylisoquinoline **117a** as a light-yellow solid (626 mg, 71%).

^{1}H NMR (500 MHz, Chloroform-*d*) *δ_H = 8.52 (s, 1H, H_3), 8.02 (d, J = 8.3 Hz, 1H, H_9), 7.97 (d, J = 7.2 Hz, 1H, H_6), 7.71 (ddd, J = 8.4, 6.9, 1.2 Hz, 1H, H_7), 7.58 (ddd, J = 8.2, 6.9, 1.2 Hz, 1H, H_8), 3.68 (m, 4H, H_{12}), 3.36 (t, J = 5.0 Hz, 4H, H_{13}), 1.50 (s, 9H, H_{16}).*

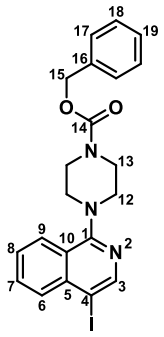
^{13}C NMR (126 MHz, Chloroform-*d*) *δ_C = 161.6 (Quat., C_1), 155.0 (Quat., C_{14}), 148.4 (CH, C_3), 138.7 (Quat., C_5), 131.6 (CH, C_6 & C_7), 127.5 (CH, C_8), 126.0 (CH, C_9), 123.2 (Quat., C_{10}), 89.2 (Quat., C_4), 80.1 (Quat., C_{15}), 51.4 (CH_2, C_{13}), 44.2 (CH_2, C_{12}), 28.6 (CH_3, C_{16}).*

FTIR (Chloroform-*d*) ν/cm^{-1} *= 2975, 2924, 2854, 1693, 1550, 1493, 1403, 1365, 1239, 1166, 1122, 1016, 870, 764, 732, 681.*

HRMS (ESI$^+$) *calculated for $C_{18}H_{22}IN_3O_2$ = 440.0826, mass found = 440.0829.*

Melting point *111–113 °C.*

Benzyl 4-(4-iodoisoquinolin-1-yl)piperazine-1-carboxylate, 117b



Following general procedure K, using chloroisoquinoline **116a** (255 mg, 0.88 mmol, 1.0 eq.) and 1-Cbz-piperazine (252 µL, 1.32 mmol, 1.5 eq.). The reaction mixture was stirred at 100 °C for 48 h. When poured onto ice water and filtrated, the desired piperazinylisoquinoline **117c** was obtained as a melty light-brown solid (323 mg, 77%).

^{1}H NMR (400 MHz, Chloroform-*d*) *δ_H = 8.52 (s, 1H, H_3), 8.01 (dd, J = 8.4, 1.3 Hz, 1H, H_9), 7.96 (dd, J = 8.4, 1.2 Hz, 1H, H_6), 7.70 (ddd, J = 8.3, 6.9, 1.3 Hz, 1H, H_7), 7.57 (ddd, J = 8.2, 6.9, 1.2 Hz, 1H, H_8), 7.36 (m, 5H, H_{17}, H_{18} & H_{19}), 5.19 (s, 2H, H_{15}), 3.77 (m, 4H, H_{12}), 3.37 (m, 4H, H_{13}).*

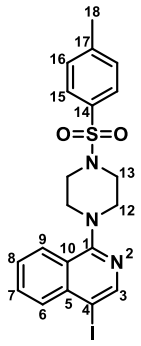
^{13}C NMR (101 MHz, Chloroform-*d*) *δ_C = 161.5 (Quat., C_1), 155.5 (Quat., C_{14}), 148.5 (CH, C_3), 138.6 (Quat., C_5), 136.7 (Quat., C_{16}), 131.5 (CH, C_6), 131.4 (CH, C_7), 128.6 (CH, C_{18}), 128.2 (CH, C_{19}), 128.0 (CH, C_{17}), 127.5 (CH, C_8), 125.8 (CH, C_9), 123.1 (Quat., C_{10}), 89.4 (Quat., C_4), 67.4 (CH_2, C_{15}), 51.3 (CH_2, C_{13}), 44.0 (CH_2, C_{12}).*

FTIR (Chloroform-*d*) ν/cm^{-1} *= 2850, 1699, 1549, 1493, 1406, 1371, 1236, 1122, 1015, 909, 764, 731, 698.*

HRMS (ESI$^+$) *calculated for $C_{21}H_{20}IN_3O_2$ = 474.0673, mass found = 474.0671.*

Melting point *melts at room temperature (20–25 °C).*

4-Iodo-1-(4-tosylpiperazin-1-yl)isoquinoline, 117c



Following general procedure K, using chloroisoquinoline **116a** (255 mg, 0.88 mmol, 1.0 eq.) and 1-tosyl-piperazine hydrochloride (365 mg, 1.32 mmol, 1.5 eq.). The reaction mixture was stirred at 100 °C for 48 h. When poured onto ice water and filtrated, piperazinylisoquinoline **117b** was obtained as an off-white solid (373 mg, 86%).

^{1}H NMR (400 MHz, Chloroform-*d*) *δ_H = 8.48 (s, 1H, H_3), 7.84 (dt, J = 8.4, 0.9 Hz, 1H, H_9), 7.84 (dt, J = 8.4, 1.0 Hz, 1H, H_6), 7.71 (d, J = 8.3 Hz, 2H, H_{15}), 7.67 (m, 1H, H_7), 7.52 (m, 1H, H_8), 7.37 (d, J = 8.1 Hz, 2H, H_{16}), 3.48 (t, 4H, H_{12}), 3.26 (t, J = 4.8 Hz, 4H, H_{13}), 2.46 (s, 3H, H_{18}).*

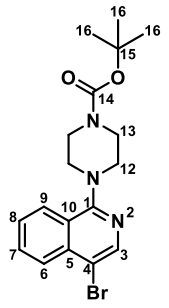
^{13}C NMR (101 MHz, Chloroform-*d*) *δ_C = 161.0 (Quat., C_1), 148.5 (CH, C_3), 144.0 (Quat., C_{17}), 138.7 (Quat., C_5), 132.8 (Quat., C_{14}), 131.6 (CH, C_9), 131.5 (CH, C_7), 130.0 (CH, C_{16}), 128.0 (CH, C_{15}), 127.5 (CH, C_8), 125.6 (CH, C_6), 122.9 (Quat., C_{10}), 89.5 (Quat., C_4), 50.8 (CH_2, C_{12}), 46.1 (CH_2, C_{13}), 21.7 (CH_3, C_{18}).*

FTIR (Chloroform-*d*) ν/cm^{-1} *= 2957, 2921, 2852, 1723, 1550, 1493, 1404, 1348, 1262, 1165, 1097, 1018, 947, 929, 800, 765, 728, 681, 648.*

HRMS (ESI$^+$) *calculated for $C_{20}H_{20}IN_3O_2S$ = 494.0394, mass found = 494.0390.*

Melting point *184–186 °C.*

***tert*-Butyl 4-(4-bromoisoquinolin-1-yl)piperazine-1-carboxylate, 117d**



Following general procedure K, using isoquinoline **116b** (243 mg, 1.0 mmol, 1.0 eq.) and 1-Boc-piperazine (279 mg, 1.5 mmol, 1.5 eq.). The reaction mixture was stirred at 80 °C for 24 h. The crude mixture was purified by column chromatography (15 g silica, 85:15 pentane/ethyl acetate) to yield the desired piperazylisoquinoline **117d** as a beige solid (199 mg, 51%).

^{1}H NMR (500 MHz, Chloroform-*d*) *δ_H = 8.31 (s, 1H, H_3), 8.11 (d, J = 8.4 Hz, 1H, H_9), 8.09 (d, J = 8.4 Hz, 1H, H_6), 7.75 (ddd, J = 8.3, 6.9, 1.2 Hz, 1H, H_7), 7.59 (ddd, J = 8.2, 6.9, 1.2 Hz, 1H, H_8), 3.69 (dd, J = 6.2, 4.0 Hz, 4H, H_{12}), 3.35 (t, J = 5.1 Hz, 4H, $H_{13.}$), 1.50 (s, 9H, H_{16}).*

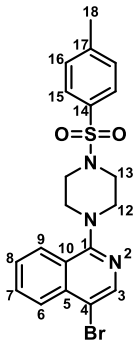
^{13}C NMR (126 MHz, Chloroform-*d*) *δ_C = 160.8 (Quat., C_1), 155.0 (Quat., C_{14}), 142.1 (CH, C_3), 136.6 (Quat., C_5), 131.2 (CH, C_7), 127.4 (CH, C_9), 126.9 (CH, C_8), 125.8 (CH, C_6), 123.0 (Quat., C_{10}), 113.5 (Quat., C_4), 80.1 (Quat., C_{15}), 51.5 (CH_2, C_{13}), 44.2 (CH_2, C_{12}), 28.6 (CH_3, C_{16}).*

FTIR (Chloroform-*d*) ν/cm^{-1} *= 2975, 2925, 2854, 1693, 1553, 1495, 1403, 1365, 1280, 1236, 1166, 1077, 1017, 874, 765, 732, 681.*

HRMS (ESI$^+$) *calculated for $C_{18}H_{22}BrN_3O_2$ = 392.0968, mass found = 392.0964.*

Melting point *118–120 °C.*

4-Bromo-1-(4-tosylpiperazin-1-yl)isoquinoline, 117e



Following general procedure K, using chloroisoquinoline **116b** (121 mg, 0.5 mmol, 1.0 eq.) and 1-tosyl-piperazine hydrochloride (208 mg, 0.75 mmol, 1.5 eq.). The reaction mixture was stirred at 100 °C for 48 h. When poured onto ice water and filtrated, the desired piperazinylisoquinoline **117e** was obtained as a light-orange solid (224 mg, quant.).

^{1}H NMR (400 MHz, Chloroform-*d*) *δ_H = 8.27 (s, 1H, H_3), 8.08 (dt, J = 8.3, 0.9 Hz, 1H, H_9), 7.90 (dt, J = 8.4, 1.0 Hz, 1H, H_6), 7.71 (m, 3H, H_{15} & H_7), 7.52 (ddd, J = 8.2, 6.9, 1.3 Hz, 1H, H_8), 7.37 (d, J = 8.0 Hz, 2H, H_{16}), 3.47 (m, 4H, H_{12}), 3.27 (m, 4H, H_{13}), 2.46 (s, 3H, H_{18}).*

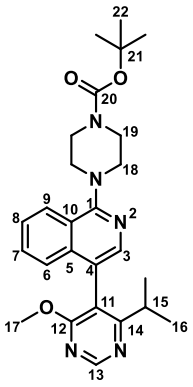
^{13}C NMR (101 MHz, Chloroform-*d*) *δ_C = 159.9 (Quat., C_1), 143.7 (Quat., C_{17}), 141.9 (CH, C_3), 136.2 (Quat., C_5), 132.5 (Quat., C_{14}), 130.8 (CH, C_7), 129.6 (CH, C_{16}), 127.7 (CH, C_{15}), 127.0 (CH, C_8), 126.6 (CH, C_9), 125.2 (CH, C_6), 122.4 (Quat., C_{10}), 113.4 (Quat., C_4), 50.5 (CH_2, C_{12}), 45.8 (CH_2, C_{13}), 21.4 (CH_3, C_{18}).*

FTIR (Chloroform-*d*) ν/cm^{-1} = *2921, 2851, 1495, 1443, 1404, 1348, 1263, 1238, 1165, 1097, 1018, 952, 766, 728, 650.*

HRMS (ESI$^+$) *calculated for $C_{20}H_{20}BrN_3O_2S$ = 446.0532, mass found = 446.0531.*

Melting point *144–146 °C.*

tert-Butyl 4-(4-(4-isopropyl-6-methoxypyrimidin-5-yl)isoquinolin-1-yl)piperazine-1-carboxylate, 119



Following general procedure M, using iodoisoquinoline **117a** (100 mg, 0.23 mmol, 1.0 eq.) and stannylpyrimidine **86** (201 mg, 0.2 mmol, 2.0 eq). The crude mixture was purified by column chromatography twice (20 g silica, ethyl acetate/pentane, 2:8 to 3:7. *Then* 10 g silica, 7:3 toluene/diethyl ether) to yield biarylpyrimidine **119** as a yellow oil (103 mg, 98%).

^{1}H NMR (500 MHz, Chloroform-*d*) *δ_H = 8.90 (s, 1H, H_{13}), 8.20 (d, J = 8.1 Hz, 1H, H_6), 7.98 (s, 1H, H_3), 7.59 (m, 3H, H_7, H_8 & H_9), 3.86 (s, 3H, H_{17}), 3.77 (s, 4H, H_{18}), 3.49 (s, 4H, H_{19}), 2.74 (m, 1H, H_{15}), 1.54 (s, 9H, H_{22}), 1.20 (d, J = 6.7 Hz, 3H, H_{16}), 1.09 (d, J = 6.7 Hz, 3H, H_{16}).*

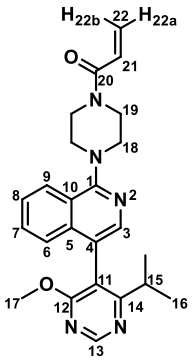
^{13}C NMR (101 MHz, Chloroform-*d*) *δ_C = 174.6 (Quat., C_{14}), 168.1 (Quat., C_{12}), 161.4 (Quat., C_1), 157.8 (CH, C_{13}), 155.0 (Quat., C_{20}), 141.1 (CH, C_3), 137.1 (Quat., C_5), 130.2 (CH, C_7/C_8), 126.5 (CH, C_7/C_8), 125.8 (CH, C_6), 124.8 (CH, C_9), 121.4 (Quat., C_{10}), 120.1 (Quat., C_{11}), 114.8 (Quat., C_4), 79.9 (Quat., C_{21}), 54.1 (CH_3, C_{17}), 51.3 (CH_2, C_{19}), 43.5 (CH_2, C_{18}), 31.8 (CH, C_{15}), 28.5 (CH_3, C_{22}), 22.2 (CH_3, C_{16}), 21.5 (CH_3, C_{16}).*

FTIR (Chloroform-*d*) ν/cm^{-1} *= 2971, 1696, 1556, 1503, 1464, 1403, 1246, 1167, 1049, 1017, 884, 771.*

HRMS (ESI$^+$) *calculated for $C_{26}H_{33}N_5O_3$ = 464.2656, mass found = 464.2652.*

Chiral HPLC *(Chiralpak IC, 4 % IPA, 96 % hexane, 1.0 mL/min, λ = 254 nm, 10 μL injection)* τ_R^1*= 20.4 min,* τ_R^2 *= 22.4 min (racemate).*

1-(4-(4-(4-Isopropyl-6-methoxypyrimidin-5-yl)isoquinolin-1-yl)piperazin-1-yl)prop-2-en-1-one, 120[243]



Deprotection: A solution of Boc-piperazinylisoquinoline **119** (20 mg, 0.04 mmol, 1.0 eq.) in hydrogen chloride – 1.25 M in methanol (2.0 mL) was stirred in a vial at room temperature for 1.5 h. The reaction mixture was concentrated *in vacuo* and the resulting crude brown solid was taken to the next step without any purification.

Acylation: The crude deprotected amine was dissolved in triethylamine (67 µL, 0.48 mmol, 11.1 eq.) and dichloromethane (3 mL). The resulting solution was cooled to 0 °C and a solution of acryloyl chloride in dichloromethane (0.013 M, 3.7 mL) was carefully added to the mixture. The ice bath was removed and the mixture was stirred at room temperature for 1.5 h. The reaction was quenched with saturated sodium bicarbonate (5 mL) and extracted with dichloromethane (3 × 5 mL). The combined organic layers were washed with saturated sodium bicarbonate (2 × 10 mL) and brine (10 mL), dried over anhydrous magnesium sulfate, filtered and concentrated *in vacuo*. The resulting yellow crude solid was purified by column chromatography (5 g silica, dichloromethane/methanol 97:3) to yield probe **120** as a sticky yellow solid (11 mg, 61%).

^{1}H NMR (500 MHz, Chloroform-*d*) *δ_H = 8.90 (s, 1H, H_{13}), 8.21 (m, 1H, H_6), 7.98 (s, 1H, H_3), 7.62 (m, 2H, H_7 & H_8), 7.31 (m, 1H, H_9), 6.69 (dd, J = 16.8, 10.5 Hz, 1H, H_{21}), 6.38 (dd, J = 16.8, 1.9 Hz, 1H,*

H_{22b}), 5.79 (dd, J = 10.5, 1.9 Hz, 1H, H_{22a}), 3.98 (m, 4H, H_{19}), 3.85 (s, 3H, H_{17}), 3.57 (m, 4H, H_{18}), 2.74 (hept, J = 6.7 Hz, 1H, H_{15}), 1.20 (d, J = 6.8 Hz, 3H, H_{16}), 1.09 (d, J = 6.7 Hz, 3H, H_{16}).

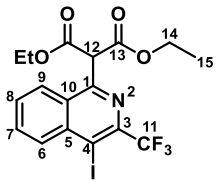
^{13}C NMR (126 MHz, Chloroform-*d*) *δ_C = 174.6 (Quat., C_{14}), 168.1 (Quat., C_{20}), 165.9 (Quat., C_{12}), 161.0 (Quat., C_1), 158.0 (CH, C_{13}), 140.8 (CH, C_3), 137.3 (CH, C_5), 130.6 (CH, C_7/C_8), 128.4 (CH_2, C_{22}), 127.6 (CH, C_{21}), 126.9 (CH, C_7/C_8), 125.9 (CH, C_6), 125.1 (CH, C_9 & Quat., C_4), 121.3 (Quat., C_{10}), 120.6 (Quat., C_{11}), 54.3 (CH_3, C_{17}), 51.1 (CH_2, C_{18}), 46.0 (CH_2, C_{19}), 42.3 (CH, C_{19}), 31.9 (CH, C_{15}), 22.3 (CH_3, C_{16}), 21.5 (CH_3, C_{16}).*

FTIR (Chloroform-*d*) ν/cm^{-1} *= 2982, 1647, 1614, 1567, 1503, 1463, 1376, 1236, 1049, 1014, 957, 773, 730.*

HRMS (ESI$^+$) *calculated for $C_{24}H_{25}N_5O_2$ = 418.2238, mass found = 418.2236.*

Chiral HPLC *(Chiralpak IC, 20 % IPA, 80 % hexane, 1.0 mL/min, λ = 254 nm, 10 μL injection) τ_R^1= 44.5 min, τ_R^2 = 47.8 min (racemate).*

Diethyl 2-(4-iodo-3-(trifluoromethyl)isoquinolin-1-yl)malonate, 121a



Following general procedure N, using iodoisoquinoline **71a** (250 mg, 0.7 mmol, 1.0 eq) and diethyl malonate **16a** (213 µL, 1.4 mmol, 2.0 eq.). The crude white solid was purified by column chromatography (18 g silica, pentane/ethyl acetate, 95:5 to 8:2) to yield arylated malonate **121a** as an off-white solid (251 mg, 75%).

^{1}H NMR (500 MHz, Chloroform-*d*) *δ_H = 8.45 (d, J = 8.8 Hz, 1H, H_9), 7.91 (d, J = 8.5 Hz, 1H, H_6), 7.87 (ddd, J = 8.5, 6.9, 1.2 Hz, 1H, H_7), 7.79 (ddd, J = 8.3, 7.0, 1.2 Hz, 1H, H_8), 5.52 (s, 1H, H_{12}), 4.30 (qd, J = 7.1, 2.1 Hz, 4H, H_{14}), 1.27 (t, J = 7.1 Hz, 6H, H_{15}).*

^{13}C NMR (126 MHz, Chloroform-*d*) *δ_C = 166.9 (Quat., C_{13}), 153.2 (Quat., C_1), 143.5 (q, J = 33.3 Hz, Quat., C_3), 139.1 (Quat., C_5), 134.2 (CH, C_9), 132.7 (CH, C_7), 130.8 (CH, C_8), 128.6 (Quat., C_{10}), 125.1 (CH, C_6), 122.0 (q, J = 275.5 Hz, Quat., C_{11}), 96.4 (CH, C_4), 62.5 (CH_2, C_{14}), 58.7 (CH, C_{12}), 14.1 (CH_3, C_{15}).*

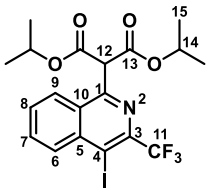
^{19}F NMR (377 MHz, Chloroform-*d*) *δ_F = -63.3.*

FTIR (Chloroform-*d*) ν/cm^{-1} *= 2983, 1736, 1446, 1395, 1369, 1305, 1236, 1172, 1134, 1035, 952, 865, 764.*

HRMS (ESI$^+$) *calculated for $C_{17}H_{15}F_3INO_4$ = 482.0071, mass found = 482.0067.*

Melting point *94–96 °C.*

Diisopropyl 2-(4-iodo-3-(trifluoromethyl)isoquinolin-1-yl)malonate, 121b



Following general procedure N, using iodoisoquinoline **71a** (250 mg, 0.7 mmol, 1.0 eq), and diisopropyl malonate **16b** (266 µL, 1.4 mmol, 2.0 eq.). The crude solid was purified by column chromatography (20 g silica, 9:1 pentane/ethyl acetate) to yield arylated malonate **121b** as a yellow solid (311 mg, quant.).

^{1}H NMR (400 MHz, Chloroform-*d*) *δ_H = 8.43 (d, J = 8.6 Hz, 1H, H_9), 7.89 (d, J = 8.4 Hz, 1H, H_6), 7.85 (m, 1H, H_7), 7.77 (m, 1H, H_8), 5.47 (s, 1H, H_{12}), 5.17 (p, J = 6.3 Hz, 2H, H_{14}), 1.28 (d, J = 4.6 Hz, 6H, H_{15}), 1.26 (d, J = 4.6 Hz, 6H, H_{15}).*

^{13}C NMR (101 MHz, Chloroform-*d*) *δ_C = 166.4 (Quat., C_{13}), 153.6 (Quat., C_1), 143.5 (q, J = 33.6 Hz, Quat., C_3), 139.0 (Quat., C_5), 134.2 (CH, C_9), 132.6 (CH, C_7), 130.7 (CH, C_8), 128.6 (Quat., C_{10}), 125.0 (CH, C_6), 122.1 (q, J = 275.4 Hz, Quat., C_{11}), 96.2 (Quat., C_4), 70.3 (CH, C_{14}), 58.9 (CH, C_{12}), 21.6 (CH_3, C_{15}).*

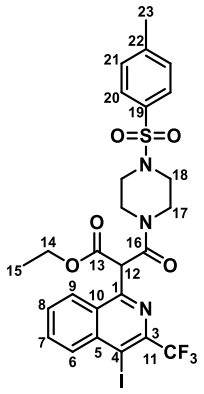
^{19}F NMR (377 MHz, Chloroform-*d*) *δ_F = -63.1.*

FTIR (Chloroform-*d*) ν/cm^{-1} *= 2983, 1727, 1446, 1330, 1302, 1259, 1170, 1131, 1099, 941, 808, 746, 631.*

HRMS (ESI$^+$) *calculated for $C_{19}H_{19}F_3INO_4$ = 510.0384, mass found = 510.0382.*

Melting point *70–72 °C.*

Ethyl 2-(4-iodo-3-(trifluoromethyl)isoquinolin-1-yl)-3-oxo-3-(4-tosylpiperazin-1-yl)propanoate, 122a[256]



A mixture of arylated malonate **121a** (50 mg, 0.10 mmol, 1.0 eq.), 1-tosylpiperazine hydrochloride (42 mg, 0.15 mmol, 1.5 eq.) and 4-(dimethylamino)pyridine (37 mg, 0.30 mmol, 3.0 eq.) in dimethylsulfoxide (2.0 mL) was allowed to stir at 100 °C for 22 h. The reaction mixture was allowed to cool down to room temperature, diluted with ethyl acetate (5 mL), washed with water (3 × 5 mL), and brine (3 × 5 mL). The organic layer was dried over anhydrous magnesium sulfate, filtered and concentrated *in vacuo*. The resulting amber oil was purified by column chromatography (12 g silica, 6:4 pentane/ethyl acetate) to yield amide **122a** as an amber oil (39 mg, 56%).

^{1}H NMR (400 MHz, Chloroform-*d*) δ_H = 8.40 (d, *J* = 8.1 Hz, 1H, H_9), 8.00 (d, *J* = 9.1 Hz, 1H, H_6), 7.85 (ddd, *J* = 8.4, 6.9, 1.2 Hz, 1H, H_7), 7.75 (ddd, *J* = 8.2, 6.9, 1.2 Hz, 1H, H_8), 7.54 (d, *J* = 8.3 Hz, 2H, H_{21}), 7.32 (d, *J* = 7.9 Hz, 2H, H_{20}), 5.61 (s, 1H, H_{12}), 4.22 (qd, *J* = 7.1, 5.7 Hz, 2H, H_{14}), 3.90 (m, 1H, H_{17}), 3.64 (m, 1H, H_{17}), 3.47 (m, 2H, H_{17}), 3.08 (m, 1H, H_{18}), 2.89 (m, 2H, H_{18}), 2.62 (m, 1H, H_{18}), 2.46 (s, 3H, H_{23}), 1.18 (t, *J* = 7.1 Hz, 3H, H_{15}).

^{19}F NMR (377 MHz, Chloroform-*d*) δ_F = -63.2.

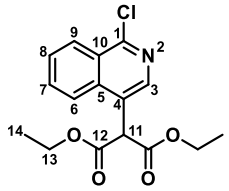
^{13}C NMR (101 MHz, Chloroform-*d*) δ_C = 167.5 (Quat., C_{13}), 164.7 (Quat., C_{16}), 153.3 (Quat., C_1), 144.2 (Quat., C_{22}), 143.1 (q, *J* = 33.1 Hz, Quat., C_3), 139.1 (Quat., C_5), 134.1 (CH, C_9), 132.9 (CH, C_7),

132.3 (Quat., C_{19}), 130.9 (CH, C_8), 130.0 (CH, C_{20}), 128.6 (Quat., C_{10}), 127.7 (CH, C_{21}), 125.6 (CH, C_6), 121.8 (q, *J* = 275.5 Hz, Quat., C_{11}), 96.6 (Quat., C_4), 62.5 (CH_2, C_{14}), 58.3 (CH, C_{12}), 45.8 (m, CH_2, C_{17}/C_{18}), 41.9 (CH_2, C_{17}/C_{18}), 21.7 (CH_3, C_{23}), 14.0 (CH_3, C_{15}).

FTIR ($CDCl_3$) ν/cm^{-1} = 2919, 1740, 1655, 1444, 1349, 1237, 1166, 1135, 947, 947, 727, 650.

HRMS (ESI^+) *calculated for $C_{26}H_{25}F_3IN_3O_5S$ = 676.0584, mass found = 678.4782.*

Diethyl 2-(1-chloroisoquinolin-4-yl)malonate, 124[86]



Following general procedure N, using iodoisoquinoline **116a** (250 mg, 0.86 mmol, 1.0 eq.) and diethyl malonate **16a** (263 µL, 1.72 mmol, 2.0 eq.). The crude solid was purified by column chromatography (25 g silica, pentane/ethyl acetate, 9:1 to 8:2) to yield arylated malonate **124** as a yellow oil (274 mg, 99%).

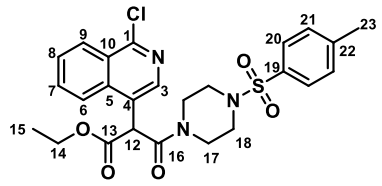
^{1}H NMR (400 MHz, Chloroform-*d*) *δ_H = 8.40 (d, J = 8.5 Hz, 1H, H_6), 8.31 (s, 1H, H_3), 7.98 (d, J = 8.5 Hz, 1H, H_9), 7.80 (ddt, J = 8.4, 6.7, 1.4 Hz, 1H, H_8), 7.71 (m, 1H, H_7), 5.19 (m, 1H, H_{11}), 4.25 (m, 4H, H_{13}), 1.25 (td, J = 7.1, 1.3 Hz, 6H, H_{14}).*

^{13}C NMR (101 MHz, Chloroform-*d*) *δ_C = 167.6 (Quat., C_{12}), 152.5 (Quat., C_1), 142.6 (CH, C_3), 136.4 (Quat., C_5), 131.8 (CH, C_8), 128.6 (CH, C_7), 127.4 (CH, C_6), 126.9 (Quat., C_{10}), 123.8 (Quat., C_4), 123.5 (CH, C_9), 62.5 (CH_2, C_{13}), 53.2 (CH, C_{11}), 14.1 (CH_3, C_{14}).*

FTIR (Chloroform-*d*) ν/cm^{-1} *= 2982, 1732, 1558, 1504, 1368, 1322, 1175, 1029, 928, 767, 686, 646.*

HRMS (ESI$^+$) *calculated for $C_{16}H_{16}ClNO_4$ = 322.0841, mass found = 322.0838.*

Ethyl 2-(1-chloroisoquinolin-4-yl)-3-oxo-3-(4-tosylpiperazin-1-yl)propanoate, 125



Following general procedure K, using chloroisoquinoline **124** (50 mg, 0.26 mmol, 1.0 eq.) and 1-tosylpiperazine hydrochloride (65 mg, 0.23 mmol, 1.5 eq.). The reaction mixture was stirred at 80 °C for 18 h. The crude amber oil was purified by column chromatography (12 g silica, pentane/ethyl acetate, 3:7 to 1:1) to yield amide **125** as an orange oil (16 mg, 20%).

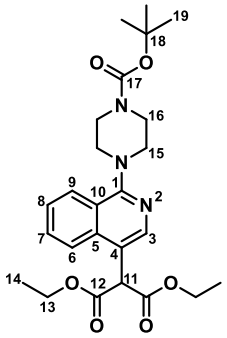
^{1}H NMR (600 MHz, Chloroform-*d*) δ_H = 8.41 (d, *J* = 8.4 Hz, 1H, H_6), 8.11 (s, 1H, H_3), 7.87 (d, *J* = 8.4 Hz, 1H, H_9), 7.79 (ddd, *J* = 8.4, 6.9, 1.3 Hz, 1H, H_7), 7.72 (ddd, *J* = 8.1, 6.9, 1.1 Hz, 1H, H_8), 7.53 (d, *J* = 8.2 Hz, 2H, H_{20}), 7.33 (d, *J* = 7.9 Hz, 2H, H_{21}), 5.23 (s, 1H, H_{12}), 4.19 (m, 2H, H_{14}), 3.85 (m, 1H, H_{17}), 3.70 (m, 1H, H_{17}), 3.32 (m, 2H, H_{17}), 3.11 (m, 1H, H_{18}), 2.89 (m, 2H, H_{18}), 2.47 (s, 4H, H_{18} & H_{23}), 1.18 (t, *J* = 7.1 Hz, 3H, H_{15}).

^{13}C NMR (151 MHz, Chloroform-*d*) δ_C = 167.8 (Quat., C_{13}), 166.0 (Quat., C_{12}), 152.7 (Quat., C_1), 144.5 (Quat., C_{22}), 142.2 (CH, C_3), 136.0 (Quat., C_5), 132.3 (Quat., C_{19}), 132.2 (CH, C_7), 130.1 (CH, C_{21}), 128.9 (CH, C_8), 127.7 (CH, C_{20}), 127.7 (CH, C_6), 126.9 (Quat., C_{10}), 123.7 (Quat., C_4), 122.8 (CH, C_9), 62.6 (CH_2, C_{14}), 51.9 (CH, C_{12}), 45.8 (CH_2, C_{17}/C_{18}), 45.7 (CH_2, C_{17}/C_{18}), 45.6 (CH_2, C_{17}/C_{18}), 41.9 (CH_2, C_{17}), 21.8 (CH_3, C_{23}), 14.1 (CH_3, C_{15}).

FTIR (Chloroform-*d*) ν/cm^{-1} = 2919, 2851, 1733, 1654, 1504, 1444, 1166, 1019, 908, 726, 648.

HRMS (ESI$^+$) *calculated for $C_{25}H_{26}ClN_3O_5S$ = 516.1355, mass found = 516.1353.*

Diethyl 2-(1-(4-(*tert*-butoxycarbonyl)piperazin-1-yl)isoquinolin-4-yl)malonate, 126a



Following general procedure N, using iodoisoquinoline **117a** (50 mg, 0.11 mmol, 1.0 eq.) and diethyl malonate **16a** (35 µL, 0.23 mmol, 2.0 eq.). The crude solid was purified by column chromatography (8 g silica, pentane/ethyl acetate, 9:1 to 8:2) to yield arylated malonate **126a** as a yellow oil (30 mg, 56%). Unreacted isoquinoline **117a** was also recovered (18 mg, 36%, 92% brsm).

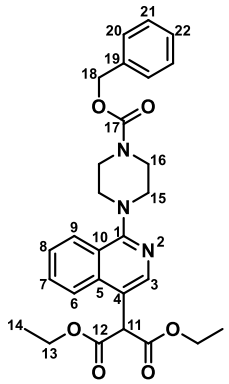
^{1}H NMR (600 MHz, Chloroform-*d*) *δ_H = 8.14 (s, 1H, H_3), 8.13 (d, J = 9.3 Hz, 1H, H_9), 7.87 (d, J = 8.6 Hz, 1H, H_6), 7.67 (m, 1H, H_7), 7.54 (m, 1H, H_8), 5.11 (s, 1H, H_{11}), 4.24 (p, J = 6.9 Hz, 4H, H_{13}), 3.69 (t, J = 5.2 Hz, 4H, H_{15}), 3.38 (t, J = 5.1 Hz, 4H, H_{16}), 1.49 (s, 9H, H_{19}), 1.25 (t, J = 7.2 Hz, 6H, H_{14}).*

^{13}C NMR (151 MHz, Chloroform-*d*) *δ_C = 168.3 (Quat., C_{12}), 161.6 (Quat., C_1), 155.1 (Quat., C_{17}), 141.8 (CH, C_3), 136.6 (Quat., C_5), 130.5 (CH, C_7), 126.4 (CH, C_9), 126.2 (CH, C_8), 123.6 (CH, C_6), 121.7 (Quat., C_{10}), 118.6 (Quat., C_4), 80.1 (Quat., C_{18}), 62.2 (CH_2, C_{13}), 53.4 (CH, C_{11}), 51.4 (CH_2, C_{16}), 43.9 (d, J = 133.6 Hz, CH_2, C_{15}), 28.6 (CH_3, C_{19}), 14.2 (CH_3, C_{14}).*

FTIR (Chloroform-*d*) ν/cm^{-1} *= 2977, 2929, 1733, 1695, 1508, 1453, 1406, 1366, 1246, 1167, 1020, 772, 684*.

HRMS (ESI$^+$) *calculated for $C_{25}H_{33}N_3O_6$ = 472.2442, mass found = 472.2438.*

Diethyl 2-(1-(4-((benzyloxy)carbonyl)piperazin-1-yl)isoquinolin-4-yl)malonate, 126b



Following general procedure N, using iodoisoquinoline **117b** (52 mg, 0.11 mmol, 1.0 eq.) and diethyl malonate **16a** (35 µL, 0.23 mmol, 2.0 eq.). The crude solid was purified by column chromatography (8 g silica, pentane/ethyl acetate, 8:2 to 6:4) to yield arylated malonate **126b** as a yellow oil (27 mg, 51%). Unreacted isoquinoline **117a** was also recovered (18 mg, 35%, 86% brsm).

When using 30mol% of catalyst, iodoisoquinoline **117b** (250 mg, 0.53 mmol, 1.0 eq.) diethyl malonate **16a** (322 µL, 1.05 mmol, 2.0 eq.), arylated malonate **126b** was obtained as a yellow oil (200 mg, 75%).

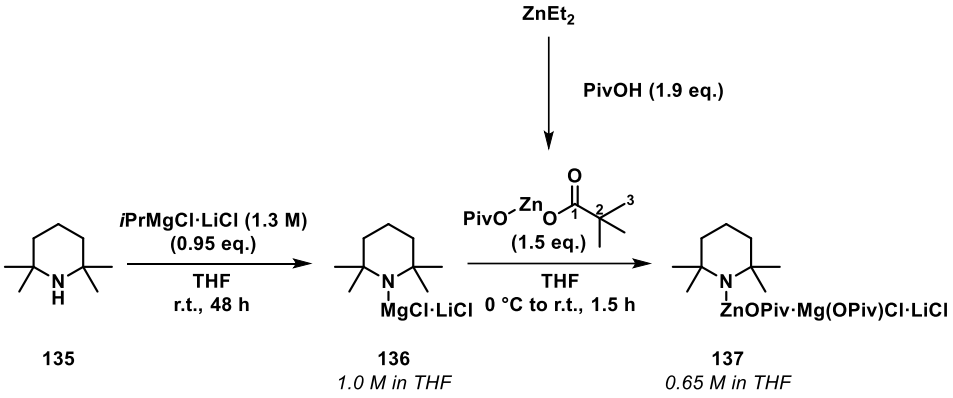
^{1}H NMR (600 MHz, Chloroform-*d*) δ_H = 8.14 (s, 1H, H_3), 8.12 (d, *J* = 8.2 Hz, 1H, H_6), 7.88 (d, *J* = 8.5 Hz, 1H, H_9), 7.67 (ddd, *J* = 8.4, 6.9, 1.3 Hz, 1H, H_7), 7.54 (ddd, *J* = 8.2, 6.9, 1.1 Hz, 1H, H_8), 7.36 (m, 5H, $H_{20,}$ H_{21} & H_{22}), 5.19 (s, 2H, H_{18}), 5.11 (s, 1H, H_{11}), 4.24 (m, 4H, H_{13}), 3.78 (m, 4H, H_{15}), 3.40 (m, 4H, H_{16}), 1.26 (m, 6H, H_{14}).

^{13}C NMR (151 MHz, Chloroform-*d*) δ_C = 168.3 (Quat., C_{12}), 166.2 (Quat., C_1), 161.6 (Quat., C_5), 155.6 (Quat., C_{17}), 141.8 (CH, C_3), 138.9 (Quat. C_5), 136.8 (Quat., C_{19}), 130.5 (CH, C_7), 128.7 (CH, C_{20}/C_{21}/C_{22}), 128.2 (CH, C_{20}/C_{21}/C_{22}), 128.1 (CH, C_{20}/C_{21}/C_{22}), 126.4 (CH, C_8), 126.1 (CH, C_6), 123.6 (CH, C_9), 121.6 (Quat., C_{10}), 118.8 (Quat., C_4), 67.4 (CH_2, C_{18}), 62.2 (CH_2, C_{13}), 53.3 (CH, C_{11}), 51.3 (CH_2, C_{16}), 44.1 (CH_2, C_{15}), 14.2 (CH_3, C_{14}).

FTIR (Chloroform-*d*) ν/cm^{-1} = 2982, 1732, 1698, 1557, 1508, 1410, 1370, 1240, 1147, 1022, 909.

HRMS (ESI$^+$) *calculated for $C_{28}H_{31}N_3O_6$ = 506.2284, mass found = 506.2272.*

TMPZnOPiv·Mg(OPiv)Cl·LiCl, 137



Preparation of zinc pivalate, $Zn(OPiv)_2$: Following literature procedures.[303,304] A flame-dried three-necked round bottom flask, equipped with a glass stopper, a rubber septum and, an outlet to a Schlenk line, was loaded with pivalic acid (2.04 g, 20 mmol, 1.9 eq.), and purged with argon three times. Anhydrous tetrahydrofuran (120 mL) was added, and the resulting solution was cooled to 0 °C. A solution of diethyl zinc (1.0 M in hexane, 10.5 mL, 10.5 mmol, 1.0 eq.) in anhydrous tetrahydrofuran (120 mL) was added dropwise *via* cannula over the course of *ca.* 30 min, with vigorous stirring under argon atmosphere. The ice bath was removed and the solution was stirred for an extra hour at room temperature to give a thick white slurry. The solvent was removed under reduced pressure and the resulting solid was dried at 200 °C under vacuum overnight to give the desired product as a white fluffy solid (2.8 g, 99%).

^{1}H NMR (400 MHz, Dimethylsulfoxide-d_6) *δ_H = 1.08 (s, 18H, H_3).*

^{13}C NMR (101 MHz, Dimethylsulfoxide-d_6) *δ_C = 184.2 (Quat., C_1), 38.0 (Quat., C_2), 28.5 (CH_3, C_3).*

FTIR (neat) ν/cm^{-1} *= 2962, 2929, 1608, 1587, 1534, 1483, 1458, 1427, 1379, 1362, 1229, 1032, 938, 898, 792, 610.*

The spectral data matches that reported in the literature.[304]

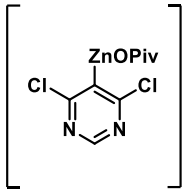
Preparation of TMPMgCl·LiCl, 136: Following a literature procedure.[269] A flame-dried, argon-purged Schlenk tube was loaded with *i*PrMgCl·LiCl (25 mL, 1.3 M in THF, 32.5 mmol, 0.95 eq). The solution was vigorously stirred and 2,2,6,6-tetramethylpiperidine **135** (5.8 mL, 34.2 mmol, 1.0 eq.) was slowly added dropwise. The resulting mixture was stirred at room temperature until no more gas evolution was observed (66 h).

The resulting solution was titrated *via* colorimetric titration by loading benzoic acid (122 mg, 1.0 mmol) and 4-(phenylazo)diphenyl amine (3.0 mg) into a flame-dried Schlenk tube. The vessel was purged with argon three times and anhydrous tetrahydrofuran (1.0 mL) was added. The prepared TMPMgCl·LiCl **136** solution was added dropwise until the mixture went from orange to dark violet (added volume: 0.98 mL *i.e.* a 1.0 M solution).

Preparation of TMPZnOPiv·Mg(OPiv)Cl·LiCl, 137: Following a literature procedure.[267] TMPMgCl·LiCl **136** (7.1 mL, 0.63 M, 7.1 mmol, 1.0 eq.) was transferred *via* cannula into a flame-dried, argon-purged round bottom flask. The solution was cooled to 0 °C, and $Zn(OPiv)_2$ (2.0 g, 7.5 mmol, 1.05 eq.) was added in one portion under an argon flow. The resulting solution was stirred and allowed to slowly warm up to room temperature over 1.5 h (melting ice bath). Anhydrous tetrahydrofuran was added (1.5 mL).

The resulting solution was titrated *via* colorimetric titration by loading benzoic acid (122 mg, 1.0 mmol) and 4-(phenylazo)diphenyl amine (3.0 mg) into a flame-dried schlenk tube. The vessel was purged with argon three times and anhydrous tetrahydrofuran (1.0 mL) was added. The prepared TMPZnOPiv ·Mg(OPiv)Cl·LiCl **137** solution was added dropwise until the mixture went from orange to dark violet (added volume: 1.59 mL *i.e.* a 0.63 M solution).

(4,6-Dichloropyrimidin-5-yl) (oxo) (pivaloyl)zinc, 134

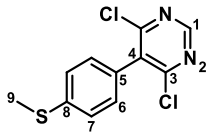


A flame-dried Schlenk tube was loaded with 4,6-dichloropyrimidine **133** (149 mg, 1.0 mmol, 1.0 eq.). The reaction vessel was purged with argon three times and anhydrous tetrahydrofuran (2 mL) was added. TMPZnOPiv·Mg(OPiv)·LiCl **137** (1.75 mL, 0.63 M in THF, 1.1 mmol, 1.1 eq.) was added dropwise under argon and the resulting solution was stirred at room temperature for 30 minutes. The solvent was removed *in vacuo* and an orange solid was collected (916 mg).

The orange solid was titrated using a 1 M solution of iodine in tetrahydrofuran: a flame-dried Schlenk tube was loaded with a portion of the orange solid (250 mg). The vessel was purged with argon three times and anhydrous tetrahydrofuran (1.5 mL) was added. A 1 M iodine solution in anhydrous tetrahydrofuran was added dropwise until the iodine colour persisted (added volume: 0.13 mL *i.e.* a concentration in active zinc species of 0.52 mmol/g and a 48% yield in **134**).

Compound **134** could not be characterised, but its synthesis was confirmed by reacting it with 4-iodothioanisole **138.**

4,6-Dichloro-5-(4-(methylthio)phenyl)pyrimidine, 139



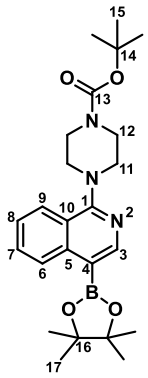
Following a literature procedure.[267] A flame-dried schlenk tube was loaded with 5-(4,6-dichloropyrimidinyl)zinc pivalate **134** (250 mg, *c.a.* 0.13 mmol, 1.25 eq.), 4-iodothioanisole **138** (26 mg, 0.1 mmol, 1.0 eq.), bis(tribenzylideneacetone)Pd(0) (3 mg, 4 mol %) and tris(2-furyl)phosphine (2 mg, 8 mol %). The vessel was purged with argon three times, and argon-sparged anhydrous tetrahydrofuran (0.5 mL) was added. The resulting suspension was stirred at room temperature for 2 h. The reaction was quenched with saturated aqueous ammonium chloride (2 mL) and extracted with diethyl ether (3 × 2 mL). The combined organic layers were dried over anhydrous magnesium sulfate, filtered, and concentrated *in vacuo* to yield the crude product as an orange sticky oil. The mixture was dissolved in deuterated chloroform and dibromomethane (10 µL, 0.14 mmol) was added. A quantitative ^{1}H NMR allowed to estimate an NMR yield of 15% and a starting material recovery of 30%.

^{1}H NMR (400 MHz, Chloroform-*d*) *δ_H = 8.77 (s, 1H, H_1), 7.36 (d, J = 8.2 Hz, 2H, H_6), 7.22 (d, J = 8.2 Hz, 2H, H_7), 2.54 (s, 3H, H_9).*

LRMS (ESI$^+$) *calculated for $C_{11}H_8Cl_2N_2S$ = 270.9858, mass found = 271.0.*

The spectral data matches that reported in the literature.[267]

***tert*-Butyl 4-(4-(4,4,5,5-tetramethyl-1,3,2-dioxaborolan-2-yl)isoquinolin-1-yl)piperazine-1-carboxylate, 141**



Boronic acid-pinacol ester formation:[254] Bromoisoquinoline **116b** (250 mg, 1.0 mmol, 1.0 eq.), bis(pinacolato)diboron (524 mg, 2.06 mmol, 2.0 eq.), potassium acetate (304 mg, 3.1 mmol, 3.0 eq.) and [1,1'-bis(diphenylphosphino)ferrocene]dichloropalladium(II), in complex with dichloromethane (42 mg, 0.05 mmol, 5 mol%) were weighed into a flame-dried two-necked round bottom flask equipped with a condenser. The reaction vessel was purged with argon three times, and argon-sparged anhydrous 1,4-dioxane (10 mL) was added. The resulting slurry was heated to 100 °C and stirred for 20 h. The red reaction mixture was filtered over Celite® and the solid was washed with ethyl acetate (100 mL). The resulting organic solution was washed with water (3 × 75 mL) and brine (75 mL), dried over anhydrous magnesium sulfate and concentrated *in vacuo*. The resulting brown solid was purified by column chromatography (40 g silica in ethyl acetate/pentane, 5:95 to 1:9) to yield an amber sticky solid (330 mg). Boronic acid pinacol ester **140** was identified in the mixture (**HRMS (ESI$^+$)** *calculated for $C_{15}H_{17}BClNO_2$ = 290.1114, mass found = 290.1115).*

SNAr reaction: *Following general procedure L,* using pinacol ester **140** (330 mg), 1-Boc-piperazine (193 mg, 1.03 mmol). The reaction mixture was stirred at 80 °C for 18 h. The crude amber oil was

purified by column chromatography (20 g silica, pentane/ethyl acetate, 9:1 to 8:2) to yield the piperazinyl isoquinoline **141** as an amber oil (98 mg, 22% over 2 steps).

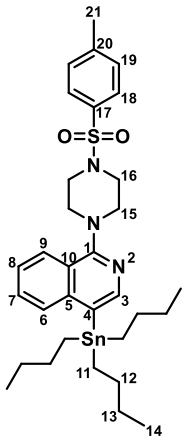
^{1}H NMR (400 MHz, Chloroform-*d*) *δ_H = 8.64 (d, J = 8.5 Hz, 1H, H_6), 8.62 (s, 1H, H_3), 8.04 (ddd, J = 8.4, 1.4, 0.7 Hz, 1H, H_9), 7.65 (ddd, J = 8.3, 6.9, 1.3 Hz, 1H, H_8), 7.48 (ddd, J = 8.3, 6.8, 1.3 Hz, 1H, H_7), 3.68 (m, 4H, H_{11}), 3.44 (m, 4H, H_{12}), 1.49 (s, 9H, H_{15}), 1.39 (s, 12H, H_{17}).*

^{13}C NMR (101 MHz, Chloroform-*d*) *δ_C = 163.2 (Quat., C_1), 154.9 (Quat., C_{13}), 150.0 (CH, C_3), 141.5 (Quat., C_5), 130.1 (CH, C_8), 128.2 (CH, C_6), 128.2 (Quat., C_4), 125.7 (CH, C_9), 125.4 (CH, C_7), 120.5 (Quat., C_{10}), 83.6 (Quat., C_{16}), 79.9 (Quat., C_{14}), 50.8 (CH_2, C_{12}), 43.2 (CH_2, C_{11}), 28.5 (CH_3, C_{15}), 24.9 (CH_3, C_{17}).*

FTIR (Chloroform-*d*) ν/cm^{-1} *= 2979, 1696, 1574, 1502, 1404, 1345, 1238, 1124, 1020, 957, 855, 772, 731.*

HRMS (ESI$^+$) *calculated for $C_{24}H_{34}B_{23}N_3O_4$ = 440.2717, mass found = 440.2710.*

1-(4-Tosylpiperazin-1-yl)-4-(tributylstannyl)isoquinoline, 144



A flame-dried Schlenk tube was loaded with bromoisoquinoline **117e** (180 mg, 0.40 mmol, 1.0 eq.) and anhydrous tetrahydrofuran (4 mL) under argon atmosphere. The resulting solution was cooled to –78 °C, and *n*-butyllithium (2.5 M in hexanes, 0.176 mL, 0.44 mmol, 1.1 eq.) was slowly added under argon. The resulting dark-orange solution was allowed to stir at –78 °C for 1 h. Tributyltin chloride (0.119 mL, 2.4 mmol, 1.1 eq.) was added dropwise and the resulting mixture was stirred at –78 °C for an hour, allowed to warm up to room temperature, and stirred for an extra 18 h. The reaction mixture was quenched with saturated aqueous ammonium chloride (5 mL) and extracted with dichloromethane (2 × 10 mL). The combined organic layers were washed with 1 M aqueous potassium fluoride (3 × 20 mL), brine (20 mL), dried over anhydrous magnesium sulfate, and concentrated *in vacuo*. The resulting crude mixture was purified by column chromatography (30 g silica, 8:2 pentane/ethyl acetate 8:2) to yield the desired product as an amber oil, in a mixture with tributyltin impurities. The amber oil was stirred in 1 M aqueous sodium hydroxide for 10 min, extracted with ethyl acetate, dried over anhydrous magnesium sulfate, filtered over silica and concentrated *in vacuo*. The desired boronic acid pinacol ester **144** was obtained as an amber oil (46 mg, 17%).

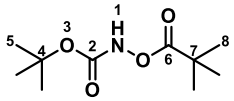
^{1}H NMR (400 MHz, Chloroform-*d*) δ_H = 8.13 (s, 1H, H_3), 7.93 (d, *J* = 8.3 Hz, 1H, H_6), 7.73 (d, *J* = 8.3 Hz, 2H, H_{18}), 7.65 (m, 1H, H_9), 7.60 (ddd, *J* = 8.2, 6.7, 1.3 Hz, 1H, H_8), 7.45 (ddd, *J* = 8.3, 6.7, 1.4 Hz, 1H, H_7), 7.38 (d, *J* = 8.0 Hz, 2H, H_{19}), 3.48 (m, 4H, H_{15}), 3.29 (m, 4H, H_{16}), 2.47 (s, 3H, H_{21}), 1.53 (m, 6H, H_{12}), 1.30 (m, 6H, H_{13}), 1.17 (m, 6H, H_{11}), 0.86 (t, *J* = 7.3 Hz, 9H, H_{14}).

^{13}C NMR (101 MHz, Chloroform-*d*) δ_C = 161.1 (Quat., C_1), 147.6 (CH, C_3), 143.9 (Quat., C_{20}), 143.7 (Quat., C_5), 142.1 (Quat., C_{17}), 133.0 (Quat., C_4), 129.9 (CH, C_{19}), 129.8 (CH, C_9), 129.7 (CH, C_8), 128.1 (CH, C_{18}), 126.0 (CH, C_7), 125.8 (CH, C_6), 122.1 (Quat., C_{10}), 50.7 (CH_2, C_{15}), 46.3 (CH_2, C_{16}), 28.0 (CH_2, C_{12}), 17.7 (CH_2, C_{13}), 13.7 (CH_2, C_{11}), 10.4 (CH_3, C_{14}).

FTIR (Chloroform-*d*) ν/cm^{-1} = 2956, 2920, 2850, 1552, 1493, 1457, 1399, 1379, 1354, 1261, 1166, 1018, 952, 766, 728, 683, 649.

HRMS (ESI$^+$) *calculated for $C_{42}H_{47}N_3O_2SSn$ = 658.2482, mass found = 658.2488.*

<u>*tert*-Butyl (pivaloyloxy)carbamate, 152</u>



Following a literature procedure.[273] Pivalic anhydride (20 mL, 99 mmol, 1.2 eq.) was added in one portion to a solution of *tert*-butylhudroxycarbamate **151** (11.0 g, 83 mmol, 1.0 eq.) in chloroform (225 mL). The resulting clear solution was heated to reflux and stirred for 16 h. The reaction mixture was then allowed to cool down to room temperature, quenched with saturated aqueous sodium bicarbonate (100 mL), and diluted with dichloromethane (100 mL). The organic layer was collected, washed with saturated aqueous sodium bicarbonate (3 × 100 mL), dried over anhydrous magnesium sulfate, filtered and concentrated *in vacuo*. The desired carbamate **152** was collected as a white solid (18.0 g, quant.).

^{1}H NMR (400 MHz, Chloroform-*d*) δ_H = 7.84 (s, 1H, H_1), 1.47 (s, 9H, H_5), 1.28 (s, 9H, H_8).

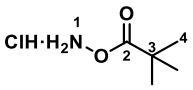
^{13}C NMR (101 MHz, Chloroform-*d*) δ_C = 177.6 (Quat., C_6), 155.5 (Quat., C_2), 82.9 (Quat., C_4), 38.0 (Quat., C_7), 27.8 (CH_3, C_5), 26.8 (CH_3, C_8).

FTIR (Chloroform-*d*) ν/cm^{-1} = 3292, 2979, 1776, 1737, 1480, 1460, 1369, 1395, 1250, 1166, 1100, 1007, 854, 774.

HRMS (ESI$^+$) *calculated for $C_{10}H_{19}NO_4Na$ = 240.1206, mass found = 240.1208 $[M+Na]^+$.*

Melting point *54–56 °C.*

<u>*O*-(Pivaloyl)hydroxylammonium chloride, 153</u>



Following a literature procedure.[275] Ethereal hydrogen chloride (2 M, 200 mmol, 5.0 eq.) was transferred *via* cannula into a solution of carbamate **152** (8.80 g, 42 mmol, 1.0 eq.) in anhydrous diethyl ether (12 mL) at 0 °C, under argon. The reaction mixture was allowed to slowly warm up to room temperature and stirred for 48 h. The resulting white suspension was cooled down to 0 °C, the precipitate was filtered off, washed with ice-cold anhydrous diethyl ether (3 × 100 mL), and dried *in vacuo* to yield the ammonium chloride salt **153** as a white solid (2.70 g, 43%).

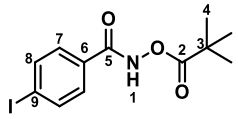
^{1}H NMR (400 MHz, Dimethylsulfoxide-*d_6*) *δ_H = 9.39 (br s, 3H, H_1), 1.19 (s, 9H, H_4).*

^{13}C NMR (101 MHz, Dimethylsulfoxide-*d_6*) *δ_C = 179.3 (Quat., C_2), 37.9 (Quat., C_3), 27.1 (CH_3, C_4).*

Melting point *> 300 °C.*

The spectral data matches that reported in the literature.[275]

4-Iodo-*N*-(pivaloyloxy)benzamide, 155a



Following a literature procedure.[272] A solution of *O*-(pivaloyl)hydroxylammonium chloride **153** (845 mg, 5.5 mmol, 1.45 eq.) in triethyl amine (1.4 mL, 10 mmol, 2.0 eq.) and tetrahydrofuran (25 mL) was cooled to 0 °C, and 4-iodobenzoyl chloride **154a** (845 mg, 5.0 mmol, 1.0 eq.) was added in one portion. The resulting mixture was stirred at 0 °C for 6 h, allowed to warm up to room temperature and concentrated *in vacuo*. Saturated aqueous sodium bicarbonate (30 mL) and ethyl acetate (30 mL) were added. The organic layer was collected, washed with brine (30 mL), dried over anhydrous magnesium sulfate, filtrated, and concentrated *in vacuo*. The resulting orange solid was recrystallized from ethyl acetate in hexane to yield the desired benzamide **155a** as a white solid (1.20 g, 69%).

^{1}H NMR (600 MHz, Methanol-*d*$_4$) *δ_H = 7.88 (d, J = 8.5 Hz, 1H, H_8), 7.57 (d, J = 8.5 Hz, 1H, H_7), 1.34 (s, 9H, H_4).*

^{13}C NMR (151 MHz, Methanol-*d*$_4$) *δ_C = 177.5 (Quat., C_2), 167.2 (Quat., C_5), 139.2 (CH, C_8), 132.2 (Quat., C_6), 130.1 (CH, C_7), 100.1 (Quat., C_9), 39.4 (Quat., C_3), 27.5 (CH_3, C_4).*

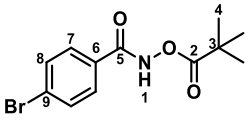
FTIR (neat) ν/cm^{-1} *= 3156, 2975, 1780, 1647, 1586, 1560, 1527, 1480, 1073, 1030, 1005, 872, 809, 743.*

HRMS (ESI$^+$) *calculated for $C_{12}H_{14}INO_3$ = 348.0087, mass found = 348.0092.*

Melting point *122–124 °C (lit. 152–153 °C).*

The spectral data matches that reported in the literature.[272]

4-Bromo-*N*-(pivaloyloxy)benzamide, 155b



Following a literature procedure.[272] A solution of *O*-(pivaloyl)hydroxylammonium chloride **153** (338 mg, 2.9 mmol, 1.45 eq.) in triethyl amine (1.1 mL, 7.6 mmol, 2.0 eq.) and tetrahydrofuran (10 mL) was cooled to 0 °C, and 4-bromobenzoyl chloride **154b** (439 mg, 2.0 mmol, 1.0 eq.) was added in one portion. The resulting mixture was stirred at 0 °C for 2 h, allowed to warm up to room temperature and concentrated *in vacuo*. Saturated aqueous sodium bicarbonate (12 mL) and ethyl acetate (12 mL) were added. The organic layer was collected, washed with brine (30 mL), dried over anhydrous magnesium sulfate, filtrated, and concentrated *in vacuo*. The resulting orange solid was recrystallized from ethyl acetate in hexane to yield the desired benzamide **155b** as a white solid (341 mg, 57%).

^{1}H NMR (400 MHz, Chloroform-*d*) *δ_H = 9.62 (s, 1H, H_1), 7.65 (d, J = 8.7 Hz, 2H, H_7), 7.56 (d, J = 8.6 Hz, 2H, H_8), 1.34 (s, 9H, H_4).*

^{13}C NMR (101 MHz, Chloroform-*d*) *δ_C = 177.2 (Quat., C_2), 166.0 (Quat., C_5), 132.2 (CH, C_8), 129.8 (Quat., C_6), 129.1 (CH, C_7), 127.7 (Quat., C_9), 38.6 (Quat., C_3), 27.1 (CH_3, C_4).*

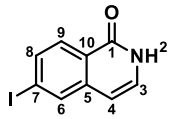
FTIR (neat) ν/cm^{-1} *= 3199, 2976, 1781, 1662, 1591, 1480, 1073, 1012, 902, 841, 746.*

HRMS (ESI$^+$) *calculated for $C_{12}H_{14}BrNO_3$ = 300.0230, mass found = 300.0230.*

Melting point *124–126 °C (lit. 141–142 °C).*

The spectral data matches that reported in the literature.[272]

6-Iodoisoquinolin-1(2*H*)-one, 156a



Following a literature procedure.[272] Benzamide **155a** (694 mg, 2.0 mmol, 1.0 eq.), $[Cp^*RhCl_2]_2$ (12 mg, 0.02 mmol, 1 mol%) and caesium acetate (116 mg, 0.60 mmol, 30 mol%) were added into a flame-dried microwave vial. The vessel was sealed and purged with argon three times. Degassed anhydrous methanol (10 mL) was added, followed by vinyl acetate (276 µL, 3.0 mmol, 1.5 eq.), and the resulting orange suspension was heated to 45 °C and stirred for 16 h. The solvent was removed and the resulting orange slurry was triturated in diethyl ether/methanol 2:1 to yield the desired isoquinolinone **156a** as an off-white solid (313 mg, 66%).

^{1}H NMR (600 MHz, Dimethylsulfoxide-*d_6*) *δ_H = 11.32 (s, 1H, H_2), 8.13 (d, J = 1.7 Hz, 1H, H_6), 7.90 (d, J = 8.4 Hz, 1H, H_9), 7.78 (dd, J = 8.4, 1.7 Hz, 1H, H_8), 7.20 (dd, J = 7.3, 4.2 Hz, 1H, H_3), 6.49 (d, J = 7.1 Hz, 1H, H_4).*

^{13}C NMR (151 MHz, Dimethylsulfoxide-*d_6*) δ_C = *161.6 (Quat., C_1), 139.5 (Quat., C_5), 134.8 (CH, C_8), 134.6 (CH, C_6), 130.2 (CH, C_3), 128.5 (CH, C_9), 125.1 (Quat., C_{10}), 103.4 (CH, C_4), 100.7 (Quat., C_7).*

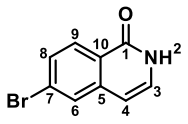
FTIR (neat) ν/cm^{-1} = *3011, 2969, 1658, 1633, 1586, 1529, 1494, 1238, 814, 784, 677, 612.*

HRMS (ESI$^+$) *calculated for C_9H_6INO = 269.8421, mass found = 269.8417.*

Melting point *decomposition ca. 228–232°C (lit. decomposition 231 °C).*

The spectral data matches that reported in the literature.[272]

6-Bromoisoquinolin-1(2*H*)-one, 156b



Following a literature procedure.[272] Benzamide **155b** (321 mg, 0.91 mmol, 1.0 eq.), $[Cp^*RhCl_2]_2$ (6 mg, 0.01 mmol, 1 mol %) and caesium acetate (58 mg, 0.30 mmol, 30 mol %) were added into a flame-dried microwave vial. The vessel was sealed and purged with argon three times. Argon-sparged anhydrous methanol (5.0 mL) was added, followed by vinyl acetate (138 µL, 1.5 mmol, 1.5 eq.), and the resulting orange suspension was heated to 45 °C and stirred for 16 h. The solvent was removed and the resulting orange slurry was triturated in diethyl ether/methanol 2:1 to yield the desired isoquinolinone **156b** as an off-white solid (137 mg, 67 %).

^{1}H NMR (600 MHz, Dimethylsulfoxide-*d_6*) *δ_H = 11.39 (s, 1H, H_2), 8.08 (d, J = 8.5 Hz, 1H, H_9), 7.95 (d, J = 2.0 Hz, 1H, H_6), 7.61 (dd, J = 8.6, 2.0 Hz, 1H, H_8), 7.23 (d, J = 7.2 Hz, 1H, H_3), 6.53 (d, J = 7.1 Hz, 1H, H_4).*

^{13}C NMR (151 MHz, Dimethylsulfoxide-*d_6*) *δ_C = 161.4 (Quat., C_1), 139.6 (Quat., C_5), 130.6 (CH, C_3), 129.2 (CH, C_8), 129.0 (CH, C_9), 128.4 (CH, C_6), 126.3 (Quat., C_{10}), 124.9 (Quat., C_7), 103.6 (CH, C_4).*

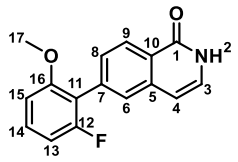
FTIR (neat) ν/cm^{-1} *= 2853, 1670, 1636, 1596, 1241, 826, 768, 674.*

HRMS (ESI$^+$) *calculated for C_9H_6BrNO = 223.9706, mass found = 223.9707.*

Melting point *decomposition ca. 260–262 °C (no lit. data).*

The spectral data matches that reported in the literature.[272]

6-(2-Fluoro-6-methoxyphenyl)isoquinolin-1(2*H*)-one, 160



Following general procedure M, using 6-iodoisoquinoline **156a** (2 × 150 mg[**], 1.1 mmol, 1.0 eq.) and organostannane **162** (2 × 460 mg, 2.2 mmol, 2.0 eq). The reaction mixtures were stirred at 80 °C for 48 h. The combined crude mixtures were purified by column chromatography (60 g silica, 6:4 ethyl acetate/pentane) to yield the title product **160** as a white solid (196 mg, 66%).

^{1}H NMR (600 MHz, Dimethylsulfoxide-*d*$_6$) δ_H = 11.25 (s, 1H, H_2), 8.21 (d, *J* = 8.2 Hz, 1H, H_9), 7.62 (m, 1H, H_8), 7.42 (m, 2H, H_{14} & H_6), 7.19 (dd, *J* = 7.1, 5.6 Hz, 1H, H_3), 7.01 (dd, *J* = 8.4, 1.1 Hz, 1H, H_{13}), 6.95 (ddd, *J* = 9.3, 8.4, 0.9 Hz, 1H, H_{15}), 6.56 (d, *J* = 7.1 Hz, 1H, H_4), 3.75 (s, 3H, H_{17}).

^{13}C NMR (151 MHz, Dimethylsulfoxide-*d*$_6$) δ_C = 161.6 (Quat., C_1), 159.4 (d, *J* = 242.8 Hz, Quat., C_{12}), 157.5 (d, *J* = 6.9 Hz, Quat., C_{16}), 137.7 (Quat., C_5), 135.4 (Quat., C_7), 131.5 (d, *J* = 9.8 Hz, CH, C_{14}), 130.1 (d, *J* = 10.8 Hz, CH, C_8), 129.2 (CH, C_3), 128.7 (d, *J* = 11.5 Hz, CH, C_6), 126.3 (CH, C_9), 125.1 (Quat., C_{10}), 117.1 (d, *J* = 17.8 Hz, Quat., C_{11}), 107.9 (d, *J* = 22.9 Hz, CH, C_{13}), 107.7 (d, *J* = 2.7 Hz, CH, C_{15}), 104.6 (CH, C_4), 56.2 (CH_3, C_{17}).

^{19}F NMR (377 MHz, Dimethylsulfoxide-*d*$_6$) δ_F = -115.7 (dd, *J* = 9.5, 7.0 Hz).

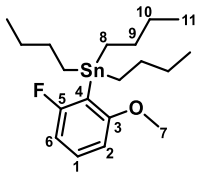
FTIR (neat) ν/cm^{-1} = 2920, 1663, 1639, 1476, 1450, 1235, 1120, 1082, 794, 782, 761, 723, 695.

HRMS (ESI$^+$) *calculated for $C_{16}H_{12}FNO_2$ = 270.0925, mass found = 270.0927.*

[**] Two separate reaction vessels. After stirring for 66 h, the reaction mixture were both filtrated over the same Celite® pad and taken worked-up/purified together from then on.

Melting point *decomposition ca. 159–161 °C.*

Tributyl(2-fluoro-6-methoxyphenyl)stannane, 162[248]



A flame-dried round-bottom flask was loaded with 2-bromo-3-fluoroanisole **161** (1.0 g, 4.9 mmol, 1.0 eq.) and anhydrous tetrahydrofuran (50 mL), under argon atmosphere. The resulting solution was cooled to –78 °C, and *n*-butyllithium (2.5 M in hexanes, 2.1 mL, 5.4 mmol, 1.1 eq.) was added dropwise. The resulting dark-orange solution was allowed to stir at –78 °C for 1 h. Tributyltin chloride (1.5 mL, 5.4 mmol, 1.1 eq.) was added dropwise, the resulting mixture was stirred at –78 °C for 1 h, allowed to warm up to room temperature, and stirred for an extra 16 h. The reaction mixture was quenched with saturated aqueous ammonium chloride (50 mL) and extracted with dichloromethane (2 × 50 mL). The combined organic layers were washed with 1 M potassium fluoride (3 × 50 mL, at least 1 min per wash) brine (100 mL), dried over anhydrous magnesium sulfate, concentrated *in vacuo*. The resulting crude mixture was dried under high vacuum to yield the desired organostannane **162** in a mixture with tributyltin chloride (2.1 g, 88% NMR purity, 91% yield) as a light-yellow oil that was used in the following Stille coupling without further purification.

^{1}H NMR (400 MHz, Chloroform-*d*) *δ_H = 7.25 (td, J = 8.1, 7.1 Hz, 1H, H_1), 6.65 (ddd, J = 8.2, 6.4, 0.7 Hz, 1H, H_6), 6.61 (d, J = 8.1 Hz, 1H, H_2), 3.78 (s, 3H, H_7), 1.54 (m, 6H, H_9), 1.33 (m, 6H, H_{10}), 1.12 (m, 6H, H_8), 0.90 (t, J = 7.3 Hz, 9H, H_{11}).*

^{13}C NMR (101 MHz, Chloroform-*d*) *δ_C = 168.1 (d, J = 235.0 Hz, Quat., C_5), 165.4 (d, J = 19.5 Hz, Quat., C_3), 131.2 (d, J = 9.3 Hz, CH, C_1), 115.2 (d, J = 47.7 Hz, Quat., C_4), 107.8 (d, J = 29.0 Hz, CH,*

C_6), 105.2 (d, J = 2.8 Hz, CH, C_2), 55.5 (CH_3, C_7), 29.2 (CH_2, C_9), 27.4 (CH_2, C_{10}), 13.8 (CH_2, C_8), 11.2 (d, J = 2.3 Hz, CH_3, C_{11}).

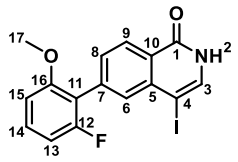
^{19}F NMR (377 MHz, Chloroform-*d*) *δ_F = -94.2.*

FTIR ($CDCl_3$) ν/cm^{-1} *= 2956, 2923, 2854, 1687, 1591, 1547, 1431, 1253, 1220, 1077, 772, 733.*

HRMS (ESI$^-$) *calculated for $C_{15}H_{25}FOSn$ = 359.0828, mass found = 359.0827 $[M\text{-}Bu\text{-}H]^-$.*

The spectral data matches that reported in the literature.[305]

6-(2-Fluoro-6-methoxyphenyl)-4-iodoisoquinolin-1(2*H*)-one, 163



Following general procedure H, using isoquinoline **160** (120 mg, 0.45 mmol, 1.0 eq.). The desired 4-iodoisoquinolinone **163** was obtained as a volatile[††] dark brown solid (142 mg, 81%).

^{1}H NMR (600 MHz, Dimethylsulfoxide-*d_6*) *δ_H = 11.55 (m, 1H, H_2), 8.23 (d, J = 8.1 Hz, 1H, H_9), 7.64 (m, 1H, H_6), 7.60 (t, J = 1.3 Hz, 1H, H_3), 7.55 (m, 1H, H_8), 7.47 (td, J = 8.4, 6.8 Hz, 1H, H_{14}), 7.05 (d, J = 8.4 Hz, 1H, H_{15}), 6.98 (ddd, J = 9.4, 8.4, 0.9 Hz, 1H, H_{13}), 3.78 (s, 3H, H_{17}).*

^{13}C NMR (151 MHz, Dimethylsulfoxide-*d_6*) *δ_C = 160.9 (Quat., C_1), 159.4 (d, J = 243.3 Hz, Quat., C_{12}), 157.4 (d, J = 6.6 Hz, Quat., C_{16}), 137.2 (Quat., C_5), 136.5 (Quat., C_7), 135.9 (CH, C_6), 131.7 (CH, C_3), 130.5 (d, J = 10.9 Hz, CH, C_{14}), 129.8 (CH, C_8), 127.1 (CH, C_9), 125.8 (Quat., C_{10}), 116.6 (d, J = 17.4 Hz, Quat., C_{11}), 108.1 (d, J = 22.8 Hz, CH, C_{13}), 107.9 (d, J = 2.7 Hz, CH, C_{15}), 70.2 (Quat., C_4), 56.3 (CH_3, C_{17}).*

^{19}F NMR (377 MHz, Dimethylsulfoxide-*d_6*) *δ_F = -115.9 (dd, J = 9.5, 7.1 Hz).*

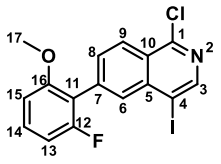
FTIR (neat) ν/cm^{-1} *= 2981, 1649, 1620, 1472, 1232, 1078, 719, 626.*

HRMS (ESI$^+$) *calculated for $C_{16}H_{11}FINO_2$ = 395.9891, mass found = 395.9884.*

Melting point *246–248 °C.*

[††] Volatility was observed under reduced pressure (10–100 mbar) at 40–50 °C.

1-Chloro-6-(2-fluoro-6-methoxyphenyl)-4-iodoisoquinoline, 164



Following general procedure J, using isoquinolinone **163** (245 mg, 0.62 mmol, 1.0 eq.). The reaction mixture was stirred at 90 °C for 16 h. The desired chloroisoquinoline **164** was obtained as a volatile[‡‡] brown solid (239 mg, 93%).

^{1}H NMR (600 MHz, Dimethylsulfoxide-*d_6*) *δ_H = 8.78 (s, 1H, H_3), 8.33 (d, J = 8.7 Hz, 1H, H_9), 8.03 (s, 1H, H_6), 7.91 (d, J = 8.6 Hz, 1H, H_8), 7.51 (td, J = 8.5, 6.9 Hz, 1H, H_{14}), 7.09 (d, J = 8.4 Hz, 1H, H_{15}), 7.02 (t, J = 9.0 Hz, 1H, H_{13}), 3.80 (s, 3H, H_{17}).*

^{13}C NMR (151 MHz, Dimethylsulfoxide-*d_6*) *δ_C = 159.4 (d, J = 244.1 Hz, Quat., C_{12}), 157.4 (d, J = 6.5 Hz, Quat., C_{16}), 151.1 (Quat., C_1), 149.0 (CH, C_3), 137.8 (Quat., C_5), 136.5 (Quat., C_7), 133.0 (CH, C_8), 132.5 (CH, C_6), 131.0 (d, J = 10.8 Hz, CH, C_{14}), 126.4 (CH, C_9), 126.0 (Quat., C_{10}), 115.9 (d, J = 17.0 Hz, Quat., C_{11}), 108.2 (CH, C_{15}), 108.1 (d, J = 3.9 Hz, CH, C_{13}), 96.7 (Quat., C_4), 56.4 (CH_3, C_{17}).*

^{19}F NMR (377 MHz, Dimethylsulfoxide-*d_6*) *δ_F = -116.2 (m).*

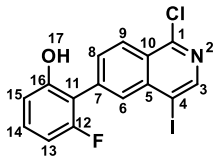
FTIR (neat) ν/cm^{-1} *= 2917, 1622, 1431, 1253, 1239, 1194, 1078, 1032, 942, 724.*

HRMS (ESI$^+$) *calculated for $C_{16}H_{10}ClFINO$ = 413.9550, mass found = 413.9551.*

Melting point *171–173 °C.*

[‡‡] Volatility was observed under reduced pressure (10–100 mbar) at 40–50 °C.

2-(1-Chloro-4-iodoisoquinolin-6-yl)-3-fluorophenol, 165[276]



Boron tribromide (1 M in dichloromethane, 0.32 mL, 0.32 mmol, 2.0 eq.) was carefully added to a solution of isoquinoline **164** (90 mg, 0.16 mmol, 1.0 eq.) in dichloromethane (3 mL) at 0 °C, under argon atmosphere. The reaction mixture was allowed to slowly warm up to room temperature over 2 h (melting ice bath) and stirred for an extra 1 h. The reaction mixture was quenched with water (5 mL) and extracted with dichloromethane (3 × 5 mL). The combined organic layers were washed with brine (2 × 10 mL), dried over anhydrous magnesium sulfate and concentrated *in vacuo* to yield phenol **165** as a brown solid (40 mg, 83%).

^{1}H NMR (600 MHz, Dimethylsulfoxide-*d*$_6$) *δ_H = 10.30 (s, 1H, H_{17}), 8.77 (s, 1H,H_3), 8.32 (d, J = 8.4 Hz, 1H, H_9), 8.09 (d, J = 1.4 Hz, 1H, H_6), 7.95 (dt, J = 8.6, 1.5 Hz, 1H, H_8), 7.32 (td, J = 8.3, 6.8 Hz, 1H, H_{14}), 6.89 (d, J = 8.3 Hz, 1H, H_{15}), 6.83 (ddd, J = 9.6, 8.3, 1.0 Hz, 1H, H_{13}).*

^{13}C NMR (151 MHz, Dimethylsulfoxide-*d*$_6$) *δ_C = 159.9 (d, J = 243.5 Hz, Quat., C_{12}), 156.0 (d, J = 6.5 Hz, Quat., C_{16}), 151.0 (Quat., C_1), 148.9 (CH, C_3), 137.8 (Quat., C_7), 137.2 (Quat., C_5), 133.1 (CH, C_8), 132.5 (CH, C_6), 130.5 (d, J = 11.0 Hz, CH, C_{14}), 126.8 (Quat., C_{10}), 126.2 (CH, C_9), 114.5 (d, J = 16.4 Hz, Quat., C_{11}), 112.1 (d, J = 2.7 Hz, CH, C_{15}), 106.2 (d, J = 22.5 Hz, CH, C_{13}), 96.8 (Quat., C_4).*

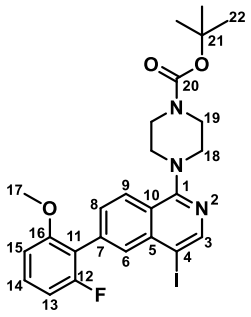
^{19}F NMR (377 MHz, Dimethylsulfoxide-*d*$_6$) *δ_F = -116.4 (m).*

FTIR (neat) ν/cm^{-1} *= 2917, 2849, 1708, 1467, 1328, 1303, 1261, 1248, 1198, 1121, 1009, 990, 903, 827, 725, 666.*

HRMS (ESI$^-$) *calculated for $C_{15}H_8ClFINO$ = 397.9250, mass found = 397.9251 [M-H]$^-$.*

Melting point *192–194 °C.*

tert-Butyl 4-(6-(2-fluoro-6-methoxyphenyl)-4-iodoisoquinolin-1-yl)piperazine-1-carboxylate, 166a



Following general procedure K, using isoquinoline **164** (99 mg, 0.24 mmol, 1.0 eq.) and 1-Boc-piperazine (66 mg, 0.36 mmol, 1.5 eq.). The reaction mixture was stirred at 90 °C for 48 h. When poured onto ice water and filtered off, piperazinylisoquinoline **166a** was isolated as an off-white solid (98 mg, 73%).

^{1}H NMR (600 MHz, Chloroform-*d*) *δ_H = 8.54 (s, 1H, H_3), 8.06 (d, J = 8.6 Hz, 1H, H_9), 8.03 (s, 1H, H_6), 7.63 (d, J = 8.6 Hz, 1H, H_8), 7.36 (td, J = 8.4, 6.5 Hz, 1H, H_{14}), 6.86 (m, 2H, H_{15} & H_{13}), 3.82 (s, 3H, H_{17}), 3.70 (t, J = 5.1 Hz, 4H, H_{18}), 3.40 (s, 4H, H_{19}), 1.50 (s, 9H, H_{22}).*

^{13}C NMR (151 MHz, Chloroform-*d*) *δ_C = 161.6 (Quat., C_1), 160.5 (d, J = 246.2 Hz, Quat., C_{12}), 158.0 (d, J = 6.6 Hz, Quat., C_{16}), 155.1 (Quat., C_{20}), 148.7 (CH, H_3), 138.7 (d, J = 3.3 Hz, Quat., C_7), 138.5 (Quat., C_5), 133.5 (CH, C_6), 130.4 (CH, C_8), 130.0 (d, J = 10.3 Hz, CH, C_{14}), 125.4 (CH, C_9), 122.4 (Quat., C_{10}), 117.6 (d, J = 17.0 Hz, Quat., C_{11}), 108.7 (d, J = 23.1 Hz, CH, C_{13}), 107.1 (d, J = 3.0 Hz, CH, C_{15}), 89.4 (Quat., C_4), 80.1 (Quat., C_{21}), 56.3 (CH_3, C_{17}), 51.4 (CH_2, C_{19}), 43.9 (d, J = 131.0 Hz, CH_2, C_{18}), 28.6 (CH_3, C_{22}).*

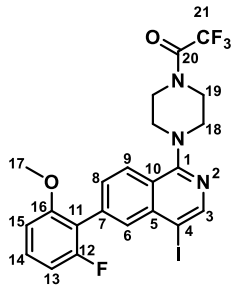
^{19}F NMR (377 MHz, Chloroform-*d*) *δ_F = -115.0.*

FTIR (Chloroform-*d*) ν/cm^{-1} *= 2919, 1694, 1620, 1552, 1496, 1406, 1365, 1328, 1278, 1228, 659.*

HRMS (ESI$^+$) *calculated for $C_{25}H_{27}FIN_3O_3$ = 564.1154, mass found = 564.1152.*

Melting point *58–60 °C.*

2,2,2-Trifluoro-1-(4-(6-(2-fluoro-6-methoxyphenyl)-4-iodoisoquinolin-1-yl)piperazin-1-yl)ethan-1-one, 166b



Following general procedure L, using isoquinoline **164** (100 mg, 0.24 mmol, 1.0 eq.), and trifluoroacetylpiperazine (66 mg, 0.36 mmol, 1.5 eq.). The reaction mixture was stirred at 100 °C for 66 h. The crude mixture was purified by column chromatography (12 g silica, 1:9 ethyl acetate/pentane) to yield piperazinylisoquinoline **166b** as an off-white solid (70 mg, 54%).

^{1}H NMR (400 MHz, Chloroform-*d*) *δ_H = 8.55 (s, 1H, H_3), 8.06 (s, 1H, H_6), 8.04 (d, J = 8.8 Hz, 1H, H_9), 7.65 (d, J = 8.6 Hz, 1H, H_8), 7.37 (td, J = 8.4, 6.5 Hz, 1H, H_{14}), 6.86 (m, 2H, H_{13} & H_{15}), 3.95 (m, 2H, H_{19}), 3.88 (t, J = 5.0 Hz, 2H, H_{19}), 3.82 (s, 3H, H_{17}), 3.51 (q, J = 5.5 Hz, 4H, H_{18}).*

^{13}C NMR (101 MHz, Chloroform-*d*) *δ_C = 160.7 (Quat., C_1), 160.5 (d, J = 246.1 Hz, Quat., C_{12}), 158.0 (d, J = 6.6 Hz, Quat., C_{16}), 155.9 (d, J = 35.8 Hz, Quat., C_{20}), 148.6 (CH, C_3), 138.6 (Quat., C_7), 135.4 (Quat., C_5), 133.7 (d, J = 1.8 Hz, CH, C_6), 130.7 (CH, C_8), 130.1 (d, J = 10.6 Hz, CH, C_{14}), 125.0 (CH., C_9), 122.2 (Quat., C_{10}), 117.5 (d, J = 17.2 Hz, Quat., C_{11}), 116.6 (q, J = 288.1 Hz, Quat., C_{21}), 108.7 (d, J = 23.2 Hz, CH, C_{13}), 107.1 (d, J = 2.9 Hz, CH, C_{15}), 90.3 (Quat., C_4), 56.3 (CH_3, C_{17}), 51.3 (CH_2, C_{18}), 51.0 (CH_2, C_{18}), 45.9 (d, J = 3.6 Hz, CH_2, C_{19}), 43.4 (CH_2, C_{19}).*

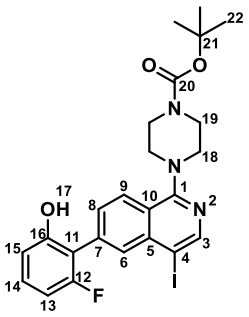
^{19}F NMR (377 MHz, Chloroform-*d*) *δ_F = -68.7 (Ar–CF_3), -115.0 (t, J = 8.0 Hz, Ar–F).*

FTIR (Chloroform-*d*) ν/cm^{-1} *= 2360, 2341, 1695, 1619, 1553, 1469, 1408, 1370, 1276, 1218, 1183, 1143, 1079, 1011, 911, 731.*

HRMS (ESI$^+$) *calculated for $C_{22}H_{18}F_4IN_3O_2$ = 560.0453, mass found = 560.0447.*

Melting point *130–132 °C.*

***tert*-Butyl 4-(6-(2-fluoro-6-hydroxyphenyl)-4-iodoisoquinolin-1-yl)piperazine-1-carboxylate, 168a**



Demethylation/deprotection:[276] Boron tribromide (1 M in dichloromethane, 0.43 mL, 0.43 mmol, 2.0 eq.) was carefully added to a solution of isoquinoline **166a** (120 mg, 0.21 mmol, 1.0 eq.) in dichloromethane (4 mL) at 0 °C, under argon atmosphere. The reaction mixture was allowed to slowly warm up to room temperature over 2 h (melting ice bath) and stirred for an extra 16 h. The reaction mixture was quenched with water (10 mL), and extracted with dichloromethane (3 × 10 mL). The combined organic layers were dried over anhydrous magnesium sulfate, filtered, and concentrated *in vacuo* to yield product **167**, resulting from the deprotection of both the anisole and Boc-piperazine, as an orange solid (77 mg, 80%) (**HRMS (ESI$^+$)** *calculated for $C_{19}H_{17}FIN_3O$ = 450.0473, mass found = 450.0478*).

Reprotection:[286] The solid was then taken up in tetrahydrofuran (1.5 mL) and di-*tert*-butyl dicarbonate (94 mg, 0.43 mmol, 2.0 eq.) was added. The resulting solution was stirred at 40 °C for 16 h, then concentrated *in vacuo*. The resulting solid was taken up in ethyl acetate (10 mL) and water (10 mL). The phases were separated and the organic layer was washed with brine (10 mL), dried over anhydrous magnesium sulfate, filtered, and concentrated *in vacuo* to yield phenol **168a** as a sticky orange goo (140 mg, yield not determined).

Reprotection (alternative):[287] The solid was then dissolved in *N,N*-dimethylformamide (2.0 mL) and di-*tert*-butyl dicarbonate (84 mg, 0.39 mmol, 1.1 eq.) was added. The resulting solution was

stirred at room temperature for 4 h (when the effervescence ceased). The mixture was diluted with ethyl acetate (20 mL), washed with water (3 × 20 mL) and brine (3 × 20 mL), dried over anhydrous magnesium sulfate, filtered, and concentrated *in vacuo* to yield phenol **168a** as a yellow oil (85 mg, 44%).

^{1}H NMR (600 MHz, Chloroform-*d*) δ_H = 8.53 (s, 1H, H_3), 8.12 (d, J = 8.7 Hz, 1H, H_9), 8.06 (s, 1H, H_6), 7.63 (d, J = 8.5 Hz, 1H,H_8), 7.28 (m, 1H, H_{14}), 6.85 (d, J = 8.2 Hz, 1H, H_{15}), 6.81 (m, 1H, H_{13}), 3.69 (dd, J = 6.5, 3.8 Hz, 4H, H_{18}), 3.38 (dd, J = 6.3, 3.8 Hz, 4H, H_{19}), 1.50 (s, 9H, H_{22}).

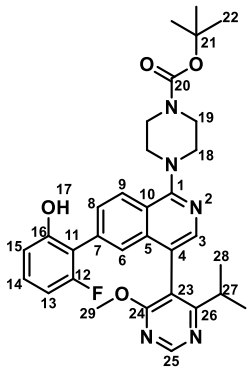
^{13}C NMR (151 MHz, Chloroform-*d*) δ_C = 161.6 (Quat., C_1), 160.4 (d, *J* = 246.5 Hz, Quat., C_{12}), 155.1 (Quat., C_{20}), 154.2 (d, *J* = 5.6 Hz, Quat., C_{16}), 149.2 (CH, C_3), 138.9 (Quat., C_5), 134.2 (Quat., C_7), 133.1 (CH, C_6), 130.2 (d, *J* = 10.7 Hz, CH, C_{14}), 129.8 (CH, C_8), 126.8 (CH, C_9), 122.7 (Quat., C_{10}), 115.9 (d, *J* = 18.3 Hz, Quat., C_{11}), 112.0 (d, *J* = 3.1 Hz, CH, C_{15}), 108.1 (d, *J* = 22.7 Hz, CH, C_{13}), 88.9 (Quat., C_4), 80.2 (Quat., C_{21}), 51.4 (CH_2, C_{19}), 43.2 (CH_2, C_{18}), 28.6 (CH_3, C_{22}).

^{19}F NMR (377 MHz, Chloroform-*d*) δ_F = -114.9.

FTIR (Chloroform-*d*) ν/cm^{-1} = 2917, 2849, 1810, 1785, 1463, 1372, 1120, 1074, 909, 733.

HRMS (ESI$^+$) *calculated for $C_{24}H_{25}FIN_3O_3$ = 550.0996, mass found = 550.1001.*

tert-Butyl 4-(6-(2-fluoro-6-hydroxyphenyl)-4-(4-isopropyl-6-methoxypyrimidin-5-yl)isoquinolin-1-yl)piperazine-1-carboxylate, 169a



Following general procedure M, using isoquinoline **168a** (80 mg, 0.15 mmol, 1.0 eq.) and stannylpyrimidine **86** (129 mg, 0.29 mmol, 2.0 eq), The resulting crude mixture was purified by column chromatography (12 g silica, ethyl acetate/pentane 1:9 to 3:7) to yield the desired biarylpyrimidine **169a** as a yellow oil (53 mg, 92% purity, 59% yield), in a mixture with deprotected piperazine **170** (see **Section III.2.2.3**). Compounds **169a** and **170** were separated by achiral semi-preparative HPLC (ZORBAX Rx-SIL, 92:8 hexane/isopropanol).

^{1}H NMR (600 MHz, Chloroform-*d*) *δ_H = 8.84 (s, 1H, H_3), 8.19 (d, J = 8.6 Hz, 1H, H_9), 7.97 (s, 1H, H_{25}), 7.55 (dd, J = 8.6, 1.6 Hz, 1H, H_8), 7.35 (td, J = 8.3, 6.1 Hz, 1H, H_{14}), 7.28 (d, J = 1.7 Hz, 1H, H_6), 7.05 (m, 2H, H_{13} & H_{15}), 3.83 (s, 3H, H_{29}), 3.74 (t, J = 5.1 Hz, 4H, H_{18}), 3.47 (t, J = 5.2 Hz, 4H, H_{19}), 2.79 (p, J = 6.7 Hz, 1H, H_{27}), 1.52 (s, 9H, H_{22}), 1.18 (d, J = 6.8 Hz, 3H, H_{28}), 1.08 (d, J = 6.7 Hz, 3H, H_{28}).*

^{13}C NMR (151 MHz, Chloroform-*d*) *δ_C = 174.7 (Quat., C_{26}), 168.1 (Quat., C_{24}), 161.3 (Quat., C_1), 160.0 (d, J = 248.3 Hz, Quat., C_{12}), 157.9 (CH, C_3), 155.2 (Quat., C_{20}), 149.4 (d, J = 5.2 Hz, Quat., C_{16}), 141.7 (CH, C_{25}), 137.0 (Quat., C_4), 132.9 (Quat., C_5), 129.7 (d, J = 9.8 Hz, CH, C_{14}), 128.5 (CH, C_8), 127.1 (CH, C_6), 125.6 (CH, C_9), 123.2 (d, J = 18.1 Hz, Quat., C_{11}), 120.7 (Quat., C_{10}), 120.5 (Quat., C_7), 118.3 (d, J = 3.4 Hz, CH, C_{15}), 114.8 (Quat., C_{23}), 113.9 (d, J = 22.6 Hz, CH, C_{13}), 80.2 (Quat., C_{21}),*

54.2 (CH_3, C_{29}), 51.0 (CH_2, C_{19}), 44.5 (CH_2, C_{18}), 31.9 (CH, C_{27}), 28.6 (CH_3, C_{22}), 22.4 (CH_3, C_{28}), 21.5 (CH_3, C_{28}).

^{19}F NMR (376 MHz, Chloroform-*d*) *δ_F = -114.5 (t, J = 7.5 Hz).*

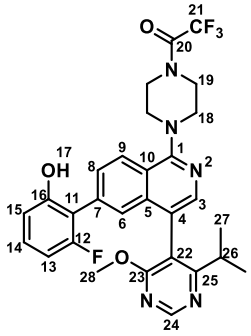
FTIR (Chloroform-*d*) ν/cm^{-1} *= 2957, 2923, 2853, 1763, 1698, 1625, 1566, 1463, 1408, 1387, 1280, 1249, 1227, 1149, 1016, 823, 693.*

HRMS (ESI$^-$) *calculated for $C_{32}H_{36}FN_5O_4$ = 572.2679, mass found = 572.2671.*

Chiral HPLC *(Chiralpak IB N-3, 5 % IPA, 95 % hexane, 1.0 mL/min, λ = 254 nm, 10 μL injection) $\tau_R{}^1$ = 7.46 min, $\tau_R{}^2$ = 8.55 min (racemate).*

Achiral HPLC *(ZORBAX Rx-SIL, 8% IPA, 92% hexane, 1.0 mL/min, λ = 254 nm, 10 μL injection) τ_R = 7.05 min.*

2,2,2-Trifluoro-1-(4-(6-(2-fluoro-6-hydroxyphenyl)-4-(4-isopropyl-6-methoxypyrimidin-5-yl)isoquinolin-1-yl)piperazin-1-yl)ethan-1-one, 169b



Demethylation:[276] Boron tribromide (1 M in dichloromethane, 0.26 mL, 0.26 mmol, 2.0 eq.) was carefully added to a solution of isoquinoline **166b** (70 mg, 0.13 mmol, 1.0 eq.) in dichloromethane (2.6 mL) at 0 °C, under argon atmosphere. The reaction mixture was allowed to slowly warm up to room temperature over 2 h (melting ice bath) and stirred for an extra 2 h. The reaction mixture was cooled back to 0 °C and carefully poured onto ice-cold saturated aqueous sodium hydrogen carbonate (10 mL). The aqueous layer was decanted and the resulting organic suspension was dissolved in ethanol, dried over anhydrous magnesium sulfate, filtered and concentrated *in vacuo* to give phenol **168b** (**HRMS (ESI$^+$)** *calculated for $C_{21}H_{16}F_4IN_3O_2$ = 546.0296, mass found = 546.0297*) and taken to the next step without any further purification.

Stille cross-coupling: *Following general procedure M,* using isoquinoline **168b** (70 mg) and stannylpyrimidine **86** (108 mg, 0.25 mmol, 2.0 eq). The resulting crude mixture was purified by column chromatography (12 g silica, ethyl acetate/pentane, 2:9 to 4:6) to yield biaryl pyrimidine **169b** as an off-white solid (23 mg, 33% over two steps).

^{1}H NMR (400 MHz, Dimethylsulfoxide-d_6) *δ_H = 10.09 (s, 1H, H_{17}), 8.85 (s, 1H, H_3), 8.27 (d, J = 8.7 Hz, 1H, H_9), 8.02 (s, 1H, H_{24}), 7.69 (d, J = 8.7 Hz, 1H, H_8), 7.23 (s, 1H, H_6), 7.18 (m, 1H, H_{14}), 6.79 (d, J*

= 8.3 Hz, 1H, H_{15}), 6.71 (t, J = 9.1 Hz, 1H, H_{13}), 3.92 (m, 4H, H_{18}), 3.77 (s, 3H, H_{28}), 3.54 (m, 4H, H_{19}), 2.64 (m, 1H, H_{26}), 1.12 (d, J = 6.7 Hz, 3H, H_{27}), 1.00 (d, J = 6.7 Hz, 3H, H_{27}).

^{13}C NMR (151 MHz, Dimethylsulfoxide-d_6) δ_C *= 173.7 (Quat., C_{25}), 167.4 (Quat., C_{23}), 160.0 (Quat., C_1), 159.9 (d, J = 243.1 Hz, Quat., C_{12}), 157.6 (CH, C_3), 154.4 (q, J = 34.7 Hz, Quat., C_{20}), 140.9 (CH, C_{24}), 136.1 (Quat., C_4), 134.0 (Quat., C_5), 129.8 (d, J = 11.1 Hz), 129.6 (CH, C_8), 125.9 (CH, C_6), 125.1 (CH, C_9), 119.7 (Quat. C_{10}), 119.2 (Quat., C_7), 116.4 (q, J = 288.6 Hz, Quat., C_{21}), 115.1 (d, J = 16.5 Hz, Quat., C_{11}), 114.1 (Quat., C_{22}), 111.9 (CH, C_{15}), 106.1 (d, J = 22.8 Hz, CH, C_{13}), 54.0 (CH, C_{28}), 50.7 (CH_2, C_{19}), 50.5 (CH_2, C_{19}), 45.5 (CH_2, C_{18}), 43.1 (CH_2, C_{18}), 31.4 (CH, C_{26}), 21.9 (CH_3, C_{27}), 21.1 (CH_3, C_{27}).*

^{19}F NMR (377 MHz, Dimethylsulfoxide-d_6) *δ_F = -67.9 (Ar–CF_3), -116.4 (t, J = 8.2 Hz, Ar–F).*

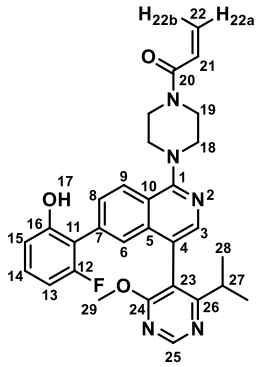
FTIR (neat) ν/cm^{-1} *= 2920, 2850, 1705, 1616, 1570, 1559, 1466, 1416, 1375, 1200, 1183, 1142, 1046, 1013, 756, 692, 670.*

HRMS (ESI$^+$) *calculated for $C_{29}H_{27}F_4N_5O_3$ = 570.2123, mass found = 570.2119.*

Chiral HPLC *(Chiralpak IA, 20 % IPA, 80 % hexane, 1.0 mL/min, λ = 254 nm, 10 μL injection) τ_R^1 = 6.15 min, τ_R^2 = 9.72 min.*

Melting point *244–246 °C.*

1-(4-(6-(2-Fluoro-6-hydroxyphenyl)-4-(4-isopropyl-6-methoxypyrimidin-5-yl)isoquinolin-1-yl)piperazin-1-yl)prop-2-en-1-one, 150



From Boc-protected starting material, 169a:[243] A solution of Boc-protected piperazine **169a** (20 mg, 0.035 mmol, 1.0 eq.) in hydrogen chloride (1.25 M in methanol, 1.75 mL) was stirred in a vial at room temperature for 2.5 h. The resulting mixture was concentrated *in vacuo* and the resulting yellow solid was dissolved in dichloromethane (6.0 mL). The resulting suspension was cooled to 0 °C and a solution of acryloyl chloride in dichloromethane (0.041 M, 1 mL) was added carefully to the mixture. The ice bath was removed and the mixture was stirred at room temperature for 2 h. The reaction was quenched with saturated aqueous sodium bicarbonate (10 mL) and extracted with dichloromethane (3 × 10 mL). The combined organic layers were washed with saturated aqueous sodium bicarbonate (2 × 20 mL) and brine (20 mL), dried over anhydrous magnesium sulfate, filtered, and concentrated *in vacuo*. The resulting off-white solid was purified by column chromatography (3 g silica, 97:3 dichloromethane/methanol) to yield probe **150** as a white solid (12 mg, 67%).

From trifluoroacetyl-protected starting material, 169b:[289] A solution of trifluoroacetyl-protected piperazine **169b** (10 mg, 0.018 mmol, 1.0 eq.) and potassium carbonate (5 mg, 0.036 mmol, 2.0 eq.) in methanol (0.8 mL) and water (0.2 mL) was stirred in a vial at 50 °C for 16 h. The resulting mixture was desiccated on a short silica plug, that was subsequently washed with 1%

triethylamine in methanol. The filtrate was concentrated *in vacuo* and the resulting yellow solid was dissolved in dichloromethane (2.6 mL). The resulting suspension was cooled to 0 °C and a solution of acryloyl chloride in dichloromethane (0.022 M, 1 mL) was added carefully to the mixture. The ice bath was removed and the mixture was stirred at room temperature for 2 h. The reaction was quenched with saturated aqueous sodium bicarbonate (5 mL) and extracted with dichloromethane (3 × 5 mL). The combined organic layers were washed with saturated aqueous sodium bicarbonate (2 × 10 mL) and brine (10 mL), dried over anhydrous magnesium sulfate, filtered, and concentrated *in vacuo*. The resulting off-white solid was purified by column chromatography (1.5 g silica, 97:3 dichloromethane/methanol) to yield probe **150** as a white solid (8 mg, 86%).

^{1}H NMR (400 MHz, Chloroform-*d*) *δ_H = 8.82 (s, 1H, H_3), 8.27 (d, J = 8.7 Hz, 1H, H_9), 7.98 (s, 1H, H_{25}), 7.67 (d, J = 8.6 Hz, 1H, H_8), 7.40 (d, J = 1.6 Hz, 1H, H_6), 7.20 (td, J = 8.3, 6.4 Hz, 1H, H_{14}), 6.80 (m, 1H, H_{15}), 6.73 (ddd, J = 9.8, 8.5, 1.3 Hz, 1H, H_{13}), 6.66 (m, 1H, H_{21}), 6.36 (dd, J = 16.8, 1.9 Hz, 1H, H_{22b}), 5.77 (dd, J = 10.5, 1.9 Hz, 1H, H_{22a}), 4.01 (m, 2H, H_{18}), 3.89 (m, 2H, H_{18}), 3.84 (s, 3H, H_{29}), 3.56 (m, 4H, H_{19}), 2.81 (p, J = 6.7 Hz, 1H, H_{27}), 1.19 (d, J = 6.8 Hz, 3H, H_{28}), 1.05 (d, J = 6.7 Hz, 3H, H_{28}).*

^{13}C NMR (101 MHz, Chloroform-*d*) *δ_C = 174.7 (Quat., C_{26}), 168.2 (Quat., C_{20}), 166.0 (Quat., C_{24}), 161.0 (Quat., C_1), 160.4 (d, J = 246.4 Hz, C_{12}), 157.9 (CH, C_3), 154.6 (d, J = 5.84 Hz, Quat., C_{16}), 141.6 (CH, C_{25}), 137.2 (Quat., C_4), 133.3 (Quat., C_5), 130.0 (d, J = 10.5 Hz, CH, C_{14}), 129.3 (CH, C_8), 128.5 (CH_2, C_{22}), 27.5 (CH, C_{21}), 126.8 (CH, C_6), 126.2 (CH, C_9), 120.7 (Quat., C_{10}), 120.5 (Quat., C_7), 116.0 (d, J = 17.7 Hz, Quat., C_{11}), 114.8 (Quat., C_{23}), 111.8 (d, J = 3.2 Hz, CH, C_{15}), 107.8 (d, J = 22.8 Hz, CH, C_{13}), 54.4 (CH_3, C_{29}), 52.0 (CH_2, C_{19}), 46.1 (CH_2, C_{18}), 42.3 (CH_2, C_{18}), 32.0 (CH, C_{27}), 22.4 (CH_3, C_{28}), 21.4 (CH_3, C_{28}).*

^{19}F NMR (376 MHz, Chloroform-*d*) *δ_H = -115.1 (t, J = 8.1 Hz).*

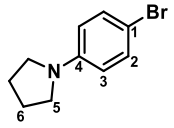
FTIR (Chloroform-*d*) ν/cm^{-1} = *2921, 2852, 2361, 1642, 1620, 1567, 1464, 1411, 1377, 1241, 1048, 1012, 912, 786, 734.*

HRMS (ESI$^+$) *calculated for $C_{30}H_{28}FN_5O_3$ = 528.2405, mass found = 528.2403.*

Chiral HPLC *(Chiralpak IA, 25 % IPA, 75 % hexane, 1.0 mL/min, λ = 254 nm, 10 μL injection) τ_R^1 = 7.27 min, τ_R^2 = 11.47 min (racemate).*

Melting point *254–256 °C.*

1-(4-Bromophenyl)pyrrolidine, 179



Following a literature procedure.[291] An oven-dried round bottom flask was loaded with a magnetic stirrer and potassium carbonate (50 g, 290 mmol, 1.0 eq.). *N,N*-dimethylformamide (290 mL) and 4-bromoaniline **178** (50 g, 290 mmol, 1.0 eq.) were added was added in sequence. The resulting black solution was sparged with argon for 30 min and kept under inert atmosphere. 1,4-Dibromobutane (38 mL, 320 mmol, 1.1 eq.) was added, and the reaction mixture was heated to 80 °C and stirred for 24 h. The reaction mixture was allowed to cool down to room temperature and poured onto ice water. The resulting precipitate was filtered off, washed abundantly with water and dried under high vacuum for several hours to yield the desired phenylpyrrolidine **179** as a brown solid (45.6 g, 69%).

^{1}H NMR (400 MHz, Chloroform-*d*) *δ_H = 7.29 (d, J = 8.9 Hz, 2H, H_2), 6.43 (d, J = 8.9 Hz, 2H, H_3), 3.25 (m, 4H, H_5), 2.02 (m, 4H, H_6).*

^{13}C NMR (101 MHz, Chloroform-*d*) *δ_C = 146.9 (Quat., C_4), 131.8 (CH, C_2), 113.3 (CH, C_3), 107.2 (Quat., C_1), 47.8 (CH_2, C_5), 25.6 (CH_2, C_6).*

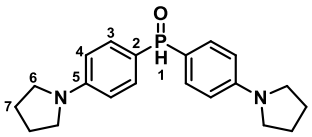
FTIR (Chloroform-*d*) ν/cm^{-1} *= 2968, 2850, 1595, 1556, 1496, 1461, 1375, 1307, 1181, 1075, 960, 802, 732.*

HRMS (ESI$^+$) *calculated for $C_{10}H_{12}Br_N$ = 226.0226, mass found = 226.0226*.

Melting point *84–86 °C.*

The spectral data matches that reported in the literature.[291]

Bis(4-(pyrrolidin-1-yl)phenyl)phosphine oxide, 180



Following a literature procedure.[291] An oven-dried round-bottom flask was loaded with pyrrolidine **179** (31.0 g, 137 mmol, 3.0 eq.) and anhydrous tetrahydrofuran (140 mL). Another oven-dried round-bottom flask, equipped with a magnetic stirrer, was loaded with magnesium turnings (3.5 g, 144 mmol, 3.15 eq.) and cooled down to 0 °C. The contents of the first round bottom-flask were added into the second *via* dropwise cannula transfer with stirring at 0 °C, under nitrogen atmosphere. Upon completion, the resulting brown solution was taken to room temperature and stirred for 2 hours under nitrogen atmosphere. The reaction mixture was cooled to 0 °C and a solution of diethyl phosphite (5.3 mL, 41.2 mmol, 1.0 eq.) in tetrahydrofuran (14 mL) was added dropwise *via* cannula transfer at 0 °C under nitrogen atmosphere. Upon completion, the resulting brown solution was taken to room temperature and stirred for 2 hours under nitrogen atmosphere. The reaction was taken back to 0 °C and quenched with 140 mL of 0.1 N aqueous hydrogen chloride. Methyl *tert*-butyl ether was added (140 mL) and the resulting gel was stirred at room temperature for an extra 5 minutes. The upper organic layer was decanted from the gel, dichloromethane (140 mL) was added, and the gel was agitated for 5 minutes. The resulting suspension was filtered over Celite®, and the solid was washed with dichloromethane (2 × 100 mL). The organic solutions were combined, dried over anhydrous magnesium sulfate, filtered and concentrated *in vacuo*. The resulting brown suspension was adsorbed onto Celite® and purified by column chromatography (300 g silica, 3:97 methanol/dichloromethane) to yield the desired phosphine oxide **180** as a peach solid (7.6 g, 54%).

^{1}H NMR (400 MHz, Chloroform-*d*) δ_H = 7.94 (d, 1H, *J* = 465.6 Hz, H_1), 7.47 (dd, *J* = 13.0, 8.7 Hz, 4H, H_3), 6.55 (dd, *J* = 8.8, 2.3 Hz, 4H, H_4), 3.29 (m, 8H, H_6), 2.00 (m, 8H, H_7).

^{13}C NMR (101 MHz, Chloroform-*d*) δ_C = 150.2 (d, *J* = 2.2 Hz, Quat., C_5), 132.4 (d, *J* = 12.8 Hz, CH, C_3), 116.6 (d, *J* = 112.8 Hz, Quat., C_2), 111.4 (d, *J* = 13.5 Hz, CH, C_4), 47.5 (CH_2, C_6), 25.5 (CH_2, C_7).

^{31}P NMR (162 MHz Chloroform-*d*) δ_P = 22.6.

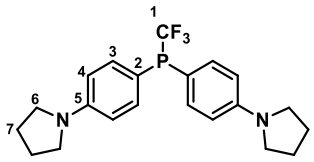
FTIR (Chloroform-*d*) ν/cm^{-1} = 2966, 2844, 1596, 1516, 1384, 1174, 1124, 928, 806, 726, 642.

HRMS (ESI$^+$) *calculated for $C_{20}H_{25}N_2OP$ = 341.1777, mass found = 341.1778.*

Melting point *185–187 °C.*

The spectral data matches that reported in the literature.[291]

1,1'-(((Trifluoromethyl)phosphanediyl)bis(4,1-phenylene))dipyrrolidine, 181



Following a literature procedure.[291] An oven-dried round-bottom flask was loaded with phosphine oxide **180** (6.8 g, 20 mmol, 1.0 eq.) and 18-crown-6 (6.3 g, 24 mmol, 1.2 eq.). The system was purged three times with nitrogen and anhydrous tetrahydrofuran (136 mL) was added. The resulting solution was cooled down to 0 °C and potassium bis(trimethylsilyl)amide (1 M in THF, 24 mL, 1.2 eq.) was added dropwise. The orange suspension was warmed up to room temperature and stirred for 30 minutes. Trimethyl(trifluoromethyl)silane (11.8 mL, 80 mmol, 4.0 eq.) was added dropwise and the suspension was stirred for 10 minutes. The system was quenched with water (100 mL) and extracted with ethyl acetate (3 × 100 mL). The combined organic layers were dried over anhydrous magnesium sulfate, filtered and concentrated *in vacuo* to yield a light-orange solid that was purified by column chromatography (150 g silica, 8:2 pentane/dichloromethane). The desired product was obtained as a white solid (491 mg, 6%, 93% brsm).

^{1}H NMR (400 MHz, Chloroform-*d*) *δ_H = 7.50 (t, J = 8.4 Hz, 4H, H_3), 6.60 (d, J = 7.6 Hz, 4H, H_4), 3.32 (m, 8H, H_6), 2.02 (m, 8H, H_7).*

^{13}C NMR (151 MHz, Chloroform-*d*) *δ_C = 149.1 (Quat., C_5), 135.6 (d, J = 22.5 Hz, CH, C_3), 133.9 (d, J = 11.5 Hz, Quat., C_2), 131.7 (qd, J = 321.6, 33.0 Hz, Quat., C_1), 112.0 (d, J = 9.1 Hz, CH, C_4), 47.7 (CH_2, C_6), 25.6 (CH_2, C_7).*

^{19}F NMR (377 MHz, Chloroform-*d*) *δ_F = -56.8 (d, J = 71.5 Hz).*

^{31}P NMR (162 MHz, Chloroform-*d*) *δ_P = -0.4 (q, J = 71.3 Hz).*

FTIR (Chloroform-*d*) ν/cm^{-1} = *2970, 2842, 1594, 1510, 1485, 1641, 1380, 1149, 1099, 1084, 808, 732.*

HRMS (ESI$^+$) *calculated for $C_{21}H_{24}F_3N_2P$ = 393.1702, mass found = 393.1007.*

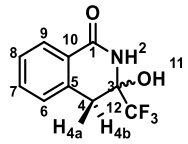
Melting point *148–150 °C.*

The spectral data matches that reported in the literature.[291]

IV.2.2.3 By-products data

This part contains the characterisations of the by-products mentioned in the main text. Some of these by-products were obtained in multiple instances and, in such cases, yields were not indicated (but were mentioned in the main text).

3-Hydroxy-3-(trifluoromethyl)-3,4-dihydroisoquinolin-1(2*H*)-one, 69



By-product in the synthesis of isoquinolinone **68**, can be dehydrated by heating in *N,N*-dimethylformamide at 150 °C for a few days to yield isoquinolinone **68**. Obtained as a white solid.

^{1}H NMR (400 MHz, Acetonitrile-d_3) *δ_H = 7.91 (dd, J = 7.8, 1.4 Hz, 1H, H_9), 7.49 (td, J = 7.5, 1.4 Hz, 1H, H_8), 7.34 (m, 1H, H_7), 7.27 (m, 1H, H_6), 7.15 (s, 1H, H_2), 4.99 (s, 1H, H_{11}), 3.38 (d, J = 16.5 Hz, 1H, H_4), 3.16 (d, J = 16.5 Hz, 1H, H_4).*

^{13}C NMR (101 MHz, Acetonitrile-d_3) *δ_C = 165.4 (Quat., C_1), 135.4 (Quat., C_5), 134.0 (CH, C_8), 129.4 (CH, C_6), 128.4 (CH, C_7), 128.3 (CH, C_9), 127.8 (Quat., C_{10}), 124.7 (q, J = 285.7 Hz, Quat., C_{12}), 82.8 (q, J = 31.3 Hz, Quat., C_3), 34.5 (CH_2, C_4).*

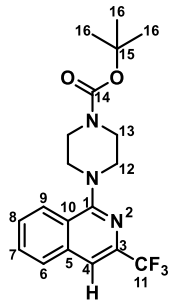
^{19}F NMR (377 MHz, Chloroform-*d*) *δ_F = -85.0*.

FTIR (neat) ν/cm^{-1} *= 3258, 2981, 1684, 1606, 1465, 1389, 1313, 1257, 1241, 1201, 1171, 1140, 1080, 998, 936, 892, 736, 719, 639*.

HRMS (ESI$^+$) *calculated for $C_{10}H_6F_3NO_2$ = 230.0434, mass found = 230.0433.*

Melting point *164–166 °C.*

<u>*tert*-Butyl 4-(3-(trifluoromethyl)isoquinolin-1-yl)piperazine-1-carboxylate, 88</u>



Resulting from the dehalogenation of **76a** and **76d** in the Suzuki-Miyaura, "Willis" and Stille cross-coupling reactions, and the proto-deborylation of **107b**. Obtained as a white solid.

^{1}H NMR (500 MHz, Chloroform-*d*) *δ_H = 8.11 (dd, J = 8.4, 1.2 Hz, 1H, H_9), 7.86 (dd, J = 8.2, 1.3 Hz, 1H, H_6), 7.71 (ddd, J = 8.2, 6.9, 1.3 Hz, 1H, H_7), 7.65 (m, 2H, H_8 & H_4), 3.69 (m, 4H, H_{12}), 3.47 (m, 4H, H_{13}), 1.50 (s, 9H, H_{16}).*

^{13}C NMR (126 MHz, Chloroform-*d*) *δ_C = 161.4 (Quat., C_1), 155.0 (Quat., C_{14}), 139.7 (q, J = 34.0 Hz, H_3), 137.7 (Quat., C_5), 130.8 (CH, C_7), 128.5 (CH, C_6), 128.3 (CH, C_8), 125.6 (CH, C_9), 122.6 (Quat., C_{10}), 122.3 (q, J = 272.9 Hz, Quat., C_{11}), 113.4 (q, J = 3.7 Hz, CH, C_4), 80.1 (Quat., C_{15}), 51.1 (d, J = 113.3 Hz, CH_2, C_{13}), 43.7 (d, J = 110.3 Hz, CH_2, C_{12}), 28.6 (CH_3, C_{16}).*

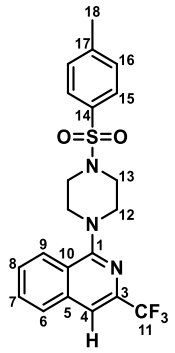
^{19}F NMR (377 MHz, Chloroform-*d*) *δ_F = -68.2.*

FTIR ($CDCl_3$) ν/cm^{-1} *= 2977, 1693, 1566, 1407, 1247, 1130, 1076, 1016, 944, 865, 756, 683.*

HRMS (ESI$^+$) *calculated for $C_{19}H_{22}F_3N_3O_2$ = 382.1737, mass found = 382.1739.*

Melting point *108–111 °C.*

1-(4-Tosylpiperazin-1-yl)-3-(trifluoromethyl)isoquinoline, 105



Resulting from the de-halogenation of **76c** in the Miyaura borylation reaction, and the proto-deborylation of the resulting product **107a**. Obtained as a light-orange solid.

^{1}H NMR (400 MHz, Chloroform-*d*) *δ_H = 7.95 (d, J = 8.4 Hz, 1H, H_9), 7.84 (d, J = 8.1 Hz, 1H, H_6), 7.71 (d, J = 8.3 Hz, 2H, H_{15}), 7.68 (m, 1H, H_7), 7.63 (s, 1H, H_4), 7.59 (ddd, J = 8.4, 7.0, 1.3 Hz, 1H, H_8), 7.37 (d, J = 8.0 Hz ,2H, H_{16}), 3.60 (m, 4H, H_{12}), 3.28 (m, 4H, H_{13}), 2.46 (s, 3H, H_{18}).*

^{13}C NMR (126 MHz, Chloroform-*d*) *δ_C[§§] = 160.8 (Quat., C_1), 144.0 (Quat., C_{17}), 137.8 (Quat., C_5), 132.9 (Quat., C_{14}), 130.8 (CH, C_7), 129.9 (CH, C_{16}), 128.6 (CH, C_6), 128.4 (CH, C_8), 128.1 (CH, C_{15}), 125.4 (CH, C_9), 122.3 (Quat., C_{10}), 113.7 (CH, C_4), 50.5 (CH_2, C_{12}), 45.9 (CH_2, C_{13}), 21.7 (CH_3, C_{18}).*

^{19}F NMR (377 MHz, Chloroform-*d*) *δ_F = -68.2.*

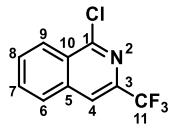
FTIR (Chloroform-*d*) ν/cm^{-1} *= 2875, 2833, 2367, 1133, 1101, 950, 691.*

HRMS (ESI$^+$) *calculated for $C_{21}H_{20}F_3N_3O_2S$ = 436.1301, mass found = 436.1301.*

Melting point *190–192 °C.*

[§§] Not enough material to see C_3 and C_{11}, but their presence was confirmed by the Ar–CF_3 signal on the ^{19}F NMR.

1-Chloro-3-(trifluoromethyl)isoquinoline, 108



Resulting from the dehalogenation of **71a** in the Miyaura borylation and malonate α-arylation reactions. Was also willingly obtained by chlorinating isoquinolinone **68** following general procedure J. Obtained as an off-white solid.

^{1}H NMR (500 MHz, Chloroform-*d*) *δ_H = 8.44 (dd, J = 8.5, 1.4 Hz, 1H, H_9), 8.04 (s, 1H, H_4), 7.99 (d, J = 7.8 Hz, 1H, H_6), 7.87 (m, 2H, H_7 & H_8).*

^{13}C NMR (126 MHz, Chloroform-*d*) *δ_C = 152.8 (Quat., C_1), 140.6 (q, J = 35.7 Hz, Quat., C_3), 137.1 (Quat., C_5), 132.6 (CH, C_8), 130.9 (CH, C_7), 128.3 (CH, C_6), 128.2 (Quat., C_{10}), 126.9 (CH, C_9), 121.5 (q, J = 273.2 Hz, Quat., C_{11}), 118.7 (q, J = 3.5 Hz, Quat., C_4).*

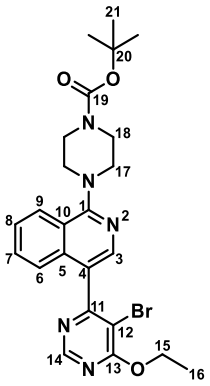
^{19}F NMR (377 MHz, Chloroform-*d*) *δ_F = -67.5.*

FTIR (Chloroform-*d*) ν/cm^{-1} *= 2981, 1562, 1494, 1458, 1423, 1316, 1284, 1247, 1211, 1167, 1128, 1089, 986, 905, 864, 783, 688, 620.*

HRMS (ESI$^+$) *calculated for $C_{10}H_5ClF_3N$ = 232.0135, mass found = 232.0138.*

Melting point *55–57 °C.*

***tert*-Butyl 4-(4-(5-bromo-6-ethoxypyrimidin-4-yl)isoquinolin-1-yl)piperazine-1-carboxylate, 143**



5-bromo-4,6-dichloropyrimidine **142a** (19 mg, 0.08 mmol, 1.2 eq.), tetrakis(triphenylhosphine)palladium(0) (8 mg, 10 mol%) and potassium carbonate (14 mg, 0.14 mmol, 2.0 eq.) were added to a Schlenk tube under argon atmosphere. The vessel was backfilled with argon three times and an argon-sparged solution of boronic ester **141** (30 mg, 0.07 mmol, 1.0 eq.) in toluene (1 mL) and ethanol (0.25 mL) was added. Argon-sparged water (0.25 mL) was added, the reaction mixture was heated to 120 °C and stirred vigorously for 18 h. The reaction mixture was allowed to cool down to room temperature and extracted with ethyl acetate (3 × 5 mL). The combined organic layers were washed with water (3 × 5 mL) and brine (10 mL), dried over anhydrous magnesium sulfate, filtered and concentrated *in vacuo*. The resulting crude mixture was purified by column chromatography (12 g silica, ethyl acetate/pentane, 1:9 to 1:1) to yield coupling by-product **143** as an orange oil (11 mg, 21%).

^{1}H NMR (600 MHz, Chloroform-*d*) *δ_H = 8.75 (s, 1H, H_3), 8.21 (s, 1H, H_{14}), 8.15 (d, J = 8.3 Hz, 1H, H_6), 7.65 (m, 1H, H_8), 7.55 (d, J = 8.3 Hz, 1H, H_9), 7.31 (m, 1H, H_7), 4.62 (q, J = 7.1 Hz, 2H, H_{15}), 3.73 (m, 4H, H_{17}), 3.50 (m, 4H, H_{18}), 1.53 (t, J = 7.1 Hz, 3H, H_{16}), 1.51 (s, 9H, H_{21}).*

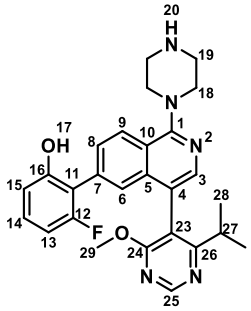
^{13}C NMR (151 MHz, Chloroform-*d*) *δ_C = 166.4 (CH, C_{14}), 158.4 (Quat., C_{13}), 156.0 (CH, C_3), 155.0 (Quat., C_{11}), 153.2 (Quat., C_{19}), 134.6 (CH, C_8), 130.5 (Quat., C_5), 128.1 (CH, C_9), 126.1 (CH, C_6),*

125.3 (CH, C_9) 124.7 (Quat., C_4), 121.0 (Quat., C_{10}), 108.4 (Quat., C_{12}), 80.2 (Quat., C_{20}), 64.6 (CH_2, C_{15}), 51.3 (CH_2, C_{18}), 44.4 (CH_2, C_{17}), 28.6 (CH_3, C_{21}), 14.5 (CH_3, C_{16}).

FTIR (Chloroform-*d*) ν/cm^{-1} = *2923, 2853, 1696, 1553, 1407, 1245, 1167, 1097, 1019, 884, 790, 771, 695*.

HRMS (ESI$^+$) *calculated for $C_{24}H_{28}BrN_5O_3$ = 516.1429, mass found = 516.1427.*

3-Fluoro-2-(4-(4-isopropyl-6-methoxypyrimidin-5-yl)-1-(piperazin-1-yl)isoquinolin-6-yl)phenol, 170



Resulting from the incomplete reprotection of piperazine **167** with di-*tert*-butyl dicarbonate. Isolated from **169a** *via* achiral preparative HPLC (ZORBAX Rx-SIL, 92:8 hexane/isopropanol). Obtained as a white solid.

^{1}H NMR (500 MHz, Chloroform-*d*) *δ_H = 8.84 (d, J = 4.2 Hz, 1H, H_3), 8.23 (d, J = 8.7 Hz, 1H, H_9), 7.92 (s, 1H, H_{25}), 7.51 (dd, J = 8.7, 1.7 Hz, 1H, H_8), 7.35 (td, J = 8.3, 6.0 Hz, 1H, H_{14}), 7.24 (d, J = 1.6 Hz, 1H), H_6, 7.04 (m, 2H, H_{13} & H_{15}), 3.83 (d, J = 1.0 Hz, 3H, H_{29}), 3.21 (s, 8H, H_{18} & H_{19}), 2.83 (m, 1H, H_{27}), 1.55 (s, 9H, H_{22}), 1.18 (d, J = 6.8 Hz, 3H, H_{28}), 1.08 (d, J = 6.7 Hz, 3H, H_{28}).*

^{19}F NMR (376 MHz, Chloroform-*d*) *δ_F = -114.4 (t, J = 7.5 Hz).*

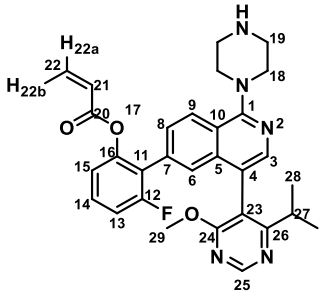
FTIR (Chloroform-*d*) ν/cm^{-1} *= 2981, 1762, 1558, 1464, 1386, 1250, 1149, 1059, 965, 742, 669.*

Chiral HPLC *(Chiralpak IB N-3, 5 % IPA, 95 % hexane, 1.0 mL/min, λ = 254 nm, 10 μL injection) τ_R^1 = 5.32 min, τ_R^2 = 5.74 min (racemate).*

Achiral HPLC *(ZORBAX Rx-SIL, 8% IPA, 92% hexane, 1.0 mL/min, λ = 254 nm, 10 μL injection) τ_R = 7.05 min.*

Not enough material was obtained for ^{13}C NMR, HRMS analysis or melting point measurement.

3-Fluoro-2-(4-(4-isopropyl-6-methoxypyrimidin-5-yl)-1-(piperazin-1-yl)isoquinolin-6-yl)phenyl acrylate, 171



Obtained as the product of the deprotection/*N*-acylation sequence of **169a**, when triethylamine was used. Obtained as a white solid (2 mg, 27%).

^{1}H NMR (500 MHz, Chloroform-*d*) *δ_H = 8.84 (s, 1H, H_3), 8.20 (d, J = 8.6 Hz, 1H, H_9), 7.91 (s, 1H, H_{25}), 7.45 (dd, J = 9.1, 2.0 Hz, 1H, H_8), 7.37 (m, 1H, H_{14}), 7.20 (s, 1H, H_6), 7.07 (m, 1H, H_{15}), 7.00 (m, 1H, H_{13}), 6.29 (dd, J = 17.2, 1.2 Hz, 1H, H_{22b}), 5.99 (dd, J = 17.3, 10.4 Hz, 1H, H_{21}), 5.81 (dd, J = 10.4, 1.2 Hz, 1H, H_{22a}), 3.83 (s, 3H, H_{29}), 3.21 (d, J = 1.4 Hz, 8H, H_{18} & H_{19}), 2.82 (p, J = 6.8 Hz, 1H, H_{27}), 1.20 (s, 6H, H_{28}).*

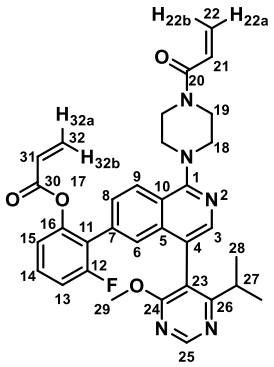
^{19}F NMR (377 MHz, Chloroform-*d*) *δ_F = -114.0 (m).*

FTIR (Chloroform-*d*) ν/cm^{-1} *= 2919, 2850, 2360, 1752, 1623, 1566, 1387, 1146, 1052, 656, 613*.

HRMS (ESI$^+$) *calculated for $C_{30}H_{28}FN_5O_3$ = 528.2405, mass found = 528.2403.*

Not enough material was obtained for a ^{13}C NMR or melting point measurement.

2-(1-(4-Acryloylpiperazin-1-yl)-4-(4-isopropyl-6-methoxypyrimidin-5-yl)isoquinolin-6-yl)-3-fluorophenyl acrylate, 172



Obtained as the product of the double acylation of substrate **169a**, when triethylamine was used. Obtained as a light-yellow oil (2 mg, 25%).

^{1}H NMR (500 MHz, Chloroform-*d*) *δ_H = 8.85 (s, 1H, H_3), 8.18 (d, J = 8.7 Hz, 1H, H_9), 7.97 (s, 1H, H_{25}), 7,53 (m, 1H, H_6), 7.46 (td, J = 7.8, 2.5 Hz, 1H, H_8), 7.38 (m, 1H, H_{15}), 7.08 (m, 1H, H_{14}), 7.02 (m, 1H, H_{13}), 6.67 (dd, J = 16.8, 10.5 Hz, 1H, H_{21}), 6.36 (dd, J = 16.8, 1.9 Hz, 1H, H_{22b}), 6.31 (dd, J = 17.3, 1.2 Hz, 1H, H_{32b}), 6.00 (dd, J = 17.3, 10.4 Hz, 1H, H_{31}), 5.83 (dd, J = 10.4, 1.2 Hz, 1H, H_{32a}), 5.77 (dt, J = 10.5, 1.7 Hz, 1H, H_{22a}), 4.00 (s, 2H, H_{19}), 3.86 (d, J = 14.4 Hz, 2H, H_{19}), 3.83 (d, J = 1.2 Hz, 3H, H_{29}), 3.54 (s, 4H, H_{18}), 2.77 (h, J = 6.5 Hz, 1H, H_{27}), 1.18 (d, J = 6.8 Hz, 3H, H_{28}), 1.05 (d, J = 6.7 Hz, 3H, H_{28}).*

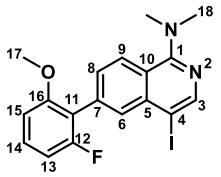
^{19}F NMR (377 MHz, Chloroform-*d*) *δ_F = -114.1 (m).*

FTIR (Chloroform-*d*) ν/cm^{-1} *= 3734, 2922, 2851, 2361, 1750, 1647, 1566, 1463, 1376, 1241, 1143, 1051, 641, 614.*

HRMS (ESI$^+$) *calculated for $C_{33}H_{28}FN_5O_4$ = 582.2511, mass found = 582.2504.*

Not enough material was obtained for a ^{13}C NMR.

6-(2-Fluoro-6-methoxyphenyl)-4-iodo-*N,N*-dimethylisoquinolin-1-amine, 173



Obtained as a byproduct in the SNAr reaction involving chloroisoquinoline **164** and trifluoroacetylpiperazine. Resulted from the thermal degradation of *N,N*-dimethylformamide (solvent) and addition of the resulting dimethylamine on the chloro site. Obtained as a light-yellow solid (12 mg, 24%).

^{1}H NMR (400 MHz, Chloroform-*d*) *δ_H = 8.46 (s, 1H, H_3), 8.08 (d, J = 8.6 Hz, 1H, H_9), 8.00 (s, 1H, H_6), 7.58 (d, J = 8.7 Hz, 1H, H_8), 7.35 (td, J = 8.4, 6.5 Hz, 1H, H_{14}), 6.85 (m, 2H, H_{13} & H_{15}), 3.82 (s, 3H, H_{17}), 3.13 (s, 6H, H_{18})*

^{13}C NMR (101 MHz, Chloroform-*d*) *δ_C = 171.2 (Quat., C_1), 162.1 (Quat., C, 160.4 (d, J = 246.0 Hz, Quat., C_{12}), 157.9 (d, J = 6.7 Hz, Quat., C_{16}), 148.3 (CH, C_3), 138.3 (Quat., C_7), 134.6 (Quat., C_5), 133.1 (d, J = 1.7 Hz, CH, C_6), 129.7 (d, J = 10.7 Hz, CH, C_{14}), 129.3 (CH, C_8), 126.1 (CH, C_9), 121.8 (Quat., C_{10}), 117.7 (d, J = 17.4 Hz, Quat., C_{11}), 108.5 (d, J = 23.2 Hz, CH, C_{13}), 106.9 (d, J = 3.0 Hz, CH, C_{15}), 86.6 (Quat., C_4), 56.2 (CH_3, C_{17}), 43.1 (CH_3, C_{18})*

^{19}F NMR (377 MHz, Chloroform-*d*) *δ_F = -114.9 (t, J = 7.9 Hz).*

FTIR (Chloroform-*d*) ν/cm^{-1} *= 2919, 2849, 2360, 1619, 1579, 1551, 1501, 1469, 1439, 1365, 1274, 1238, 1207, 1279, 1062, 909, 781, 730.*

HRMS (ESI$^+$) *calculated for $C_{18}H_{16}FIN_2O$ = 423.0325, mass found = 423.0373.*

Melting point *118–120 °C.*

IV.3 Rotational barriers

Rotational barriers were determined by thermal racemisation at specific temperatures. The appropriate compound (1 to 2 mg) was dissolved in *m*-xylene and heated to the desired temperature (T) and stirred at the latter for as long as necessary to observe a significant decrease of enantiomeric excess. 10 µL aliquots were removed at specific time points, diluted in 1:1 2-propanol/hexane (100–200 µL), and analysed by chiral HPLC. The e.e. values of the samples were collected and $ln\,(\frac{1}{ee})$ was ploted against time (t). The following equations then allowed to determine the half-life of racemization ($t_{1/2}^{rac}$) and the rotational barrier ($\Delta G_{T\,(K)}^{\ddagger}$).

$$\ln\left(\frac{1}{e.e.}\right) = 2k_{ent}t + C = k_{rac}t + C$$

k_{ent} being the enantiomerisation constant

$k_{rac} = \frac{1}{2}k_{ent}$ being the racemisation constant

$$t_{1/2}^{rac} = \frac{\ln(2)}{k_{rac}}$$

The Eyring equation:

$$\Delta G_T^{\ddagger} = -RTln\left(\frac{k_{ent}h}{k_BT}\right)$$

$$R = 8.314\,J \cdot K^{-1} \cdot mol^{-1}$$
$$h = 6.626 \cdot 10^{-34} J \cdot s$$
$$k_B = 1.381 \cdot 10^{-23} J \cdot K^{-1}$$

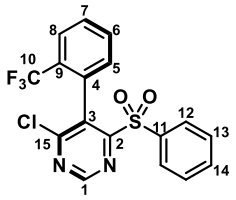
With R being the gas constant, h being Planck's constant and k_B being Boltzmann's constant.

(*S*)-4-Chloro-6-(phenylsulfonyl)-5-(2-(trifluoromethyl)phenyl)pyrimidine, 20

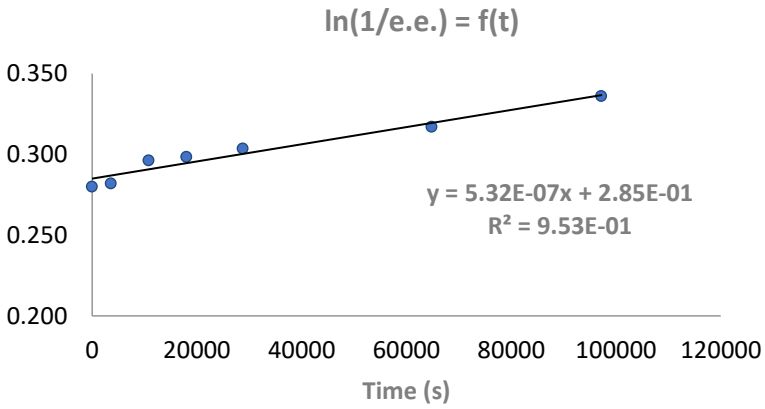
As measured by Lucia Staroňova.[87]

Determined at 130 °C (403 K).

Chiral HPLC *(Chiralpak ADH, 20% IPA, 80% hexane, 1.0 mL/min, λ = 250 nm, 10 µL injection).*



time (h)	time (s)	% major ent.	% minor ent.	ln(1/e.e.)
0	0	87.79	12.21	0.280
1	3600	87.71	12.29	0.282
3	10800	87.18	12.82	0.296
5	18000	87.1	12.90	0.298
8	28800	86.91	13.09	0.304
18	64800	86.41	13.59	0.317
27	97200	85.73	14.27	0.336



$$k_{rac} = 2_{kent} = 5.32 \times 10^{-7}\ s^{-1}$$

$$t_{1/2}^{rac} = \frac{\ln(2)}{k_{rac}} = 15.1\ days\ (at\ 403\ K)$$

Using the Eyring equation:

$$\Delta G_T^{\ddagger} = -RTln\left(\frac{k_{ent}h}{k_BT}\right)$$

= 15.1 × 10^4 J.mol^{-1} (at 403 K)

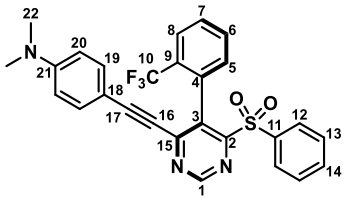
= 36.0 kcal.mol^{-1} (at 403 K)

(*S*)-*N*,*N*-Dimethyl-4-((6-(phenylsulfonyl)-5-(2-(trifluoromethyl)phenyl)pyrimidin-4-yl)ethynyl)aniline, 22a

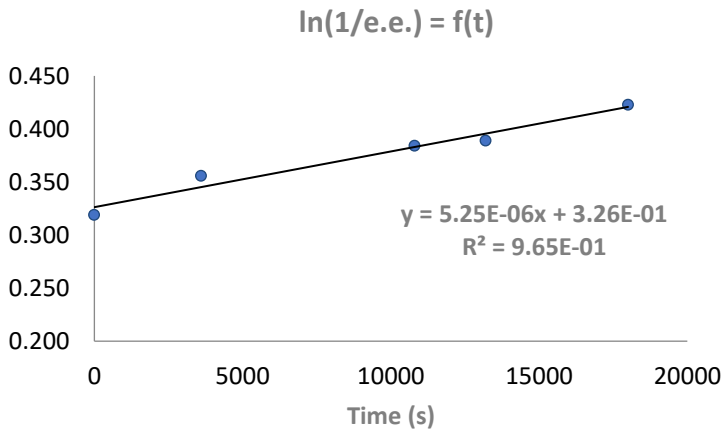
As measured by Lucia Staroňova.[87]

Determined at 130 °C (403 K).

Chiral HPLC *(Chiralpak ADH, 30% IPA, 70% hexane, 1.0 mL/min, λ = 250 nm, 10 µL injection).*



time (h)	time (s)	% major ent.	% minor ent.	ln(1/e.e.)
0	0	86.34	13.66	0.319
1	3600	85.03	14.97	0.356
3	10800	84.05	15.95	0.384
3.667	13201	83.89	16.11	0.389
5	18000	82.76	17.24	0.423



$$k_{rac} = 2_{kent} = 5.25 \times 10^{-6}\ s^{-1}$$

$$t_{1/2}^{rac} = \frac{\ln(2)}{k_{rac}} = 1.5\ days\ (at\ 403\ K)$$

$$\Delta G_T^{\ddagger} = -RTln\left(\frac{k_{ent}h}{k_B T}\right)$$

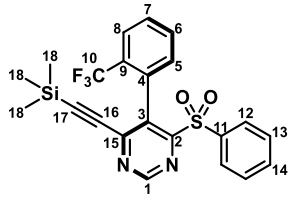
= 14.3 × 10^4 J.mol^{-1} (at 403 K)

= 34.1 kcal.mol^{-1} (at 403 K)

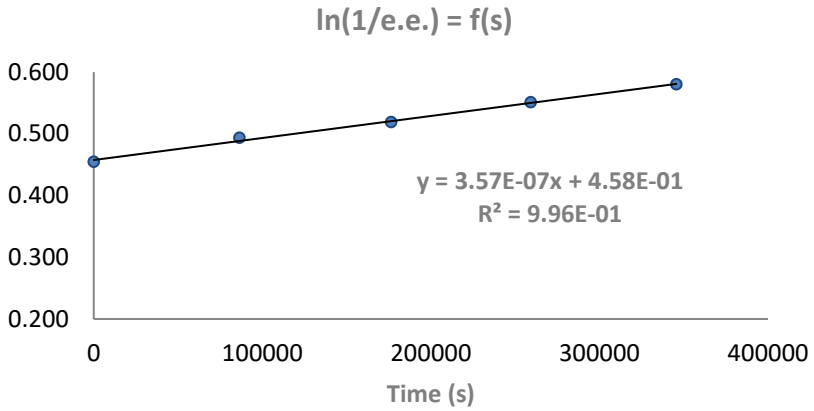
(*S*)-4-(Phenylsulfonyl)-5-(2-(trifluoromethyl)phenyl)-6-((trimethylsilyl)ethynyl)pyrimidine, 22b

Determined at 80 °C (353 K).

Chiral HPLC *(Chiralpak ADH, 5% IPA, 95% hexane, 1.0 mL/min, λ = 250 nm, 10 μL injection).*



time (h)	time (s)	% major ent.	% minor ent.	ln(1/e.e.)
0	0	80.94	19.06	0.454
24	86400	80.53	19.47	0.493
49	176400	79.76	20.24	0.519
72	259200	78.82	21.18	0.551
96	345600	78.00	22.00	0.580



$k_{rac} = 2_{kent} = 3.57 \times 10^{-7}\ s^{-1}$

$t_{1/2}^{rac} = \dfrac{\ln(2)}{k_{rac}} = 22.4\ days\ (at\ 353\ K)$

$\Delta G_T^{\ddagger} = -RTln\left(\dfrac{k_{ent}h}{k_B T}\right)$

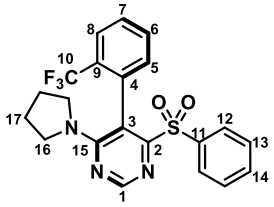
= 13.3 × 10^4 J.mol^{-1} (at 353 K)

= 31.9 kcal.mol^{-1} (at 353 K)

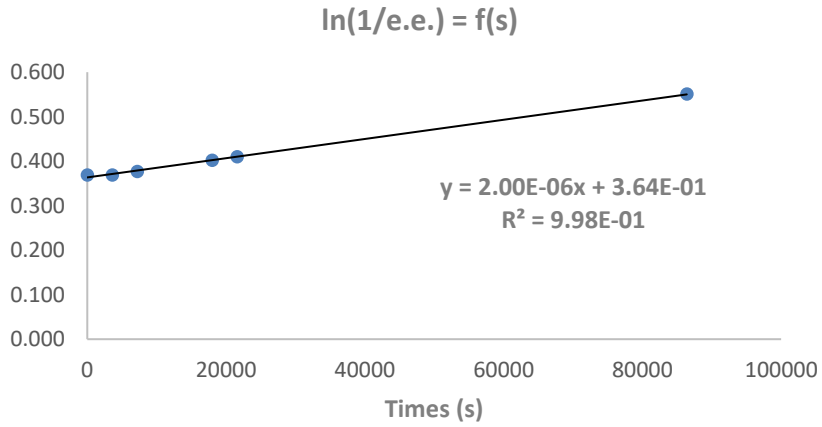
***(R)*-4-(Phenylsulfonyl)-6-(pyrrolidin-1-yl)-5-(2-(trifluoromethyl)phenyl)pyrimidine, 25**

Determined at 120 °C (343 K).

Chiral HPLC *(Chiralpak ADH, 30 % IPA, 70 % hexane, 1.0 mL/min, λ = 226 nm, 10 μL injection).*



time (h)	time (s)	% major ent.	% minor ent.	ln(1/e.e.)
0	0	84.58	15.42	0.369
1	3600	84.48	15.52	0.369
2	7200	84.30	15.70	0.377
5	18000	83.45	16.55	0.402
6	21600	83.20	16.80	0.509
24	86400	78.83	21.17	0.551



$k_{rac} = 2_{kent} = 2.00 \times 10^{-6}\ s^{-1}$

$t_{1/2}^{rac} = \dfrac{\ln(2)}{k_{rac}} = 4\ days\ (at\ 393\ K)$

$\Delta G_T^{\ddagger} = -RTln\left(\dfrac{k_{ent}h}{k_BT}\right)$

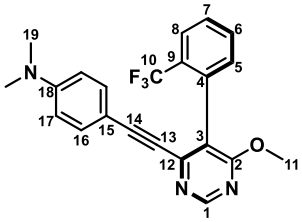
= 14.2 × 10^4 J.mol^{-1} (at 393 K)

= 34.0 kcal.mol^{-1} (at 393 K)

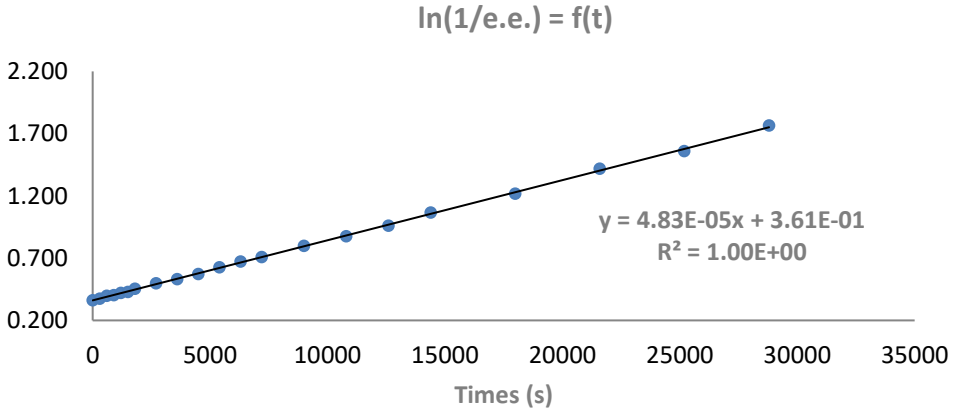
(*S*)-4-((6-Methoxy-5-(2-(trifluoromethyl)phenyl)pyrimidin-4-yl)ethynyl)-N,N-dimethylaniline, 37a

Determined at 80 °C (353 K).

Chiral HPLC *(Chiralpak ADH, 20% IPA, 80% hexane, 1.0 mL/min, λ = 250 nm, 10 μL injection)*



time (min)	time (s)	% major ent.	% minor ent.	ln(1/e.e.)
0	0	84.87	15.13	0.360
15	900	83.46	16.54	0.402
30	1800	81.67	18.13	0.454
45	2700	80.39	80.39	0.498
60	3600	79.38	20.62	0.532
120	7200	74.63	25.37	0.708
180	10800	72.50	29.18	0.876
240	14400	67.22	32.78	1.066
300	18000	64.79	35.21	1.218
360	21600	62.12	37.88	1.417
420	25200	60.51	39.49	1.560
480	28800	58.57	41.43	1.764



$k_{rac} = 2_{kent} = 4.83 \times 10^{-5}\ s^{-1}$

$t_{1/2}^{rac} = \dfrac{\ln(2)}{k_{rac}} = 4\ hours\ (at\ 353\ K)$

$\Delta G_T^{\ddagger} = -RTln\left(\dfrac{k_{ent}h}{k_BT}\right)$

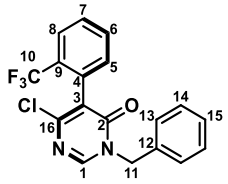
= 11.8 × 10^4 J.mol^{-1} (at 353 K)

= 28.2 kcal.mol^{-1} (at 353 K)

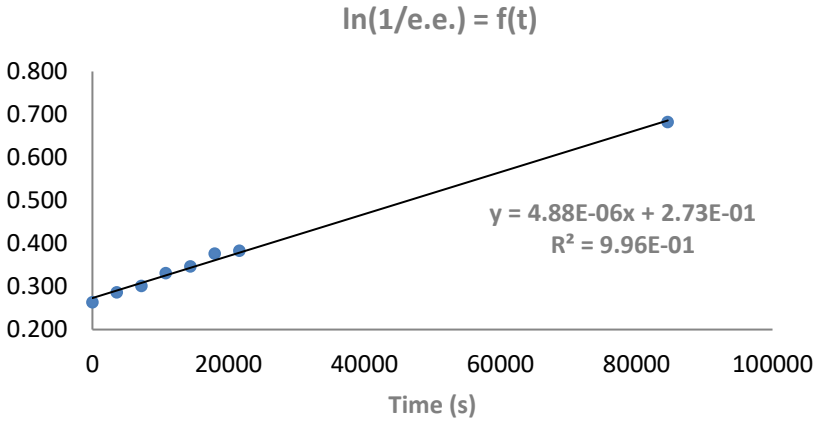
(*S*)-4-(Benzyloxy)-6-chloro-5-(2-(trifluoromethyl)phenyl)pyrimidine, 40a

Determined at 80 °C (353 K).

Chiral HPLC *(Chiralpak ADH, 20% IPA, 80% hexane, 1.0 mL/min, λ = 250 nm, 10 μL injection).*



time (h)	time (s)	% major ent.	% minor ent.	ln(1/e.e.)
0	0	88.45	11.55	0.360
1	3600	87.55	12.45	0.286
2	7200	87.00	13.00	0.301
3	10800	85.92	14.08	0.331
4	14400	85.36	14.64	0.346
5	18000	84.32	15.68	0.377
6	21600	84.10	15.90	0.383
23.5	84600	75.29	24.71	0.682



$k_{rac} = 2_{kent} = 4.88 \times 10^{-6}\ s^{-1}$

$t_{1/2}^{rac} = \dfrac{\ln(2)}{k_{rac}} = 1.6\ days\ (at\ 353\ K)$

$\Delta G_T^{\ddagger} = -RTln\left(\dfrac{k_{ent}h}{k_BT}\right)$

= 12.5 × 10^4 J.mol^{-1} (at 353 K)

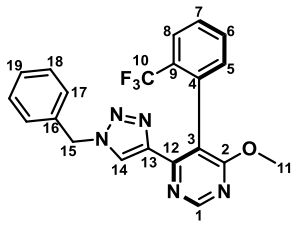
= 29.8 kcal.mol^{-1} (at 353 K)

4-(1-Benzyl-1*H*-1,2,3-triazol-4-yl)-6-methoxy-5-(2-(trifluoromethyl)phenyl)pyrimidine, 42a

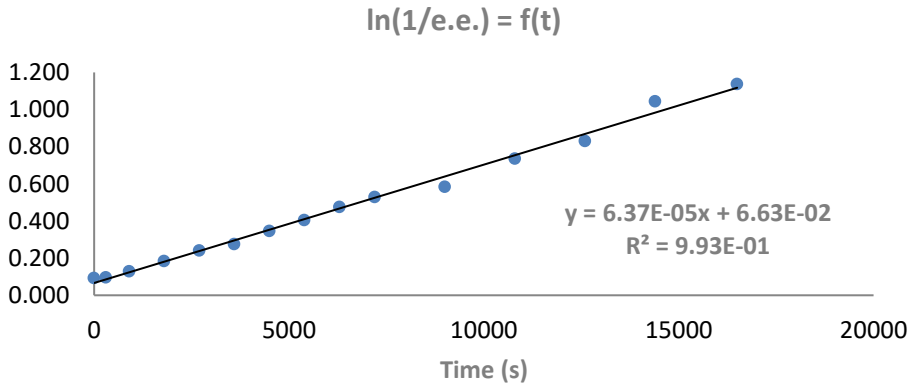
As measured by Alistair Ross.[108]

Determined at 120 °C (393 K).

Chiral HPLC *(Chiralpak IC, 2% IPA, 98% hexane, 1.0 mL/min, λ = 250 nm, 10 μL injection)*



time (min)	time (s)	% major ent.	% minor ent.	ln(1/e.e.)
0	0	95.53	4.47	0.094
5	300	95.42	4.58	0.096
15	900	93.91	6.09	0.130
30	1800	91.57	8.43	0.185
45	2700	89.29	10.71	0.241
60	3600	87.95	12.05	0.276
75	4500	85.35	14.65	0.347
90	5400	83.37	16.63	0.404
105	6300	81.07	18.93	0.476
120	7200	79.43	20.57	0.530
150	9000	77.87	22.13	0.584
180	12600	73.96	26.04	0.736
240	14400	67.6	32.4	1.044
275	16500	66.03	33.97	1.138



$k_{rac} = 2_{kent} = 6.37 \times 10^{-5}\ s^{-1}$

$t_{1/2}^{rac} = \dfrac{\ln(2)}{k_{rac}} = 3.0\ hours\ (at\ 393\ K)$

$$\Delta G_T^{\ddagger} = -RTln\left(\frac{k_{ent}h}{k_B T}\right)$$

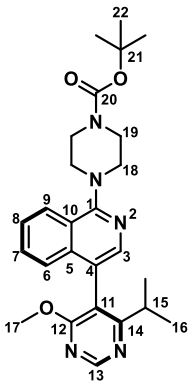
= 13.1 × 10^4 J.mol^{-1} (at 393 K)

= 31.3 kcal.mol^{-1} (at 393 K)

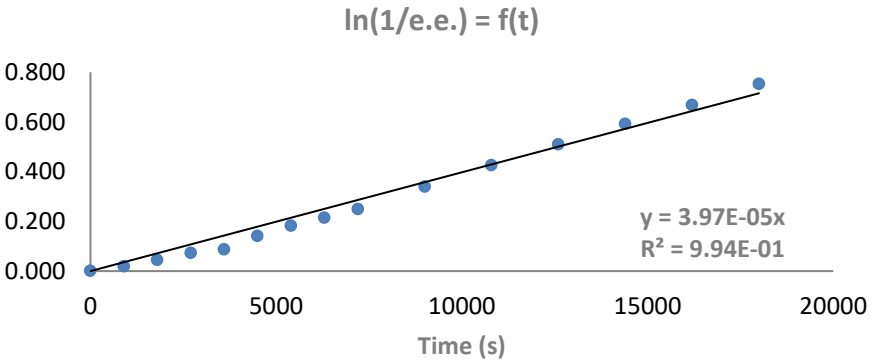
tert-Butyl 4-(4-(4-isopropyl-6-methoxypyrimidin-5-yl)isoquinolin-1-yl)piperazine-1-carboxylate, 119

Determined at 80 °C (353 K).

Chiral HPLC *(Chiralpak ADH, 4% IPA, 96% hexane, 1.0 mL/min, λ = 254 nm, 50 μL injection).*



time (min)	time (s)	% major ent.	% minor ent.	ln(1/e.e.)
0	0	100	0.00	0.000
15	900	99.0	0.91	0.018
30	1800	97.83	2.17	0.044
45	2700	96.49	3.51	0.073
60	3600	95.87	4.13	0.086
75	4500	93.46	6.54	0.140
90	5400	91.69	8.31	0.182
105	6300	90.37	9.63	0.214
120	7200	89.00	11.00	0.248
150	9000	85.62	14.38	0.339
180	10800	82.69	17.31	0.425
210	12600	80.07	19.93	0.508
240	14400	77.66	22.34	0.592
270	16200	75.65	24.35	0.667
300	18000	73.57	26.43	0.752



$k_{rac} = 2_{kent} = 3.97 \times 10^{-5}\ s^{-1}$

$t_{1/2}^{rac} = \dfrac{\ln(2)}{k_{rac}} = 4\ hours\ 48\ min\ (at\ 353\ K)$

$\Delta G_T^{\ddagger} = -RTln\left(\dfrac{k_{ent}h}{k_B T}\right)$

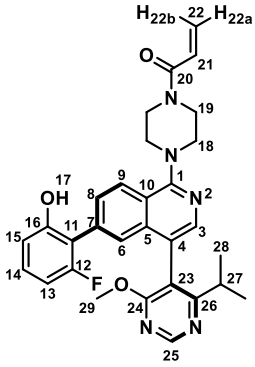
= 11.9 × 10^4 J.mol^{-1} (at 353 K)

= 28.4 kcal.mol^{-1} (at 353 K)

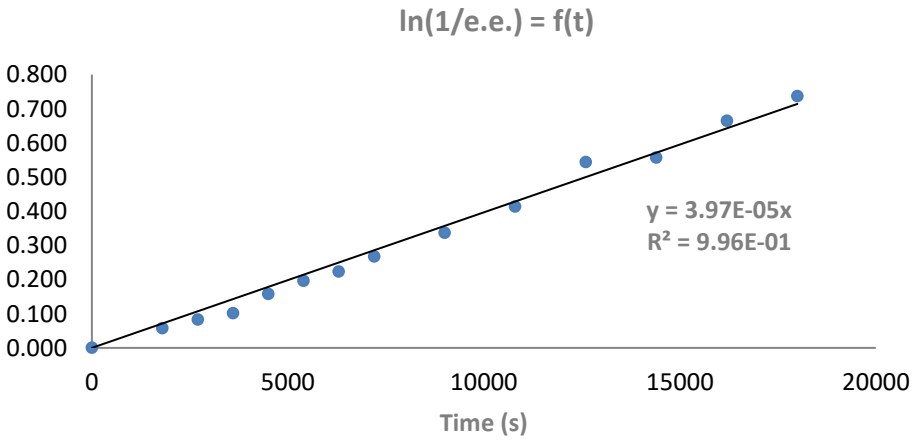
1-(4-(6-(2-Fluoro-6-hydroxyphenyl)-4-(4-isopropyl-6-methoxypyrimidin-5-yl)isoquinolin-1-yl)piperazin-1-yl)prop-2-en-1-one, 150

Determined at 80 °C (353 K).

Chiral HPLC *(Chiralpak IA, 25% IPA, 75% hexane, 1.0 mL/min, λ = 254 nm, 50 μL injection).*



time (min)	time (s)	% major ent.	% minor ent.	ln(1/e.e.)
0	0	100	0.00	0.000
30	1800	97.21	2.79	0.057
45	2700	96.05	3.95	0.082
60	3600	95.18	4.82	0.101
75	4500	92.73	7.27	0.157
90	5400	91.12	8.88	0.196
105	6300	90.01	9.99	0.223
120	7200	88.29	11.71	0.267
150	9000	85.73	14.27	0.336
180	10800	83.06	16.94	0.414
210	12600	79.02	20.98	0.544
240	14400	78.66	21.34	0.557
270	16200	75.73	24.27	0.664
300	18000	73.93	26.07	0.737



$k_{rac} = 2_{kent} = 3.97 \times 10^{-5}\ s^{-1}$

$t_{1/2}^{rac} = \dfrac{\ln(2)}{k_{rac}} = 4\ hours\ 48\ min\ (at\ 353\ K)$

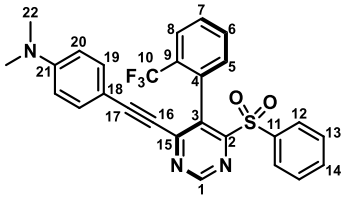
$\Delta G_T^{\ddagger} = -RTln\left(\dfrac{k_{ent}h}{k_B T}\right)$

= 11.9 × 10^4 J.mol^{-1} (at 353 K)

= 28.4 kcal.mol^{-1} (at 353 K)

IV.4 X-Ray Crystallography

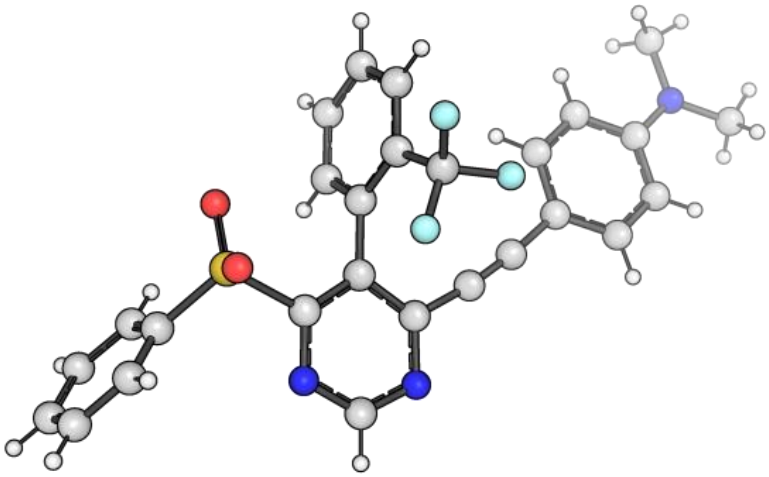
(*S*)-*N*,*N*-Dimethyl-4-((6-(phenylsulfonyl)-5-(2-(trifluoromethyl)phenyl)pyrimidin-4-yl)ethynyl)aniline, 22a

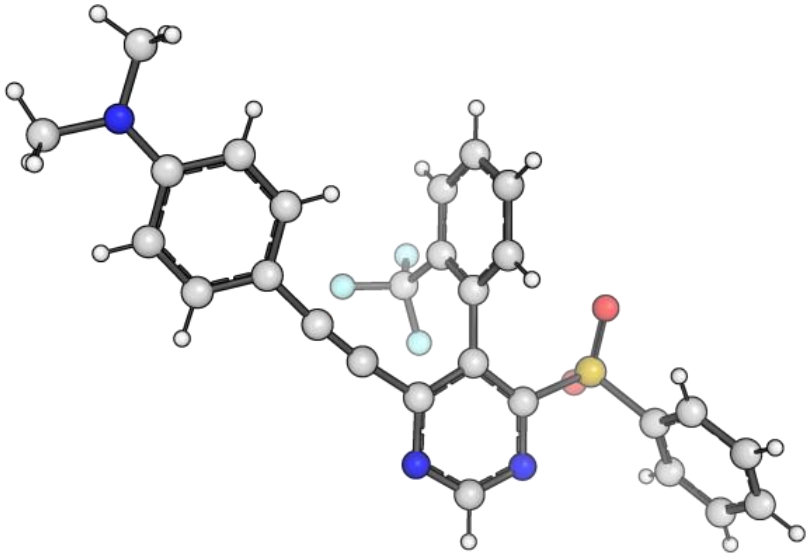


Yellow needles of X-ray quality were grown by slow evaporation of a solution of **22a** (30 mg, 97:3 e.r.) in 2-propanol. The Flack x parameter was refined to -0.023(14). Bayesian analysis of the Bijvoet pairs gave the Hooft y parameter as -0.015(6).

Identification Code	012OS20	
Empirical Formula	C27 H20 F3 N3 O2 S	
M_r	507.53	
Temperature	150 K	
Wavelength	λ = 1.54180 Å (Cu K_α)	
Crystal System	Monoclinic	
Space Group	P 2_1	
Unit Cell Dimensions	a = 7.95200(10) Å	α = 90°
	B = 9.60450(10) Å	β = 95.2671(10)°
	c = 31.4531(4) Å	γ = 90°
Volume	2392.09(5) ($Å^3$)	
Z	4	
Density (Calculated)	1.409 Mg m^{-3}	
Absorption Coefficient	1.677 mm^{-1}	
Crystal Size	0.05 x 0.08 x 0.18 mm^3	
Theta range for data collection	4.235 to 76.176°	
Index Ranges	-9<=h<=8 , -11<=k<=12 , -39<=l<=38	
Reflections Collected	32489	
Independent Reflections	9883 [R(int) = 0.032]	

Completeness to theta = 74.652°	99.7%
Absorption Correction	multi-scan
Refinement method	Full-matrix least-squares on F^2
Goodness-of-fit on F^2	1.0378
Final R indices [I>2sigma(I)]	R1 = 0.0374, wR2 = 0.1035
R indices (all data)	R1 = 0.0416, wR2 = 0.1082
Flack x parameter	-0.023(14)
Hooft y parameter	-0.015(6)





Part IV

Bibliography

V. Bibliography

[1] C. W. Murray, D. C. Rees, *Nat. Chem. 2009 13* **2009**, *1*, 187–192.

[2] B. C. Doak, R. S. Norton, M. J. Scanlon, *Pharmacol. Ther.* **2016**, *167*, 28–37.

[3] C. A. Lipinski, F. Lombardo, B. W. Dominy, P. J. Feeney, *Adv. Drug Deliv. Rev.* **2001**, *46*, 3–26.

[4] M. P. Gleeson, *J. Med. Chem.* **2008**, *51*, 817–834.

[5] M. C. Wenlock, R. P. Austin, P. Barton, A. M. Davis, P. D. Leeson, *J. Med. Chem.* **2003**, *46*, 1250–1256.

[6] H. J. Verheij, *Mol. Divers.* **2006**, *10*, 377–388.

[7] M. Vieth, M. G. Siegel, R. E. Higgs, I. A. Watson, D. H. Robertson, K. A. Savin, G. L. Durst, P. A. Hipskind, *J. Med. Chem.* **2004**, *47*, 224–232.

[8] J. D. Hughes, J. Blagg, D. A. Price, S. Bailey, G. A. DeCrescenzo, R. V. Devraj, E. Ellsworth, Y. M. Fobian, M. E. Gibbs, R. W. Gilles, N. Greene, E. Huang, T. Krieger-Burke, J. Loesel, T. Wager, L. Whiteley, Y. Zhang, *Bioorg. Med. Chem. Lett.* **2008**, *18*, 4872–4875.

[9] P. D. Leeson, B. Springthorpe, *Nat. Rev. Drug Discov. 2007 611* **2007**, *6*, 881–890.

[10] D. A. Erlanson, S. W. Fesik, R. E. Hubbard, W. Jahnke, H. Jhoti, *Twenty Years on: The Impact of Fragments on Drug Discovery*, Nature Publishing Group, **2016**.

[11] R. S. Bohacek, C. McMartin, W. C. Guida, *Med. Res. Rev.* **1996**, *16*, 3–50.

[12] Q. Li, *Front. Mol. Biosci.* **2020**, *7*, 180.

[13] L. Ruddigkeit, R. Van Deursen, L. C. Blum, J. L. Reymond, *J. Chem. Inf. Model.* **2012**, *52*, 2864–2875.

[14] A. Schuffenhauer, S. Ruedisser, A. Marzinzik, W. Jahnke, P. Selzer, E. Jacoby, *Curr. Top. Med. Chem.* **2005**, *5*, 751–762.

[15] M. Congreve, R. Carr, C. Murray, H. Jhoti, *Drug Discov. Today* **2003**, *8*, 876–877.

[16] H. Jhoti, G. Williams, D. C. Rees, C. W. Murray, *Nat. Rev. Drug Discov.* **2013**, *12*, 644.

[17] P. D. Leeson, S. A. St-Gallay, *Nat. Rev. Drug Discov.* **2011**, *10*, 749–765.

[18] G. Bollag, J. Tsai, J. Zhang, C. Zhang, P. Ibrahim, K. Nolop, P. Hirth, *Nat. Rev. Drug Discov.* **2012**, *11*, 873–886.

[19] A. J. Souers, J. D. Leverson, E. R. Boghaert, S. L. Ackler, N. D. Catron, J. Chen, B. D. Dayton, H. Ding, S. H. Enschede, W. J. Fairbrother, D. C. S. Huang, S. G. Hymowitz, S. Jin, S. L. Khaw, P. J. Kovar, L. T. Lam, J. Lee, H. L. Maecker, K. C. Marsh, K. D. Mason, M. J. Mitten, P. M. Nimmer, A. Oleksijew, C. H. Park, C. M. Park, D. C. Phillips, A. W. Roberts, D. Sampath, J. F. Seymour, M. L. Smith, G. M. Sullivan, S. K. Tahir, C. Tse, M. D. Wendt, Y. Xiao, J. C. Xue, H. Zhang, R. A. Humerickhouse, S. H. Rosenberg, S. W. Elmore, *Nat. Med.* **2013**, *19*, 202–208.

[20] T. Oltersdorf, S. W. Elmore, A. R. Shoemaker, R. C. Armstrong, D. J. Augeri, B. A. Belli, M. Bruncko, T. L. Deckwerth, J. Dinges, P. J. Hajduk, M. K. Joseph, S. Kitada, S. J. Korsmeyer, A. R. Kunzer, A. Letai, C. Li, M. J. Mitten, D. G. Nettesheim, S. C. Ng, P. M. Nimmer, J. M. O'Connor, A. Oleksijew, A. M. Petros, J. C. Reed, W. Shen, S. K. Tahir, C. B. Thompson, K. J. Tomaselli, B. Wang, M. D. Wendt, H. Zhang, S. W. Fesik, S. H. Rosenberg, *Nature* **2005**, *435*, 677–681.

[21] U. S. F. and D. A. (FDA), "FDA approves new drug for chronic lymphocytic leukemia in patients with a specific chromosomal abnormality," can be found under https://www.fda.gov/news-events/press-announcements/fda-approves-new-drug-chronic-lymphocytic-leukemia-patients-specific-chromosomal-abnormality, **2016**.

[22] U. S. F. and D. A. (FDA), "FDA approves first therapy for rare joint tumor," can be found under https://www.fda.gov/news-events/press-announcements/fda-approves-first-therapy-rare-joint-tumor, **2019**.

[23] U. S. F. and D. A. (FDA), “FDA approves first targeted therapy for metastatic bladder cancer,” can be found under https://www.fda.gov/news-events/press-announcements/fda-approves-first-targeted-therapy-metastatic-bladder-cancer, **2019**.

[24] U. S. F. and D. A. (FDA), “FDA Approves First Targeted Therapy for Lung Cancer Mutation Previously Considered Resistant to Drug Therapy,” can be found under https://www.fda.gov/news-events/press-announcements/fda-approves-first-targeted-therapy-lung-cancer-mutation-previously-considered-resistant-drug, **2021**.

[25] B. A. Lanman, J. R. Allen, J. G. Allen, A. K. Amegadzie, K. S. Ashton, S. K. Booker, J. J. Chen, N. Chen, M. J. Frohn, G. Goodman, D. J. Kopecky, L. Liu, P. Lopez, J. D. Low, V. Ma, A. E. Minatti, T. T. Nguyen, N. Nishimura, A. J. Pickrell, A. B. Reed, Y. Shin, A. C. Siegmund, N. A. Tamayo, C. M. Tegley, M. C. Walton, H. L. Wang, R. P. Wurz, M. Xue, K. C. Yang, P. Achanta, M. D. Bartberger, J. Canon, L. S. Hollis, J. D. McCarter, C. Mohr, K. Rex, A. Y. Saiki, T. San Miguel, L. P. Volak, K. H. Wang, D. A. Whittington, S. G. Zech, J. R. Lipford, V. J. Cee, *J. Med. Chem.* **2020**, *63*, 52–65.

[26] Y. Shin, J. W. Jeong, R. P. Wurz, P. Achanta, T. Arvedson, M. D. Bartberger, I. D. G. Campuzano, R. Fucini, S. K. Hansen, J. Ingersoll, J. S. Iwig, J. R. Lipford, V. Ma, D. J. Kopecky, J. McCarter, T. San Miguel, C. Mohr, S. Sabet, A. Y. Saiki, A. Sawayama, S. Sethofer, C. M. Tegley, L. P. Volak, K. Yang, B. A. Lanman, D. A. Erlanson, V. J. Cee, *ACS Med. Chem. Lett.* **2019**, *10*, 1302–1308.

[27] M. M. Hann, A. R. Leach, G. Harper, *J. Chem. Inf. Comput. Sci.* **2001**, *41*, 856–864.

[28] T. J. Ritchie, S. J. F. Macdonald, *Drug Discov. Today* **2009**, *14*, 1011–1020.

[29] F. Lovering, J. Bikker, C. Humblet, *J. Med. Chem.* **2009**, *52*, 6752–6756.

[30] C. S. Leung, S. S. F. Leung, J. Tirado-Rives, W. L. Jorgensen, *J. Med. Chem.* **2012**, *55*, 4489–4500.

[31] P. D. Edwards, J. S. Albert, M. Sylvester, D. Aharony, D. Andisik, O. Callaghan, J. B. Campbell, R. A. Carr, G. Chessari, M. Congreve, M. Frederickson, R. H. A. Folmer, S. Geschwindner, G. Koether, K. Kolmodin, J. Krumrine, R. C. Mauger, C. W. Murray, L. L. Olsson, S. Patel, N. Spear, G. Tian, *J. Med. Chem.* **2007**, *50*, 5912–5925.

[32] A. D. Morley, A. Pugliese, K. Birchall, J. Bower, P. Brennan, N. Brown, T. Chapman, M. Drysdale, I. H. Gilbert, S. Hoelder, A. Jordan, S. V. Ley, A. Merritt, D. Miller, M. E. Swarbrick, P. G. Wyatt, *Drug Discov. Today* **2013**, *18*, 1221–1227.

[33] G. H. Christie, J. Kenner, *J. Chem. Soc. Trans.* **1923**, *123*, 779–785.

[34] J. Clayden, P. Johnson, J. H. Pink, M. Helliwell, *J. Org. Chem.* **2000**, *65*, 7033–7040.

[35] P. Eveleigh, E. C. Hulme, C. Schudt, N. J. M. Birdsall, *Mol. Pharmacol.* **1989**, *35*, 477–483.

[36] X. Fu, M. B. Hossain, F. J. Schmitz, D. Van der Helm, *J. Org. Chem.* **1997**, *62*, 3810–3819.

[37] P. W. Glunz, *Bioorganic Med. Chem. Lett.* **2018**, *28*, 53–60.

[38] N. Z. Burns, I. N. Krylova, R. N. Hannoush, P. S. Baran, *J. Am. Chem. Soc.* **2009**, *131*, 9172–9173.

[39] S. R. LaPlante, L. D. Fader, K. R. Fandrick, D. R. Fandrick, O. Hucke, R. Kemper, S. P. F. Miller, P. J. Edwards, *J. Med. Chem.* **2011**, *54*, 7005–7022.

[40] A. Zask, J. Murphy, G. A. Ellestad, *Chirality* **2013**, *25*, 265–274.

[41] C. Rosini, L. Franzini, A. Raffaelli, P. Salvadori, *Synthesis (Stuttg).* **1992**, *6*, 503–517.

[42] M. McCarthy, P. J. Guiry, *Tetrahedron* **2001**, *57*, 3809–3844.

[43] A. Miyashita, A. Yasuda, H. Takaya, K. Toriumi, T. Ito, T. Souchi, R. Noyori, *J. Am. Chem. Soc.* **2002**, *102*, 7932–7934.

[44] R. Noyori, H. Takaya, *Acc. Chem. Res.* **2002**, *23*, 345–350.

[45] S. Hoffmann, A. Majeed Seayad, B. List, D.-C. S. Hoffmann, A. M. Seayad, B. List, *Angew. Chem. Int. Ed.* **2005**, *44*, 7424–7427.

[46] T. Akiyama, Y. Tamura, J. Itoh, H. Morita, K. Fuchibe, *Synlett* **2006**, *2006*, 0141–0143.

[47] J. Seayad, A. M. Seayad, B. List, *J. Am. Chem. Soc.* **2006**, *128*, 1086–1087.

[48] G. Adair, S. Mukherjee, B. List, *Aldrichimica Acta* **2008**, *41*, 31–39.

[49] R. Armstrong, M. D. Smith, Catalytic Asymmetric Reactions Employing Chiral Cations (PhD Thesis), University of Oxford, **2017**.

[50] M. Ōki, *Top. Stereochem.* **1983**, *14*, 1–81.

[51] S. Fabro, R. L. Smith, R. T. Williams, *Nat. 1967 2155098* **1967**, *215*, 296–296.

[52] T. Eriksson, S. Björkman, B. Roth, Å. Fyge, P. Höuglund, *Chirality* **1995**, *7*, 44–52.

[53] M. Reist, P. A. Carrupt, E. Francotte, B. Testa, *Chem. Res. Toxicol.* **1998**, *11*, 1521–1528.

[54] I. Agranat, H. Caner, J. Caldwell, *Nat. Rev. Drug Discov. 2002 110* **2002**, *1*, 753–768.

[55] J. Clayden, W. J. Moran, P. J. Edwards, S. R. Laplante, *Angew. Chem. Int. Ed.* **2009**, *48*, 6398–6401.

[56] C. S. Chen, W. R. Shieh, P. H. Lu, S. Harriman, C. Y. Chen, *Biochim. Biophys. Acta - Protein Struct. Mol. Enzymol.* **1991**, *1078*, 411–417.

[57] T. Nguyen, *C&EN Glob. Enterp.* **2018**, *96*, 22–25.

[58] S. T. Toenjes, J. L. Gustafson, *Future Med. Chem.* **2018**, *10*, 409–422.

[59] S. R. LaPlante, P. J. Edwards, L. D. Fader, A. Jakalian, O. Hucke, *ChemMedChem* **2011**, *6*, 505–513.

[60] J. S. Albert, D. Andisik, H. Barthlow, P. R. Bernstein, R. A. Bialecki, R. Dedinas, B. T. Dembofsky, D. Hill, K. Kirkland, G. M. Koether, B. J. Kosmider, C. Ohnmacht, W. Palmer, W. Potts, W. Rumsey, L. Shen, A. Shenvi, S. Sherwood, D. Aharony, P. J. Warwick, K. Russell, *J. Med. Chem.* **2002**, *45*, 3972–3983.

[61] J. S. Albert, C. Ohnmacht, P. R. Bernstein, W. L. Rumsey, D. Aharony, B. B. Masek, B. T. Dembofsky, G. M. Koether, W. Potts, J. L. Evenden, *Tetrahedron* **2004**, *60*, 4337–4347.

[62] F. C. Tucci, T. Hu, M. F. Mesleh, A. Bokser, E. Allsopp, T. D. Gross, Z. Guo, Y. F. Zhu, R. S. Struthers, N. Ling, C. Chen, *Chirality* **2005**, *17*, 559–564.

[63] A. Palani, S. Shapiro, J. W. Clader, W. J. Greenlee, S. Vice, S. McCombie, K. Cox, J. Strizki, B. M. Baroudy, *Bioorg. Med. Chem. Lett.* **2003**, *13*, 709–712.

[64] J. Porter, A. Payne, B. de Candole, D. Ford, B. Hutchinson, G. Trevitt, J. Turner, C. Edwards, C. Watkins, I. Whitcombe, J. Davis, C. Stubberfield, *Bioorg. Med. Chem. Lett.* **2009**, *19*, 230–233.

[65] J. Porter, A. Payne, I. Whitcombe, B. de Candole, D. Ford, R. Garlish, A. Hold, B. Hutchinson, G. Trevitt, J. Turner, C. Edwards, C. Watkins, J. Davis, C. Stubberfield, *Bioorg. Med. Chem. Lett.* **2009**, *19*, 1767–1772.

[66] P. Wu, T. E. Nielsen, M. H. Clausen, *Trends Pharmacol. Sci.* **2015**, *36*, 422–439.

[67] D. E. Smith, I. Marquez, M. E. Lokensgard, A. L. Rheingold, D. A. Hecht, J. L. Gustafson, *Angew. Chem. Int. Ed.* **2015**, *54*, 11754–11759.

[68] J. Chandrasekhar, R. Dick, J. Van Veldhuizen, D. Koditek, E. I. Lepist, M. E. McGrath, L. Patel, G. Phillips, K. Sedillo, J. R. Somoza, J. Therrien, N. A. Till, J. Treiberg, A. G. Villasenὶor, Y. Zherebina, S. Perreault, *J. Med. Chem.* **2018**, *61*, 6858–6868.

[69] J. Dai, C. Wang, S. C. Traeger, L. Discenza, M. T. Obermeier, A. A. Tymiak, Y. Zhang, *J. Chromatogr. A* **2017**, *1487*, 116–128.

[70] U.S. National Library of Medicine, “Efficacy and Safety Study of BMS-986142 in Patients With Moderate to Severe Rheumatoid Arthritis,” can be found under https://clinicaltrials.gov/ct2/show/NCT02638948, **2019**.

[71] R. J. Armstrong, M. D. Smith, *Angew. Chem. Int. Ed.* **2014**, *53*, 12822–12826.

[72] J. D. Jolliffe, R. J. Armstrong, M. D. Smith, *Nat. Chem.* **2017**, *9*, 558–562.

[73] A. Fugard, Enantioselective Synthesis of Non-Biaryl Atropisomers, University of Oxford,

2019.

[74] B. A. Jones, T. Balan, J. D. Jolliffe, C. D. Campbell, M. D. Smith, *Angew. Chem. Int. Ed.* **2019**, *58*, 4596–4600.

[75] J. M. Keith, J. F. Larrow, E. N. Jacobsen, *Adv. Synth. Catal.* **2001**, *343*, 5–26.

[76] H. Pellissier, *Tetrahedron* **2003**, *59*, 8291–8327.

[77] W. R. Pitt, D. M. Parry, B. G. Perry, C. R. Groom, *J. Med. Chem.* **2009**, *52*, 2952–2963.

[78] A. P. Taylor, R. P. Robinson, Y. M. Fobian, D. C. Blakemore, L. H. Jones, O. Fadeyi, *Org. Biomol. Chem.* **2016**, *14*, 6611–6637.

[79] G. Z. Zheng, C. H. Lee, J. K. Pratt, R. J. Perner, M. Q. Jiang, A. Gomtsyan, M. A. Matulenko, Y. Mao, J. R. Koenig, K. H. Kim, S. Muchmore, H. Yu, K. Kohlhaas, K. M. Alexander, S. McGaraughty, K. L. Chu, C. T. Wismer, J. Mikusa, M. F. Jarvis, K. Marsh, E. A. Kowaluk, S. S. Bhagwat, A. O. Stewart, *Bioorg. Med. Chem. Lett.* **2001**, *11*, 2071–2074.

[80] M. A. Matulenko, E. S. Paight, R. R. Frey, A. Gomtsyan, S. DiDomenico, M. Jiang, C. H. Lee, A. O. Stewart, H. Yu, K. L. Kohlhaas, K. M. Alexander, S. McGaraughty, J. Mikusa, K. C. Marsh, S. W. Muchmore, C. L. Jakob, E. A. Kowaluk, M. F. Jarvis, S. S. Bhagwat, *Bioorganic Med. Chem.* **2007**, *15*, 1586–1605.

[81] B. A. Lanman, J. Chen, A. B. Reed, V. J. Cee, L. Liu, D. J. Kopecky, P. Lopez, R. P. Wurz, T. T. Nguyen, S. Booker, N. Nishimura, Y. Shin, N. A. Tamayo, J. G. Allen, J. R. Allen, *KRas G12C Inhibitors and Methods of Using the Same*, **2018**, US20180334454.

[82] B. A. Lanman, S. Booker, C. Goodman, A. B. Reed, J. D. Low, H.-L. Wang, A. E. Minatti, R. P. Wurz, V. J. Cee, *Inhibitors of KRAS G12C and Methods of Using the Same*, **2019**, WO2019051291.

[83] H. L. Yale, *J. Med. Chem.* **2002**, *1*, 121–133.

[84] D. T. Wong, F. P. Bymaster, E. A. Engleman, *Life Sci.* **1995**, *57*, 411–441.

[85] T. D. Penning, J. J. Talley, S. R. Bertenshaw, J. S. Carter, P. W. Collins, S. Docter, M. J. Graneto, L. F. Lee, J. W. Malecha, J. M. Miyashiro, R. S. Rogers, D. J. Rogier, S. S. Yu, G. D. Anderson, E. G. Burton, J. N. Cogburn, S. A. Gregory, C. M. Koboldt, W. E. Perkins, K. Seibert, A. W. Veenhuizen, Y. Y. Zhang, P. C. Isakson, *J. Med. Chem.* **1997**, *40*, 1347–1365.

[86] S. F. Yip, H. Y. Cheung, Z. Zhou, F. Y. Kwong, *Org. Lett.* **2007**, *9*, 3469–3472.

[87] L. Staroňova, M. D. Smith, P. E. Brennan, Atropisomeric Fragments in Drug Discovery and Probe Compound Development (Rotation Report), University of Oxford, **2018**.

[88] K. Sonogashira, *J. Organomet. Chem.* **2002**, *653*, 46–49.

[89] R. Chinchilla, C. Nájera, *Chem. Rev.* **2007**, *107*, 874–922.

[90] K. S. England, C. J. Schofield, A Potent and Selective Inhibitor of a Histone Demethylase (PhD Thesis), University of Oxford, **2016**.

[91] M. Pérez-Rodríguez, A. A. C. Braga, M. Garcia-Melchor, M. H. Pérez-Temprano, J. A. Casares, G. Ujaque, A. R. De Lera, R. Álvarez, F. Maseras, P. Espinet, *J. Am. Chem. Soc.* **2009**, *131*, 3650–3657.

[92] N. Miyaura, K. Yamada, A. Suzuki, *Tetrahedron Lett.* **1979**, *20*, 3437–3440.

[93] D. Blakemore, *RSC Drug Discov. Ser.* **2016**, *2016-January*, 1–69.

[94] E. ichi Negishi, D. E. Van Horn, T. Yoshida, *J. Am. Chem. Soc.* **1985**, *107*, 6639–6647.

[95] D. M. Knapp, E. P. Gillis, M. D. Burke, *J. Am. Chem. Soc.* **2009**, *131*, 6961–6963.

[96] M. M. Cardenas, S. T. Toenjes, C. J. Nalbandian, J. L. Gustafson, *Org. Lett.* **2018**, *20*, 2037–2041.

[97] A. Baron, G. Sandford, R. Slater, D. S. Yufit, J. A. K. Howard, A. Vong, *J. Org. Chem.* **2005**, *70*, 9377–9381.

[98] R. Fu, X. Xu, Q. Dang, F. Chen, X. Bai, *Org. Lett.* **2007**, *9*, 571–574.

[99] L. Zheng, F. Yang, Q. Dang, X. Bai, *Org. Lett.* **2008**, *10*, 889–892.

[100] W. Cowden, N. Jacobsen, *Aust. J. Chem.* **1979**, *32*, 2049–2057.

[101] M. Abarbri, J. L. Parrain, A. Duchêne, J. Thibonnet, *Synthesis (Stuttg).* **2006**, *2006*, 2951–2970.

[102] W. Li, L. Gao, Z. Yue, J. Zhang, *Adv. Synth. Catal.* **2015**, *357*, 2651–2655.

[103] Y. Guan, S. V. Shree Sowndarya, L. C. Gallegos, P. C. St. John, R. S. Paton, *Chem. Sci.* **2021**, *12*, 12012–12026.

[104] V. V. Rostovtsev, L. G. Green, V. V. Fokin, K. B. Sharpless, *ChemInform* **2002**, *33*, 45–45.

[105] J. Hou, X. Liu, J. Shen, G. Zhao, P. G. Wang, *Expert Opin. Drug Discov.* **2012**, *7*, 489–501.

[106] S. G. Agalave, S. R. Maujan, V. S. Pore, *Chem. – An Asian J.* **2011**, *6*, 2696–2718.

[107] C. Zhang, L. M. F. Gomes, T. Zhang, T. Storr, *Can. J. Chem.* **2018**, *96*, 78–82.

[108] A. Ross, B. Danet, M. D. Smith, P. E. Brennan, Developing a One-Pot Click Chemistry (CuAAC) – SNAr Sequence for the Synthesis of a Potential Adenosine Kinase (AK) Inhibitor (Part II Thesis), Oxford, **2021**.

[109] H. M. R. Hoffmann, *J. Chem. Soc.* **1965**, 6753–6761.

[110] D. L. Comins, G. Jianhua, *Tetrahedron Lett.* **1994**, *35*, 2819–2822.

[111] S. Ferrer, D. P. Naughton, I. Parveen, M. D. Threadgill, *J. Chem. Soc. Perkin Trans. 1* **2002**, *2*, 335–340.

[112] Y. G. Wang, E. C. Barnes, *ACS Omega* **2018**, *3*, 4557–4572.

[113] T. Vol, G. C. Hopkins, J. P. Jonak, lb J. Harry Minnemeyer, H. Tieckelmann, C. Hopkins, J. P. Jonak, H. Tieckelmann, H. J. Minnemeyer, A. Smiley, K. Blackwood, D. C. Iffland, F. Ramirez, A. P. Paul, *J. Org. Chem.* **2002**, *32*, 4040–4044.

[114] J. J. Harvey, *Nature* **1964**, *204*, 1104–1105.

[115] W. H. Kirsten, L. A. Mayer, *JNCI J. Natl. Cancer Inst.* **1967**, *39*, 311–335.

[116] B. K. Krueger, M. P. Blaustein, R. W. Ratzlaff, J. Barhanin, A. Schmid, A. Lombet, K. P.

Wheeler, M. Lazdunski, J. C. Eliory, J. Biol, A. R. Drummond, J. A. Benson, I. B. Levitan, L. K. Kaczmarek, K. R. Jenifings, F. Strumwasser, A. C. Nairn, U. Walter, F. D. Wilson, P. Greengard, E. Kandel, J. Schwartz, E. Santos, D. Martin-Zanca, E. A. Premkumar Reddy Marco Pierotti, G. Della Porta, M. Barbacid, *Science* **1984**, *223*, 661–664.

[117] M. Hajdúch, S. Jančík, J. Drábek, D. Radzioch, *J. Biomed. Biotechnol.* **2010**, *2010*, DOI 10.1155/2010/150960.

[118] B. Papke, C. J. Der, *Science* **2017**, *355*, 1158–1163.

[119] P. Liu, Y. Wang, X. Li, *Acta Pharm. Sin. B* **2019**, *9*, 871–879.

[120] D. Uprety, A. A. Adjei, *Cancer Treat. Rev.* **2020**, *89*, 102070.

[121] A. D. Cox, S. W. Fesik, A. C. Kimmelman, J. Luo, C. J. Der, *Nat. Rev. Drug Discov.* **2014**, *13*, 828–851.

[122] M. Barbacid, *Annu. Rev. Biochem.* **1987**, *56*, 779–827.

[123] O. Vögler, J. M. Barceló, C. Ribas, P. V. Escribá, *Biochim. Biophys. Acta - Biomembr.* **2008**, *1778*, 1640–1652.

[124] B. B. Friday, A. A. Adjei, *Biochim. Biophys. Acta - Rev. Cancer* **2005**, *1756*, 127–144.

[125] J. Gao, J. Liao, G. Y. Yang, *Am. J. Transl. Res.* **2009**, *1*, 312.

[126] C. H. Heldin, *Cell* **1995**, *80*, 213–223.

[127] J. Schlessinger, *Cell* **2000**, *103*, 211–225.

[128] P. M. Campbell, C. J. Der, *Semin. Cancer Biol.* **2004**, *14*, 105–114.

[129] G. Buhrman, G. Holzapfel, S. Fetics, C. Mattos, *Proc. Natl. Acad. Sci.* **2010**, *107*, 4931–4936.

[130] K. Scheffzek, M. R. Ahmadian, W. Kabsch, L. Wiesmüller, A. Lautwein, F. Schmitz, A. Wittinghofer, *Science* **1997**, *277*, 333–338.

[131] J. Downward, *Nat. Rev. Cancer 2003 31* **2003**, *3*, 11–22.

[132] E. Castellano, J. Downward, *Genes Cancer* **2011**, *2*, 261.

[133] B. Magnuson, B. Ekim, D. C. Fingar, *Biochem. J.* **2012**, *441*, 1–21.

[134] H. Singh, D. L. Longo, B. A. Chabner, *J. Clin. Oncol.* **2015**, *33*, 3650–3659.

[135] Y. Pylayeva-Gupta, E. Grabocka, D. Bar-Sagi, *Nat. Rev. Cancer 2011 1111* **2011**, *11*, 761–774.

[136] A. Matikas, D. Mistriotis, V. Georgoulias, A. Kotsakis, *Crit. Rev. Oncol. Hematol.* **2017**, *110*, 1–12.

[137] H. J. N. Andreyev, A. R. Norman, D. Cunningham, J. R. Oates, P. A. Clarke, *JNCI J. Natl. Cancer Inst.* **1998**, *90*, 675–684.

[138] P. Keohavong, M. . A. DeMichele, A. C. Melacrinos;, R. J. Landreneau, R. J. Weyant, J. M. Siegfried, *Clin. Cancer Res.* **1996**, *2*, 411–418.

[139] My Cancer Genome, "KRAS G12D," can be found under https://www.mycancergenome.org/content/alteration/kras-g12d/, **2019**.

[140] My Cancer Genome, "KRAS G12V," can be found under https://www.mycancergenome.org/content/alteration/kras-g12v/, **2018**.

[141] My Cancer Genome, "KRAS G12C," can be found under https://www.mycancergenome.org/content/alteration/kras-g12c/, **2019**.

[142] Mirati Therapeutics Inc., "KRAS Inhibitors | Mirati Therapeutics, Inc.," can be found under https://www.mirati.com/science/programs/kras-inhibitors/, **2022**.

[143] C. Caulin, T. Nguyen, M. A. Longley, Z. Zhou, X. J. Wang, D. R. Roop, *Cancer Res.* **2004**, *64*, 5054–5058.

[144] L. Vitale-Cross, P. Amornphimoltham, G. Fisher, A. A. Molinolo, J. S. Gutkind, *Cancer Res.* **2004**, *64*, 8804–8807.

[145] M. A. Collins, J. C. Brisset, Y. Zhang, F. Bednar, J. Pierre, K. A. Heist, C. J. Galbán, S. Galbán, M. P. di Magliano, *PLoS One* **2012**, *7*, e49707.

[146] I. Becher, M. M. Savitski, M. F. Savitski, C. Hopf, M. Bantscheff, G. Drewes, *ACS Chem. Biol.*

2013, *8*, 599–607.

[147] P. Haluska, G. K. Dy, A. A. Adjei, *Eur. J. Cancer* **2002**, *38*, 1685–1700.

[148] T. F. Gajewski, A. K. S. Salama, D. Niedzwiecki, J. Johnson, G. Linette, C. Bucher, M. A. Blaskovich, S. M. Sebti, F. Haluska, *J. Transl. Med.* **2012**, *10*, 1–8.

[149] S. Luger, V. X. Wang, E. Paietta, R. P. Ketterling, W. Rybka, H. M. Lazarus, M. R. Litzow, J. M. Rowe, R. A. Larson, F. R. Appelbaum, M. S. Tallman, *Blood* **2015**, *126*, 1308–1308.

[150] E. Van Cutsem, H. van de Velde, P. Karasek, H. Oettle, W. L. Vervenne, A. Szawlowski, P. Schoffski, S. Post, C. Verslype, H. Neumann, H. Safran, Y. Humblet, J. Perez Ruixo, Y. Ma, D. Von Hoff, *J. Clin. Oncol.* **2004**, *22*, 1430–1438.

[151] A. A. Adjei, A. Mauer, L. Bruzek, R. S. Marks, S. Hillman, S. Geyer, L. J. Hanson, J. J. Wright, C. Erlichman, S. H. Kaufmann, E. E. Vokes, *J. Clin. Oncol.* **2003**, *21*, 1760–1766.

[152] Y. Zhu, S. Sharma, L. B. Saltz, N. Kemeny, D. P. Kelsen, D. Ilson, E. O'Reilly, S. Zaknoen, C. Baum, P. Statkevich, E. Hollywood, *Ann. Oncol.* **2002**, *13*, 1067–1071.

[153] E. Winquist, M. J. Moore, K. N. Chi, D. S. Ernst, H. Hirte, S. North, J. Powers, W. Walsh, T. Boucher, R. Patton, L. Seymour, *Urol. Oncol. Semin. Orig. Investig.* **2005**, *23*, 143–149.

[154] E. S. Kim, M. S. Kies, F. V. Fossella, B. S. Glisson, S. Zaknoen, P. Statkevich, R. F. Munden, C. Summey, K. M. W. Pisters, V. Papadimitrakopoulou, M. Tighiouart, A. Rogatko, F. R. Khuri, *Cancer* **2005**, *104*, 561–569.

[155] T. B. Karasic, E. G. Chiorean, S. M. Sebti, P. J. O'Dwyer, *Target. Oncol.* **2019**, *14*, 613–618.

[156] B. Papke, S. Murarka, H. A. Vogel, P. Martín-Gago, M. Kovacevic, D. C. Truxius, E. K. Fansa, S. Ismail, G. Zimmermann, K. Heinelt, C. Schultz-Fademrecht, A. Al Saabi, M. Baumann, P. Nussbaumer, A. Wittinghofer, H. Waldmann, P. I. H. Bastiaens, *Nat. Commun.* **2016**, *7*, 1–9.

[157] J. M. Llovet, S. Ricci, V. Mazzaferro, P. Hilgard, E. Gane, J.-F. Blanc, A. C. de Oliveira, A. Santoro, J.-L. Raoul, A. Forner, M. Schwartz, C. Porta, S. Zeuzem, L. Bolondi, T. F. Greten, P.

R. Galle, J.-F. Seitz, I. Borbath, D. Häussinger, T. Giannaris, M. Shan, M. Moscovici, D. Voliotis, J. Bruix, *N. Engl. J. Med.* **2008**, *359*, 378–390.

[158] B. Escudier, T. Eisen, W. M. Stadler, C. Szczylik, S. Oudard, M. Siebels, S. Negrier, C. Chevreau, E. Solska, A. A. Desai, F. Rolland, T. Demkow, T. E. Hutson, M. Gore, S. Freeman, B. Schwartz, M. Shan, R. Simantov, R. M. Bukowski, *N. Engl. J. Med.* **2007**, *356*, 125–134.

[159] M. S. Brose, C. M. Nutting, B. Jarzab, R. Elisei, S. Siena, L. Bastholt, C. De La Fouchardiere, F. Pacini, R. Paschke, Y. K. Shong, S. I. Sherman, J. W. A. Smit, J. Chung, C. Kappeler, C. Peña, I. Molnár, M. J. Schlumberger, *Lancet* **2014**, *384*, 319–328.

[160] A. Hauschild, J. J. Grob, L. V. Demidov, T. Jouary, R. Gutzmer, M. Millward, P. Rutkowski, C. U. Blank, W. H. Miller, E. Kaempgen, S. Martín-Algarra, B. Karaszewska, C. Mauch, V. Chiarion-Sileni, A. M. Martin, S. Swann, P. Haney, B. Mirakhur, M. E. Guckert, V. Goodman, P. B. Chapman, *Lancet* **2012**, *380*, 358–365.

[161] V. Subbiah, M. E. Cabanillas, R. J. Kreitman, Z. A. Wainberg, J. Y. Cho, B. Keam, J. H. M. Schellens, J. C. Soria, P. Y. Wen, C. Zielinski, G. Urbanowitz, B. Mookerjee, D. Wang, F. Rangwala, *J. Clin. Oncol.* **2018**, *36*, 7–13.

[162] D. M. Hyman, I. Puzanov, V. Subbiah, J. E. Faris, I. Chau, J.-Y. Blay, J. Wolf, N. S. Raje, E. L. Diamond, A. Hollebecque, R. Gervais, M. E. Elez-Fernandez, A. Italiano, R.-D. Hofheinz, M. Hidalgo, E. Chan, M. Schuler, S. F. Lasserre, M. Makrutzki, F. Sirzen, M. L. Veronese, J. Tabernero, J. Baselga, *N. Engl. J. Med.* **2015**, *373*, 726–736.

[163] R. Dummer, P. A. Ascierto, H. J. Gogas, A. Arance, M. Mandala, G. Liszkay, C. Garbe, D. Schadendorf, I. Krajsova, R. Gutzmer, V. Chiarion-Sileni, C. Dutriaux, J. W. B. de Groot, N. Yamazaki, C. Loquai, L. A. Moutouh-de Parseval, M. D. Pickard, V. Sandor, C. Robert, K. T. Flaherty, *Lancet Oncol.* **2018**, *19*, 603–615.

[164] S. Kopetz, A. Grothey, R. Yaeger, E. Van Cutsem, J. Desai, T. Yoshino, H. Wasan, F. Ciardiello,

F. Loupakis, Y. S. Hong, N. Steeghs, T. K. Guren, H.-T. Arkenau, P. Garcia-Alfonso, P. Pfeiffer, S. Orlov, S. Lonardi, E. Elez, T.-W. Kim, J. H. M. Schellens, C. Guo, A. Krishnan, J. Dekervel, V. Morris, A. Calvo Ferrandiz, L. S. Tarpgaard, M. Braun, A. Gollerkeri, C. Keir, K. Maharry, M. Pickard, J. Christy-Bittel, L. Anderson, V. Sandor, J. Tabernero, *N. Engl. J. Med.* **2019**, *381*, 1632–1643.

[165] S. M. Wilhelm, C. Carter, L. Y. Tang, D. Wilkie, A. McNabola, H. Rong, C. Chen, X. Zhang, P. Vincent, M. McHugh, Y. Cao, J. Shujath, S. Gawlak, D. Eveleigh, B. Rowley, L. Liu, L. Adnane, M. Lynch, D. Auclair, I. Taylor, R. Gedrich, A. Voznesensky, B. Riedl, L. E. Post, G. Bollag, P. A. Trail, *Cancer Res.* **2004**, *64*, 7099–7109.

[166] S. Cascinu, R. Berardi, A. Sobrero, P. Bidoli, R. Labianca, S. Siena, D. Ferrari, S. Barni, E. Aitini, V. Zagonel, F. Caprioni, F. Villa, S. Mosconi, L. Faloppi, G. Tonini, C. Boni, P. Conte, F. Di Costanzo, M. Cinquini, *Dig. Liver Dis.* **2014**, *46*, 182–186.

[167] H. L. Kindler, K. Wroblewski, J. A. Wallace, M. J. Hall, G. Locker, S. Nattam, E. Agamah, W. M. Stadler, E. E. Vokes, *Invest. New Drugs* **2012**, *30*, 382–386.

[168] P. I. Poulikakos, C. Zhang, G. Bollag, K. M. Shokat, N. Rosen, *Nature* **2010**, *464*, 427–430.

[169] D. Planchard, B. Besse, H. J. M. Groen, S. M. S. Hashemi, J. Mazieres, T. M. Kim, E. Quoix, P. J. Souquet, F. Barlesi, C. Baik, L. C. Villaruz, R. J. Kelly, S. Zhang, M. Tan, E. Gasal, L. Santarpia, B. E. Johnson, *J. Thorac. Oncol.* **2022**, *17*, 103–115.

[170] P. A. Ascierto, G. A. McArthur, B. Dréno, V. Atkinson, G. Liszkay, A. M. Di Giacomo, M. Mandalà, L. Demidov, D. Stroyakovskiy, L. Thomas, L. de la Cruz-Merino, C. Dutriaux, C. Garbe, Y. Yan, M. Wongchenko, I. Chang, J. J. Hsu, D. O. Koralek, I. Rooney, A. Ribas, J. Larkin, *Lancet Oncol.* **2016**, *17*, 1248–1260.

[171] A. M. Gross, P. L. Wolters, E. Dombi, A. Baldwin, P. Whitcomb, M. J. Fisher, B. Weiss, A. Kim, M. Bornhorst, A. C. Shah, S. Martin, M. C. Roderick, D. C. Pichard, A. Carbonell, S. M. Paul, J.

Therrien, O. Kapustina, K. Heisey, D. W. Clapp, C. Zhang, C. J. Peer, W. D. Figg, M. Smith, J. Glod, J. O. Blakeley, S. M. Steinberg, D. J. Venzon, L. A. Doyle, B. C. Widemann, *N. Engl. J. Med.* **2020**, *382*, 1430–1442.

[172] J. Rinehart, A. A. Adjei, P. M. LoRusso, D. Waterhouse, J. R. Hecht, R. B. Natale, O. Hamid, M. Varterasian, P. Asbury, E. P. Kaldjian, S. Gulyas, D. Y. Mitchell, R. Herrera, J. S. Sebolt-Leopold, M. B. Meyer, *J. Clin. Oncol.* **2004**, *22*, 4456–4462.

[173] J. D. Hainsworth, C. L. Cebotaru, V. Kanarev, T. E. Ciuleanu, D. Damyanov, P. Stella, H. Ganchev, G. Pover, C. Morris, V. Tzekova, *J. Thorac. Oncol.* **2010**, *5*, 1630–1636.

[174] K. Kawaguchi, K. Igarashi, T. Murakami, T. Kiyuna, T. M. Lwin, H. K. Hwang, J. C. Delong, B. M. Clary, M. Bouvet, M. Unno, R. M. Hoffman, K. Kawaguchi, K. Igarashi, T. Murakami, T. Kiyuna, T. M. Lwin, H. K. Hwang, J. C. Delong, B. M. Clary, M. Bouvet, M. Unno, R. M. Hoffman, *Oncotarget* **2017**, *8*, 47490–47496.

[175] K. Kawaguchi, K. Igarashi, K. Miyake, T. M. Lwin, M. Miyake, T. Kiyuna, H. K. Hwang, T. Murakami, J. C. Delong, S. R. Singh, B. Clary, M. Bouvet, M. Unno, R. M. Hoffman, *Tissue Cell* **2018**, *52*, 124–128.

[176] J. R. Infante, B. G. Somer, J. O. Park, C. P. Li, M. E. Scheulen, S. M. Kasubhai, D. Y. Oh, Y. Liu, S. Redhu, K. Steplewski, N. Le, *Eur. J. Cancer* **2014**, *50*, 2072–2081.

[177] O. K. Mirzoeva, E. A. Collisson, P. M. Schaefer, B. Hann, Y. K. Hom, A. H. Ko, W. M. Korn, *Mol. Cancer Ther.* **2013**, *12*, 2213–2225.

[178] S. Pant, J. C. Bendell, R. J. Sullivan, G. Shapiro, M. Millward, G. Mi, E. Yuen, M. D. Willard, D. Wang, S. Joseph, W. T. McMillen, S. V. Bhagwat, R. V. Tiu, M. R. Patel, *J. Clin. Oncol.* **2019**, *37*, 3001–3001.

[179] N. T. Ihle, R. Lemos, P. Wipf, A. Yacoub, C. Mitchell, D. Siwak, G. B. Mills, P. Dent, D. L. Kirkpatrick, G. Powis, *Cancer Res.* **2009**, *69*, 143–150.

[180] J. A. Engelman, L. Chen, X. Tan, K. Crosby, A. R. Guimaraes, R. Upadhyay, M. Maira, K. McNamara, S. A. Perera, Y. Song, L. R. Chirieac, R. Kaur, A. Lightbown, J. Simendinger, T. Li, R. F. Padera, C. García-Echeverría, R. Weissleder, U. Mahmood, L. C. Cantley, K. K. Wong, *Nat. Med.* **2008**, *14*, 1351–1356.

[181] A. W. Tolcher, K. Khan, M. Ong, U. Banerji, V. Papadimitrakopoulou, D. R. Gandara, A. Patnaik, R. D. Baird, D. Olmos, C. R. Garrett, J. M. Skolnik, E. H. Rubin, P. D. Smith, P. Huang, M. Learoyd, K. A. Shannon, A. Morosky, E. Tetteh, Y. M. Jou, K. P. Papadopoulos, V. Moreno, B. Kaiser, T. A. Yap, L. Yan, J. S. De Bono, in *Clin. Cancer Res.*, American Association For Cancer Research Inc., **2015**, pp. 739–748.

[182] Y. Xing, N. U. Lin, M. A. Maurer, H. Chen, A. Mahvash, A. Sahin, A. Akcakanat, Y. Li, V. Abramson, J. Litton, M. Chavez-Macgregor, V. Valero, S. A. Piha-Paul, D. Hong, K. A. Do, E. Tarco, D. Riall, A. K. Eterovic, G. M. Wulf, L. C. Cantley, G. B. Mills, L. A. Doyle, E. Winer, G. N. Hortobagyi, A. M. Gonzalez-Angulo, F. Meric-Bernstam, *Breast Cancer Res.* **2019**, *21*, 1–12.

[183] R. C. Hillig, B. Sautier, J. Schroeder, D. Moosmayer, A. Hilpmann, C. M. Stegmann, N. D. Werbeck, H. Briem, U. Boemer, J. Weiske, V. Badock, J. Mastouri, K. Petersen, G. Siemeister, J. D. Kahmann, D. Wegener, N. Böhnke, K. Eis, K. Graham, L. Wortmann, F. Von Nussbaum, B. Bader, *Proc. Natl. Acad. Sci. U. S. A.* **2019**, *116*, 2551–2560.

[184] Y. N. P. Chen, M. J. Lamarche, H. M. Chan, P. Fekkes, J. Garcia-Fortanet, M. G. Acker, B. Antonakos, C. H. T. Chen, Z. Chen, V. G. Cooke, J. R. Dobson, Z. Deng, F. Fei, B. Firestone, M. Fodor, C. Fridrich, H. Gao, D. Grunenfelder, H. X. Hao, J. Jacob, S. Ho, K. Hsiao, Z. B. Kang, R. Karki, M. Kato, J. Larrow, L. R. La Bonte, F. Lenoir, G. Liu, S. Liu, D. Majumdar, M. J. Meyer, M. Palermo, L. Perez, M. Pu, E. Price, C. Quinn, S. Shakya, M. D. Shultz, J. Slisz, K. Venkatesan, P. Wang, M. Warmuth, S. Williams, G. Yang, J. Yuan, J. H. Zhang, P. Zhu, T. Ramsey, N. J. Keen, W. R. Sellers, T. Stams, P. D. Fortin, *Nature* **2016**, *535*, 148–152.

[185] M. J. Lamarche, M. Acker, A. Argintaru, D. Bauer, J. Boisclair, H. Chan, C. H. T. Chen, Y. N. Chen, Z. Chen, Z. Deng, M. Dore, D. Dunstan, J. Fan, P. Fekkes, B. Firestone, M. Fodor, J. Garcia-Fortanet, P. D. Fortin, C. Fridrich, J. Giraldes, M. Glick, D. Grunenfelder, H. X. Hao, M. Hentemann, S. Ho, A. Jouk, Z. B. Kang, R. Karki, M. Kato, N. Keen, R. Koenig, L. R. Labonte, J. Larrow, G. Liu, S. Liu, D. Majumdar, S. Mathieu, M. J. Meyer, M. Mohseni, R. Ntaganda, M. Palermo, L. Perez, M. Pu, T. Ramsey, J. Reilly, P. Sarver, W. R. Sellers, M. Sendzik, M. D. Shultz, J. Slisz, K. Slocum, T. Smith, S. Spence, T. Stams, C. Straub, V. Tamez, B. B. Toure, C. Towler, P. Wang, H. Wang, S. L. Williams, F. Yang, B. Yu, J. H. Zhang, S. Zhu, *J. Med. Chem.* **2020**, *63*, 13578–13594.

[186] Z. Song, M. Wang, Y. Ge, X. P. Chen, Z. Xu, Y. Sun, X. F. Xiong, *Acta Pharm. Sin. B* **2021**, *11*, 13–29.

[187] J. Bendell, S. Ulahannan, M. Koczywas, J. Brahmer, A. Capasso, S. G. Eckhardt, M. Gordon, C. McCoach, M. Nagasaka, K. Ng, J. Pacheco, J. Riess, A. Spira, C. Steuer, R. Dua, S. Chittivelu, S. Masciari, Z. Wang, X. Wang, S. H. Ou, *Eur. J. Cancer* **2020**, *138*, S8–S9.

[188] B. O'Leary, R. S. Finn, N. C. Turner, *Nat. Rev. Clin. Oncol. 2016 137* **2016**, *13*, 417–430.

[189] M. Puyol, A. Martín, P. Dubus, F. Mulero, P. Pizcueta, G. Khan, C. Guerra, D. Santamaría, M. Barbacid, *Cancer Cell* **2010**, *18*, 63–73.

[190] J. W. Goldman, J. Mazieres, F. Barlesi, M. Koczywas, K. H. Dragnev, T. Göksel, A. B. Cortot, N. Girard, C. Wesseler, H. Bischoff, E. Nadal, K. Park, S. Lu, A. Taus, M. Cobo, K. Hurt, A. Chiang, A. Hossain, W. J. John, L. G. Paz-Ares, *https://doi.org/10.1200/JCO.2018.36.15_suppl.9025* **2018**, *36*, 9025–9025.

[191] Z. Y. Dong, W. Z. Zhong, X. C. Zhang, J. Su, Z. Xie, S. Y. Liu, H. Y. Tu, H. J. Chen, Y. L. Sun, Q. Zhou, J. J. Yang, X. N. Yang, J. X. Lin, H. H. Yan, H. R. Zhai, L. X. Yan, R. Q. Liao, S. P. Wu, Y. L. Wu, *Clin. Cancer Res.* **2017**, *23*, 3012–3024.

[192] J. Cong, X. Wang, X. Zheng, D. Wang, B. Fu, R. Sun, Z. Tian, H. Wei, *Cell Metab.* **2018**, *28*, 243–255.

[193] Y. Wan, Y. Zhang, G. Wang, P. M. Mwangi, H. Cai, R. Li, *Front. Oncol.* **2020**, *10*, 1326.

[194] U. Sahin, E. Derhovanessian, M. Miller, B. P. Kloke, P. Simon, M. Löwer, V. Bukur, A. D. Tadmor, U. Luxemburger, B. Schrörs, T. Omokoko, M. Vormehr, C. Albrecht, A. Paruzynski, A. N. Kuhn, J. Buck, S. Heesch, K. H. Schreeb, F. Müller, I. Ortseifer, I. Vogler, E. Godehardt, S. Attig, R. Rae, A. Breitkreuz, C. Tolliver, M. Suchan, G. Martic, A. Hohberger, P. Sorn, J. Diekmann, J. Ciesla, O. Waksmann, A. K. Brück, M. Witt, M. Zillgen, A. Rothermel, B. Kasemann, D. Langer, S. Bolte, M. Diken, S. Kreiter, R. Nemecek, C. Gebhardt, S. Grabbe, C. Höller, J. Utikal, C. Huber, C. Loquai, Ö. Türeci, *Nature* **2017**, *547*, 222–226.

[195] K. Sakamoto, Y. Kamada, T. Sameshima, M. Yaguchi, A. Niida, S. Sasaki, M. Miwa, S. Ohkubo, J. ichi Sakamoto, M. Kamaura, N. Cho, A. Tani, *Biochem. Biophys. Res. Commun.* **2017**, *484*, 605–611.

[196] A. Niida, S. Sasaki, K. Yonemori, T. Sameshima, M. Yaguchi, T. Asami, K. Sakamoto, M. Kamaura, *Bioorg. Med. Chem. Lett.* **2017**, *27*, 2757–2761.

[197] S. Sogabe, Y. Kamada, M. Miwa, A. Niida, T. Sameshima, M. Kamaura, K. Yonemori, S. Sasaki, J. I. Sakamoto, K. Sakamoto, *ACS Med. Chem. Lett.* **2017**, *8*, 732–736.

[198] K. Sakamoto, T. Masutani, T. Hirokawa, *Sci. Rep.* **2020**, *10*, 1–16.

[199] G. Fumagalli, R. J. Carbajo, J. W. M. Nissink, J. Tart, R. Dou, A. P. Thomas, D. R. Spring, *J. Med. Chem.* **2021**, *64*, 17287–17303.

[200] J. M. Ostrem, U. Peters, M. L. Sos, J. A. Wells, K. M. Shokat, *Nature* **2013**, *503*, 548–551.

[201] M. P. Patricelli, M. R. Janes, L. S. Li, R. Hansen, U. Peters, L. V. Kessler, Y. Chen, J. M. Kucharski, J. Feng, T. Ely, J. H. Chen, S. J. Firdaus, A. Babbar, P. Ren, Y. Liu, *Cancer Discov.* **2016**, *6*, 316–329.

[202] G. A. Hobbs, A. Wittinghofer, C. J. Der, *Cancer Cell* **2016**, *29*, 251–253.

[203] P. Lito, M. Solomon, L. S. Li, R. Hansen, N. Rosen, *Science* **2016**, *351*, 604–608.

[204] M. R. Janes, J. Zhang, L. S. Li, R. Hansen, U. Peters, X. Guo, Y. Chen, A. Babbar, S. J. Firdaus, L. Darjania, J. Feng, J. H. Chen, S. Li, S. Li, Y. O. Long, C. Thach, Y. Liu, A. Zarieh, T. Ely, J. M. Kucharski, L. V. Kessler, T. Wu, K. Yu, Y. Wang, Y. Yao, X. Deng, P. P. Zarrinkar, D. Brehmer, D. Dhanak, M. V. Lorenzi, D. Hu-Lowe, M. P. Patricelli, P. Ren, Y. Liu, *Cell* **2018**, *172*, 578-589.e17.

[205] J. Canon, K. Rex, A. Y. Saiki, C. Mohr, K. Cooke, D. Bagal, K. Gaida, T. Holt, C. G. Knutson, N. Koppada, B. A. Lanman, J. Werner, A. S. Rapaport, T. San Miguel, R. Ortiz, T. Osgood, J. R. Sun, X. Zhu, J. D. McCarter, L. P. Volak, B. E. Houk, M. G. Fakih, B. H. O'Neil, T. J. Price, G. S. Falchook, J. Desai, J. Kuo, R. Govindan, D. S. Hong, W. Ouyang, H. Henary, T. Arvedson, V. J. Cee, J. R. Lipford, *Nature* **2019**, *575*, 217–223.

[206] D. R. Gentile, M. K. Rathinaswamy, M. L. Jenkins, S. M. Moss, B. D. Siempelkamp, A. R. Renslo, J. E. Burke, K. M. Shokat, *Cell Chem. Biol.* **2017**, *24*, 1455–1466.

[207] D. S. Hong, M. G. Fakih, J. H. Strickler, J. Desai, G. A. Durm, G. I. Shapiro, G. S. Falchook, T. J. Price, A. Sacher, C. S. Denlinger, Y.-J. Bang, G. K. Dy, J. C. Krauss, Y. Kuboki, J. C. Kuo, A. L. Coveler, K. Park, T. W. Kim, F. Barlesi, P. N. Munster, S. S. Ramalingam, T. F. Burns, F. Meric-Bernstam, H. Henary, J. Ngang, G. Ngarmchamnanrith, J. Kim, B. E. Houk, J. Canon, J. R. Lipford, G. Friberg, P. Lito, R. Govindan, B. T. Li, *N. Engl. J. Med.* **2020**, *383*, 1207–1217.

[208] F. Skoulidis, B. T. Li, G. K. Dy, T. J. Price, G. S. Falchook, J. Wolf, A. Italiano, M. Schuler, H. Borghaei, F. Barlesi, T. Kato, A. Curioni-Fontecedro, A. Sacher, A. Spira, S. S. Ramalingam, T. Takahashi, B. Besse, A. Anderson, A. Ang, Q. Tran, O. Mather, H. Henary, G. Ngarmchamnanrith, G. Friberg, V. Velcheti, R. Govindan, *N. Engl. J. Med.* **2021**, *384*, 2371–2381.

[209] J. B. Fell, J. P. Fischer, B. R. Baer, J. Ballard, J. F. Blake, K. Bouhana, B. J. Brandhuber, D. M. Briere, L. E. Burgess, M. R. Burkard, H. Chiang, M. J. Chicarelli, K. Davidson, J. J. Gaudino, J. Hallin, L. Hanson, K. Hee, E. J. Hicken, R. J. Hinklin, M. A. Marx, M. J. Mejia, P. Olson, P. Savechenkov, N. Sudhakar, T. P. Tang, G. P. Vigers, H. Zecca, J. G. Christensen, *ACS Med. Chem. Lett.* **2018**, *9*, 1230–1234.

[210] J. Hallin, L. D. Marx, Matthew A. Engstom, L. Hargis, A. Calinisan, R. Aranda, A. C. Burns, D. M. Briere, V. Sudhakar, Niranjan Bowcut, B. R. Baer, J. F. Blake, M. R. Bruckard, J. B. Fell, J. P. Fischer, T. P. Tang, L. Wollenberg, G. P. Vigers, P. Olson, J. G. Christensen, in *Poster Present. AACR-NCI-EORTC 2019*, Mirati Therapeutics, Boston, Massachusetts, **2019**.

[211] J. B. Fell, J. P. Fischer, B. R. Baer, J. F. Blake, K. Bouhana, D. M. Briere, K. D. Brown, L. E. Burgess, A. C. Burns, M. R. Burkard, H. Chiang, M. J. Chicarelli, A. W. Cook, J. J. Gaudino, J. Hallin, L. Hanson, D. P. Hartley, E. J. Hicken, G. P. Hingorani, R. J. Hinklin, M. J. Mejia, P. Olson, J. N. Otten, S. P. Rhodes, M. E. Rodriguez, P. Savechenkov, D. J. Smith, N. Sudhakar, F. X. Sullivan, T. P. Tang, G. P. Vigers, L. Wollenberg, J. G. Christensen, M. A. Marx, *J. Med. Chem.* **2020**, *63*, 6679–6693.

[212] J. Hallin, L. D. Engstrom, L. Hargi, A. Calinisan, R. Aranda, D. M. Briere, N. Sudhakar, V. Bowcut, B. R. Baer, J. A. Ballard, M. R. Burkard, J. B. Fell, J. P. Fischer, G. P. Vigers, Y. Xue, S. Gatto, J. Fernandez-Banet, A. Pavlicek, K. Velastagui, R. C. Chao, J. Barton, M. Pierobon, E. Baldelli, E. F. Patricoin, D. P. Cassidy, M. A. Marx, I. I. Rybkin, M. L. Johnson, S. H. Ignatius, P. Lito, K. P. Papadopoulos, P. A. Jänne, P. Olson, J. G. Christensen, *Cancer Discov.* **2020**, *10*, 54–71.

[213] D. Hong, L. Bazhenova, B. C. Cho, S. Sen, M. Ponz-Sarvise, R. Heist, Z. Zimmerman, X. Le, D. Xuan, Z. Junming, J. Lee, D. Mckinney, M. Ranaghan, B. Mcmillan, M. Brousseau, M. O'keefe, J. Moroco, R. Singh, B. Besnik, P. Mccarren, K. Mulvaney, W. Sellers, A. Ianari, P. A. Jä Nne, I.

I. Rybkin, A. I. Spira, G. J. Riely, K. P. Papadopoulos, J. K. Sabari, M. L. Johnson, R. S. Heist, M. Barve, J. M. Pacheco, T. A. Leal, K. Velastegui, C. Cornelius, P. Olson, J. G. Christensen, T. Kheoh, R. C. Chao, S. H. I. Ou, *Eur. J. Cancer* **2020**, *138*, S1–S2.

[214] M. L. Johnson, S. H. I. Ou, M. Barve, I. I. Rybkin, K. P. Papadopoulos, T. A. Leal, K. Velastegui, J. G. Christensen, T. Kheoh, R. C. Chao, J. Weiss, *Eur. J. Cancer* **2020**, *138*, S2.

[215] Mirati Therapeutics Inc., "U.S. Food and Drug Administration (FDA) Accepts Mirati Therapeutics' New Drug Application for Adagrasib as Treatment of Previously Treated KRASG12C-Mutated Non-Small Cell Lung Cancer," can be found under https://www.prnewswire.com/news-releases/us-food-and-drug-administration-fda-accepts-mirati-therapeutics-new-drug-application-for-adagrasib-as-treatment-of-previously-treated-krasg12c-mutated-non-small-cell-lung-cancer-301483014.html, **2022**.

[216] Mirati Therapeutics Inc., "Pipeline," can be found under https://www.mirati.com/science/pipeline/, **2022**.

[217] G. Budwell, "Why Mirati Therapeutics Stock Is Plunging Today," can be found under https://www.fool.com/investing/2022/02/16/why-mirati-therapeutics-stock-is-plunging-today/, **2022**.

[218] A. K. Kwan, G. A. Piazza, A. B. Keeton, C. A. Leite, *J. Exp. Clin. Cancer Res.* **2022**, *41*, 1–23.

[219] X. Wang, S. Allen, J. F. Blake, V. Bowcut, D. M. Briere, A. Calinisan, J. R. Dahlke, J. B. Fell, J. P. Fischer, R. J. Gunn, J. Hallin, J. Laguer, J. D. Lawson, J. Medwid, B. Newhouse, P. Nguyen, J. M. O'Leary, P. Olson, S. Pajk, L. Rahbaek, M. Rodriguez, C. R. Smith, T. P. Tang, N. C. Thomas, D. Vanderpool, G. P. Vigers, J. G. Christensen, M. A. Marx, *J. Med. Chem.* **2022**, *65*, 3123–3133.

[220] S.-B. Peng, C. Si, Y. Zhang, R. D. Van Horn, X. Lin, X. Gong, L. Huber, G. Donoho, C. Curtis, J. M. Strelow, W. P. Bocchinfuso, D. Guo, S. L. Boulet, D. Barda, D. Manglicmot, M.-B. D. Saflor,

J. Wang, J. Xiao, M. J. Chalmers, L. Burns, R. J. Linder, B. L. Ackermann, P. D. Cornwell, L. Zhou, D. McCann, J. Henry, *Cancer Res.* **2021**, *81*, 1259–1259.

[221] U.S. National Library of Medicine, "Study of LY3537982 in Cancer Patients With a Specific Genetic Mutation (KRAS G12C)," can be found under https://clinicaltrials.gov/ct2/show/NCT04956640, **2021**.

[222] U.S. National Library of Medicine, "A Study to Evaluate the Safety, Pharmacokinetics, and Activity of GDC-6036 Alone or in Combination in Participants With Advanced or Metastatic Solid Tumors With a KRAS G12C Mutation," can be found under https://clinicaltrials.gov/ct2/show/NCT04449874, **2020**.

[223] U.S. National Library of Medicine, "Study of JDQ443 in Patients With Advanced Solid Tumors Harboring the KRAS G12C Mutation," can be found under https://clinicaltrials.gov/ct2/show/NCT04699188, **2021**.

[224] U.S. National Library of Medicine, "Study to Evaluate D-1553 in Subjects With Solid Tumors," can be found under https://clinicaltrials.gov/ct2/show/NCT04585035, **2020**.

[225] U.S. National Library of Medicine, "A Study to Test Different Doses of BI 1823911 Alone and Combined With Other Medicines in People With Different Types of Advanced Cancer With KRAS Mutation," can be found under https://clinicaltrials.gov/ct2/show/NCT04973163, **2021**.

[226] J. D. Vasta, D. M. Peacock, Q. Zheng, J. A. Walker, Z. Zhang, C. A. Zimprich, M. R. Thomas, M. T. Beck, B. F. Binkowski, C. R. Corona, M. B. Robers, K. M. Shokat, *Nat. Chem. Biol. 2022* **2022**, 1–9.

[227] Amgen, "Amgen Announces First Clinical Data Evaluating Novel Investigational KRASG12C Inhibitor AMG 510 At ASCO 2019," can be found under https://www.prnewswire.com/news-releases/amgen-announces-first-clinical-data-

evaluating-novel-investigational-krasg12c-inhibitor-amg-510-at-asco-2019-300860318.html, **2019**.

[228] J. K. Stille, *Angew. Chemie Int. Ed. English* **1986**, *25*, 508–524.

[229] K. Yamamoto, T. Hayashi, M. Kumada, J. Organometal, see J. D Morrison, H. S. Mosher, L. H. Sommer, J. E. Lyons, H. Fujimoto, Y. Kiso, K. Yamamoto, K. Tamao, M. Kumada, *J. Am. Chem. Soc.* **2002**, *94*, 4374–4376.

[230] S. Xu, E. I. Negishi, *Acc. Chem. Res.* **2016**, *49*, 2158–2168.

[231] J. Langham, Barry, P. Alexander, Rikki, C. Head, John, M. Linsley, Janeen, R. Porter, John, C. Archibald, Sarah, J. Warlow, Graham, *3-Substituted Isoquinolin-1-Yl Derivatives*, **2001**, WO2001019233A1.

[232] C. O. Usifoh, *J. Heterocycl. Chem.* **2001**, *38*, 597–600.

[233] S. A. Gamage, J. A. Spicer, G. W. Rewcastle, J. Milton, S. Sohal, W. Dangerfield, P. Mistry, N. Vicker, P. A. Charlton, W. A. Denny, *J. Med. Chem.* **2002**, *45*, 740–743.

[234] C. Yang, F. Mehmood, T. L. Lam, S. L. F. Chan, Y. Wu, C. S. Yeung, X. Guan, K. Li, C. Y. S. Chung, C. Y. Zhou, T. Zou, C. M. Che, *Chem. Sci.* **2016**, *7*, 3123–3136.

[235] O. Baudoin, *Eur. J. Org. Chem.* **2005**, *2005*, 4223–4229.

[236] D. Zhang, Q. Wang, *Coord. Chem. Rev.* **2015**, *286*, 1–16.

[237] Q. Zhao, C. Li, C. H. Senanayake, W. Tang, *Chem. - A Eur. J.* **2013**, *19*, 2261–2265.

[238] H. Yang, J. Sun, W. Gu, W. Tang, *J. Am. Chem. Soc.* **2020**, *142*, 8036–8043.

[239] T. Markovic, B. N. Rocke, D. C. Blakemore, V. Mascitti, M. C. Willis, *Org. Lett.* **2017**, *19*, 6033–6035.

[240] T. Markovic, B. N. Rocke, D. C. Blakemore, V. Mascitti, M. C. Willis, *Chem. Sci.* **2017**, *8*, 4437–4442.

[241] S. Ayesa, J. Bylund, K. Ersmark, L. Salvadoroden, F. Sehgelmeble, *Respiratory Syncytial Virus*

Inhibitors, **2018**, WO2018038667.

[242] A. Ansari, S. Satalkar, V. Patil, A. S. Shete, S. Kaur, A. Gupta, S. Singh, M. Raja, D. L. Severance, S. Bernales, S. Chakravarty, D. T. Hung, S. M. Pham, F. J. Herrera, R. Rai, *Bioorganic Med. Chem. Lett.* **2017**, *27*, 217–222.

[243] L. Li, J. Feng, T. Wu, P. Ren, Y. Liu, Y. Liu, Y. O. Long, *Inhibitors of KRAS G12C*, **2015**, WO2015054572.

[244] P. Forzatti, L. Lietti, *Catal. Today* **1999**, *52*, 165–181.

[245] C. H. Bartholomew, *Appl. Catal. A Gen.* **2001**, *212*, 17–60.

[246] J. B. Brenneman, E. B. Krall, M. Schlabach, A. A. Wylie, *Substituted Pyrazolopyrimidines and Substituted Purines and Their Use as Ubiquitin-Specific Processing Protease 1*, **2020**, WO2020132269A1.

[247] C. P. Seath, J. W. B. Fyfe, J. J. Molloy, A. J. B. Watson, *Angew. Chem. Int. Ed.* **2015**, *54*, 9976–9979.

[248] V. Koch, M. Nieger, S. Bräse, *Adv. Synth. Catal.* **2017**, *359*, 832–840.

[249] L. Wu, E. Drinkel, F. Gaggia, S. Capolicchio, A. Linden, L. Falivene, L. Cavallo, R. Dorta, *Chem. - A Eur. J.* **2011**, *17*, 12886–12890.

[250] R. Martin, S. L. Buchwald, *Acc. Chem. Res.* **2008**, *41*, 1461–1473.

[251] S. P. H. Mee, V. Lee, J. E. Baldwin, *Angew. Chem. Int. Ed.* **2004**, *43*, 1132–1136.

[252] H. Scheible, M. Dyroff, A. Seithel-Keuth, E. Harrison-Moench, N. Mammasse, A. Port, A. Bachmann, J. Dong, J. J. van Lier, W. Tracewell, D. Mitchell, *Clin. Transl. Sci.* **2021**, *14*, 2420–2430.

[253] S. Allen, M. L. Boys, A. Cook, J. Gaudino, R. J. Hinklin, E. Laird, O. T. McNulty, A. T. Metcalf, R. Newhouse, J. E. Robinson, *Bicyclic Fused Pyridine Compunds As Inhibitors of TAM Kinases*, **2019**, WO2019113190.

[254] T. Ishiyama, M. Murata, N. Miyaura, *J. Org. Chem.* **1995**, *60*, 7508–7510.

[255] **段文虎**, **耿美玉**, 赵彬, **丁健**, **艾菁**, **范珺**, **彭霞**, 严伟, 陈奕, *Pyrazolo [3,4-b] Pyridines and the Preparation Method of Indazole Compounds and Purposes*, **2016**, CN106146493.

[256] S. W. Andrews, S. Aronow, J. F. Blake, B. J. Brandhuber, J. Collier, A. Cook, J. Haas, Y. Jiang, G. R. Kolakowski, E. A. McFaddin, M. L. McKenney, O. T. McNulty, A. T. Metcalf, D. A. Moreno, G. A. Ramann, L. Ren, T. P. Tang, S. M. Walls, *Substituted Pyrazolo[1,5-a]Pyridine Compounds as RET Kinase Inhibitors*, **2018**, WO2018071454.

[257] L. Li, J. Feng, T. Wu, Y. Liu, Y. Wang, P. Ren, L. Liu, *Covalent Inhibitors of KRas*, **2018**, WO2018218070.

[258] R. D. Caldwell, H. Qiu, B. C. Askew, A. T. Bender, N. Brugger, M. Camps, M. Dhanabal, V. Dutt, T. Eichhorn, A. S. Gardberg, A. Goutopoulos, R. Grenningloh, J. Head, B. Healey, B. L. Hodous, B. R. Huck, T. L. Johnson, C. Jones, R. C. Jones, I. Mochalkin, F. Morandi, N. Nguyen, M. Meyring, J. R. Potnick, D. C. Santos, R. Schmidt, B. Sherer, A. Shutes, K. Urbahns, A. V. Follis, A. A. Wegener, S. C. Zimmerli, L. Liu-Bujalski, *J. Med. Chem.* **2019**, *62*, 7643–7655.

[259] R. Gedye, F. Smith, K. Westaway, H. Ali, L. Baldisera, L. Laberge, J. Rousell, *Tetrahedron Lett.* **1986**, *27*, 279–282.

[260] L. Bai, J. X. Wang, Y. Zhang, *Green Chem.* **2003**, *5*, 615–617.

[261] A. K. Sharma, K. Gowdahalli, J. Krzeminski, S. Amin, *J. Org. Chem.* **2007**, *72*, 8987–8989.

[262] A. Cohen, M. D. Crozet, P. Rathelot, P. Vanelle, *Green Chem.* **2009**, *11*, 1736–1742.

[263] W. P. Mai, B. Sun, L. Q. You, L. R. Yang, P. Mao, J. W. Yuan, Y. M. Xiao, L. B. Qu, *Org. Biomol. Chem.* **2015**, *13*, 2750–2755.

[264] J. G. Kettle, S. K. Bagal, S. Bickerton, M. S. Bodnarchuk, J. Breed, R. J. Carbajo, D. J. Cassar, A. Chakraborty, S. Cosulich, I. Cumming, M. Davies, A. Eatherton, L. Evans, L. Feron, S. Fillery, E.

S. Gleave, F. W. Goldberg, S. Harlfinger, L. Hanson, M. Howard, R. Howells, A. Jackson, P. Kemmitt, J. K. Kingston, S. Lamont, H. J. Lewis, S. Li, L. Liu, D. Ogg, C. Phillips, R. Polanski, G. Robb, D. Robinson, S. Ross, J. M. Smith, M. Tonge, R. Whiteley, J. Yang, L. Zhang, X. Zhao, *J. Med. Chem.* **2020**, *63*, 4468–4483.

[265] N. Madhyastha, S. K. Samantha, S. Dittakavi, M. Markose, S. R. Mallurwar, M. Zainuddin, R. Mullangi, *Biomed. Chromatogr.* **2021**, *35*, e5043.

[266] U. S. F. and D. A. (FDA), "Highlights of Prescribing Information (LUMAKRAS)," can be found under www.fda.gov/medwatch., **2021**.

[267] C. I. Stathakis, S. M. Manolikakes, P. Knochel, *Org. Lett.* **2013**, *15*, 1302–1305.

[268] P. Knochel, J. J. Almena Perea, P. Jones, *Tetrahedron* **1998**, *54*, 8275–8319.

[269] C. J. Rohbogner, A. J. Wagner, G. C. Clososki, P. Knochel, *Org. Synth.* **2009**, *86*, 374.

[270] K. Xu, C. Li, X. Zhang, Z. Zhang, *Compound Containing Pyridine as Core and Application Thereof in Organic Electroluminescent Devices*, **2018**, CN107880031.

[271] B. Wu, S. Basu, S. Meng, X. Wang, M. Hu, *Curr. Drug Metab.* **2012**, *12*, 900–916.

[272] N. J. Webb, S. P. Marsden, S. A. Raw, *Org. Lett.* **2014**, *16*, 4718–4721.

[273] N. Guimond, S. I. Gorelsky, K. Fagnou, *J. Am. Chem. Soc.* **2011**, *133*, 6449–6457.

[274] S. Rakshit, C. Grohmann, T. Besset, F. Glorius, *J. Am. Chem. Soc.* **2011**, *133*, 2350–2353.

[275] L. Legnani, G. Prina-Cerai, T. Delcaillau, S. Willems, B. Morandi, *Science* **2018**, *362*, 434–439.

[276] S. Liu, Y. Wang, Y. Yuan, C. Cen, R. Bao, *Nitrogen-Containing Heterocyclic Derivative Regulator, Preparation Method Therefor and Application Thereof*, **2020**, WO2020239077.

[277] R. L. Burwell, *Chem. Rev.* **2002**, *54*, 615–685.

[278] H. Rapoport, C. H. Lovell, B. M. Tolbert, J. Am Chem, J. A. Lawson, J. I. DeGraw, *J. Med. Chem.* **2002**, *20*, 165–166.

[279] L. Zuo, S. Yao, W. Wang, W. Duan, *Tetrahedron Lett.* **2008**, *49*, 4054–4056.

[280] J. F. W. McOmie, D. E. West, *Org. Synth.* **1969**, *49*, 50.

[281] T. Javorskis, E. Orentas, *J. Org. Chem.* **2017**, *82*, 13423–13439.

[282] T. T. Bui, H. K. Kim, *Synlett* **2020**, *31*, 997–1002.

[283] J. Omprakash Rathi, G. Subray Shankarling, *ChemistrySelect* **2020**, *5*, 6861–6893.

[284] Y. Yang, Y. Yu, X. Li, J. Li, Y. Wu, J. Yu, J. Ge, Z. Huang, L. Jiang, Y. Rao, M. Yang, *J. Med. Chem.* **2017**, *60*, 1994–2005.

[285] R. Francke, G. Schnakenburg, S. R. Waldvogel, *Org. Lett.* **2010**, *12*, 4288–4291.

[286] D. A. Hay, C. M. Rogers, O. Fedorov, C. Tallant, S. Martin, O. P. Monteiro, S. Müller, S. Knapp, C. J. Schofield, P. E. Brennan, *Medchemcomm* **2015**, *6*, 1381–1386.

[287] L. J. Gao, J. S. Schwed, L. Weizel, S. De Jonghe, H. Stark, P. Herdewijn, *Bioorg. Med. Chem. Lett.* **2013**, *23*, 132–137.

[288] S. Bartoli, K. B. Jensen, J. D. Kilburn, *J. Org. Chem.* **2003**, *68*, 9416–9422.

[289] H. Bian, K. Chevalier, P. J. Connolly, C. M. Flores, S.-C. Lin, L. Liu, J. Mabus, M. J. Macielag, M. E. McDonnell, P. M. Pitis, S.-P. Zhang, Y.-M. Zhang, B. Zhu, J. Clemente, *Azetidinyl Diamides as Monocyglycerol Lipase Inhibitors and Their Preparation and Use in the Treatment of Diseases*, **2010**, WO2010124086.

[290] L. A. Nguyen, H. He, C. Pham-Huy, *Int. J. Biomed. Sci.* **2006**, *2*, 85–100.

[291] X. Zhang, K. G. Nottingham, C. Patel, J. V. Alegre-Requena, J. N. Levy, R. S. Paton, A. McNally, *Nat. 2021 5947862* **2021**, *594*, 217–222.

[292] G. B. Kauffman, L. Y. Fang, N. Viswanathan, G. Townsend, *Inorg. Synth.* **2006**, *22*, 101–103.

[293] B. J. Cosier, A. M. Glazer, *J. Appl. Crystallogr.* **1986**, *19*, 105–107.

[294] P. Parois, R. I. Cooper, A. L. Thompson, *Chem. Cent. J.* **2015**, *9*, 1–14.

[295] R. I. Cooper, A. L. Thompson, D. J. Watkin, *J. Appl. Crystallogr.* **2010**, *43*, 1100–1107.

[296] L. Palatinus, G. Chapuis, *J. Appl. Crystallogr.* **2007**, *40*, 786–790.

[297] H. D. Flack, G. Bernardinelli, D. A. Clemente, A. Linden, A. L. Spek, *Acta Crystallogr. Sect. B Struct. Sci.* **2006**, *62*, 695–701.

[298] H. D. Flack, *Acta Crystallogr. Sect. A* **1983**, *39*, 876–881.

[299] R. W. W. Hooft, L. H. Straver, A. L. Spek, *J. Appl. Crystallogr.* **2008**, *41*, 96.

[300] Research Collaboratory for Structural Bioinformatics, "RCSB PDB: Homepage," can be found under https://www.rcsb.org/, **2020**.

[301] Schrödinger, "A Chemist's Guide to Maestro," can be found under https://www.schrodinger.com/sites/default/files/s3/mkt/Documentation/2021-2/docs/Documentation.htm#academy_tutorials/AChemistsGuideToMaestro/A Chemist s Guide to Maestro.htm, **2020**.

[302] J. Sikorski, R. Durley, D. Mischke, E. Reinhard, Y. Fobian, M. Toffelson, L. Wang, M. Grapperhaus, B. Hickory, M. Massa, M. Norton, W. Vernier, B. Parnas, M. Promo, A. Hamme, D. Spangle, M. Rueppel, *Substituted N,N-Disubstituted Diamino Compounds Useful for Inhibiting Cholesteryl Ester Transfer Protein Activity*, **2001**, US20020120011A1.

[303] L. Song, H. Yao, L. Zhu, R. Tong, *Org. Lett.* **2013**, *15*, 6–9.

[304] M. Ellwart, *Org. Synth.* **2018**, *95*, 127–141.

[305] H. Yoshida, R. Yoshida, K. Takaki, *Angew. Chem. Int. Ed.* **2013**, *52*, 8629–8632.

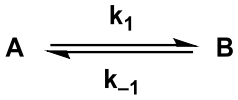
Part V

Appendix

VI. Appendix

Appendix A – Origin of rate of racemisation equation[49]

Let A be the major enantiomer in an enantioenriched sample undergoing racemisation, where B is the minor enantiomer. Let k_1 and k_{-1} be the rate constants associated with the interconversion of A to B and B to A respectively.



The rate of change of [A] would then be

$$\frac{d[A]}{dt} = -k_1[A] + k_{-1}[B]$$

In the context of an enantiomerisation process, it can be assumed that $k_1 = k_{-1} = k_{ent}$

$$\frac{d[A]}{dt} = k_{ent}([B] - [A])$$

The conservation of mass implies that, at any given time t, [A] + [B] = $[A_0]$ + $[B_0]$, where $[A_0]$ and $[B_0]$ are the initial concentrations in A and B, respectively (t = 0). Therefore, [B] = $[A_0]$ + $[B_0]$ – [A], and by incorporating this into the equation above, we get:

$$\frac{d[A]}{dt} = k_{ent}([A_0] + [B_0] - 2[A])$$

$$\frac{dA}{[A_0] + [B_0] - 2[A]} = k_{ent}dt$$

Integrating this equation gives

$$\int_{[A_0]}^{[A]} \frac{d[A]}{[A_0] + [B_0] - 2[A]} = k_{ent} \int_o^t dt$$

$$\left[-\frac{1}{2} ln\left([A_0] + [B_0] - 2[A]\right) \right]_{[A_0]}^{[A]} = k_{ent}[t]_0^t$$

$$-\frac{1}{2} ln\left([A_0] + [B_0] - 2[A]\right) + \frac{1}{2} ln([A_0] + [B_0] - 2[A_0]) = k_{ent}t$$

Rearranging the equation

$$ln\left(\frac{[B_0] - [A_0]}{[A_0] + [B_0] - 2[A]}\right) = 2k_{ent}t$$

Reinjecting the conservation of mass in the denominator ($[A_0] + [B_0] - [A] = [B]$)

$$ln\left(\frac{[B_0] - [A_0]}{[B] - [A]}\right) = 2k_{ent}t$$

Multiplying the numerator and denominator by [A] + [B] and rearranging the equation

$$ln\left(\frac{[B_0] - [A_0]}{[A] + [B]} \times \frac{[A] + [B]}{[B] - [A]}\right) = 2k_{ent}t$$

Separating the logarithms and using the conservation of mass once again

$$ln\left(\frac{[B_0] - [A_0]}{[A_0] + [B_0]}\right) + ln\left(\frac{[A] + [B]}{[B] - [A]}\right) = 2k_{ent}t$$

Rearranging the equation above

$$ln\left(\frac{[A] + [B]}{[B] - [A]}\right) = 2k_{ent}t + ln\left(\frac{[A_0] + [B_0]}{[B_0] - [A_0]}\right)$$

By definition, the enantiomeric excess (ee) of a system where A is the major enantiomer and B is the minor enantiomer is

$$ee = \frac{[B] - [A]}{[A] + [B]}$$

Therefore, with ee_0 as the initial enantiomeric excess (t = 0) and $k_{rac} = 2k_{ent}$

$$ln\left(\frac{1}{ee}\right) = 2k_{ent}t + ln\left(\frac{1}{ee_0}\right) = k_{rac}t + \ ln\left(\frac{1}{ee_0}\right)$$

Thus, $ln\frac{1}{ee} = f(t)$ is a straight line.

The half-life of racemisation is defined as the time $t_{1/2}^{rac}$ when ee = 0.5 = 1/2, assuming $ee_0 = 1$

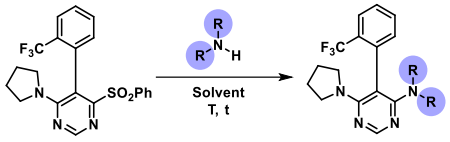
$$ln\left(\frac{1}{1/2}\right) = k_{rac}t_{1/2}^{rac} + ln\left(\frac{1}{1}\right)$$

Therefore

$$ln(2) = k_{rac}t_{1/2}^{rac}$$

$$t_{1/2}^{rac} = \frac{ln\,(2)}{k_{rac}}$$

Appendix B – Failed attempts at SNAr on the sulfonyl group



25
rac.

31x
x=a..b

R_2NH	Additive(s)	Solvent	Temperature	Duration	Result
Morpholine	N/A	Neat	100 °C	48 h	No reaction
Morpholine	N/A	Neat	120 °C	96 h	No reaction
Morpholine	K_2CO_3	DMF	120 °C	16 h	No reaction
Morpholine	DIPEA	DMF	120 °C	16 h	No reaction
Et_2NH	N/A	Neat	r.t.	96 h	No reaction
Et_2NH	N/A	Neat	120 °C	96 h	No reaction
Et_2NH	DIPEA	DMF	r.t.	16 h	No reaction
Et_2NH	DIPEA	DMF	120 °C	16 h	No reaction
Et_2NH	KOH (aq.) nBu$_4$NBr (10 mol%)	PhMe/H_2O	r.t.	16 h	No reaction

Appendix C – MPLS PGR Student Log – Impact of the Coronavirus (COVID-19) Public Health Emergency

The University and the MPLS Division are aware that the current situation with the coronavirus (COVID-19) public health emergency will have a very significant effect on PGR students, including on their research projects. We are working on policies and procedures to deal with the impacts, but it will help us and you if there is clear information on how the situation has an impact on you as it progresses. We have therefore prepared this template log for you to use to help you to keep track of how the situation affects your research progression over time. If you keep this up to date it will provide important information for us to ensure that you receive any additional time and support you need at a later stage.

This log is designed to be completed by you, the student, but you should share this with your supervisor and work on content collaboratively if required. Supervisors can include their own comments in the additional details column if required. Please ensure it is clear where information is a supervisor contribution.

Please save this document with your name and student number so that we can easily trace it to you if necessary.

Student name (family, first name): Danet, Benjamin **Student number:** 2354037

Department: Chemistry (Chemistry Research Laboratory) **Programme of Study:** SBM CDT

Supervisor: Martin D. Smith, Paul E. Brennan.

Event start date	Event end date	Brief description	Level of impact	Additional details
18/3/20	*13/07/20*	*Lockdown – Staying at home*	*High*	*Was constrained to stay at home for almost 4 months due to the international pandemic. My work being exclusively lab-based, I was not able to achieve any progress during this time.*
14/07/20	*22/08/20*	*Resumed work (1 week on/ 1 week off)*	*Medium*	*Due to the 3 (then 4) people per lab limit, the members of the group switch places so that everyone gets the same amount of time in the lab, which leads to some weeks where I am unable to carry out any lab work*
23/08/20	*07/09/20*	*Quarantine – Staying at home*	*High*	*Had to quarantine for 14 days after visiting family in France during August and the government implemented a self-isolation policy for people coming back to the United Kingdom whilst I was there.*
08/09/20	*17/10/20*	*Resumed work on/off (2 weeks on/ 1 week off)*	*Medium*	*Due to the 3 (then 4) people per lab limit, the members of the group switch places so that everyone gets the same amount of time in the lab, which leads to some weeks where I am unable to carry out any lab work.*
18/10/20	*02/01/21*	*Work in AM/PM shift*	*Medium*	*Back to the lab every day, but only on AM/PM shifts due to the*

				increasing number of people in the lab and the limitation on occupancy. (AM shift = 7 am – 2.15 pm; PM shift = 2.40 pm – 10 pm).
03/01/21	*13/01/21*	*Quarantine – Staying at home*	*High*	*Had to quarantine for 10 days after visiting family in France for Christmas.*
14/01/21	*31/05/21*	*Work in AM/PM shift*	*Medium*	*Back to the lab every day, but only on AM/PM shifts due to the increasing number of people in the lab and the limitation on occupancy. (AM shift = 6 am – 2.15 pm; PM shift = 2.40 pm – 12 am).*
01/06/21	*19/07/21*	*Work 4 to 4.5 days a week (out of 5)*	*Low*	*Maximum occupancy in the lab was allowed to 6, so shift work was abandoned and full-time work was possible again. However, to accommodate 7 people on that schedule half a day 2/3 weeks and a full day 1/3 week had to be taken off.*
20/07/21	*19/11/21*	*Normal working hours*	*None*	*Back to normal working hours in the lab*
20/11/21	*25/11/21*	*Self-isolation / close contact*	*High*	*Advised to stay out of the lab after being a close contact. Waiting for confirmation of no infection.*
26/11/21	*14/02/22*	*Normal working hours*	*None*	*Back to normal working hours in the lab*